NETTER'S Correlative Imaging

Abdominal & Pelvic Anatomy

DREW A. TORIGIAN
MARY KITAZONO HAMMELL

With online access at
www.NetterReference.com

F. Netter M.D.

ELSEVIER
SAUNDERS

NETTER'S

Correlative Imaging: Abdominal and Pelvic Anatomy

Volume Editors

DREW A. TORIGIAN, MD, MA
Department of Radiology
Hospital of the University of Pennsylvania
Philadelphia, Pennsylvania

MARY KITAZONO HAMMELL, MD
Department of Radiology
Hospital of the University of Pennsylvania
Philadelphia, Pennsylvania

Series Editor

NANCY M. MAJOR, MD
Director of Diagnostic Imaging
Orthopaedic Associates of Allentown
Allentown, Pennsylvania

Illustrations by
Frank H. Netter, MD

Contributing Illustrators
Kristen Wienandt Marzejon, MAMS
Carlos A.G. Machado, MD

ELSEVIER
SAUNDERS

ELSEVIER
SAUNDERS

1600 John F. Kennedy Blvd.
Ste. 1800
Philadelphia, PA 19103-2899

NETTER'S CORRELATIVE IMAGING: ABDOMINAL AND PELVIC ANATOMY

ISBN: 978-1-4377-3654-0

Notices

Knowledge and best practice in this field are constantly changing. As new research and experience broaden our understanding, changes in research methods, professional practices, or medical treatment may become necessary.

Practitioners and researchers must always rely on their own experience and knowledge in evaluating and using any information, methods, compounds, or experiments described herein. In using such information or methods they should be mindful of their own safety and the safety of others, including parties for whom they have a professional responsibility.

With respect to any drug or pharmaceutical products identified, readers are advised to check the most current information provided (i) on procedures featured or (ii) by the manufacturer of each product to be administered, to verify the recommended dose or formula, the method and duration of administration, and contraindications. It is the responsibility of practitioners, relying on their own experience and knowledge of their patients, to make diagnoses, to determine dosages and the best treatment for each individual patient, and to take all appropriate safety precautions.

To the fullest extent of the law, neither the Publisher nor the authors, contributors, or editors, assume any liability for any injury and/or damage to persons or property as a matter of products liability, negligence or otherwise, or from any use or operation of any methods, products, instructions, or ideas contained in the material herein.

ISBN: 978-1-4377-3654-0

Senior Content Strategist: Elyse O'Grady
Content Development Manager: Marybeth Thiel
Publishing Services Manager: Patricia Tannian
Senior Project Manager: John Casey
Senior Design Manager: Lou Forgione
Illustrations Manager: Karen Giacomucci

Last digit is the print number: 9 8 7 6 5 4 3 2 1

To my parents, Andrew and Rose Torigian, who have always supported and encouraged me and whom I love and respect beyond words, to my sisters, Christine and Cathy, whom I love and am very proud of, and to their beautiful children, Sammy, Sierra, and Elizabeth who are just full of wonder and curiosity, and to God who in His infinite grace and mercy has shown me unconditional love through His Son, Jesus Christ.

DAT

To my parents, Lloyd and Jody Kitazono, who are both my foundation and my inspiration, and to my husband, Darren Hammell, who is my heart, my reason, and my balance.

MKH

About the Artists

FRANK H. NETTER, MD

Frank H. Netter was born in 1906 in New York City. He studied art at the Art Student's League and the National Academy of Design before entering medical school at New York University, where he received his medical degree in 1931. During his student years, Dr. Netter's notebook sketches attracted the attention of the medical faculty and other physicians, allowing him to augment his income by illustrating articles and textbooks. He continued illustrating as a sideline after establishing a surgical practice in 1933, but he ultimately opted to give up his practice in favor of a full-time commitment to art. After service in the United States Army during World War II, Dr. Netter began his long collaboration with the CIBA Pharmaceutical Company (now Novartis Pharmaceuticals). This 45-year partnership resulted in the production of the extraordinary collection of medical art so familiar to physicians and other medical professionals worldwide.

In 2005 Elsevier, Inc., purchased the Netter Collection and all publications from Icon Learning Systems. Over 50 publications featuring the art of Dr. Netter are now available through Elsevier, Inc. (in the US: www.us.elsevierhealth.com/Netter and outside the US: www.elsevierhealth.com).

Dr. Netter's works are among the finest examples of the use of illustration in the teaching of medical concepts. The 13-book *Netter Collection of Medical Illustrations*, which includes the greater part of the more than 20,000 paintings created by Dr. Netter, became and remains one of the most famous medical works ever published. *The Netter Atlas of Human Anatomy*, first published in 1989, presents the anatomical paintings from the Netter Collection. Now translated into 16 languages, it is the anatomy atlas of choice among medical and health professions students the world over.

The Netter illustrations are appreciated not only for their aesthetic qualities, but also, more important, for their intellectual content. As Dr. Netter wrote in 1949, ". . . clarification of a subject is the aim and goal of illustration. No matter how beautifully painted, how delicately and subtly rendered a subject may be, it is of little value as a *medical illustration* if it does not serve to make clear some medical point." Dr. Netter's planning, conception, point of view, and approach are what inform his paintings and what makes them so intellectually valuable.

Frank H. Netter, MD, physician and artist, died in 1991.

Learn more about the physician-artist whose work has inspired the Netter Reference collection: http://www.netterimages.com/artist/netter.htm

CARLOS MACHADO, MD

Carlos Machado was chosen by Novartis to be Dr. Netter's successor. He continues to be the main artist contributing to the Netter collection of medical illustrations.

Self-taught in medical illustration, cardiologist Carlos Machado has contributed meticulous updates to some of Dr. Netter's original plates and has created many paintings of his own in the style of Netter as an extension of the Netter collection. Dr. Machado's photorealistic expertise and his keen insight into the physician-patient relationship informs his vivid and unforgettable visual style. His dedication to researching each topic and subject he paints places him among the premier medical illustrators at work today.

Learn more about his background and see more of his art at: http://www.netterimages.com/artist/machado.htm

KRISTEN WIENANDT MARZEJON, MAMS

Kristen Wienandt Marzejon is a certified medical illustrator with a master's degree from the University of Illinois at Chicago's Biomedical Visualization graduate program. Her passion for both art and science from an early age makes her perfectly suited to this gratifying profession. She started her career as a staff illustrator at Rush University Medical Center in Chicago and then committed to self-employed status in 2001. She offers medical illustration and graphic design services to a variety of clients in the medical arena.

The work of Frank Netter has been a valuable part of Kristen's medical library throughout her 20-year career. That said, she is honored to continue the Netter tradition by producing work authentic to his distinctive style.

About the Editors

Drew A. Torigian, MD, MA, began his career in radiology as a resident in training at the Hospital of the University of Pennsylvania. After completing a 2 year body and musculoskeletal research MRI fellowship at Penn, he subsequently remained on faculty for 8 years. His interest in human anatomy first began in elementary school, as he used to check out and read the few illustrated human anatomy books that were available at the library. This interest was reinforced when he was a medical student at the NYU School of Medicine, as well as during his residency and fellowship training in radiology, ultimately leading to his desire to put together this volume of the Netter anatomy series.

Dr. Torigian is a coauthor of 18 book chapters, 35 non–peer reviewed manuscripts, and 92 peer-reviewed manuscripts in the imaging literature, has been a guest editor for several issues of the journals *PET Clinics* and *Seminars in Nuclear Medicine*, and has provided multiple invited lectures on a wide variety of imaging related topics at the local and national level.

Currently, Dr. Torigian is an Associate Professor of Radiology at the University of Pennsylvania and is a member of the thoracic imaging, body CT, and body MRI sections. He has particular expertise in CT, MRI, and PET imaging, with clinical emphasis on disease conditions that affect the thorax, abdomen, and pelvis, and is involved in the education of undergraduate students, medical students, residents, fellows, and faculty locally and nationally on a wide variety of imaging-related subjects of interest. Furthermore, he is enthusiastically involved in the design and conduct of translational and clinical research involving the use of novel combined structural-functional imaging approaches for the quantitative evaluation of various disease conditions in order to advance scientific discovery and to help patients not to suffer or to suffer less.

Mary Kitazono Hammell, MD, first became interested in the field of radiology while working with Dr. Jonathan Cohen's neuroimaging lab at Princeton University, an interest that was fostered by Dr. Bill Green of Princeton Radiology. After graduating from Princeton in 2001, Mary attended the University of Southern California's Keck School of Medicine, where she worked with Dr. Patrick Colletti on various projects including an award-winning MRI Atlas of Renal Pathology, which was presented at the RSNA in 2004. After graduating from USC in 2006, Mary completed her residency in radiology at the Hospital of the University in Pennsylvania, serving as a chief resident during her final year. Mary became board-certified in diagnostic radiology in 2011, and completed a fellowship in pediatric radiology at The Children's Hospital of Philadelphia. In 2012, she joined Princeton Radiology and currently lives in Princeton, NJ, with her husband, Darren Hammell.

Acknowledgments

I would like to acknowledge my friend and colleague Dr. Evan Siegelman for teaching me clinical MRI during my radiology residency and MRI fellowship training at the University of Pennsylvania; Drs. Warren Gefter and Abass Alavi in the Department of Radiology at the University of Pennsylvania, two visionary and highly creative individuals who have been my mentors and friends over the years; and Dr. Bruce Bogart and the late Dr. Lawrence Prutkin for teaching me human anatomy during my first year in medical school at the NYU School of Medicine.

I also would like to thank Mary Kitazono for her dedication and hard work in preparing this atlas, as well as to our artist, Kristen Marzejon, whose medical illustrations would, in my opinion, make the late Dr. Frank Netter very proud.

Drew A. Torigian

I would like to sincerely thank all of the attending physicians who have tirelessly taught and encouraged me throughout my training. To name only a few: Drs. Susan Hilton, Diego Jaramillo, Jill Langer, Mary Scanlon, and Evan Siegelman, who will always be my role models for their dedication to resident education and their passion for the field of radiology.

I would also like to thank Drew Torigian for giving me the opportunity to participate in creating this atlas, and our artist, Kristen Marzejon, who worked with meticulous care on every drawing through multiple revisions.

Mary Kitazono Hammell

Preface

Thorough knowledge of human anatomy is of fundamental importance for practicing radiologists and nuclear medicine physicians, for other clinical specialists such as radiation oncologists and surgeons, amongst others, for other healthcare specialists, as well as for students of radiology and anatomy. As magnetic resonance imaging (MRI) becomes more widely utilized around the world for the detection and characterization of a wide variety of disease conditions, accurate recognition and differentiation of normal anatomical structures from those that are affected by pathology will be of paramount importance for early diagnosis and optimal individualized patient treatment planning. In particular, MRI has been shown to be very useful for the structural-based detection, characterization, and treatment response assessment of abdominopelvic pathology. It provides gross functional information through use of various imaging techniques such as diffusion-weighted imaging and magnetic resonance spectroscopy, is useful in the pediatric setting given the lack of ionizing radiation, and is complementary with molecular imaging techniques such as positron emission tomography (PET).

In this book we have provided delineation of the visible anatomical structures relevant to abdominopelvic anatomy seen on the most commonly utilized pulse sequences of MR imaging, namely T1-weighted, T2-weighted, and post-contrast fat-suppressed T1-weighted images. The imaging planes and particular pulse sequences provided in each chapter are those that are typically used in body MR imaging examinations tailored for evaluation of the abdomen, peritoneal cavity, biliary system, male pelvis, prostate gland and seminal tract, scrotum and testes, penis and male urethra, and female pelvis.

The layout generally includes one or more MR images on one page with an accompanying artist illustration on the opposite page. Wherever appropriate, normal anatomy, normal variants, diagnostic considerations, and pathologic process pearls are included with information relevant to that particular tomographic section.

The labeling of structures is the most commonly accepted language for radiologists. Occasionally, the reader will encounter a phrase in parentheses. This indicates anatomical structures/terms that are used interchangeably in the radiological and/or anatomical literature.

There are two major goals of the text design of this volume of *Netter's Correlative Imaging: Abdominal and Pelvic Anatomy*. One is to demonstrate high-quality MR imaging, allowing for clear identification of important anatomical structures on relevant pulse sequences in multiple planes that would be useful in clinical practice, along with high-quality anatomical illustrations that are reminiscent of Netter quality. The other is to provide user-friendly anatomical references and, when appropriate, to provide succinct insights about commonly encountered diagnoses and imaging challenges. Please note that the text is not meant to be inclusive of all possible pathology, but rather the focus is on presenting the anatomy in a way that has not been presented in previous anatomy and cross-sectional atlases.

It is our hope that you will find this book of human abdominal and pelvic anatomy useful and interesting for didactic and clinical purposes so that you can provide excellent care for your patients.

Drew A. Torigian, MD, MA
Mary Kitazono Hammell, MD

Contents

*For Peritoneal Cavity: Pelvis, see Chapter 3, pp. 166-205

*For Peritoneal Cavity: Pelvis, see Chapter 3, pp. 166-205

PART 1 ABDOMINAL ANATOMY

Chapter 1 OVERVIEW OF ABDOMEN

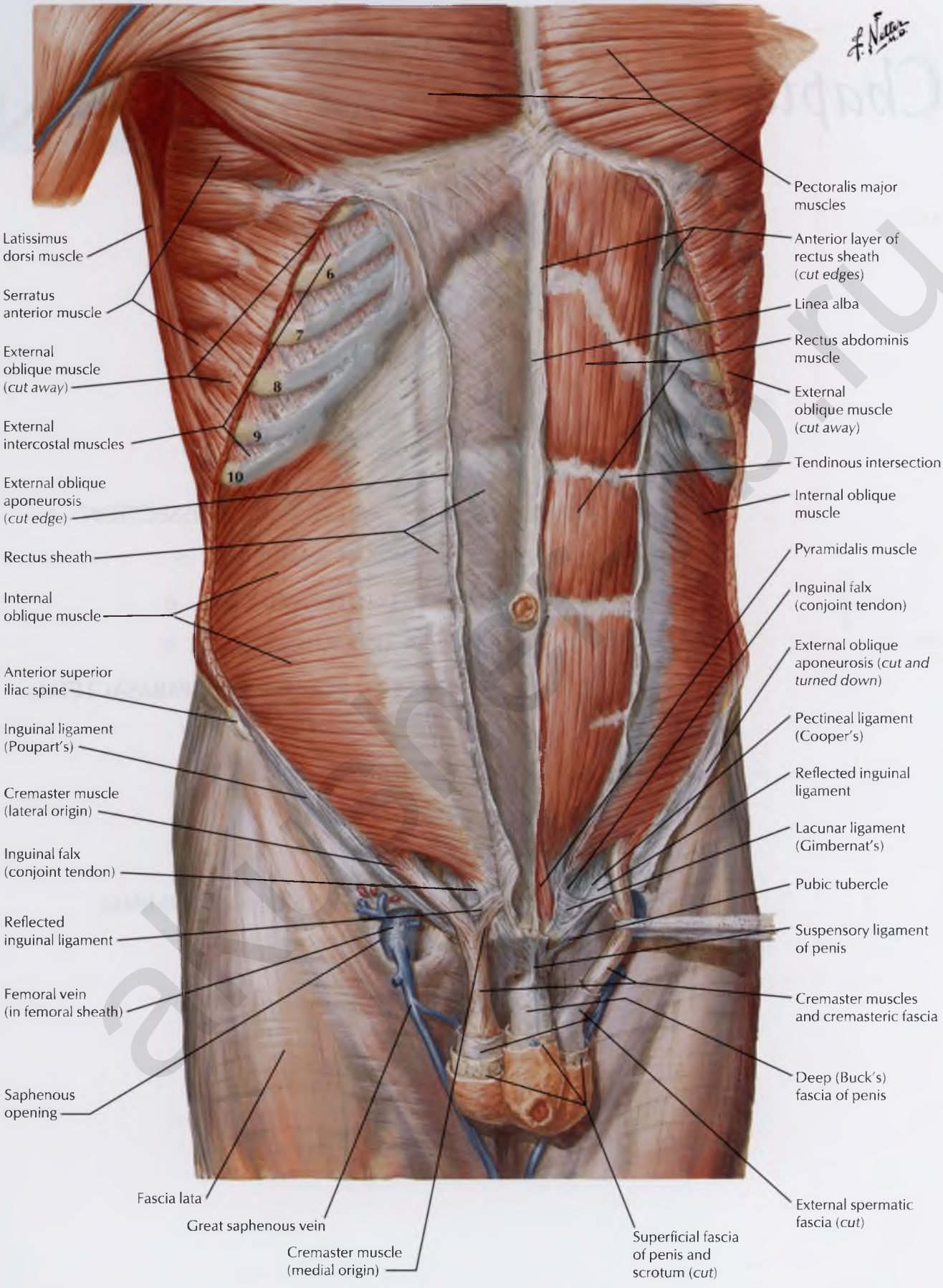
Pectoralis major muscles
Latissimus dorsi muscle
Anterior layer of rectus sheath (*cut edges*)
Serratus anterior muscle
Linea alba
Rectus abdominis muscle
External oblique muscle (*cut away*)
External oblique muscle (*cut away*)
External intercostal muscles
Tendinous intersection
External oblique aponeurosis (*cut edge*)
Internal oblique muscle
Rectus sheath
Pyramidalis muscle
Internal oblique muscle
Inguinal falx (conjoint tendon)
External oblique aponeurosis (*cut and turned down*)
Anterior superior iliac spine
Inguinal ligament (Poupart's)
Pectineal ligament (Cooper's)
Cremaster muscle (lateral origin)
Reflected inguinal ligament
Inguinal falx (conjoint tendon)
Lacunar ligament (Gimbernat's)
Pubic tubercle
Reflected inguinal ligament
Suspensory ligament of penis
Femoral vein (in femoral sheath)
Cremaster muscles and cremasteric fascia
Deep (Buck's) fascia of penis
Saphenous opening
External spermatic fascia (*cut*)
Fascia lata
Great saphenous vein
Cremaster muscle (medial origin)
Superficial fascia of penis and scrotum (*cut*)
6
7
8
9
10

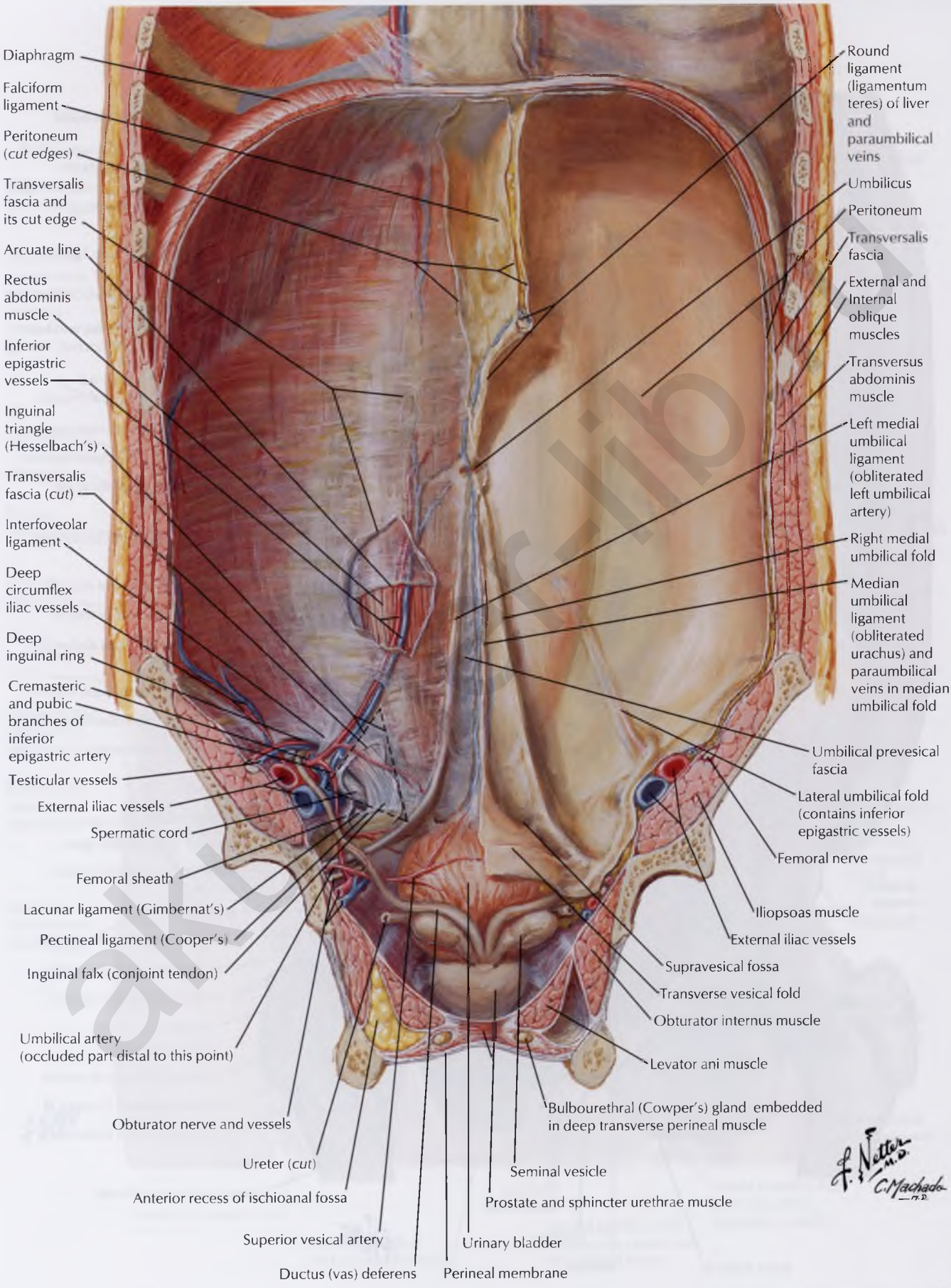

Posterior Abdominal Wall: Internal View

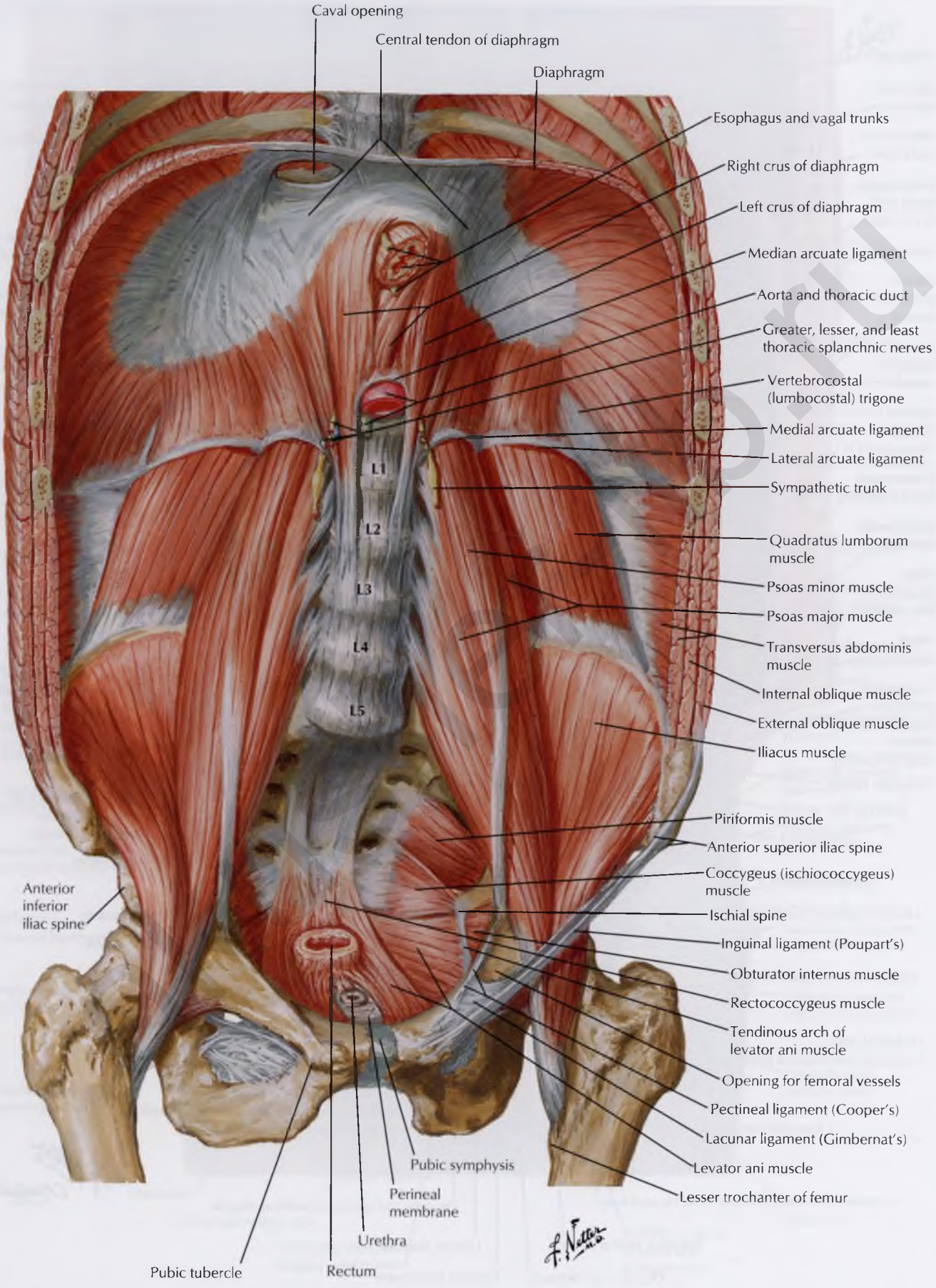

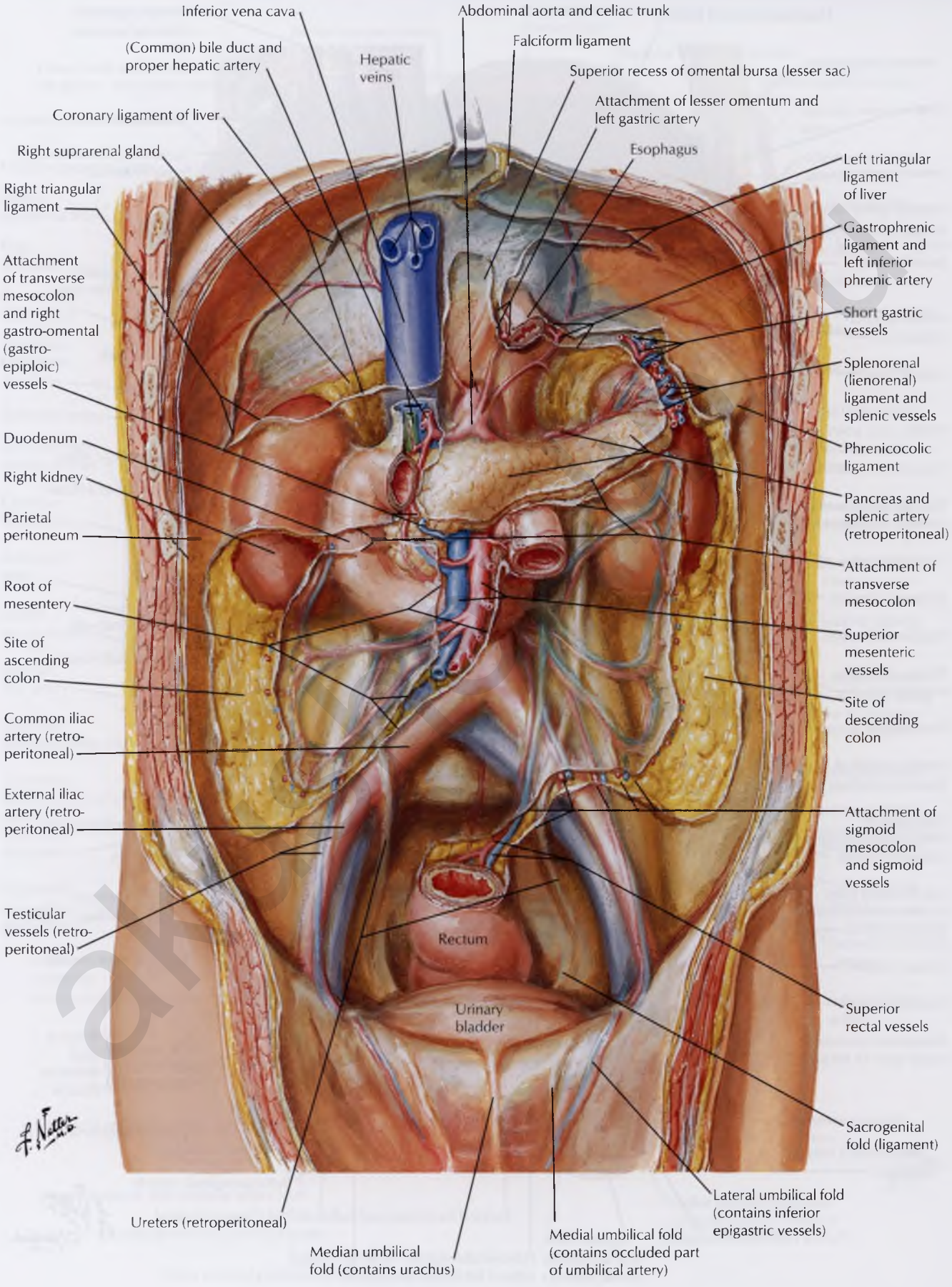
Inferior vena cava
Abdominal aorta and celiac trunk
(Common) bile duct and proper hepatic artery
Hepatic veins
Falciform ligament
Superior recess of omental bursa (lesser sac)
Attachment of lesser omentum and left gastric artery
Coronary ligament of liver
Esophagus
Right suprarenal gland
Left triangular ligament of liver
Right triangular ligament
Gastrophrenic ligament and left inferior phrenic artery
Attachment of transverse mesocolon and right gastro-omental (gastro-epiploic) vessels
Short gastric vessels
Splenorenal (lienorenal) ligament and splenic vessels
Duodenum
Phrenicocolic ligament
Right kidney
Pancreas and splenic artery (retroperitoneal)
Parietal peritoneum
Attachment of transverse mesocolon
Root of mesentery
Superior mesenteric vessels
Site of ascending colon
Site of descending colon
Common iliac artery (retro-peritoneal)
External iliac artery (retro-peritoneal)
Attachment of sigmoid mesocolon and sigmoid vessels
Testicular vessels (retro-peritoneal)
Rectum
Urinary bladder
Superior rectal vessels
Sacrogenital fold (ligament)
Lateral umbilical fold (contains inferior epigastric vessels)
Ureters (retroperitoneal)
Medial umbilical fold (contains occluded part of umbilical artery)
Median umbilical fold (contains urachus)

Abdominal Wall and Viscera: Paramedian (Parasagittal) Section

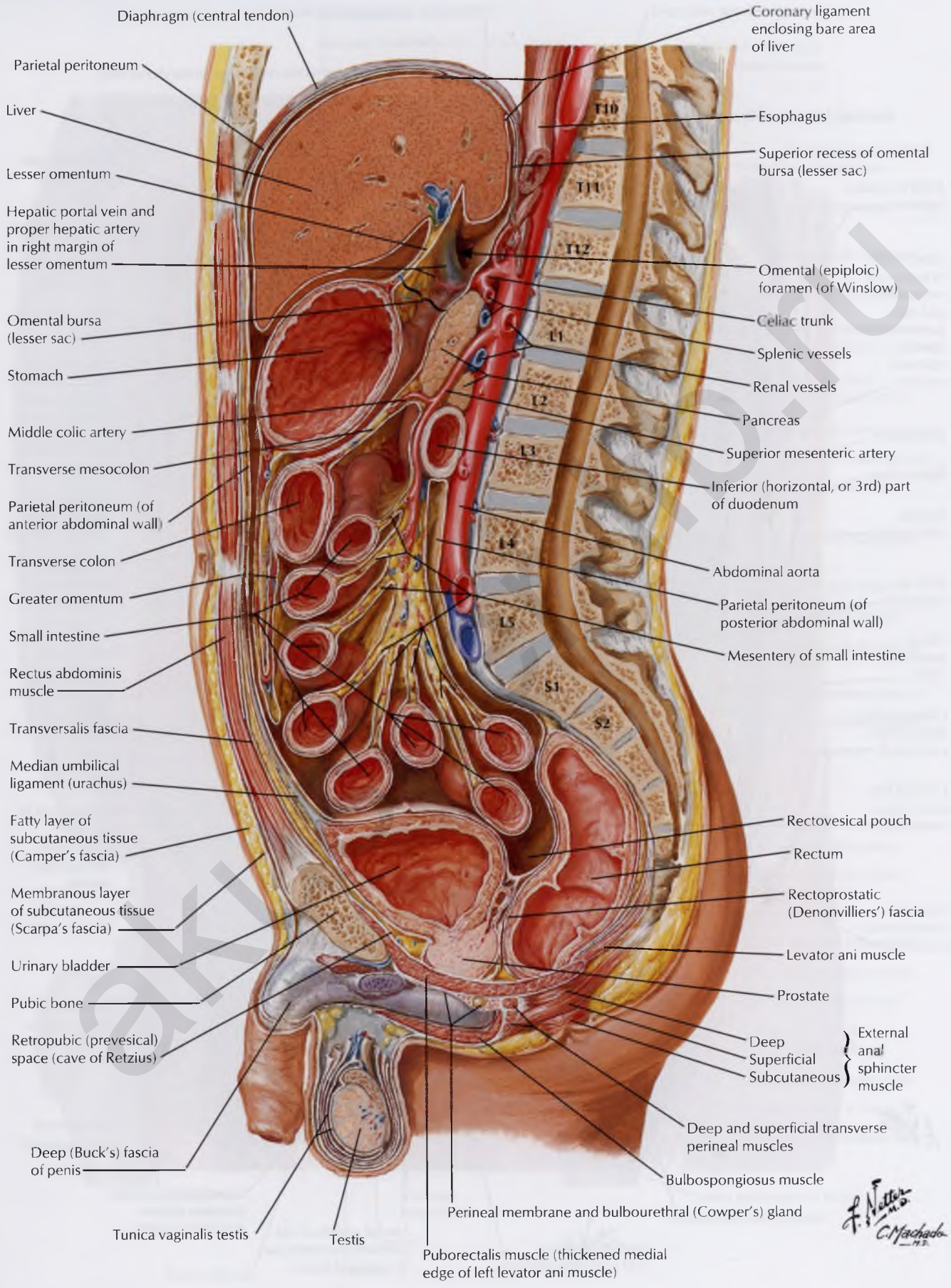

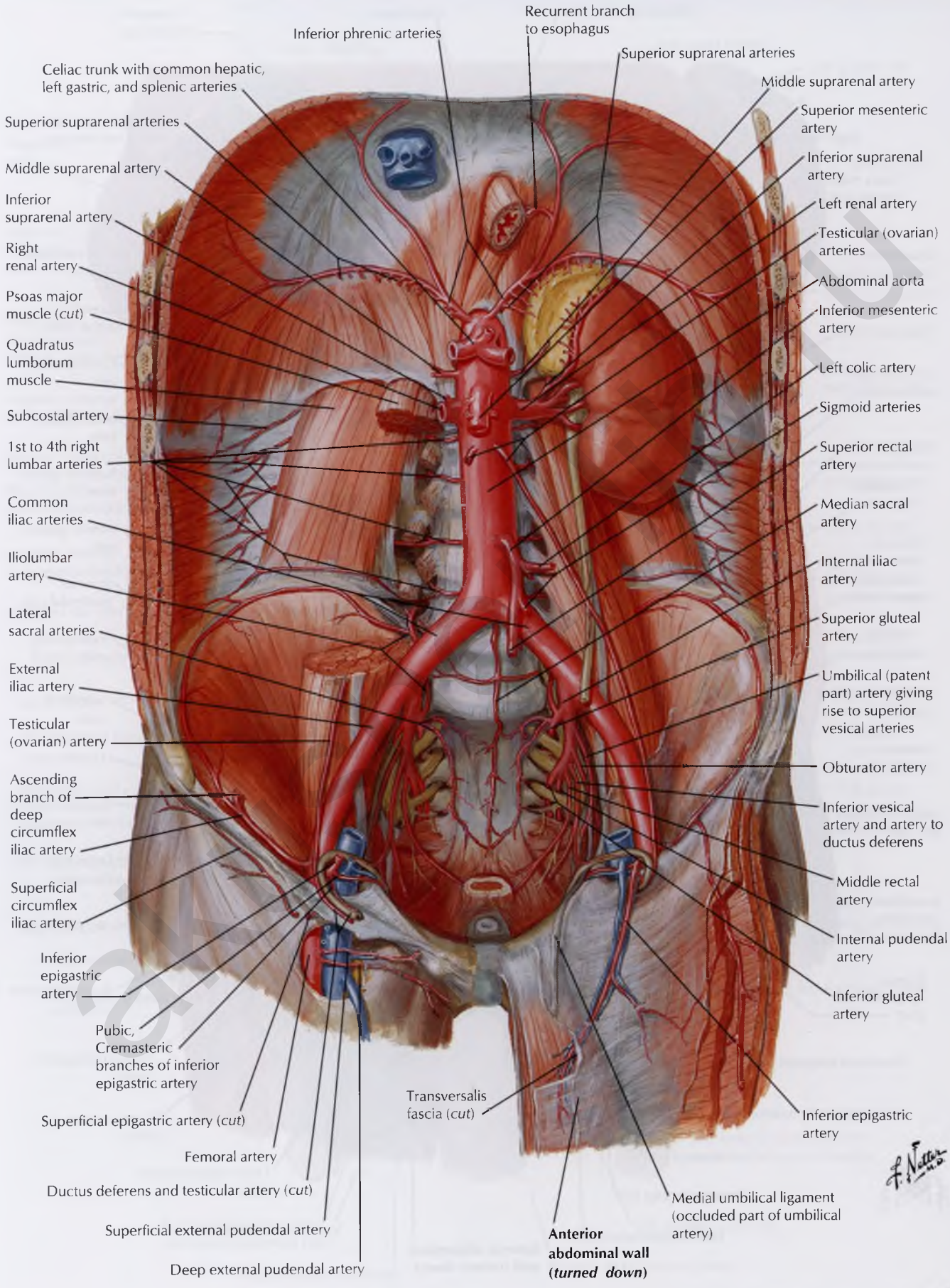
Recurrent branch to esophagus
Inferior phrenic arteries
Superior suprarenal arteries
Celiac trunk with common hepatic, left gastric, and splenic arteries
Middle suprarenal artery
Superior suprarenal arteries
Superior mesenteric artery
Middle suprarenal artery
Inferior suprarenal artery
Inferior suprarenal artery
Left renal artery
Right renal artery
Testicular (ovarian) arteries
Psoas major muscle (cut)
Abdominal aorta
Inferior mesenteric artery
Quadratus lumborum muscle
Left colic artery
Subcostal artery
Sigmoid arteries
1st to 4th right lumbar arteries
Superior rectal artery
Common iliac arteries
Median sacral artery
Iliolumbar artery
Internal iliac artery
Lateral sacral arteries
Superior gluteal artery
External iliac artery
Umbilical (patent part) artery giving rise to superior vesical arteries
Testicular (ovarian) artery
Obturator artery
Ascending branch of deep circumflex iliac artery
Inferior vesical artery and artery to ductus deferens
Superficial circumflex iliac artery
Middle rectal artery
Internal pudendal artery
Inferior epigastric artery
Inferior gluteal artery
Pubic, Cremasteric branches of inferior epigastric artery
Transversalis fascia (cut)
Inferior epigastric artery
Superficial epigastric artery (cut)
Femoral artery
Ductus deferens and testicular artery (cut)
Medial umbilical ligament (occluded part of umbilical artery)
Superficial external pudendal artery
Anterior abdominal wall (turned down)
Deep external pudendal artery

Veins of Posterior Abdominal Wall

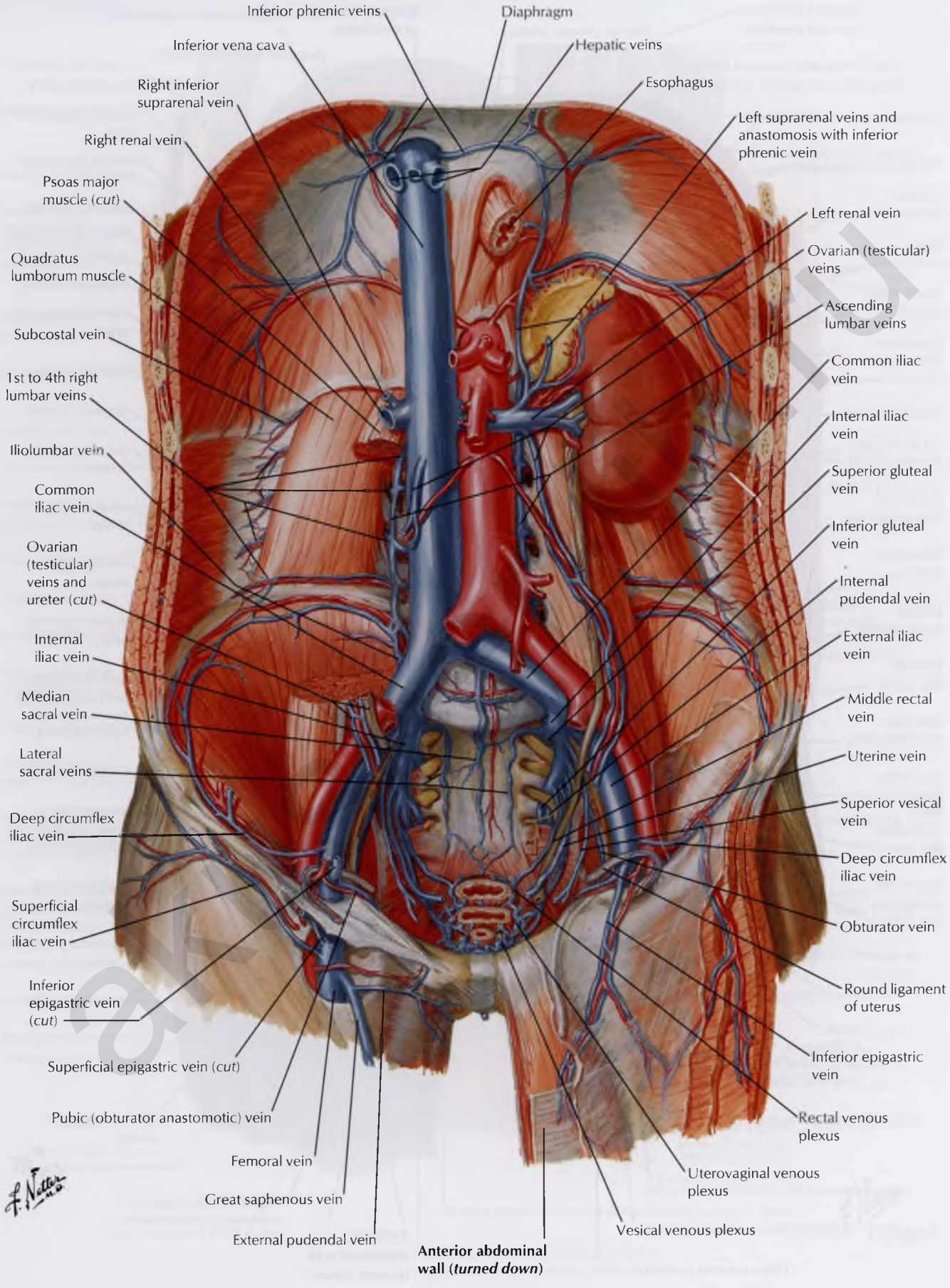

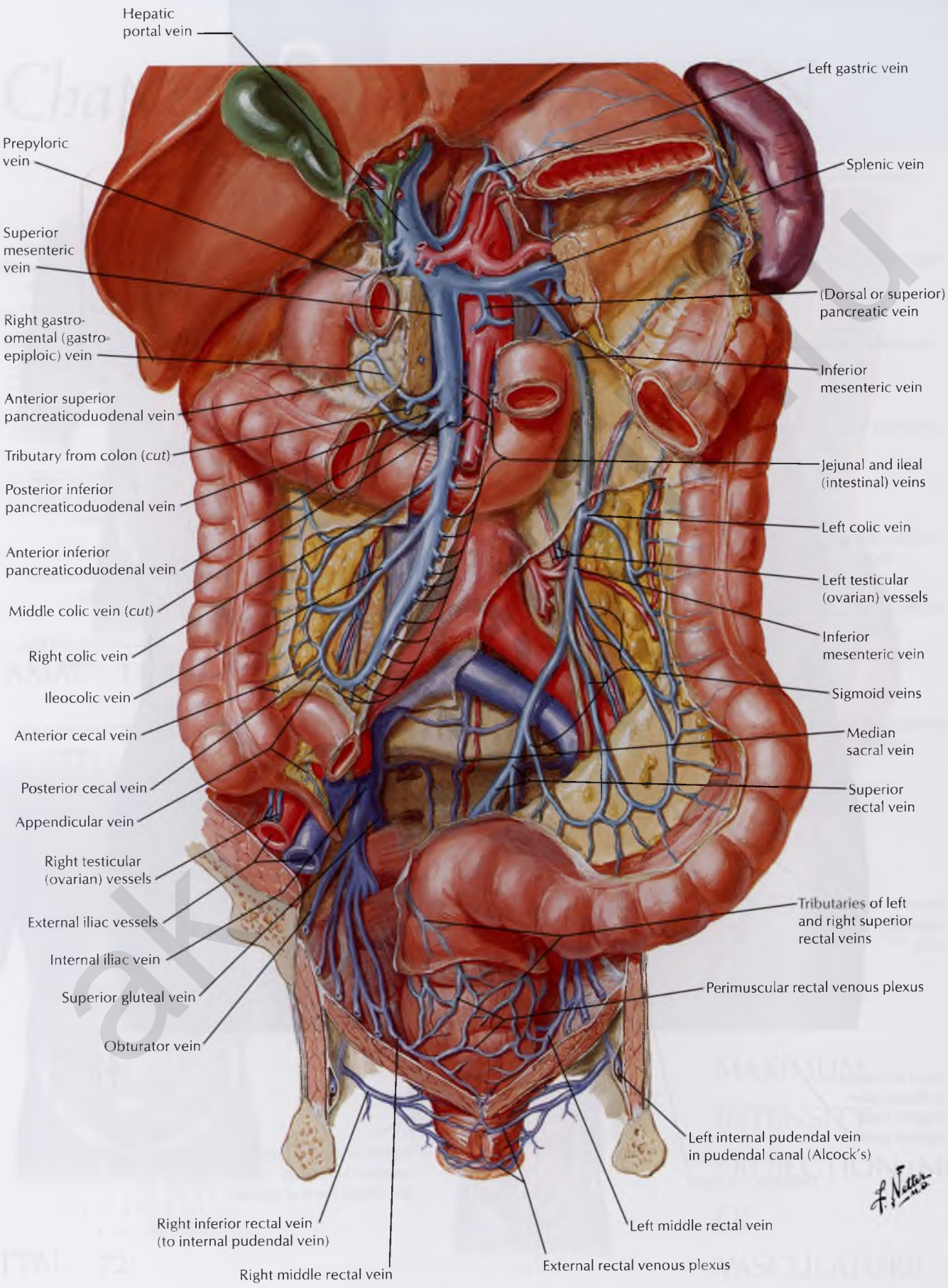
Hepatic portal vein
Left gastric vein
Prepyloric vein
Splenic vein
Superior mesenteric vein
(Dorsal or superior) pancreatic vein
Right gastro-omental (gastro-epiploic) vein
Inferior mesenteric vein
Anterior superior pancreaticoduodenal vein
Tributary from colon (cut)
Jejunal and ileal (intestinal) veins
Posterior inferior pancreaticoduodenal vein
Left colic vein
Anterior inferior pancreaticoduodenal vein
Left testicular (ovarian) vessels
Middle colic vein (cut)
Inferior mesenteric vein
Right colic vein
Sigmoid veins
Ileocolic vein
Median sacral vein
Anterior cecal vein
Superior rectal vein
Posterior cecal vein
Appendicular vein
Right testicular (ovarian) vessels
Tributaries of left and right superior rectal veins
External iliac vessels
Internal iliac vein
Perimuscular rectal venous plexus
Superior gluteal vein
Obturator vein
Left internal pudendal vein in pudendal canal (Alcock's)
Right inferior rectal vein (to internal pudendal vein)
Left middle rectal vein
Right middle rectal vein
External rectal venous plexus

Lymph Vessels and Nodes of Posterior Abdominal Wall

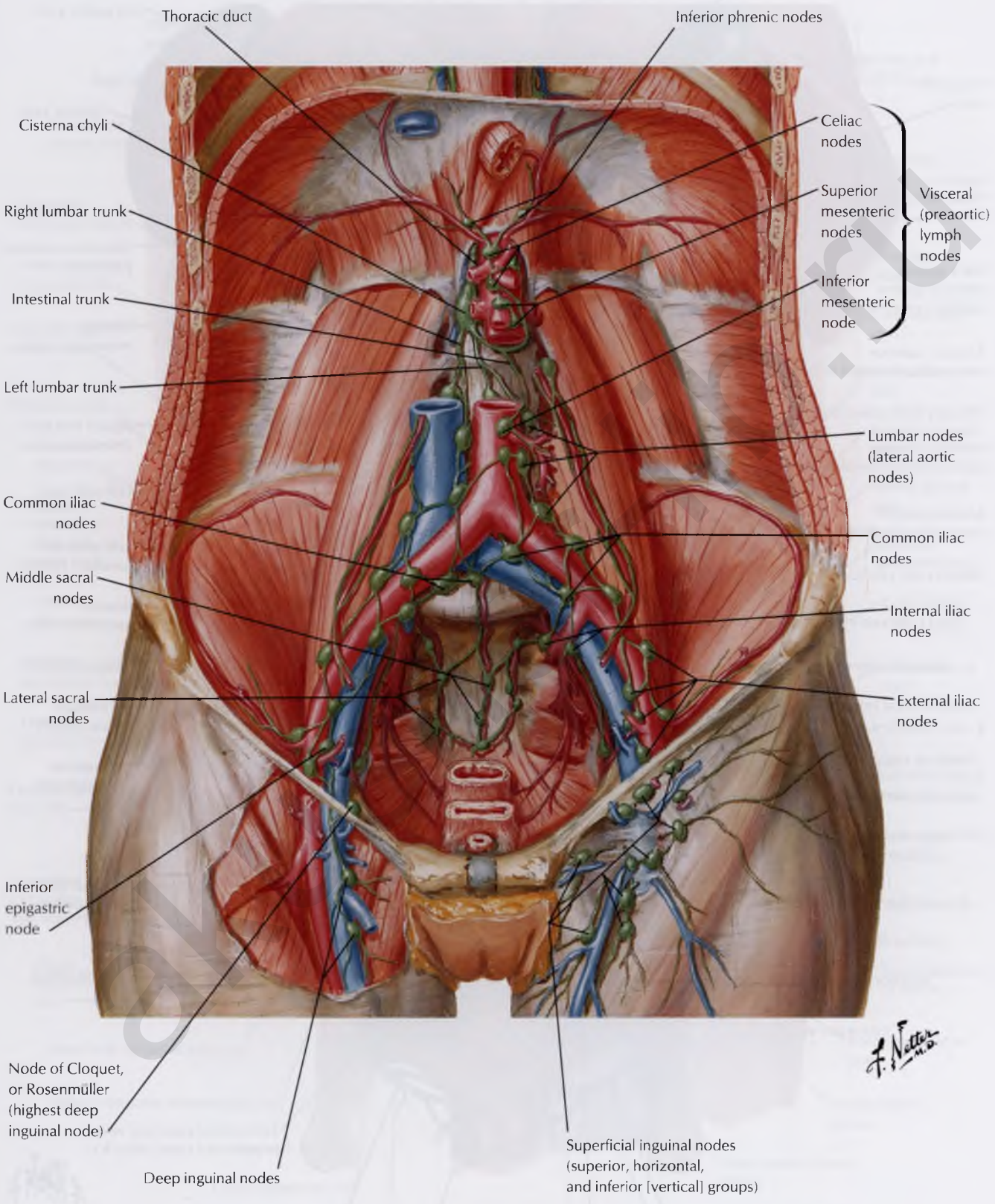

Chapter 2 ABDOMEN

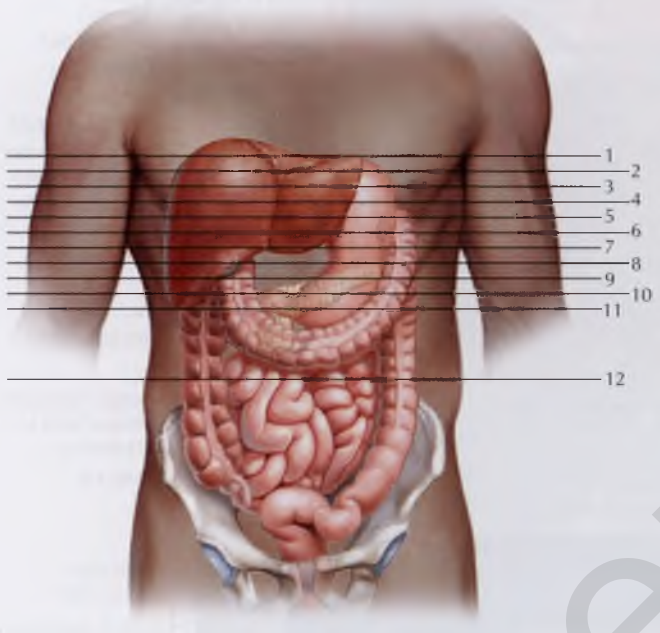

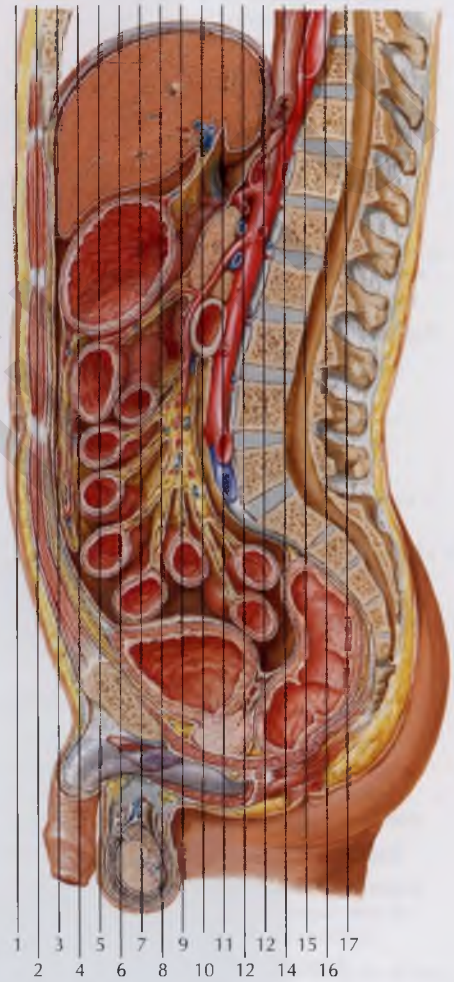

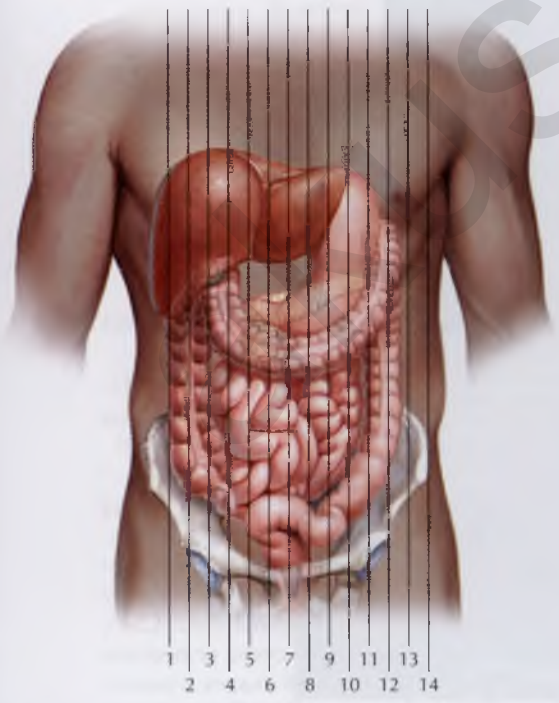

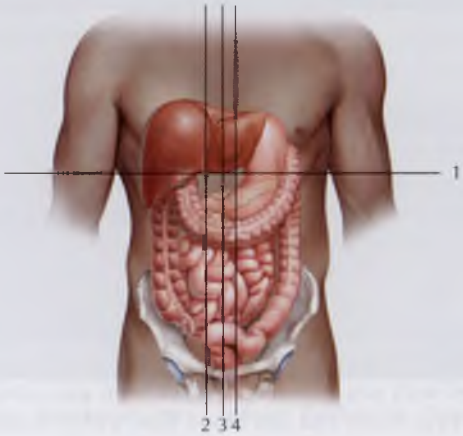

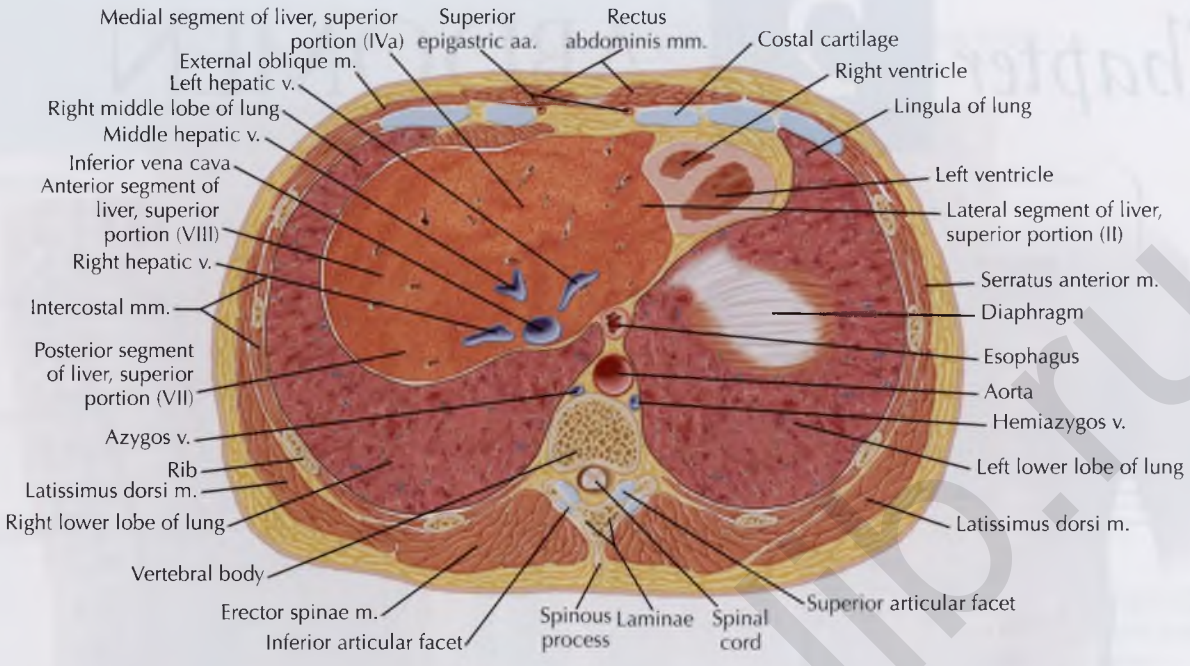

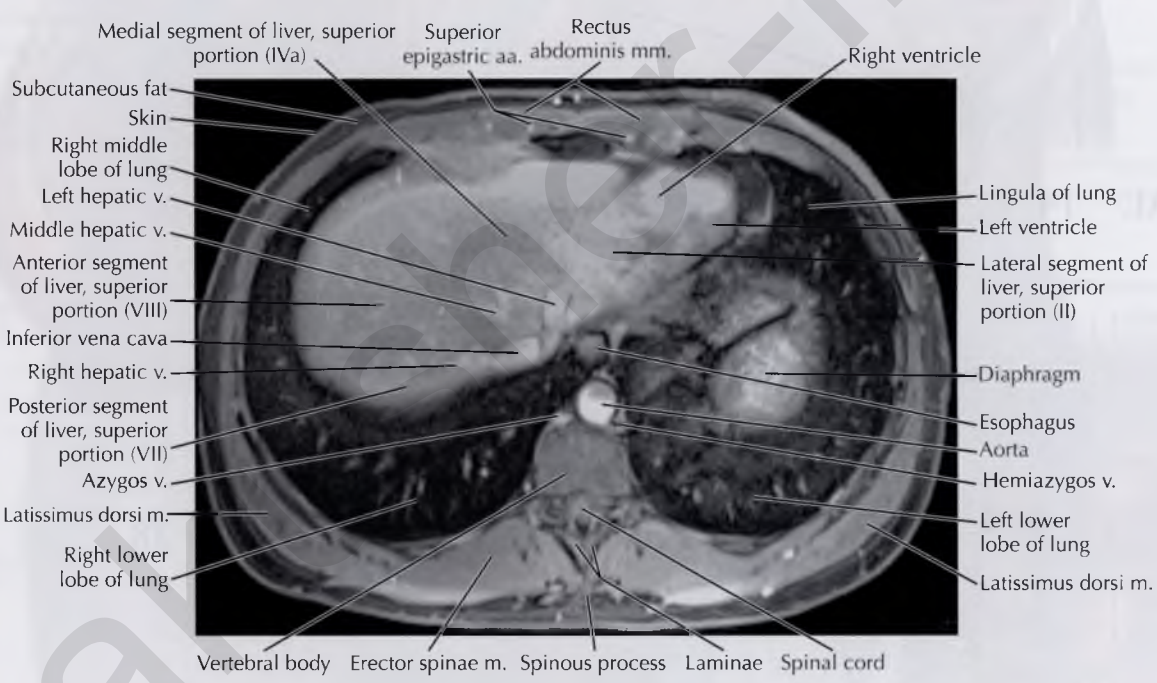

DIAGNOSTIC CONSIDERATION

In magnetic resonance imaging (MRI), all signal intensity is relative; signal intensity varies depending on the type of MR sequence. High signal intensity on T1-weighted images is typically associated with fat, proteinaceous content, subacute hemorrhage, paramagnetic substances (e.g., melanin, gadolinium), and slow blood flow within vessels. High signal intensity on T2-weighted images is typically associated with fluid, including cerebrospinal fluid (CSF), urine, bile, gastric fluid, and enteric fluid, as well as fluid-filled lesions (cyst, cystic or necrotic tumor), hemangiomas, and fat. Low signal intensity on T1- and T2-weighted images is associated with susceptibility artifact from gas, iron, and metallic objects, as well as fibrous tissue, cortical bone, and fast blood flow within vessels.

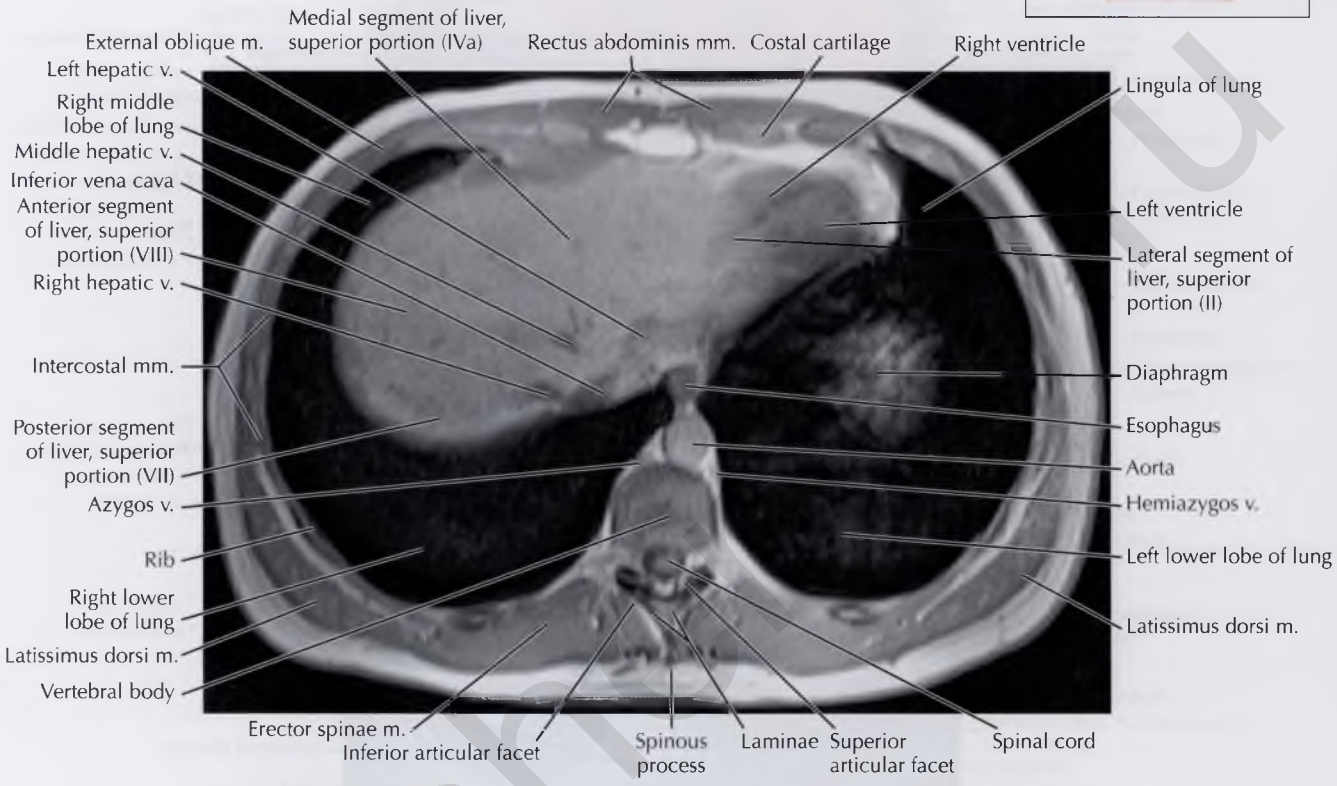
External oblique m.
Medial segment of liver, superior portion (IVa)
Rectus abdominis mm.
Costal cartilage
Right ventricle
Left hepatic v.
Right middle lobe of lung
Middle hepatic v.
Inferior vena cava
Anterior segment of liver, superior portion (VIII)
Right hepatic v.
Intercostal mm.
Posterior segment of liver, superior portion (VII)
Azygos v.
Rib
Right lower lobe of lung
Latissimus dorsi m.
Vertebral body
Lingula of lung
Left ventricle
Lateral segment of liver, superior portion (II)
Diaphragm
Esophagus
Aorta
Hemiazygos v.
Left lower lobe of lung
Latissimus dorsi m.
Erector spinae m.
Inferior articular facet
Spinous process
Laminae
Superior articular facet
Spinal cord

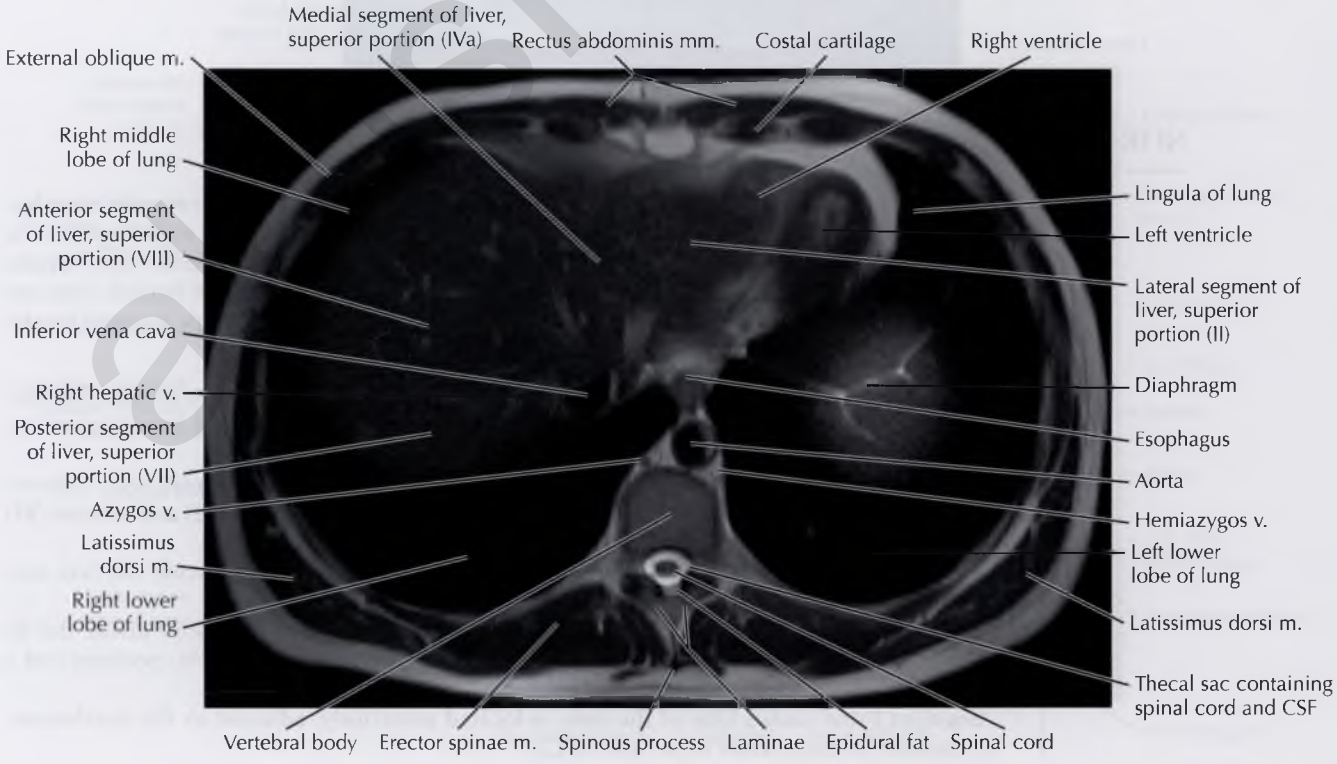
Medial segment of liver, superior portion (IVa)
Rectus abdominis mm.
Costal cartilage
Right ventricle
External oblique m.
Right middle lobe of lung
Anterior segment of liver, superior portion (VIII)
Inferior vena cava
Right hepatic v.
Posterior segment of liver, superior portion (VII)
Azygos v.
Latissimus dorsi m.
Right lower lobe of lung
Lingula of lung
Left ventricle
Lateral segment of liver, superior portion (II)
Diaphragm
Esophagus
Aorta
Hemiazygos v.
Left lower lobe of lung
Latissimus dorsi m.
Thecal sac containing spinal cord and CSF
Vertebral body
Erector spinae m.
Spinous process
Laminae
Epidural fat
Spinal cord

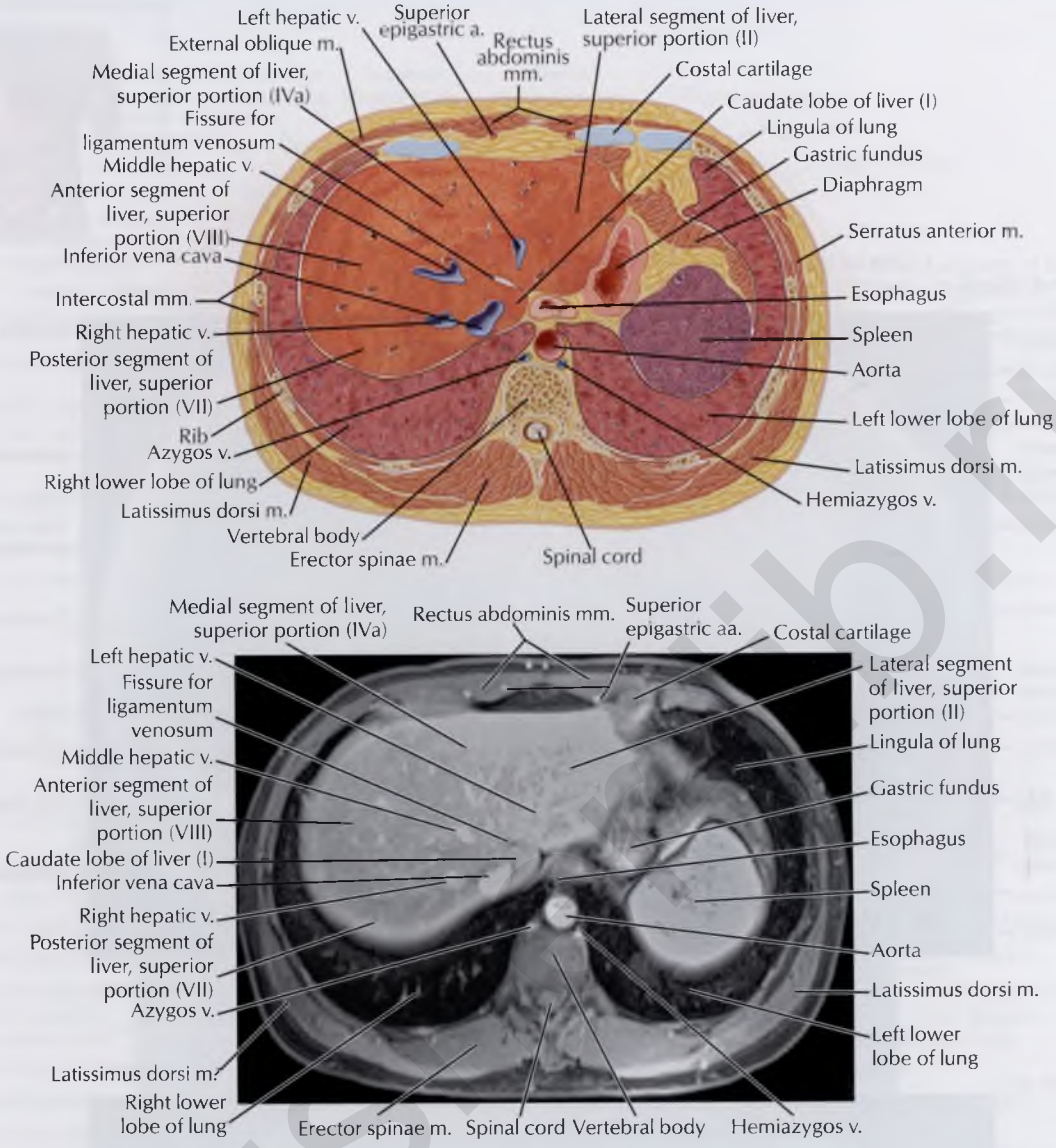

NORMAL ANATOMY

Many systems have been proposed for liver segmentation anatomy. The approach most frequently used, however, is the *Couinaud system*, which subdivides the liver into eight functionally independent segments (I-VIII). *Portal triads*, composed of branches of the portal vein, hepatic artery, and biliary ducts, are seen within the center of each segment, whereas hepatic veins are seen in the periphery. Because each hepatic segment is self-contained, a single segment can be surgically resected without injury to the remaining segments.

In this system, a transverse plane through the level of the main portal vein divides the liver into lateral, medial, anterior, and posterior segments, each with superior and inferior portions, as follows:

- The right hepatic vein divides the *right* hepatic lobe into an *anterior* segment with superior (VIII) and inferior (V) portions and a *posterior* segment with superior (VII) and inferior (VI) portions.
- The middle hepatic vein (superiorly) and gallbladder fossa (inferiorly) divide the liver into right and left hepatic lobes.
- The left hepatic vein (superiorly) and left intersegmental fissure (inferiorly) divide the *left* hepatic lobe into a *medial* segment with superior (IVa) and inferior (IVb) portions and a *lateral* segment with superior (II) and inferior (III) portions.
- Segment I, the *caudate* lobe of the liver, is located posteriorly, adjacent to the intrahepatic portion of the inferior vena cava (IVC).

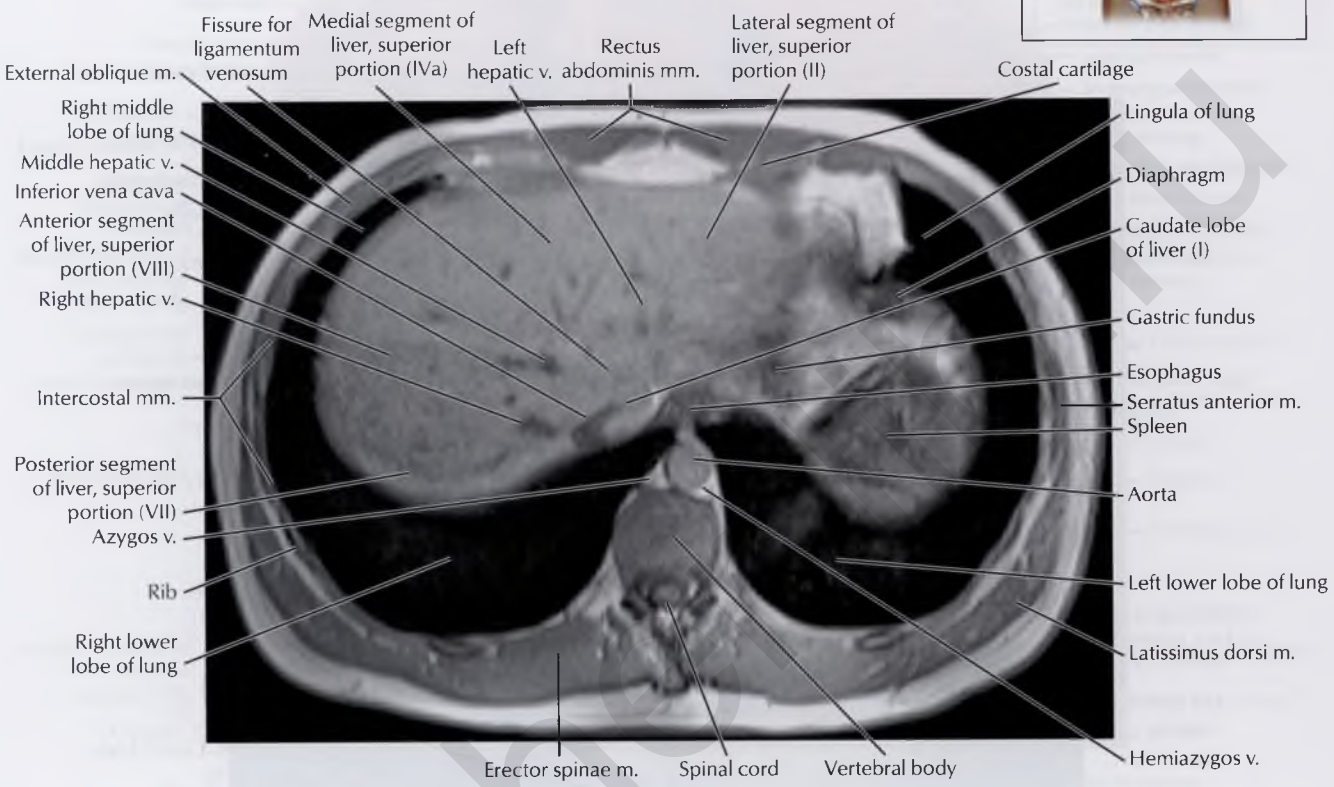
External oblique m.
Fissure for ligamentum venosum
Medial segment of liver, superior portion (IVa)
Left hepatic v.
Rectus abdominis mm.
Lateral segment of liver, superior portion (II)
Costal cartilage
Right middle lobe of lung
Middle hepatic v.
Inferior vena cava
Anterior segment of liver, superior portion (VIII)
Right hepatic v.
Intercostal mm.
Posterior segment of liver, superior portion (VII)
Azygos v.
Rib
Right lower lobe of lung
Lingula of lung
Diaphragm
Caudate lobe of liver (I)
Gastric fundus
Esophagus
Serratus anterior m.
Spleen
Aorta
Left lower lobe of lung
Latissimus dorsi m.
Hemiazygos v.
Erector spinae m.
Spinal cord
Vertebral body

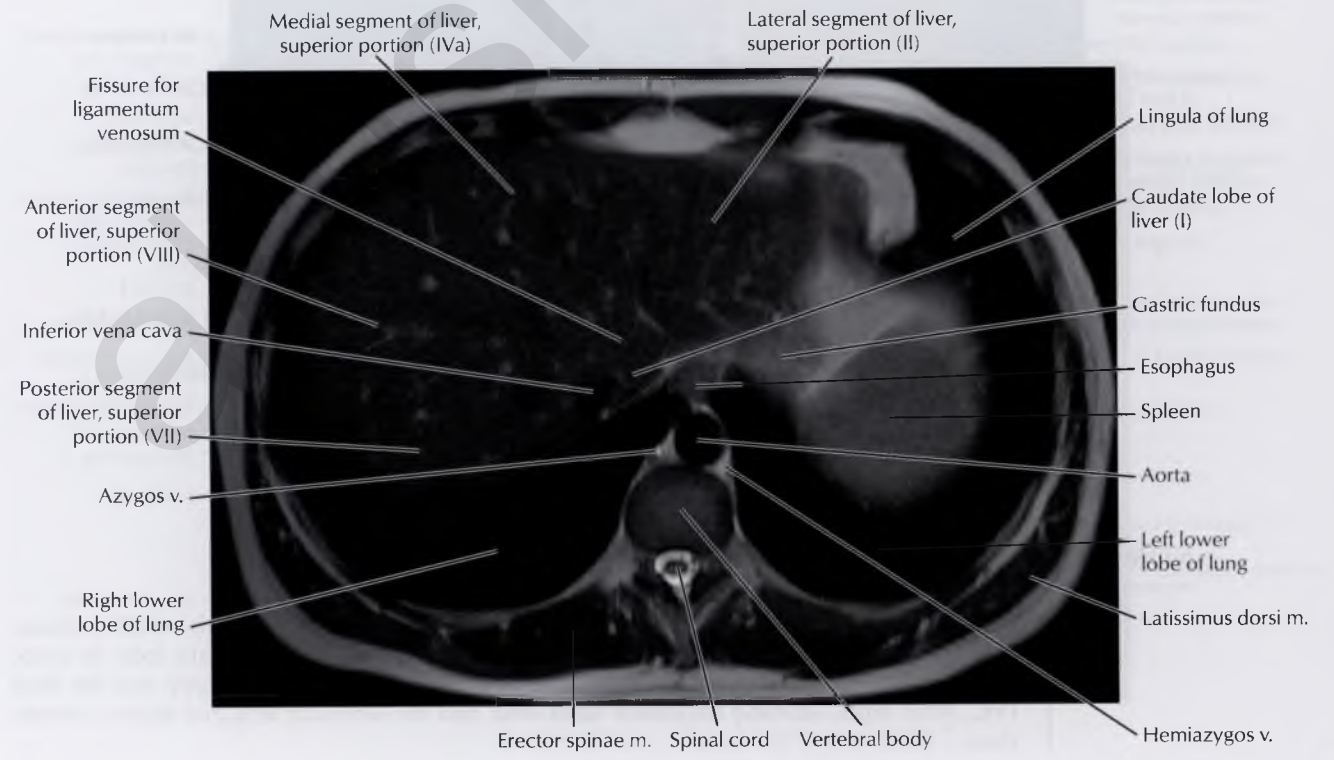
Medial segment of liver, superior portion (IVa)
Lateral segment of liver, superior portion (II)
Fissure for ligamentum venosum
Anterior segment of liver, superior portion (VIII)
Inferior vena cava
Posterior segment of liver, superior portion (VII)
Azygos v.
Right lower lobe of lung
Lingula of lung
Caudate lobe of liver (I)
Gastric fundus
Esophagus
Spleen
Aorta
Left lower lobe of lung
Latissimus dorsi m.
Hemiazygos v.
Erector spinae m.
Spinal cord
Vertebral body

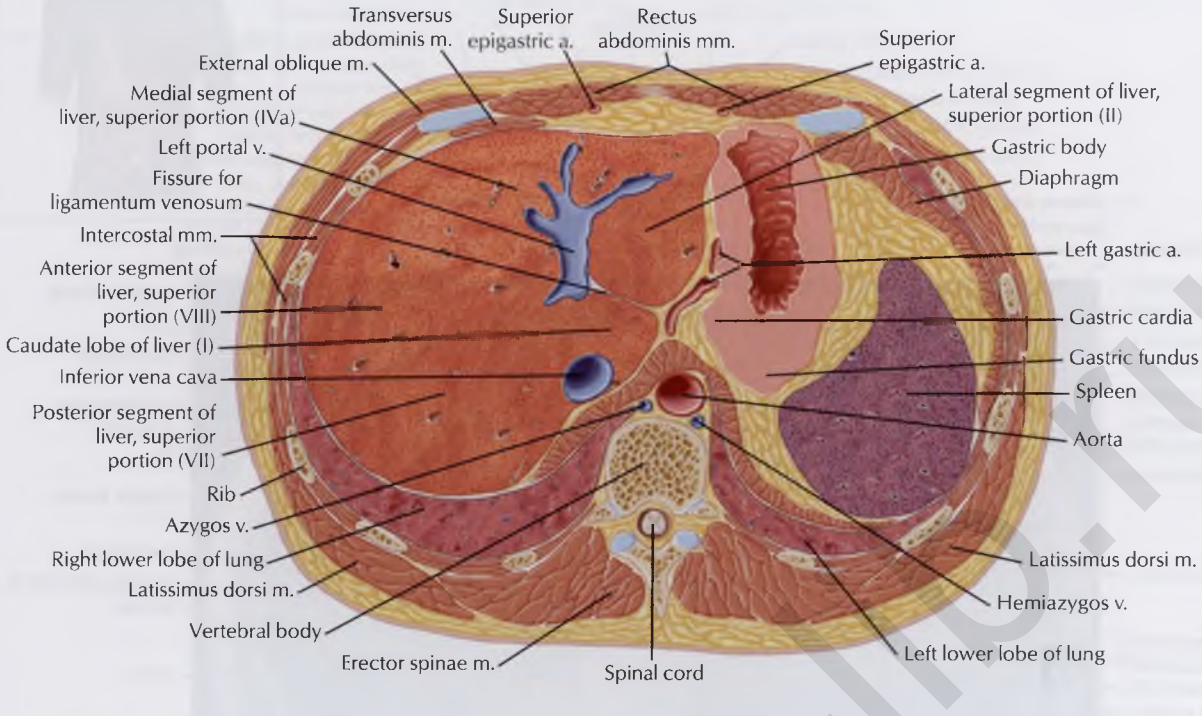

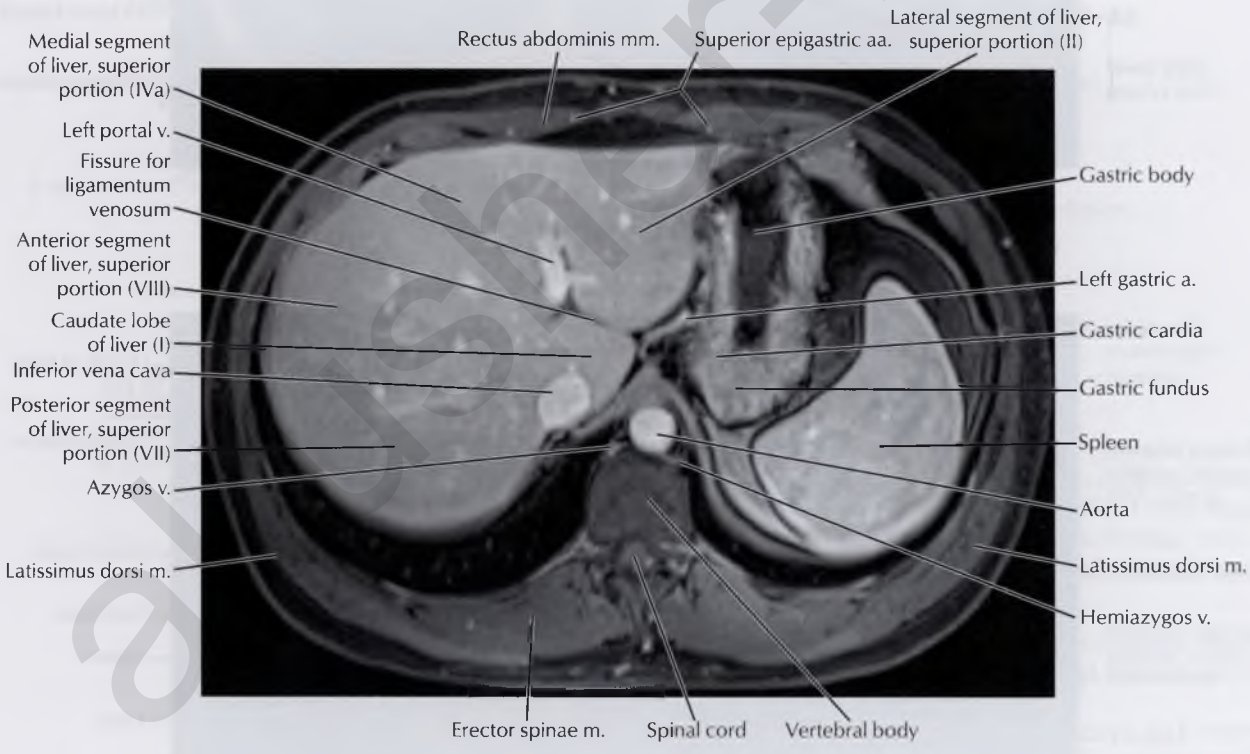

NORMAL ANATOMY

The *ligamentum venosum*, a remnant of the obliterated ductus venosus, travels within a fissure along the inferior surface of the liver between the caudate lobe and left hepatic lobe. In utero, the ductus venosus shunts oxygenated blood from the umbilical vein directly into the fetal IVC. After birth, neonatal circulation takes over, and the umbilical vein and ductus venosus close.

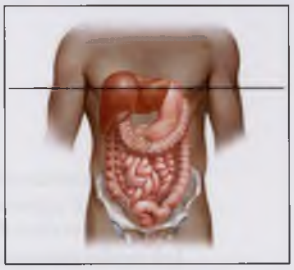

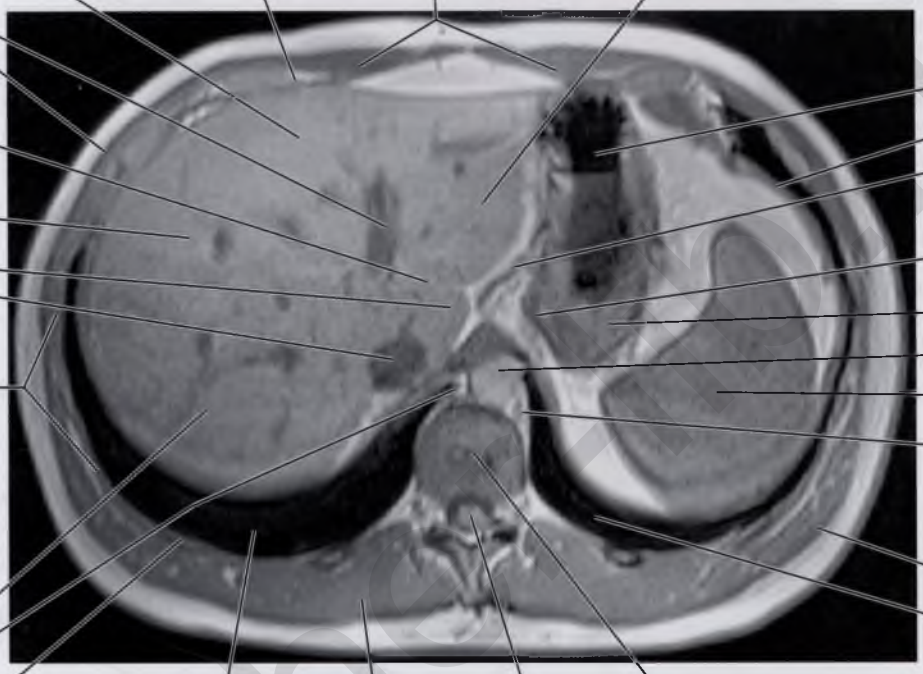
Medial segment of liver, superior portion (IVa)
Transversus abdominis m.
Rectus abdominis mm.
Lateral segment of liver, superior portion (II)
Left portal v.
External oblique m.
Fissure for ligamentum venosum
Anterior segment of liver, superior portion (VIII)
Caudate lobe of liver (I)
Inferior vena cava
Intercostal mm.
Anterior segment of liver, superior portion (VIII)
Azygos v.
Rib
Right lower lobe of lung
Erector spinae m.
Spinal cord
Vertebral body
Gastric body
Diaphragm
Left gastric a.
Gastric cardia
Gastric fundus
Aorta
Spleen
Hemiazygos v.
Latissimus dorsi m.
Left lower lobe of lung

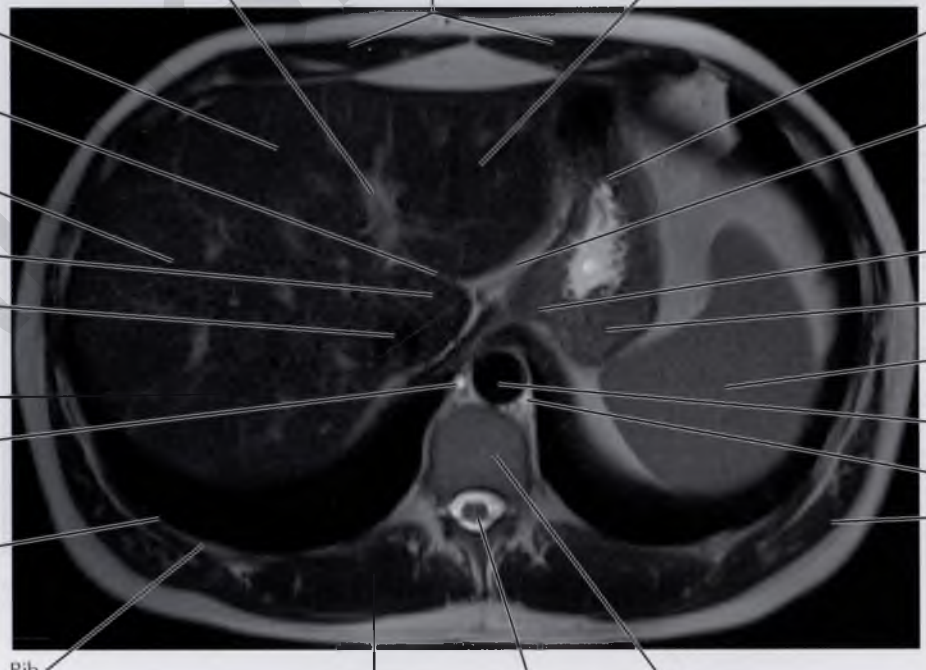
Medial segment of liver, superior portion (IVa)
Left portal v.
Rectus abdominis mm.
Lateral segment of liver, superior portion (II)
Fissure for ligamentum venosum
Anterior segment of liver, superior portion (VIII)
Caudate lobe of liver (I)
Inferior vena cava
Posterior segment of liver, superior portion (VII)
Azygos v.
Intercostal mm.
Rib
Erector spinae m.
Spinal cord
Vertebral body
Gastric body
Left gastric a.
Gastric cardia
Gastric fundus
Spleen
Aorta
Hemiazygos v.
Latissimus dorsi m.

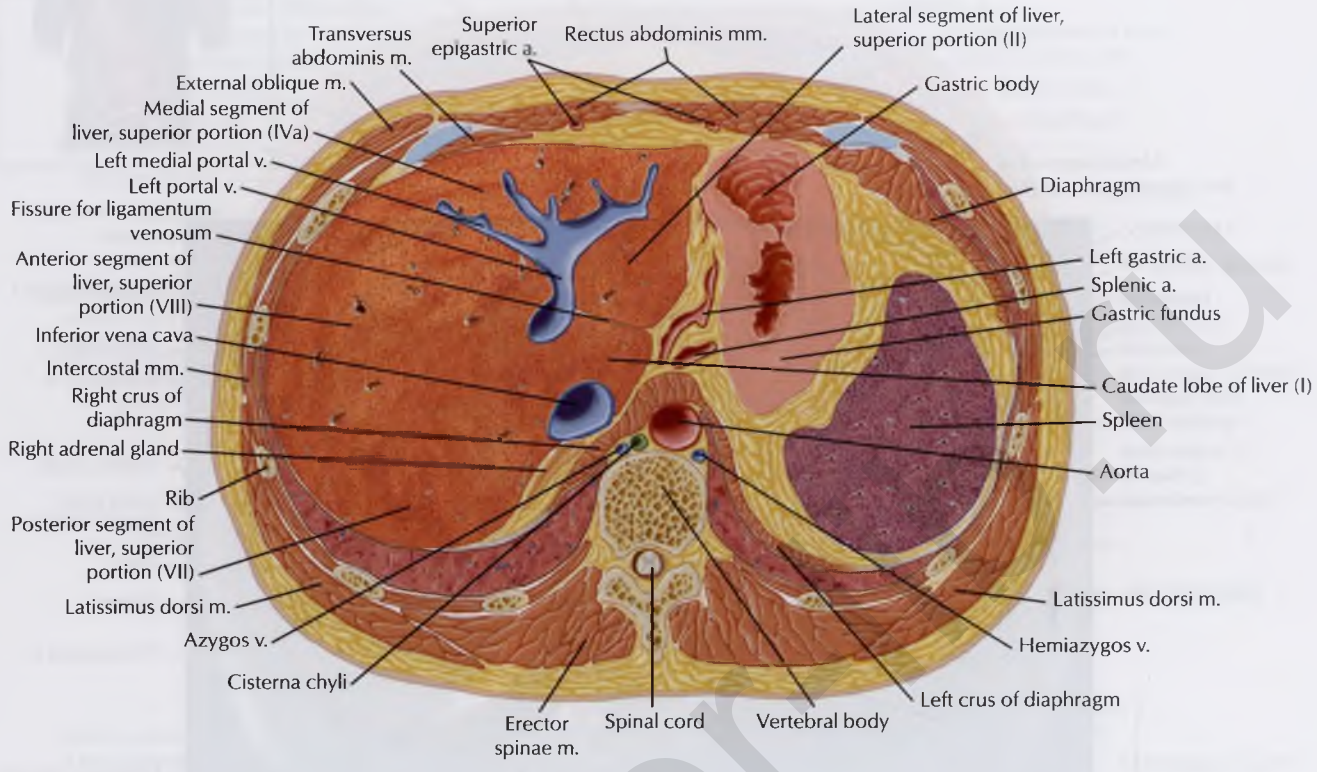
Transversus abdominis m.
Superior epigastric a.
Rectus abdominis mm.
Lateral segment of liver, superior portion (II)
External oblique m.
Gastric body
Medial segment of liver, superior portion (IVa)
Left medial portal v.
Left portal v.
Diaphragm
Fissure for ligamentum venosum
Anterior segment of liver, superior portion (VIII)
Left gastric a.
Splenic a.
Gastric fundus
Inferior vena cava
Intercostal mm.
Caudate lobe of liver (I)
Right crus of diaphragm
Spleen
Right adrenal gland
Aorta
Rib
Posterior segment of liver, superior portion (VII)
Latissimus dorsi m.
Azygos v.
Hemiazygos v.
Cisterna chyli
Left crus of diaphragm
Erector spinae m.
Spinal cord
Vertebral body

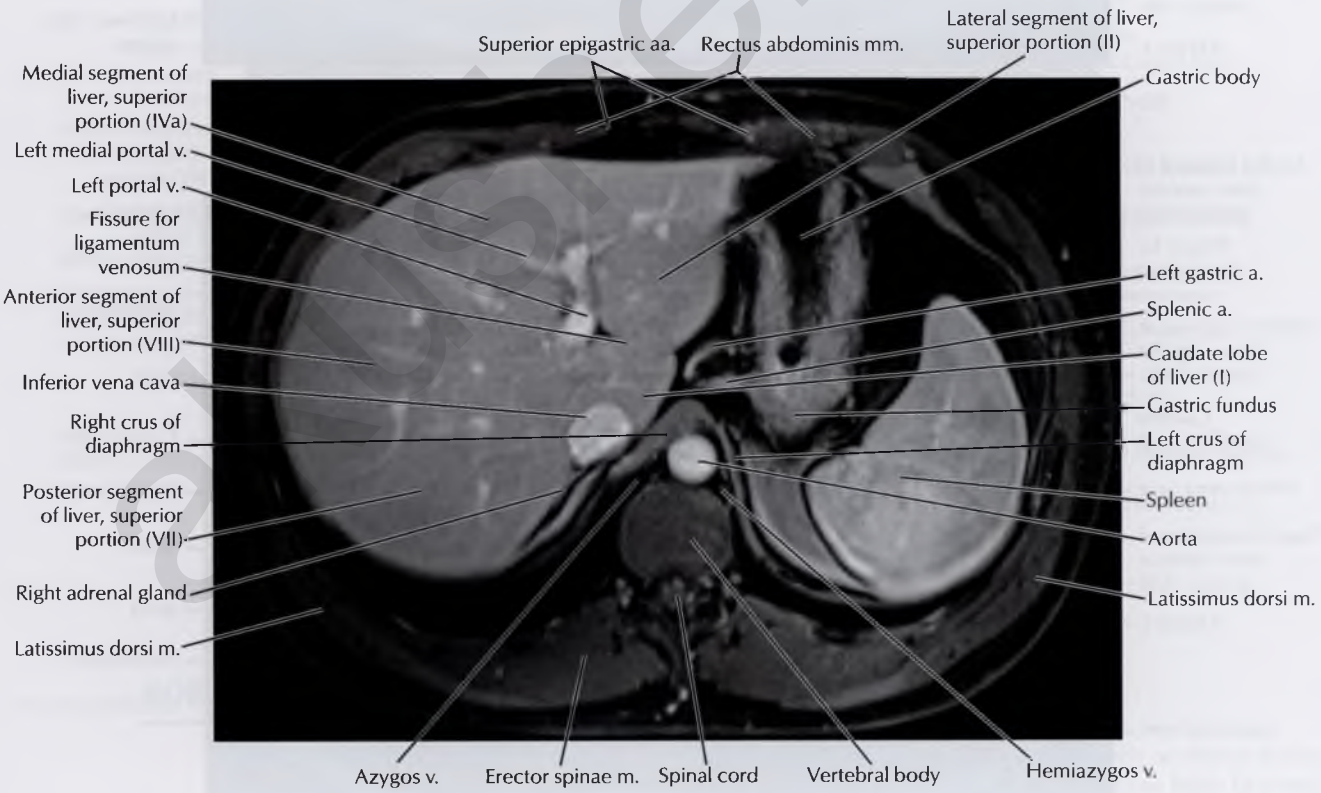
Superior epigastric aa.
Rectus abdominis mm.
Lateral segment of liver, superior portion (II)
Medial segment of liver, superior portion (IVa)
Gastric body
Left medial portal v.
Left portal v.
Fissure for ligamentum venosum
Left gastric a.
Anterior segment of liver, superior portion (VIII)
Splenic a.
Caudate lobe of liver (I)
Inferior vena cava
Gastric fundus
Right crus of diaphragm
Left crus of diaphragm
Spleen
Posterior segment of liver, superior portion (VII)
Aorta
Right adrenal gland
Latissimus dorsi m.
Latissimus dorsi m.
Azygos v.
Erector spinae m.
Spinal cord
Vertebral body
Hemiazygos v.

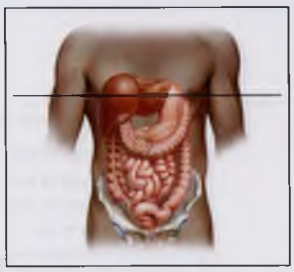

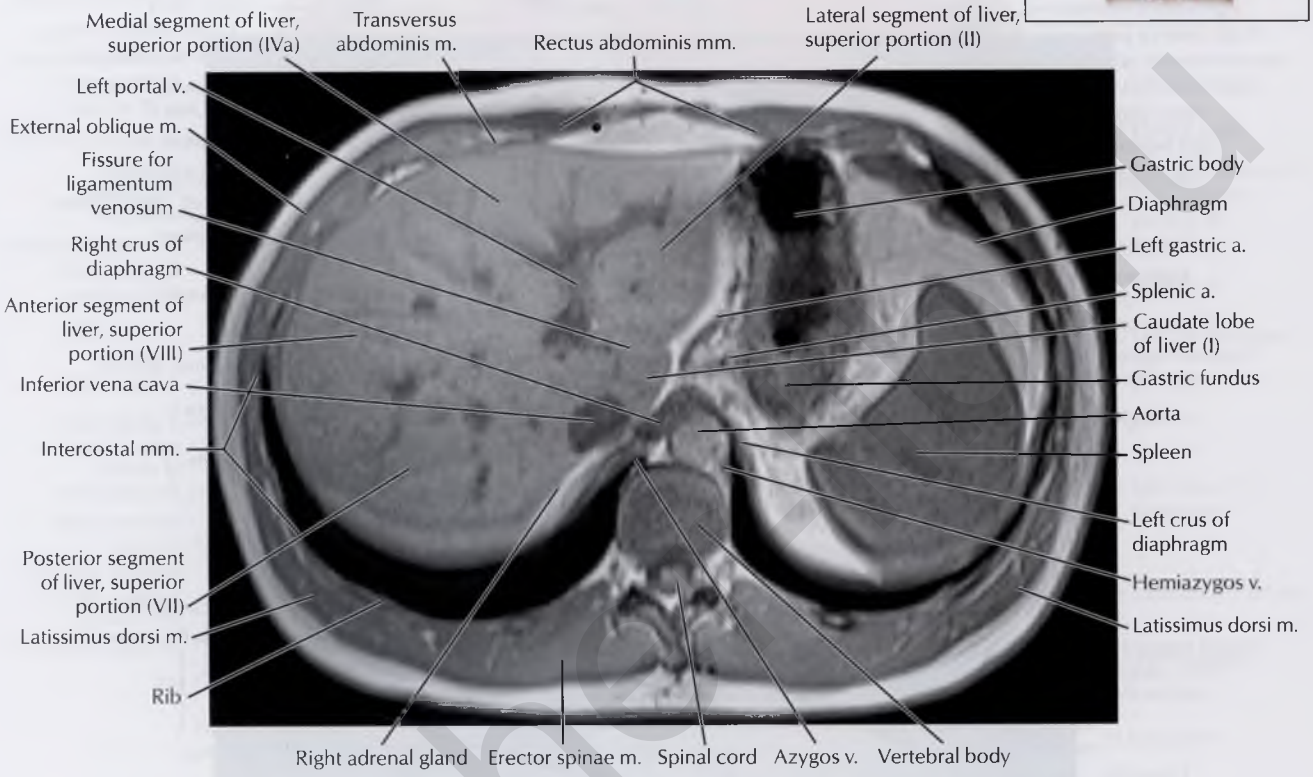
Medial segment of liver, superior portion (IVa)
Transversus abdominis m.
Rectus abdominis mm.
Lateral segment of liver, superior portion (II)
Left portal v.
External oblique m.
Fissure for ligamentum venosum
Right crus of diaphragm
Anterior segment of liver, superior portion (VIII)
Inferior vena cava
Intercostal mm.
Posterior segment of liver, superior portion (VII)
Latissimus dorsi m.
Rib
Gastric body
Diaphragm
Left gastric a.
Splenic a.
Caudate lobe of liver (I)
Gastric fundus
Aorta
Spleen
Left crus of diaphragm
Hemiazygos v.
Latissimus dorsi m.
Right adrenal gland
Erector spinae m.
Spinal cord
Azygos v.
Vertebral body

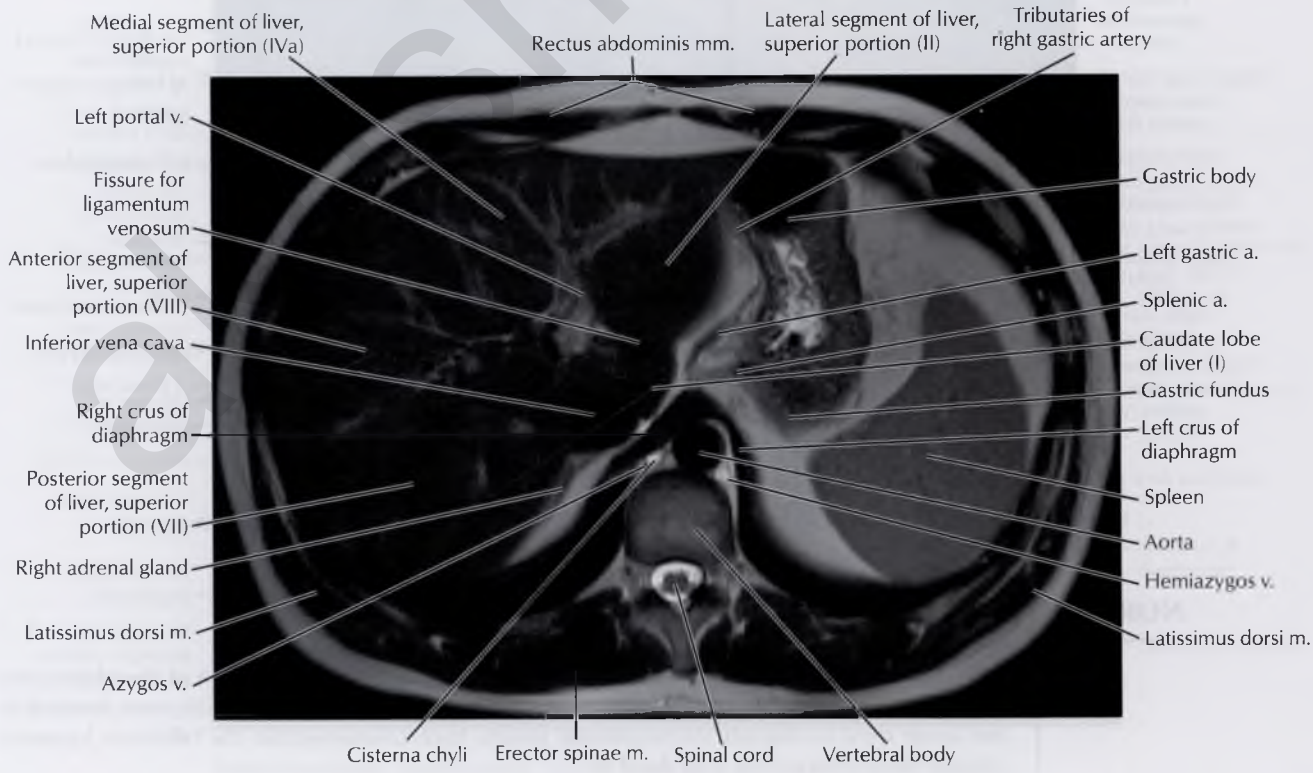
Medial segment of liver, superior portion (IVa)
Rectus abdominis mm.
Lateral segment of liver, superior portion (II)
Tributaries of right gastric artery
Left portal v.
Fissure for ligamentum venosum
Anterior segment of liver, superior portion (VIII)
Inferior vena cava
Right crus of diaphragm
Posterior segment of liver, superior portion (VII)
Right adrenal gland
Latissimus dorsi m.
Azygos v.
Gastric body
Left gastric a.
Splenic a.
Caudate lobe of liver (I)
Gastric fundus
Left crus of diaphragm
Spleen
Aorta
Hemiazygos v.
Latissimus dorsi m.
Cisterna chyli
Erector spinae m.
Spinal cord
Vertebral body

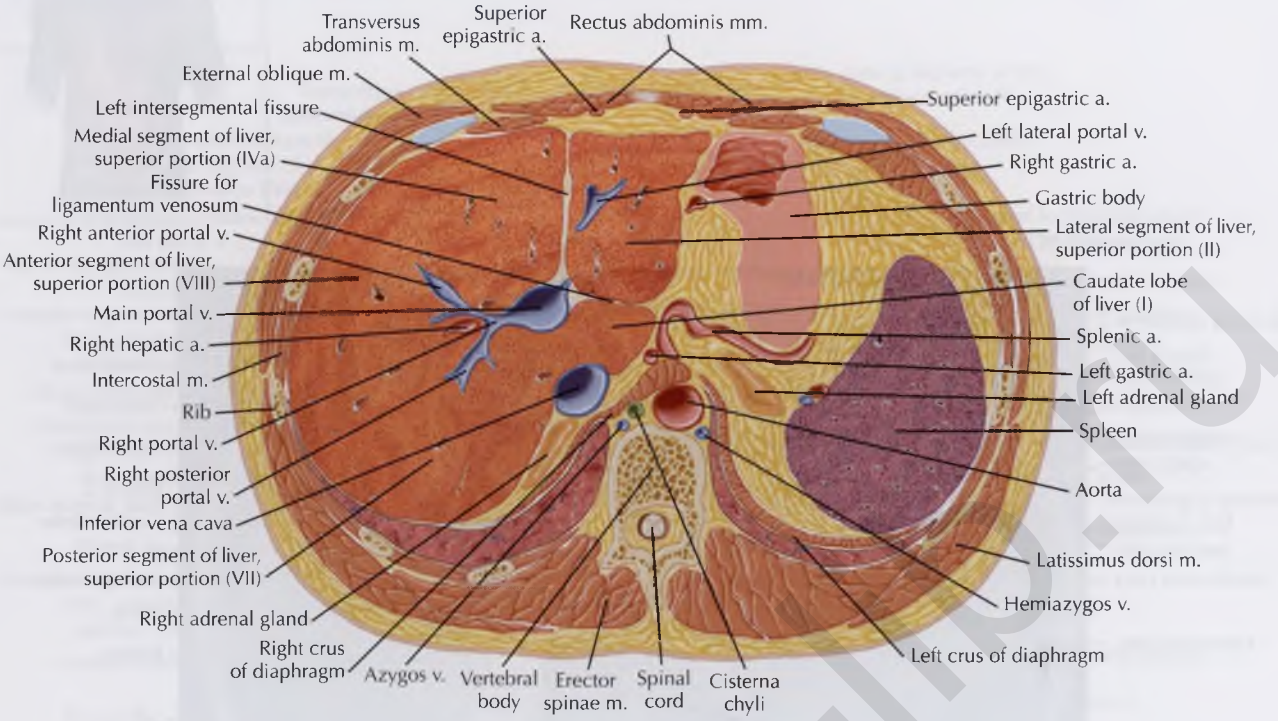

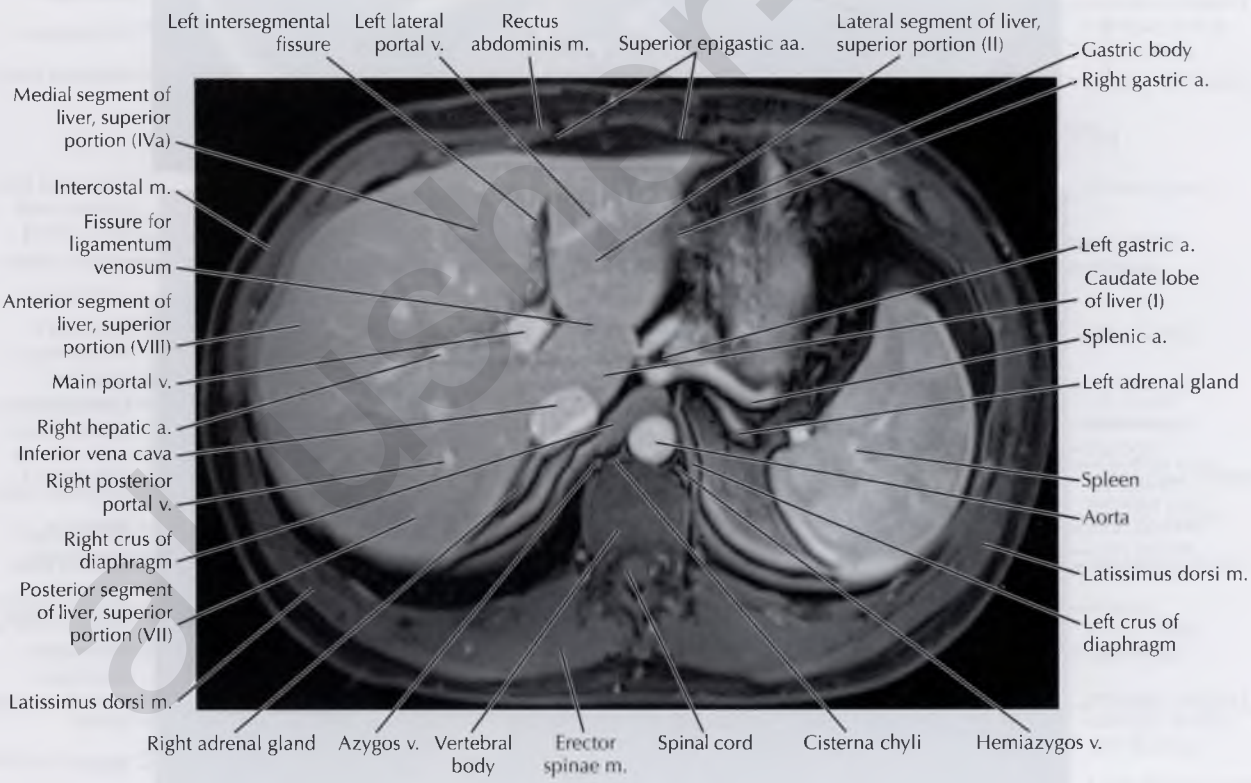

NORMAL ANATOMY

The ligamentum venosum is in continuity with *the ligamentum teres*, a remnant of the obliterated umbilical vein. The ligamentum teres travels in the fissure for the ligamentum teres, located in the lower third of the left intersegmental fissure, then courses within the falciform ligament toward the umbilicus (see also Axial 6).

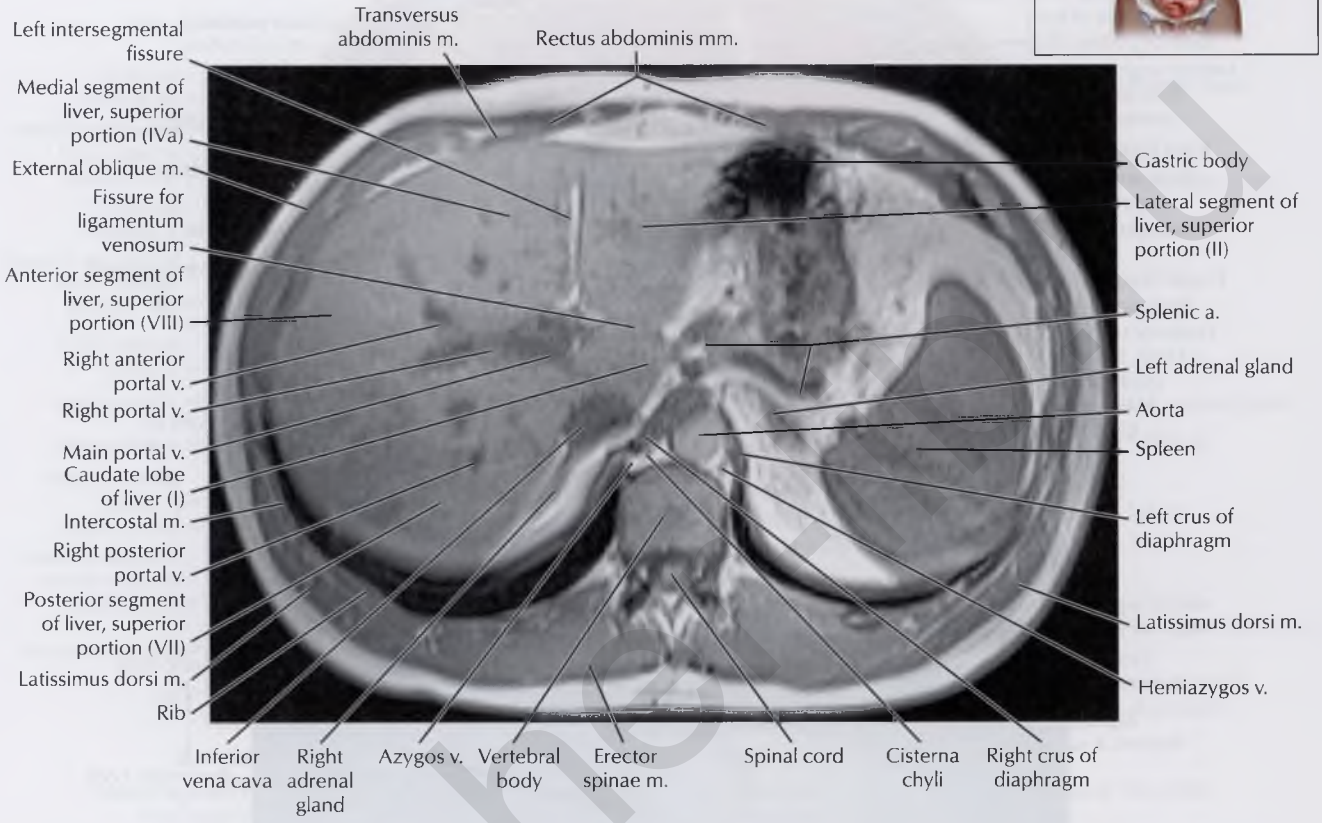
Left intersegmental fissure
Transversus abdominis m.
Rectus abdominis mm.
Medial segment of liver, superior portion (IVa)
External oblique m.
Fissure for ligamentum venosum
Anterior segment of liver, superior portion (VIII)
Right anterior portal v.
Right portal v.
Main portal v.
Caudate lobe of liver (I)
Intercostal m.
Right posterior portal v.
Posterior segment of liver, superior portion (VII)
Latissimus dorsi m.
Rib
Gastric body
Lateral segment of liver, superior portion (II)
Splenic a.
Left adrenal gland
Aorta
Spleen
Left crus of diaphragm
Latissimus dorsi m.
Hemiazygos v.
Inferior vena cava
Right adrenal gland
Azygos v.
Vertebral body
Erector spinae m.
Spinal cord
Cisterna chyli
Right crus of diaphragm

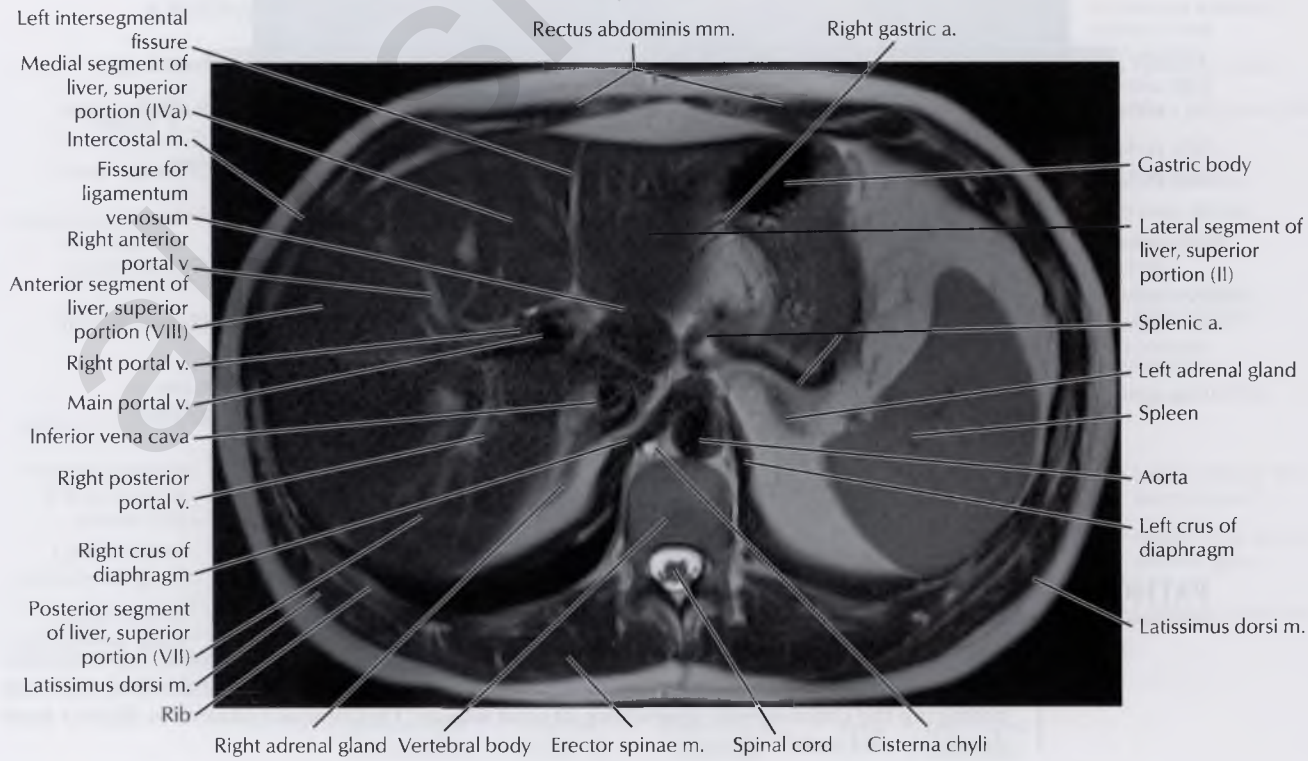
Left intersegmental fissure
Rectus abdominis mm.
Right gastric a.
Medial segment of liver, superior portion (IVa)
Intercostal m.
Fissure for ligamentum venosum
Right anterior portal v.
Anterior segment of liver, superior portion (VIII)
Right portal v.
Main portal v.
Inferior vena cava
Right posterior portal v.
Right crus of diaphragm
Posterior segment of liver, superior portion (VII)
Latissimus dorsi m.
Rib
Gastric body
Lateral segment of liver, superior portion (II)
Splenic a.
Left adrenal gland
Spleen
Aorta
Left crus of diaphragm
Latissimus dorsi m.
Right adrenal gland
Vertebral body
Erector spinae m.
Spinal cord
Cisterna chyli

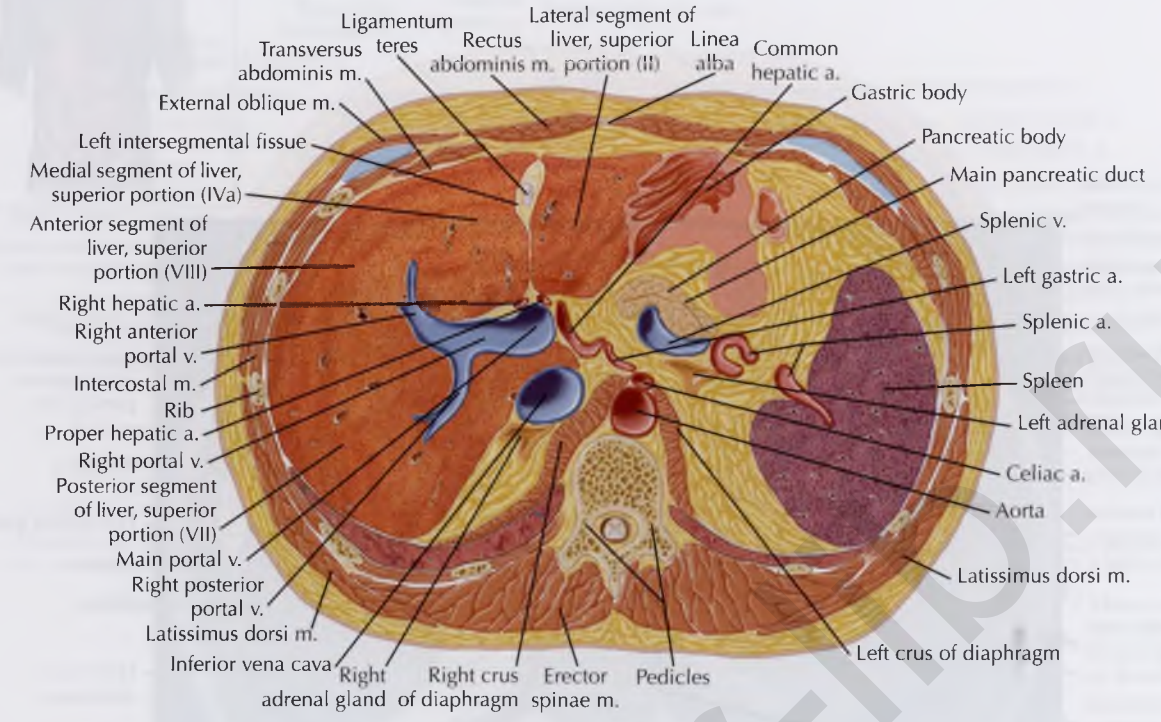

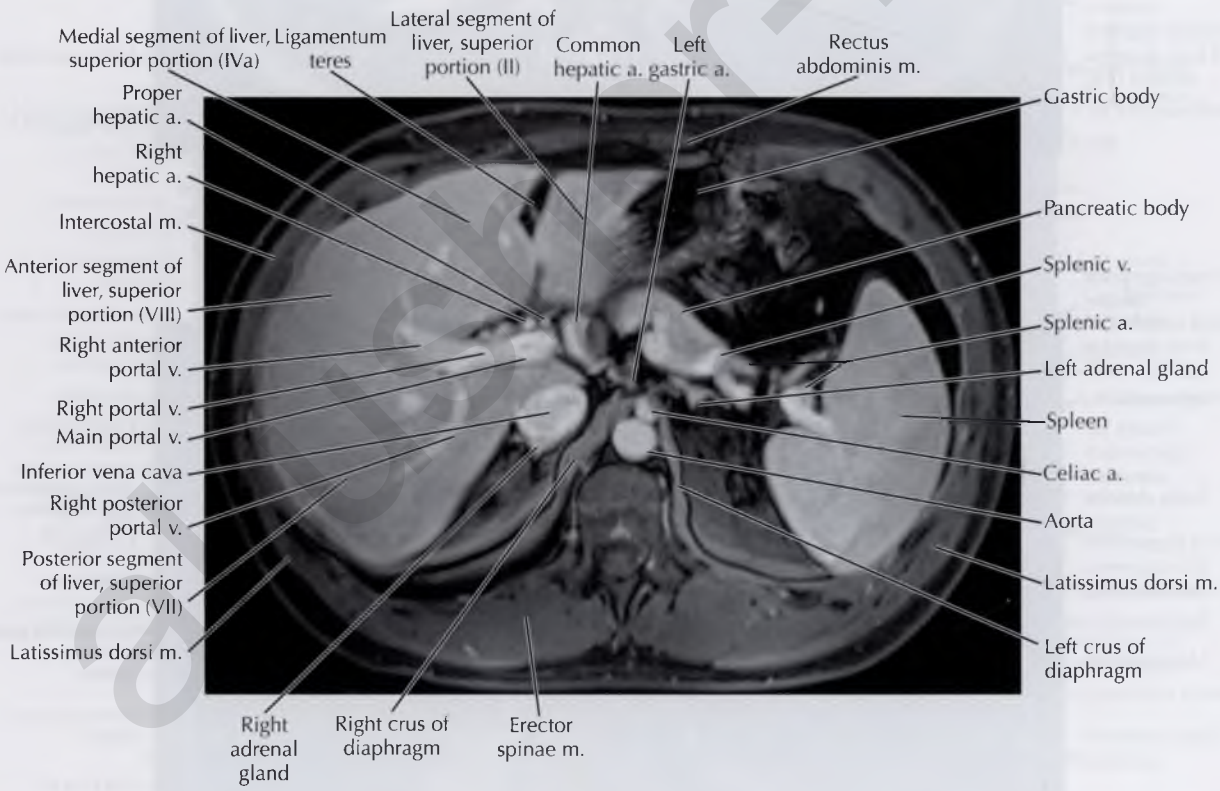

PATHOLOGIC PROCESS

An enlarged paraumbilical vein may become visible in the patient with portal hypertension, allowing for portosystemic venous collateralization within the anterior abdominal wall and producing the characteristic appearance of *caput medusae*. This venous collateral is distinct from the obliterated umbilical vein.

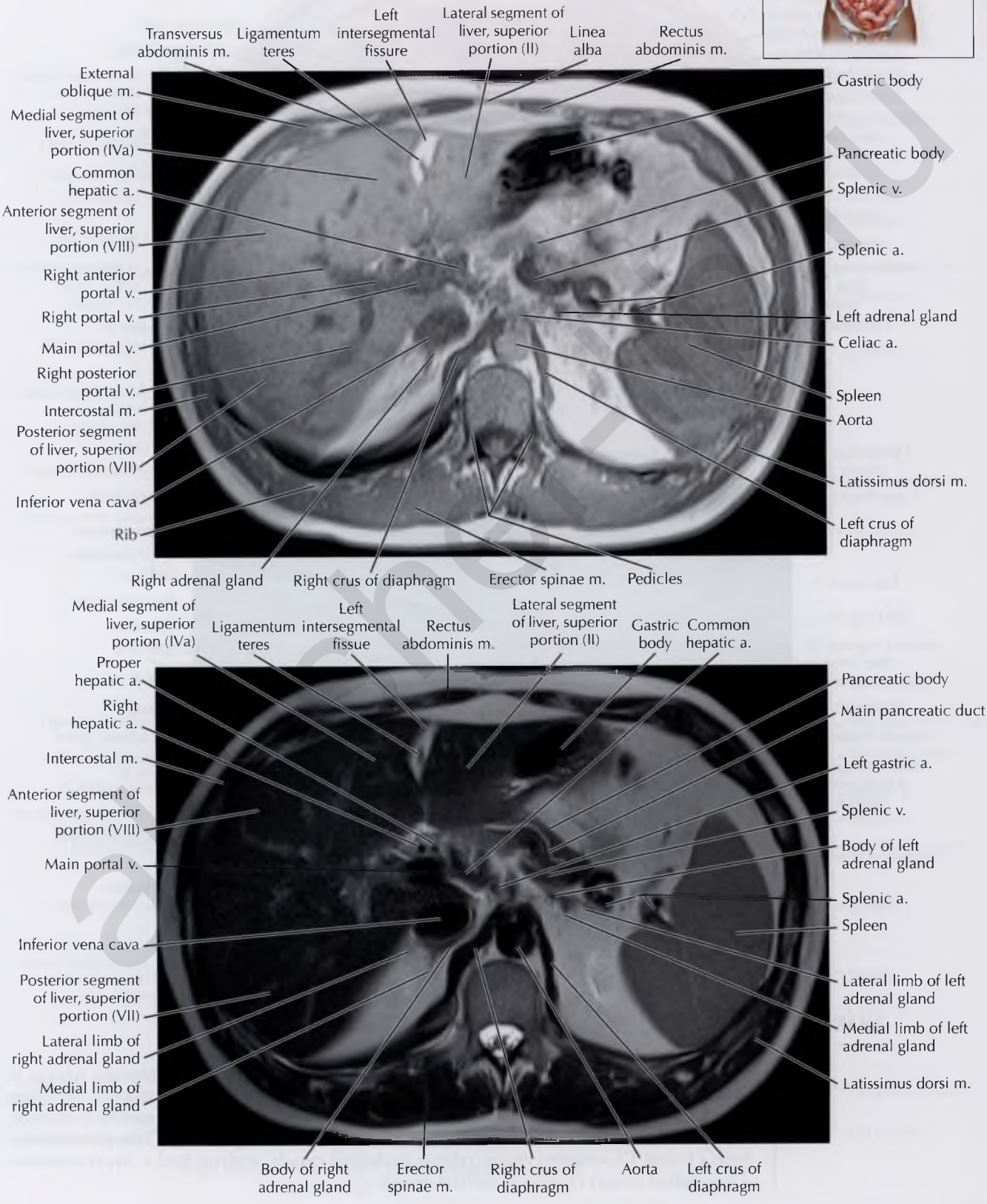
Transversus abdominis m.
Ligamentum teres
Left intersegmental fissure
Lateral segment of liver, superior portion (II)
Linea alba
Rectus abdominis m.
External oblique m.
Medial segment of liver, superior portion (IVa)
Common hepatic a.
Anterior segment of liver, superior portion (VIII)
Right anterior portal v.
Right portal v.
Main portal v.
Right posterior portal v.
Intercostal m.
Posterior segment of liver, superior portion (VII)
Inferior vena cava
Rib
Gastric body
Pancreatic body
Splenic v.
Splenic a.
Left adrenal gland
Celiac a.
Spleen
Aorta
Latissimus dorsi m.
Left crus of diaphragm
Right adrenal gland
Right crus of diaphragm
Erector spinae m.
Pedicles
Medial segment of liver, superior portion (IVa)
Ligamentum teres
Left intersegmental fissue
Rectus abdominis m.
Lateral segment of liver, superior portion (II)
Gastric body
Common hepatic a.
Proper hepatic a.
Right hepatic a.
Intercostal m.
Anterior segment of liver, superior portion (VIII)
Main portal v.
Inferior vena cava
Posterior segment of liver, superior portion (VII)
Lateral limb of right adrenal gland
Medial limb of right adrenal gland
Pancreatic body
Main pancreatic duct
Left gastric a.
Splenic v.
Body of left adrenal gland
Splenic a.
Spleen
Lateral limb of left adrenal gland
Medial limb of left adrenal gland
Latissimus dorsi m.
Body of right adrenal gland
Erector spinae m.
Right crus of diaphragm
Aorta
Left crus of diaphragm

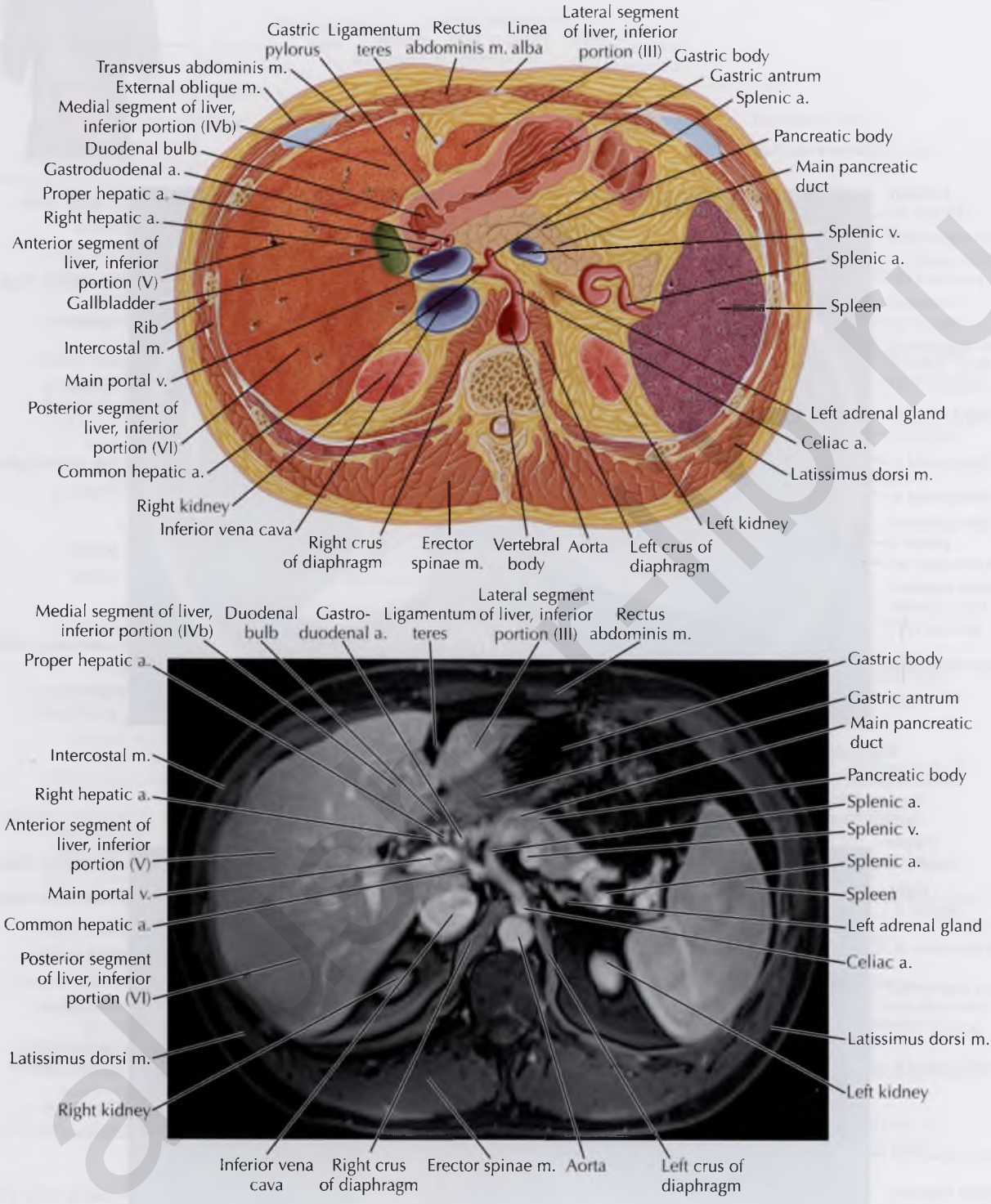

NORMAL ANATOMY

On T1-weighted MR images, the normal pancreas has the highest signal intensity relative to other parenchymal organs, because of its high protein and rough endoplasmic reticulum content, followed by the liver, then the spleen. On T2-weighted images, the pattern is reversed; the normal spleen has higher signal intensity than the liver or pancreas. Fat is hyperintense on both T1- and T2-weighted images relative to skeletal muscle, whereas fluid is hyperintense on T2-weighted images relative to skeletal muscle.

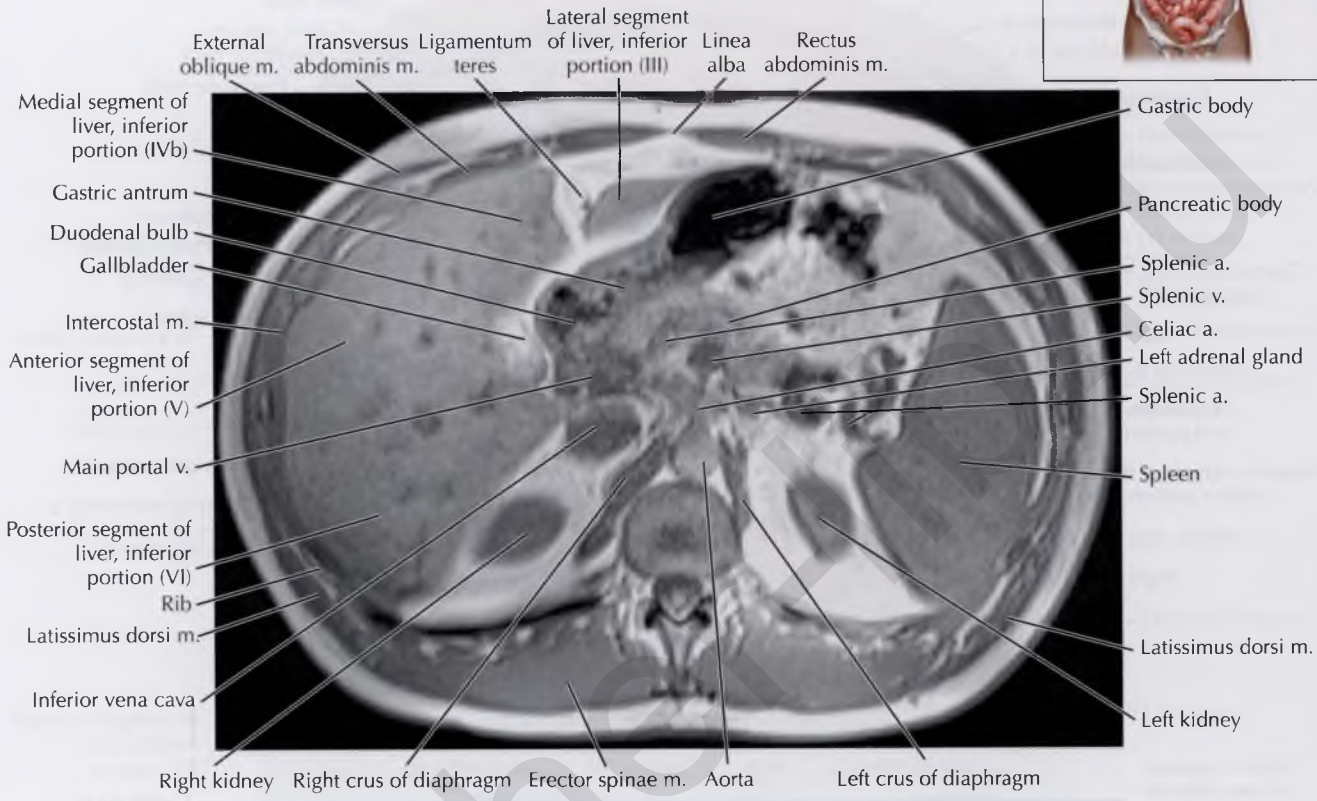
External oblique m.
Transversus abdominis m.
Ligamentum teres
Lateral segment of liver, inferior portion (III)
Linea alba
Rectus abdominis m.
Medial segment of liver, inferior portion (IVb)
Gastric antrum
Duodenal bulb
Gallbladder
Intercostal m.
Anterior segment of liver, inferior portion (V)
Main portal v.
Posterior segment of liver, inferior portion (VI)
Rib
Latissimus dorsi m.
Inferior vena cava
Gastric body
Pancreatic body
Splenic a.
Splenic v.
Celiac a.
Left adrenal gland
Splenic a.
Spleen
Latissimus dorsi m.
Left kidney
Right kidney
Right crus of diaphragm
Erector spinae m.
Aorta
Left crus of diaphragm

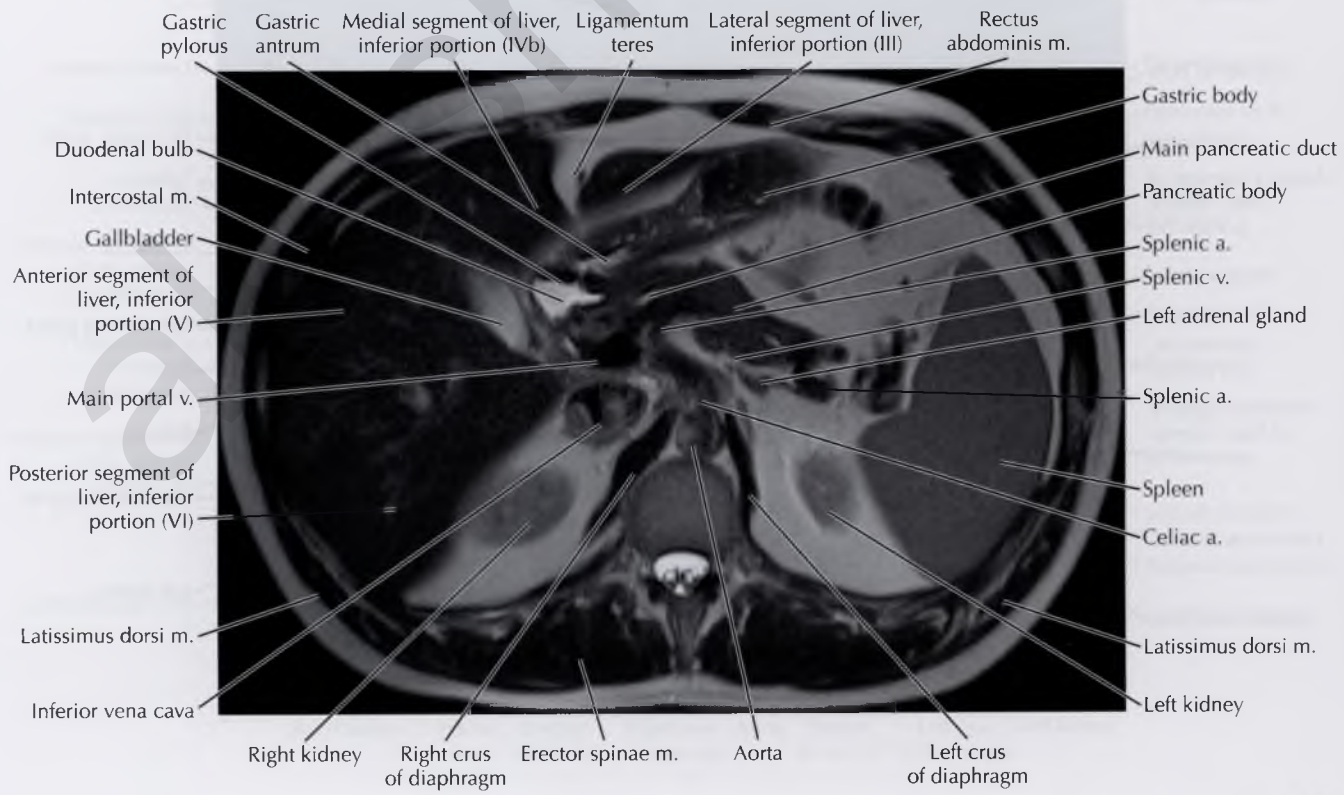
Gastric pylorus
Gastric antrum
Medial segment of liver, inferior portion (IVb)
Ligamentum teres
Lateral segment of liver, inferior portion (III)
Rectus abdominis m.
Duodenal bulb
Intercostal m.
Gallbladder
Anterior segment of liver, inferior portion (V)
Main portal v.
Posterior segment of liver, inferior portion (VI)
Latissimus dorsi m.
Inferior vena cava
Gastric body
Main pancreatic duct
Pancreatic body
Splenic a.
Splenic v.
Left adrenal gland
Splenic a.
Spleen
Celiac a.
Latissimus dorsi m.
Left kidney
Right kidney
Right crus of diaphragm
Erector spinae m.
Aorta
Left crus of diaphragm

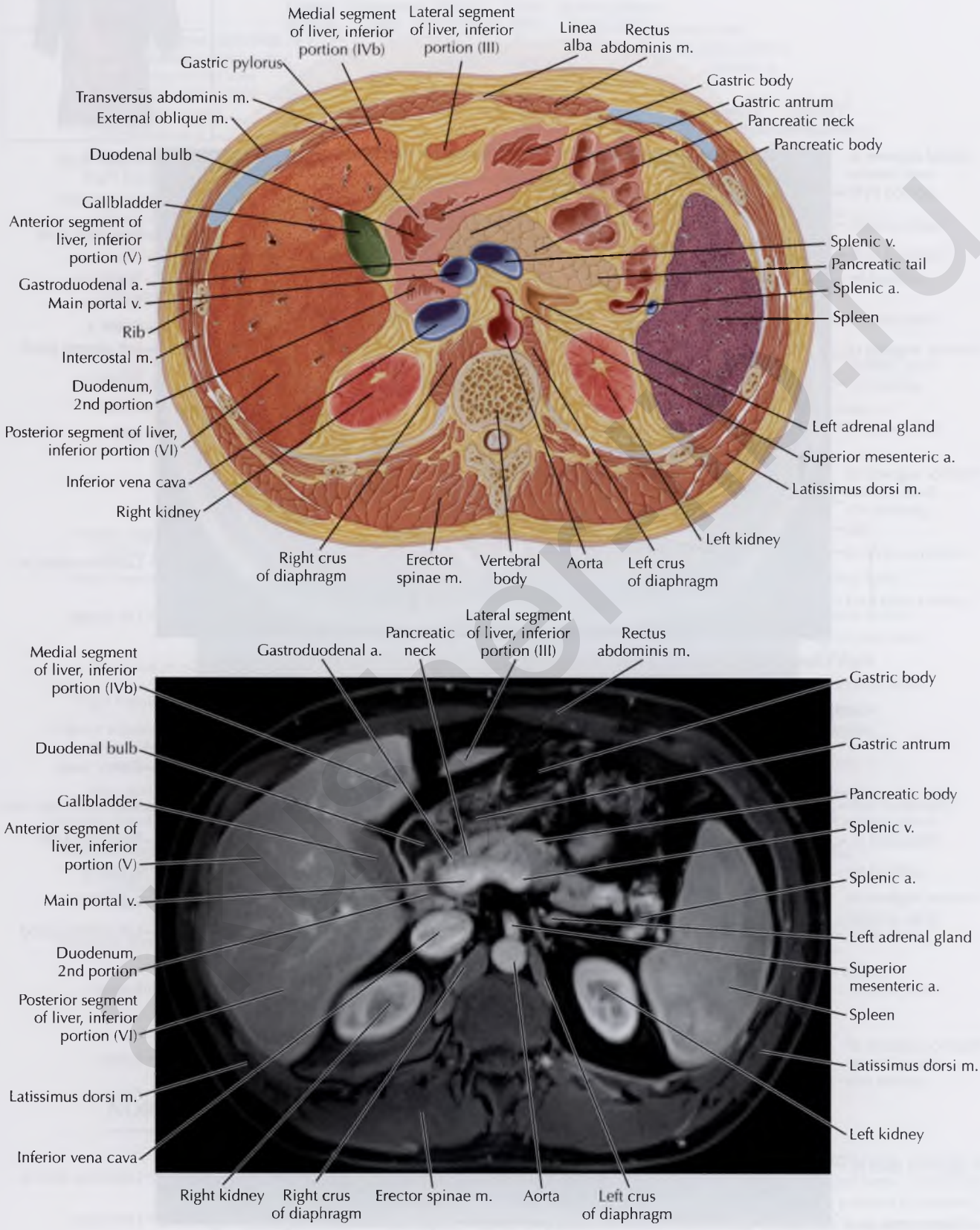
Medial segment of liver, inferior portion (IVb)
Lateral segment of liver, inferior portion (III)
Linea alba
Rectus abdominis m.
Gastric pylorus
Transversus abdominis m.
External oblique m.
Duodenal bulb
Gallbladder
Anterior segment of liver, inferior portion (V)
Gastroduodenal a.
Main portal v.
Rib
Intercostal m.
Duodenum, 2nd portion
Posterior segment of liver, inferior portion (VI)
Inferior vena cava
Right kidney
Gastric body
Gastric antrum
Pancreatic neck
Pancreatic body
Splenic v.
Pancreatic tail
Splenic a.
Spleen
Left adrenal gland
Superior mesenteric a.
Latissimus dorsi m.
Left kidney
Right crus of diaphragm
Erector spinae m.
Vertebral body
Aorta
Left crus of diaphragm
Medial segment of liver, inferior portion (IVb)
Gastroduodenal a.
Pancreatic neck
Lateral segment of liver, inferior portion (III)
Rectus abdominis m.
Duodenal bulb
Gallbladder
Anterior segment of liver, inferior portion (V)
Main portal v.
Duodenum, 2nd portion
Posterior segment of liver, inferior portion (VI)
Latissimus dorsi m.
Inferior vena cava
Gastric body
Gastric antrum
Pancreatic body
Splenic v.
Splenic a.
Left adrenal gland
Superior mesenteric a.
Spleen
Latissimus dorsi m.
Left kidney
Right kidney
Right crus of diaphragm
Erector spinae m.
Aorta
Left crus of diaphragm

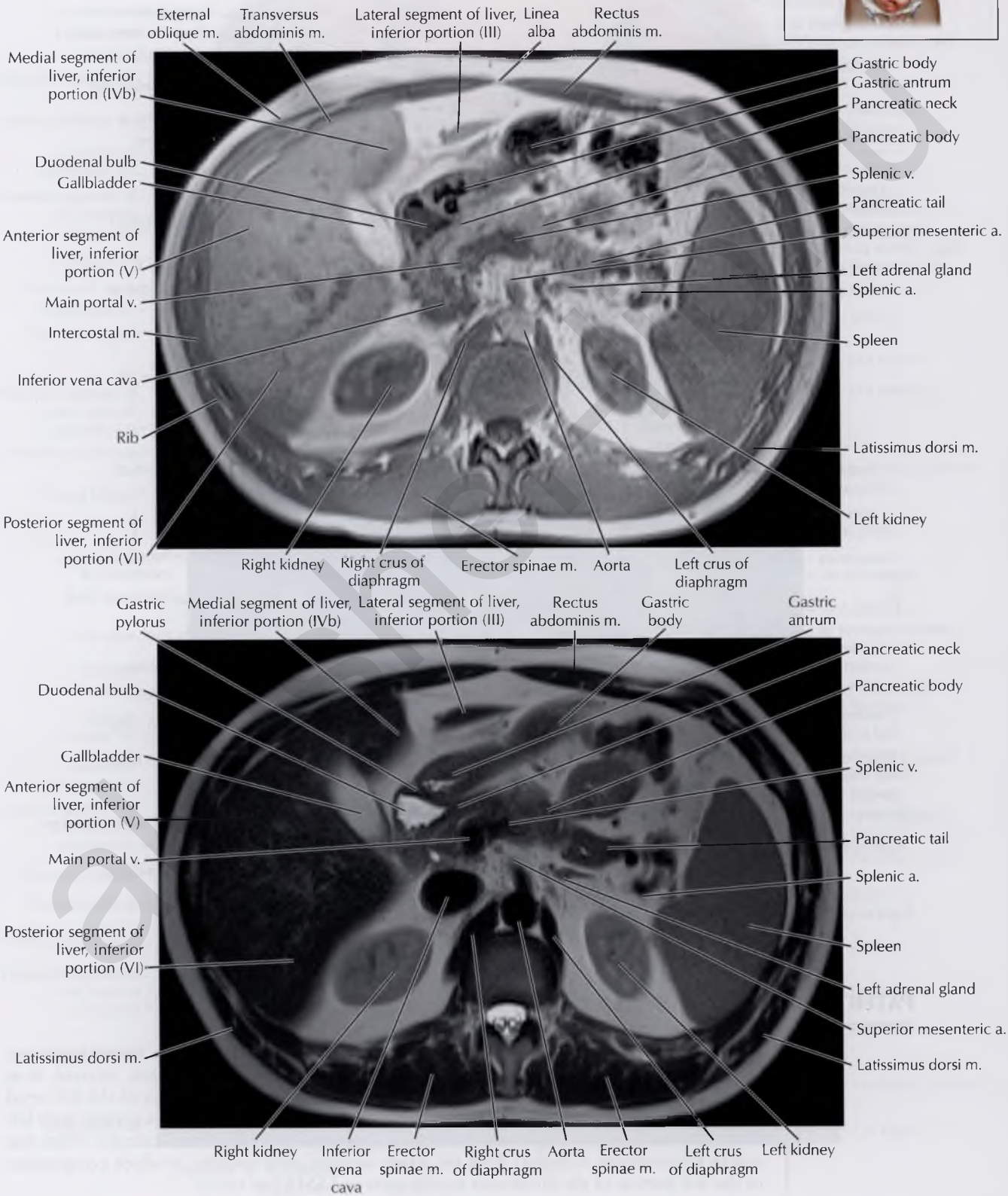
External oblique m.
Transversus abdominis m.
Lateral segment of liver, inferior portion (III)
Linea alba
Rectus abdominis m.
Medial segment of liver, inferior portion (IVb)
Duodenal bulb
Gallbladder
Anterior segment of liver, inferior portion (V)
Main portal v.
Intercostal m.
Inferior vena cava
Rib
Posterior segment of liver, inferior portion (VI)
Gastric body
Gastric antrum
Pancreatic neck
Pancreatic body
Splenic v.
Pancreatic tail
Superior mesenteric a.
Left adrenal gland
Splenic a.
Spleen
Latissimus dorsi m.
Left kidney
Right kidney
Right crus of diaphragm
Erector spinae m.
Aorta
Left crus of diaphragm
Gastric pylorus
Medial segment of liver, inferior portion (IVb)
Lateral segment of liver, inferior portion (III)
Rectus abdominis m.
Gastric body
Gastric antrum
Duodenal bulb
Gallbladder
Anterior segment of liver, inferior portion (V)
Main portal v.
Posterior segment of liver, inferior portion (VI)
Latissimus dorsi m.
Pancreatic neck
Pancreatic body
Splenic v.
Pancreatic tail
Splenic a.
Spleen
Left adrenal gland
Superior mesenteric a.
Latissimus dorsi m.
Right kidney
Inferior vena cava
Erector spinae m.
Right crus of diaphragm
Aorta
Erector spinae m.
Left crus of diaphragm
Left kidney

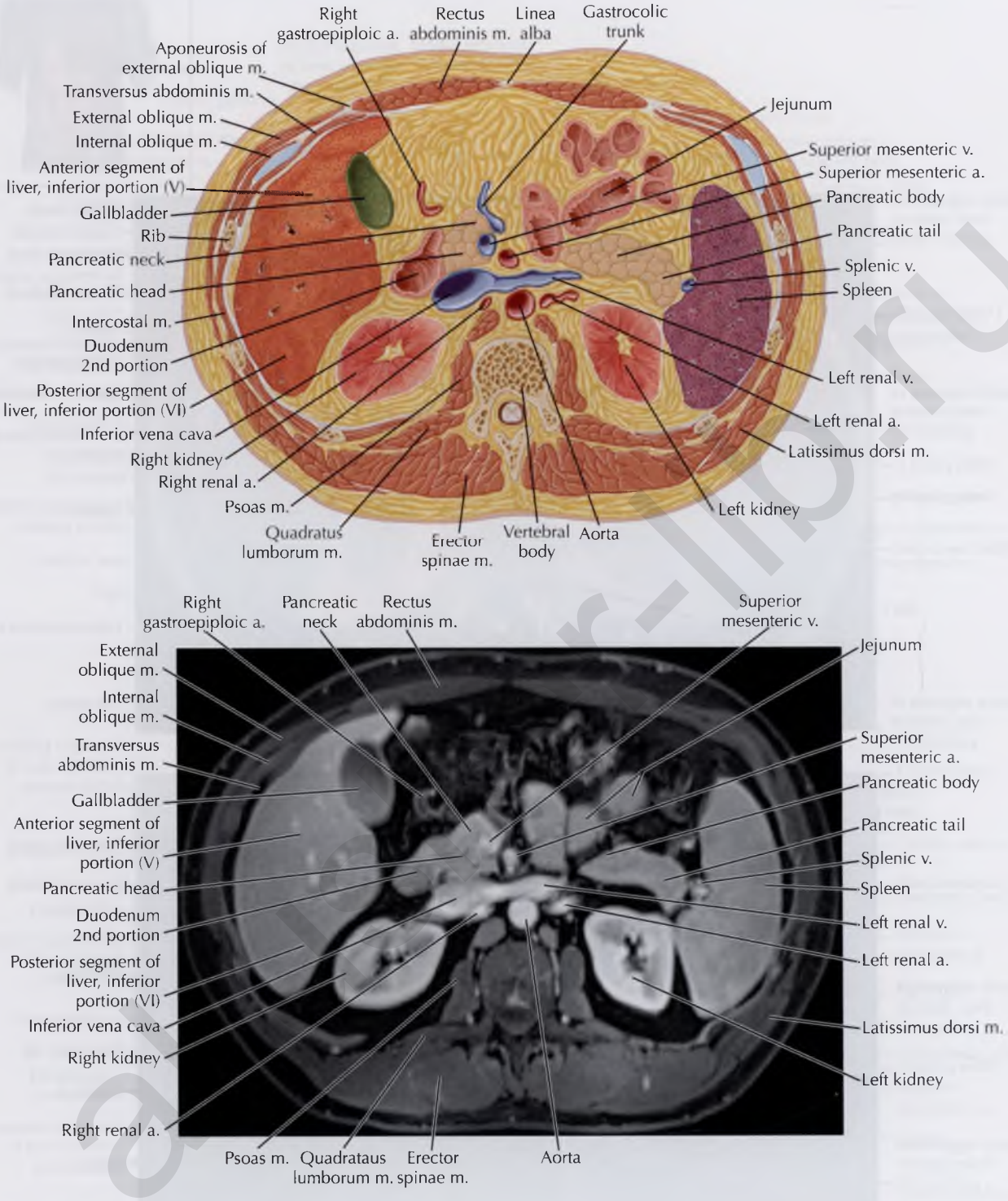

PATHOLOGIC PROCESS

Compression of the left renal vein as it passes between the aorta and superior mesenteric artery (SMA) can result in an outflow obstruction and left renal vein hypertension, referred to as *nutcracker syndrome* (or nutcracker phenomenon). In addition to compression of the left renal vein, look for perirenal varices and a unilateral left varicocele. Patients can present with left flank pain and hematuria, clinically mimicking symptoms of a left ureteral calculus. Note that nutcracker syndrome is distinct from the *superior mesenteric artery syndrome*, in which compression of the 3rd portion of the duodenum by the aorta and SMA can occur.

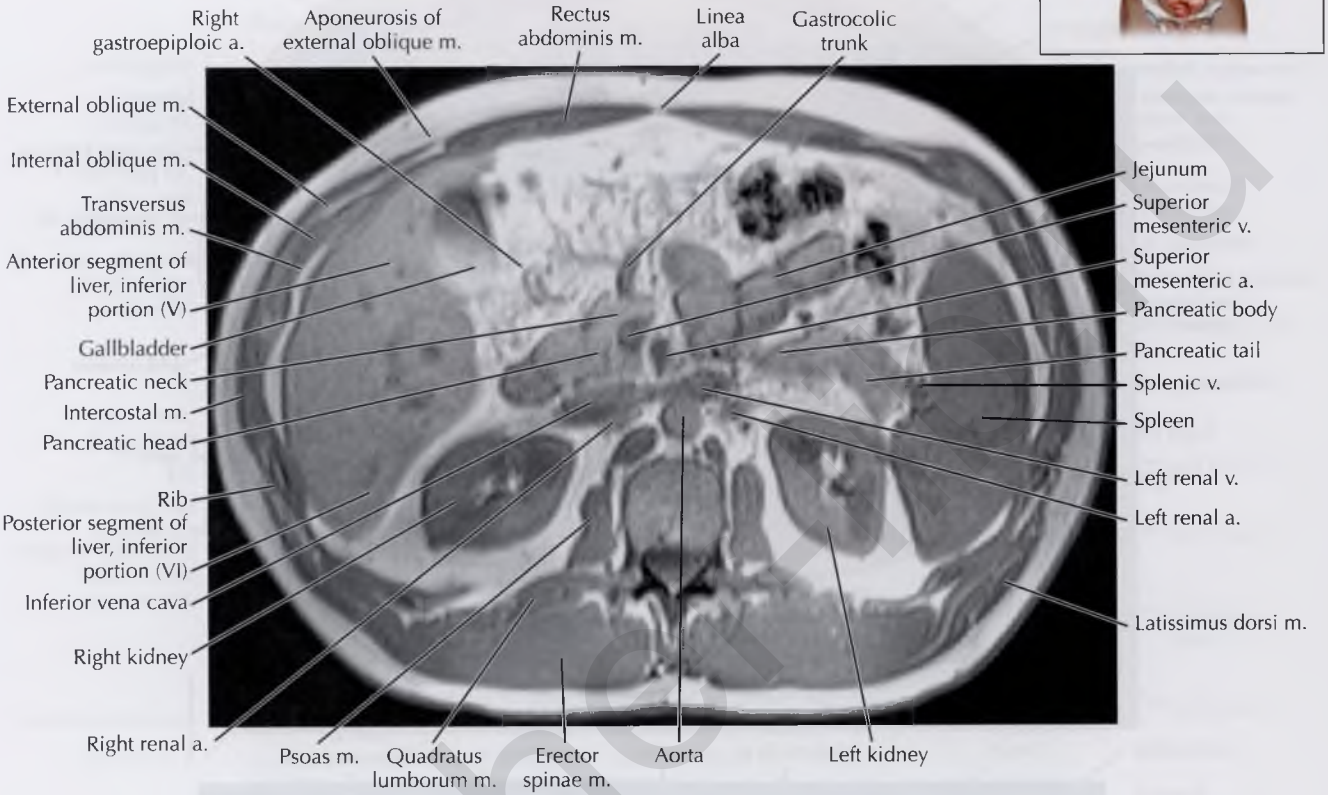
Right gastroepiploic a.
Aponeurosis of external oblique m.
Rectus abdominis m.
Linea alba
Gastrocolic trunk
External oblique m.
Internal oblique m.
Transversus abdominis m.
Anterior segment of liver, inferior portion (V)
Gallbladder
Pancreatic neck
Intercostal m.
Pancreatic head
Rib
Posterior segment of liver, inferior portion (VI)
Inferior vena cava
Right kidney
Right renal a.
Psoas m.
Quadratus lumborum m.
Erector spinae m.
Aorta
Left kidney
Jejunum
Superior mesenteric v.
Superior mesenteric a.
Pancreatic body
Pancreatic tail
Splenic v.
Spleen
Left renal v.
Left renal a.
Latissimus dorsi m.

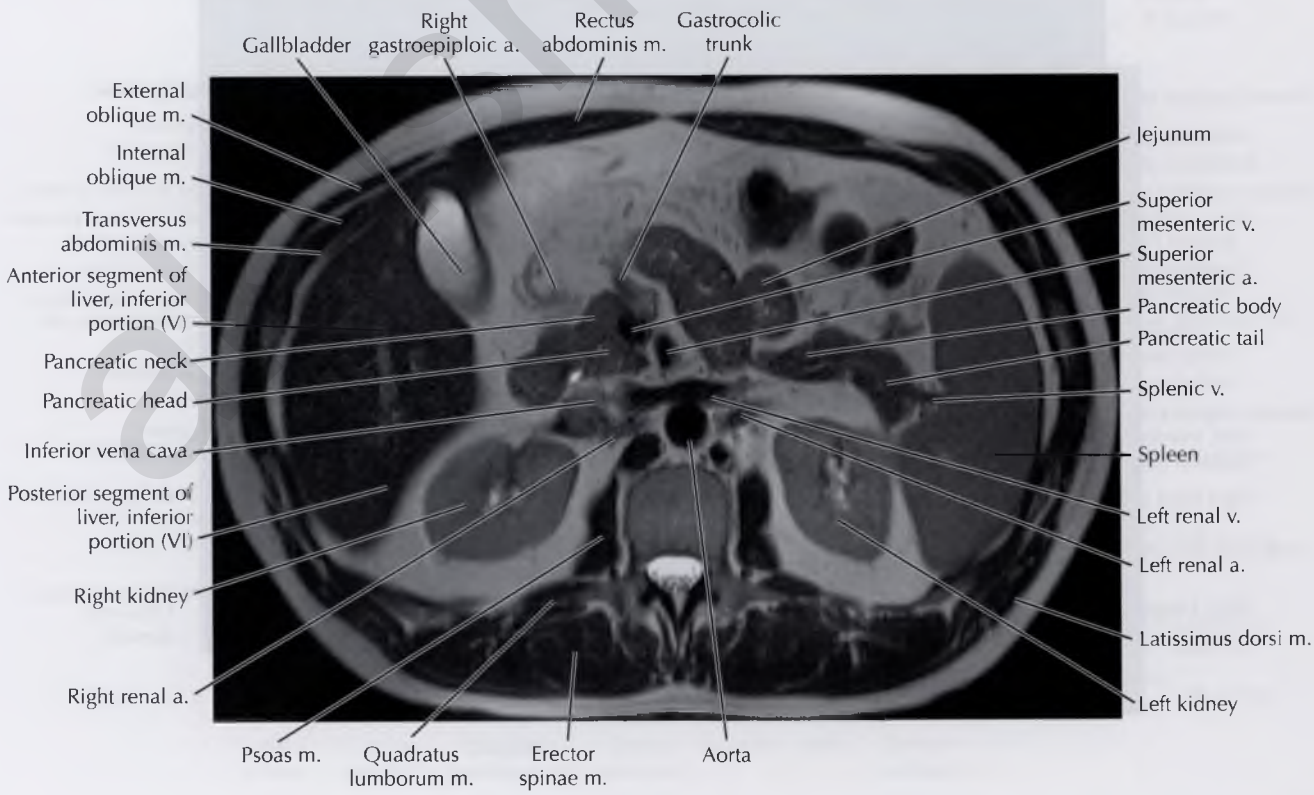
Gallbladder
Right gastroepiploic a.
Rectus abdominis m.
Gastrocolic trunk
External oblique m.
Internal oblique m.
Transversus abdominis m.
Anterior segment of liver, inferior portion (V)
Pancreatic neck
Pancreatic head
Inferior vena cava
Posterior segment of liver, inferior portion (VI)
Right kidney
Right renal a.
Psoas m.
Quadratus lumborum m.
Erector spinae m.
Aorta
Jejunum
Superior mesenteric v.
Superior mesenteric a.
Pancreatic body
Pancreatic tail
Splenic v.
Spleen
Left renal v.
Left renal a.
Latissimus dorsi m.
Left kidney

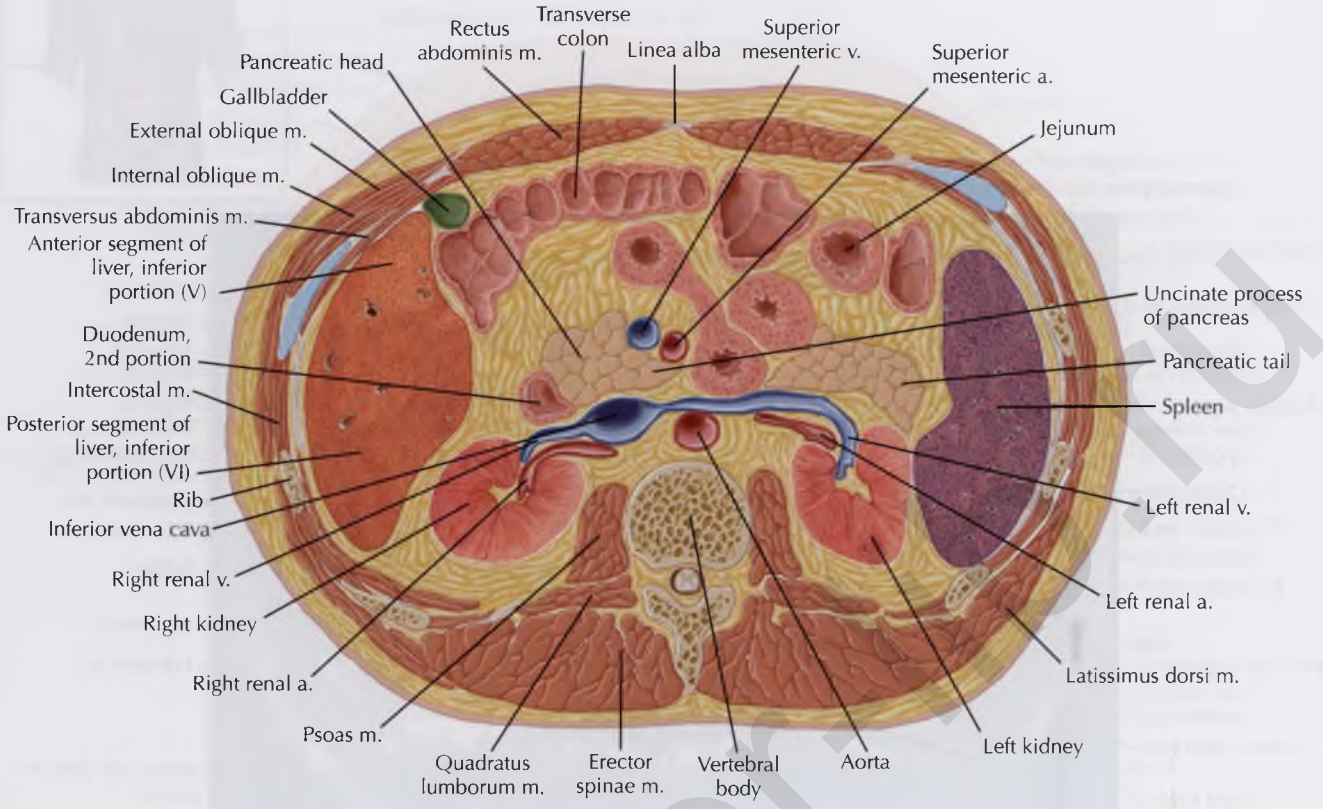
Rectus abdominis m.
Transverse colon
Linea alba
Superior mesenteric v.
Superior mesenteric a.
Pancreatic head
Gallbladder
External oblique m.
Internal oblique m.
Jejunum
Transversus abdominis m.
Anterior segment of liver, inferior portion (V)
Uncinate process of pancreas
Duodenum, 2nd portion
Pancreatic tail
Intercostal m.
Spleen
Posterior segment of liver, inferior portion (VI)
Left renal v.
Rib
Inferior vena cava
Left renal a.
Right renal v.
Right kidney
Latissimus dorsi m.
Right renal a.
Psoas m.
Left kidney
Quadratus lumborum m.
Erector spinae m.
Vertebral body
Aorta

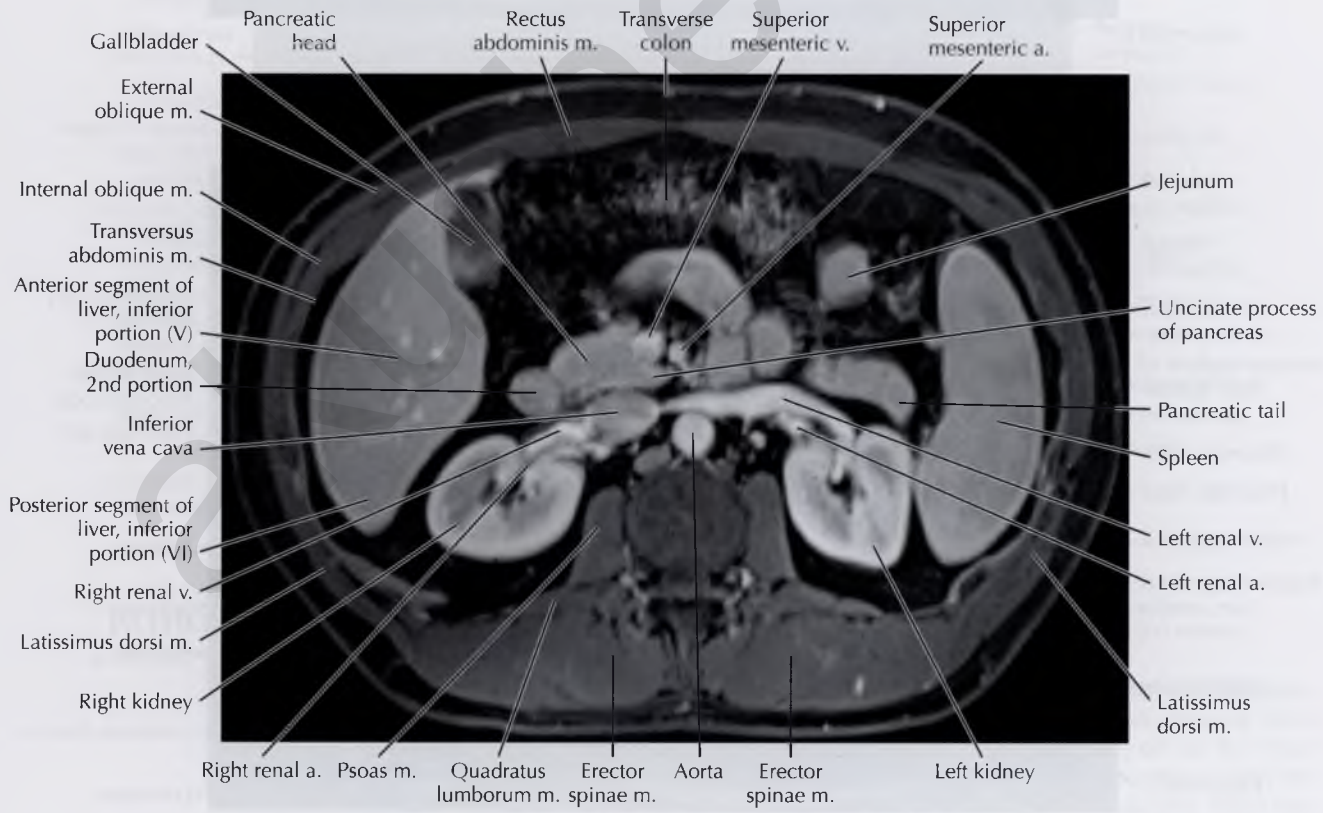
Gallbladder
Pancreatic head
Rectus abdominis m.
Transverse colon
Superior mesenteric v.
Superior mesenteric a.
External oblique m.
Internal oblique m.
Jejunum
Transversus abdominis m.
Anterior segment of liver, inferior portion (V)
Uncinate process of pancreas
Duodenum, 2nd portion
Pancreatic tail
Inferior vena cava
Spleen
Posterior segment of liver, inferior portion (VI)
Left renal v.
Right renal v.
Left renal a.
Latissimus dorsi m.
Right kidney
Latissimus dorsi m.
Right renal a.
Psoas m.
Quadratus lumborum m.
Erector spinae m.
Aorta
Erector spinae m.
Left kidney

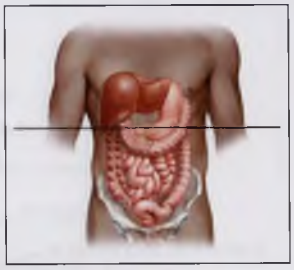

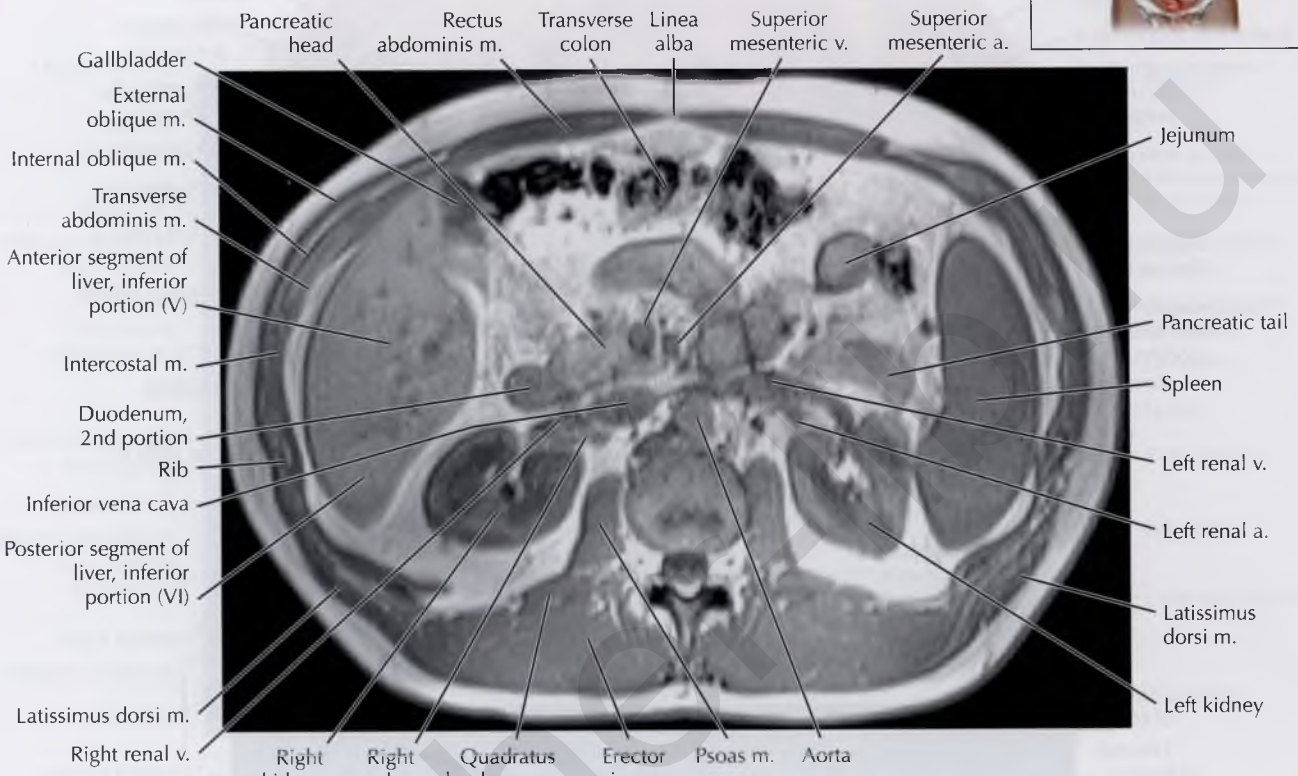
Pancreatic head
Rectus abdominis m.
Transverse colon
Linea alba
Superior mesenteric v.
Superior mesenteric a.
Gallbladder
External oblique m.
Internal oblique m.
Transverse abdominis m.
Anterior segment of liver, inferior portion (V)
Intercostal m.
Duodenum, 2nd portion
Rib
Inferior vena cava
Posterior segment of liver, inferior portion (VI)
Latissimus dorsi m.
Right renal v.
Jejunum
Pancreatic tail
Spleen
Left renal v.
Left renal a.
Latissimus dorsi m.
Left kidney
Right kidney
Right renal a.
Quadratus lumborum m.
Erector spinae m.
Psoas m.
Aorta

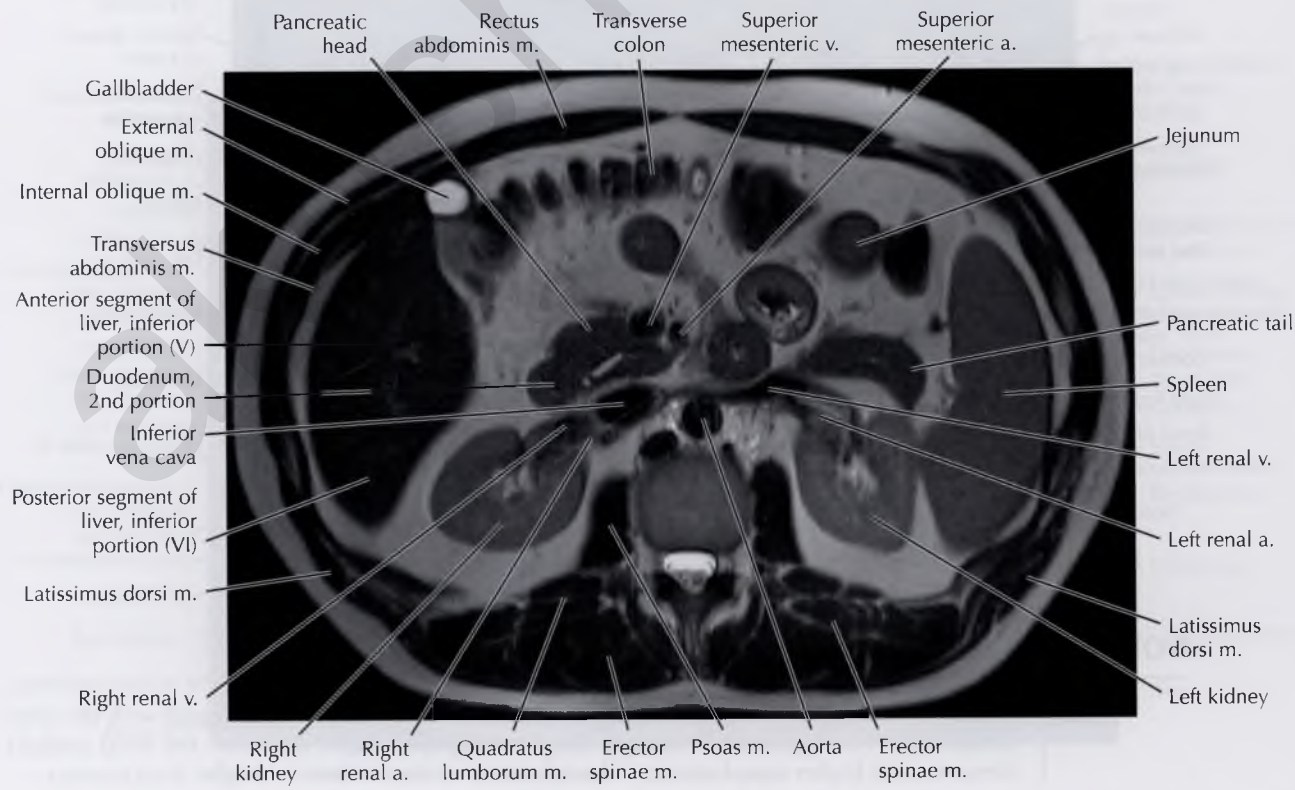
Pancreatic head
Rectus abdominis m.
Transverse colon
Superior mesenteric v.
Superior mesenteric a.
Gallbladder
External oblique m.
Internal oblique m.
Transversus abdominis m.
Anterior segment of liver, inferior portion (V)
Duodenum, 2nd portion
Inferior vena cava
Posterior segment of liver, inferior portion (VI)
Latissimus dorsi m.
Right renal v.
Jejunum
Pancreatic tail
Spleen
Left renal v.
Left renal a.
Latissimus dorsi m.
Left kidney
Right kidney
Right renal a.
Quadratus lumborum m.
Erector spinae m.
Psoas m.
Aorta
Erector spinae m.

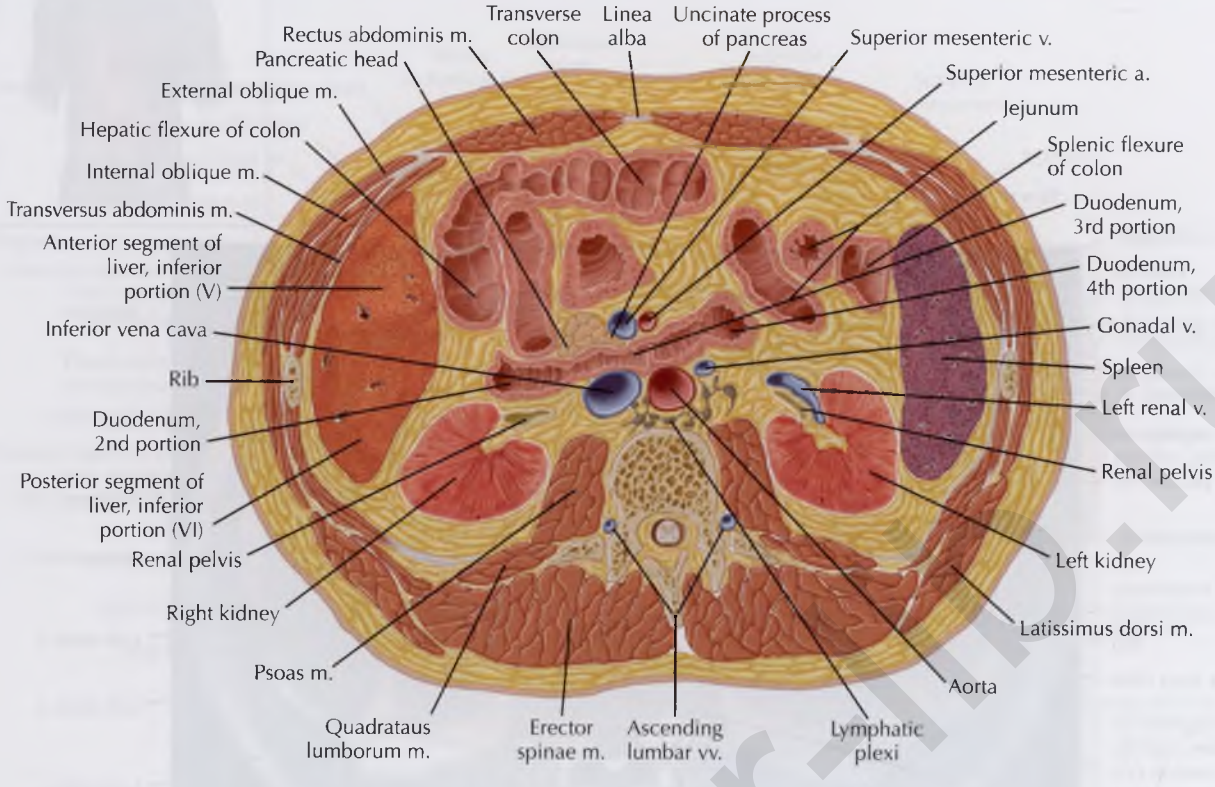

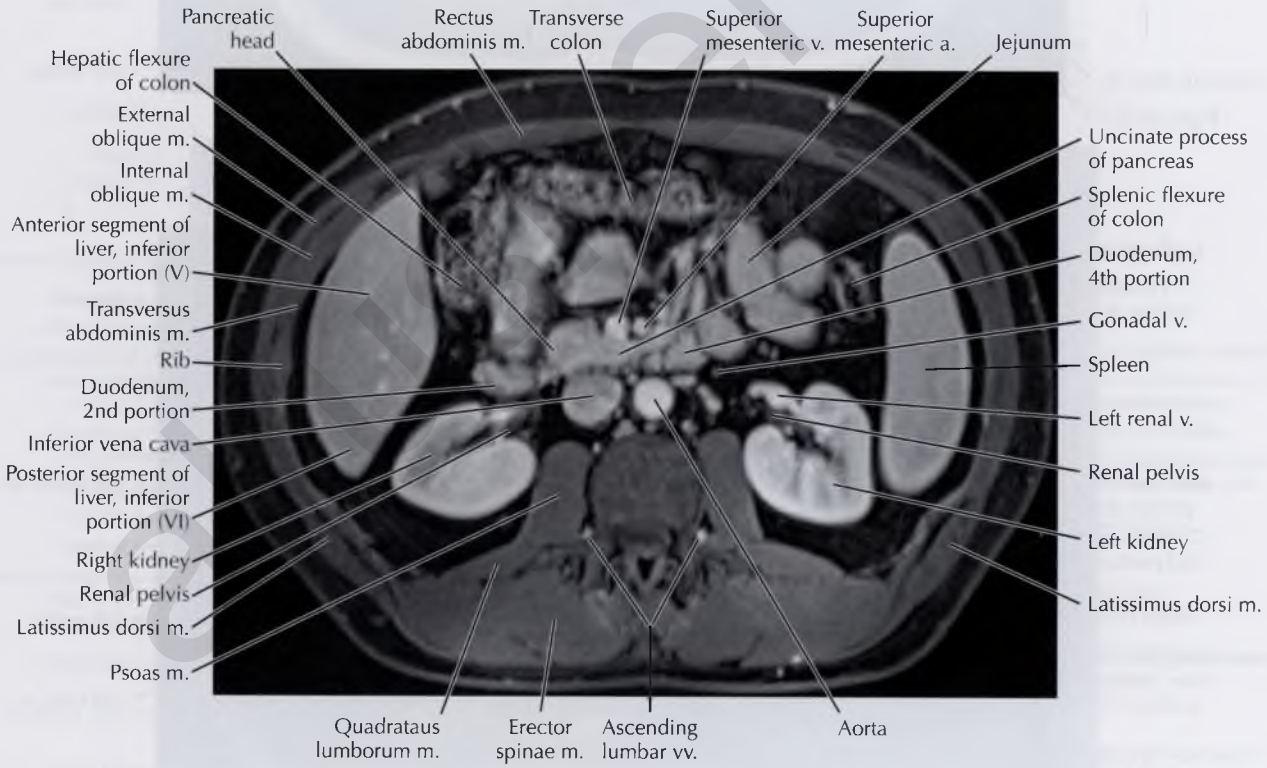

NORMAL ANATOMY

In the kidneys, the renal cortex demonstrates higher signal intensity compared with the renal medulla on T1-weighted MR images. On T2-weighted images, however, the renal medulla demonstrates higher signal intensity than the renal cortex because of higher fluid content.

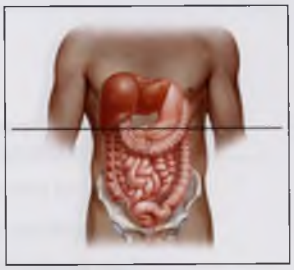

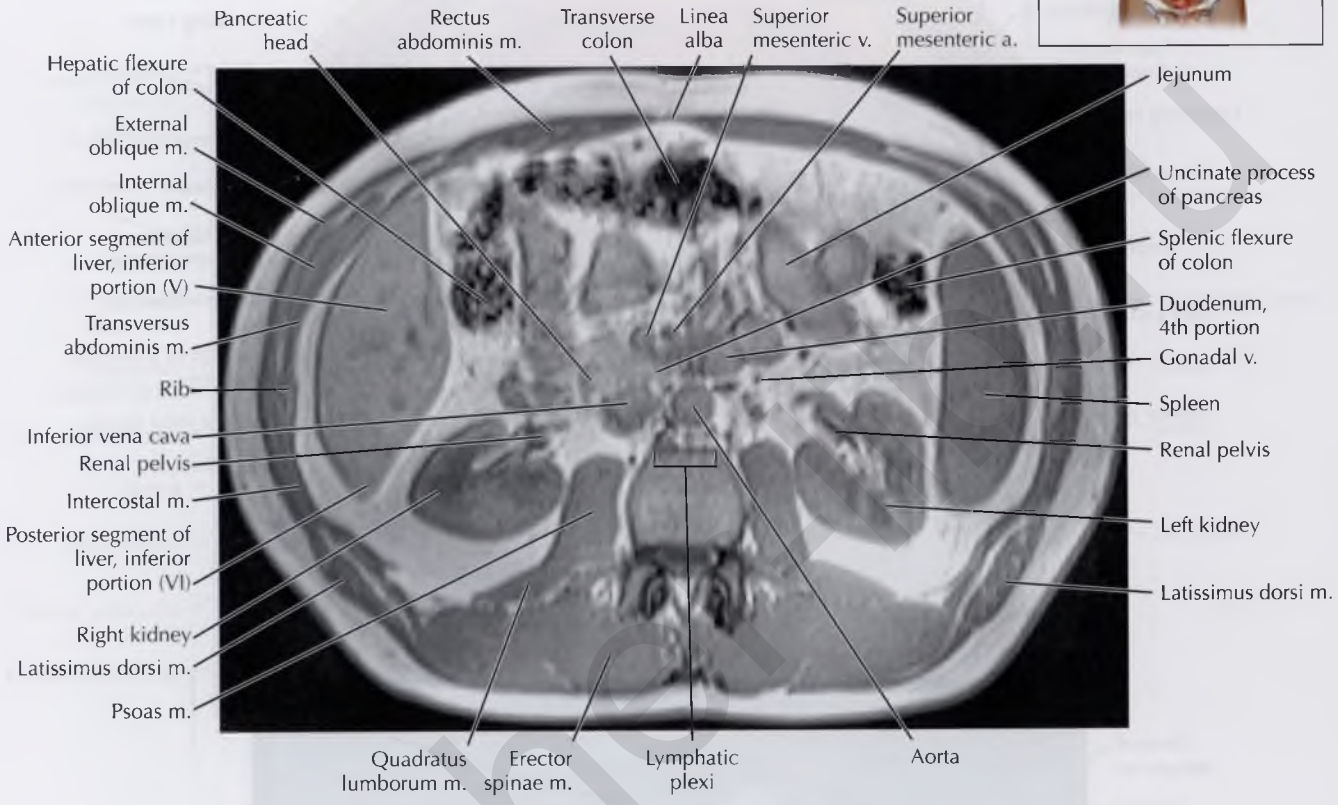
Pancreatic head
Rectus abdominis m.
Transverse colon
Linea alba
Superior mesenteric v.
Superior mesenteric a.
Hepatic flexure of colon
External oblique m.
Internal oblique m.
Anterior segment of liver, inferior portion (V)
Transversus abdominis m.
Rib
Inferior vena cava
Renal pelvis
Intercostal m.
Posterior segment of liver, inferior portion (VI)
Right kidney
Latissimus dorsi m.
Psoas m.
Jejunum
Uncinate process of pancreas
Splenic flexure of colon
Duodenum, 4th portion
Gonadal v.
Spleen
Renal pelvis
Left kidney
Latissimus dorsi m.
Quadratus lumborum m.
Erector spinae m.
Lymphatic plexi
Aorta

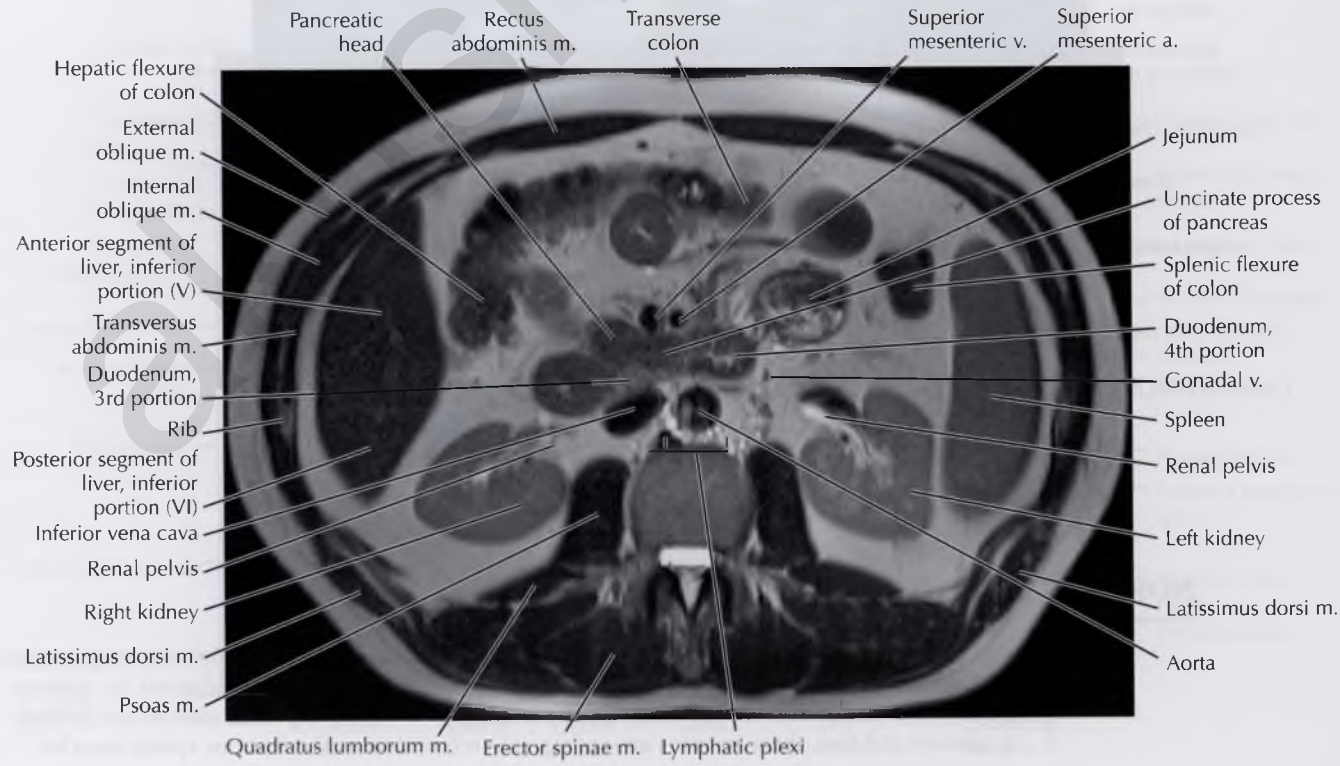
Pancreatic head
Rectus abdominis m.
Transverse colon
Superior mesenteric v.
Superior mesenteric a.
Hepatic flexure of colon
External oblique m.
Internal oblique m.
Anterior segment of liver, inferior portion (V)
Transversus abdominis m.
Duodenum, 3rd portion
Rib
Posterior segment of liver, inferior portion (VI)
Inferior vena cava
Renal pelvis
Right kidney
Latissimus dorsi m.
Psoas m.
Jejunum
Uncinate process of pancreas
Splenic flexure of colon
Duodenum, 4th portion
Gonadal v.
Spleen
Renal pelvis
Left kidney
Latissimus dorsi m.
Aorta
Quadratus lumborum m.
Erector spinae m.
Lymphatic plexi

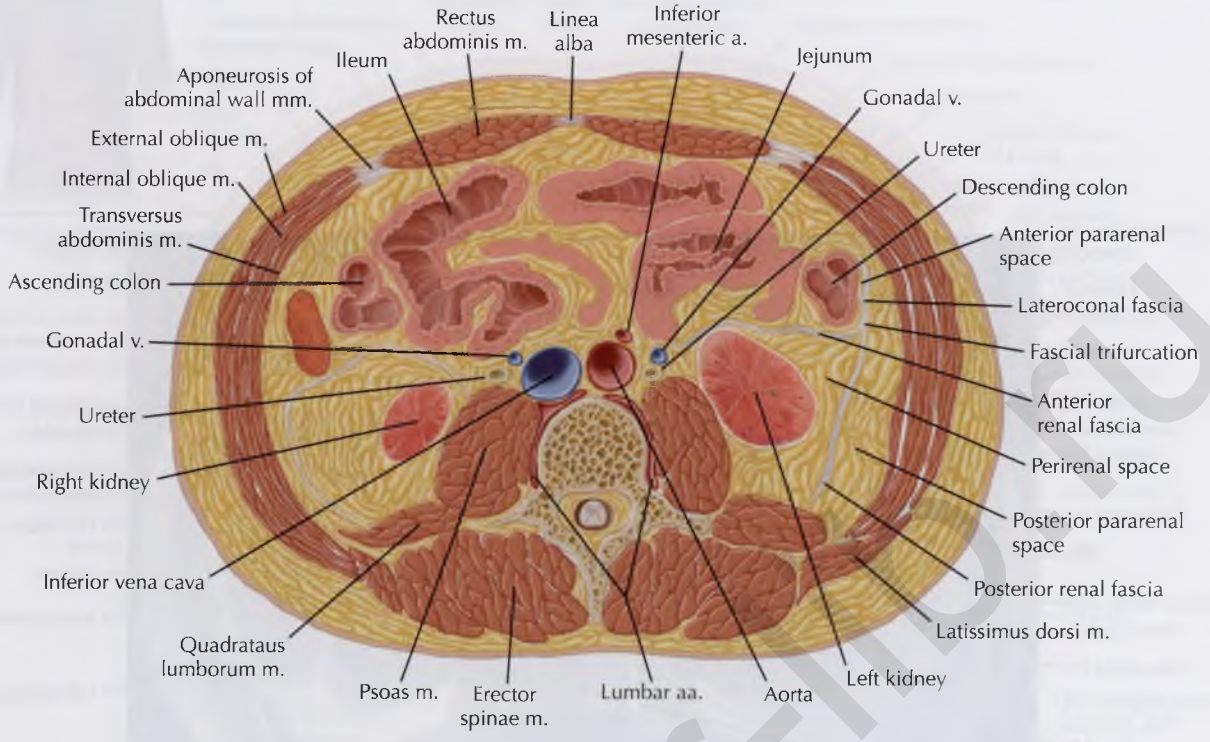

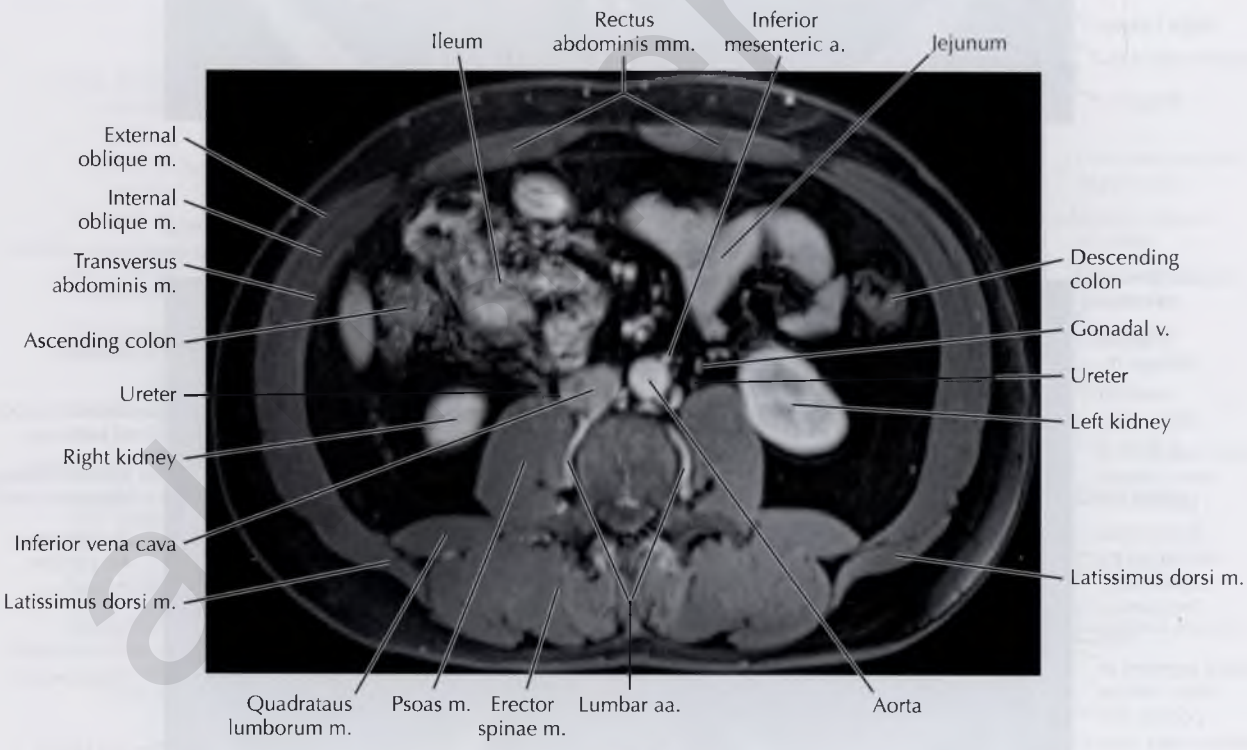

NORMAL ANATOMY

The erector spinae muscles are composed of the iliocostalis muscles (laterally), the longissimus muscles (intermediate in location), and the spinalis muscles (medially, adjacent to spinous processes of vertebrae). On MR imaging, the fascial planes separating these muscles are difficult to discern and thus these muscles are collectively referred to as the "erector spinae muscles."

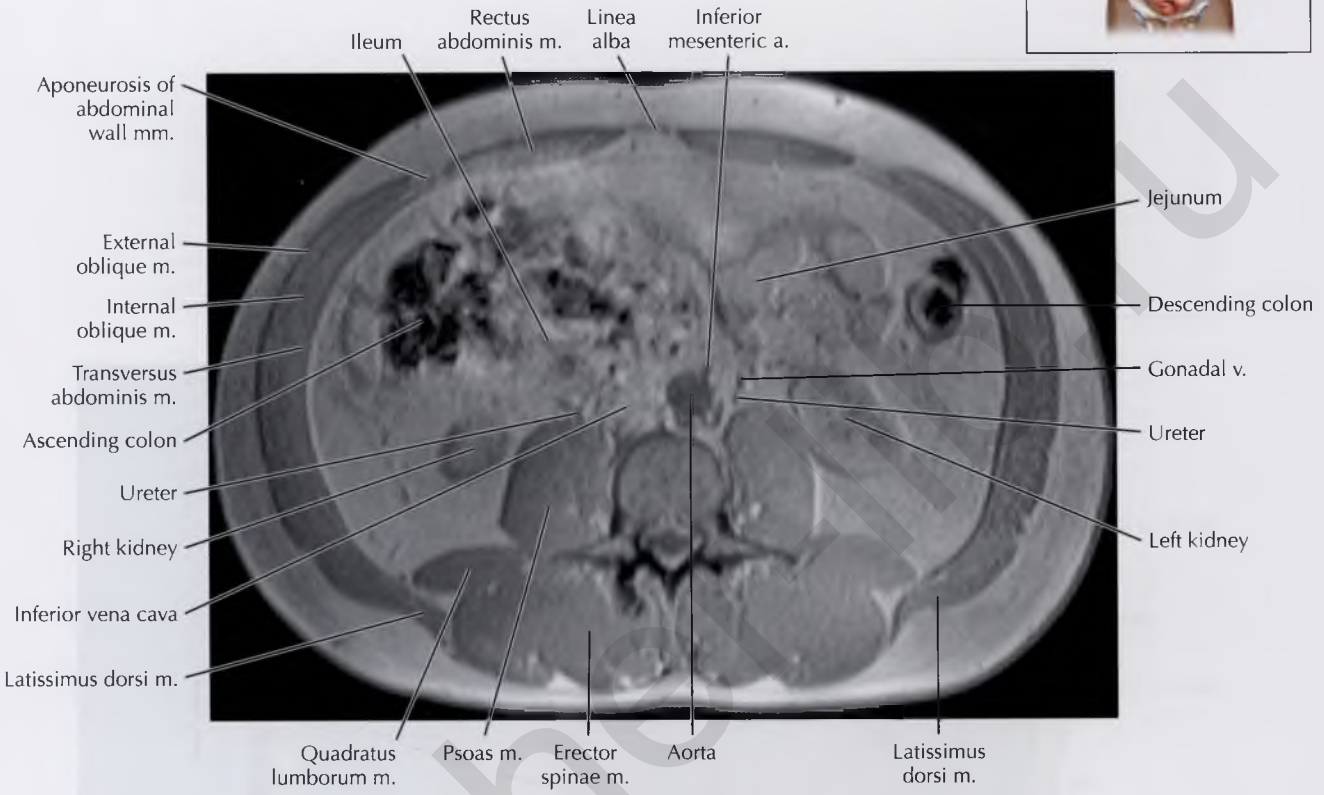
Ileum
Rectus abdominis m.
Linea alba
Inferior mesenteric a.
Aponeurosis of abdominal wall mm.
External oblique m.
Internal oblique m.
Transversus abdominis m.
Ascending colon
Ureter
Right kidney
Inferior vena cava
Latissimus dorsi m.
Jejunum
Descending colon
Gonadal v.
Ureter
Left kidney
Quadratus lumborum m.
Psoas m.
Erector spinae m.
Aorta
Latissimus dorsi m.

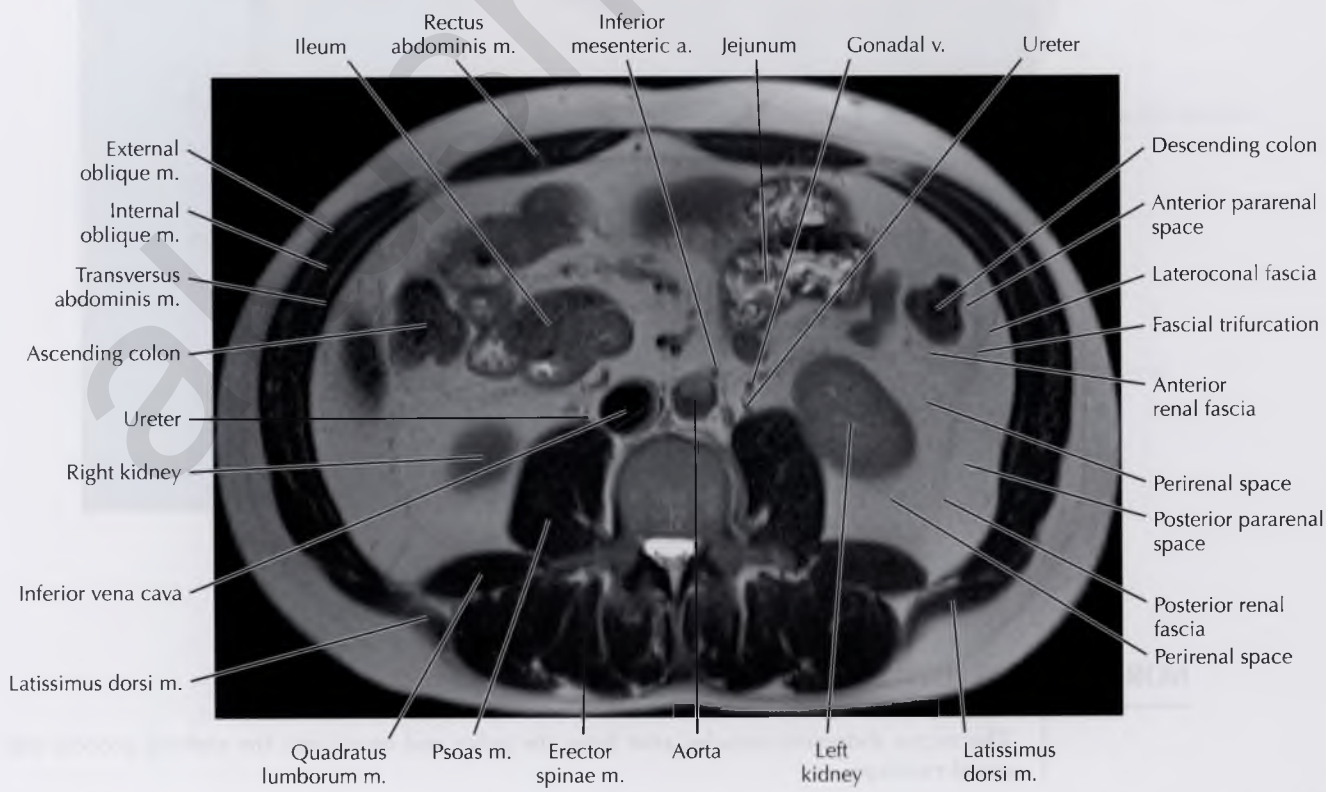
Ileum
Rectus abdominis m.
Inferior mesenteric a.
Jejunum
Gonadal v.
Ureter
External oblique m.
Internal oblique m.
Transversus abdominis m.
Ascending colon
Ureter
Right kidney
Inferior vena cava
Latissimus dorsi m.
Descending colon
Anterior pararenal space
Lateroconal fascia
Fascial trifurcation
Anterior renal fascia
Perirenal space
Posterior pararenal space
Posterior renal fascia
Perirenal space
Quadratus lumborum m.
Psoas m.
Erector spinae m.
Aorta
Left kidney
Latissimus dorsi m.

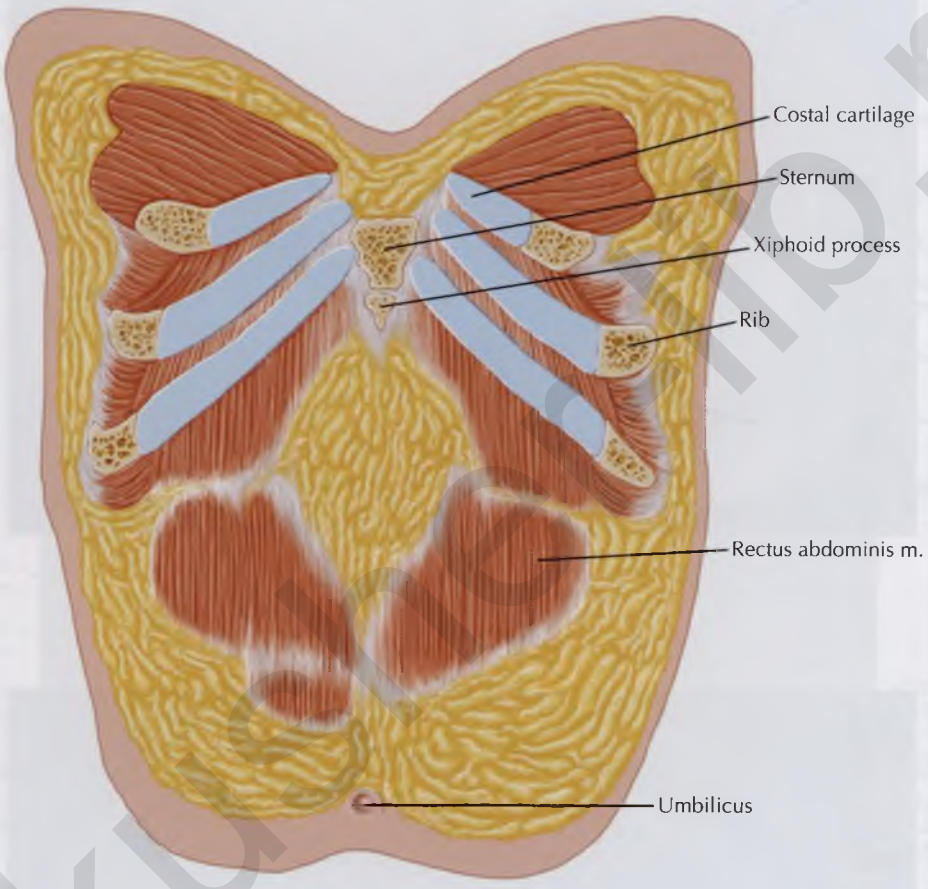

NORMAL ANATOMY

The rectus abdominis muscles arise from the pubis and insert into the xiphoid process and costal cartilages.

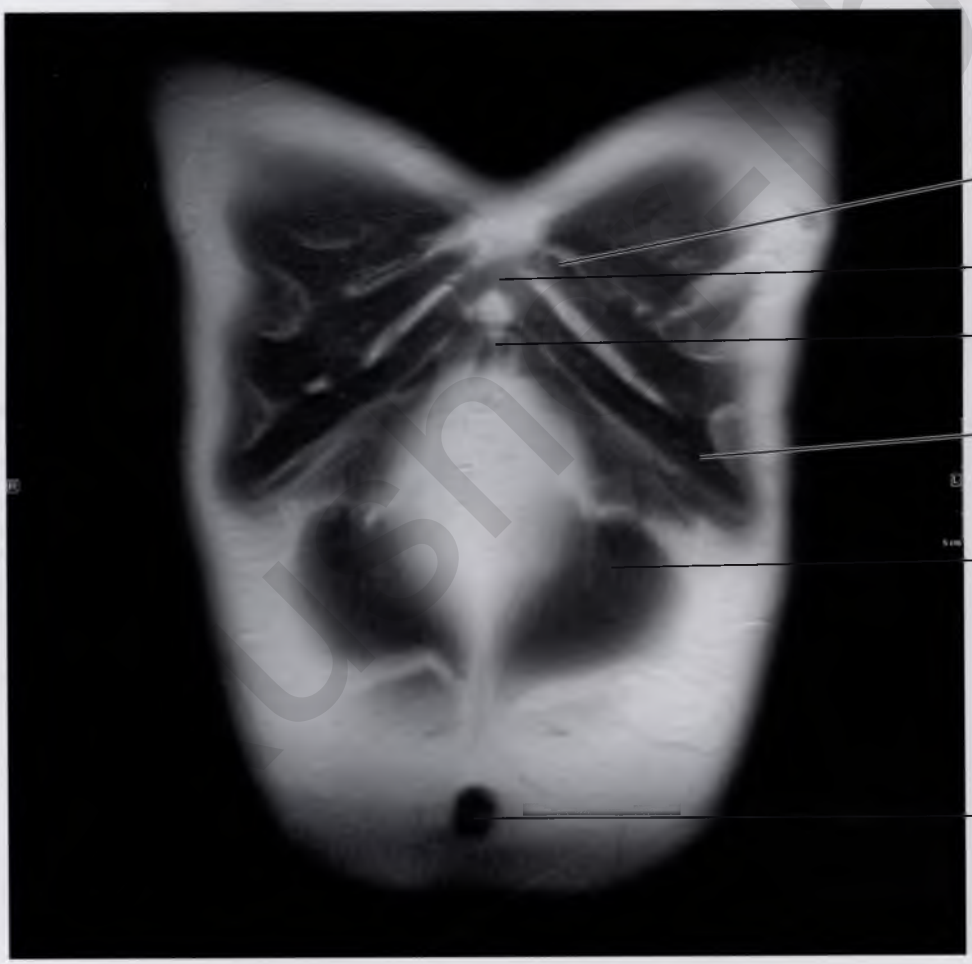
Costal cartilage
Sternum
Xiphoid process
Rib
Rectus abdominis m.
Umbilicus

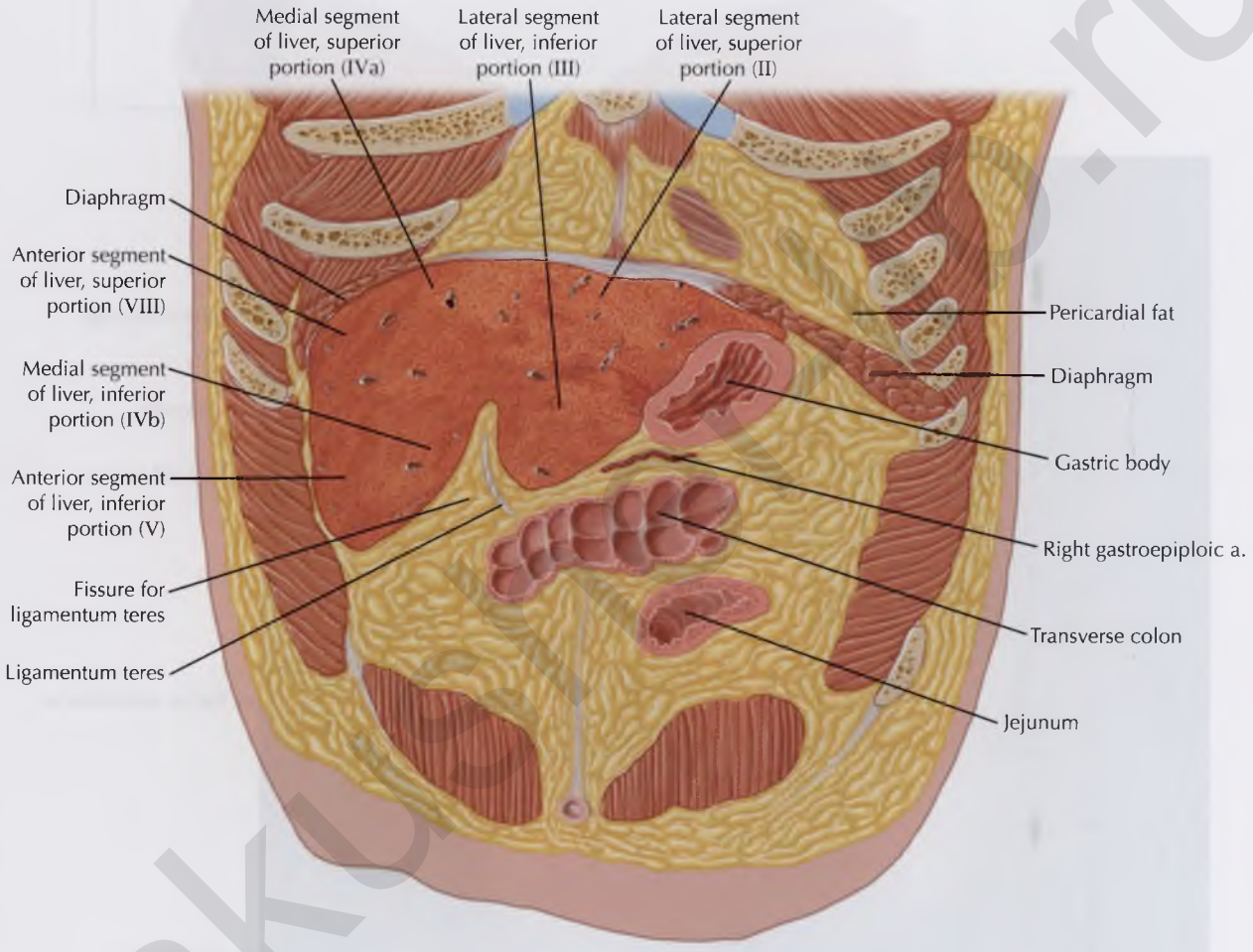
Medial segment of liver, superior portion (IVa)
Lateral segment of liver, inferior portion (III)
Lateral segment of liver, superior portion (II)
Diaphragm
Anterior segment of liver, superior portion (VIII)
Medial segment of liver, inferior portion (IVb)
Anterior segment of liver, inferior portion (V)
Fissure for ligamentum teres
Ligamentum teres
Pericardial fat
Diaphragm
Gastric body
Right gastroepiploic a.
Transverse colon
Jejunum


Medial segment of liver, superior portion (IVa)
Lateral segment of liver, inferior portion (III)
Lateral segment of liver, superior portion (II)
Diaphragm
Anterior segment of liver, superior portion (VIII)
Medial segment of liver, inferior portion (IVb)
Anterior segment of liver, inferior portion (V)
Fissure for ligamentum teres
Ligamentum teres
Pericardial fat
Diaphragm
Gastric body
Right gastroepiploic a.
Transverse colon
Jejunum

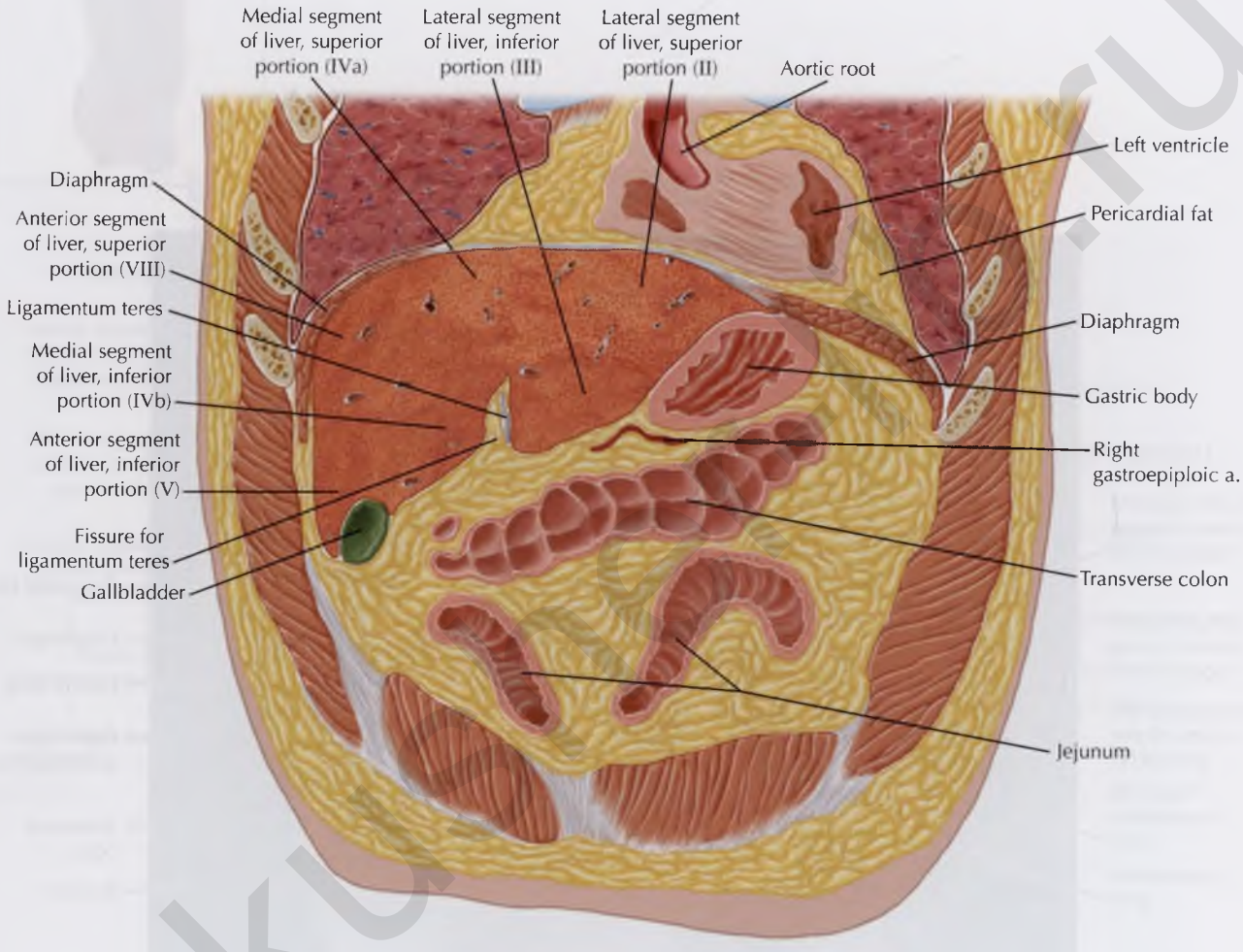

NORMAL ANATOMY

The normal thickness of the gastric wall varies greatly with distention. The gastric wall appears paper thin with effacement of the rugal folds when well distended, and up to several centimeters in thickness when collapsed.

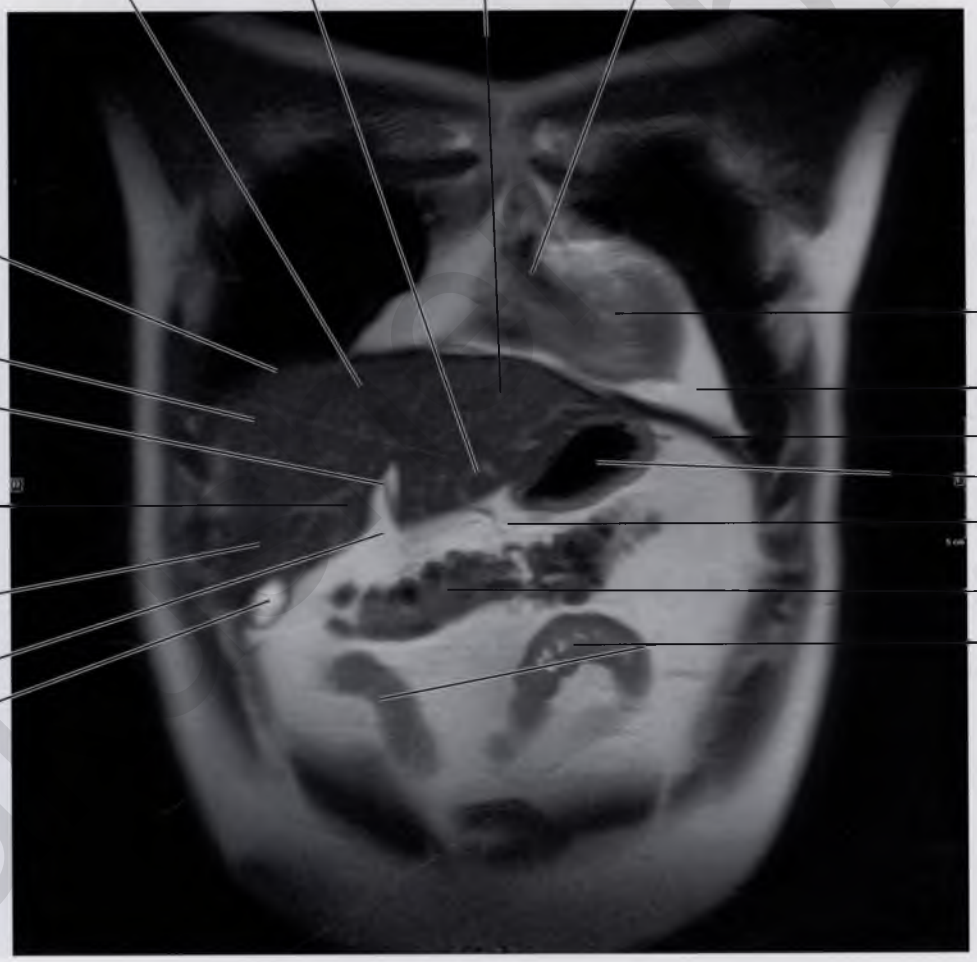
Medial segment of liver, superior portion (IVa)
Lateral segment of liver, inferior portion (III)
Lateral segment of liver, superior portion (II)
Aortic root
Diaphragm
Anterior segment of liver, superior portion (VIII)
Ligamentum teres
Medial segment of liver, inferior portion (IVb)
Anterior segment of liver, inferior portion (V)
Fissure for ligamentum teres
Gallbladder
Left ventricle
Pericardial fat
Diaphragm
Gastric body
Right gastro-epiploic a.
Transverse colon
Jejunum

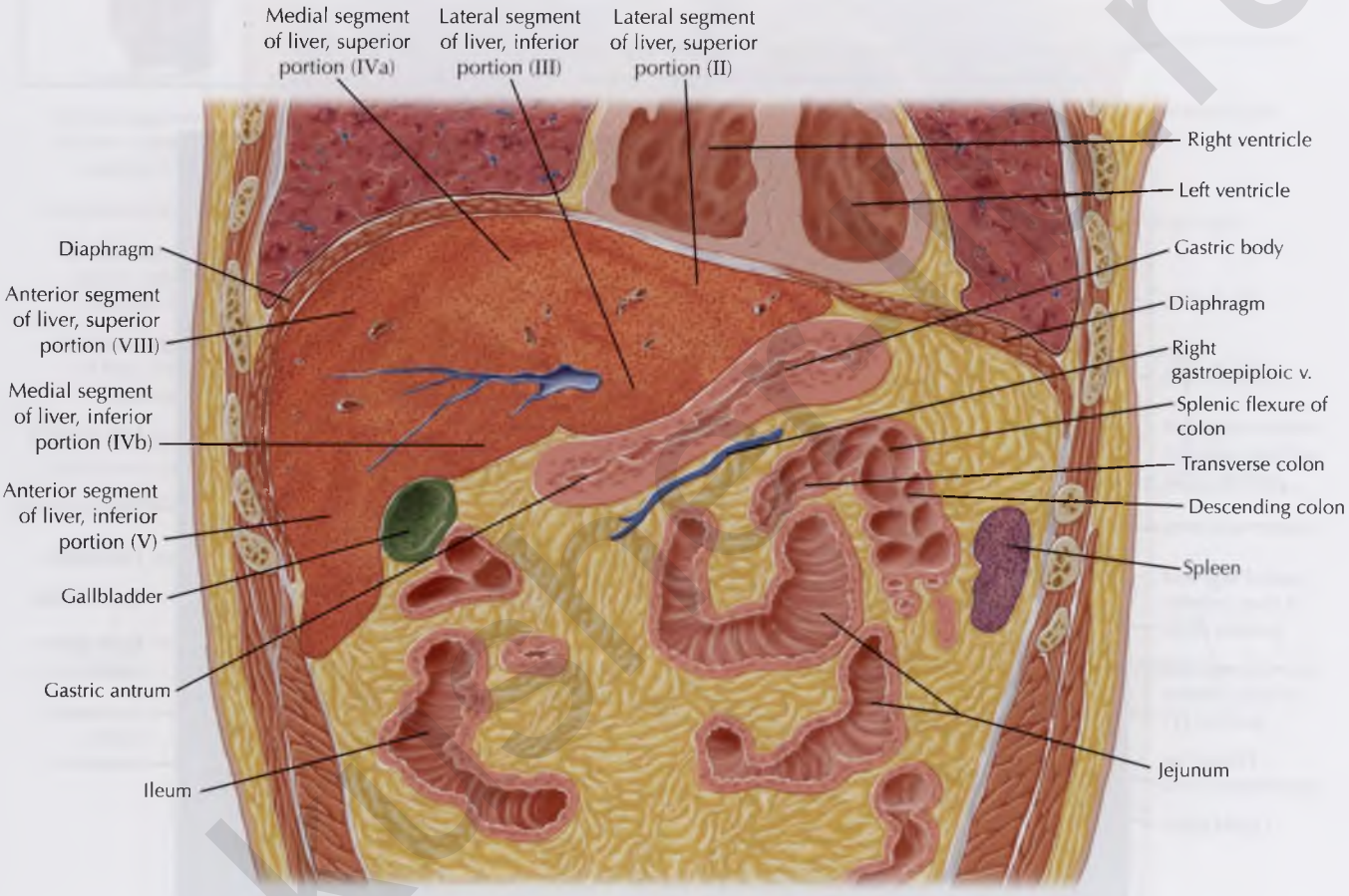
Medial segment of liver, superior portion (IVa)
Lateral segment of liver, inferior portion (III)
Lateral segment of liver, superior portion (II)
Right ventricle
Left ventricle
Diaphragm
Gastric body
Anterior segment of liver, superior portion (VIII)
Diaphragm
Right gastroepiploic v.
Medial segment of liver, inferior portion (IVb)
Splenic flexure of colon
Transverse colon
Anterior segment of liver, inferior portion (V)
Descending colon
Gallbladder
Spleen
Gastric antrum
Jejunum
Ileum

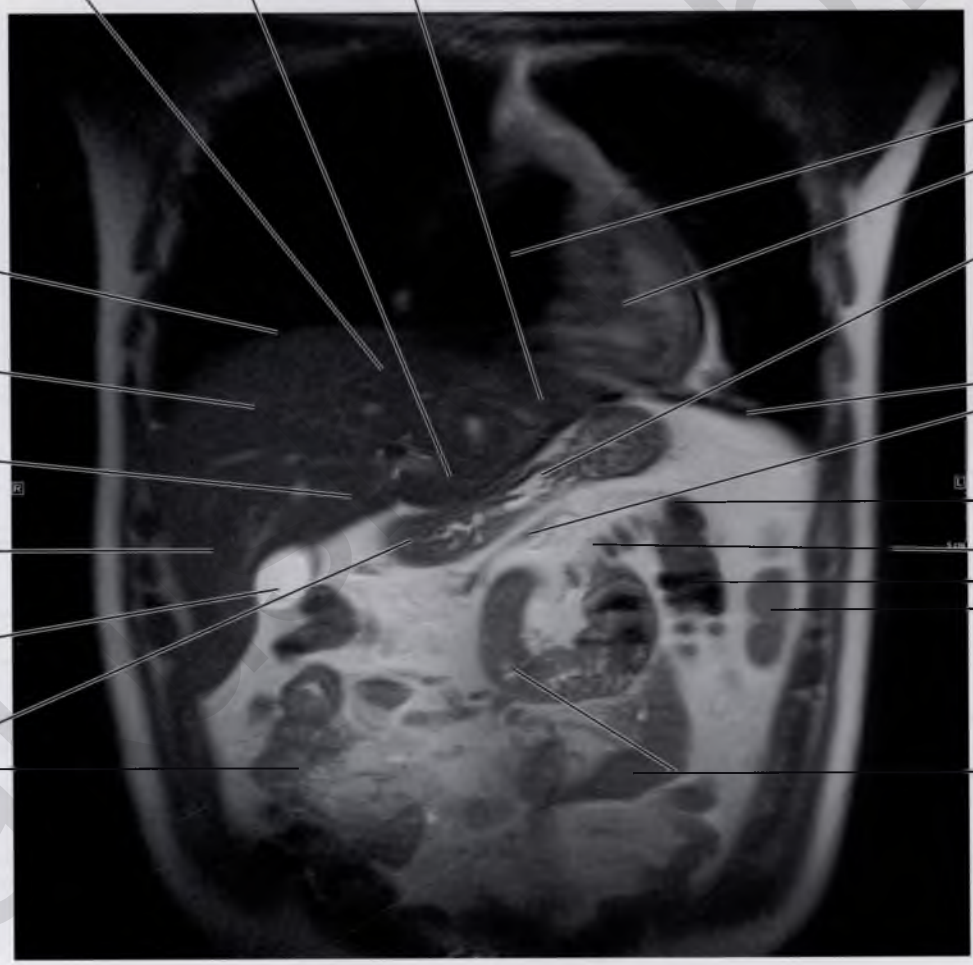
Medial segment of liver, superior portion (IVa)
Lateral segment of liver, inferior portion (III)
Lateral segment of liver, superior portion (II)
Right ventricle
Left ventricle
Gastric body
Diaphragm
Anterior segment of liver, superior portion (VIII)
Medial segment of liver, inferior portion (IVb)
Anterior segment of liver, inferior portion (V)
Gallbladder
Gastric antrum
Ileum
Diaphragm
Right gastroepiploic v.
Splenic flexure of colon
Transverse colon
Descending colon
Spleen
Jejunum

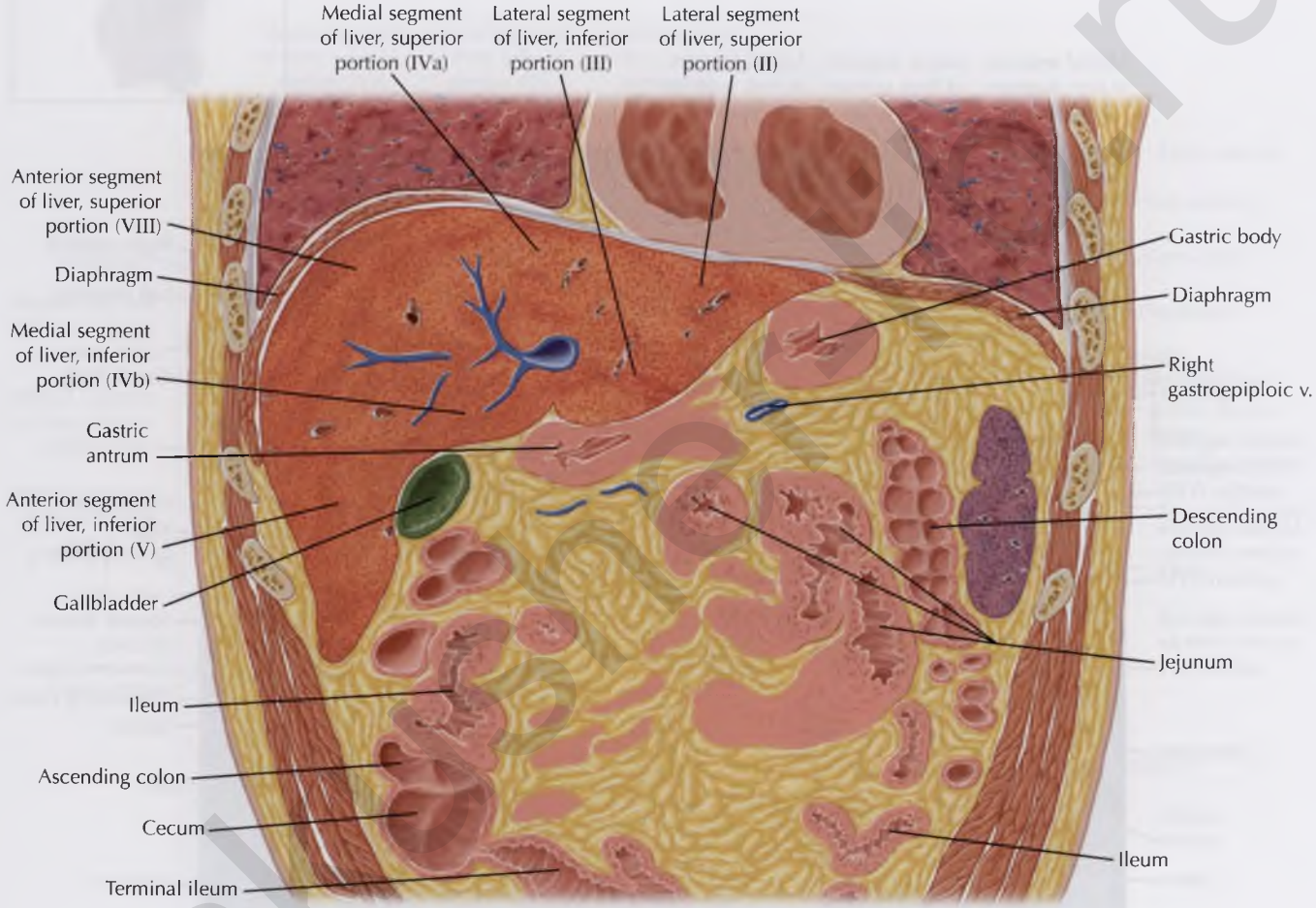
Medial segment of liver, superior portion (IVa)
Lateral segment of liver, inferior portion (III)
Lateral segment of liver, superior portion (II)
Anterior segment of liver, superior portion (VIII)
Diaphragm
Medial segment of liver, inferior portion (IVb)
Gastric antrum
Anterior segment of liver, inferior portion (V)
Gallbladder
Ileum
Ascending colon
Cecum
Terminal ileum
Gastric body
Diaphragm
Right gastroepiploic v.
Descending colon
Jejunum
Ileum

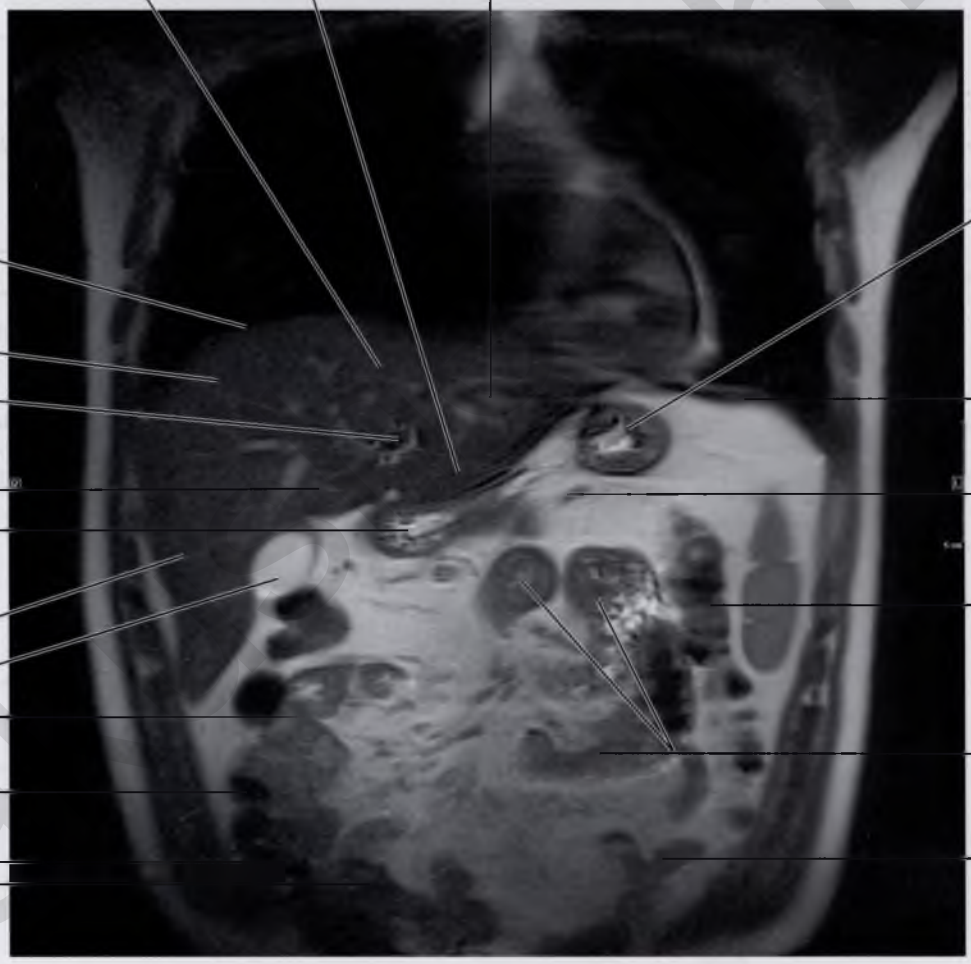
Medial segment of liver, superior portion (IVa)
Lateral segment of liver, inferior portion (III)
Lateral segment of liver, superior portion (II)
Diaphragm
Anterior segment of liver, superior portion (VIII)
Left portal vein
Medial segment of liver, inferior portion (IVb)
Gastric antrum
Anterior segment of liver, inferior portion (V)
Gallbladder
Ileum
Ascending colon
Cecum
Terminal ileum
Gastric body
Diaphragm
Right gastroepiploic v.
Descending colon
Jejunum
Ileum

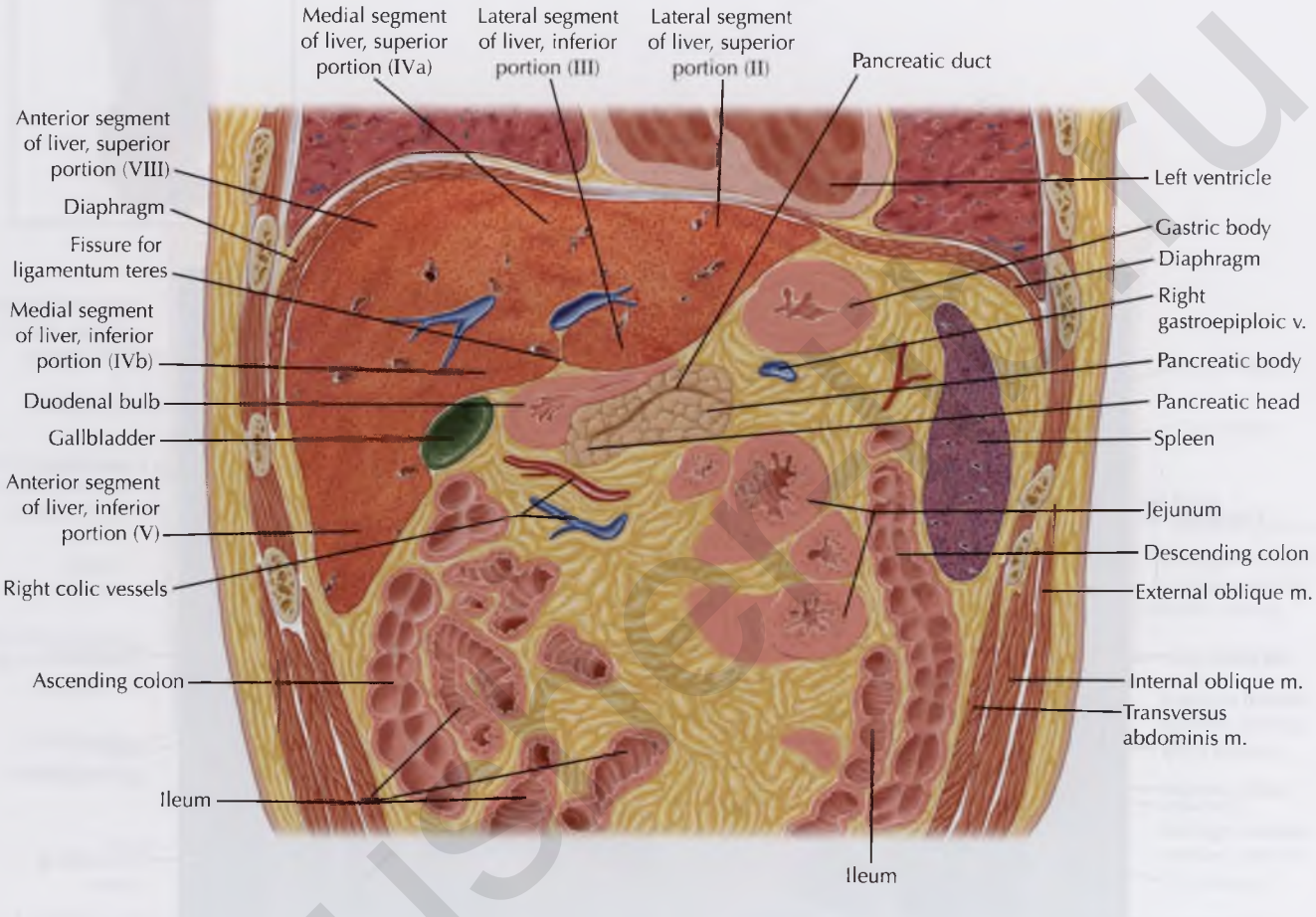

NORMAL ANATOMY

The gradual change in morphology between the jejunum and the ileum makes a precise demarcation arbitrary, although each small-bowel segment has general characteristic features. The *jejunum* is predominantly located in the left upper quadrant of the abdomen, measures up to 3.5 cm in caliber and 2 mm in wall thickness, and has four to seven folds per inch, with the height of the folds measuring 3 to 7 mm, resulting in a feathery appearance. The *ileum* is predominantly located in the right lower quadrant of the abdomen, measures up to 2.5 cm in caliber and 1 mm in wall thickness, and has less pronounced folds, with two to five folds per inch at 1.5 to 3.5 mm high.

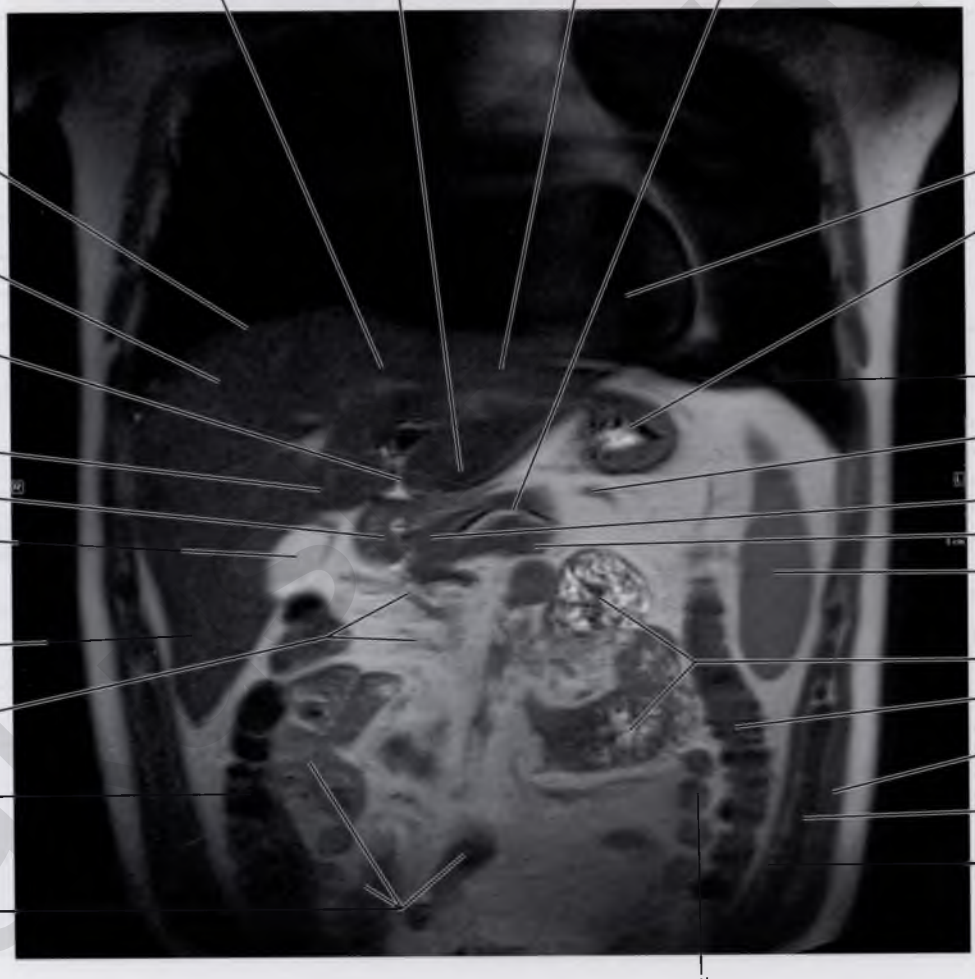
Medial segment of liver, superior portion (IVa)
Lateral segment of liver, inferior portion (III)
Lateral segment of liver, superior portion (II)
Pancreatic duct
Diaphragm
Anterior segment of liver, superior portion (VIII)
Fissure for ligamentum teres
Medial segment of liver, inferior portion (IVb)
Duodenal bulb
Gallbladder
Anterior segment of liver, inferior portion (V)
Right colic vessels
Ascending colon
Ileum
Left ventricle
Gastric body
Diaphragm
Right gastro-epiploic v.
Pancreatic head
Pancreatic body
Spleen
Jejunum
Descending colon
External oblique m.
Internal oblique m.
Transversus abdominis m.
Ileum

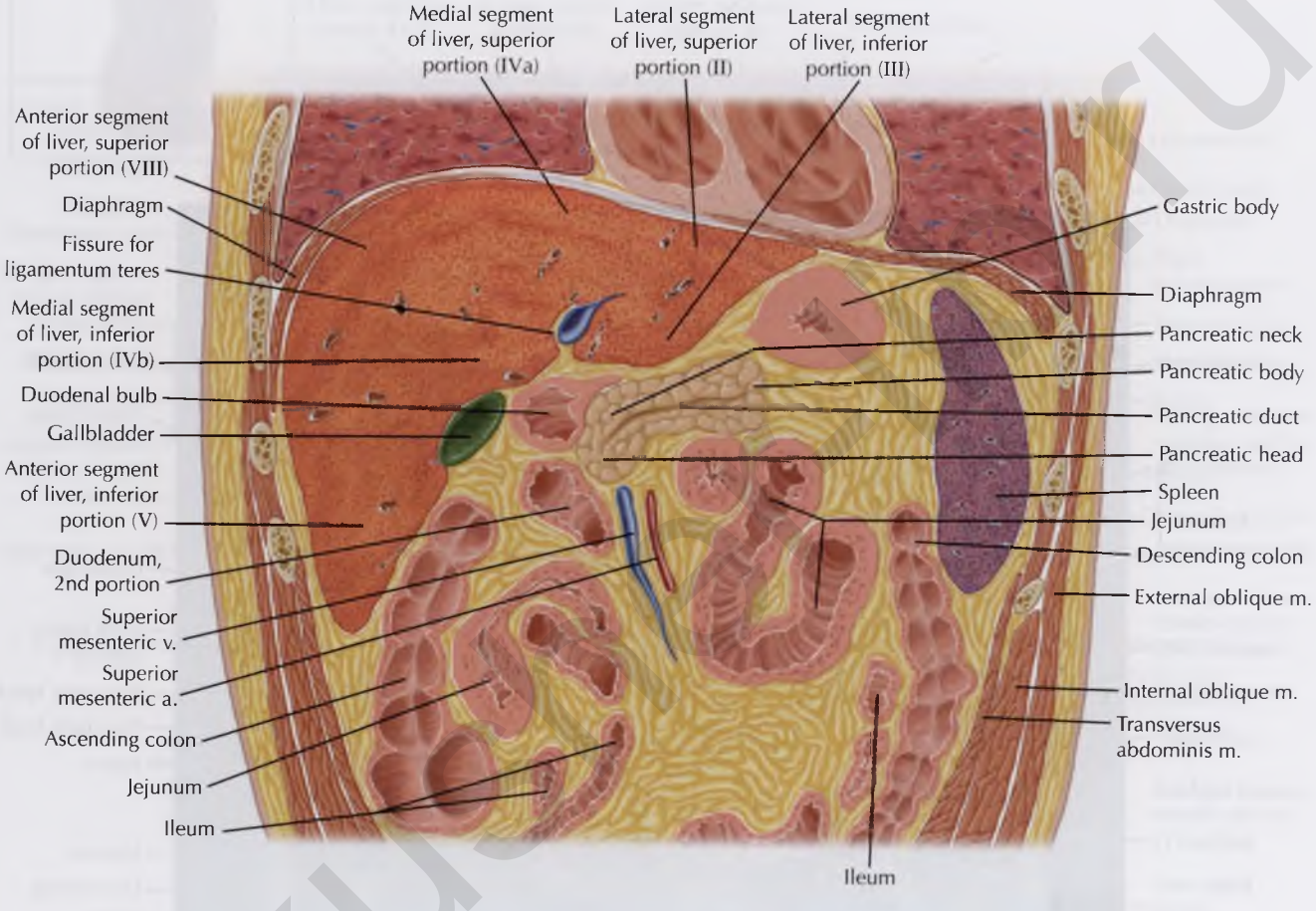

NORMAL VARIANTS

Splenic clefts are common anatomic variants that represent remnants of the grooves that originally separated the fetal lobules. Clefts are typically seen on the superior border of the spleen, are often partial, and can be as deep as 2 to 3 cm (about 1 inch). The characteristic location, a smooth contour, and the lack of associated perisplenic fluid or hemorrhage should help to distinguish a splenic cleft from a splenic laceration in the patient with abdominal trauma.

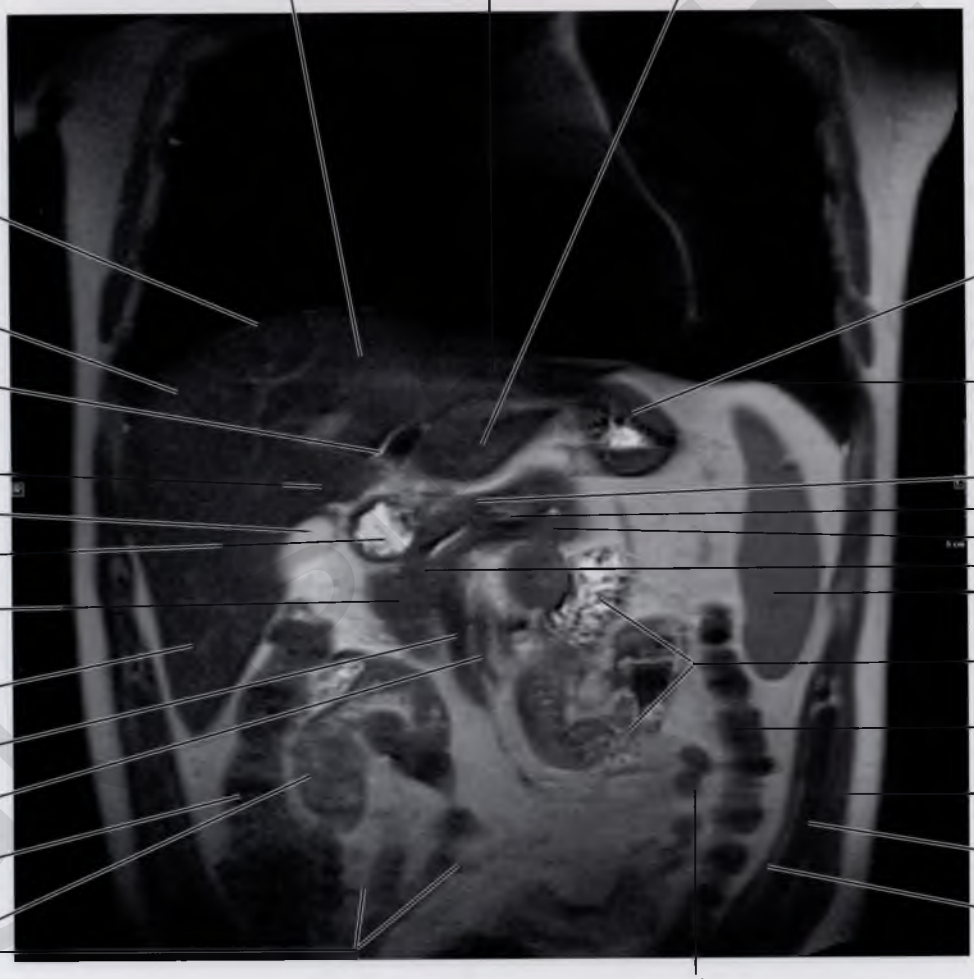
Medial segment of liver, superior portion (IVa)
Lateral segment of liver, superior portion (II)
Lateral segment of liver, inferior portion (III)
Diaphragm
Anterior segment of liver, superior portion (VIII)
Fissure for ligamentum teres
Medial segment of liver, inferior portion (IVb)
Gallbladder
Duodenal bulb
Duodenum, 2nd portion
Anterior segment of liver, inferior portion (V)
Superior mesenteric v.
Superior mesenteric a.
Ascending colon
Jejunum
Ileum
Gastric body
Diaphragm
Pancreatic neck
Pancreatic duct
Pancreatic body
Pancreatic head
Spleen
Jejunum
Descending colon
External oblique m.
Internal oblique m.
Transversus abdominis m.
Ileum

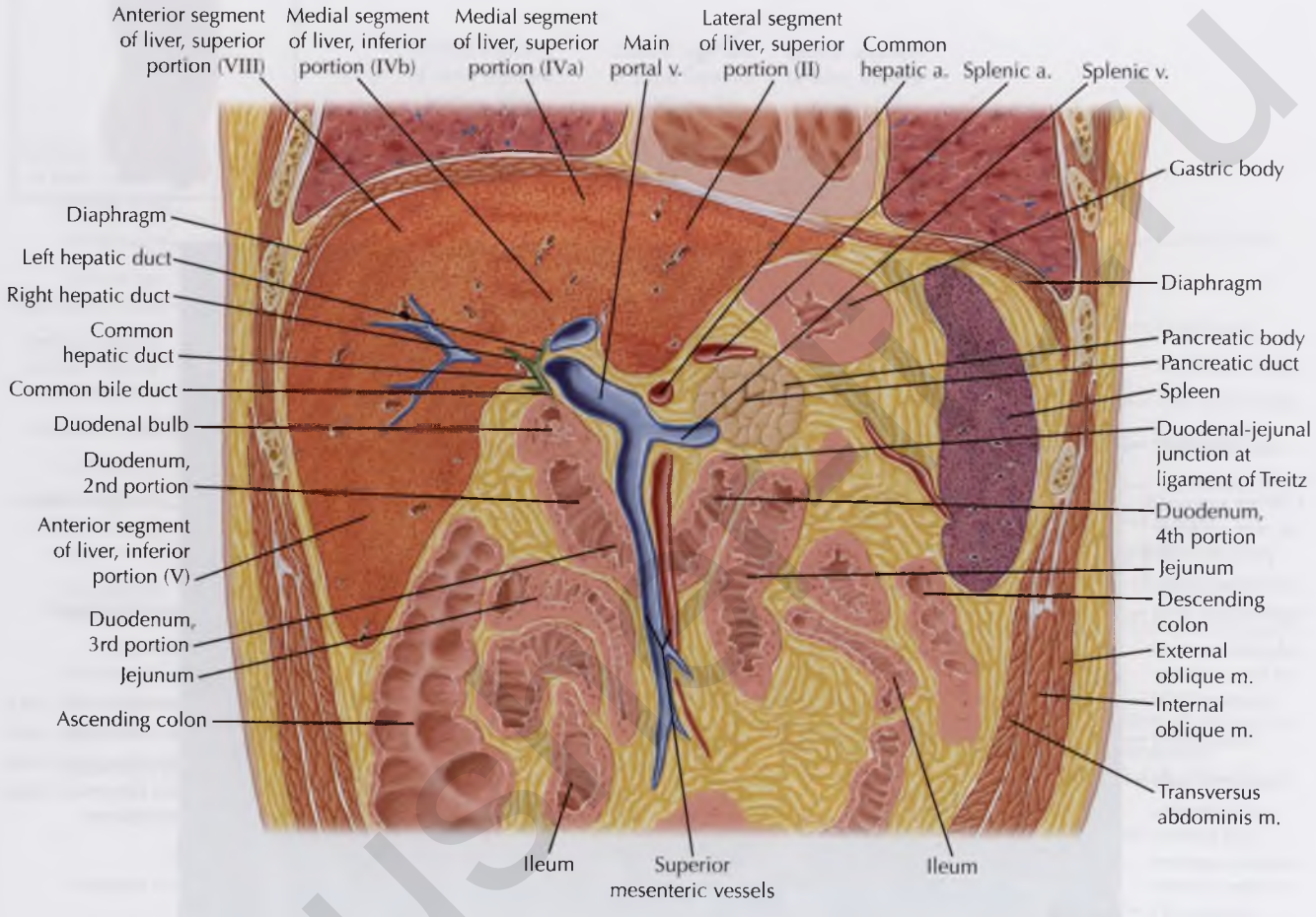

DIAGNOSTIC CONSIDERATION

Always assess the position of the duodenal-jejunal junction (at the ligament of Treitz) to make sure it is in the correct anatomic position in the left upper quadrant of the abdomen. Findings of right-sided small bowel, left-sided colon, abnormal relationship of the superior mesenteric vessels, and aplasia of the uncinate process of the pancreas are typically seen with malrotation or nonrotation of the bowel. Failure of the bowel to undergo normal embryologic rotation and fixation results in malpositioning of the bowel and a narrow base of mesenteric fixation, which is prone to *midgut volvulus*, a life-threatening disorder.


Medial segment of liver, inferior portion (IVb)
Medial segment of liver, superior portion (IVa)
Lateral segment of liver, superior portion (II)
Common hepatic a.
Splenic a.
Gastric body
Diaphragm
Anterior segment of liver, superior portion (VIII)
Left hepatic duct
Right hepatic duct
Common hepatic duct
Common bile duct
Anterior segment of liver, inferior portion (V)
Duodenal bulb
Duodenum, 2nd portion
Duodenum, 4th portion
Duodenum, 3rd portion
Jejunum
Ascending colon
Diaphragm
Pancreatic body
Pancreatic duct
Spleen
Duodenal-jejunal junction at ligament of Treitz
Jejunum
Descending colon
External oblique m.
Internal oblique m.
Transversus abdominis m.
Ileum
Superior mesenteric vessels
Ileum

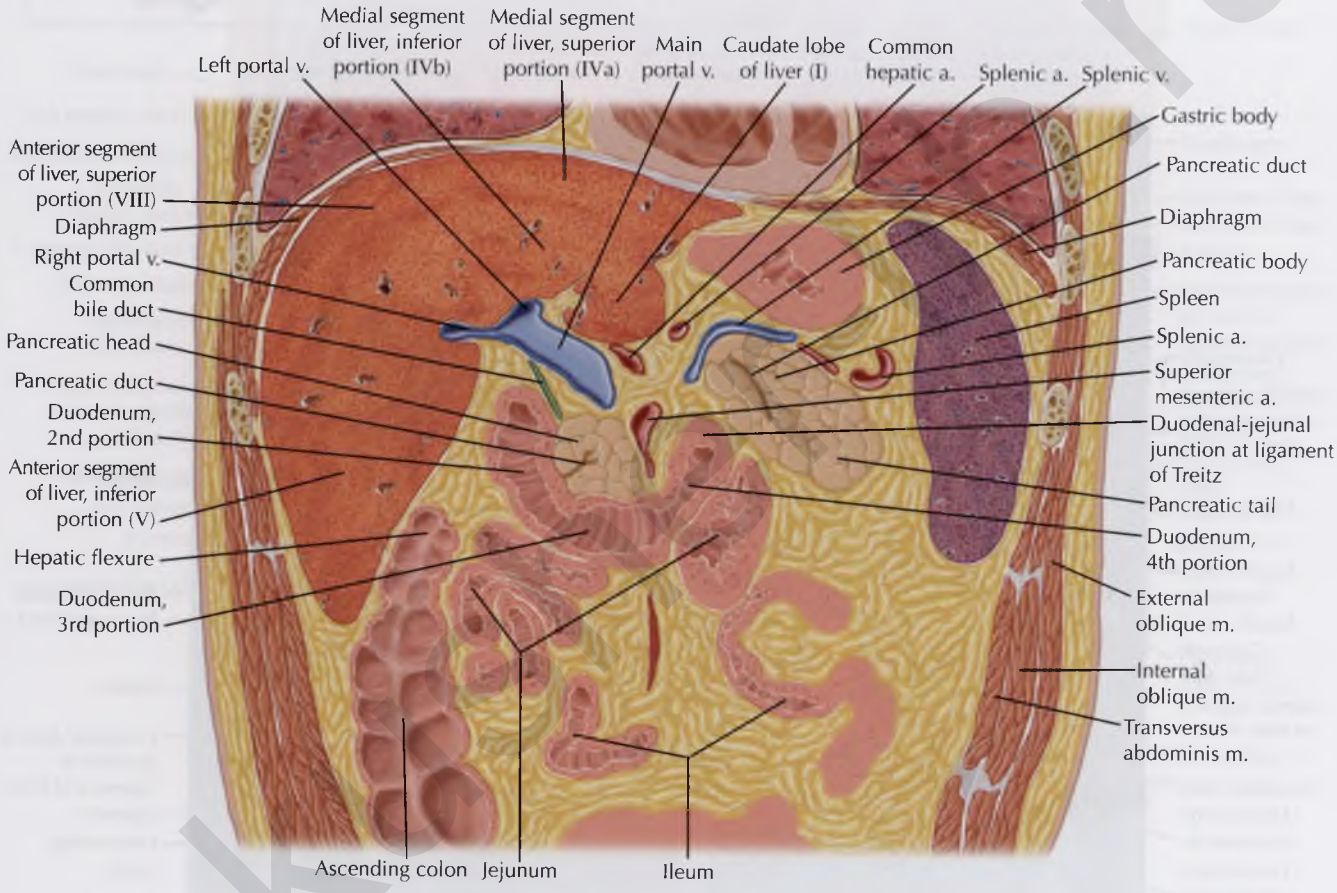
Left portal v.
Medial segment of liver, inferior portion (IVb)
Medial segment of liver, superior portion (IVa)
Main portal v.
Caudate lobe of liver (I)
Common hepatic a.
Splenic a.
Splenic v.
Gastric body
Pancreatic duct
Diaphragm
Pancreatic body
Spleen
Splenic a.
Superior mesenteric a.
Duodenal-jejunal junction at ligament of Treitz
Pancreatic tail
Duodenum, 4th portion
External oblique m.
Internal oblique m.
Transversus abdominis m.
Anterior segment of liver, superior portion (VIII)
Diaphragm
Right portal v.
Common bile duct
Pancreatic head
Pancreatic duct
Duodenum, 2nd portion
Anterior segment of liver, inferior portion (V)
Hepatic flexure
Duodenum, 3rd portion
Ascending colon
Jejunum
Ileum


Medial segment of liver, superior portion (IVa)
Caudate lobe of liver (I)
Common hepatic a.
Splenic a.
Splenic v.
Gastric body
Diaphragm
Anterior segment of liver, superior portion (VIII)
Medial segment of liver, inferior portion (IVb)
Left portal v.
Right portal v.
Main portal v.
Common bile duct
Anterior segment of liver, inferior portion (V)
Pancreatic head
Superior mesenteric a.
Duodenum, 2nd portion
Pancreatic duct
Hepatic flexure of colon
Duodenum, 3rd portion
Diaphragm
Spleen
Pancreatic duct
Pancreatic body
Pancreatic tail
Duodenal-jejunal junction at ligament of Treitz
Duodenum, 4th portion
External oblique m.
Internal oblique m.
Transversus abdominis m.
Ascending colon
Jejunum
Ileum

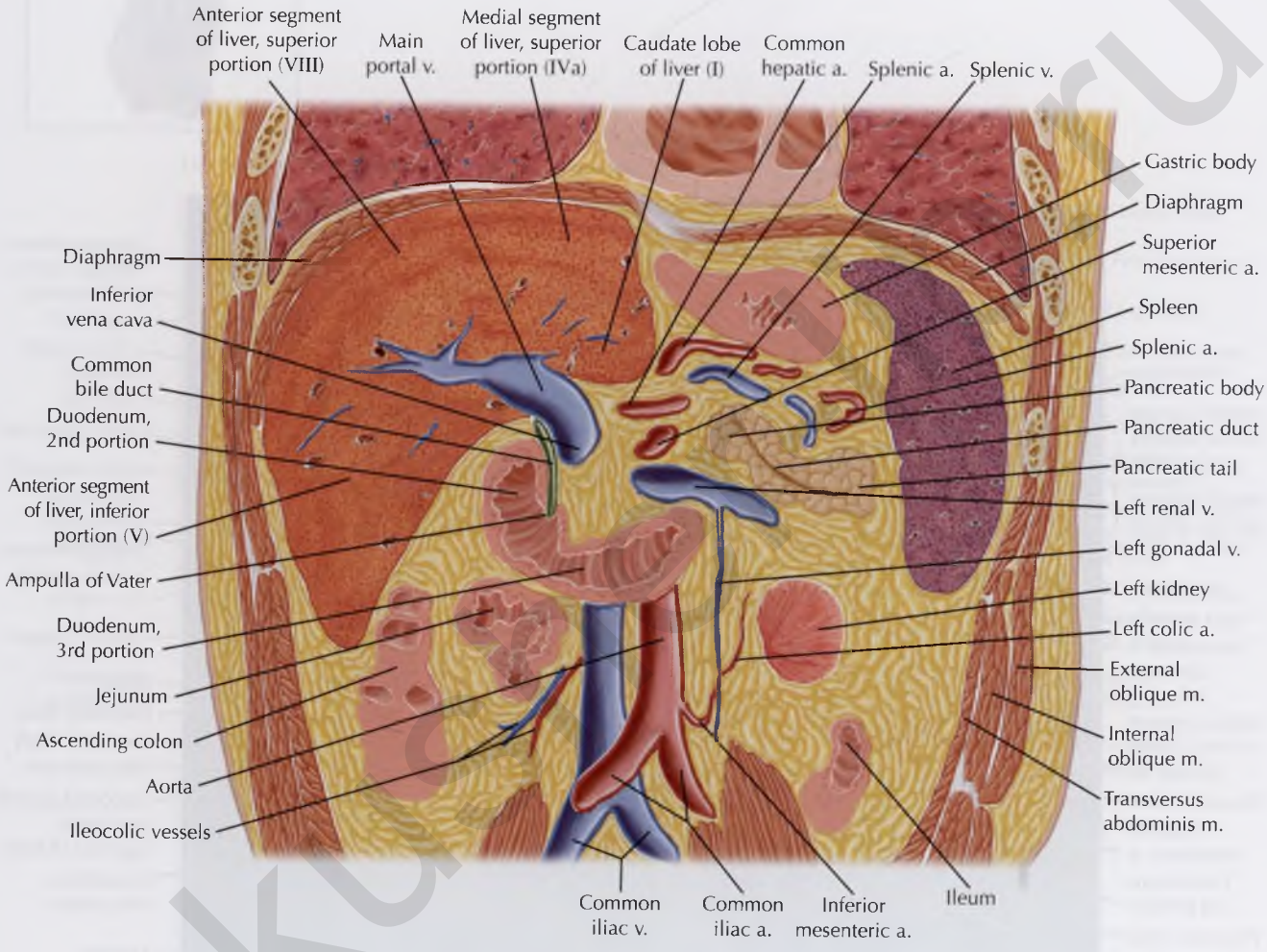

NORMAL ANATOMY

The spleen typically measures 9 to 12 cm (~4 inches) in cranial-caudal dimension in normal adults, with normal splenic size varying positively with an individual's height.


Anterior segment of liver, superior portion (VIII)
Main portal v.
Medial segment of liver, superior portion (IVa)
Caudate lobe of liver (I)
Common hepatic a.
Splenic a.
Splenic v.
Gastric body
Diaphragm
Diaphragm
Common bile duct
Superior mesenteric a.
Spleen
Anterior segment of liver, inferior portion (V)
Splenic a.
Spleen
Pancreatic body
Duodenum, 2nd portion
Pancreatic tail
Pancreatic duct
Ampulla of Vater
Left renal v.
Duodenum, 3rd portion
Left gonadal v.
Left kidney
Jejunum
Left colic a.
Ileocolic vessels
External oblique m.
Ascending colon
Internal oblique m.
Inferior vena cava
Transversus abdominis m.
Aorta
Common iliac vv.
Common iliac aa.
Inferior mesenteric a.
Ileum

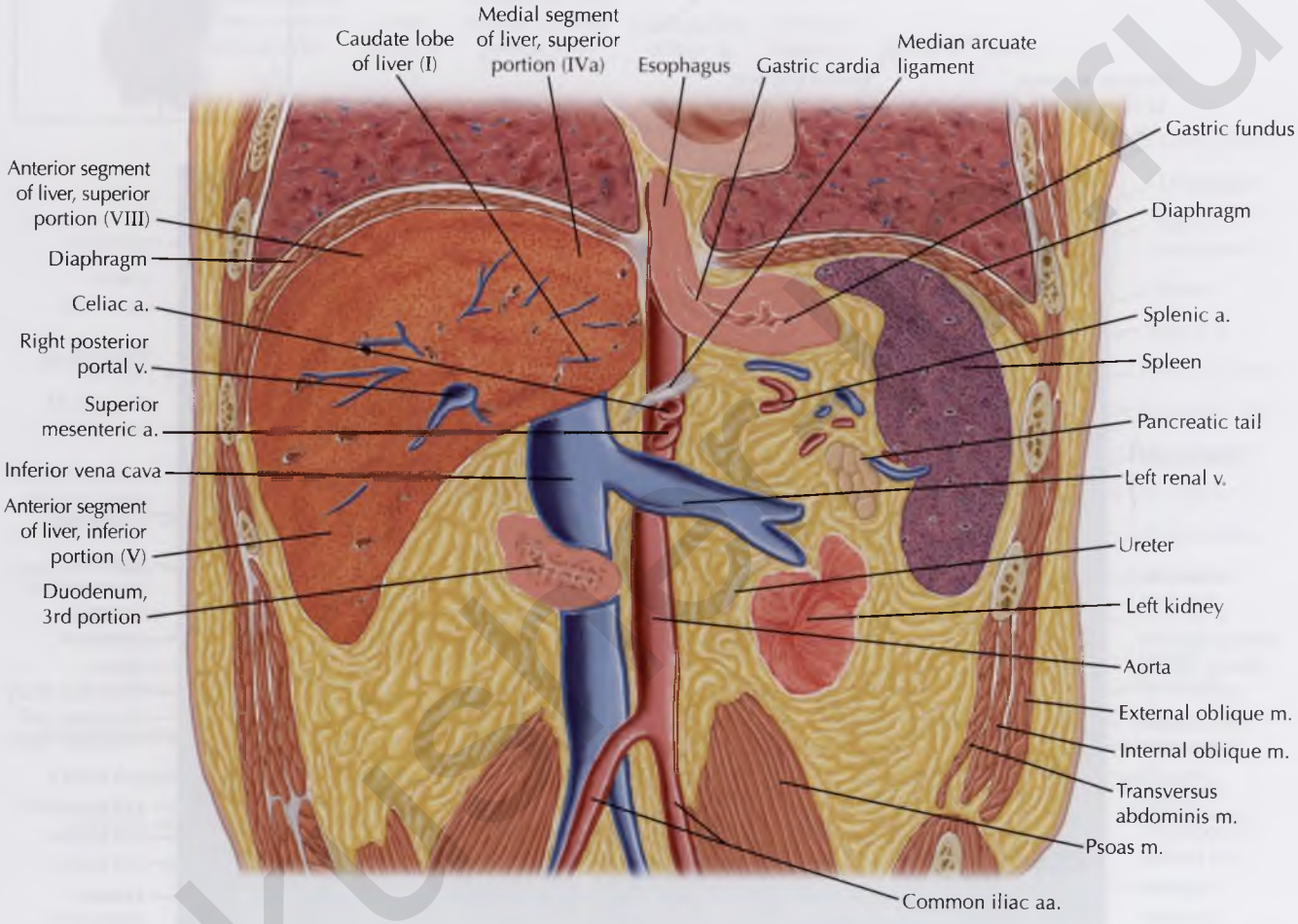

NORMAL ANATOMY

The median arcuate ligament, at the junction of the diaphragmatic crura, is best seen just above the celiac axis on coronal MR images.

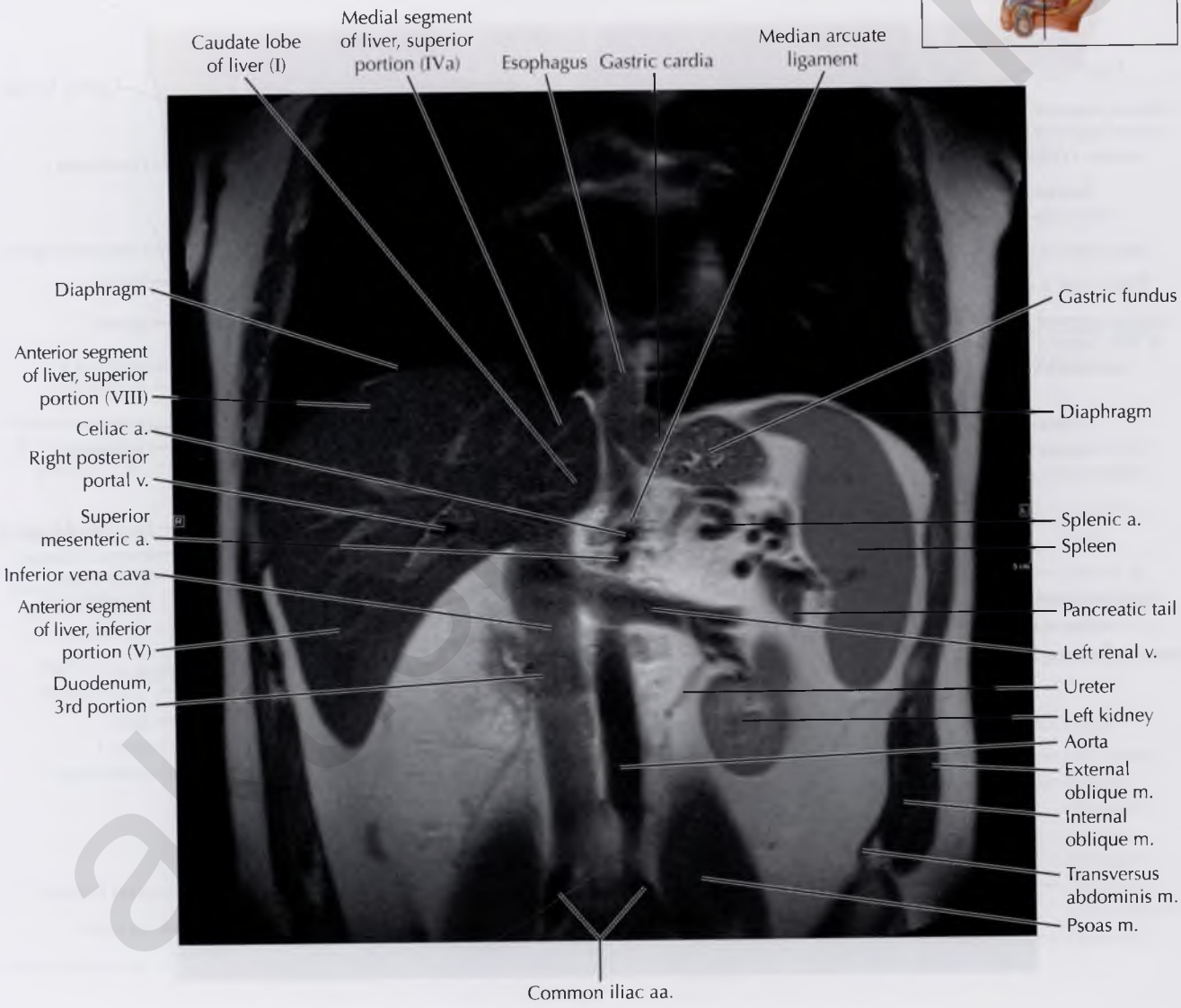
Caudate lobe of liver (I)
Medial segment of liver, superior portion (IVa)
Esophagus
Gastric cardia
Median arcuate ligament
Diaphragm
Anterior segment of liver, superior portion (VIII)
Celiac a.
Right posterior portal v.
Superior mesenteric a.
Inferior vena cava
Anterior segment of liver, inferior portion (V)
Duodenum, 3rd portion
Gastric fundus
Diaphragm
Splenic a.
Spleen
Pancreatic tail
Left renal v.
Ureter
Left kidney
Aorta
External oblique m.
Internal oblique m.
Transversus abdominis m.
Psoas m.
Common iliac aa.

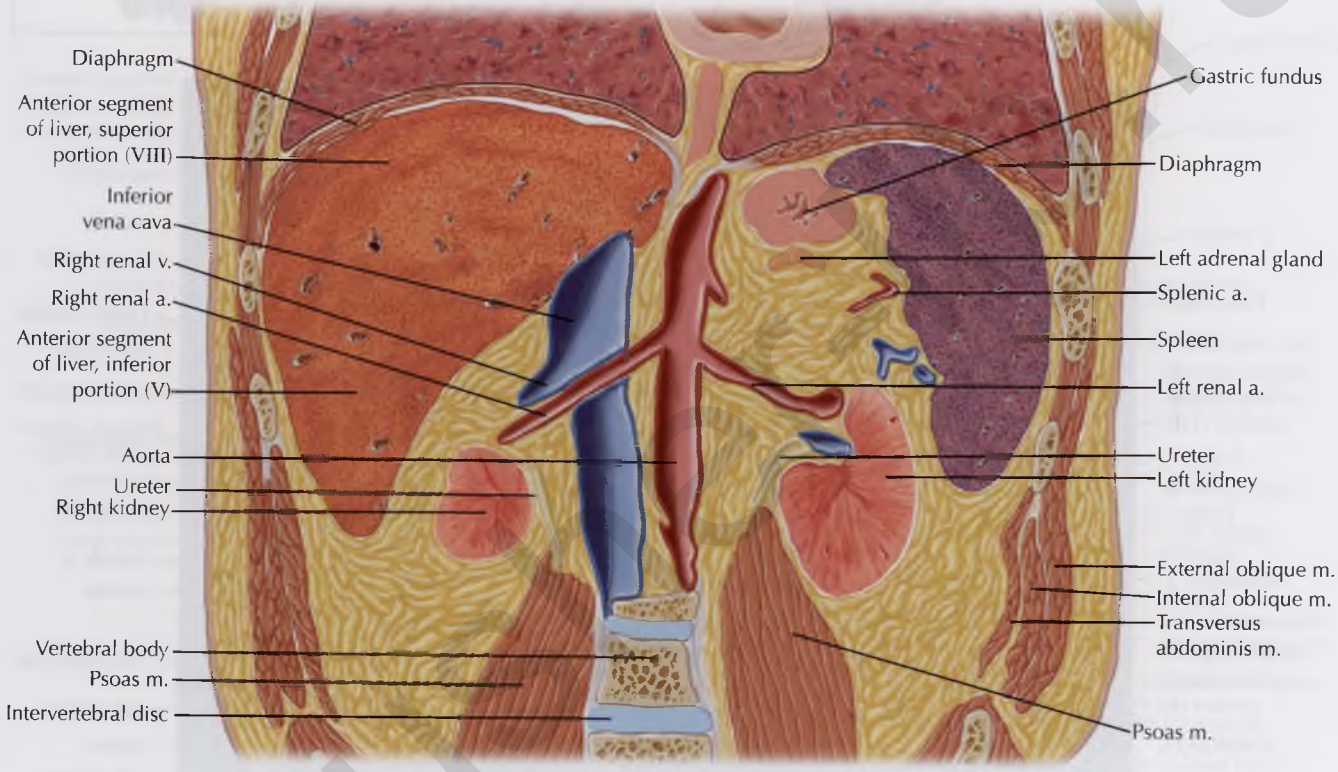

NORMAL VARIANTS

Fetal lobation of the spleen typically disappears before birth, but may persist to some degree along the medial aspect of the spleen.

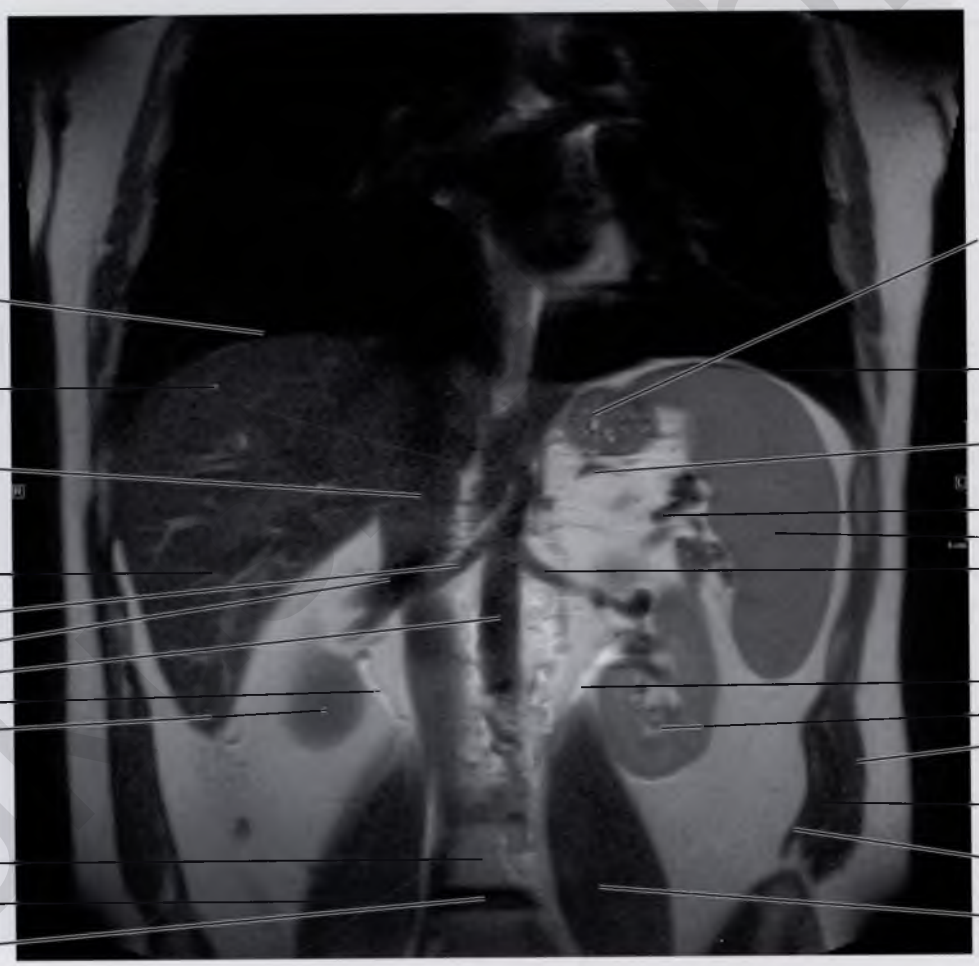
Diaphragm
Anterior segment of liver, superior portion (VIII)
Inferior vena cava
Anterior segment of liver, inferior portion (V)
Right renal a.
Right renal v.
Aorta
Ureter
Right kidney
Vertebral body
Psoas m.
Intervertebral disc
Gastric fundus
Diaphragm
Left adrenal gland
Splenic a.
Spleen
Left renal a.
Ureter
Left kidney
External oblique m.
Internal oblique m.
Transversus abdominis m.
Psoas m.

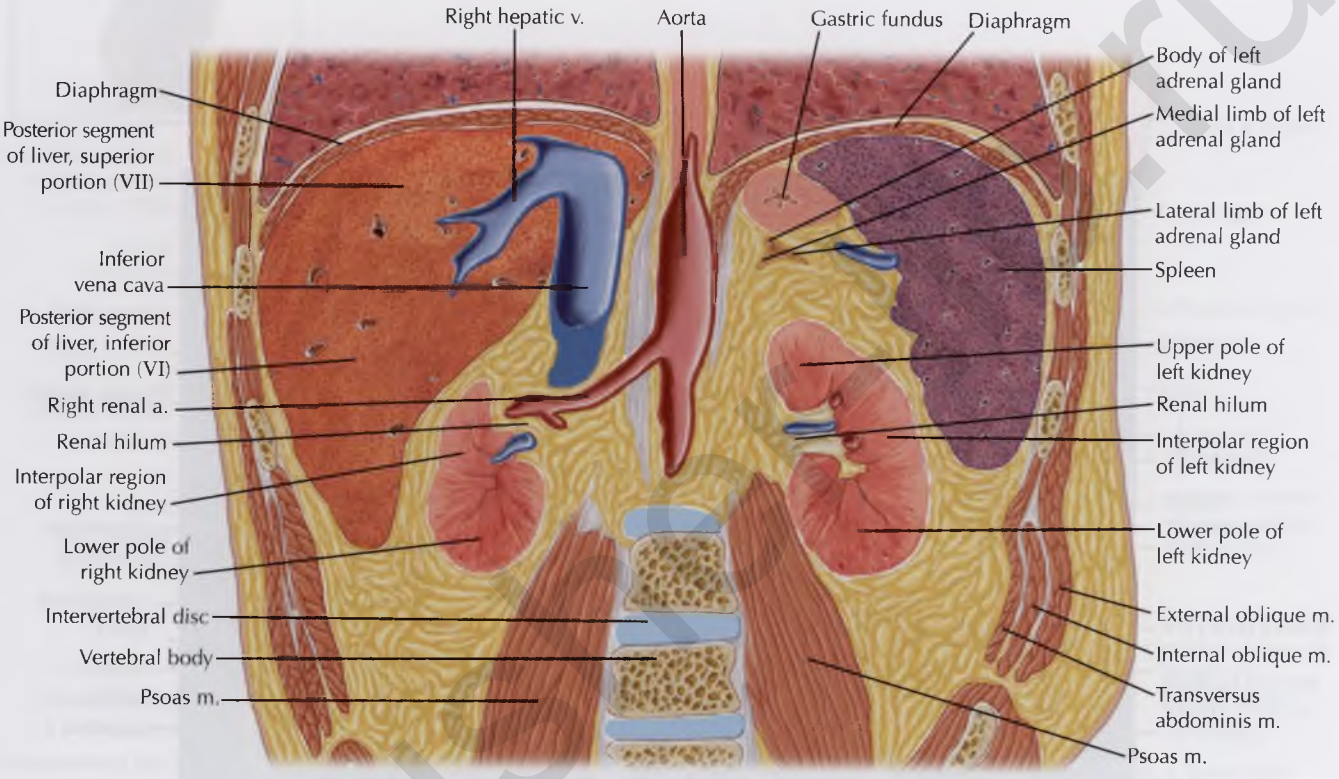

NORMAL ANATOMY

Intrahepatic veins classically coalesce into three hepatic veins that drain into the IVC superiorly. The *right hepatic vein* is typically the largest and drains directly into the IVC. The left and middle hepatic veins most often form a short common trunk before draining into the IVC, but may also drain directly into the IVC. Almost 50% of the population has an *inferior accessory* right hepatic vein that drains directly into the IVC most often from the posterior hepatic segment.


Right hepatic v.
Aorta
Gastric fundus
Diaphragm
Diaphragm
Posterior segment of liver, superior portion (VII)
Inferior vena cava
Posterior segment of liver, inferior portion (VI)
Right renal a.
Renal hilum
Interpolar region of right kidney
Lower pole of right kidney
Intervertebral disc
Vertebral body
Psoas m.
Body of left adrenal gland
Lateral limb of left adrenal gland
Medial limb of left adrenal gland
Spleen
Upper pole of left kidney
Renal hilum
Interpolar region of left kidney
Lower pole of left kidney
External oblique m.
Internal oblique m.
Transversus abdominis m.
Psoas m.

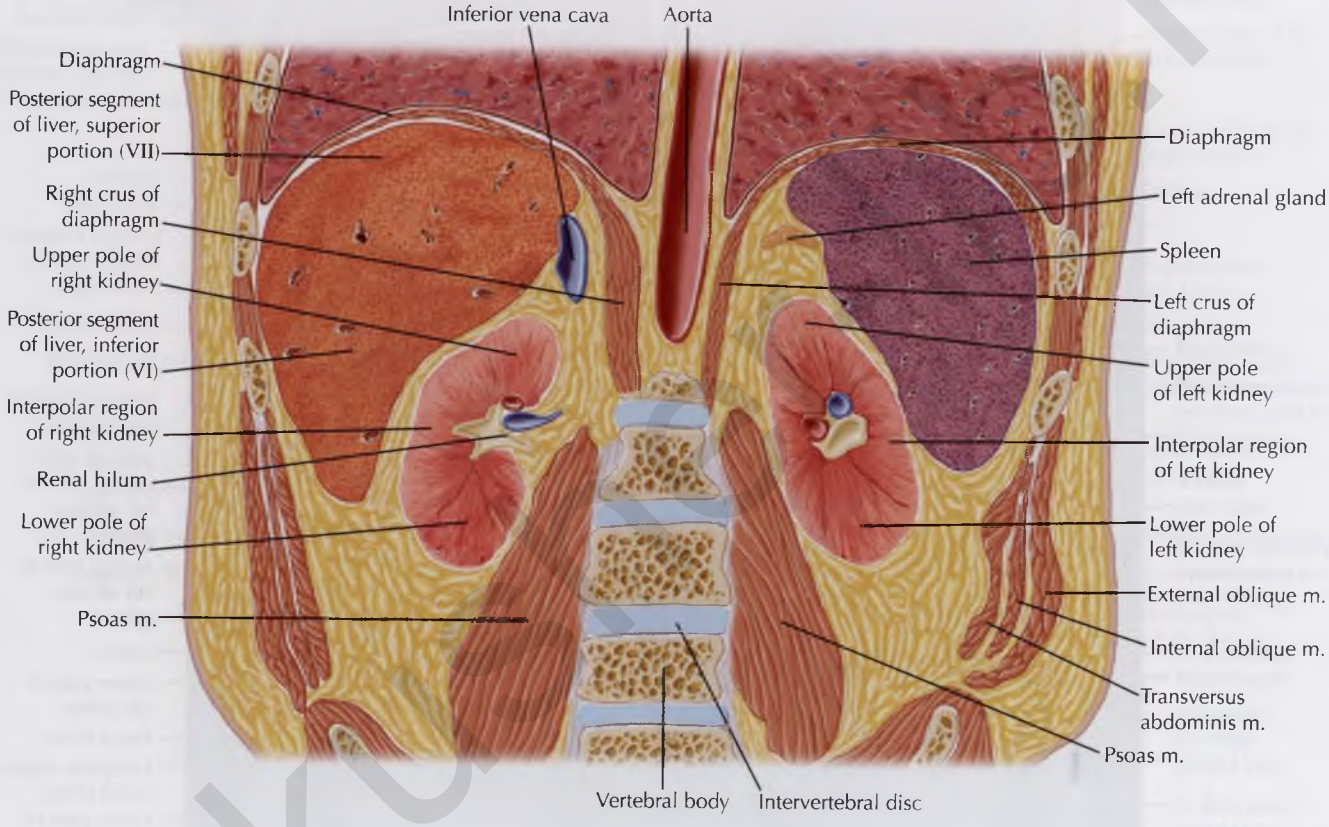
Inferior vena cava
Aorta
Diaphragm
Posterior segment of liver, superior portion (VII)
Right crus of diaphragm
Upper pole of right kidney
Posterior segment of liver, inferior portion (VI)
Interpolar region of right kidney
Renal hilum
Lower pole of right kidney
Psoas m.
Diaphragm
Left adrenal gland
Spleen
Left crus of diaphragm
Upper pole of left kidney
Interpolar region of left kidney
Lower pole of left kidney
External oblique m.
Internal oblique m.
Transversus abdominis m.
Psoas m.
Vertebral body
Intervertebral disc

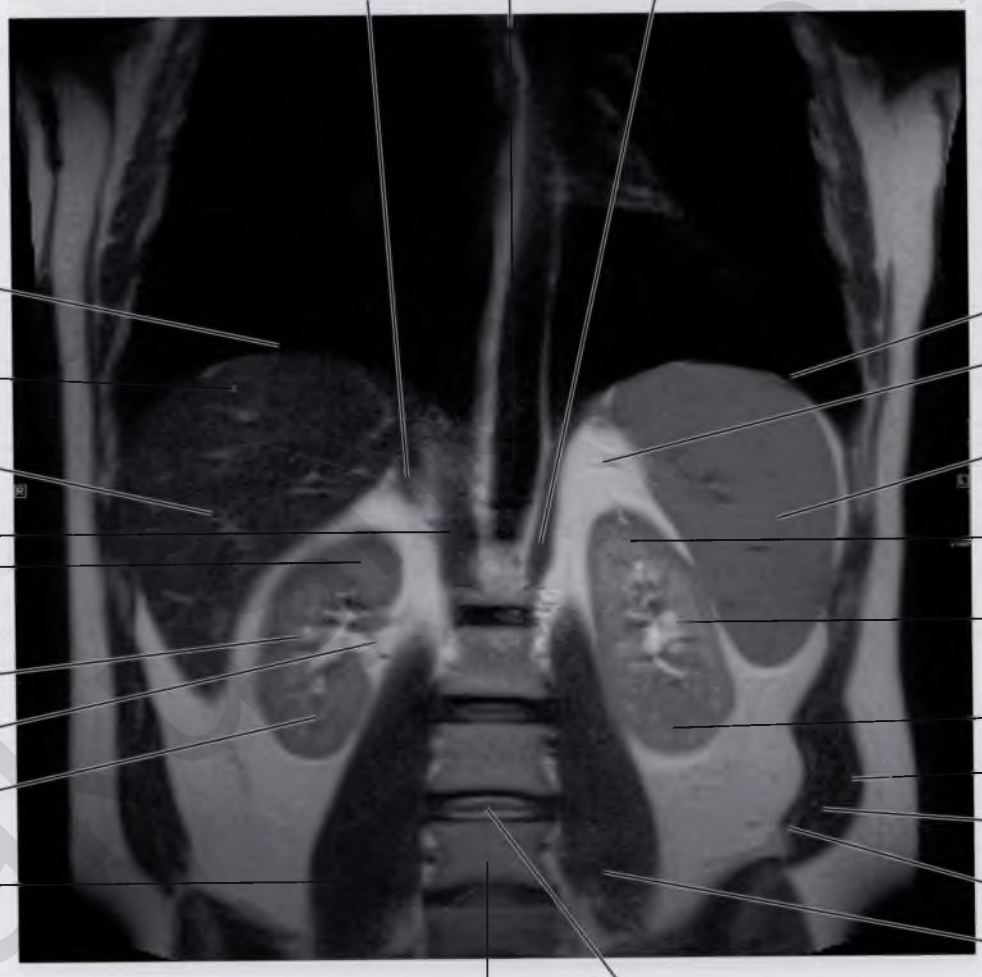
Inferior vena cava
Aorta
Left crus of diaphragm
Diaphragm
Posterior segment of liver, superior portion (VII)
Posterior segment of liver, inferior portion (VI)
Right crus of diaphragm
Upper pole of right kidney
Interpolar region of right kidney
Renal hilum
Lower pole of right kidney
Psoas m.
Diaphragm
Left adrenal gland
Spleen
Upper pole of left kidney
Interpolar region of left kidney
Lower pole of left kidney
External oblique m.
Internal oblique m.
Transversus abdominis m.
Psoas m.
Vertebral body
Intervertebral disc

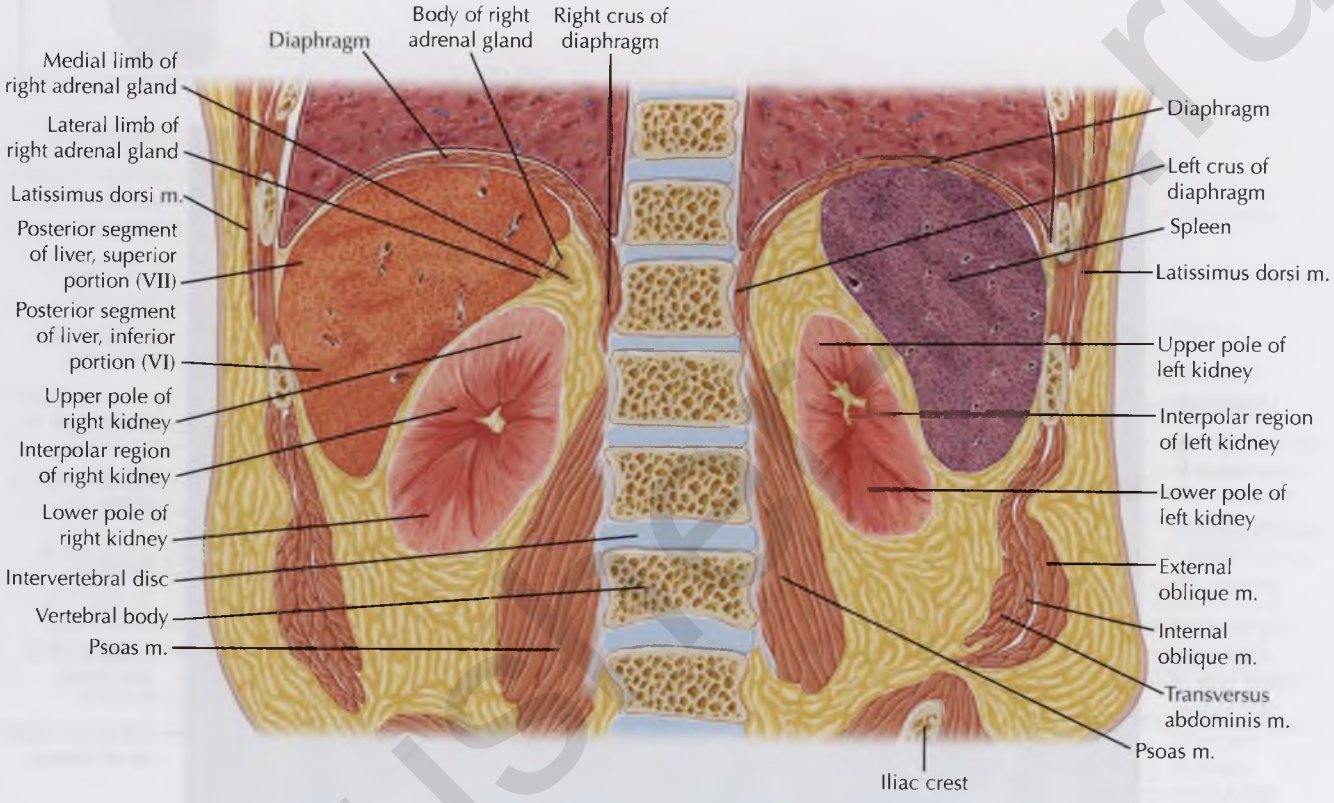

DIAGNOSTIC CONSIDERATION

Each *adrenal gland* is shaped like an inverted Y or V, with the medial and lateral limbs joining at the body of the adrenal gland. Unlike other organs in the abdomen, the adrenal glands continue to increase in volume with increasing age in both children and adults. The left adrenal gland is typically larger in volume than the right adrenal gland.


Diaphragm
Body of the right adrenal gland
Right crus of diaphragm
Posterior segment of liver, superior portion (VII)
Lateral limb of right adrenal gland
Medial limb of right adrenal gland
Posterior segment of liver, inferior portion (VI)
Upper pole of right kidney
Interpolar region of right kidney
Lower pole of right kidney
Intervertebral disc
Vertebral body
Psoas m.
Diaphragm
Spleen
Latissimus dorsi m.
Left crus of diaphragm
Upper pole of left kidney
Interpolar region of left kidney
Lower pole of left kidney
External oblique m.
Internal oblique m.
Transversus abdominis m.
Psoas m.
Iliac crest


Diaphragm
Vertebral body
Intervertebral disc
Posterior segment of liver, superior portion (VII)
Right kidney
Latissimus dorsi m.
Psoas m.
Cauda equina
Spinal nerve roots
Diaphragm
Spleen
Left kidney
Psoas m.
External oblique m.
Internal oblique m.
Transversus abdominis m.
Iliac crest


Diaphragm
Vertebral body
Intervertebral disc
Posterior segment of liver, superior portion (VII)
Right kidney
Latissimus dorsi m.
Psoas m.
Cauda equina
Spinal nerve roots
Diaphragm
Spleen
Left kidney
Psoas m.
External oblique m.
Internal oblique m.
Transversus abdominis m.
Iliac crest

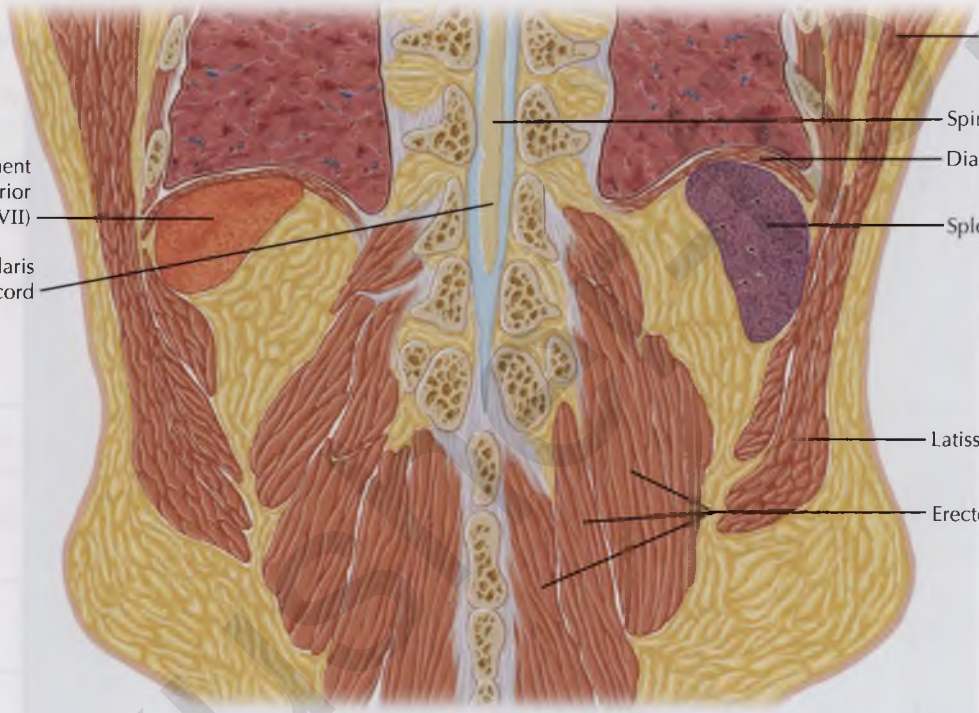
Latissimus dorsi m.
Spinal cord
Diaphragm
Posterior segment of liver, superior portion (VII)
Spleen
Conus medullaris of spinal cord
Latissimus dorsi m.
Erector spinae m.

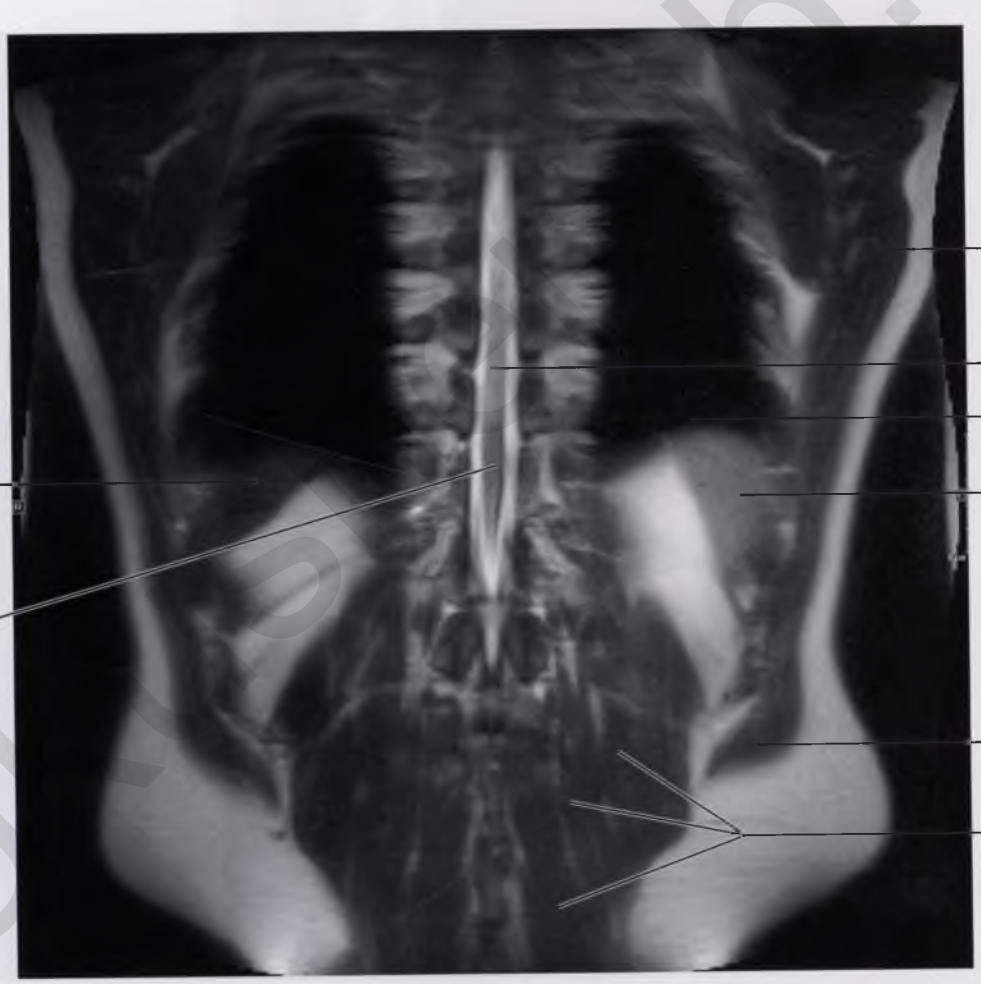
Latissimus dorsi m.
Spinal cord
Diaphragm
Posterior segment of liver, superior portion (VII)
Spleen
Conus medullaris of spinal cord
Latissimus dorsi m.
Erector spinae m.

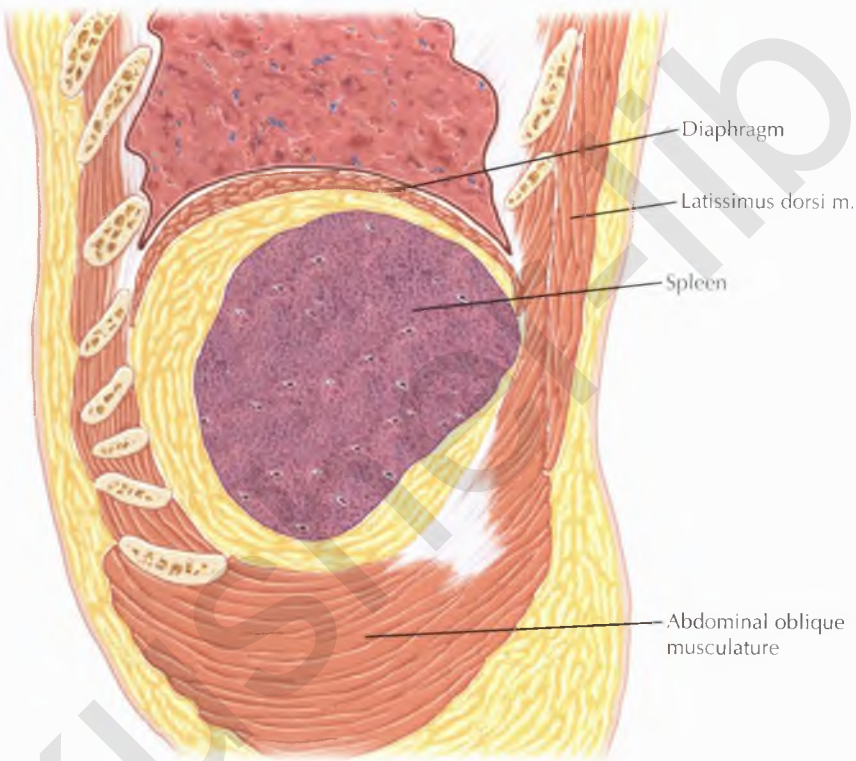
Diaphragm
Latissimus dorsi m.
Spleen
Abdominal oblique musculature

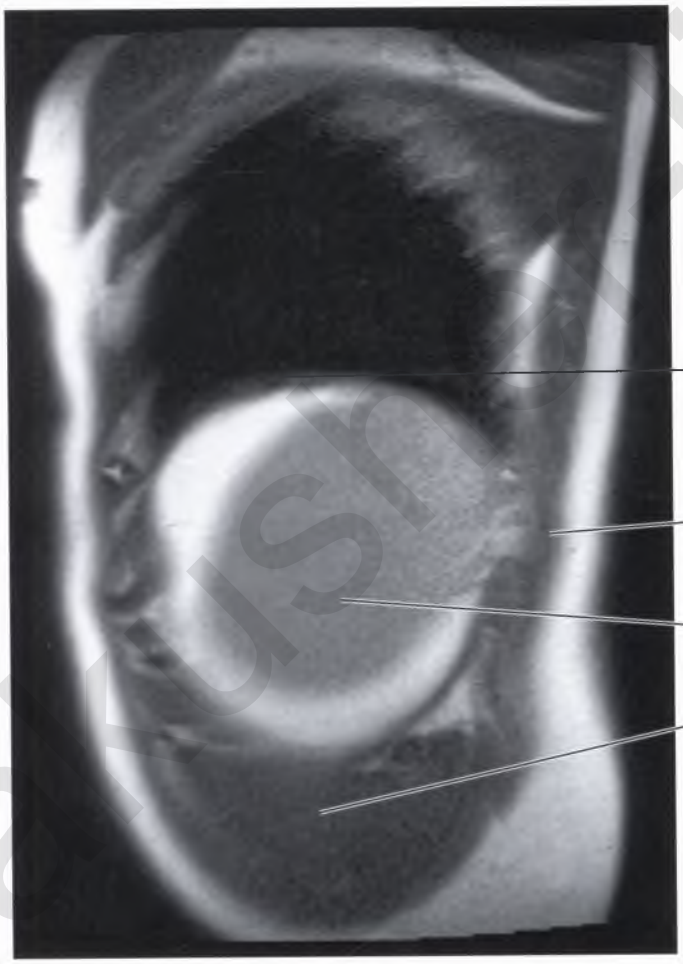
Diaphragm
Latissimus dorsi m.
Spleen
Abdominal oblique musculature

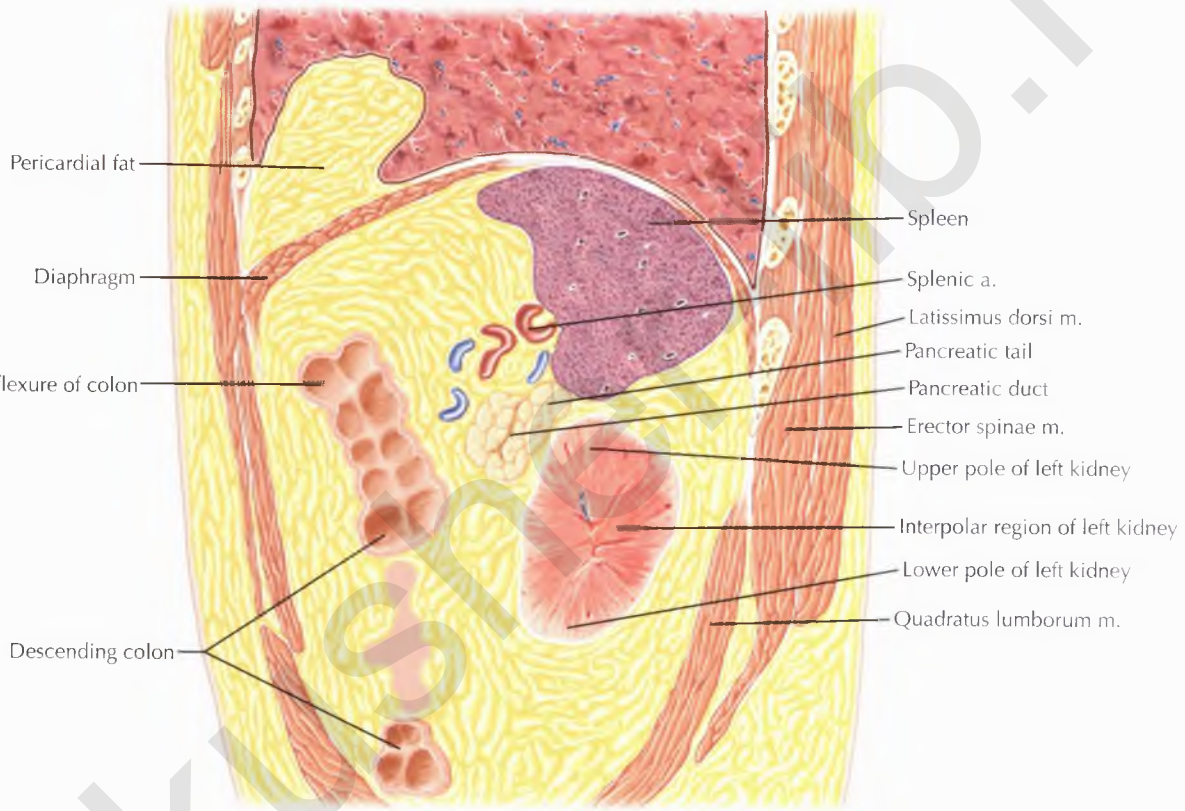
Pericardial fat
Diaphragm
Spenic flexure of colon
Descending colon
Spleen
Splenic a.
Latissimus dorsi m.
Pancreatic tail
Pancreatic duct
Erector spinae m.
Upper pole of left kidney
Interpolar region of left kidney
Lower pole of left kidney
Quadratus lumborum m.

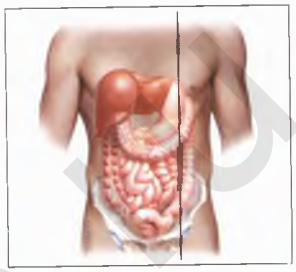

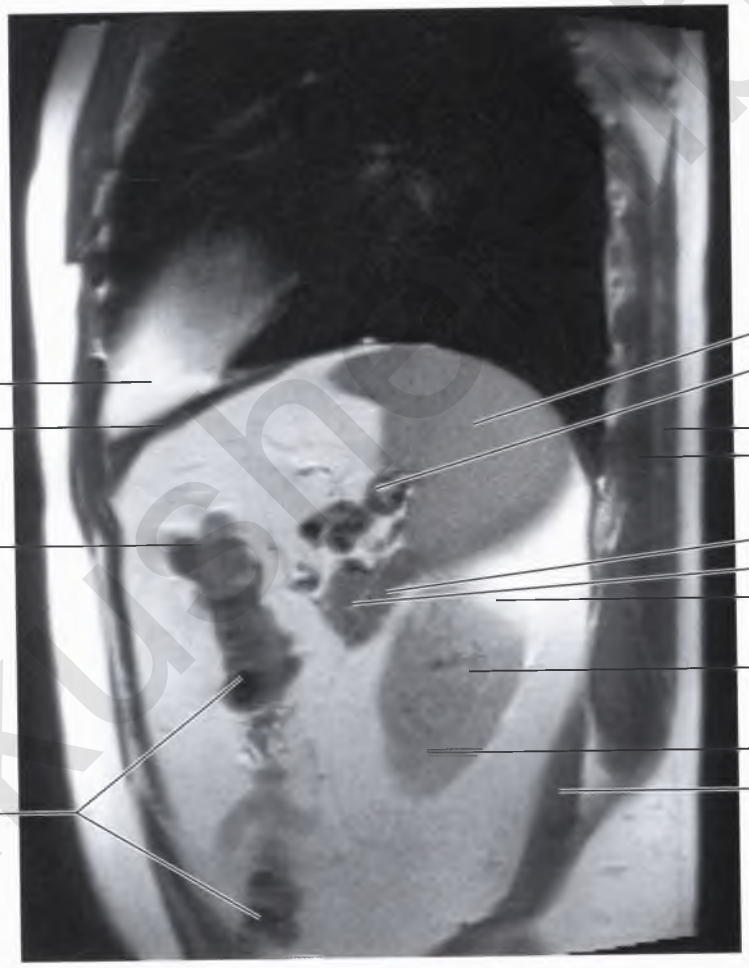

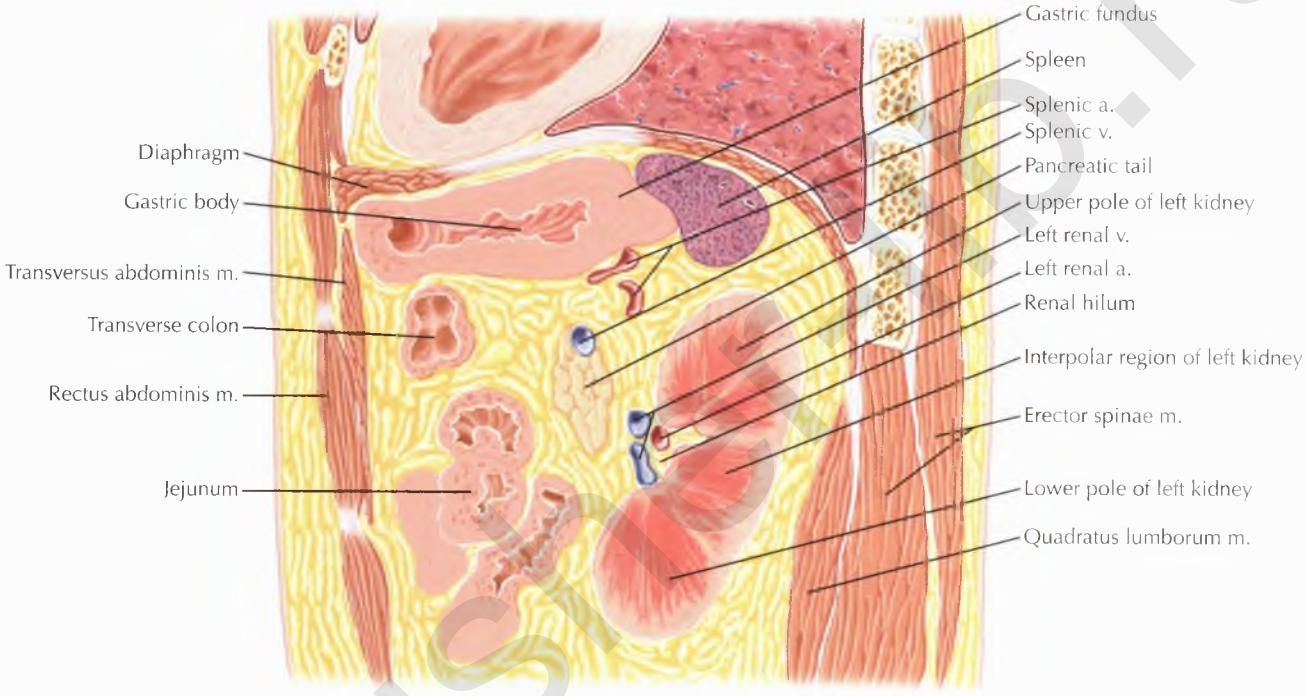

NORMAL ANATOMY

The kidneys are paired retroperitoneal organs found within the perirenal spaces, surrounded by the renal fascia. The kidneys vary in length; on MR images the average length in a male adult is 11.5 to 13.3 cm, and in a female adult, 10.5 to 12.7 cm.

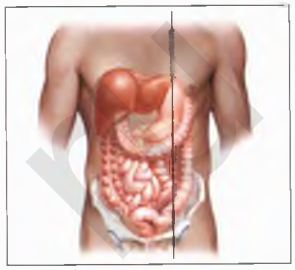

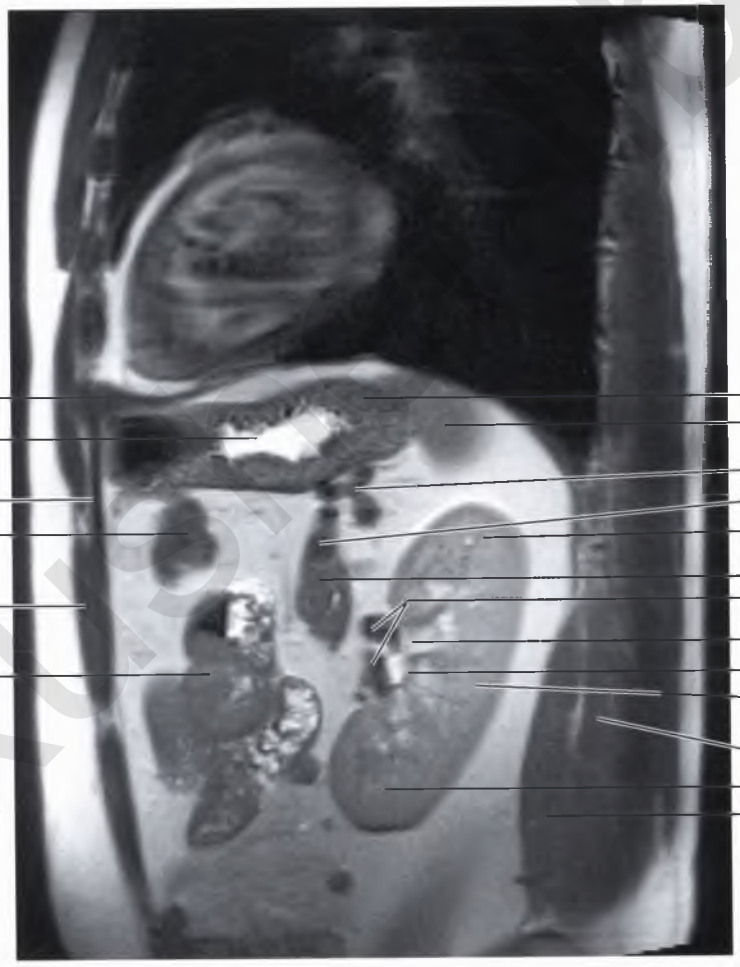

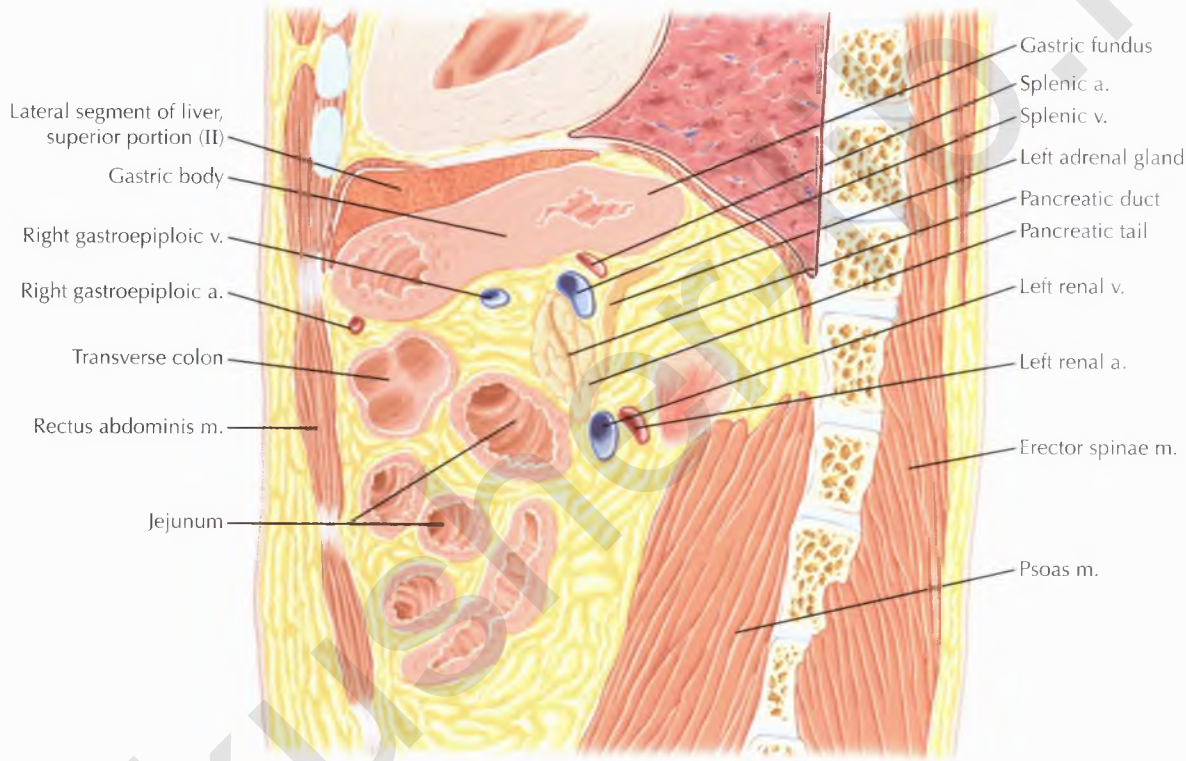
Lateral segment of liver, superior portion (II)
Gastric body
Right gastroepiploic v.
Right gastroepiploic a.
Transverse colon
Rectus abdominis m.
Jejunum
Gastric fundus
Splenic a.
Splenic v.
Left adrenal gland
Pancreatic duct
Pancreatic tail
Left renal v.
Left renal a.
Erector spinae m.
Psoas m.

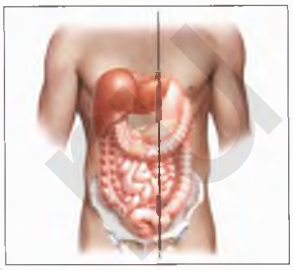

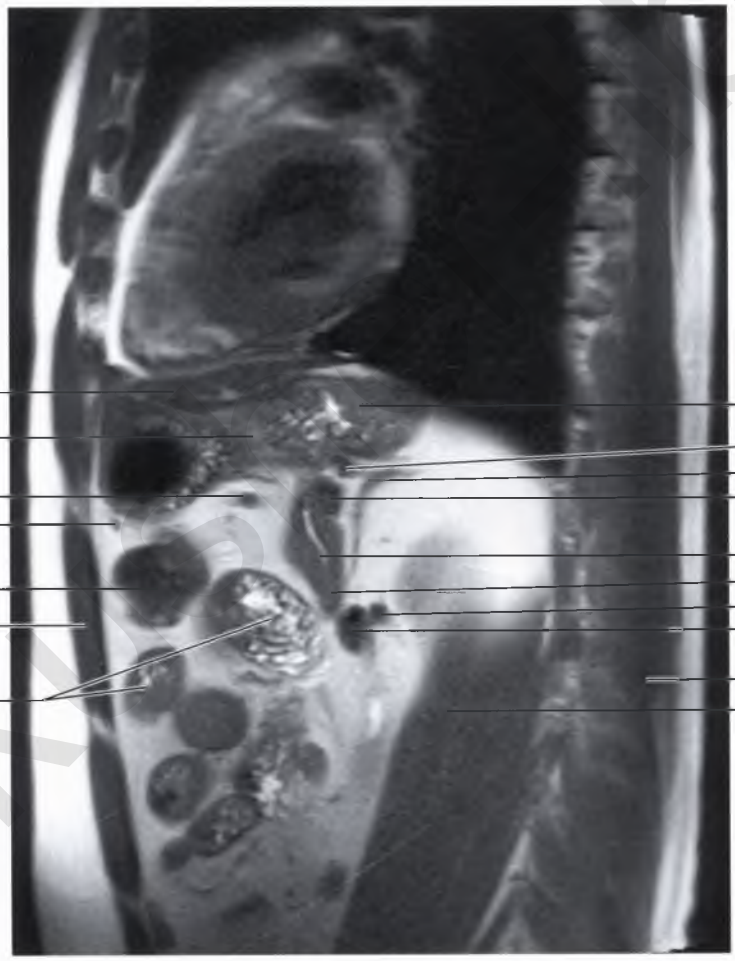
Lateral segment of liver, superior portion (II)
Gastric body
Right gastroepiploic v.
Right gastroepiploic a.
Transverse colon
Rectus abdominis m.
Jejunum
Gastric fundus
Splenic a.
Left adrenal gland
Splenic v.
Pancreatic duct
Pancreatic tail
Left renal a.
Left renal v.
Erector spinae m.
Psoas m.

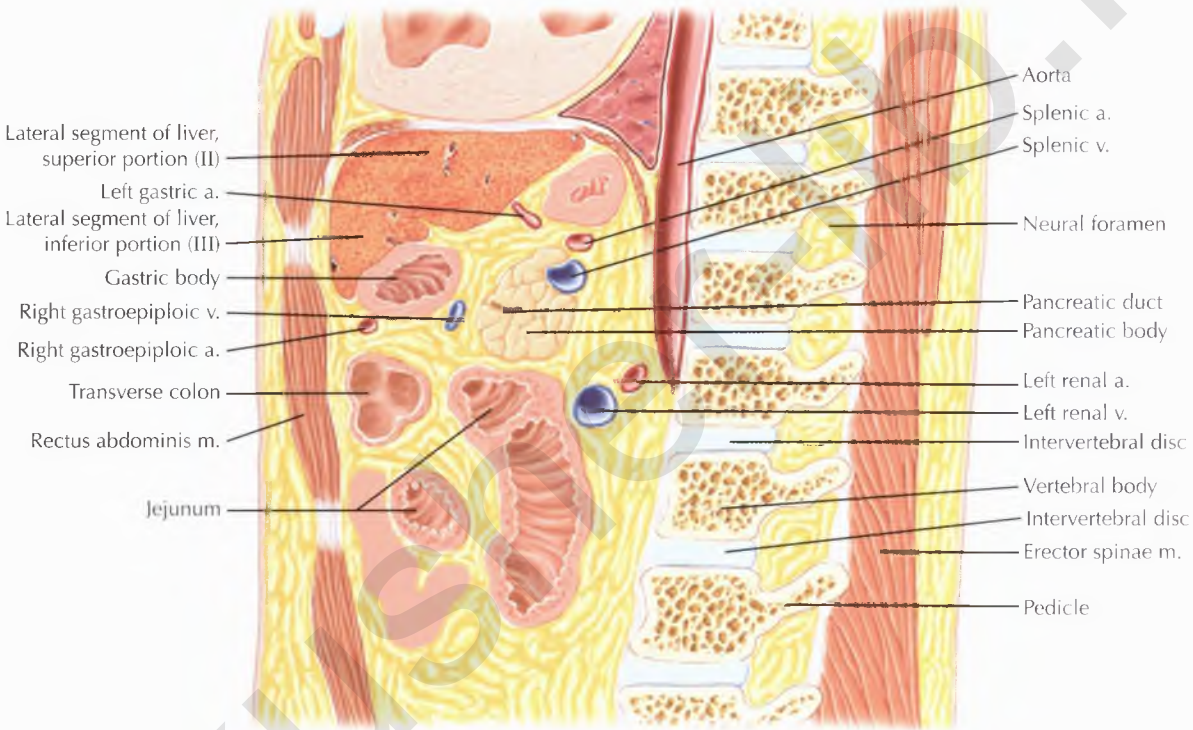

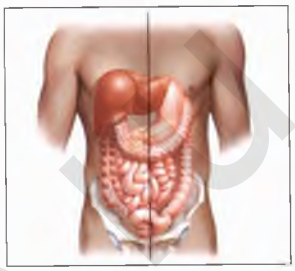


Lateral segment of liver, superior portion (II)
Left gastric a.
Lateral segment of liver, inferior portion (III)
Gastric body
Right gastroepiploic v.
Right gastroepiploic a.
Transverse colon
Rectus abdominis m.
Jejunum
Aorta
Splenic a.
Splenic v.
Neural foramen
Pancreatic duct
Pancreatic body
Left renal a.
Left renal v.
Vertebral body
Intervertebral disc
Erector spinae m.
Pedicle

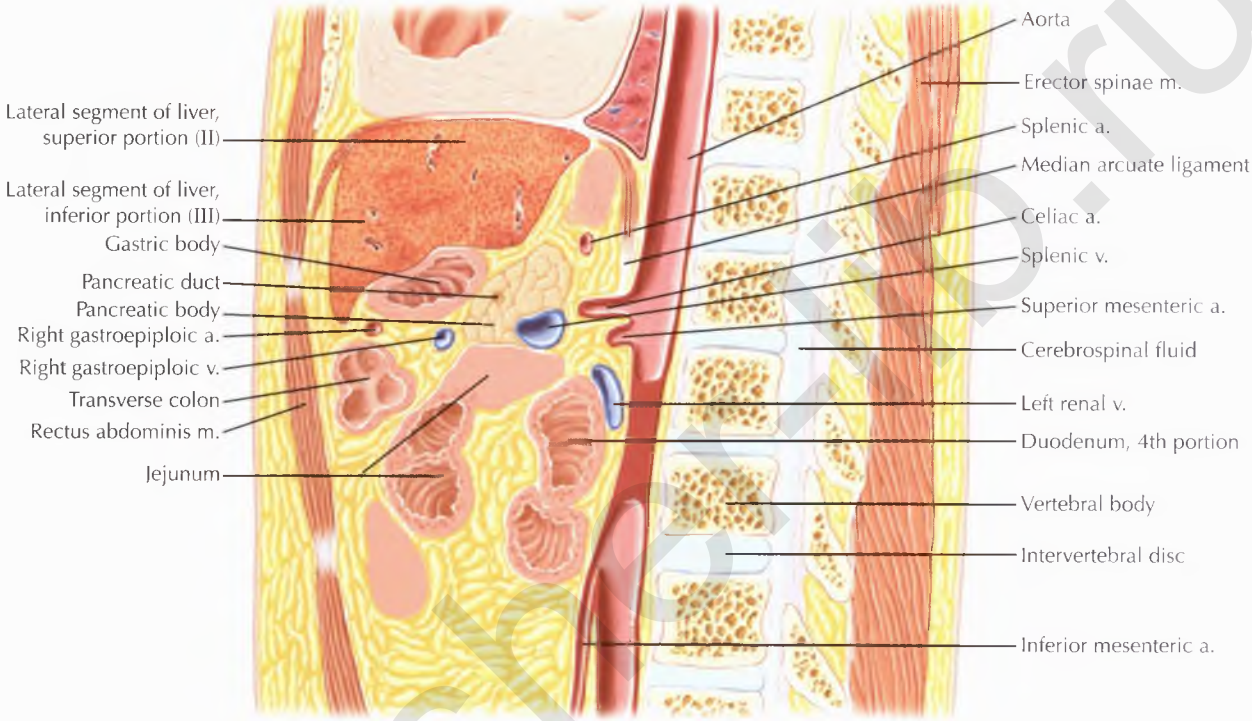

PATHOLOGIC PROCESS

In *median arcuate ligament syndrome* (also known as celiac artery compression syndrome) the median arcuate ligament compresses and narrows the celiac artery near its origin typically during end inspiration as well as during end expiration; this is best seen in the sagittal plane. This syndrome is classically seen in thin female patients presenting with postprandial epigastric pain. Characteristic findings include narrowing of the celiac axis with post-stenotic dilation, upward hooking of the celiac artery, and a prominent pancreaticoduodenal arcade.

Note that mild compression of the celiac axis seen during expiration only can be seen as a normal variant.

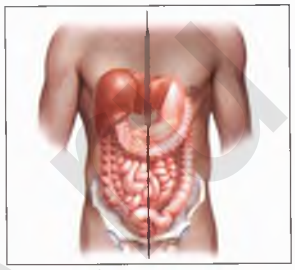

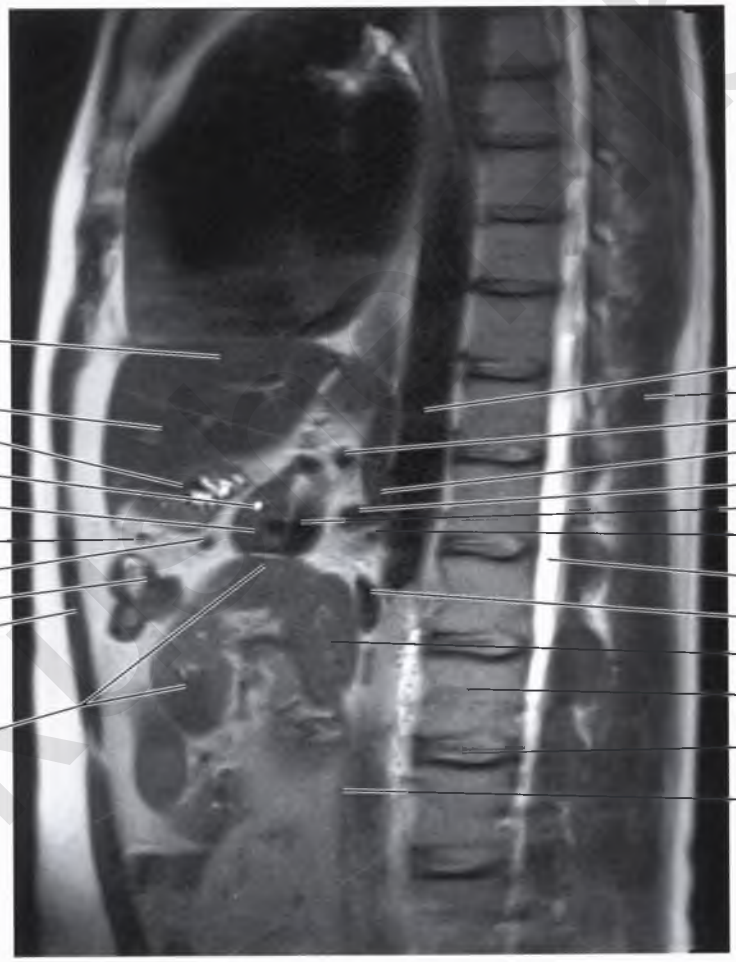
Lateral segment of liver, superior portion (II)
Lateral segment of liver, inferior portion (III)
Gastric body
Pancreatic duct
Pancreatic body
Right gastroepiploic a.
Right gastroepiploic v.
Transverse colon
Rectus abdominis m.
Jejunum
Aorta
Erector spinae m.
Splenic a.
Median arcuate ligament
Celiac a.
Splenic v.
Superior mesenteric a.
Cerebrospinal fluid
Left renal v.
Duodenum, 4th portion
Vertebral body
Intervertebral disc
Inferior mesenteric a.

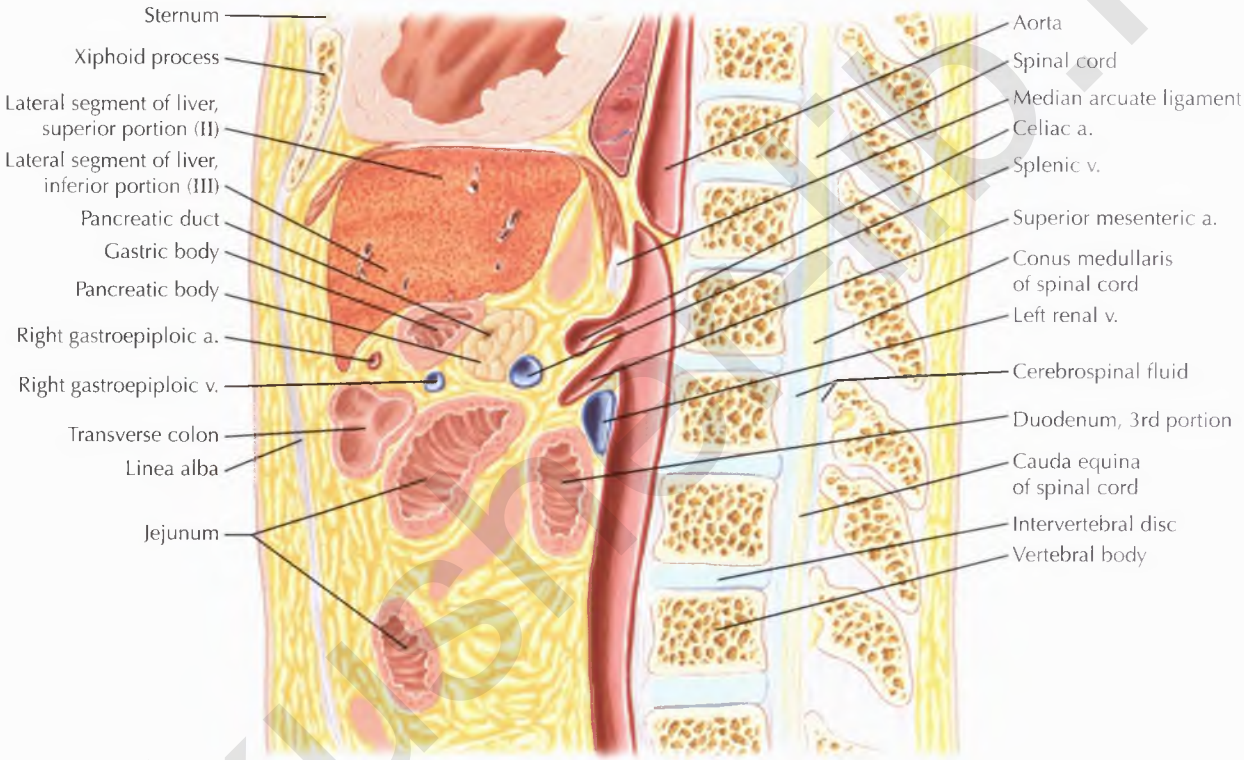

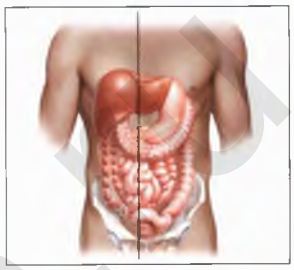

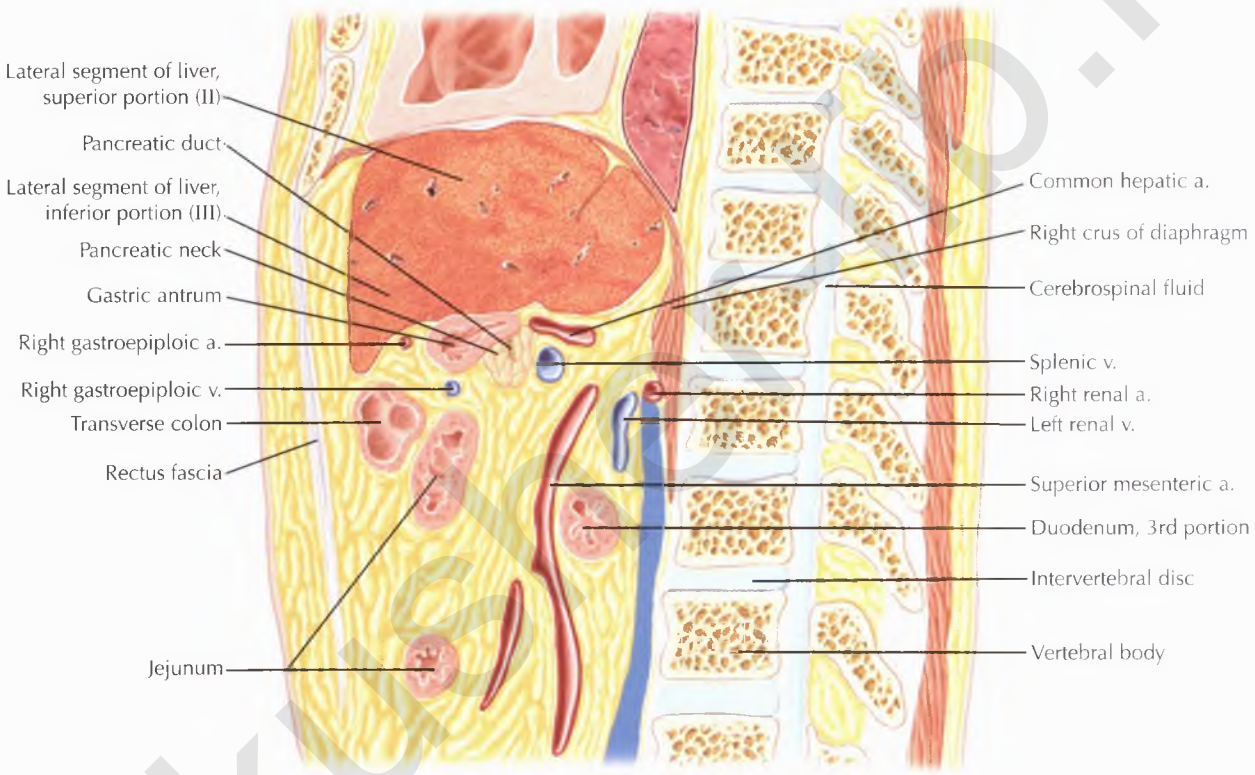

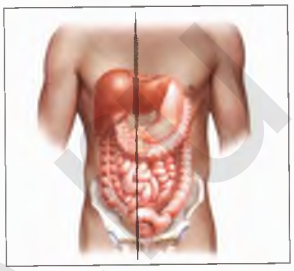

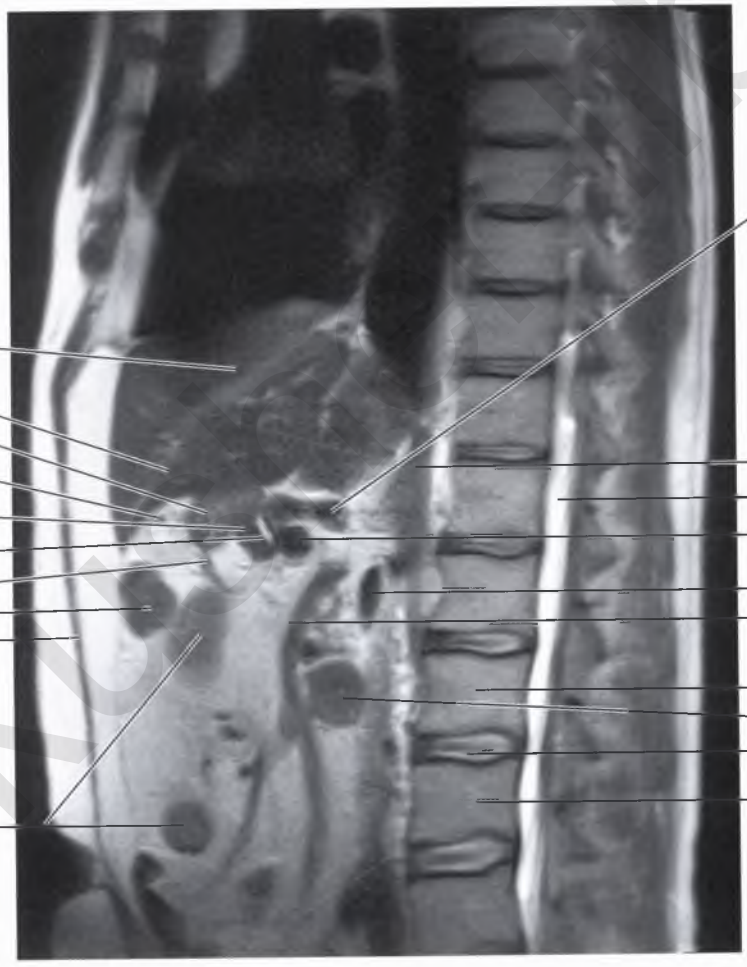
Lateral segment of liver, superior portion (II)
Lateral segment of liver, inferior portion (III)
Gastric antrum
Right gastroepiploic a.
Pancreatic body
Pancreatic duct
Right gastroepiploic v.
Transverse colon
Rectus fascia
Jejunum
Common hepatic a.
Right crus of diaphragm
Cerebrospinal fluid
Splenic v.
Left renal v.
Superior mesenteric a.
Vertebral body
Duodenum, 3rd portion
Intervertebral disc
Vertebral body

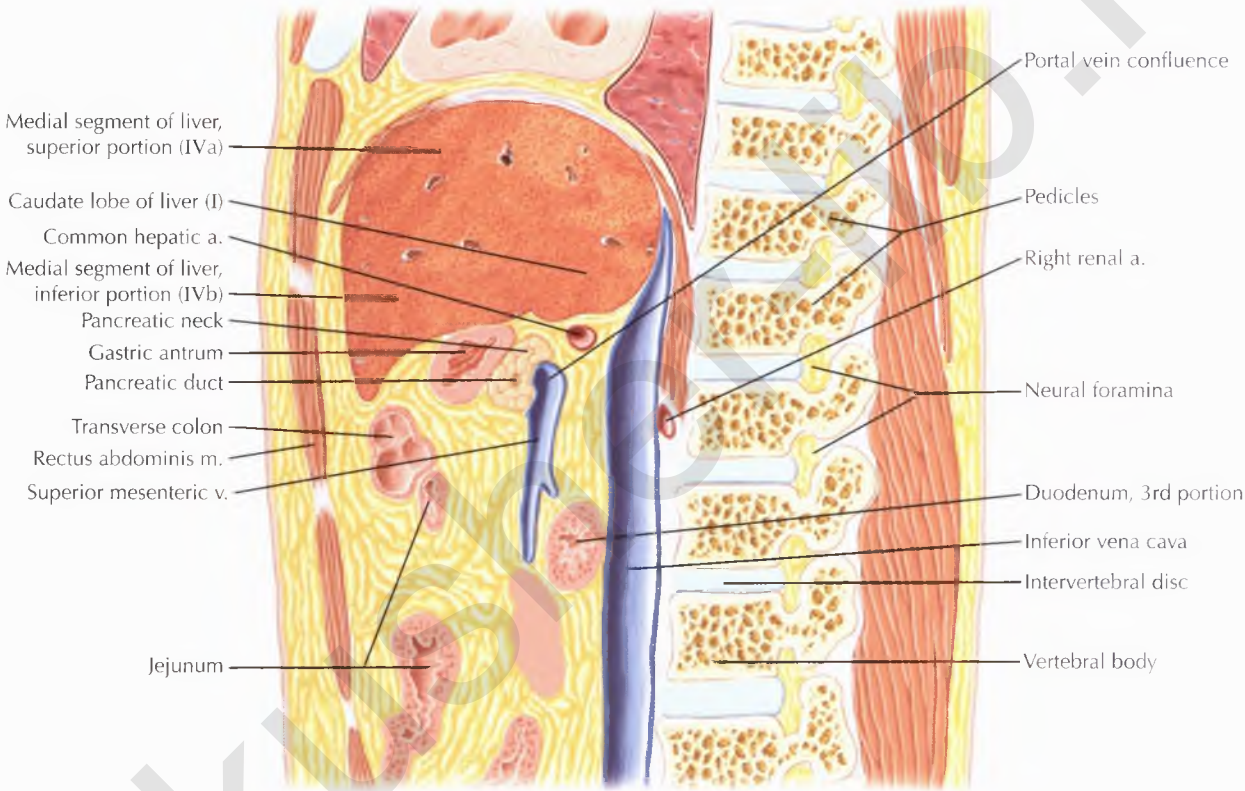

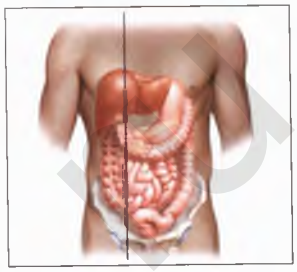

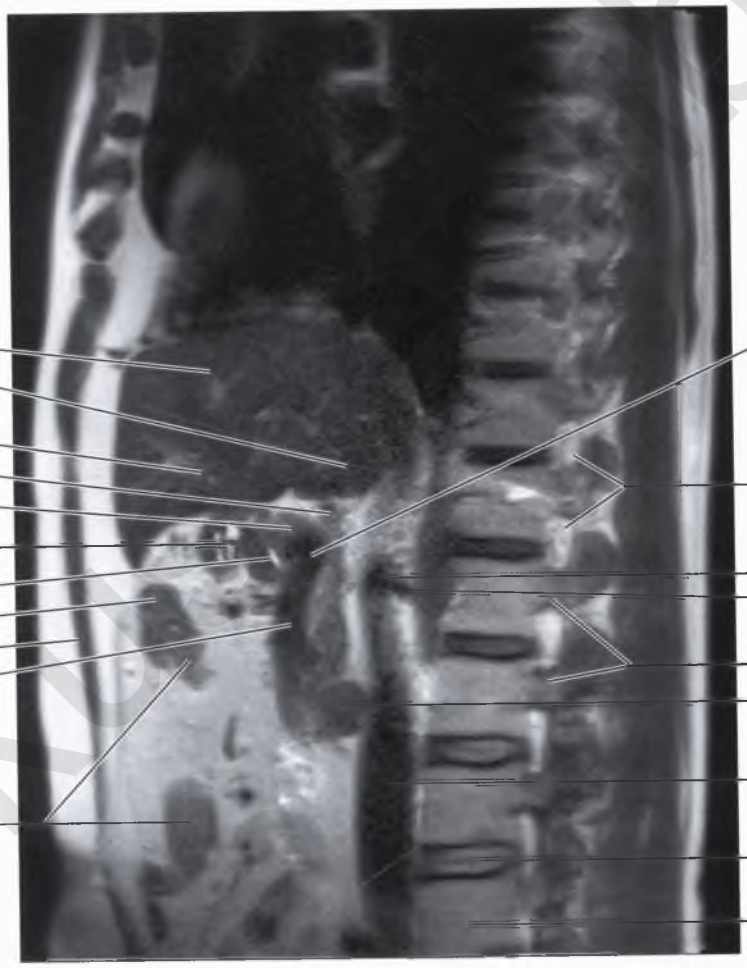
Medial segment of liver, superior portion (IVa)
Caudate lobe of liver (I)
Medial segment of liver, inferior portion (IVb)
Common hepatic a.
Pancreatic neck
Gastric antrum
Pancreatic duct
Transverse colon
Rectus abdominis m.
Superior mesenteric v.
Jejunum
Portal vein confluence
Neural foramina
Inferior vena cava
Right renal a.
Pedicles
Duodenum, 3rd portion
Inferior vena cava
Intervertebral disc
Vertebral body

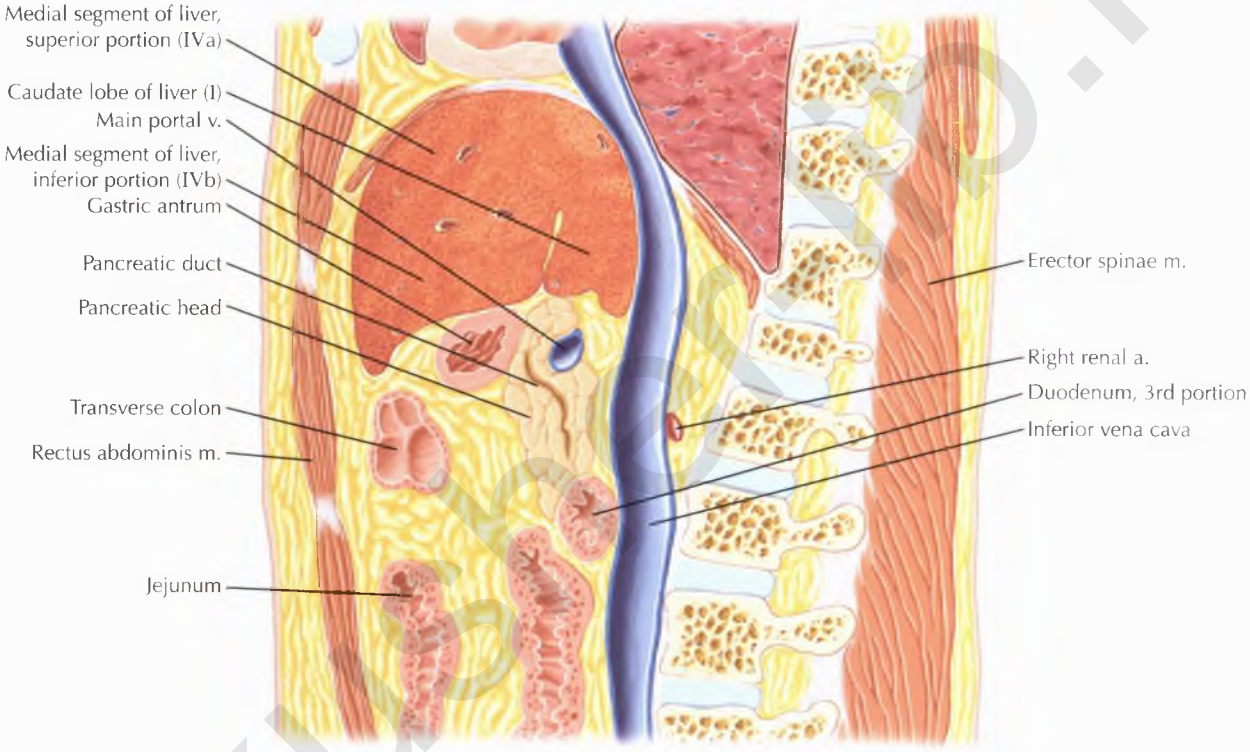

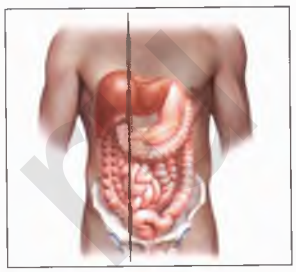


Medial segment of liver, superior portion (IVa)
Caudate lobe of liver (I)
Medial segment of liver, inferior portion (IVb)
Main portal v.
Gastric antrum
Pancreatic duct
Pancreatic head
Transverse colon
Rectus abdominis m.
Jejunum
Erector spinae
Right renal a.
Duodenum, 3rd portion
Inferior vena cava

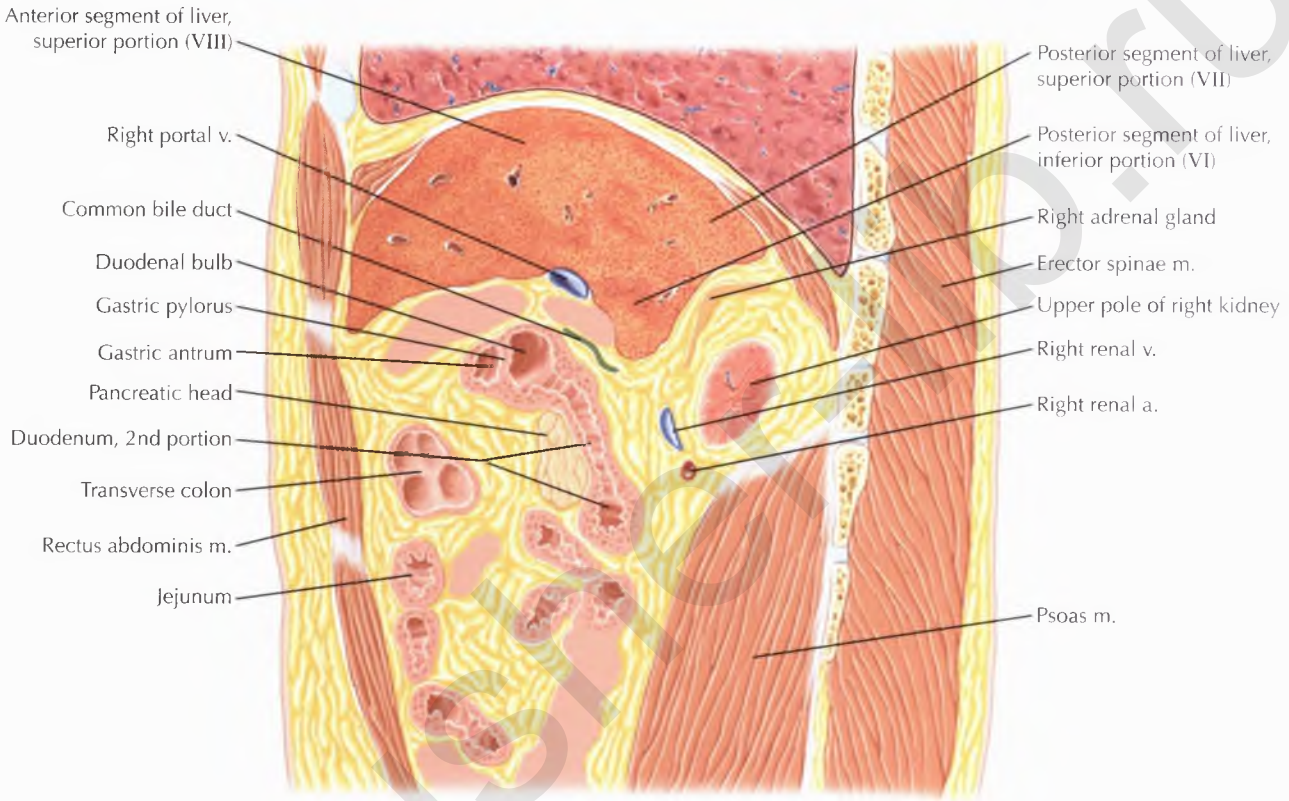

DIAGNOSTIC CONSIDERATION

Magnetic resonance imaging of the liver is usually performed in potential liver donors to assess the arterial, venous, and biliary ductal anatomy, as well as the volume of the potential graft and residual donor liver. In general, the remnant liver volume should be at least 30% of the standard liver volume to ensure sufficient liver function in the donor after transplantation.

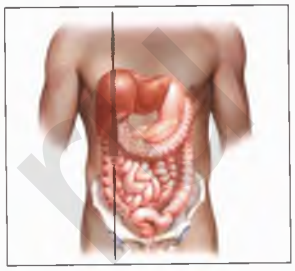

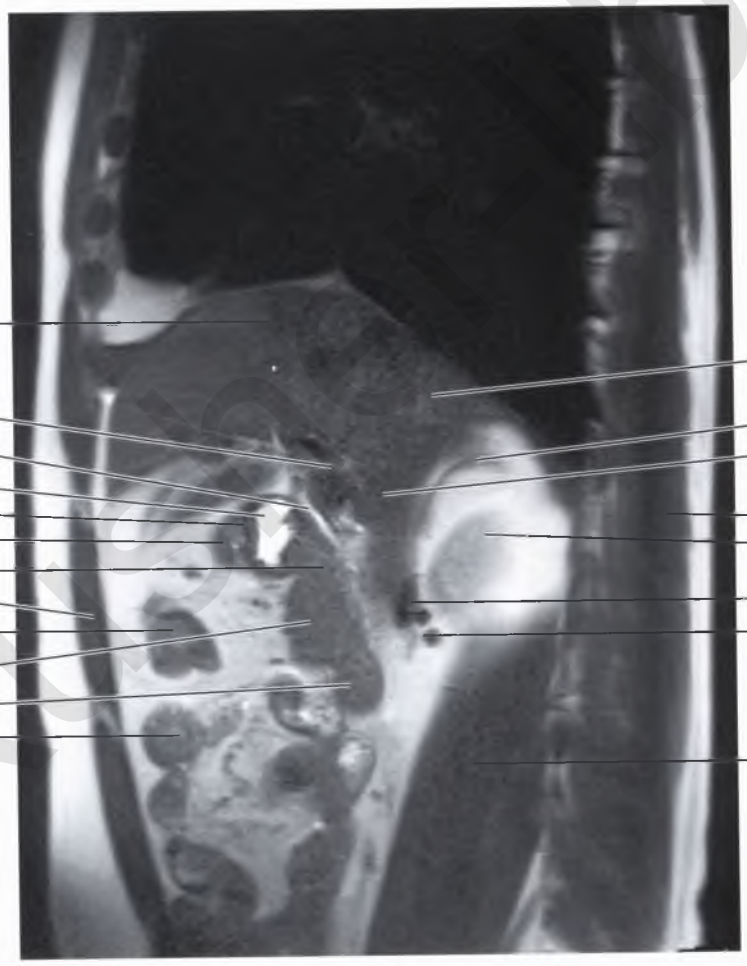

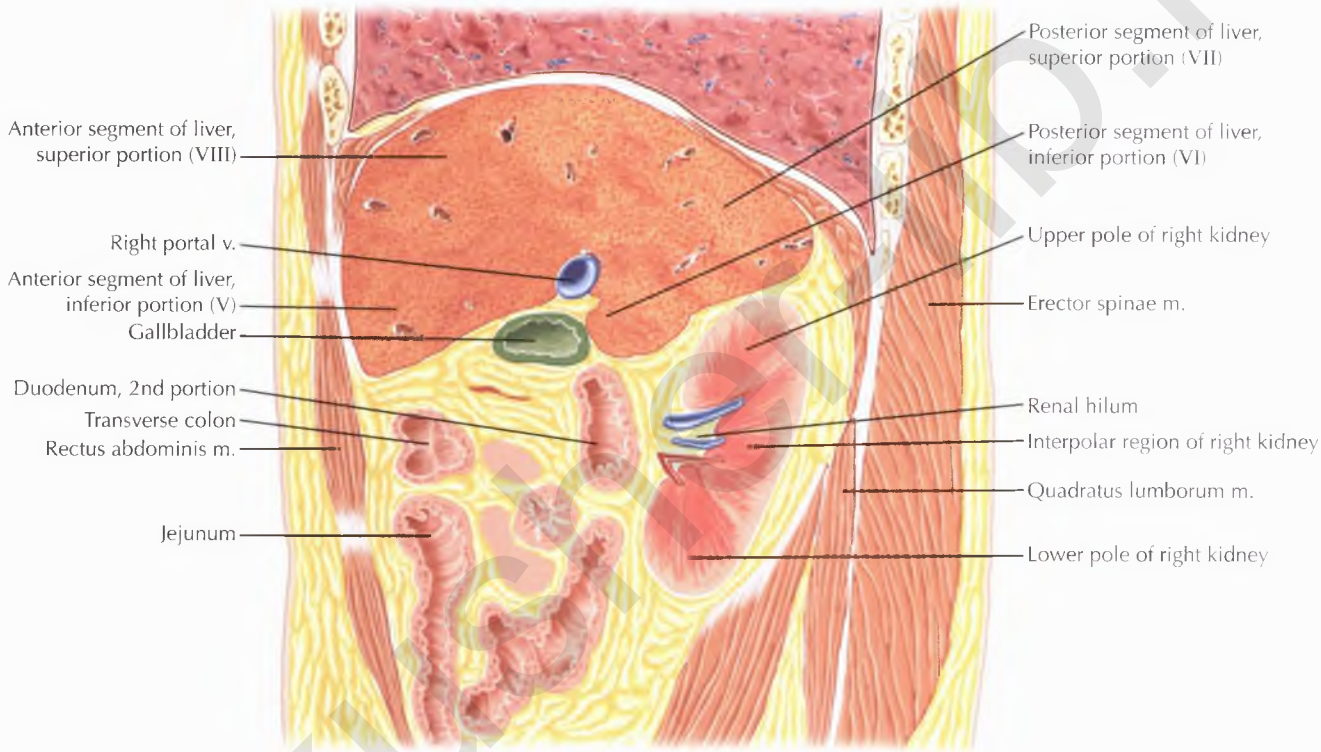

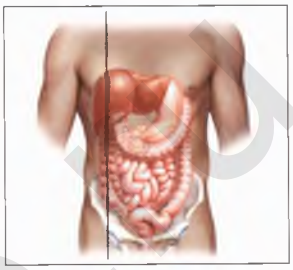

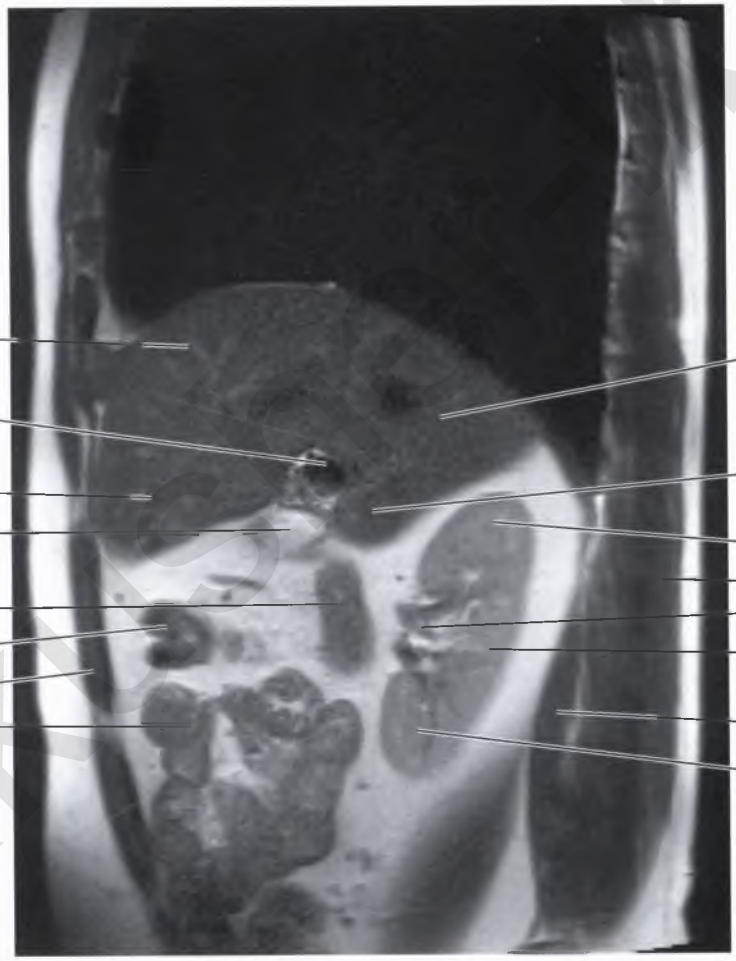

Anterior segment of liver, superior portion (VIII)

Right portal v.

Anterior segment of liver, inferior portion (V)

Gallbladder

Duodenum, 2nd portion

Transverse colon

Rectus abdominis m.

Jejunum

Posterior segment of liver, superior portion (VII)

Posterior segment of liver, inferior portion (VI)

Upper pole of right kidney

Erector spinae m.

Renal hilum

Interpolar region of right kidney

Quadratus lumborum m.

Lower pole of right kidney

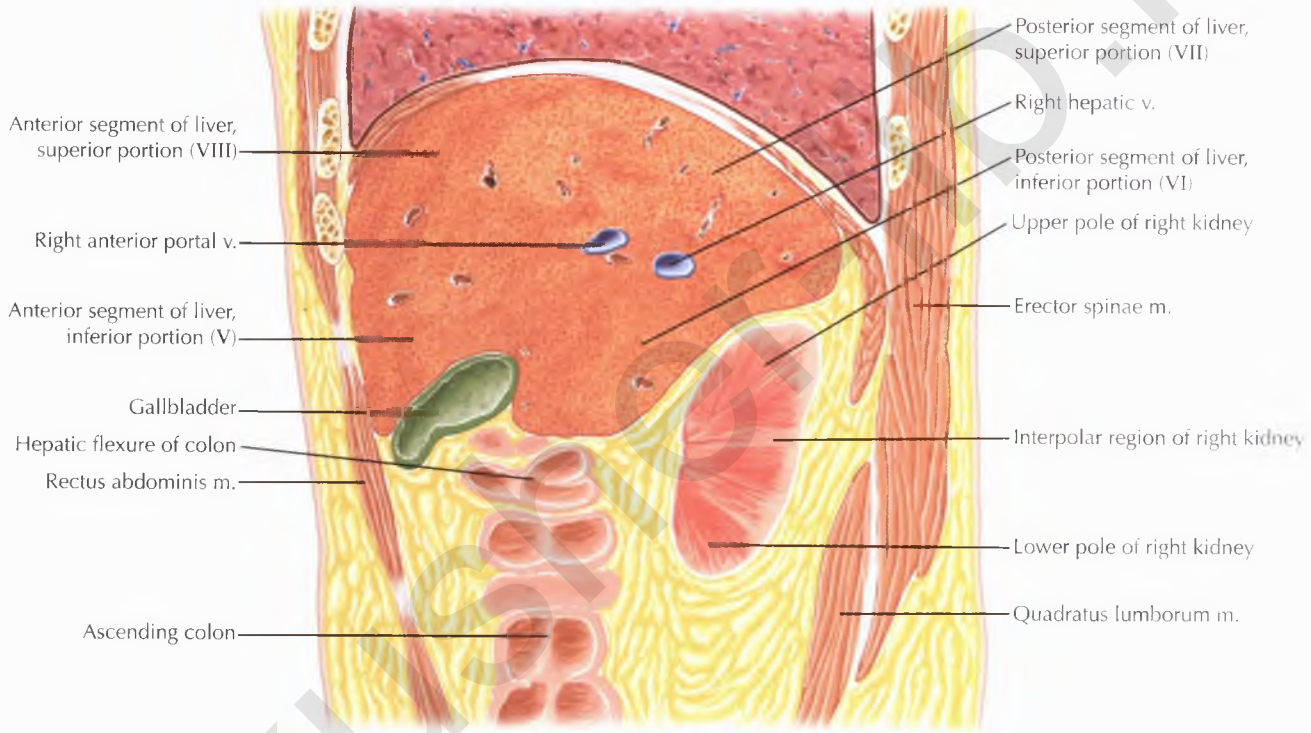
Anterior segment of liver, superior portion (VIII)
Right anterior portal v.
Anterior segment of liver, inferior portion (V)
Gallbladder
Hepatic flexure of colon
Rectus abdominis m.
Ascending colon
Posterior segment of liver, superior portion (VII)
Right hepatic v.
Posterior segment of liver, inferior portion (VI)
Upper pole of right kidney
Erector spinae m.
Interpolar region of right kidney
Lower pole of right kidney
Quadratus lumborum m.

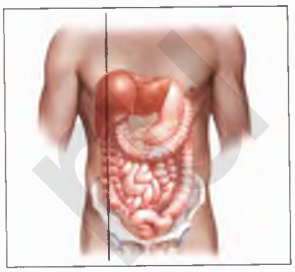

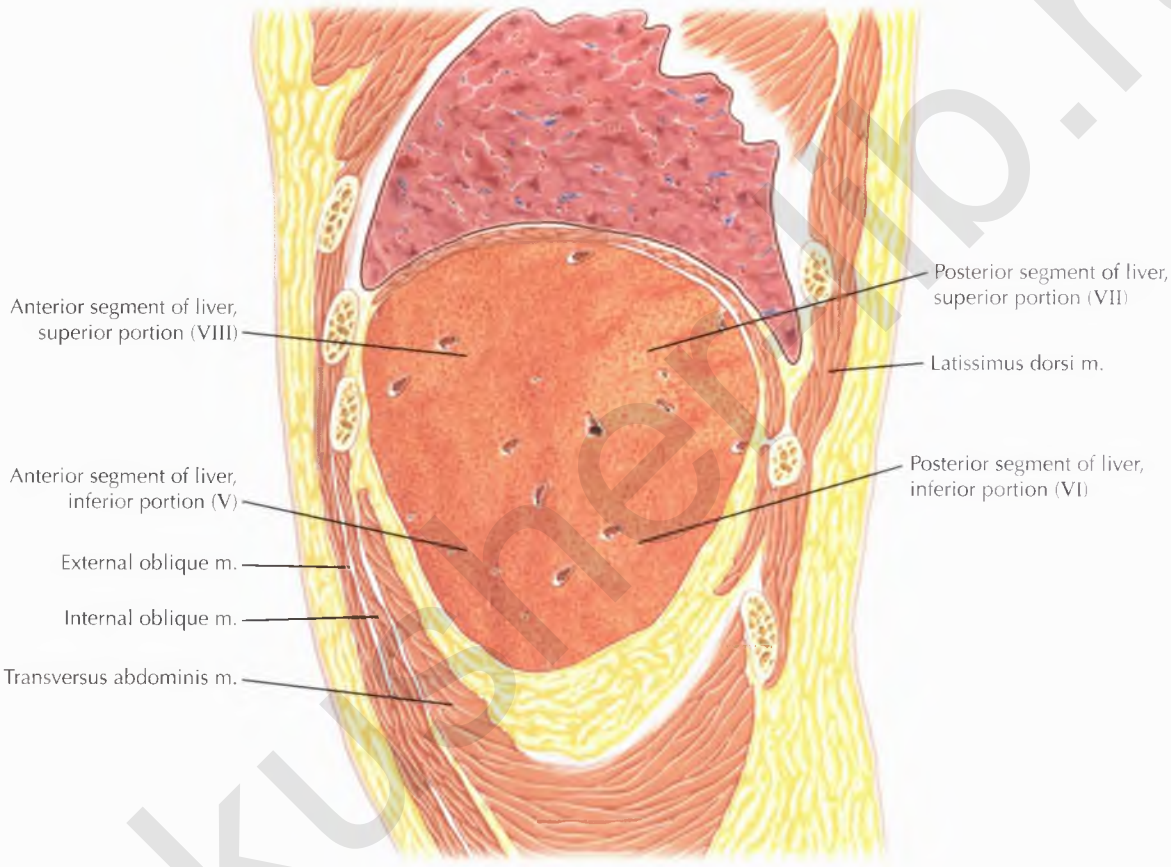

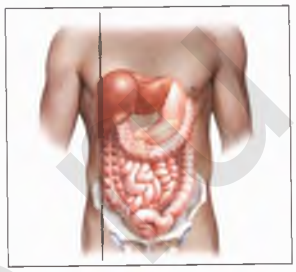

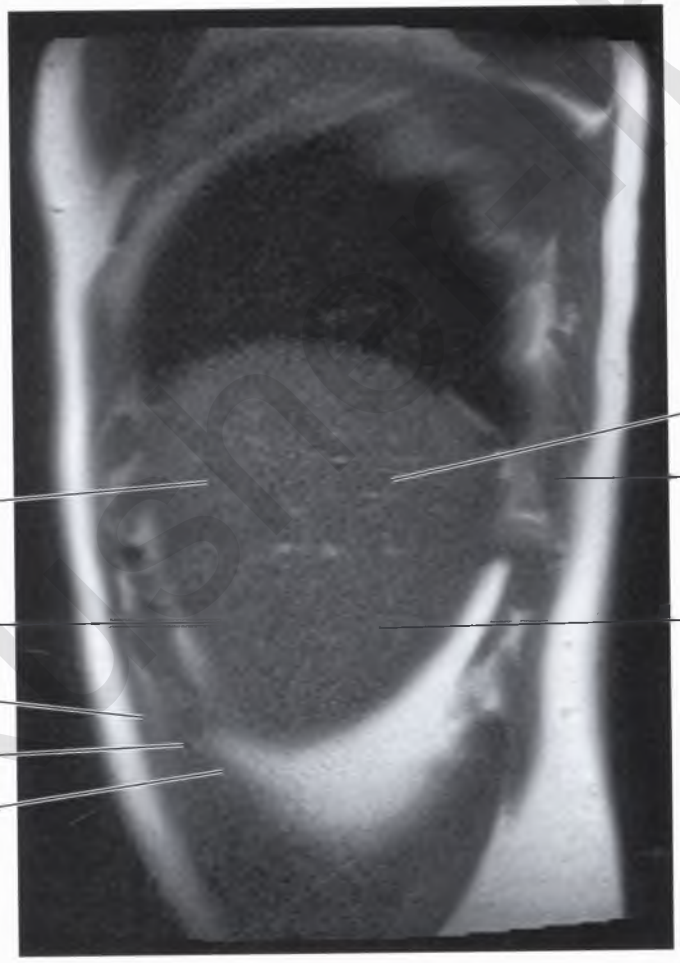
Anterior segment of liver, superior portion (VIII)
Anterior segment of liver, inferior portion (V)
External oblique m.
Internal oblique m.
Transversus abdominis m.
Posterior segment of liver, superior portion (VII)
Latissimus dorsi m.
Posterior segment of liver, inferior portion (VI)

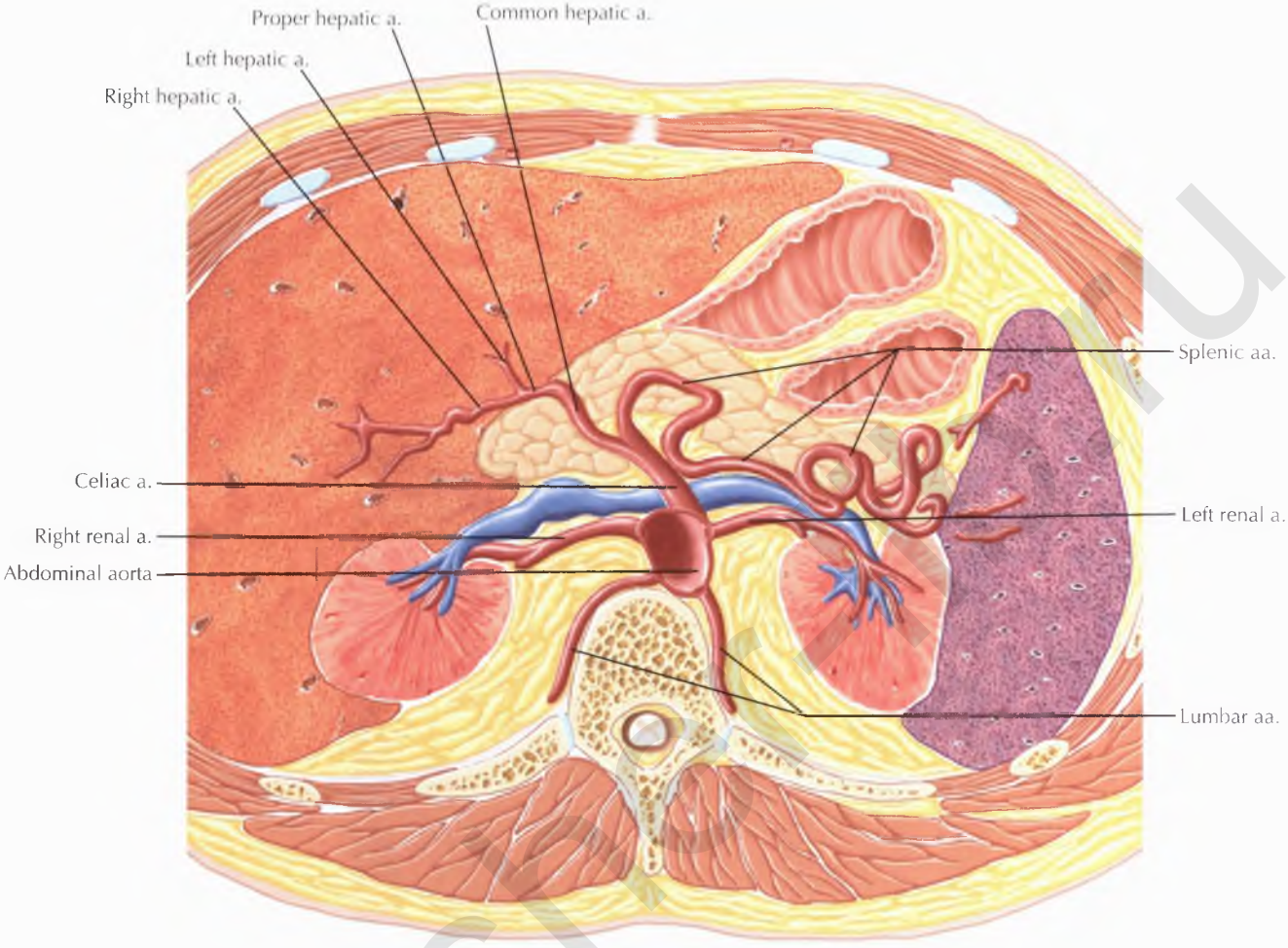

NORMAL ANATOMY

In classic celiac arterial anatomy, the common hepatic artery, left gastric artery, and splenic artery each arise from the celiac axis. The *common hepatic artery* proceeds laterally to the right and becomes the proper hepatic artery after the takeoff of the gastroduodenal artery. The *gastroduodenal artery* proceeds caudally to supply the gastric pylorus, proximal duodenum, and portions of the pancreas. The *proper hepatic artery* classically branches into the left and right hepatic arteries. The right gastric artery has a variable origin from the hepatic artery. The cystic artery to the gallbladder usually arises from the right hepatic artery.

NORMAL VARIANTS

The many hepatic arterial variants include *replaced* right and left hepatic arteries, which arise from arteries other than the proper hepatic artery, and *accessory* right and left hepatic arteries, which also arise from arteries other than the proper hepatic artery, in addition to the presence of the usual right and left hepatic arteries arising from the proper hepatic artery. The most common variants include a *replaced right hepatic artery* arising from the SMA, seen in about 20% of patients, and a *replaced left hepatic artery* arising from the left gastric artery, seen in approximately 15% of patients.

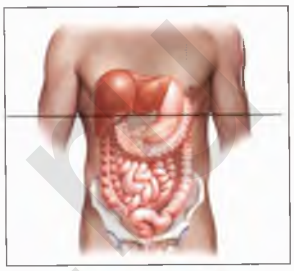

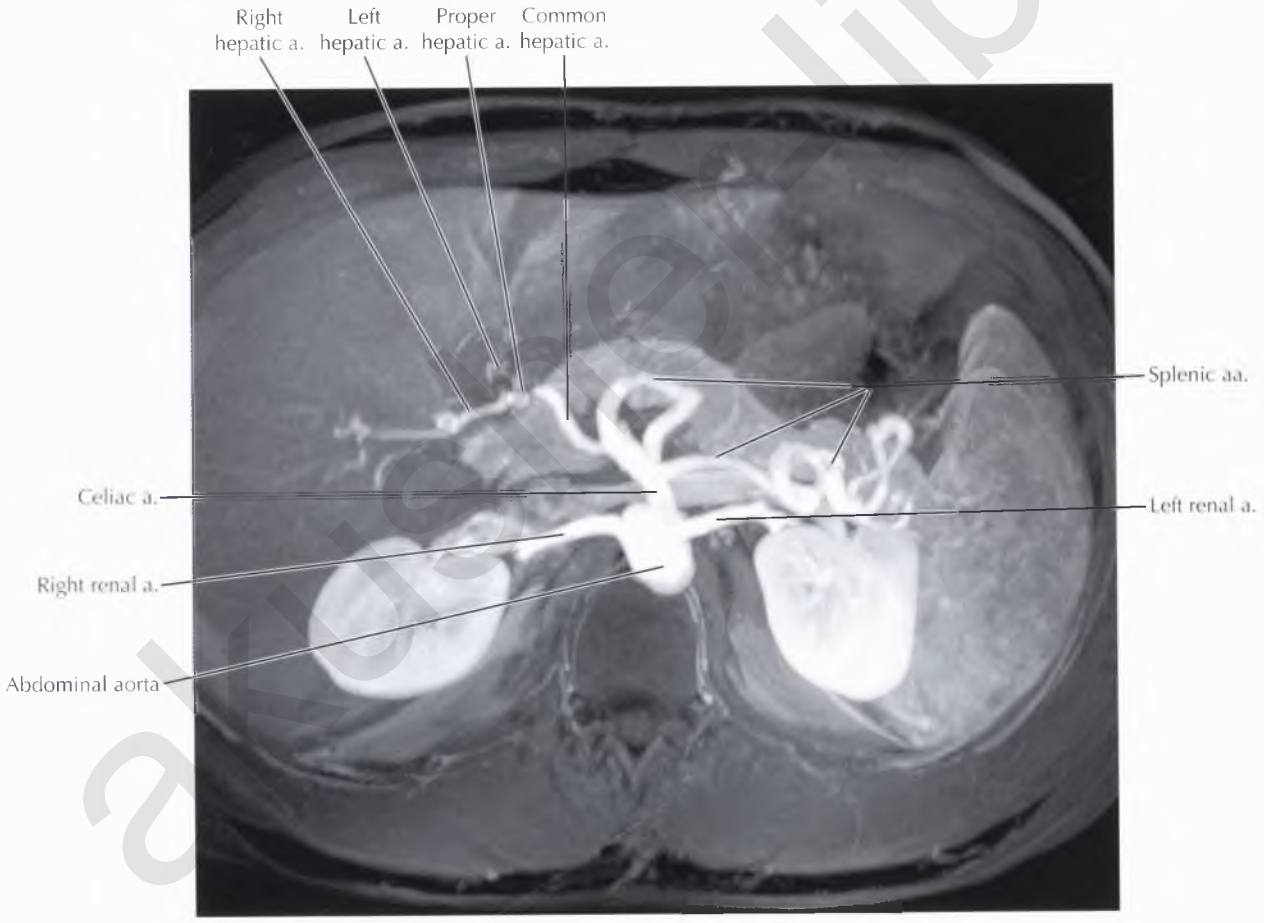
Right hepatic a.
Left hepatic a.
Proper hepatic a.
Common hepatic a.
Splenic aa.
Celiac a.
Left renal a.
Right renal a.
Abdominal aorta

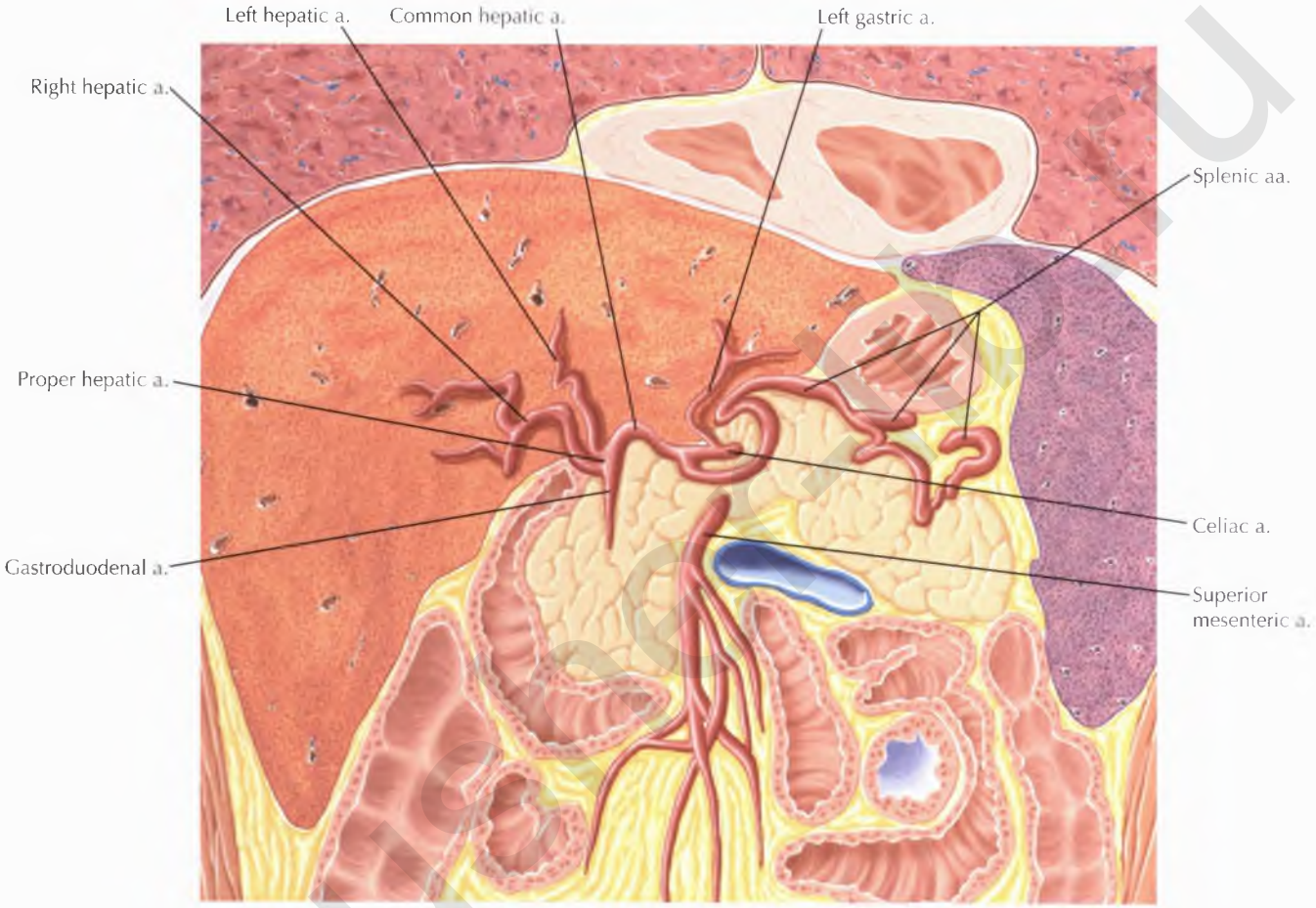

DIAGNOSTIC CONSIDERATION

Contrast-enhanced magnetic resonance angiography (MRA) of the abdomen is often performed to characterize mesenteric artery stenosis in the setting of chronic mesenteric ischemia. MRI findings include stenosis or occlusion of at least two of the three visceral arteries—celiac artery, superior mesenteric artery (SMA), and inferior mesenteric artery (IMA)—along with visualization of collateral circulation through the pancreaticoduodenal arcade (celiac artery to SMA), arc of Riolan (SMA to IMA), or marginal artery of Drummond (SMA to IMA).

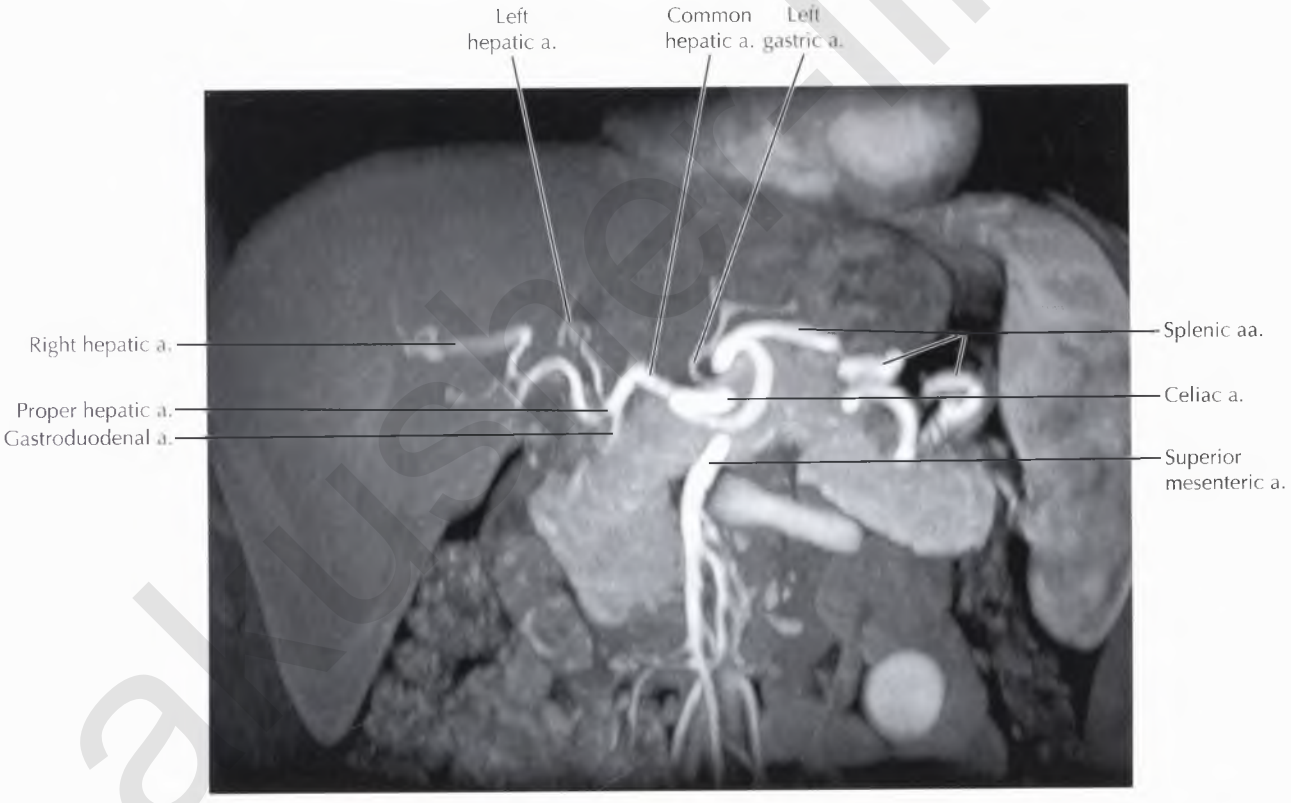

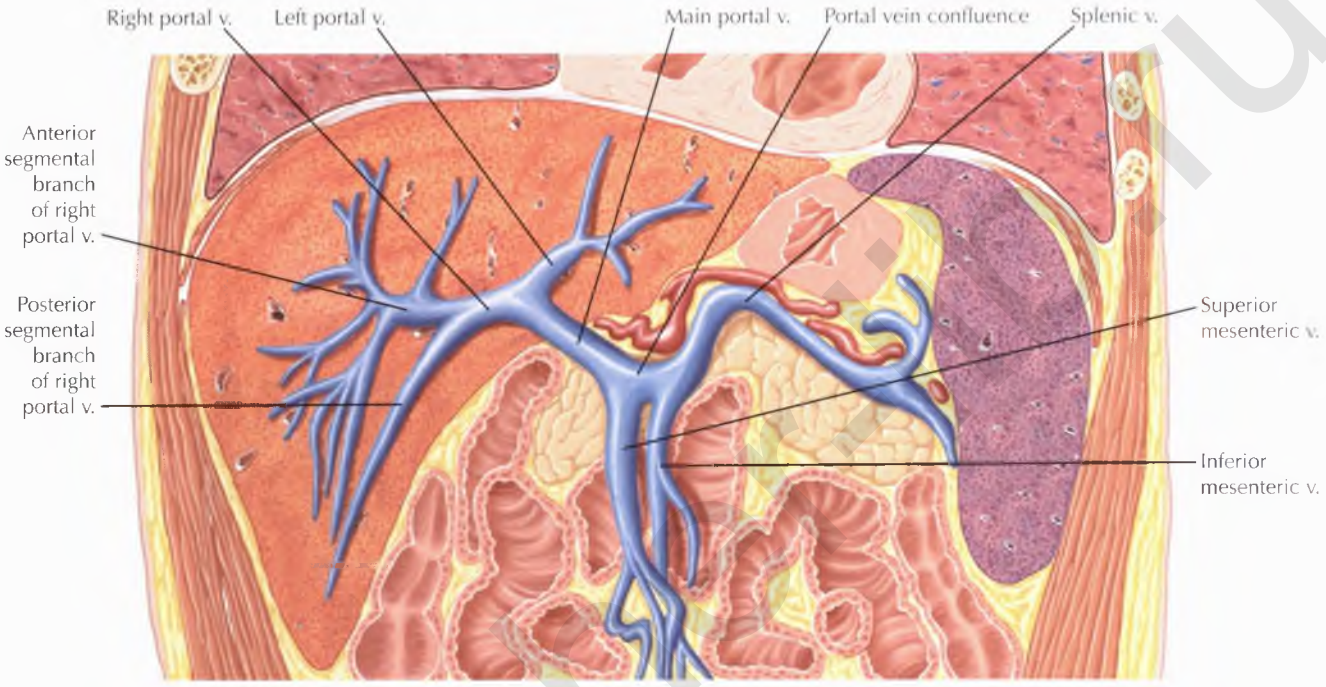

NORMAL ANATOMY

The main portal vein forms from the confluence of the superior mesenteric vein (SMV) and the splenic vein, posterior to the pancreatic neck. The inferior mesenteric vein (IMV) joins the splenic vein along its inferior aspect just before the portal vein confluence.

The main portal vein courses toward the liver within the hepatoduodenal ligament and divides into left and right portal veins near the liver hilum. The left portal vein divides into segmental branches supplying segments II, III, IVa, and IVb of the left hepatic lobe. The right portal vein divides into anterior and posterior segmental branches, then subdivides into branches supplying segments V and VIII anteriorly and segments VI and VII posteriorly. Portal vein inflow to the caudate lobe of the liver (segment I) usually arises from the left portal vein, but inflow is highly variable and may arise from the main portal vein directly or from the right portal vein.

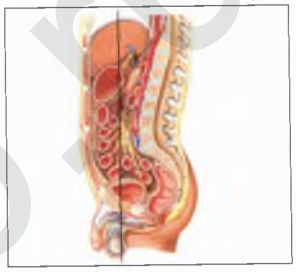

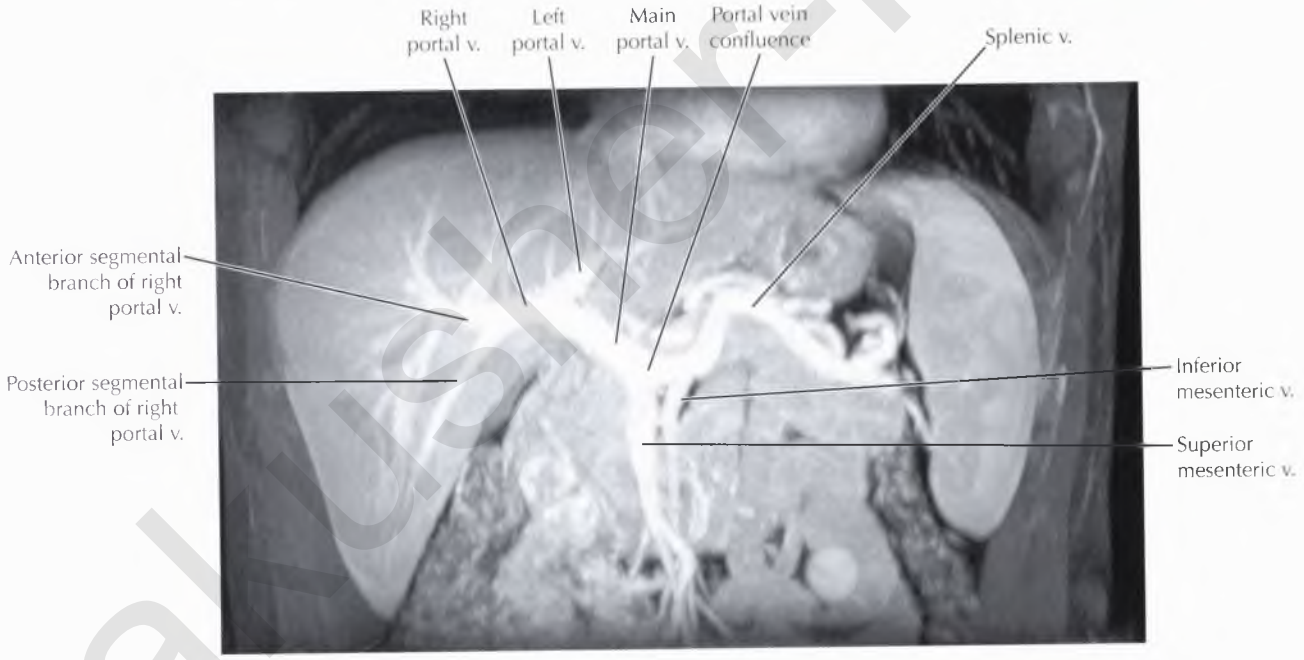

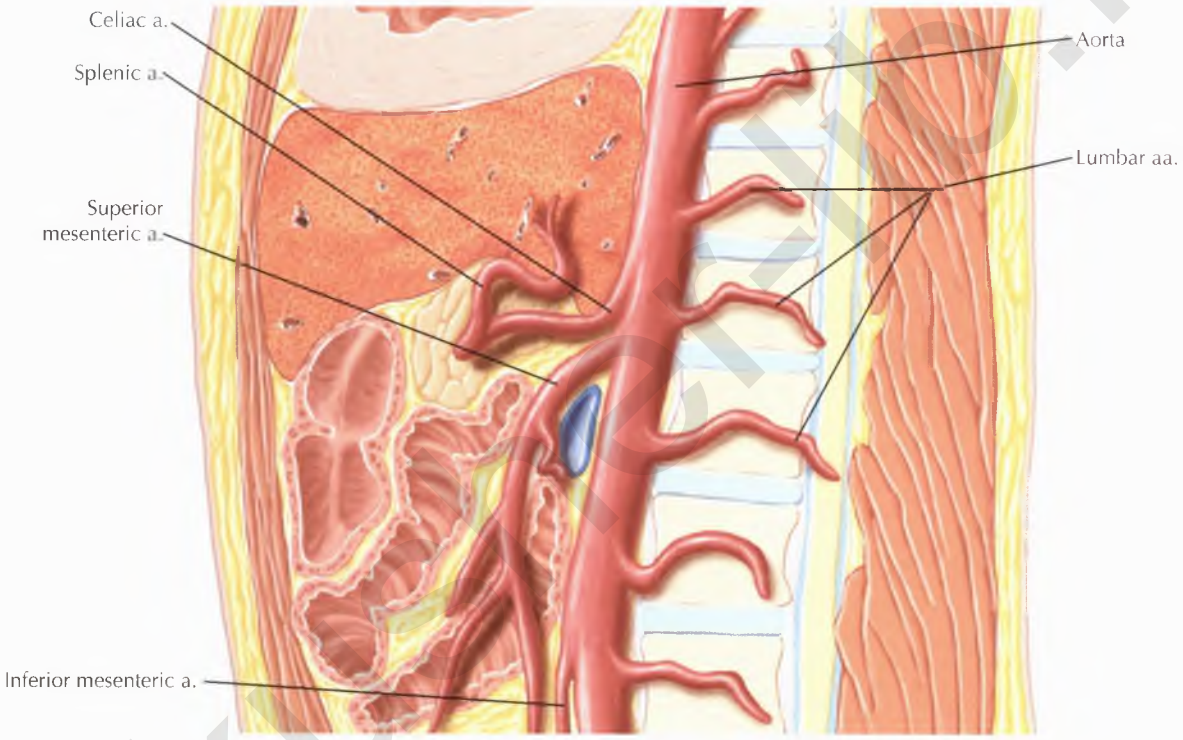

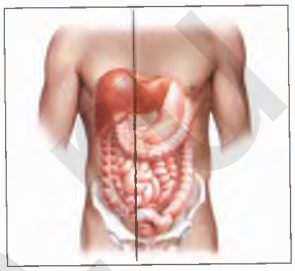


Celiac a.
Aorta
Splenic a.
Superior mesenteric a.
Lumbar aa.
Inferior mesenteric a.

Chapter 3 PERITONEAL CAVITY

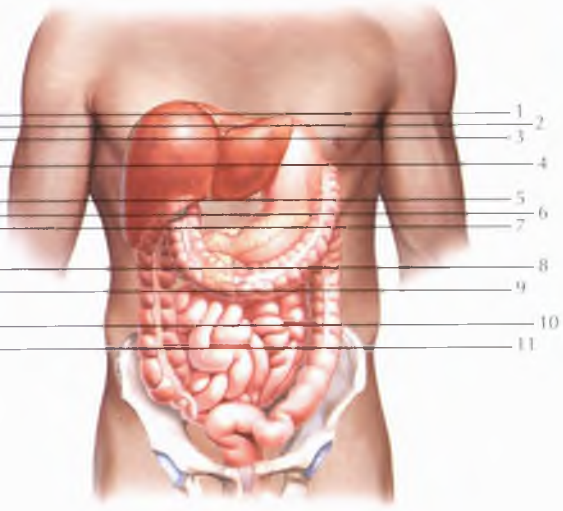

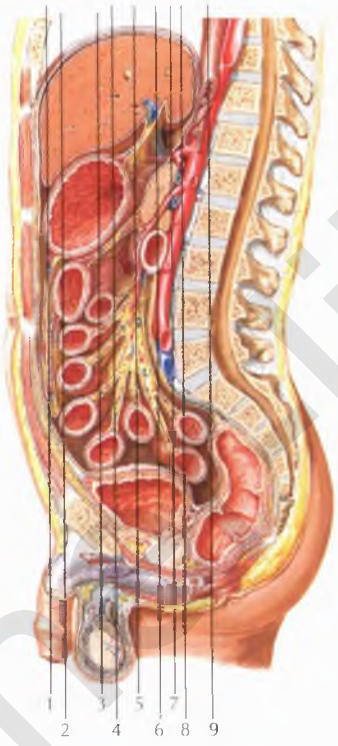

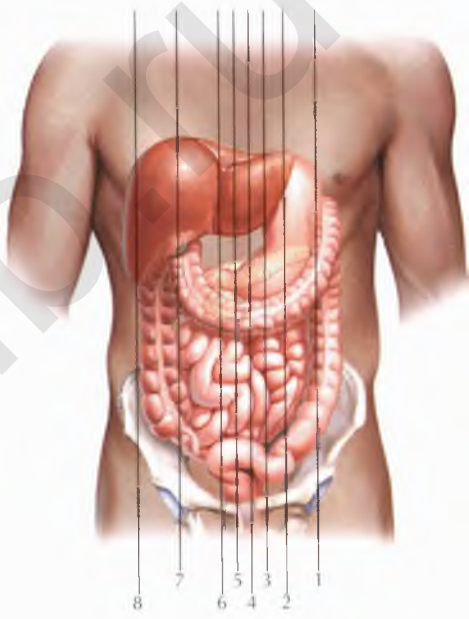

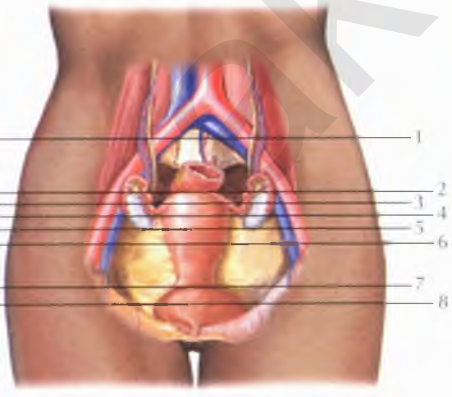

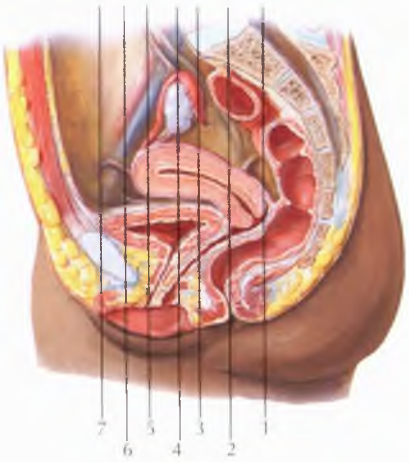

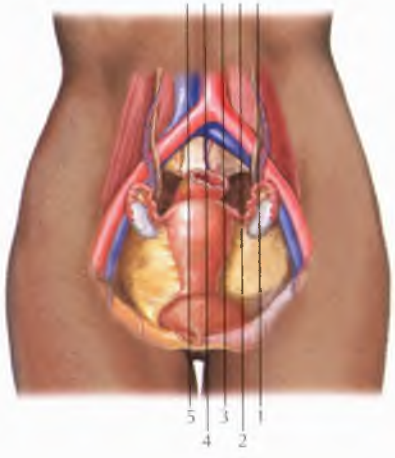

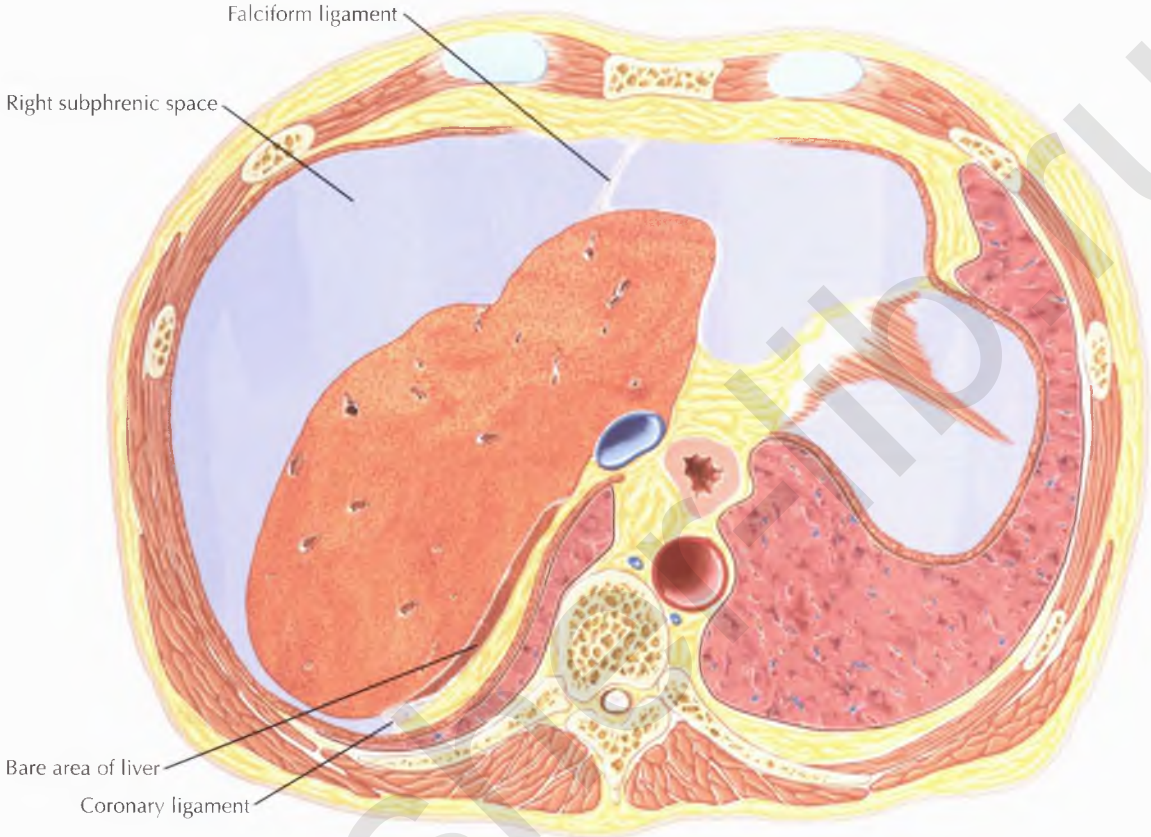

NORMAL ANATOMY

The abdominal peritoneal cavity can be divided by the transverse mesocolon into the supramesocolic and inframesocolic compartments. The *supramesocolic* compartment can be subdivided into the subphrenic spaces, subhepatic spaces, and lesser sac; the *inframesocolic* compartment can be subdivided into the infracolic and paracolic spaces. The *greater sac* of the abdominal peritoneal cavity comprises the subphrenic, subhepatic, infracolic, and paracolic spaces.

PATHOLOGIC PROCESS

The spaces in the peritoneal cavity are best demonstrated in patients with *ascites*, which distends the potential space of the peritoneal cavity and outlines the peritoneal reflections, peritoneal ligaments, mesenteries, and omenta, as demonstrated in this example.

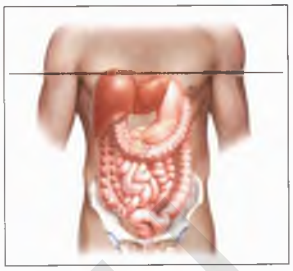

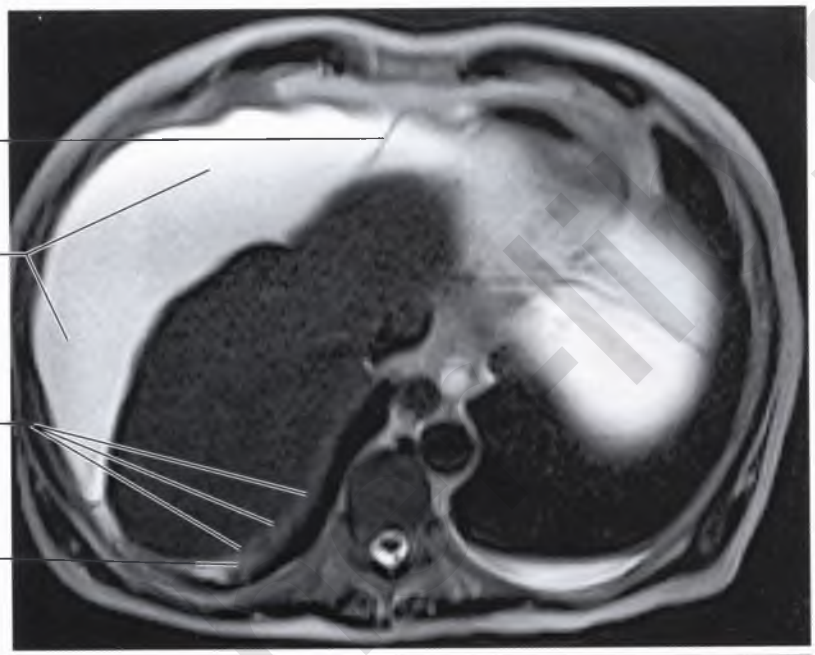
Falciform ligament
Right subphrenic space
Bare area of liver
Coronary ligament

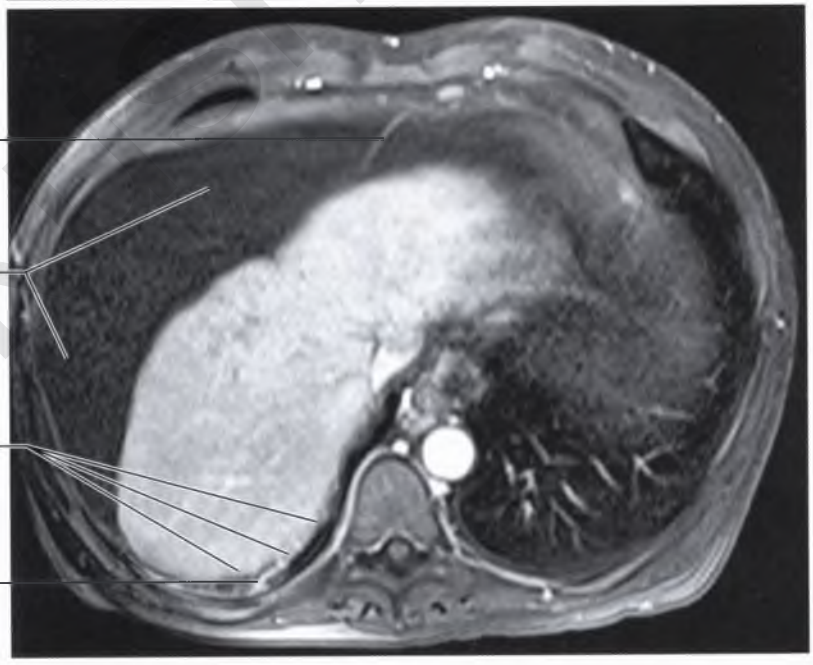
Falciform ligament
Right subphrenic space
Bare area of liver
Coronary ligament

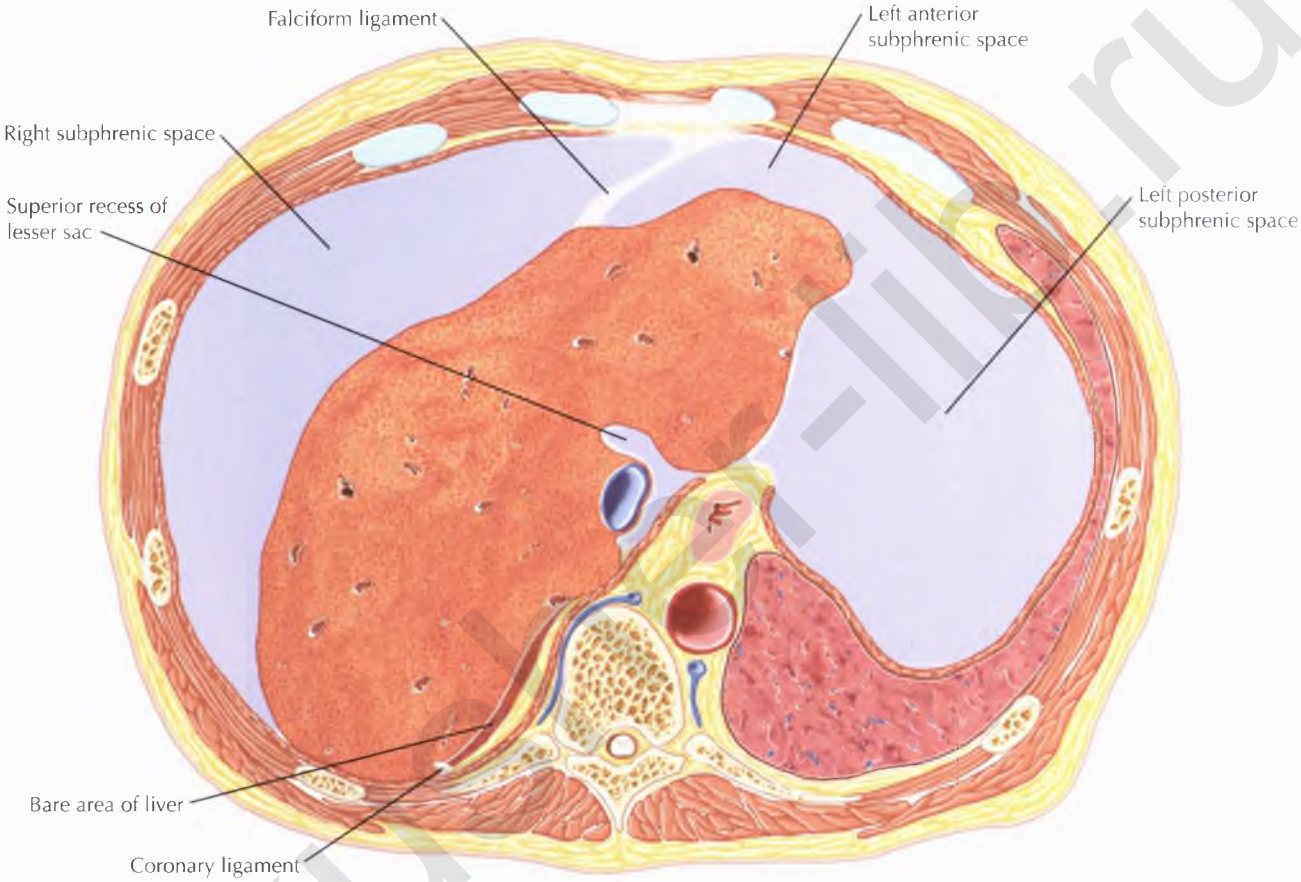

NORMAL ANATOMY

The *right subphrenic space* is bounded by the falciform ligament anteromedially and the right coronary ligament posteriorly. Posteromedial to the right coronary ligament is the *bare area of the liver*, the nonperitonealized attachment of the liver to the diaphragm, where peritoneal ascites is excluded. The bare area of the liver is continuous with the retroperitoneum.

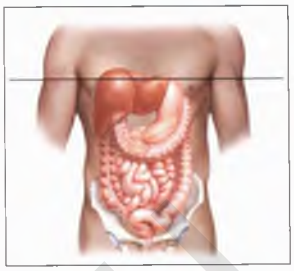

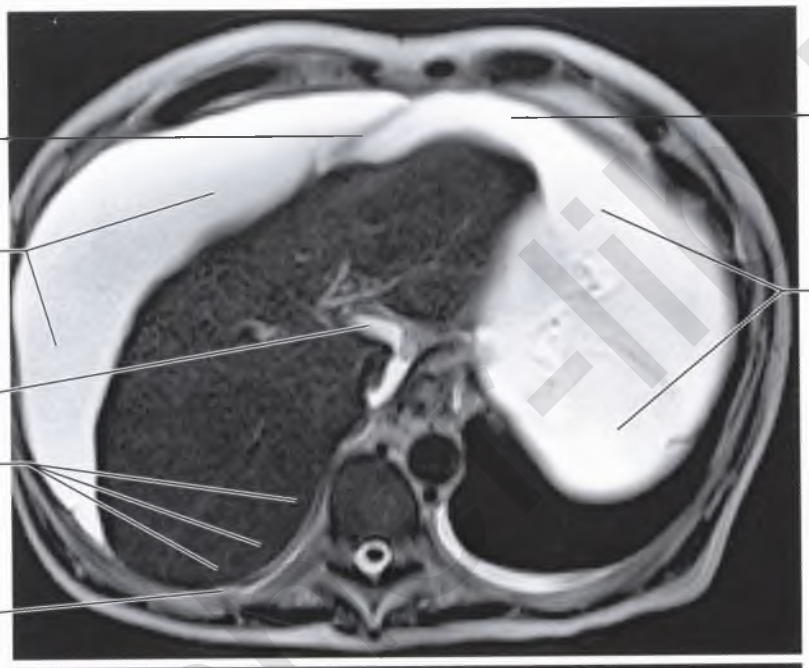
Falciform ligament
Right subphrenic space
Superior recess of lesser sac
Bare area of liver
Coronary ligament
Left anterior subphrenic space
Left posterior subphrenic space


Falciform ligament
Right subphrenic space
Superior recess of lesser sac
Bare area of liver
Coronary ligament
Left anterior subphrenic space
Left posterior subphrenic space

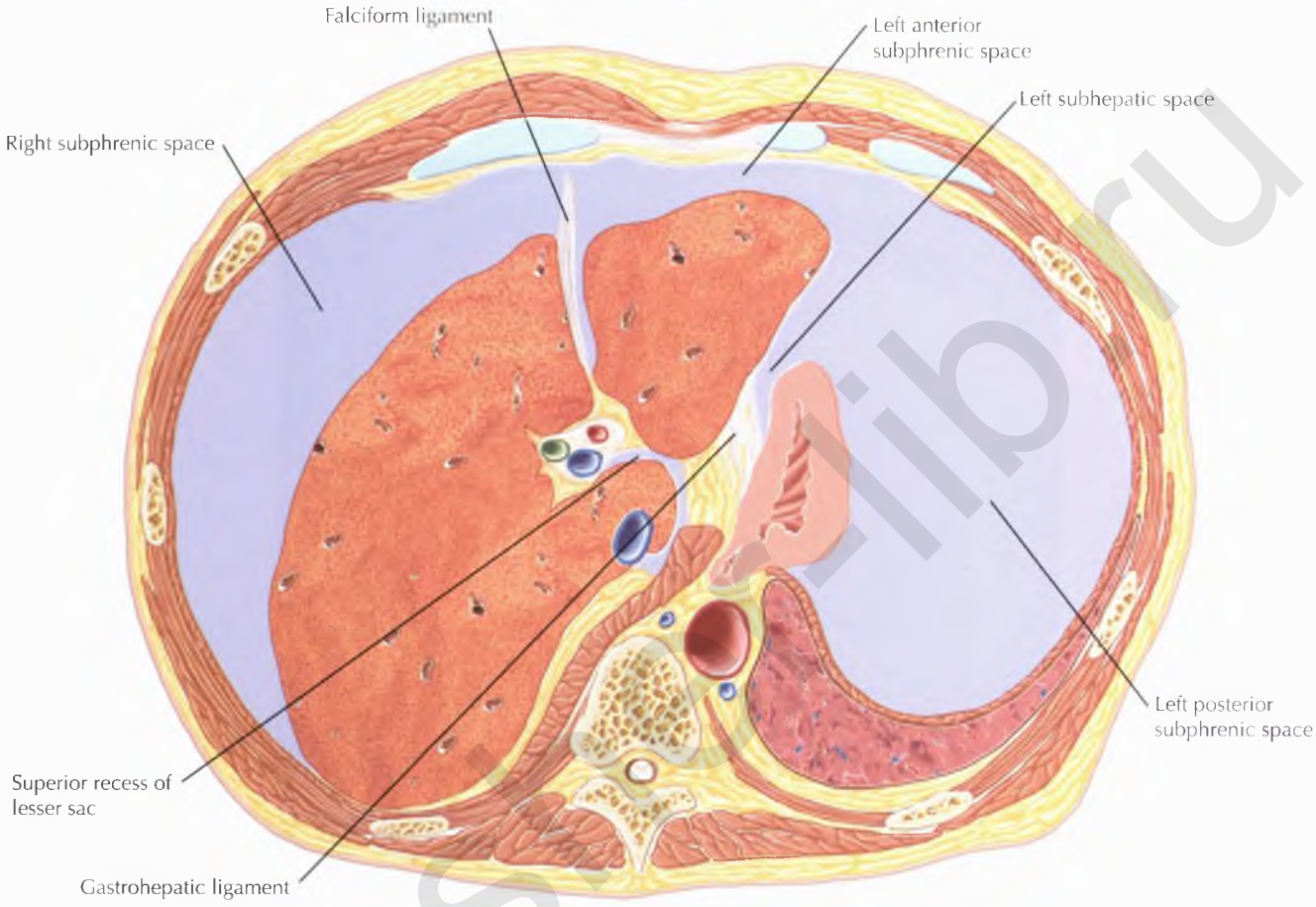

NORMAL ANATOMY

The *left anterior subphrenic space* extends from the falciform ligament anteromedially to surround the anterior left hepatic lobe and anterior gastric wall deep to the diaphragm. The inferior portion of this space, located between the left hepatic lobe posteriorly and the diaphragm anteriorly, may be considered a separate space, called the left anterior *perihepatic* space, which is bounded posteriorly by the left coronary ligament. The *left posterior subphrenic space* completely envelops the spleen and is also known as the "perisplenic space."

The *left subhepatic space*, also known as the "left posterior perihepatic space" or "gastrohepatic recess," is located between the lateral segment of the liver anteriorly and the stomach posteriorly, to the left of the gastrohepatic ligament.

The superior recess of the lesser sac is also seen at this level, adjacent to the caudate lobe of the liver (segment I).

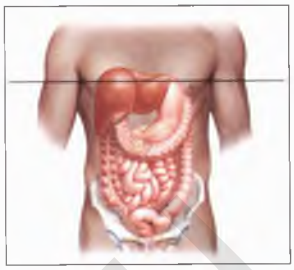

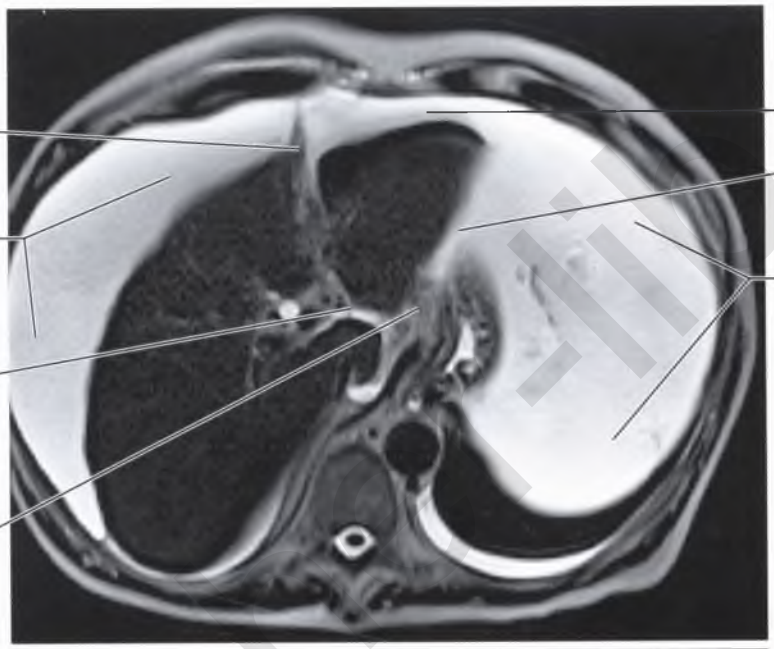
Falciform ligament
Right subphrenic space
Superior recess of lesser sac
Gastrohepatic ligament
Left anterior subphrenic space
Left subhepatic space
Left posterior subphrenic space

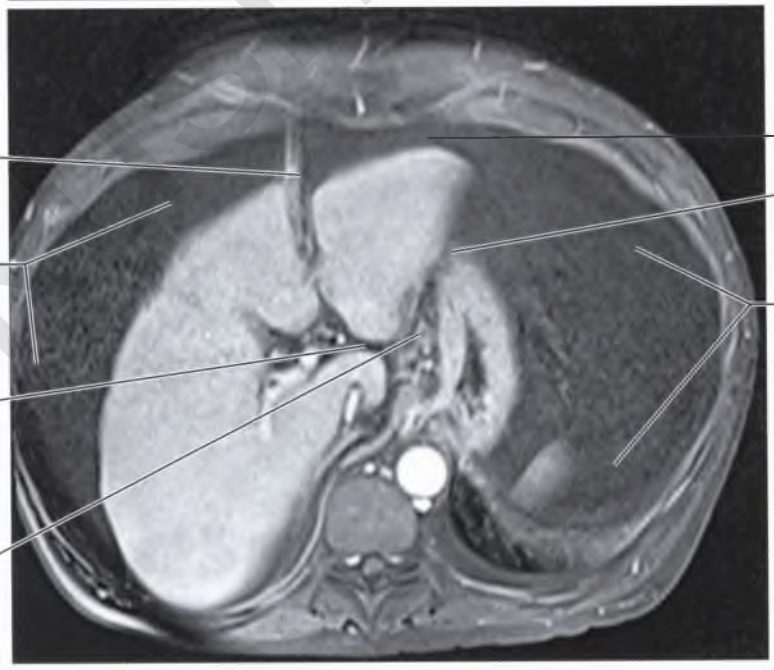
Falciform ligament
Right subphrenic space
Superior recess of lesser sac
Gastrohepatic ligament
Left anterior subphrenic space
Left subhepatic space
Left posterior subphrenic space

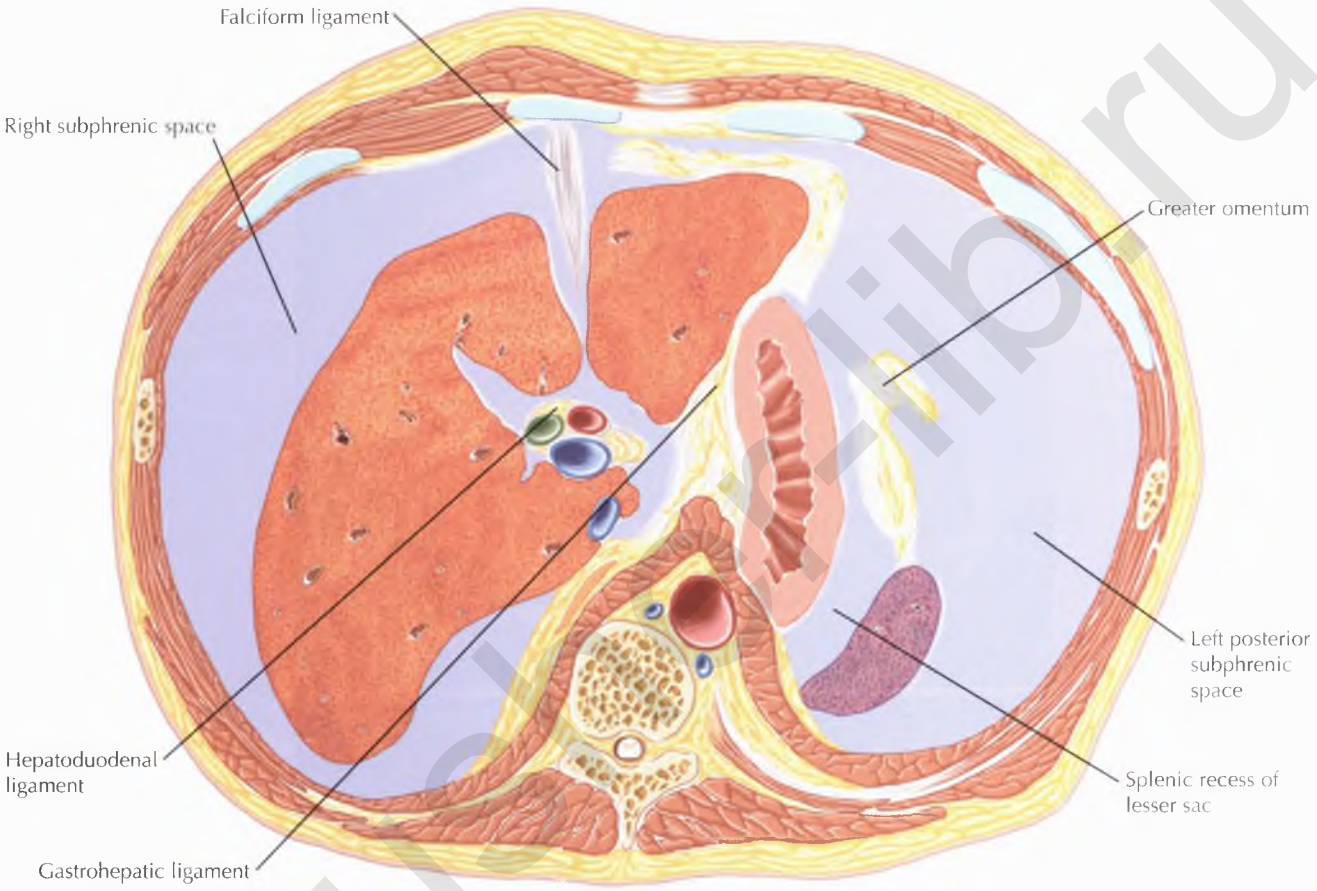

NORMAL ANATOMY

The hepatoduodenal and gastrohepatic ligaments form the lesser omentum (peritoneal fold) and can be seen at this level. The *gastrohepatic ligament* can be found by locating the left gastric artery, which runs within the ligament. The coronary vein also runs within the gastrohepatic ligament.

The *splenic recess* of the lesser sac is also seen at this level, between the gastric fundus and spleen.

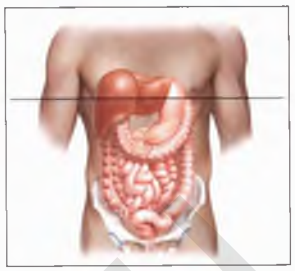

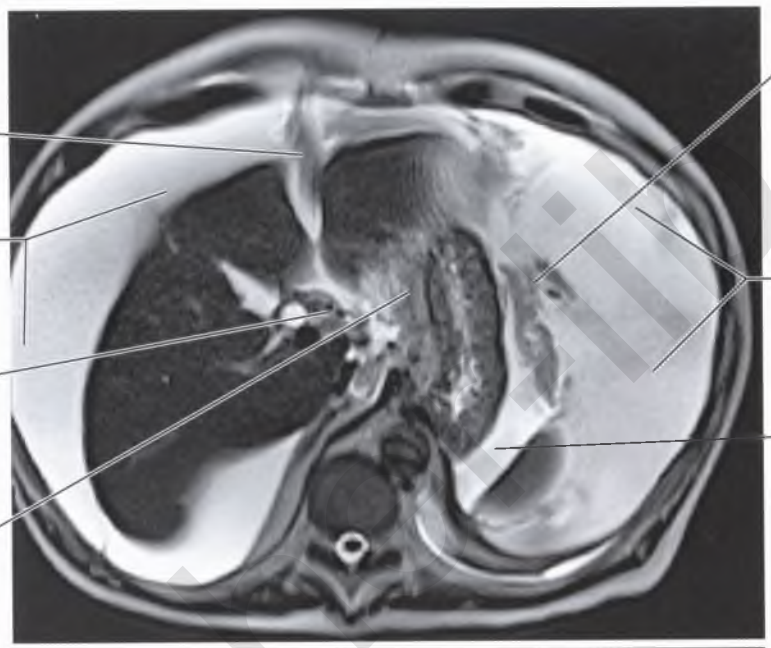

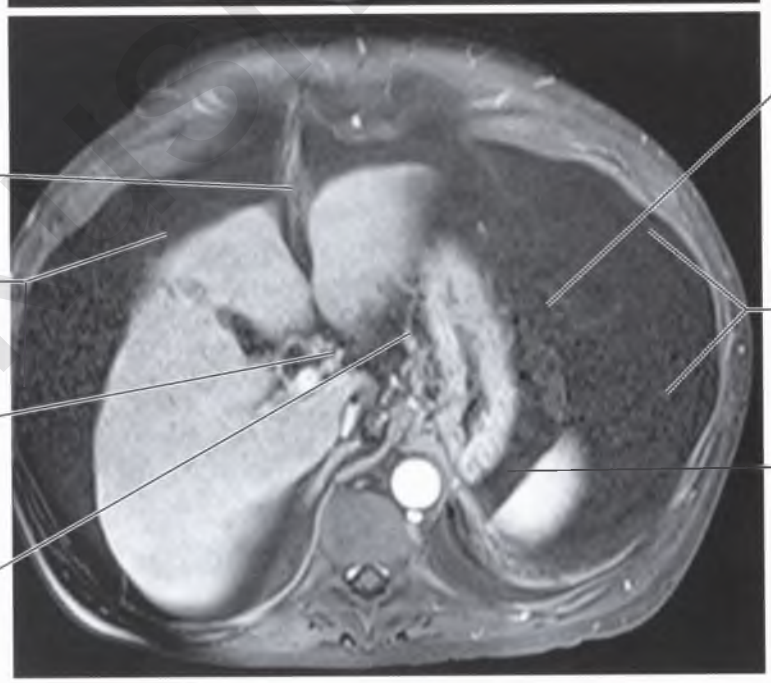

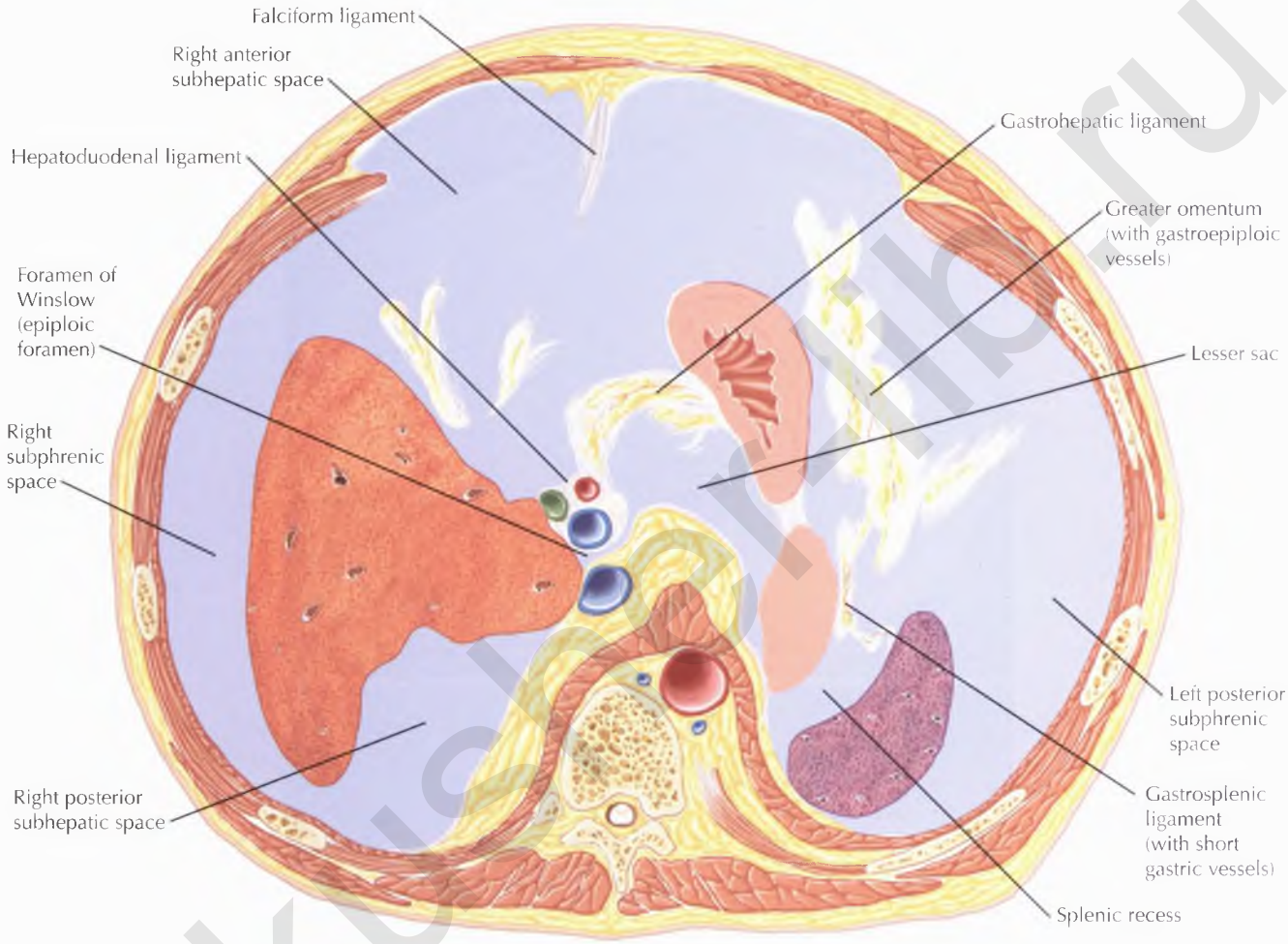

NORMAL ANATOMY

The *hepatoduodenal ligament* extends from the porta hepatis to the duodenum and contains the proper hepatic artery, main portal vein, and common bile duct. The hepatoduodenal ligament forms the anterior margin of the foramen of Winslow, also known as the *epiploic foramen*, which is the communication between the lesser and greater sacs.

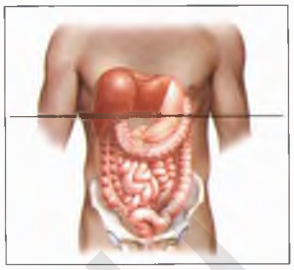

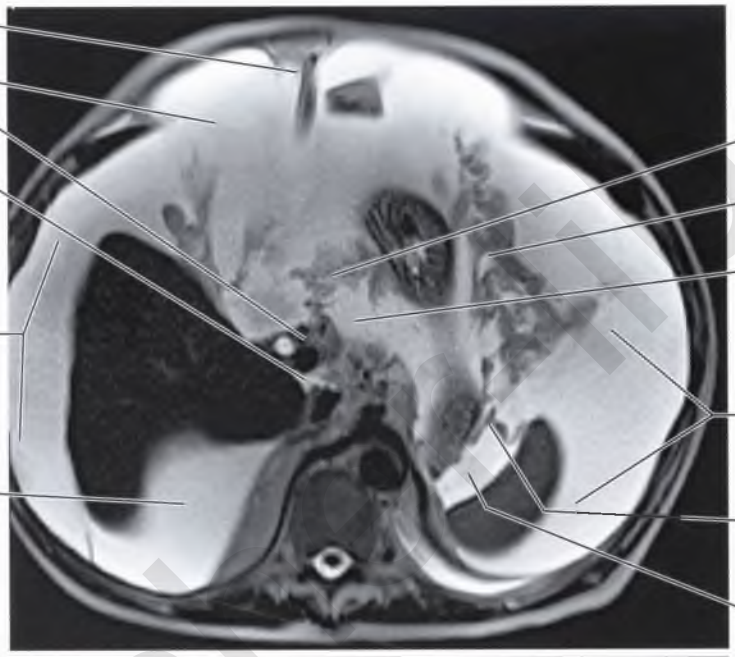
Falciform ligament
Right anterior subhepatic space
Hepatoduodenal ligament
Foramen of Winslow (epiploic foramen)
Right subphrenic space
Right posterior subhepatic space
Gastrohepatic ligament
Greater omentum (with gastroepiploic vessels)
Lesser sac
Left posterior subphrenic space
Gastrosplenic ligament (with short gastric vessels)
Splenic recess

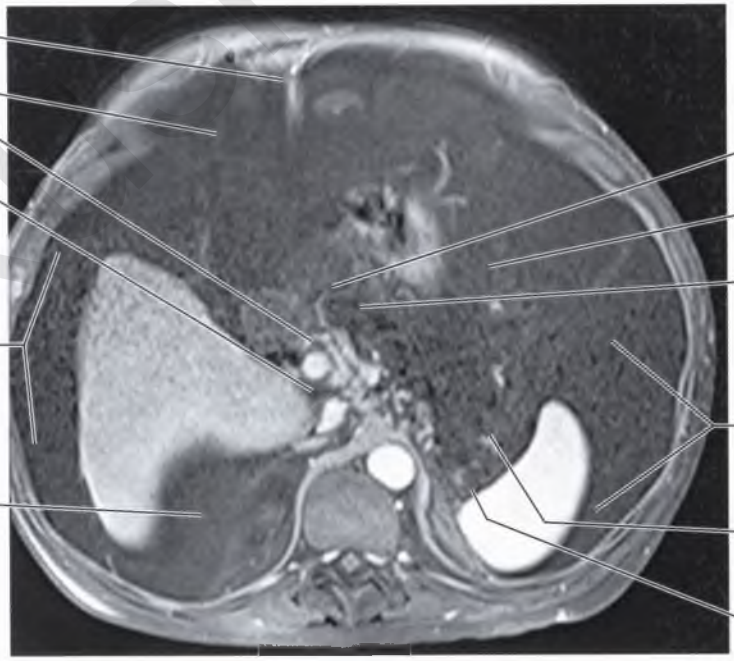
Falciform ligament
Right anterior subhepatic space
Hepatoduodenal ligament
Foramen of Winslow (epiploic foramen)
Right subphrenic space
Right posterior subhepatic space
Gastrohepatic ligament
Greater omentum (with gastroepiploic vessels)
Lesser sac
Left posterior subphrenic space
Gastrosplenic ligament (with short gastric vessels)
Splenic recess

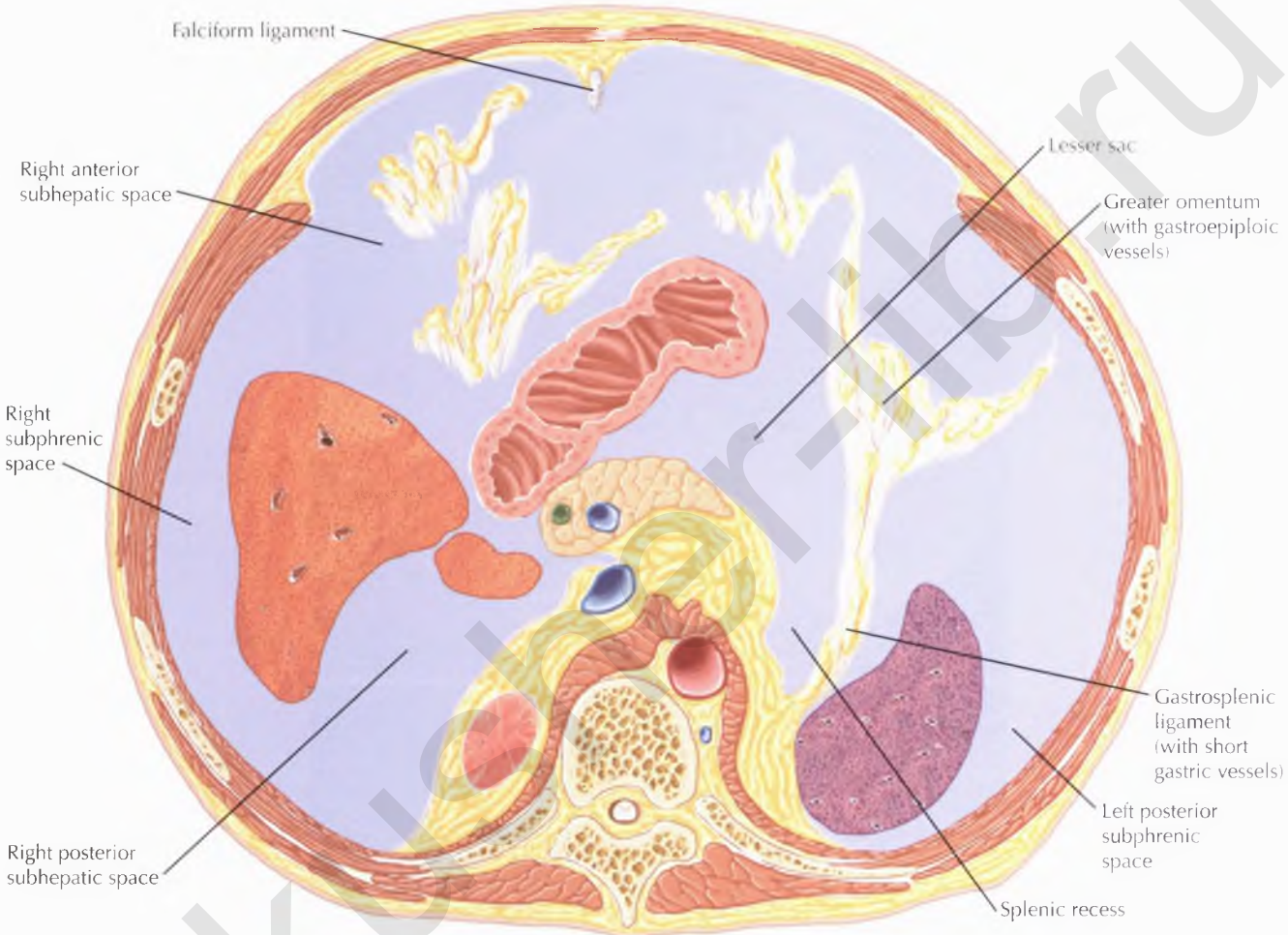

NORMAL ANATOMY

The *lesser sac* is bounded by the pancreas posteriorly, the stomach and gastrohepatic ligament anteriorly, and the gastrosplenic ligament and greater omentum laterally. Note that the gastrosplenic ligament is a part of the greater omentum.

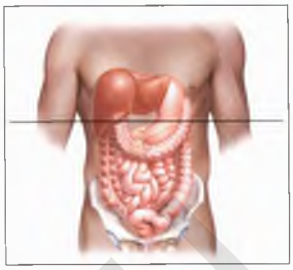

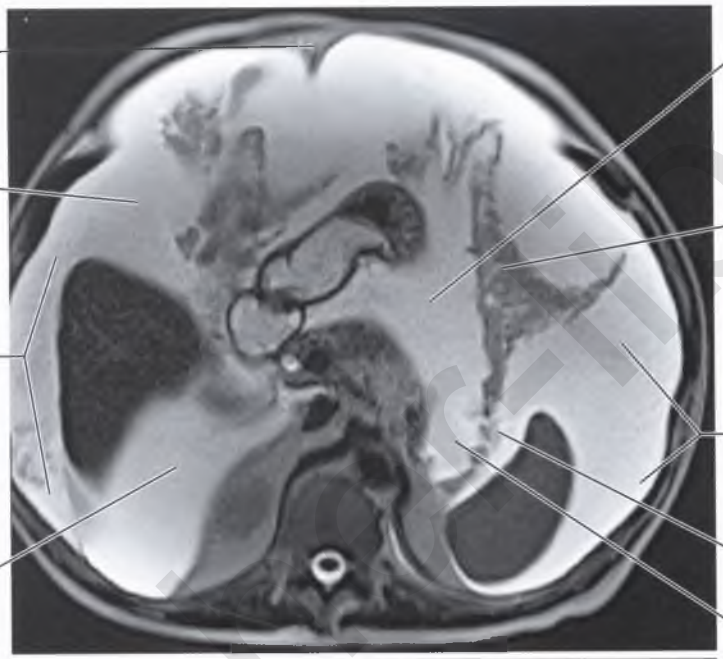
Falciform ligament
Right anterior subhepatic space
Right subphrenic space
Right posterior subhepatic space
Lesser sac
Greater omentum (with gastroepiploic vessels)
Left posterior subphrenic space
Gastrosplenic ligament (with short gastric vessels)
Splenic recess

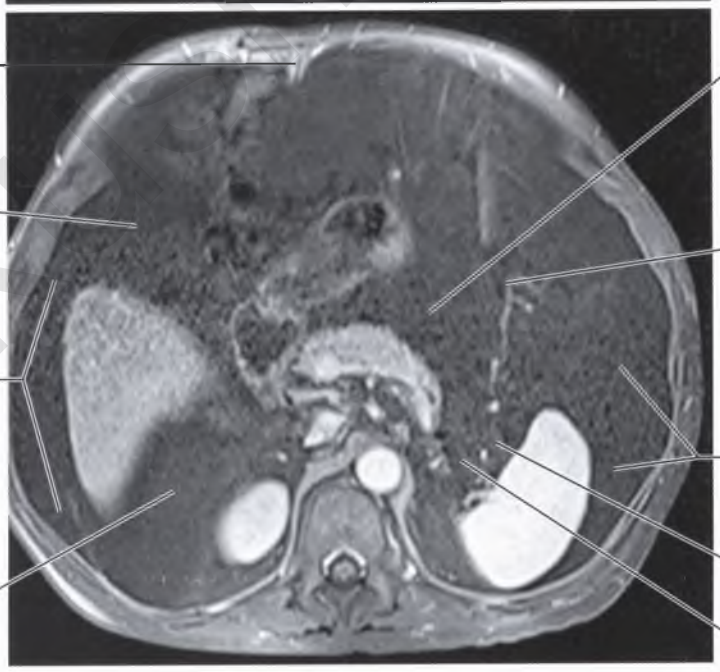
Falciform ligament
Right anterior subhepatic space
Right subphrenic space
Right posterior subhepatic space
Lesser sac
Greater omentum (with gastroepiploic vessels)
Left posterior subphrenic space
Gastrosplenic ligament (with short gastric vessels)
Splenic recess

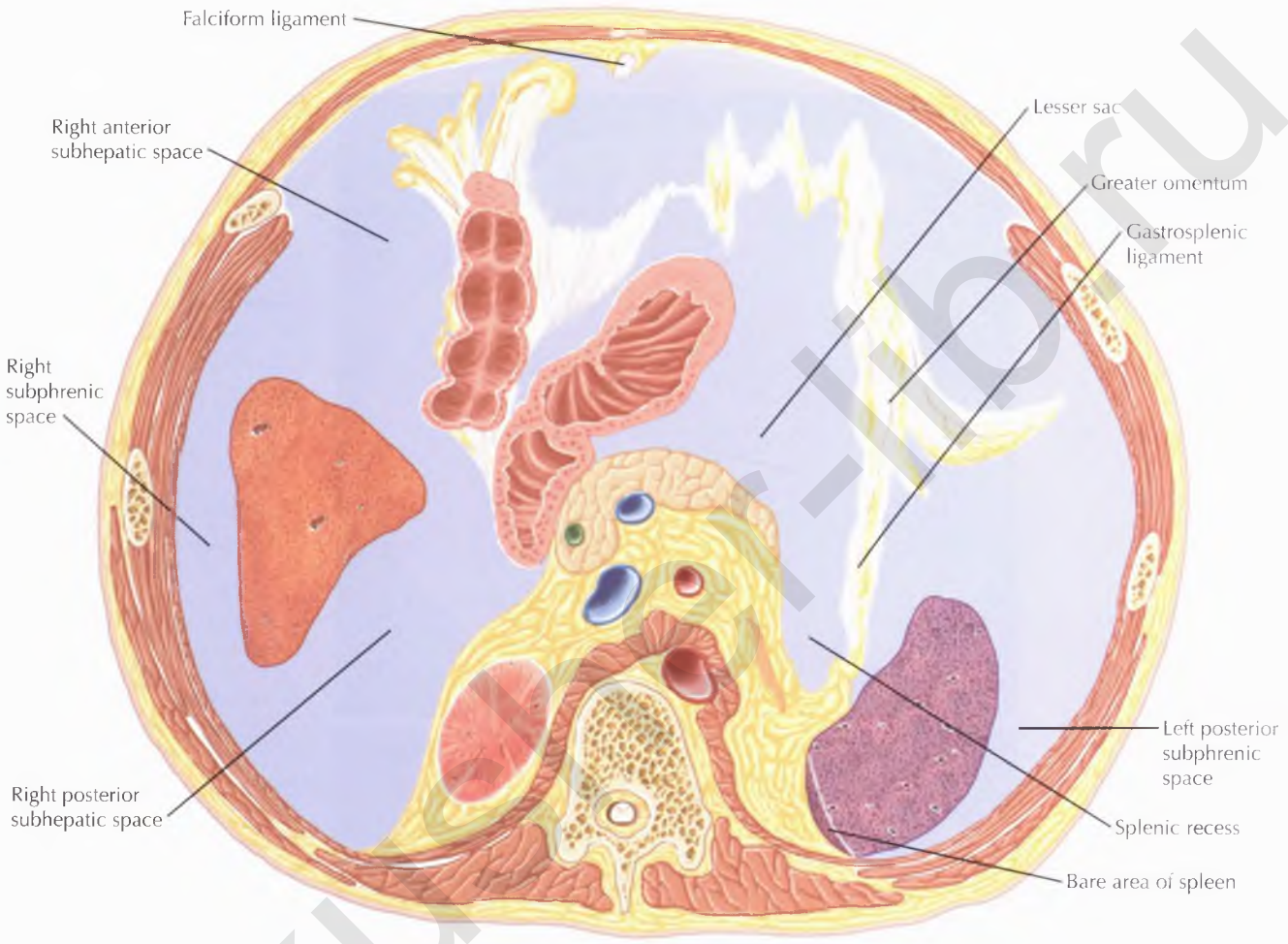

NORMAL ANATOMY

The *right subhepatic space* (with anterior and posterior portions) is bounded superiorly by the inferior right lobe of the liver and is continuous with the right subphrenic space and right paracolic space. The right *posterior* subhepatic space, also known as *Morison's pouch* or the hepatorenal space, is seen between the posterior right hepatic lobe and the right kidney, and is the most dependent portion of the abdominal peritoneal cavity in the supine position. As such, this space is a common location for peritoneal fluid to accumulate.

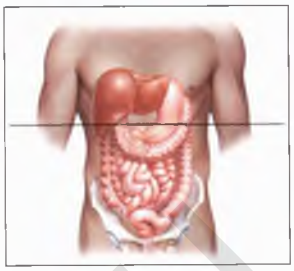

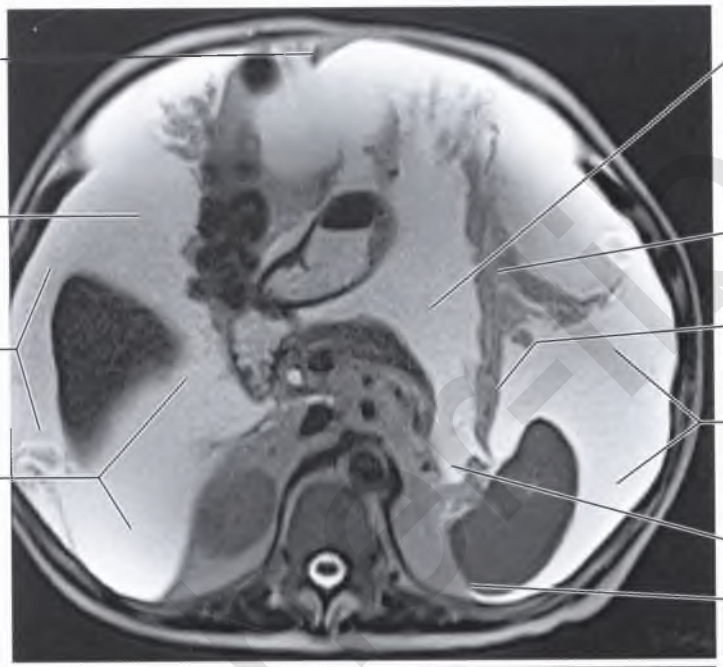

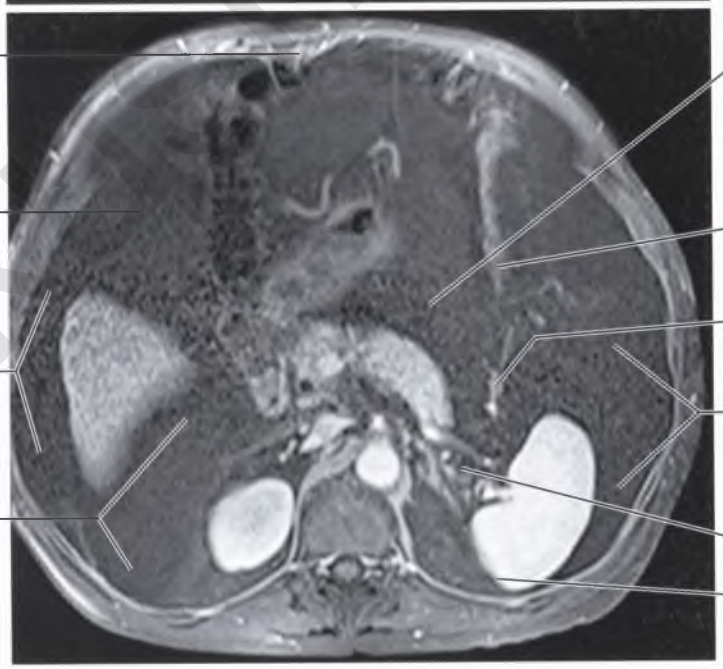

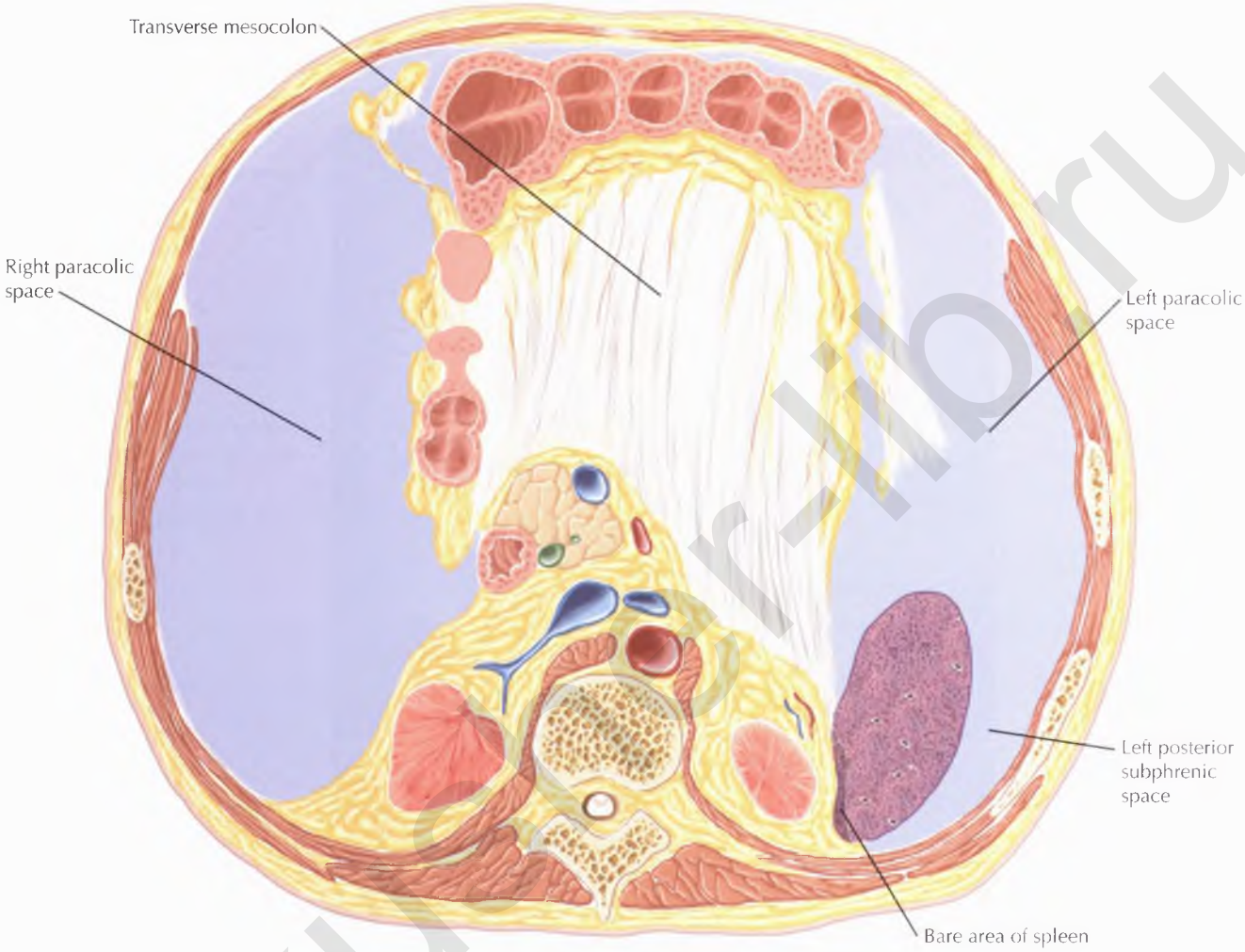

NORMAL ANATOMY

The spleen is attached posteriorly to the retroperitoneum by the splenorenal ligament, forming the bare area of the spleen. The splenic artery and vein travel within the splenorenal ligament at the splenic hilum.

The transverse mesocolon is seen extending from the anterior aspect of the retroperitoneum at the level of the pancreas to the posterior superior wall of the transverse colon, dividing the abdominal peritoneal cavity into the supramesocolic and inframesocolic compartments described earlier. This may serve as a conduit for the spread of disease from the retroperitoneum to the transverse colon, as in the patient with acute pancreatitis.

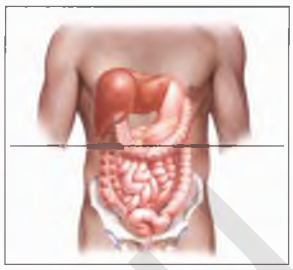

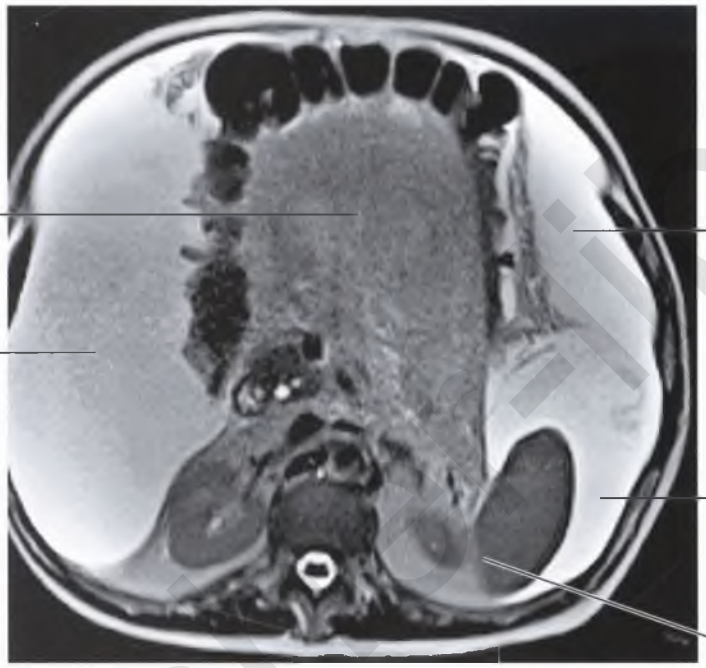

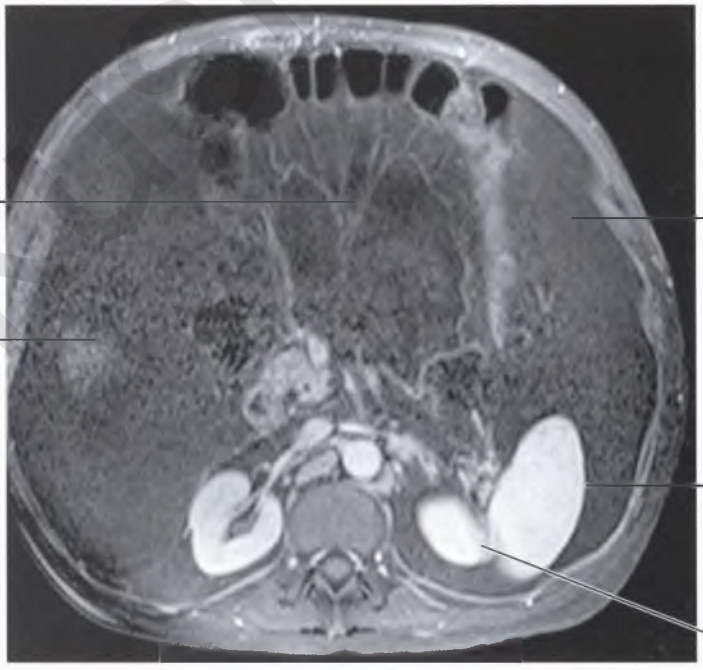

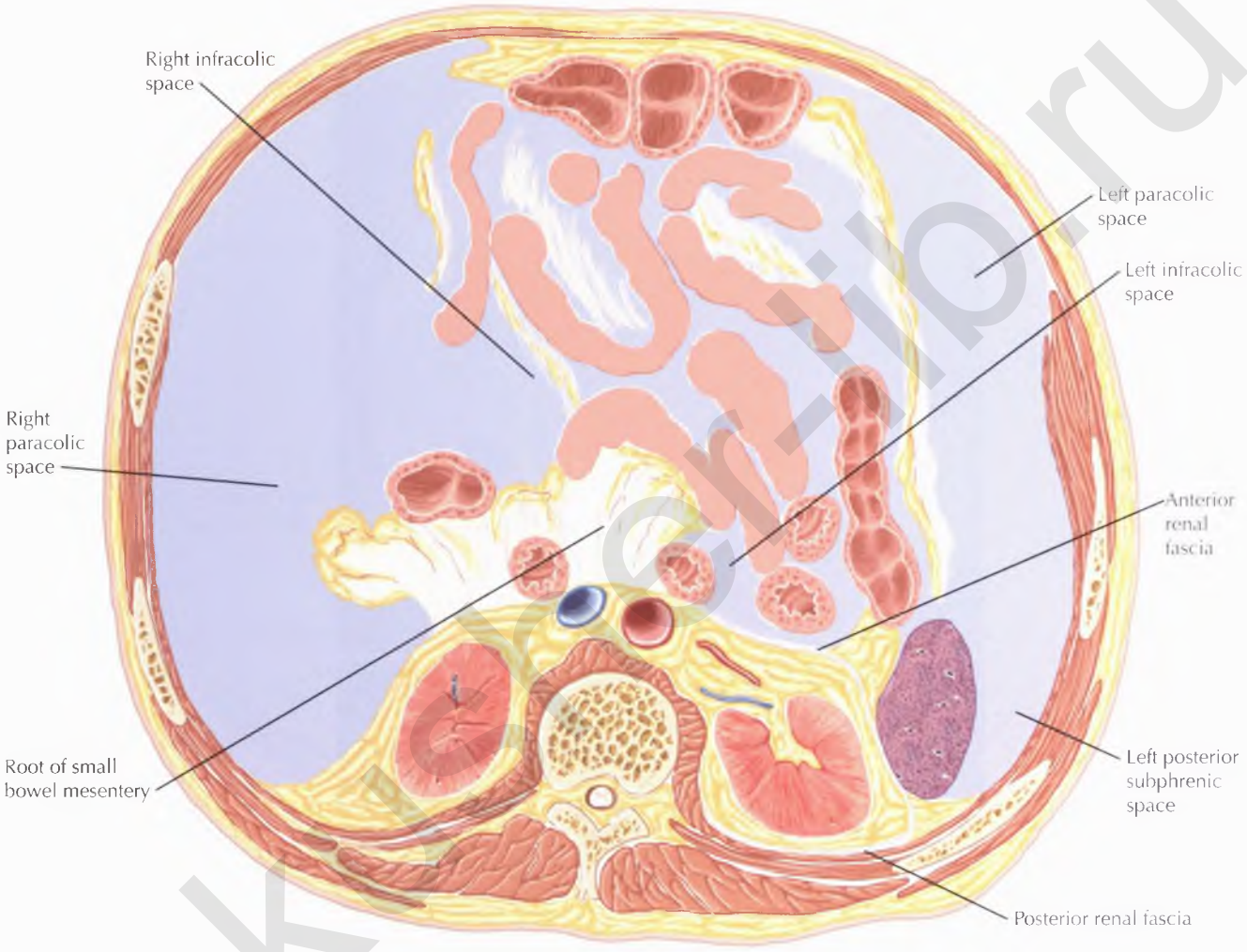

NORMAL ANATOMY

The root of the small bowel mesentery is seen at the duodenal-jejunal junction, suspended by the ligament of Treitz.

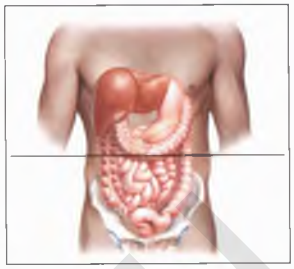

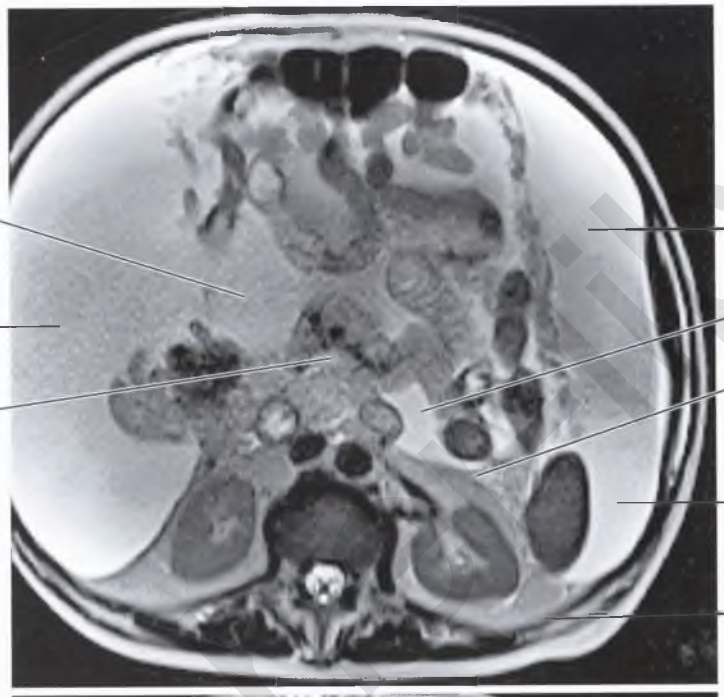

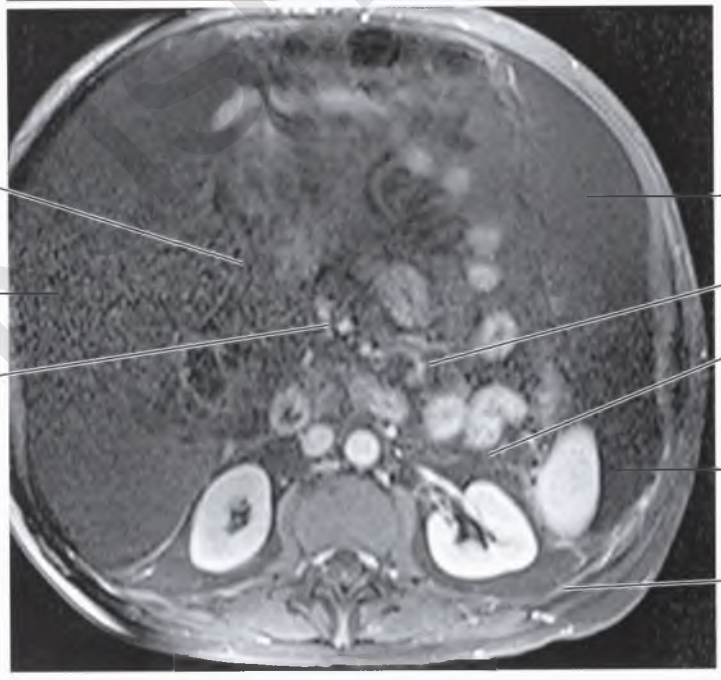

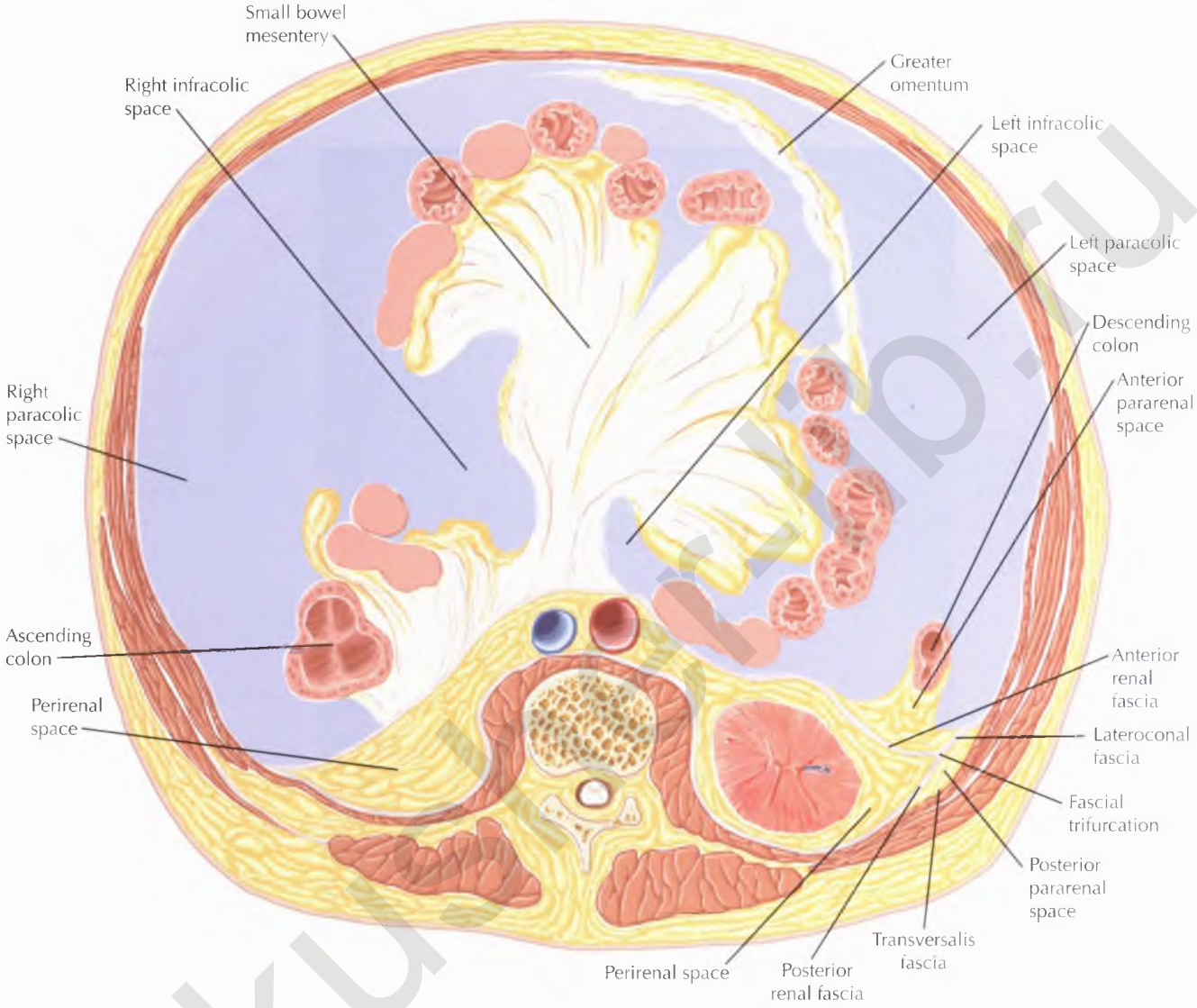

NORMAL ANATOMY

The retroperitoneum can be divided into three spaces. The *anterior pararenal space* is bounded anteriorly by the posterior parietal peritoneum and posteriorly by the *anterior renal fascia* (ARF), also called Gerota's fascia, and contains the ascending and descending colon, pancreas, and the 2nd to 4th portions of the duodenum. The *perirenal space* is formed by the ARF, the lateroconal fascia, and the *posterior renal fascia* (PRF), also known as Zuckerkandl's fascia, and contains the kidneys, adrenal glands, renal vasculature, and lymphatics, as well as the bridging renal septa of Kunin, which can serve as a conduit for disease spread through the perirenal space. The *posterior pararenal space* is bounded by the PRF and lateroconal fascia anteriorly and the transversalis fascia posteriorly, and is contiguous with the properitoneal fat anteriorly and laterally.

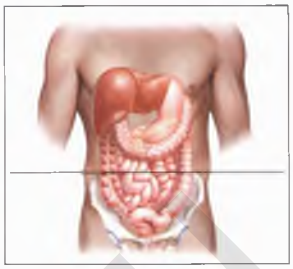

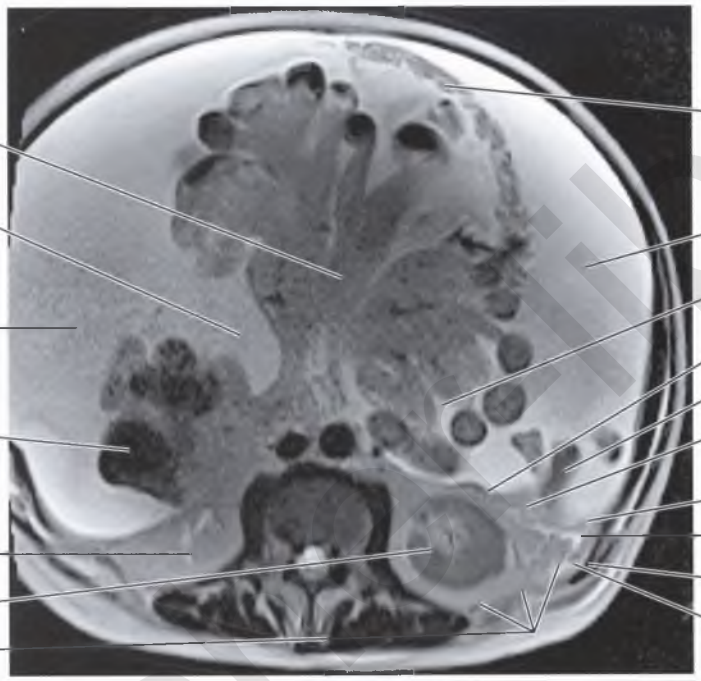

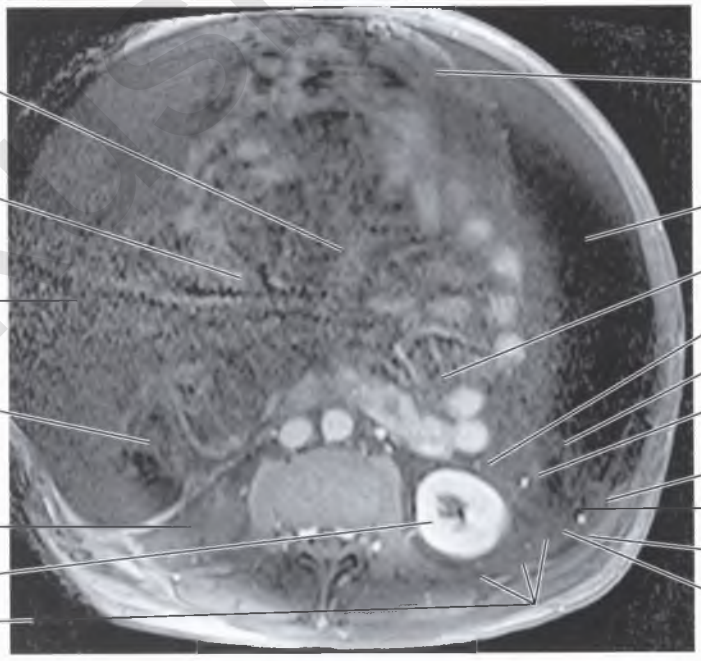

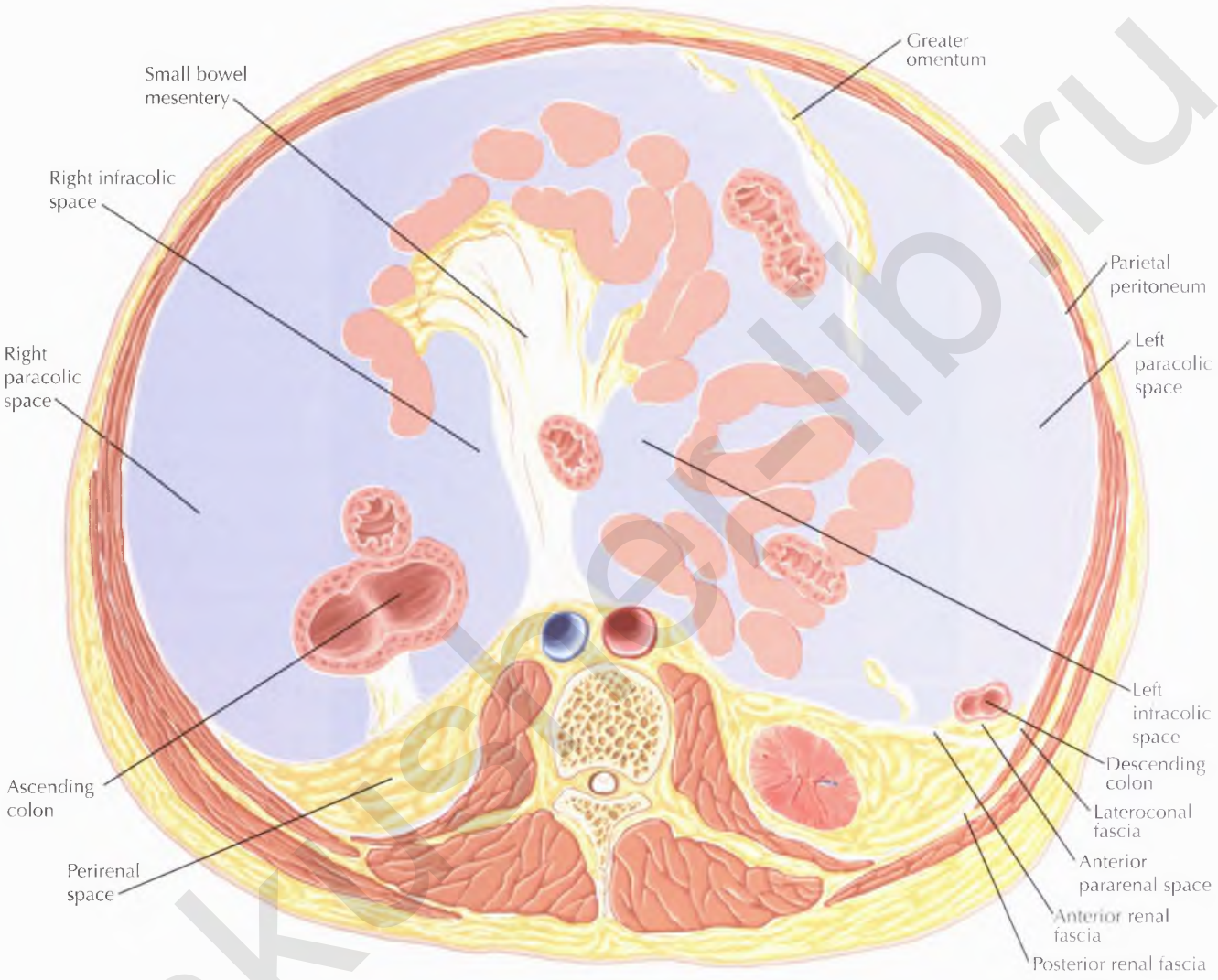

NORMAL ANATOMY

The *right infracolic space* is seen between the ascending colon and the small bowel mesentery. The *left infracolic space* is seen between the descending colon and the small bowel mesentery, and is in continuity with the pelvic peritoneal space.

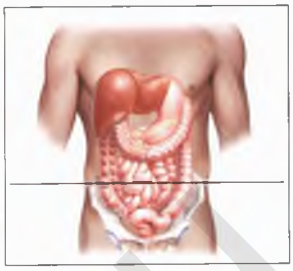

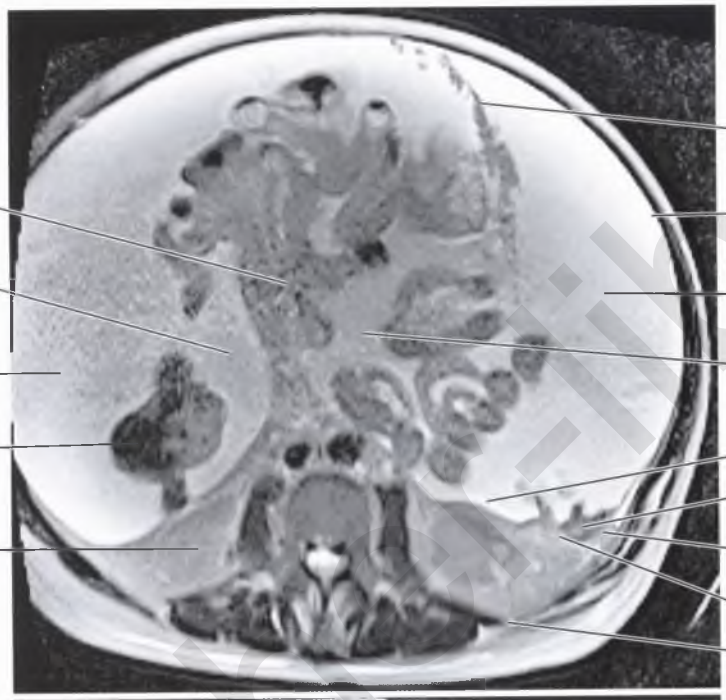

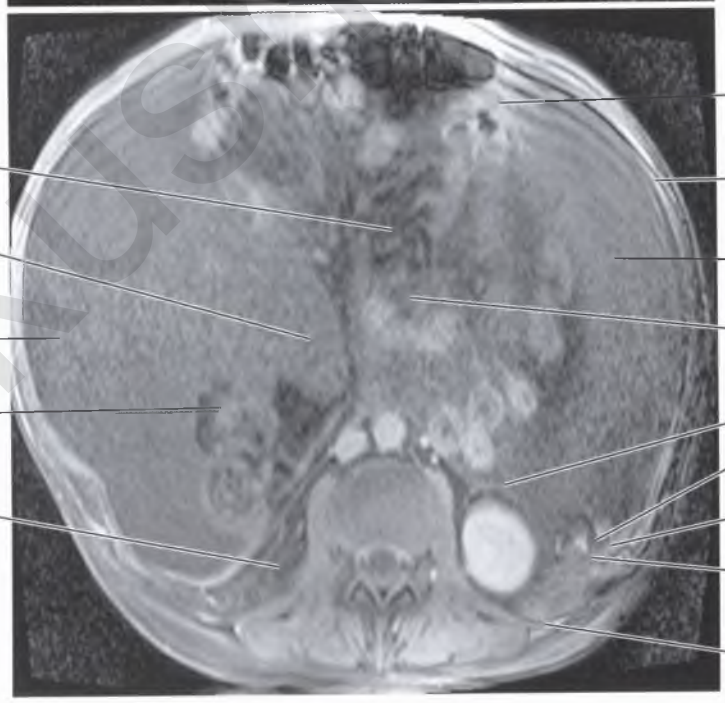

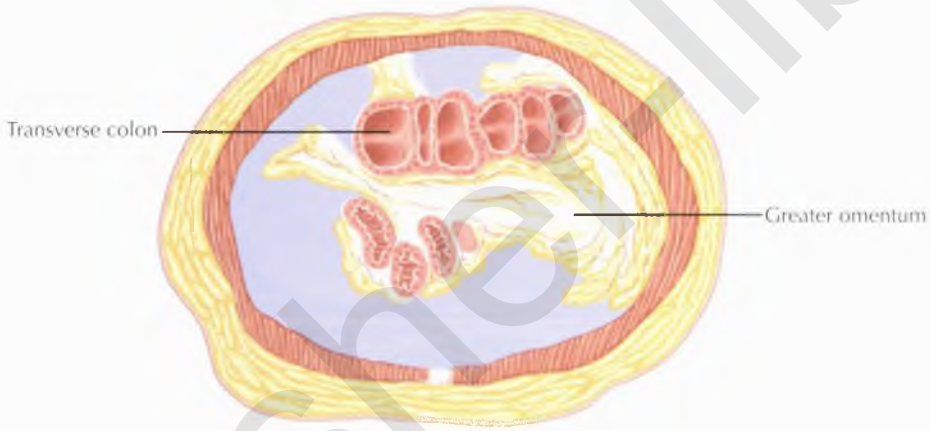

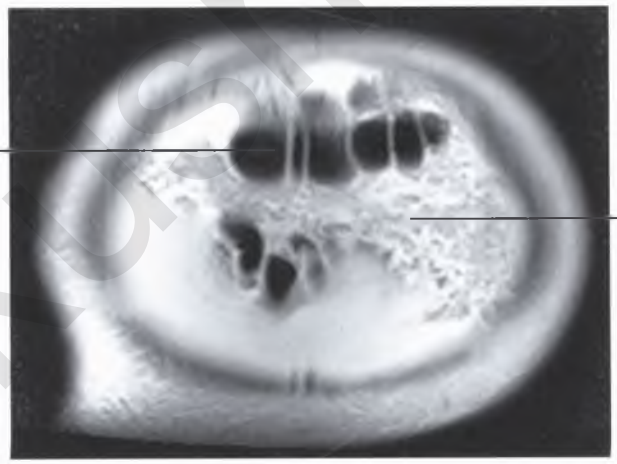

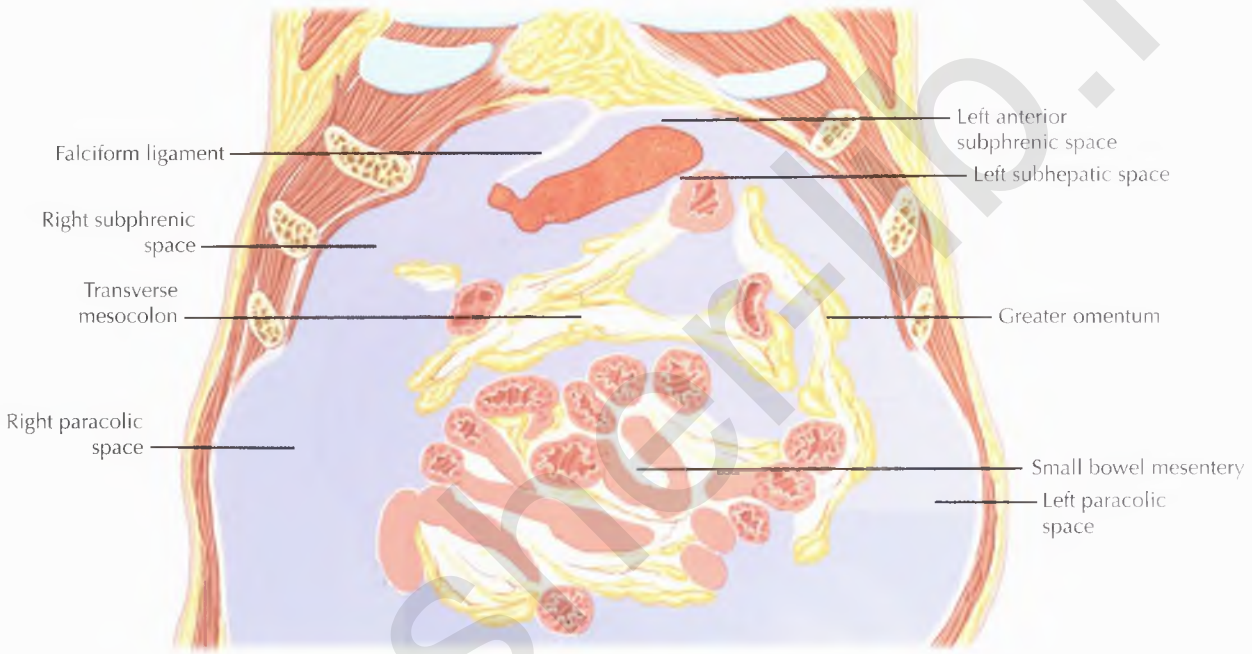

NORMAL ANATOMY

The superior and inferior portions of the peritoneal cavity communicate through the right and left paracolic spaces, also known as the "paracolic gutters," which are formed by peritoneal reflections covering the colon and the abdominal wall laterally.

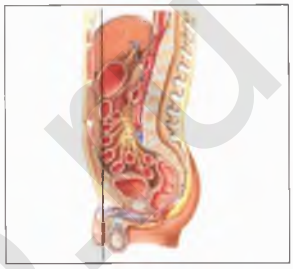

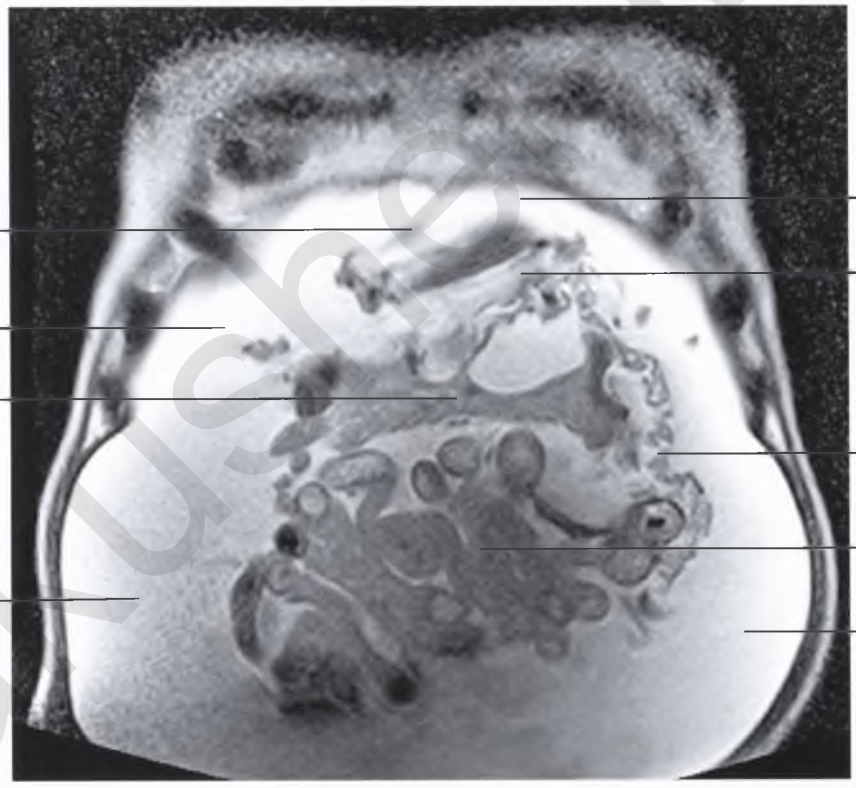
Falciform ligament
Right subphrenic space
Transverse mesocolon
Right paracolic space
Left anterior subphrenic space
Left subhepatic space
Greater omentum
Small bowel mesentery
Left paracolic space

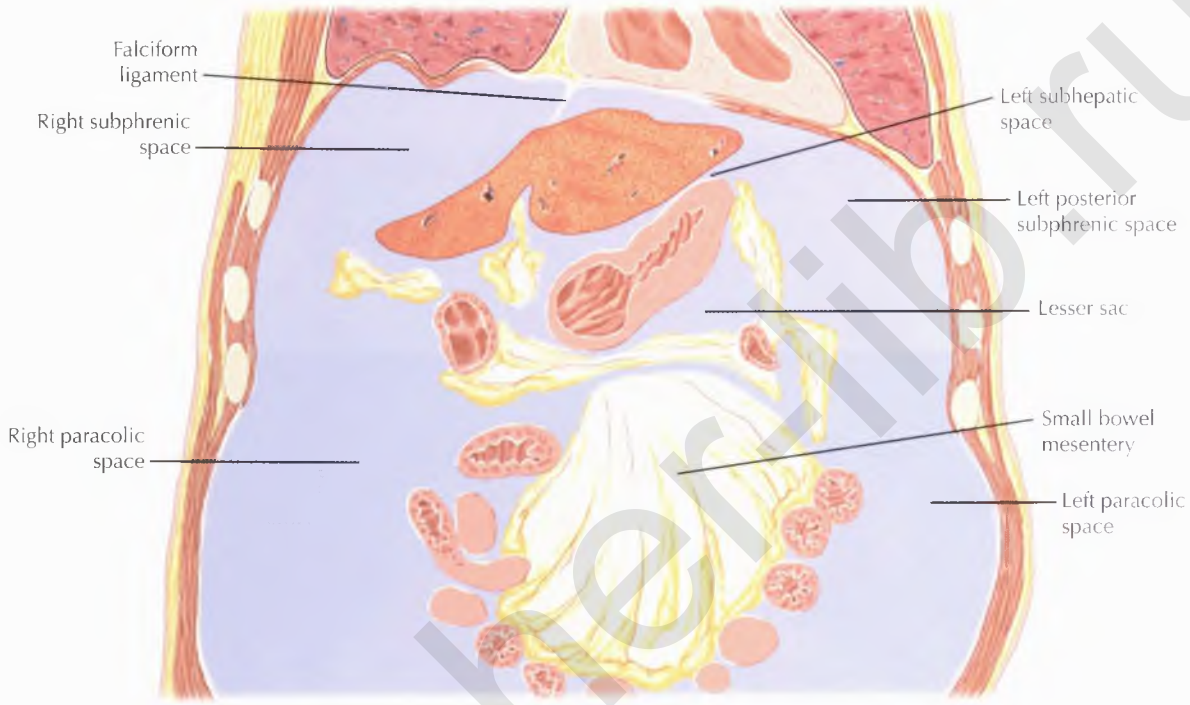

NORMAL ANATOMY

The *right subphrenic space* extends from the falciform ligament anteromedially to surround the diaphragmatic surface of the right lobe of the liver and is continuous with the right subhepatic space (seen on Abdomen Coronal 4) and the right paracolic space inferiorly. The right paracolic space communicates freely with the right pelvic peritoneal space.

The *left subphrenic space* extends from the falciform ligament anteromedially to surround the diaphragmatic surface of the left lobe of the liver and spleen, and is continuous with the left subhepatic space. The left subphrenic space is limited posteriorly and inferiorly by the splenorenal and phrenicocolic ligaments and more superiorly by the gastrosplenic ligament. Adjacent to the lateral segment of the liver, the left subhepatic space is continuous with the left subphrenic space.

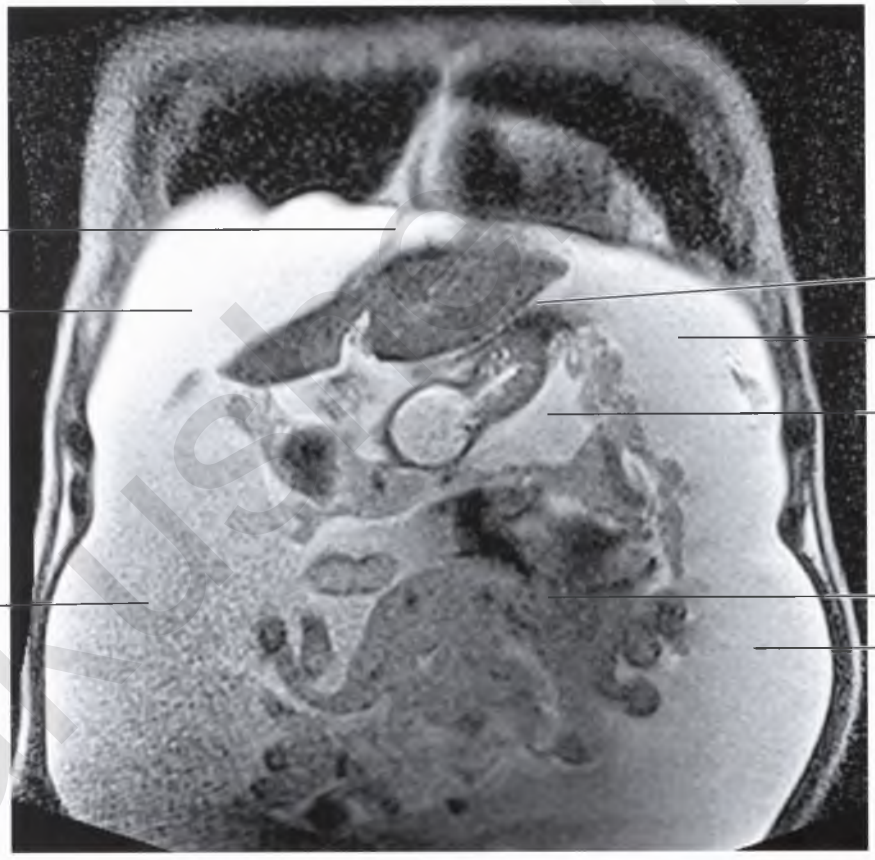
Falciform ligament
Right subphrenic space
Right paracolic space
Left subhepatic space
Left posterior subphrenic space
Lesser sac
Small bowel mesentery
Left paracolic space

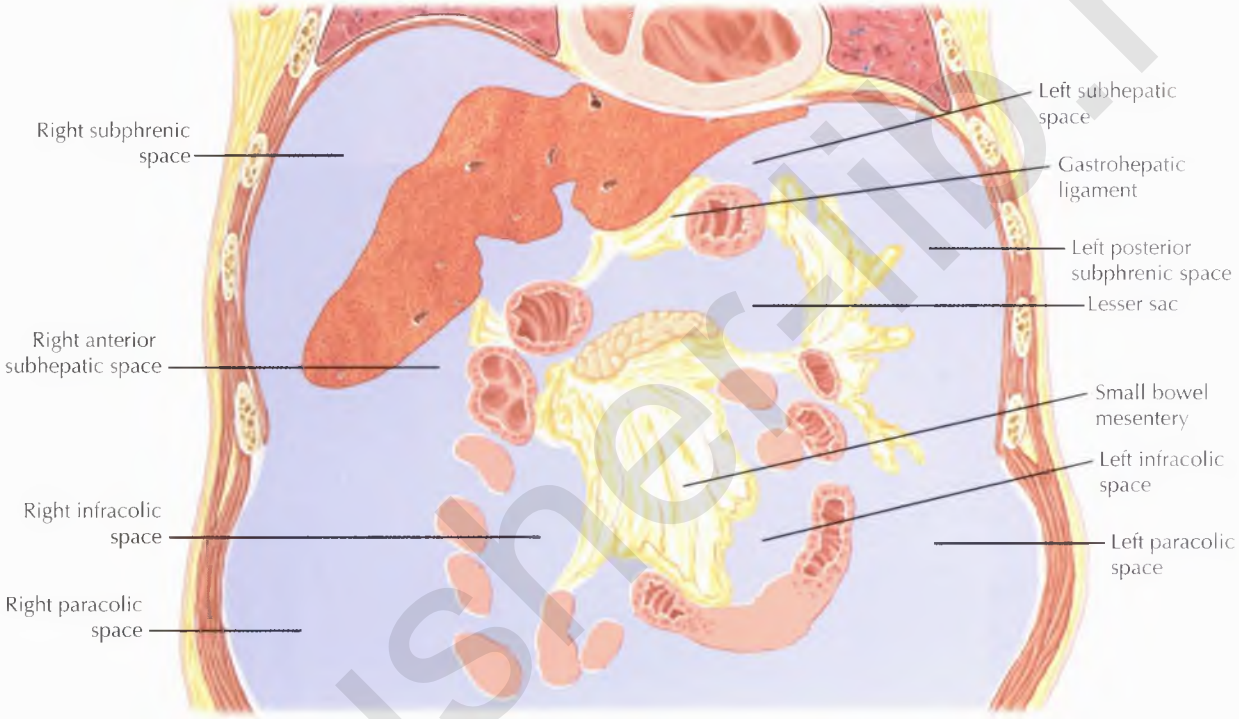

NORMAL ANATOMY

The small bowel mesentery extends from its attachment on the posterior abdominal wall at the ligament of Treitz to the right lower quadrant near the ileocecal junction.

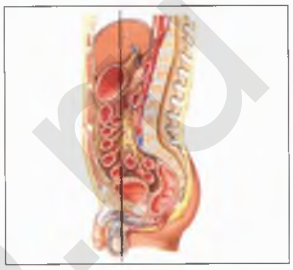


Right subphrenic space
Right anterior subhepatic space
Right infracolic space
Right paracolic space
Left subhepatic space
Gastrohepatic ligament
Left posterior subphrenic space
Lesser sac
Small bowel mesentery
Left infracolic space
Left paracolic space

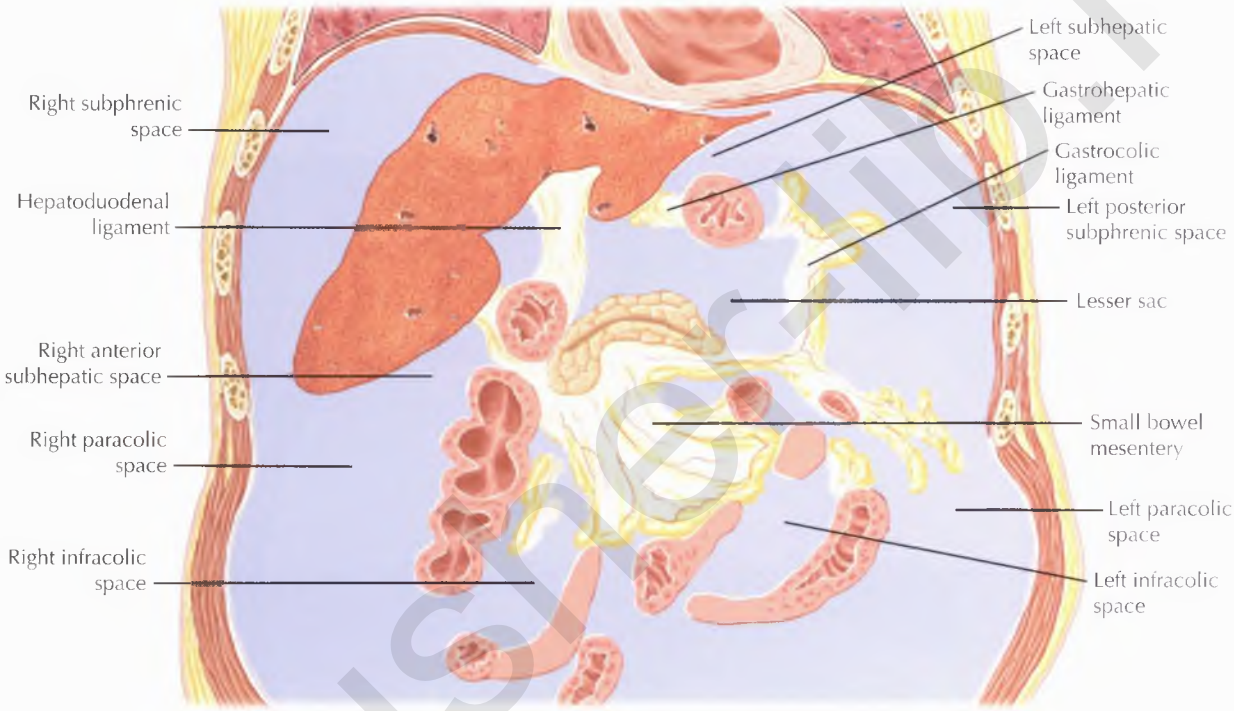

NORMAL ANATOMY

The gastrohepatic ligament is on the anterior superior margin of the lesser sac and contains the left gastric artery and coronary vein.


Right subphrenic space
Hepatoduodenal ligament
Right anterior subhepatic space
Right paracolic space
Right intracolic space
Left subhepatic space
Gastrohepatic ligament
Gastrocolic ligament
Left posterior subphrenic space
Lesser sac
Small bowel mesentery
Left paracolic space
Left infracolic space

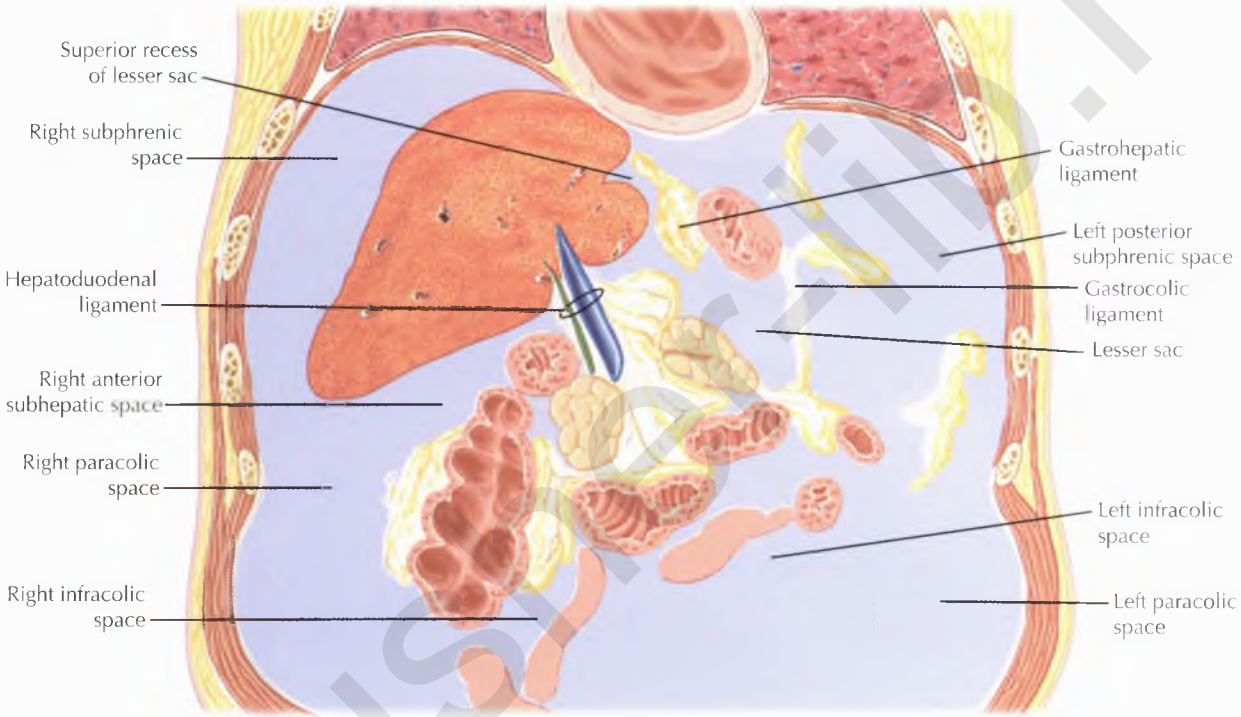

NORMAL ANATOMY

The hepatoduodenal ligament contains the main portal vein, proper hepatic artery, and common bile duct.


Superior recess of lesser sac
Right subphrenic space
Hepatoduodenal ligament
Right anterior subhepatic space
Right paracolic space
Right infracolic space
Gastrohepatic ligament
Left posterior subphrenic space
Gastrocolic ligament
Lesser sac
Left infracolic space
Left paracolic space

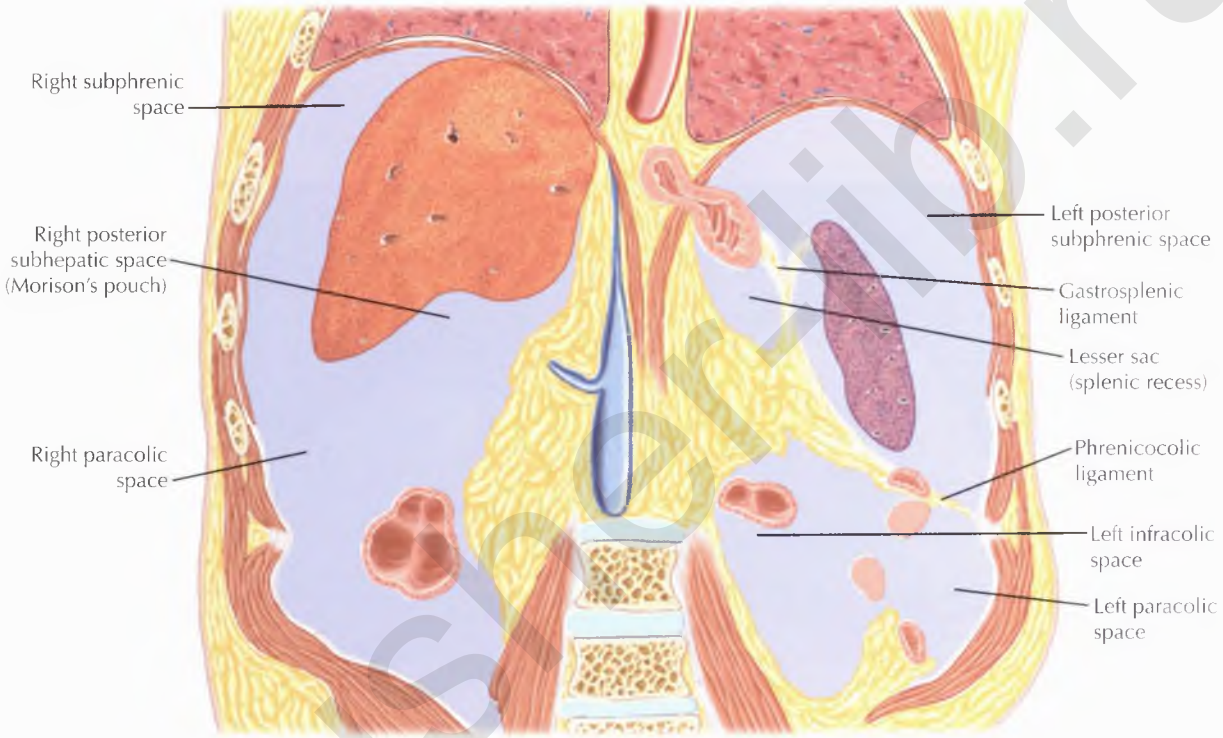

NORMAL ANATOMY

The *phrenicocolic ligament* separates the left subphrenic space from the left paracolic space, preventing direct communication. The left paracolic space is in continuity with the left infracolic space, and both communicate freely with the pelvic peritoneal space.

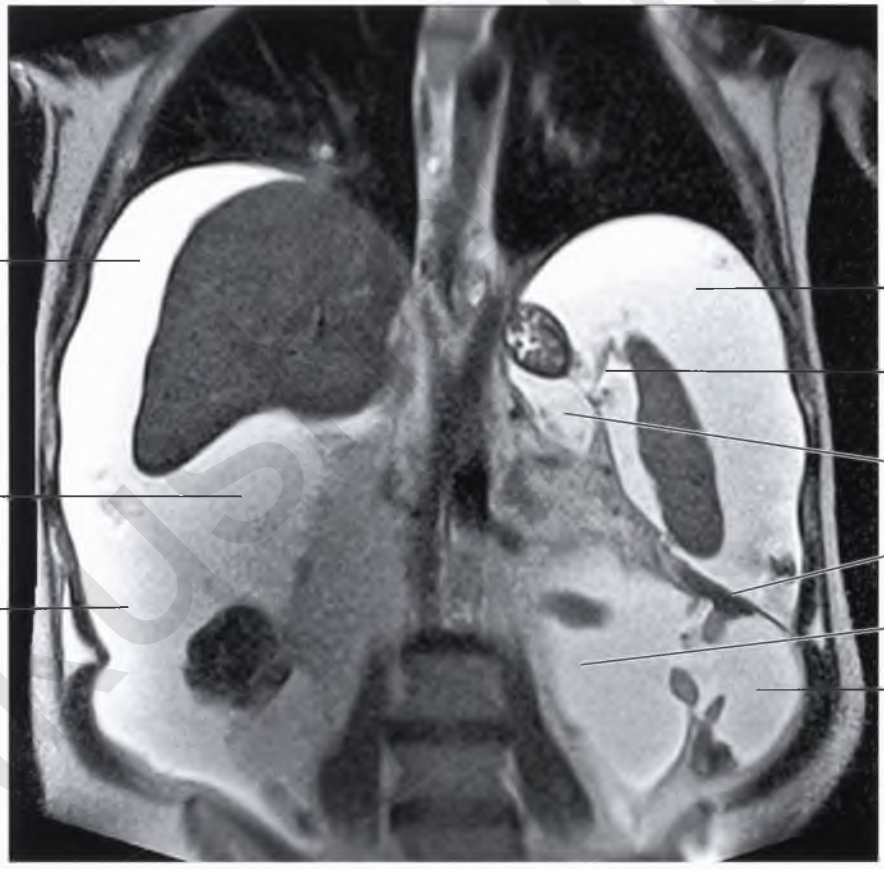
Right subphrenic space
Right posterior subhepatic space (Morison's pouch)
Right paracolic space
Left posterior subphrenic space
Gastrosplenic ligament
Lesser sac (splenic recess)
Phrenicocolic ligament
Left infracolic space
Left paracolic space

NORMAL ANATOMY

The *gastrosplenic ligament*, a part of the greater omentum, is seen extending from the gastric fundus to the splenic hilum and contains the left gastroepiploic vessels. The gastrosplenic ligament is also in continuity with the splenorenal ligament at the splenic hilum.

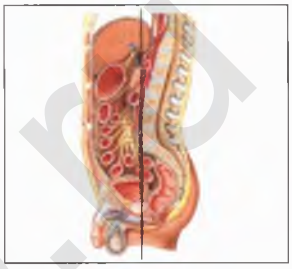

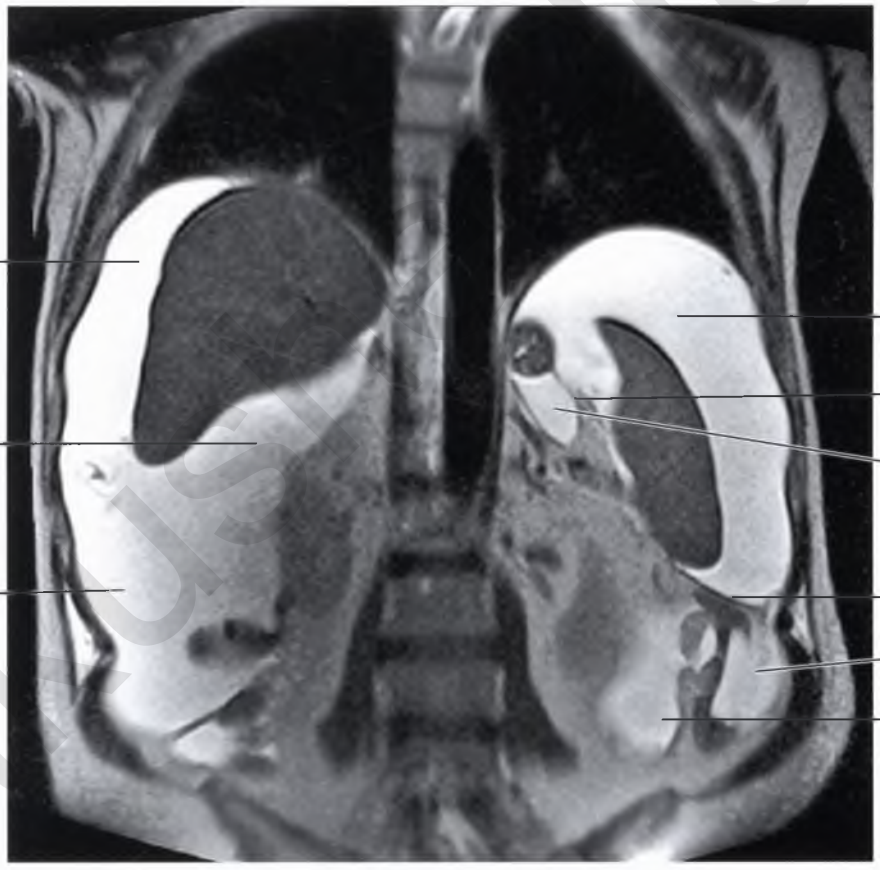
Right subphrenic space
Right posterior subhepatic space (Morison's pouch)
Right paracolic space
Left posterior subphrenic space
Gastrosplenic ligament
Lesser sac (splenic recess)
Phrenicocolic ligament
Left paracolic space
Left infracolic space

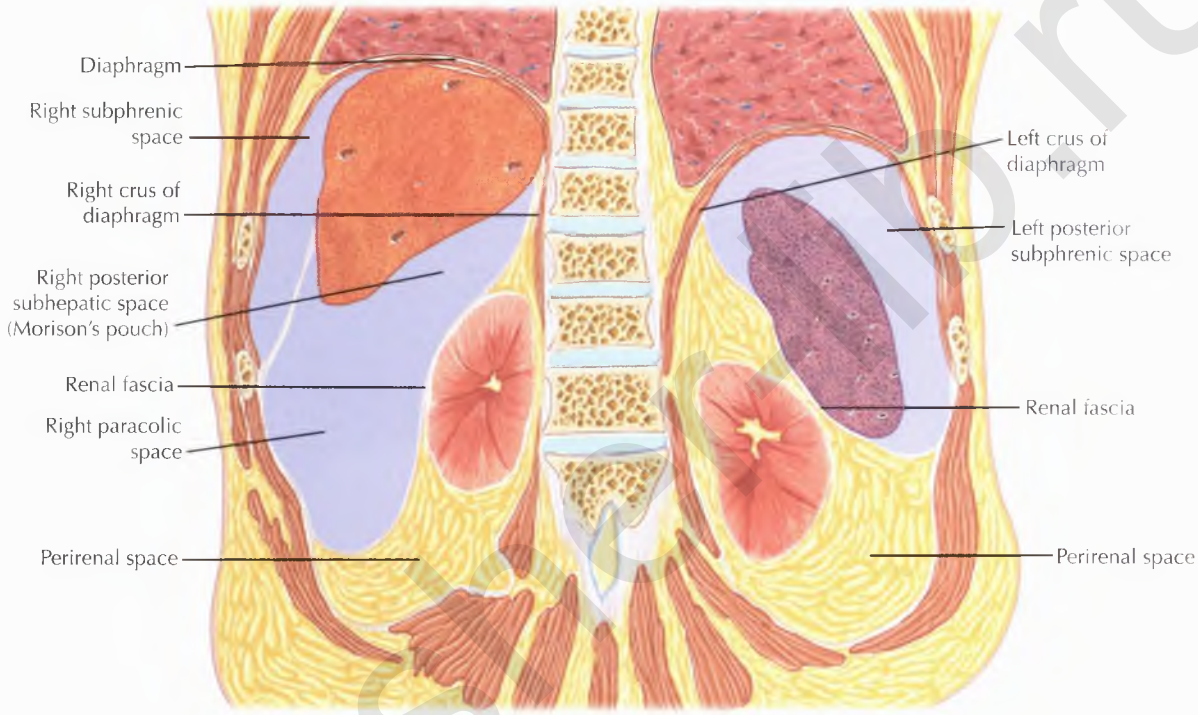

NORMAL ANATOMY

Renal fascia surrounding the cone-shaped retroperitoneal fat, kidneys, and adrenal glands within the perirenal space isolates these retroperitoneal structures from the peritoneal ascites.

DIAGNOSTIC CONSIDERATION

Masses originating in the retroperitoneum are usually malignant in etiology.

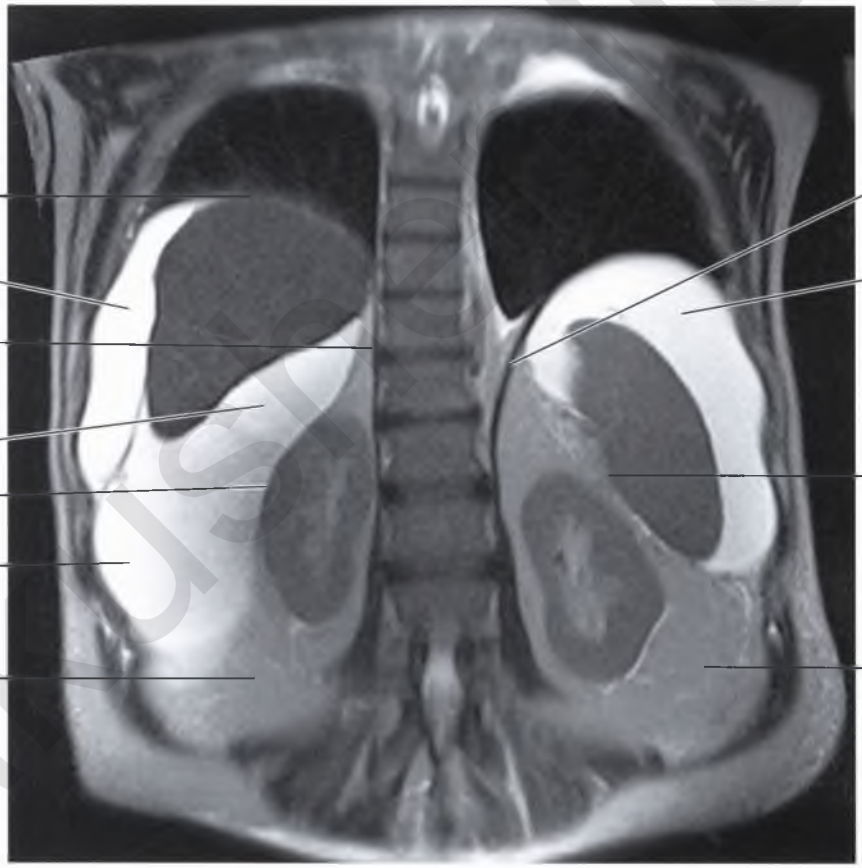

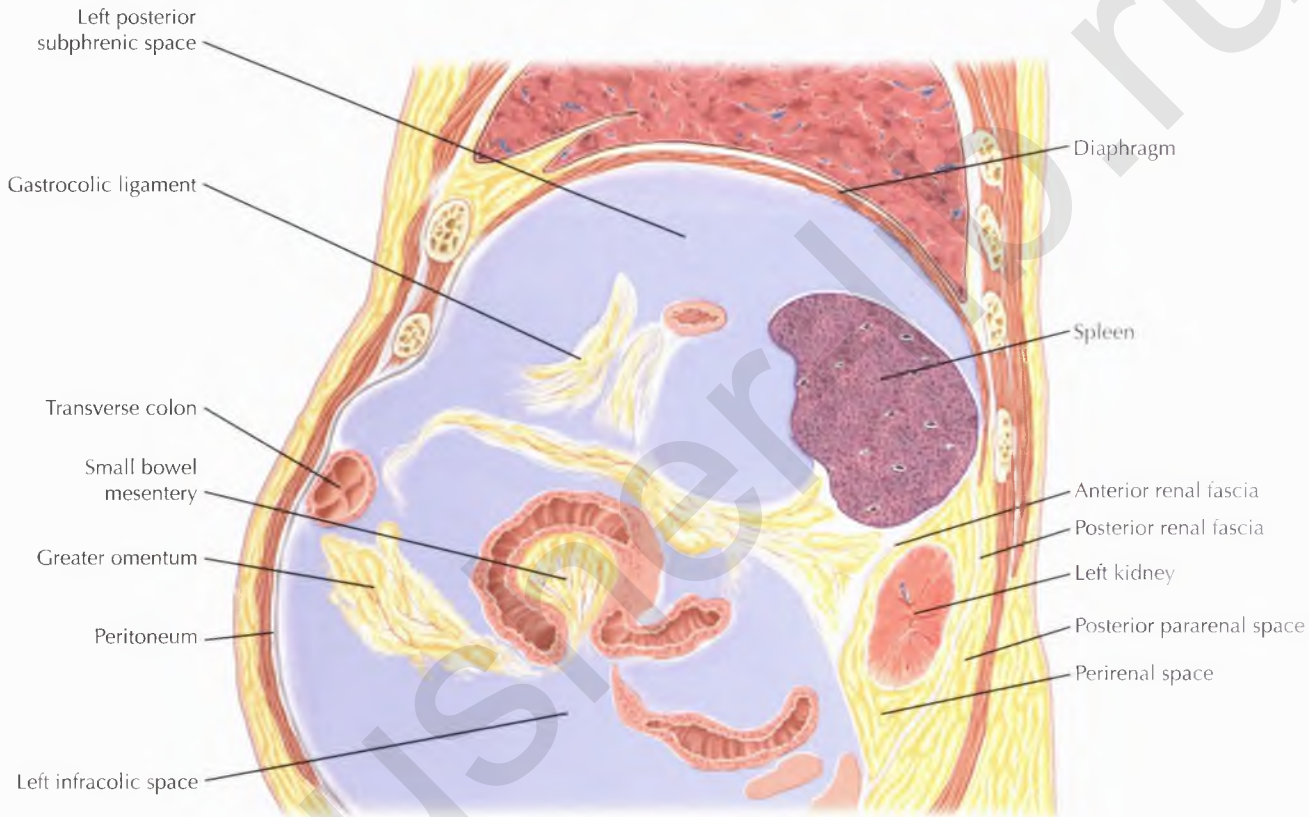

PATHOLOGIC PROCESS

The normal peritoneum is thin. Thickening of the peritoneum can be caused by peritoneal infection, inflammation, or malignancy.

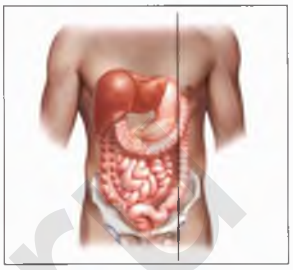

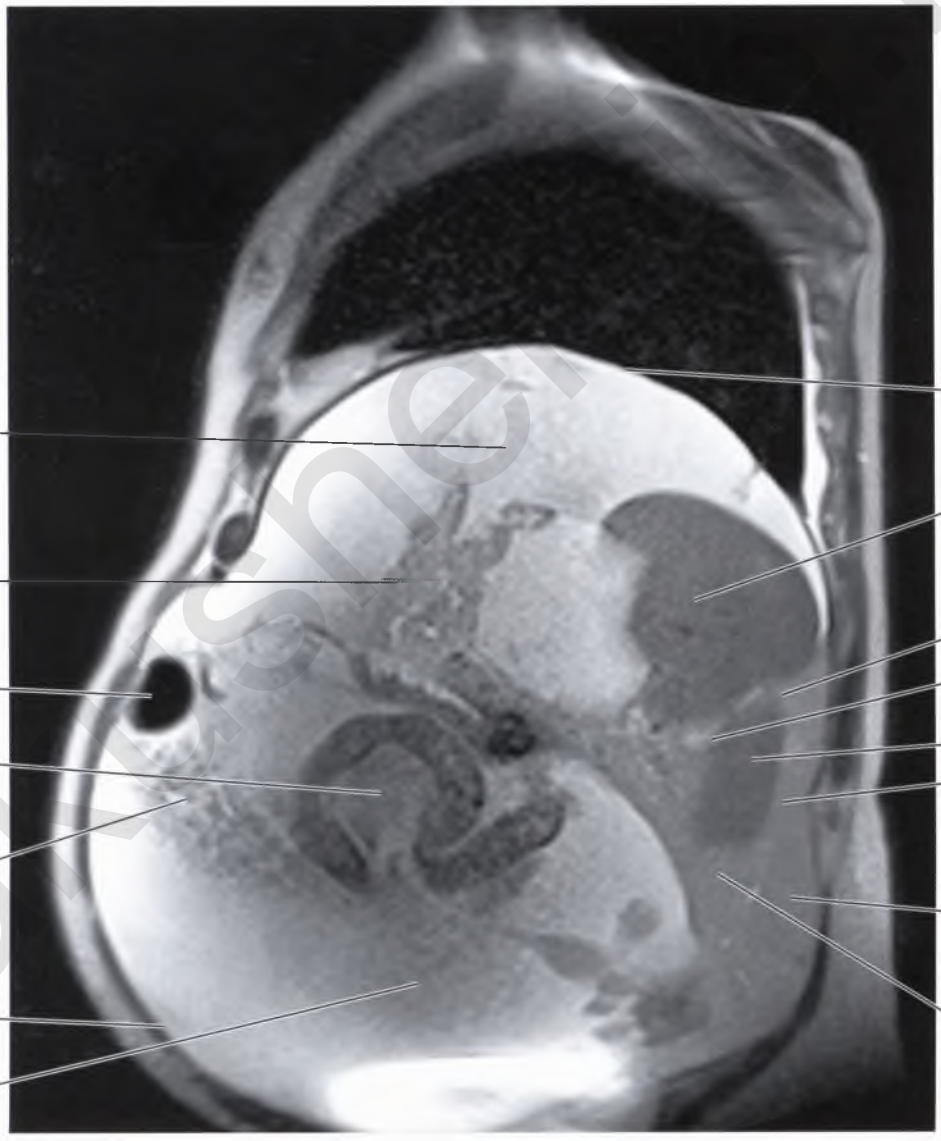
Left posterior subphrenic space
Gastrocolic ligament
Transverse colon
Small bowel mesentery
Greater omentum
Peritoneum
Left infracolic space
Diaphragm
Spleen
Perirenal space
Anterior renal fascia
Left kidney
Posterior renal fascia
Posterior pararenal space
Perirenal space

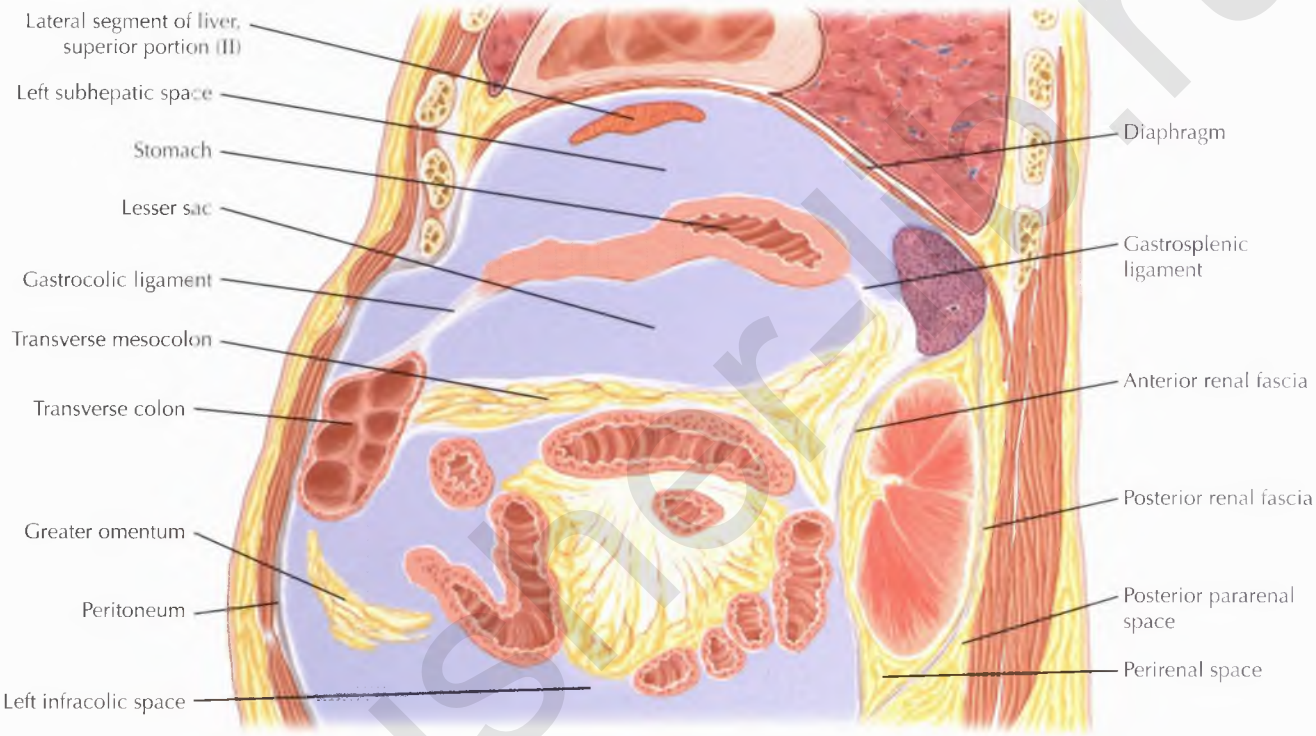

PATHOLOGIC PROCESS

The boundaries of the lesser sac are well demonstrated in the sagittal plane. Isolated ascites in the lesser sac may be caused by benign etiologies such as acute pancreatitis or by malignant etiologies; however, isolated ascites in the greater sac is usually benign.

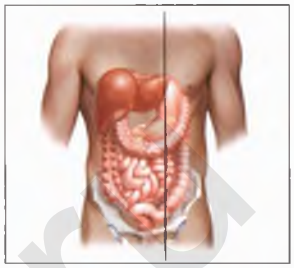


Lateral segment of liver, superior portion (II)
Left subhepatic space
Stomach
Lesser sac
Gastrocolic ligament
Transverse mesocolon
Transverse colon
Peritoneum
Greater omentum
Left infracolic space
Diaphragm
Gastrosplenic ligament
Anterior renal fascia
Perirenal space
Posterior renal fascia
Posterior pararenal space
Perirenal space

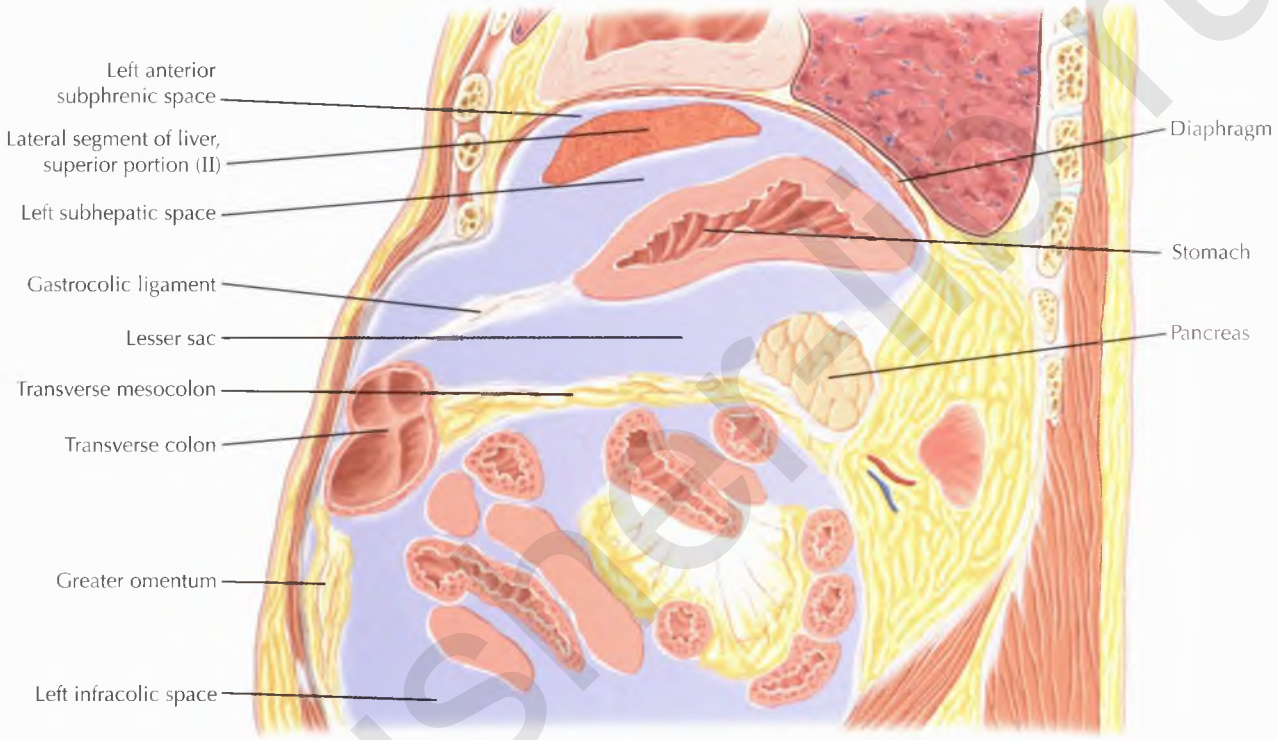

NORMAL ANATOMY

The greater omentum is composed of a double layer of peritoneum that hangs from the greater curvature of the stomach like an apron over the transverse colon and small bowel. The portion of the greater omentum extending from the stomach to the transverse colon is called the *gastrocolic ligament*.

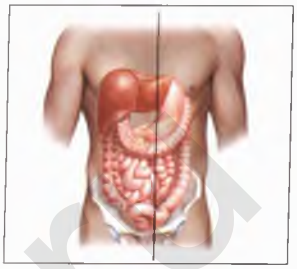

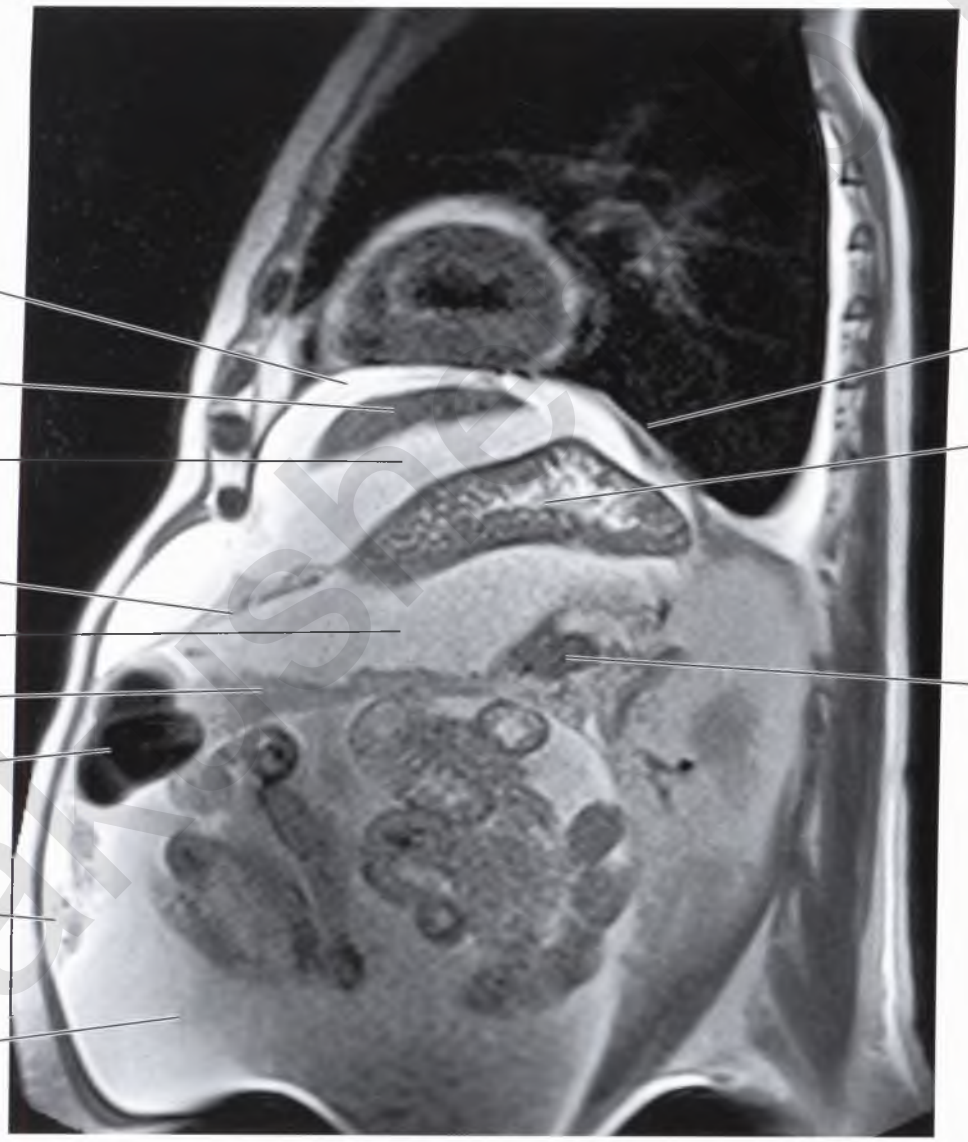
Left anterior subphrenic space
Lateral segment of liver, superior portion (II)
Left subhepatic space
Gastrocolic ligament
Lesser sac
Transverse mesocolon
Transverse colon
Greater omentum
Left infracolic space
Diaphragm
Stomach
Pancreas

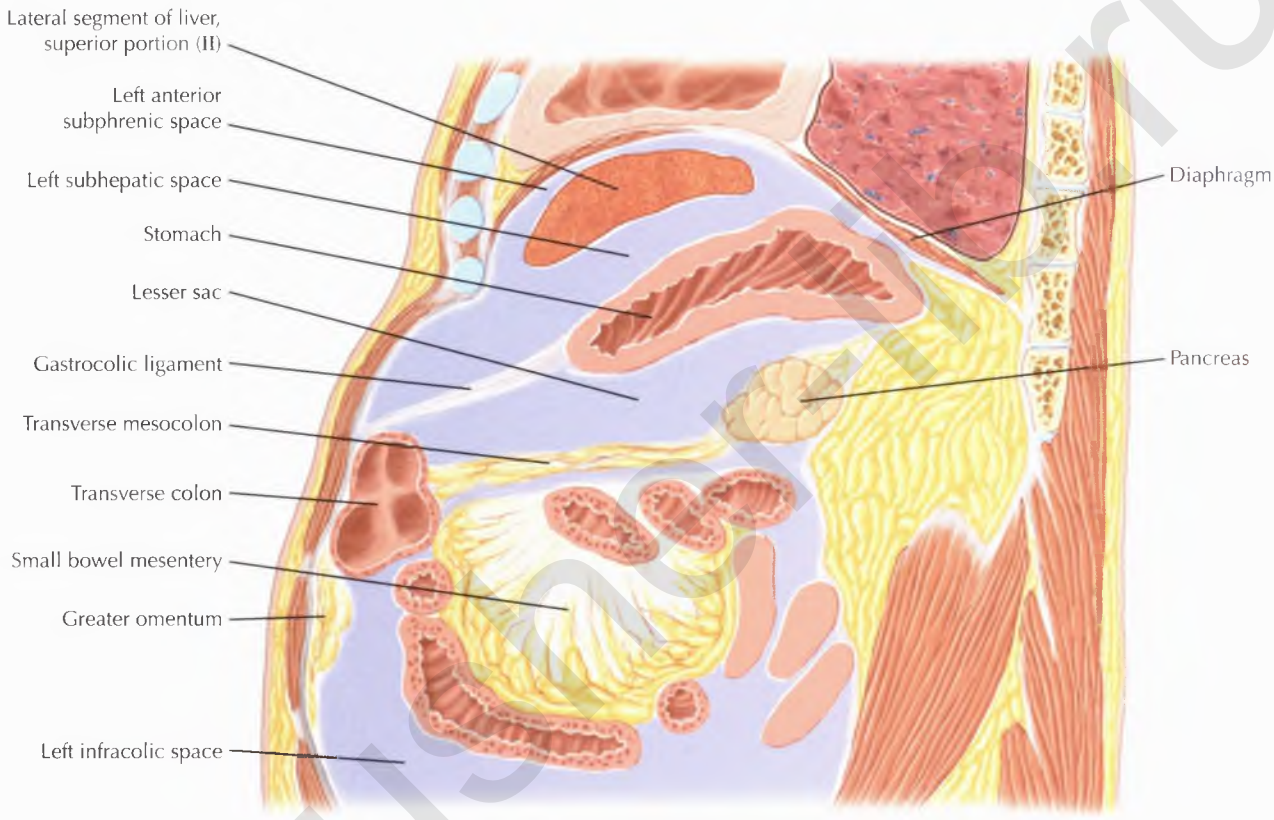

PATHOLOGIC PROCESS

Omental caking is caused by the accumulation of abnormal tissue within the omentum, usually caused by peritoneal carcinomatosis. Subtle infiltration or nodularity of the omentum is often one of the earliest signs of peritoneal carcinomatosis.

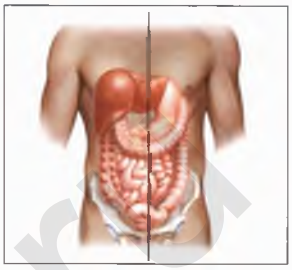


Lateral segment of liver, superior portion (II)
Left anterior subphrenic space
Left subhepatic space
Stomach
Lesser sac
Gastrocolic ligament
Transverse mesocolon
Transverse colon
Small bowel mesentery
Greater omentum
Left infracolic space
Diaphragm
Pancreas

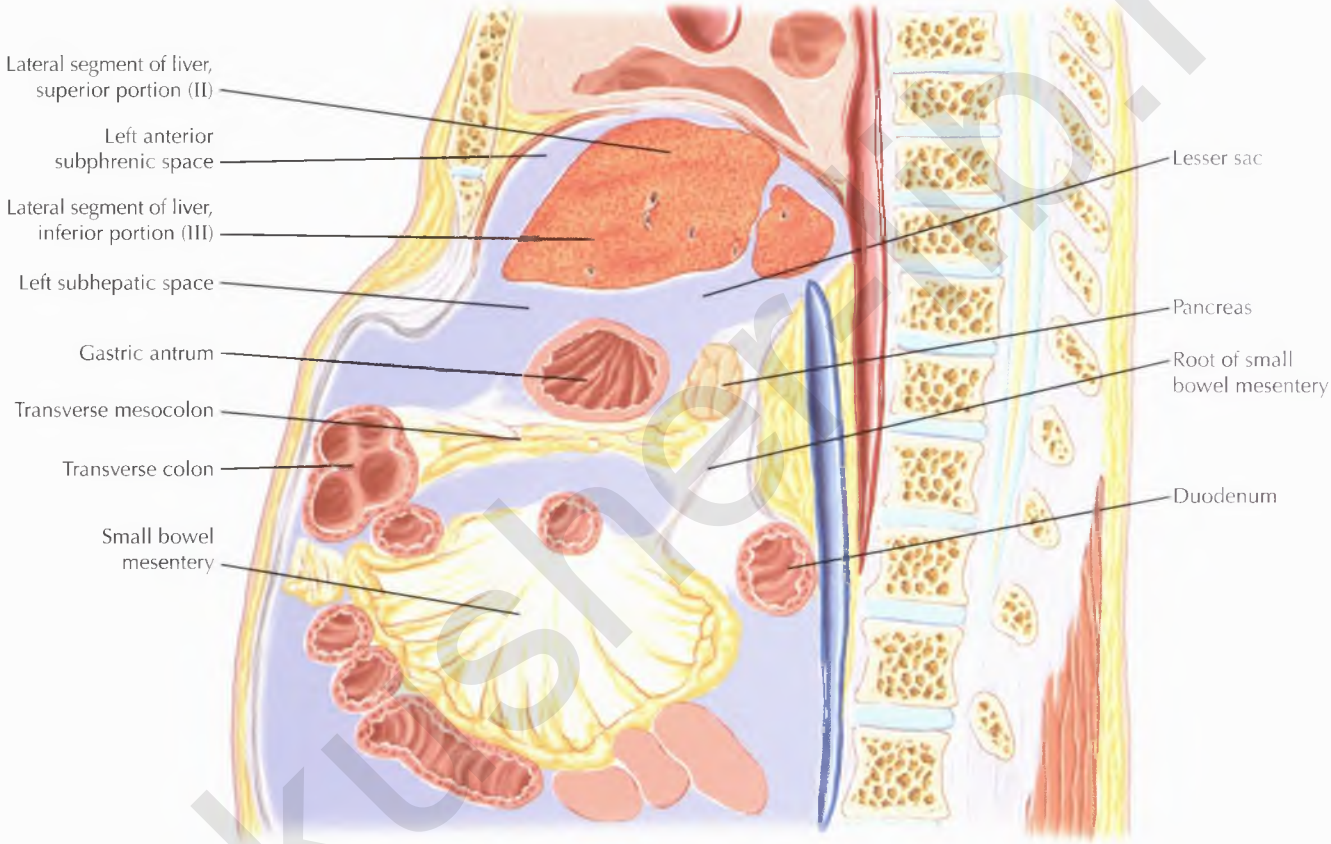
Lateral segment of liver, superior portion (II)
Left anterior subphrenic space
Lateral segment of liver, inferior portion (III)
Left subhepatic space
Gastric antrum
Transverse mesocolon
Transverse colon
Small bowel mesentery
Lesser sac
Pancreas
Root of small bowel mesentery
Duodenum

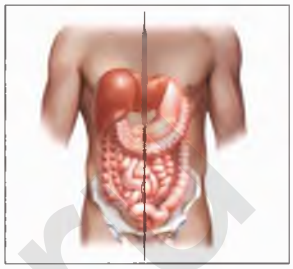


Lateral segment of liver, superior portion (II)
Left anterior subphrenic space
Lateral segment of liver, inferior portion (III)
Left subhepatic space
Gastric antrum
Transverse mesocolon
Transverse colon
Small bowel mesentery
Lesser sac
Pancreas
Root of small bowel mesentery
Duodenum

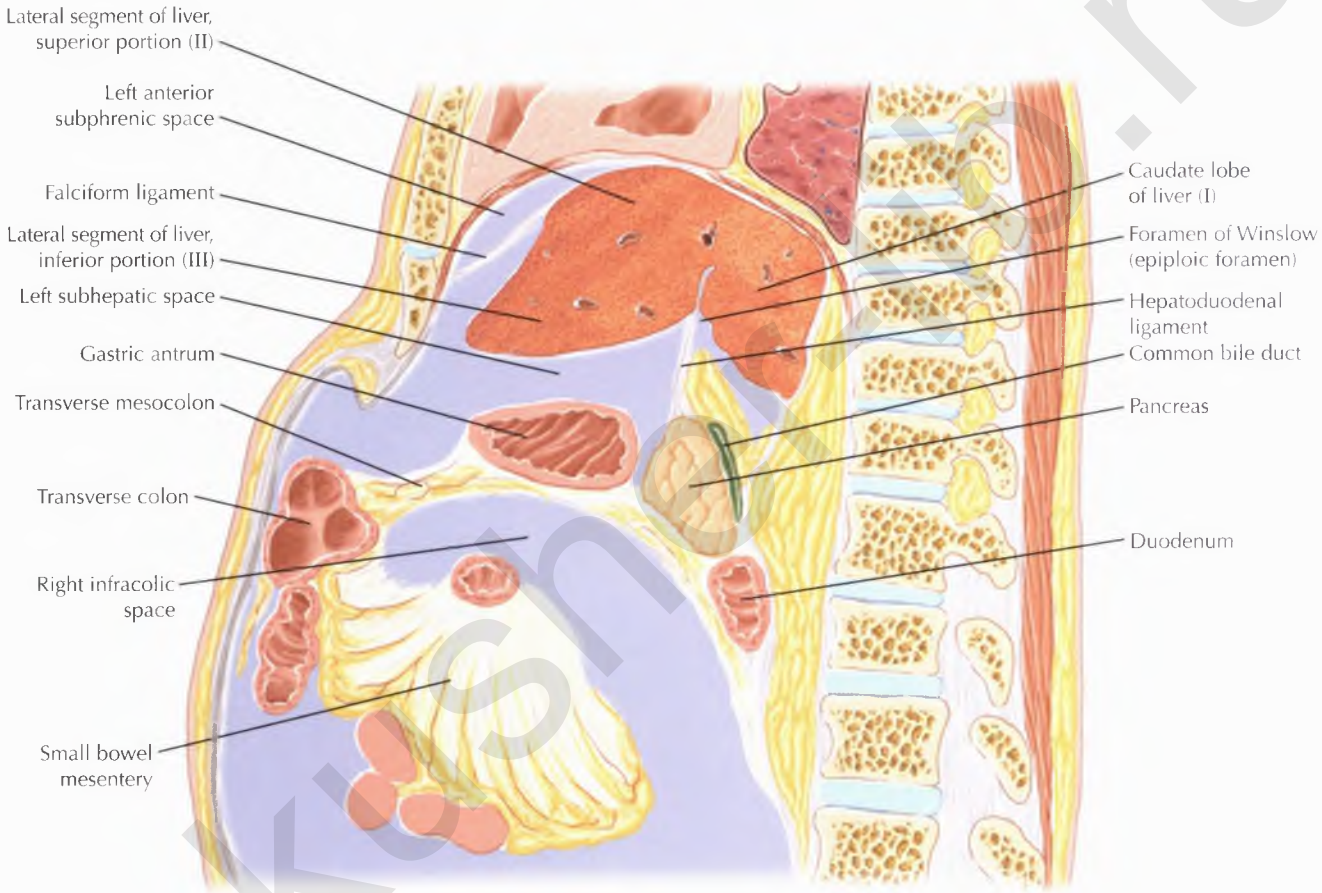
Lateral segment of liver, superior portion (II)
Left anterior subphrenic space
Falciform ligament
Lateral segment of liver, inferior portion (III)
Left subhepatic space
Gastric antrum
Transverse mesocolon
Transverse colon
Right infracolic space
Small bowel mesentery
Caudate lobe of liver (I)
Foramen of Winslow (epiploic foramen)
Hepatoduodenal ligament
Common bile duct
Pancreas
Duodenum

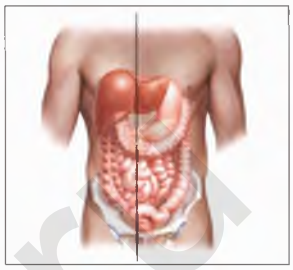

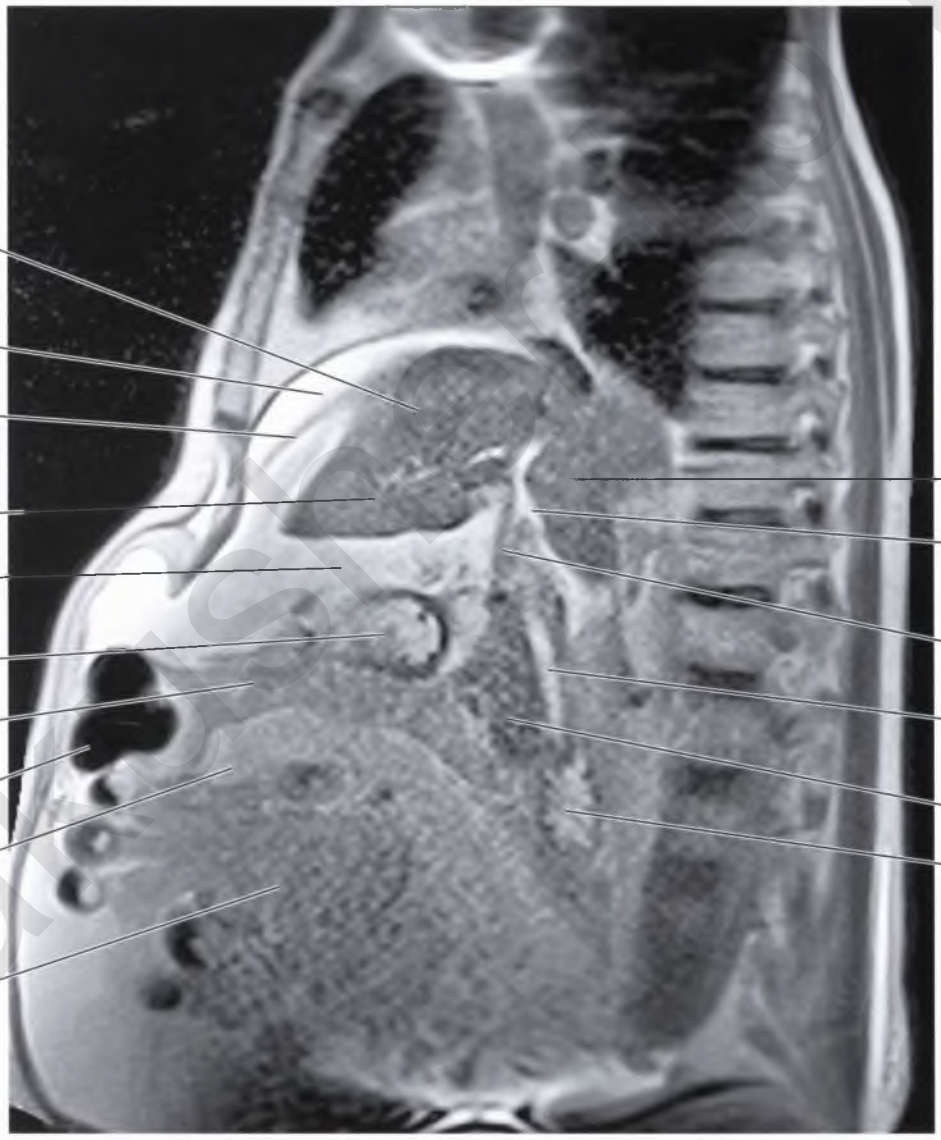
Lateral segment of liver, superior portion (II)
Left anterior subphrenic space
Falciform ligament
Lateral segment of liver, inferior portion (III)
Left subhepatic space
Gastric antrum
Transverse mesocolon
Transverse colon
Right infracolic space
Small bowel mesentery
Caudate lobe of liver (I)
Foramen of Winslow (epiploic foramen)
Hepatoduodenal ligament
Common bile duct
Pancreas
Duodenum

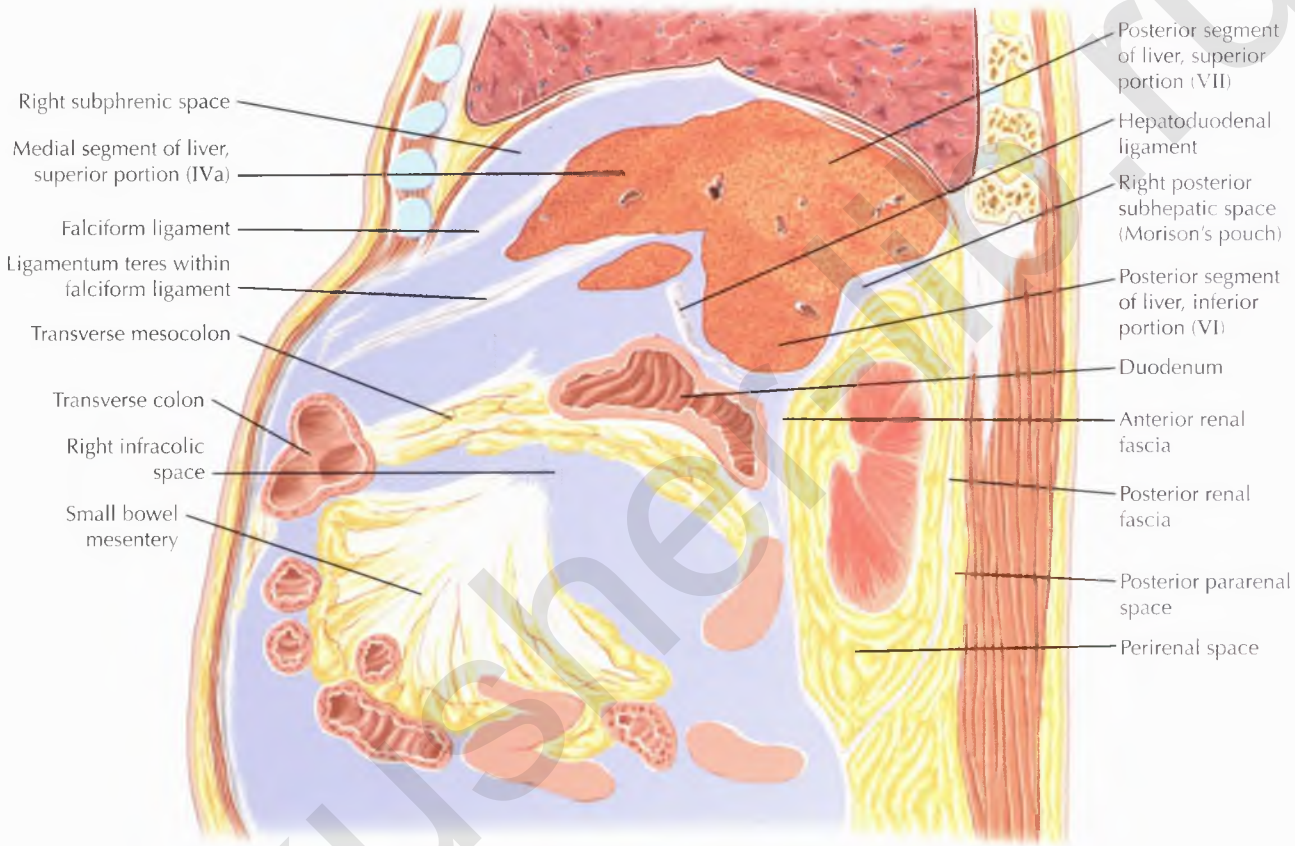

NORMAL ANATOMY

The falciform ligament is a peritoneal reflection enclosing the *ligamentum teres*, the obliterated remnant of the umbilical vein, as it travels from the umbilicus to the liver.


Right subphrenic space
Medial segment of liver, superior portion (IVa)
Falciform ligament
Ligamentum teres within falciform ligament
Transverse mesocolon
Transverse colon
Right infracolic space
Small bowel mesentery
Posterior segment of liver, superior portion (VII)
Hepatoduodenal ligament
Right posterior subhepatic space (Morison's pouch)
Perirenal space
Posterior segment of liver, inferior portion (VI)
Anterior renal fascia
Posterior renal fascia
Perirenal space
Posterior pararenal space

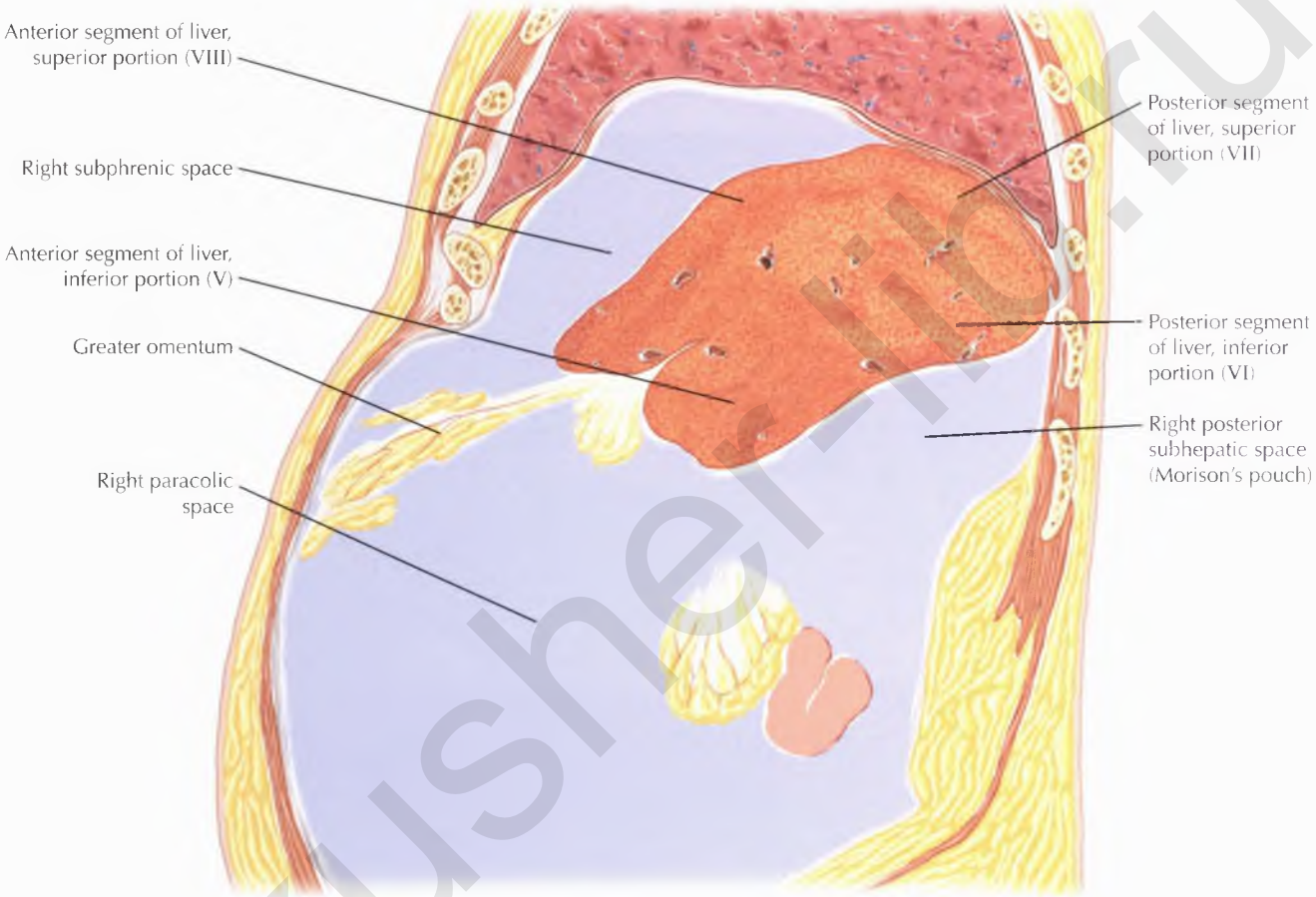

PATHOLOGIC PROCESS

Inflammatory processes and malignancies in the pelvis can spread superiorly through the right paracolic space into the right subphrenic and subhepatic spaces. However, the left phrenicocolic ligament prevents superior extension of disease from the left paracolic space into the left subphrenic and subhepatic spaces.

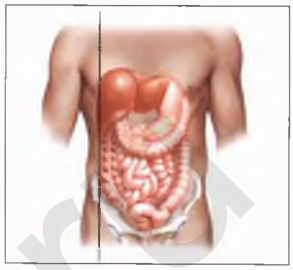


Anterior segment of liver, superior portion (VIII)
Right subphrenic space
Anterior segment of liver, inferior portion (V)
Greater omentum
Right paracolic space
Posterior segment of liver, superior portion (VII)
Posterior segment of liver, inferior portion (VI)
Right posterior subhepatic space (Morison's pouch)

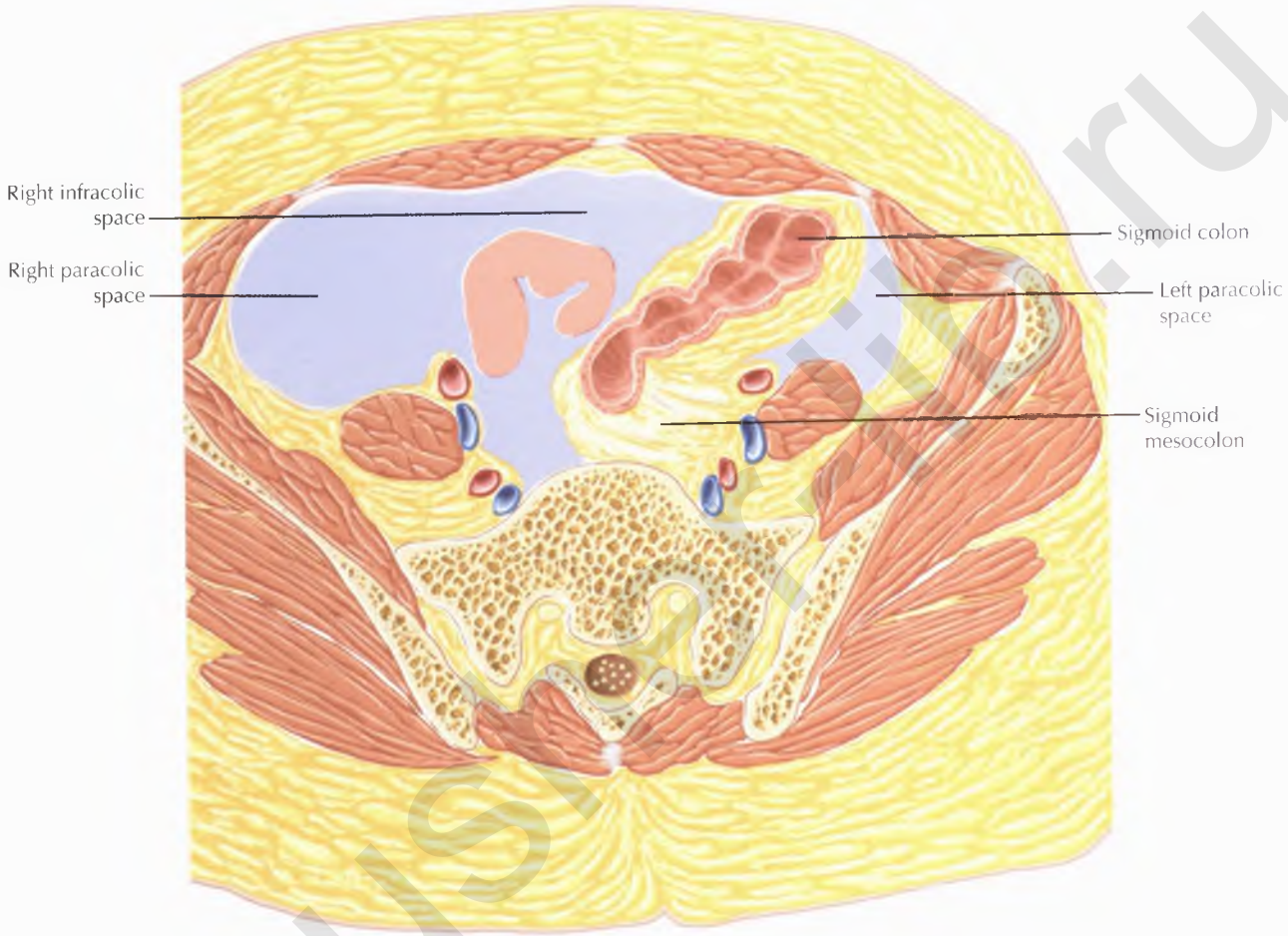

NORMAL ANATOMY

Branches from the inferior mesenteric artery and vein, including the sigmoid and superior rectal vessels, pass within the sigmoid mesocolon.

PATHOLOGIC PROCESS

The pelvic ligaments and peritoneal spaces are best appreciated in the presence of ascites, as in this example.

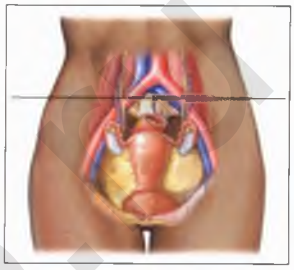

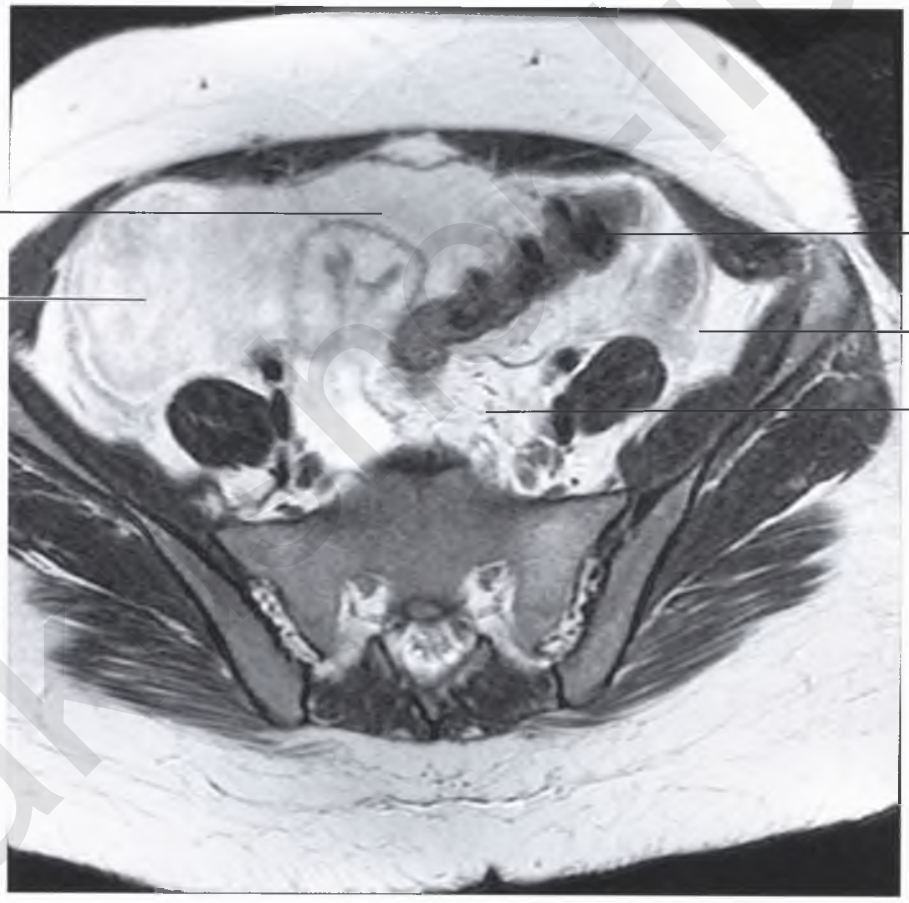
Right infracolic space
Right paracolic space
Sigmoid colon
Left paracolic space
Sigmoid mesocolon

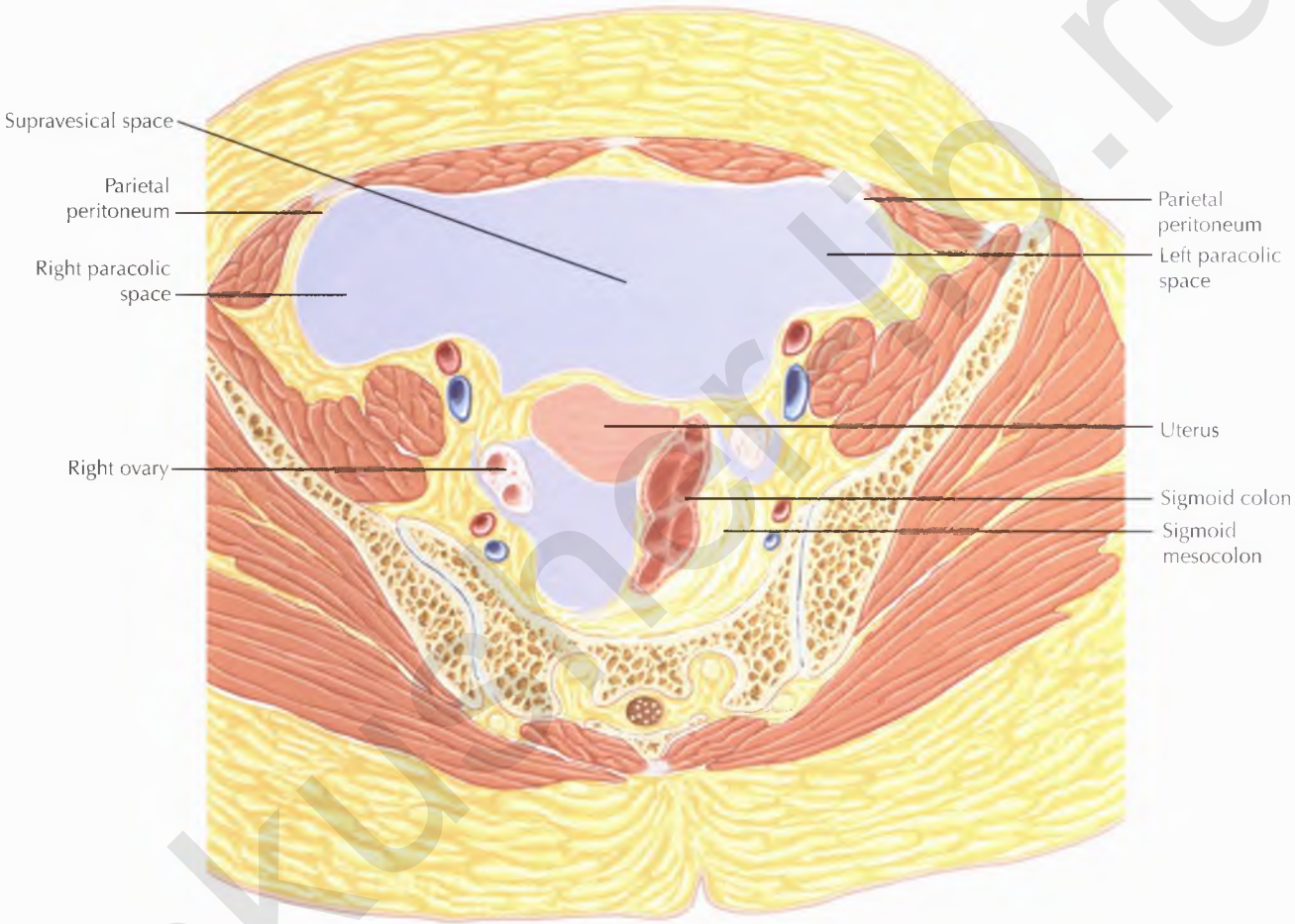

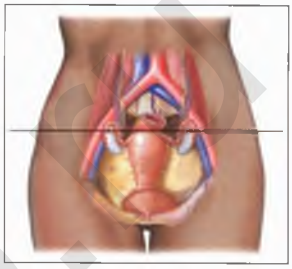

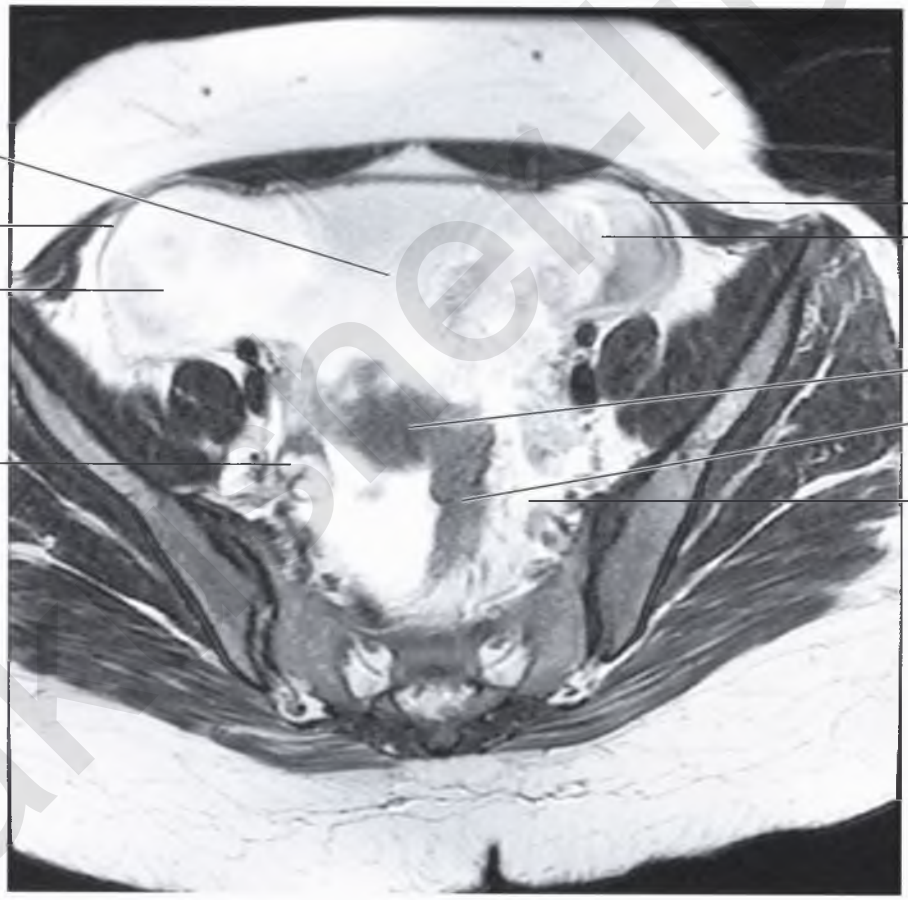
Supravesical space
Parietal peritoneum
Right paracolic space
Right ovary
Parietal peritoneum
Left paracolic space
Uterus
Sigmoid colon
Sigmoid mesocolon

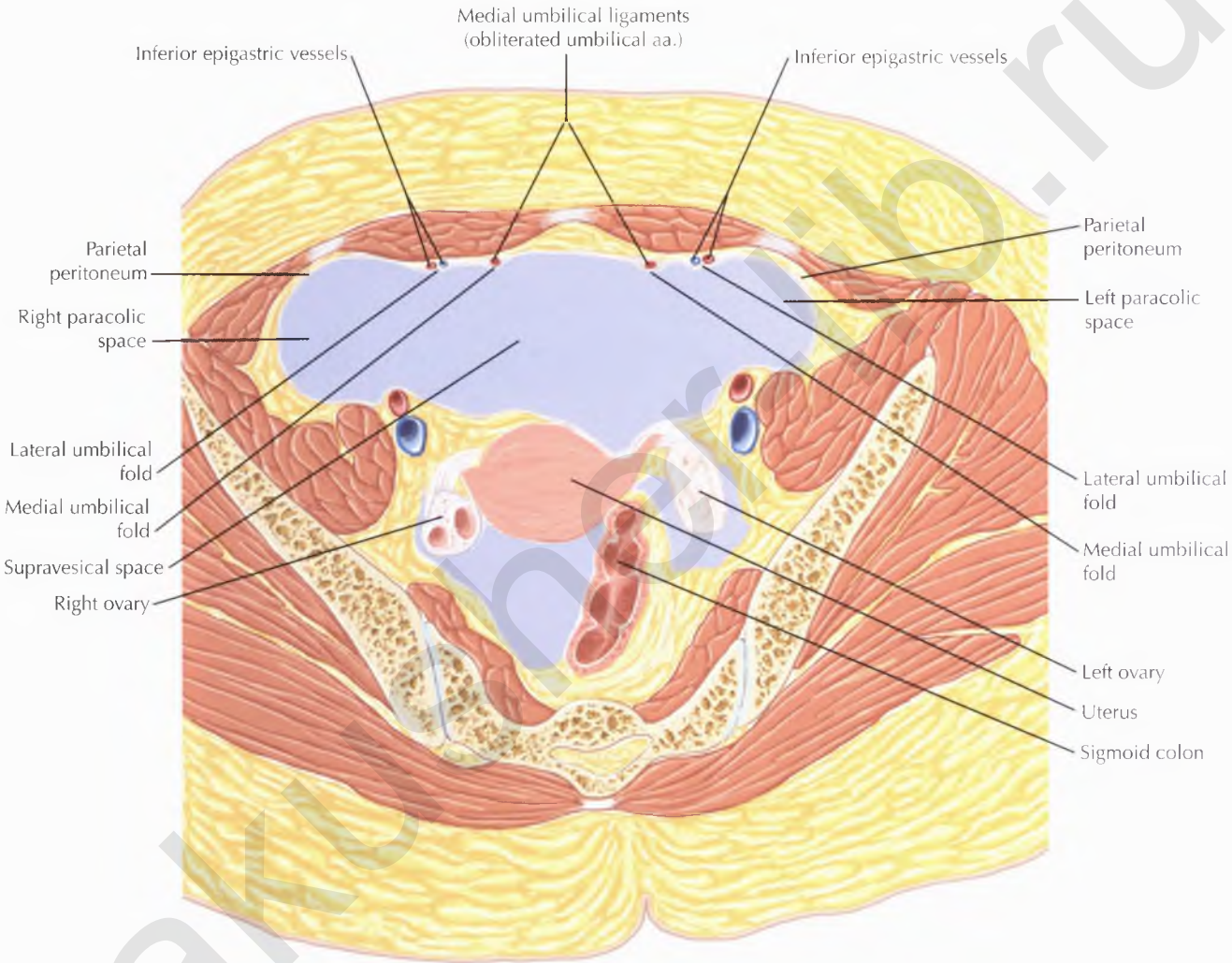

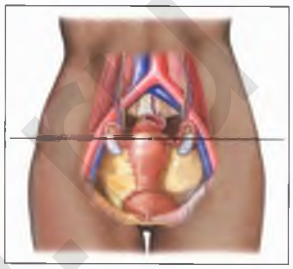

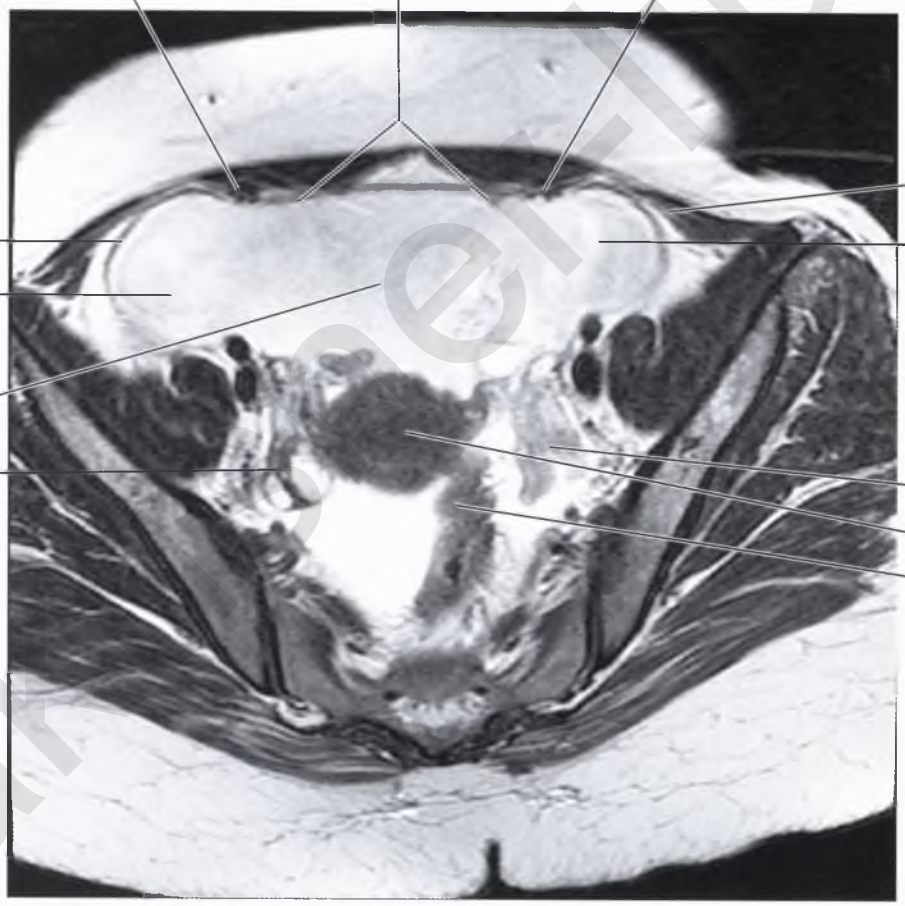

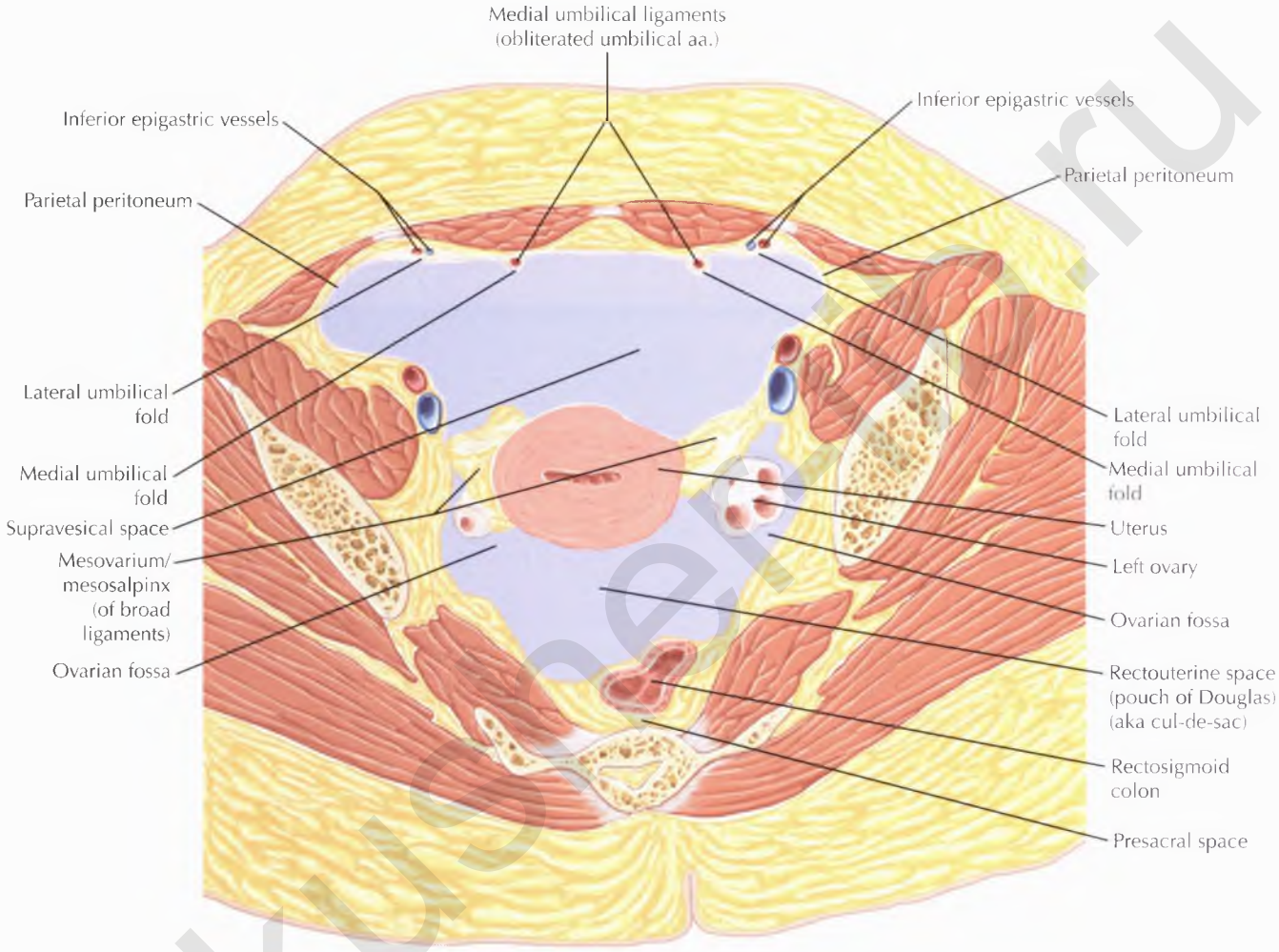

NORMAL ANATOMY

The *presacral* (or retrorectal) *space* is a fat-containing extraperitoneal space seen between the upper two thirds of the rectum and the sacrum. Presacral space tumors often arise from embryonic remnants, with *sacrococcygeal teratoma* the most common tumor arising in this region. MR imaging is useful for delineating soft tissue planes and evaluating the presence or extent of osseous invasion and nerve involvement, which is important for surgical planning.

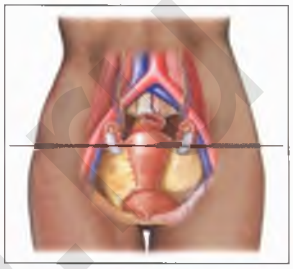

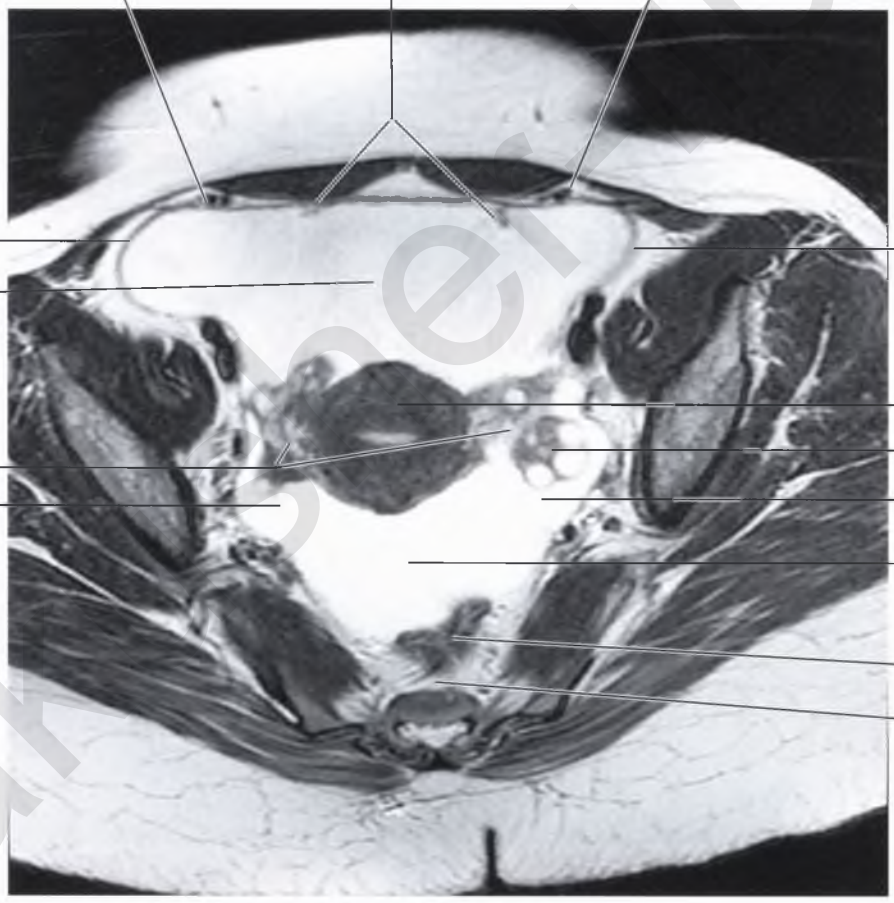
Inferior epigastric vessels (in lateral umbilical fold)
Medial umbilical ligaments (obliterated umbilical aa.) in medial umbilical folds
Inferior epigastric vessels (in lateral umbilical fold)
Parietal peritoneum
Supravesical space
Mesovarium/ mesosalpinx (of broad ligaments)
Ovarian fossa
Parietal peritoneum
Uterus
Left ovary
Ovarian fossa
Rectouterine space (pouch of Douglas) (aka cul-de-sac)
Rectosigmoid colon
Presacral space

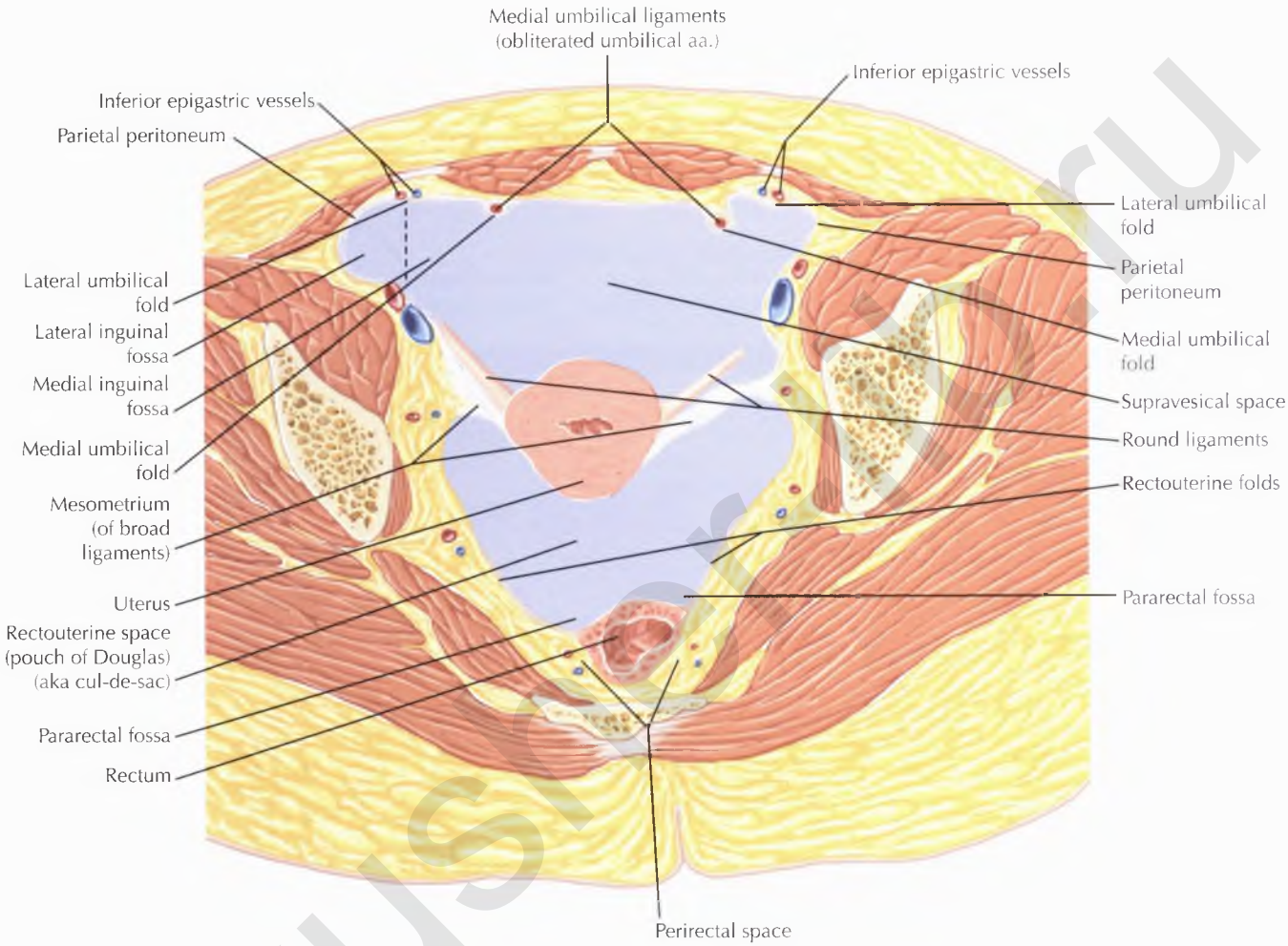

NORMAL ANATOMY

The paired *broad ligaments* are formed by two layers of peritoneum that drape over the uterus and extend laterally from the uterus to the pelvic side walls. The superior free edge of each broad ligament is formed by the fallopian tube medially and the suspensory ligament of the ovary laterally. The paired *round ligaments* are bands of fibromuscular tissue that also course within the broad ligament, attaching to the anterolateral uterine fundus and extending anteriorly through the deep inguinal ring and inguinal canal, terminating in the labia majora. Uterine and ovarian blood vessels, nerves, and lymphatics as well as a portion of the pelvic ureters also course within the broad ligaments.

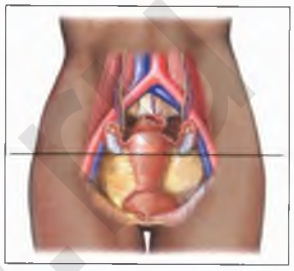

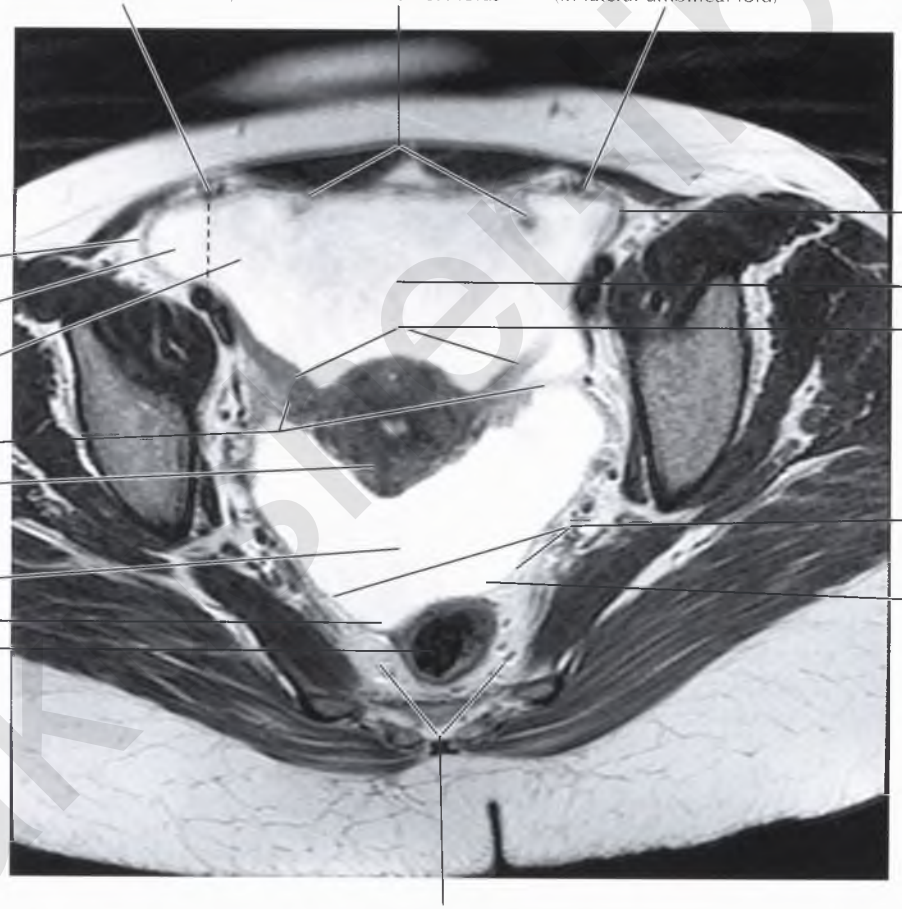
Inferior epigastric vessels (in lateral umbilical fold)
Medial umbilical ligaments (obliterated umbilical aa.) in medial umbilical folds
Inferior epigastric vessels (in lateral umbilical fold)
Parietal peritoneum
Lateral inguinal fossa
Medial inguinal fossa
Mesometrium (of broad ligaments)
Uterus
Rectouterine space (pouch of Douglas) (aka cul-de-sac)
Pararectal fossa
Rectum
Parietal peritoneum
Supravesical space
Round ligaments
Rectouterine folds
Pararectal fossa
Perirectal space

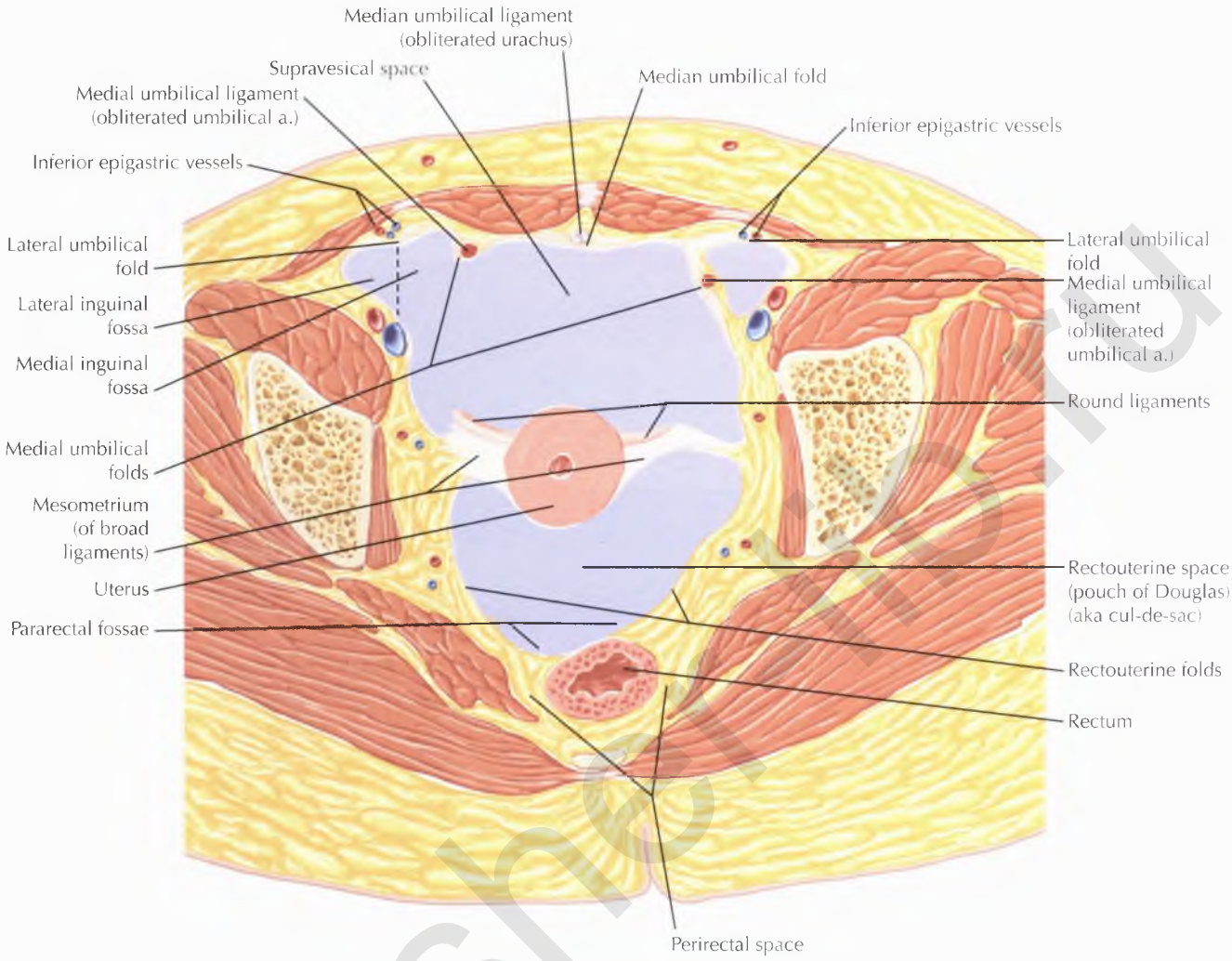

NORMAL ANATOMY

The *median umbilical ligament*, which represents the obliterated urachus, courses within the median umbilical fold, a single midline fold of peritoneum that extends from the anterosuperior bladder to the umbilicus. The paired *medial umbilical ligaments*, which represent the obliterated umbilical arteries, course within the medial umbilical folds of the peritoneum along the posterior aspect of the rectus abdominis muscles, between the median and lateral umbilical folds. Medial umbilical ligaments serve as landmarks for the superior aspect of the *umbilicovesical fascia*, a thin fascial plane triangular in configuration with apex at the umbilicus, seen anterior to the parietal peritoneum and posterior to the transversalis fascia.

The inferior epigastric vessels course within the paired lateral umbilical folds of the peritoneum, which separate the medial and lateral inguinal fossae.

DIAGNOSTIC CONSIDERATION

The deep inguinal ring lies lateral to the inferior epigastric vessels within the lateral inguinal fossa. In the patient with an indirect inguinal hernia, ascites may extend from the lateral inguinal fossa into the inguinal canal through a patent processus vaginalis testis (peritonei) in males or the "canal of Nuck" in females. In comparison, both femoral and direct inguinal hernias involve the medial inguinal fossa.

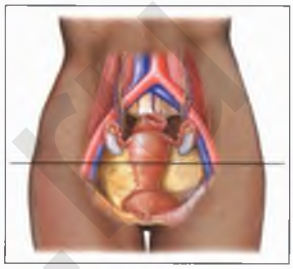

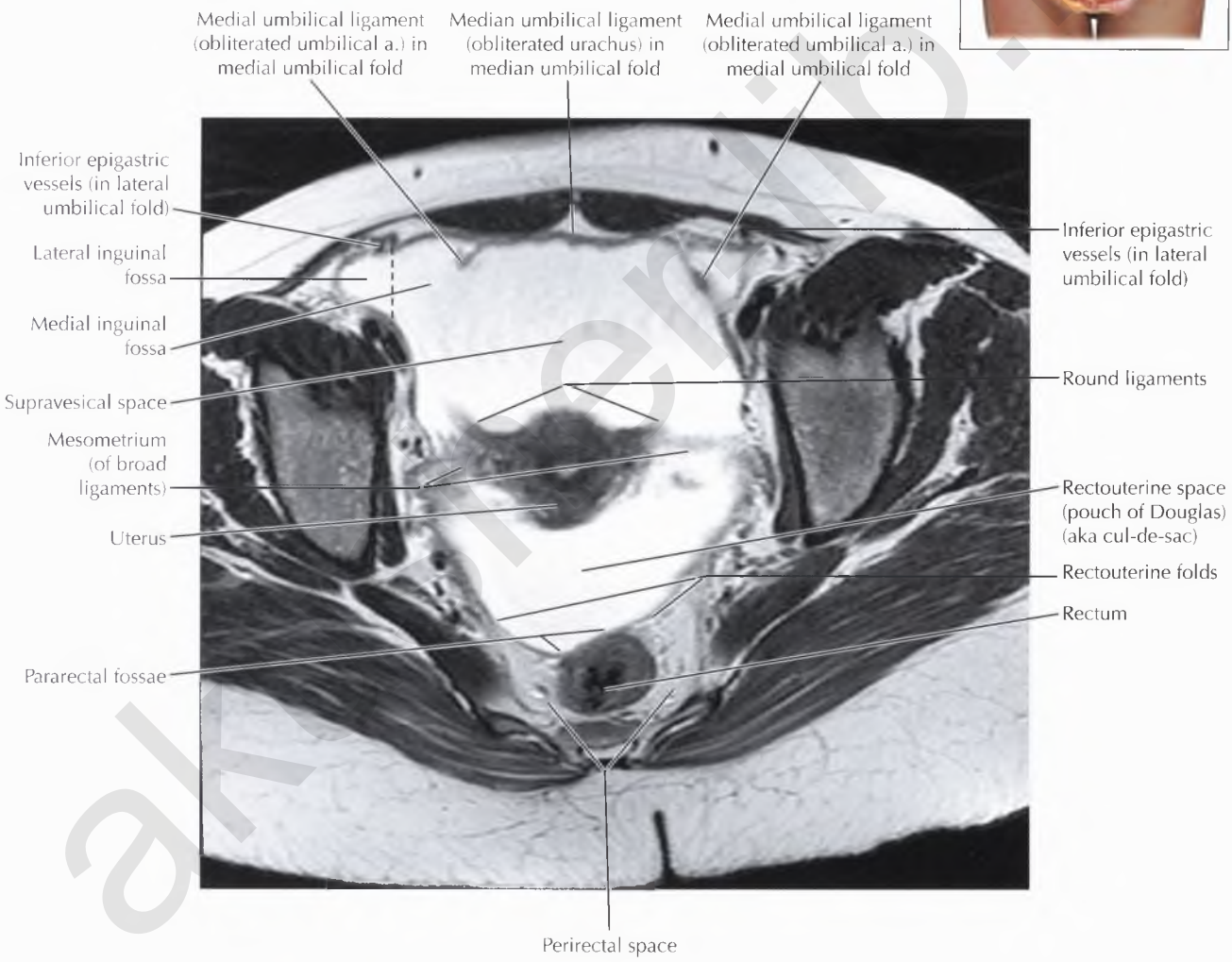
Medial umbilical ligament (obliterated umbilical a.) in medial umbilical fold
Median umbilical ligament (obliterated urachus) in median umbilical fold
Medial umbilical ligament (obliterated umbilical a.) in medial umbilical fold
Inferior epigastric vessels (in lateral umbilical fold)
Lateral inguinal fossa
Medial inguinal fossa
Supravesical space
Mesometrium (of broad ligaments)
Uterus
Pararectal fossae
Inferior epigastric vessels (in lateral umbilical fold)
Round ligaments
Rectouterine space (pouch of Douglas) (aka cul-de-sac)
Rectouterine folds
Rectum
Perirectal space

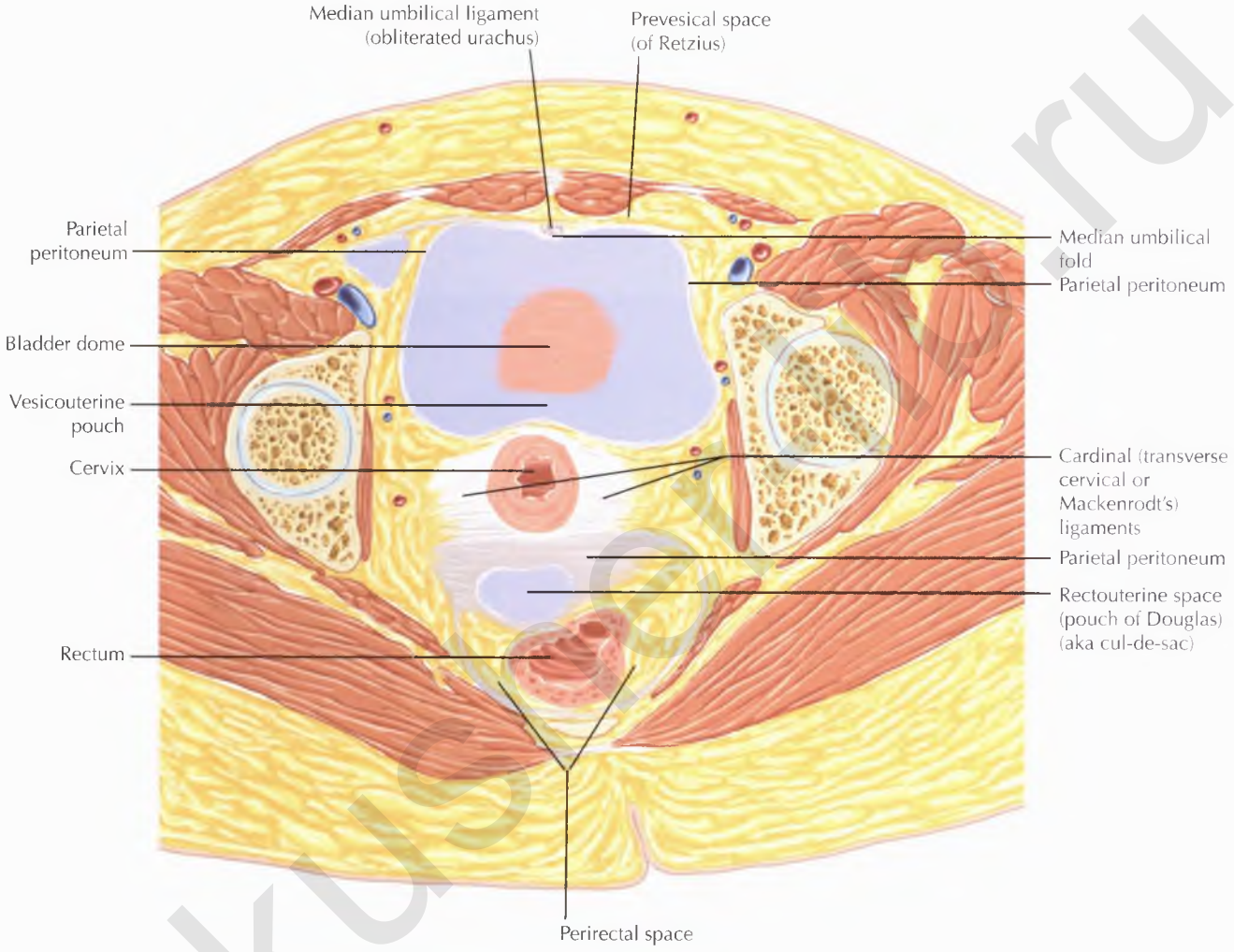

NORMAL ANATOMY

The perirectal space surrounds the rectum and is in continuity with the other major extraperitoneal spaces in the pelvis, including the prevesical space anteriorly and laterally as well as the presacral space. Denonvilliers' (rectoprostatic) fascia comprises the anterior perirectal fascia and the posterior prostatic fascia in males (see Chapter 1, Abdominal Wall and Viscera).

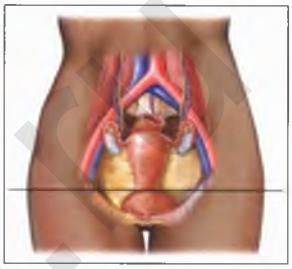

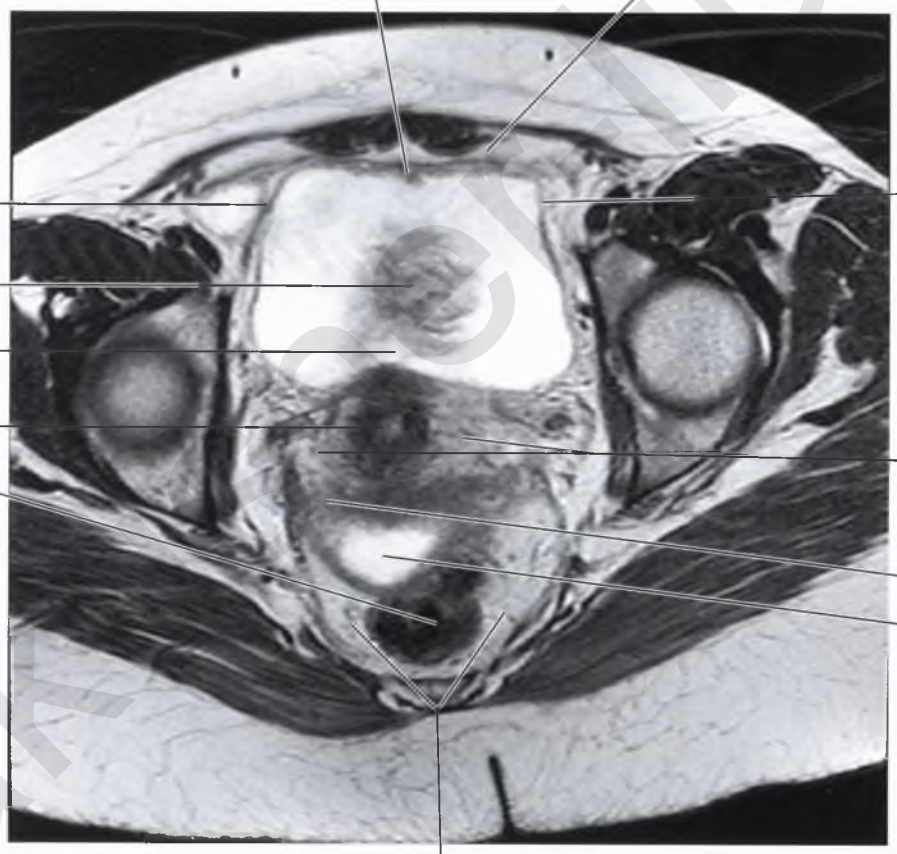
Median umbilical ligament (obliterated urachus) in median umbilical fold
Prevesical space (of Retzius)
Parietal peritoneum
Bladder dome
Vesicouterine pouch
Cervix
Rectum
Parietal peritoneum
Cardinal (transverse cervical or Mackenrodt's) ligaments
Parietal peritoneum
Rectouterine space (pouch of Douglas) (aka cul-de-sac)
Perirectal space

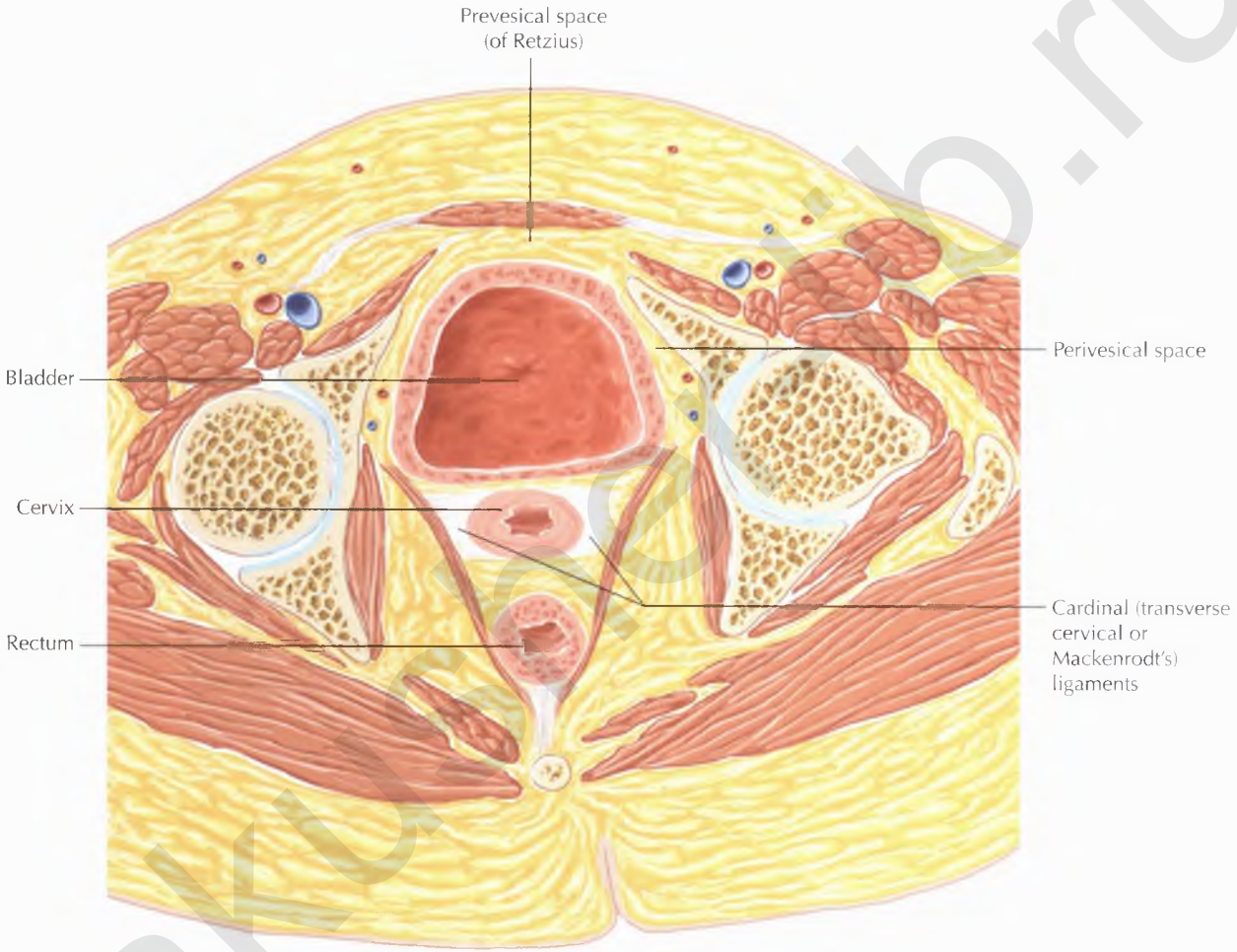
Prevesical space
(of Retzius)
Perivesical space
Bladder
Cervix
Rectum
Cardinal (transverse
cervical or
Mackenrodt's)
ligaments

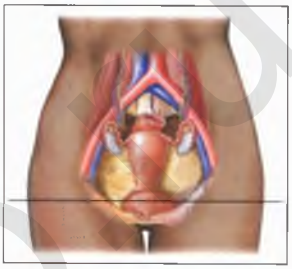

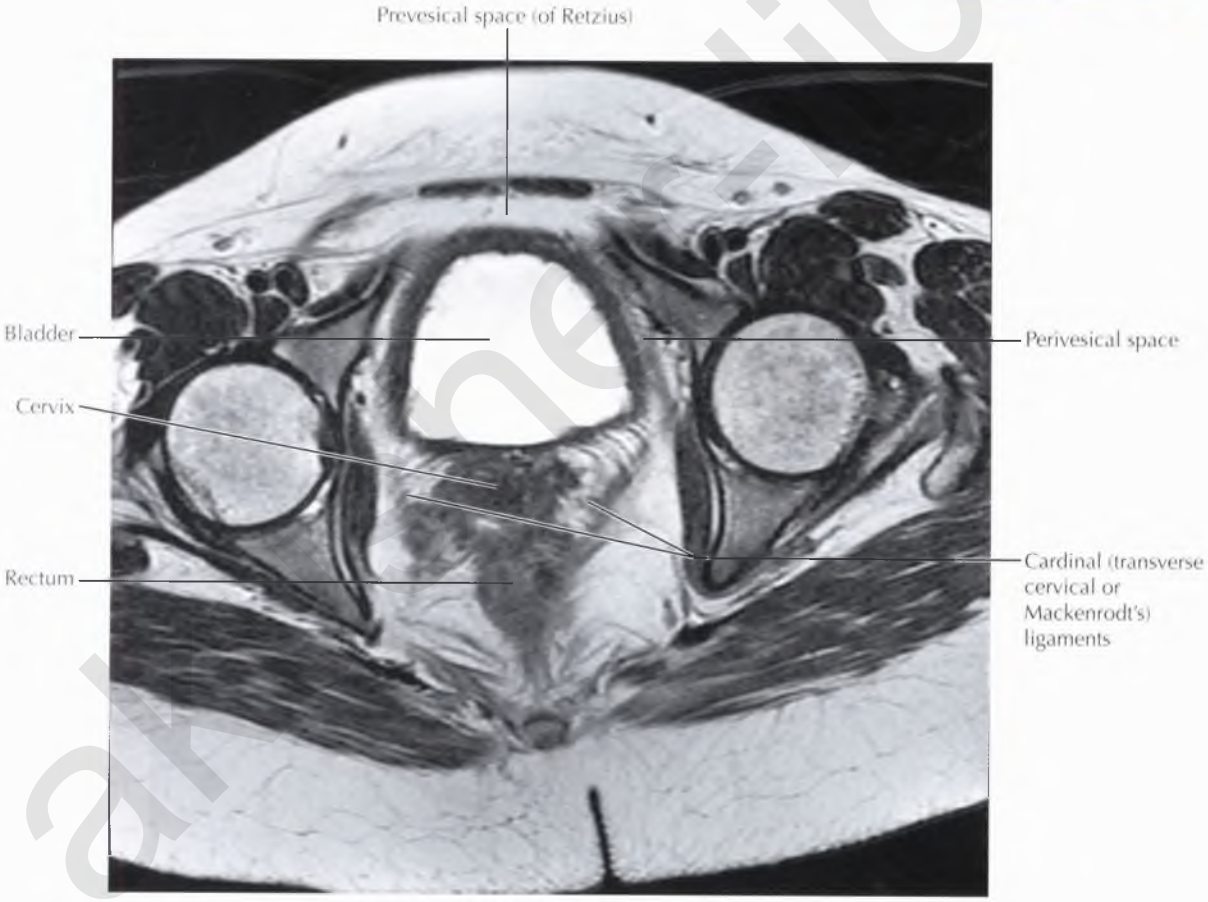
Prevesical space (of Retzius)
Bladder
Perivesical space
Cervix
Rectum
Cardinal (transverse cervical or Mackenrodt's) ligaments

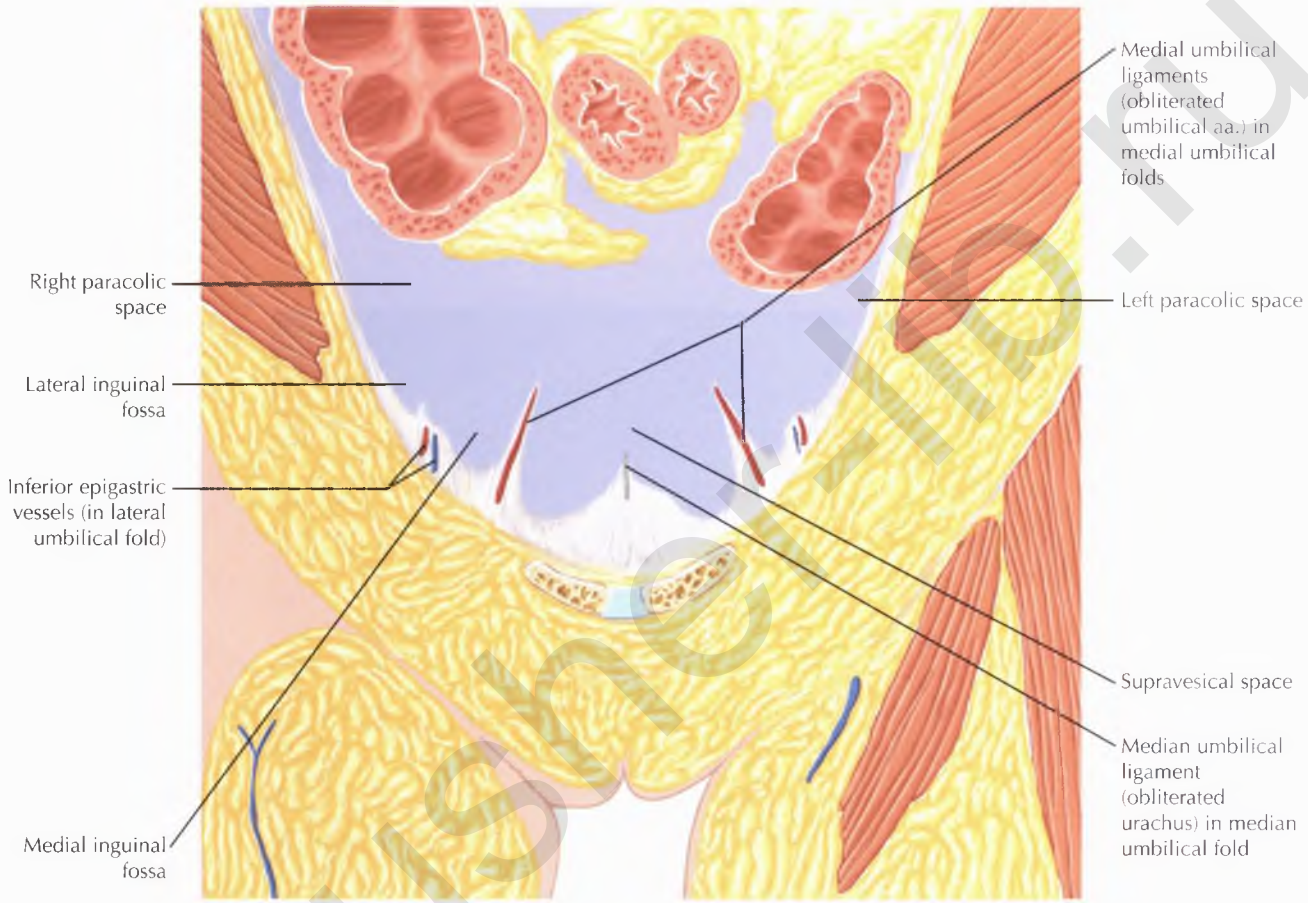

NORMAL ANATOMY

The medial and lateral umbilical folds separate the pelvic peritoneal paravesical spaces into the supravesical space, the medial inguinal fossa, and the lateral inguinal fossa (also seen on Pelvis Axials 5 and 6). The *supravesical space* is located superior to the urinary bladder and is bounded by the obliterated umbilical arteries running within the medial umbilical folds. The medial inguinal fossa is seen between the medial and lateral umbilical folds, and the lateral inguinal fossa between the lateral umbilical fold and the lateral parietal peritoneum.

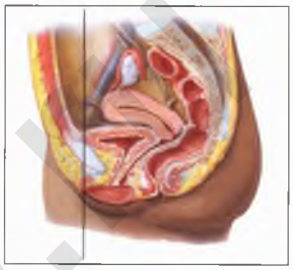


Right paracolic space
Lateral inguinal fossa
Inferior epigastric vessels (in lateral umbilical fold)
Medial inguinal fossa
Medial umbilical ligaments (obliterated umbilical aa.) in medial umbilical folds
Left paracolic space
Supravesical space
Median umbilical ligament (obliterated urachus) in median umbilical fold

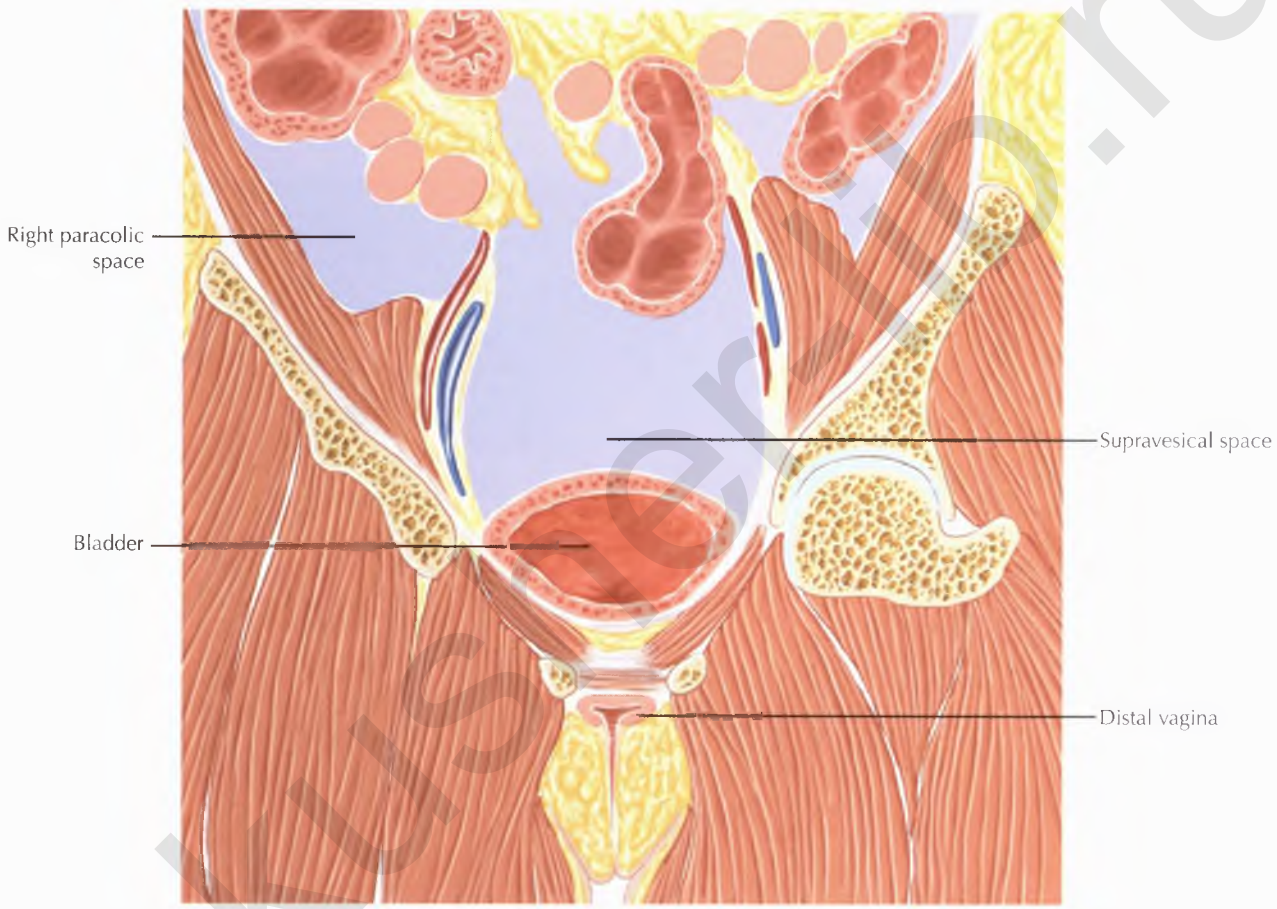
Right paracolic space
Supravesical space
Bladder
Distal vagina

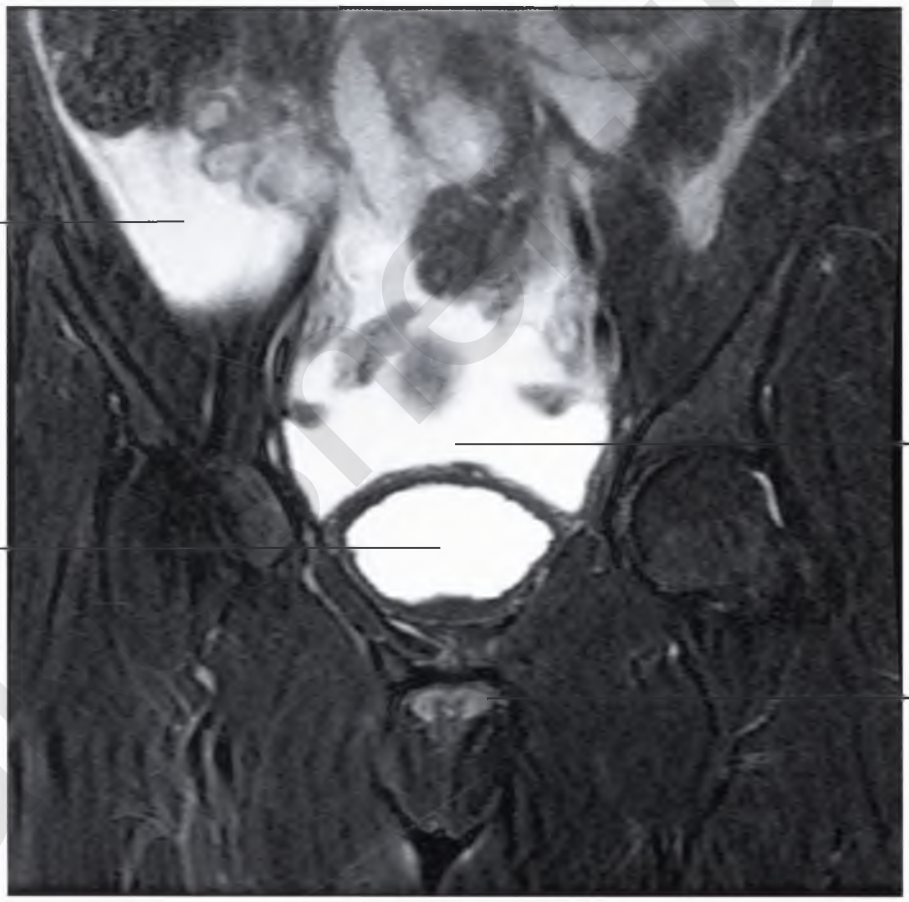
Right paracolic space
Supravesical space
Bladder
Distal vagina

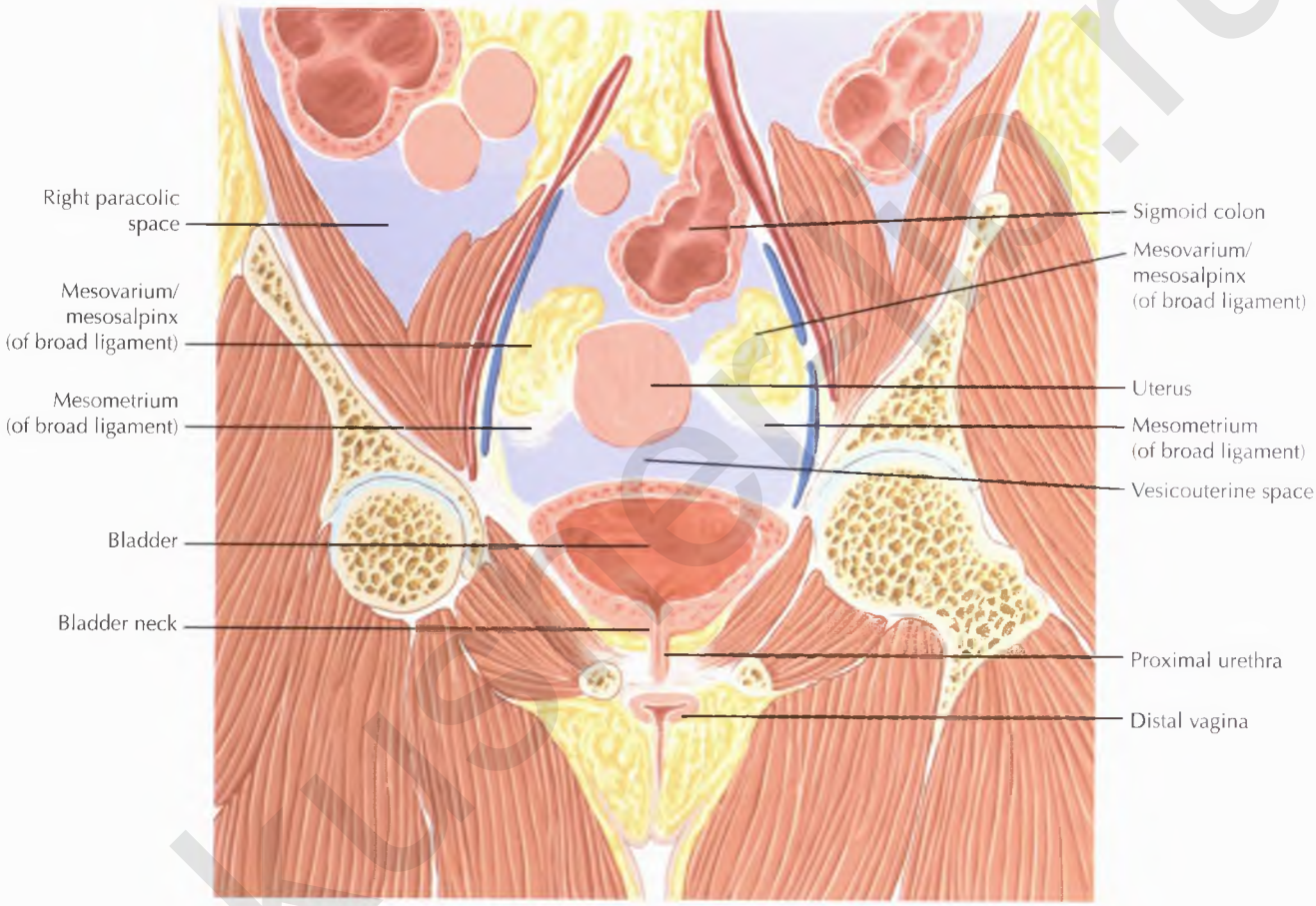

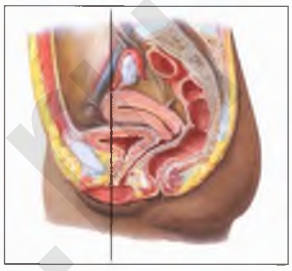

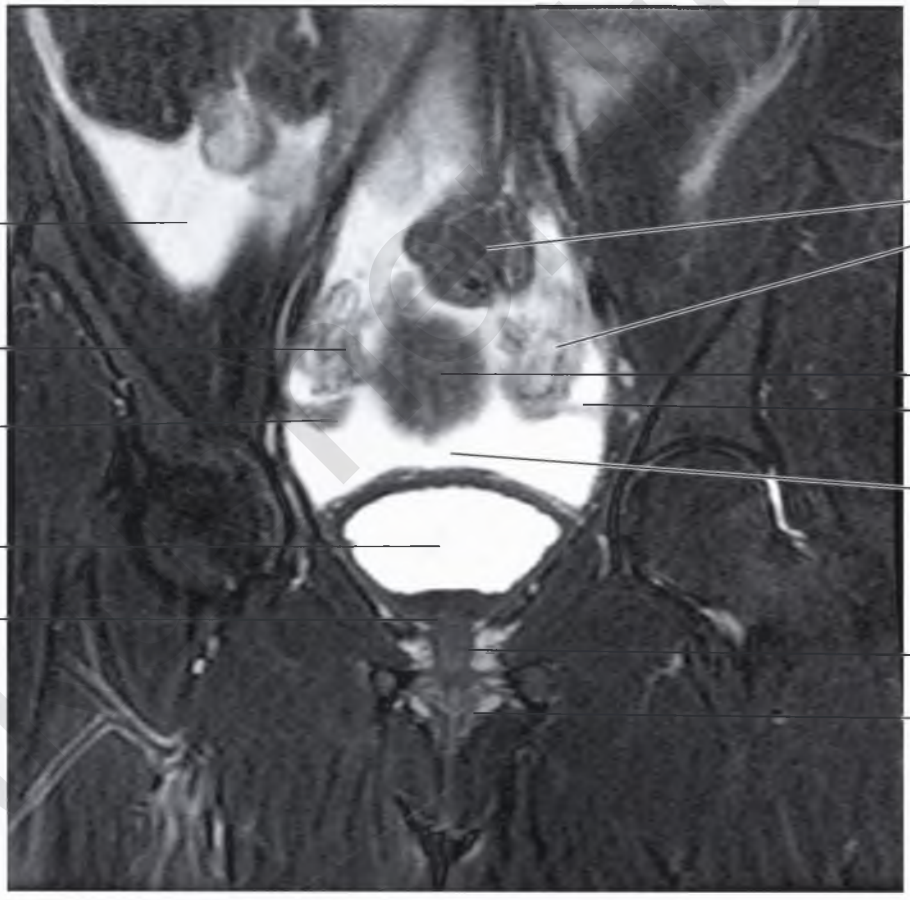
Right paracolic space
Mesovarium/ mesosalpinx (of broad ligament)
Mesometrium (of broad ligament)
Bladder
Bladder neck
Sigmoid colon
Mesovarium/ mesosalpinx (of broad ligament)
Uterus
Mesometrium (of broad ligament)
Vesicouterine space
Proximal urethra
Distal vagina

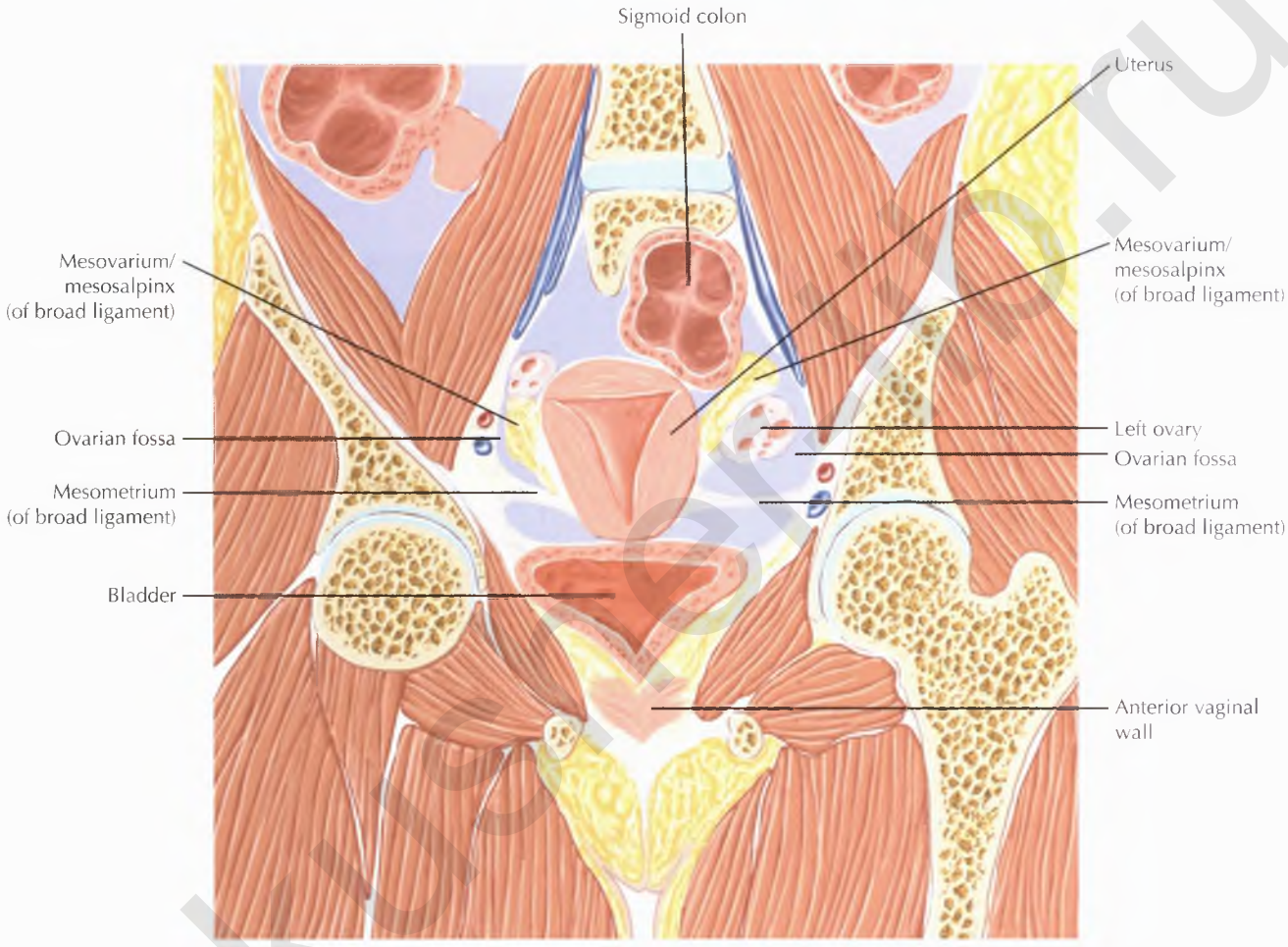

NORMAL ANATOMY

The broad ligament is subdivided into three components: the *mesometrium*, surrounding the uterus; the *mesosalpinx*, surrounding the fallopian tube; and the *mesovarium*, surrounding the ovary.

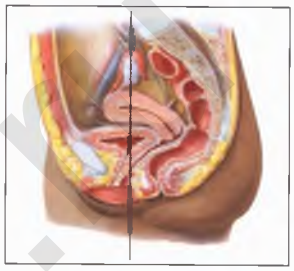

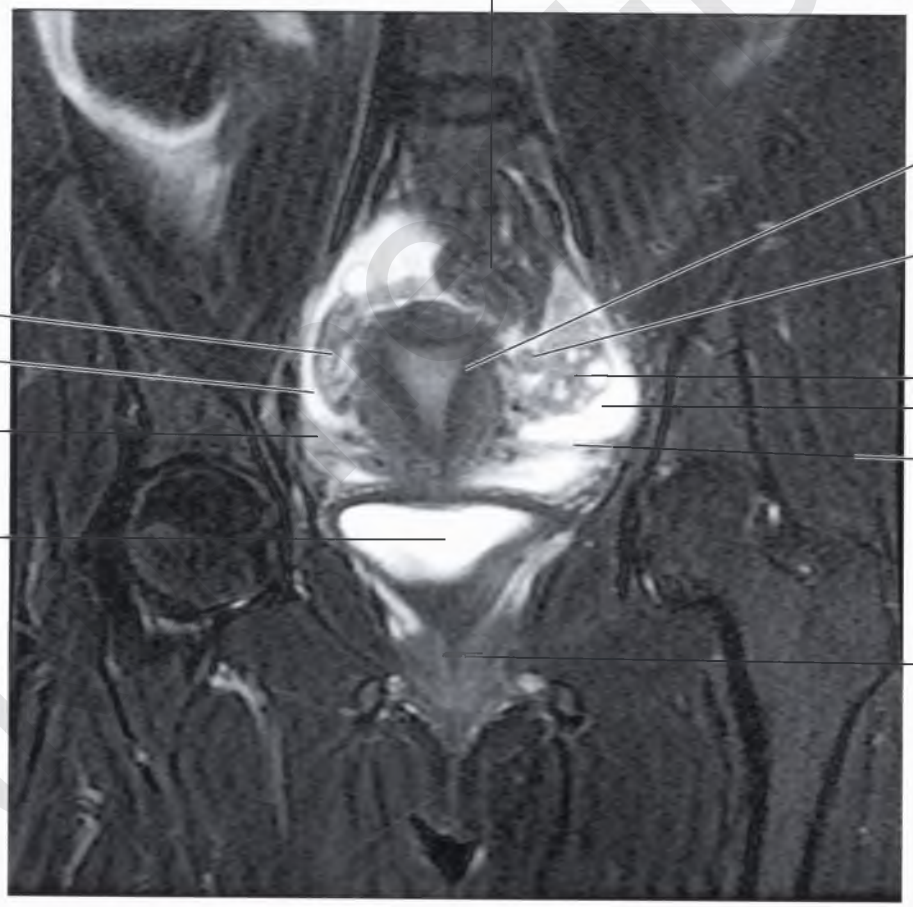
Sigmoid colon
Uterus
Mesovarium/
mesosalpinx
(of broad ligament)
Mesovarium/
mesosalpinx
(of broad ligament)
Ovarian fossa
Left ovary
Ovarian fossa
Mesometrium
(of broad ligament)
Mesometrium
(of broad ligament)
Bladder
Anterior vaginal
wall

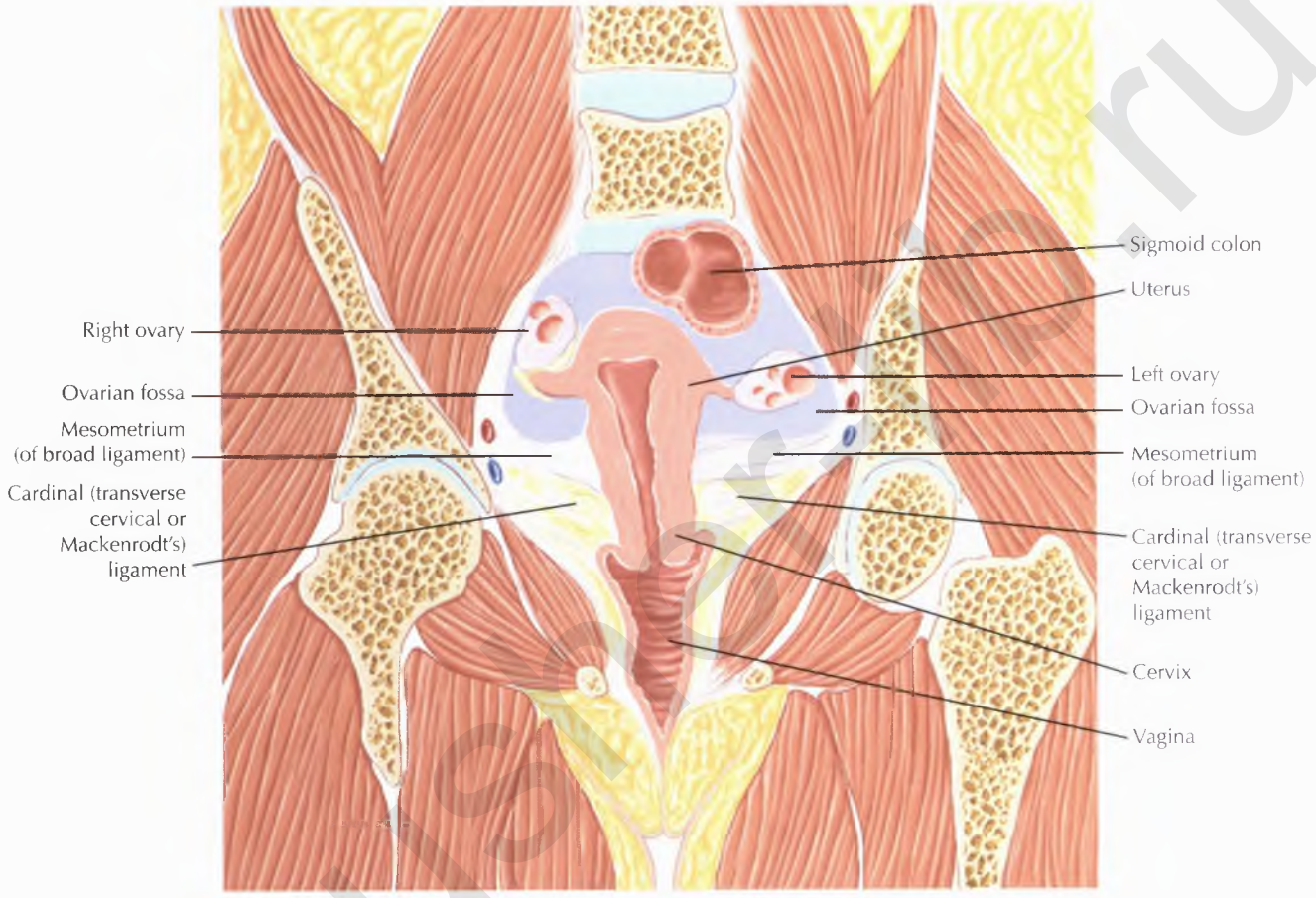

NORMAL ANATOMY

The *cardinal ligament*, also called the transverse cervical or Mackenrodt's ligament, is a triangular ligament that forms the base of the broad ligament and provides the primary support of the uterus and superior vagina. The cardinal ligament extends from the cervix to the pelvic side wall laterally, and the uterine artery runs along its superior aspect. The paired uterine arteries are branches from the anterior division of the internal iliac arteries and are the primary blood supply to the uterus.

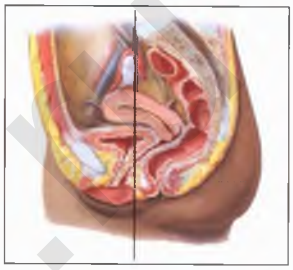

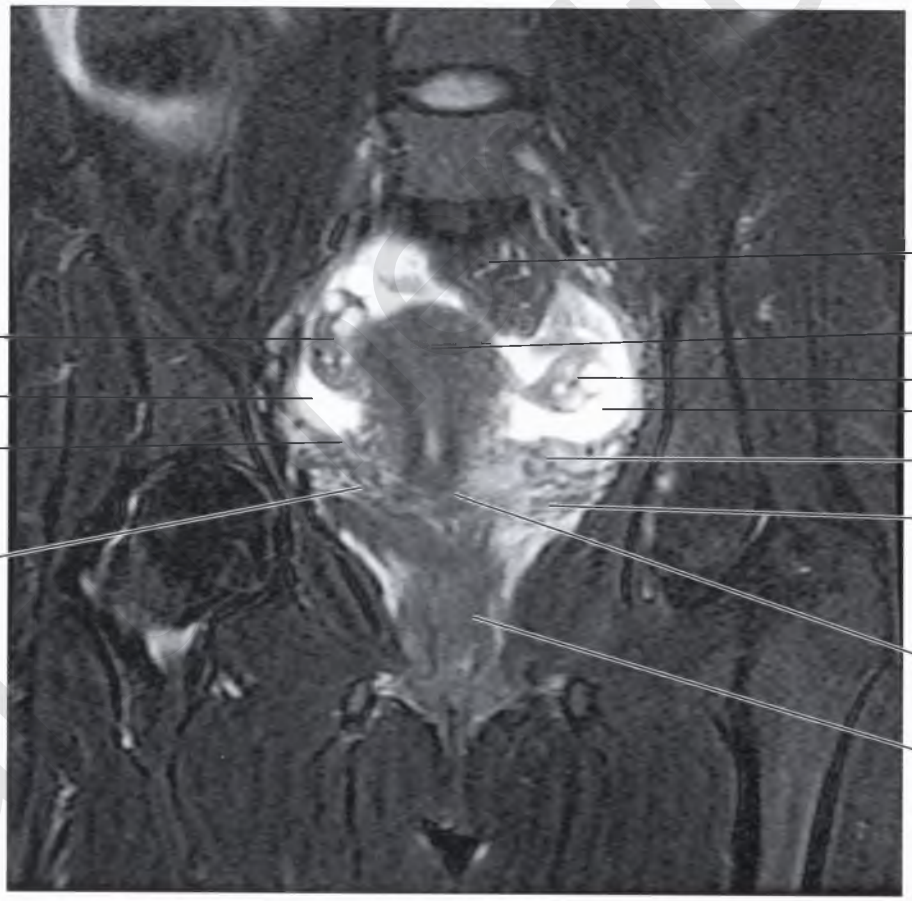
Sigmoid colon
Right ovary
Uterus
Ovarian fossa
Left ovary
Mesometrium (of broad ligament)
Ovarian fossa
Cardinal (transverse cervical or Mackenrodt's) ligament
Mesometrium (of broad ligament)
Cardinal (transverse cervical or Mackenrodt's) ligament
Cervix
Vagina

NORMAL ANATOMY

There are four recesses surrounding the vaginal portion of the cervix: a small anterior fornix, two small lateral fornices (shown here), and a deep posterior fornix (shown on Pelvis Coronal 7).

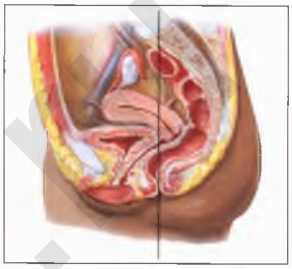

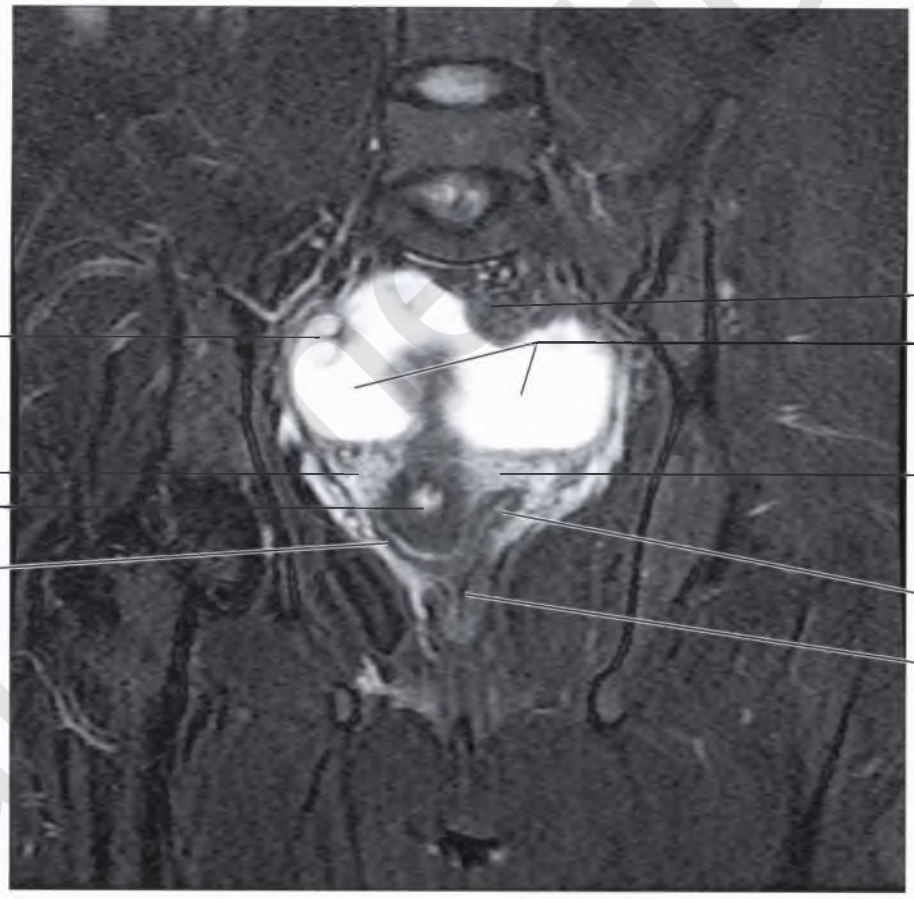
Right ovary
Cardinal (transverse cervical or Mackenrodt's) ligament
Cervix
Lateral vaginal fornix
Sigmoid colon
Rectouterine space (pouch of Douglas) (aka cul-de-sac)
Cardinal (transverse cervical or Mackenrodt's) ligament
Lateral vaginal fornix
Vagina

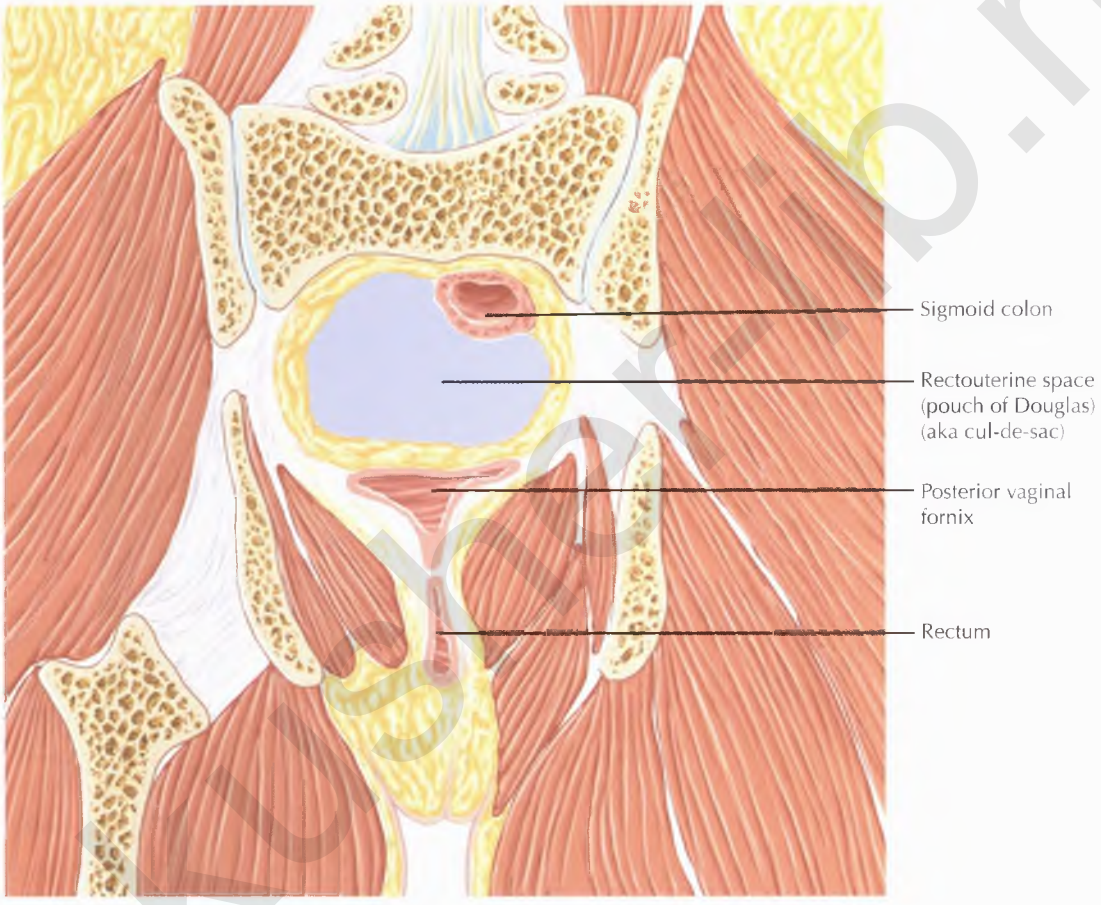

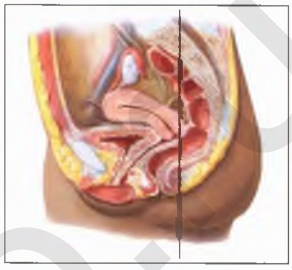

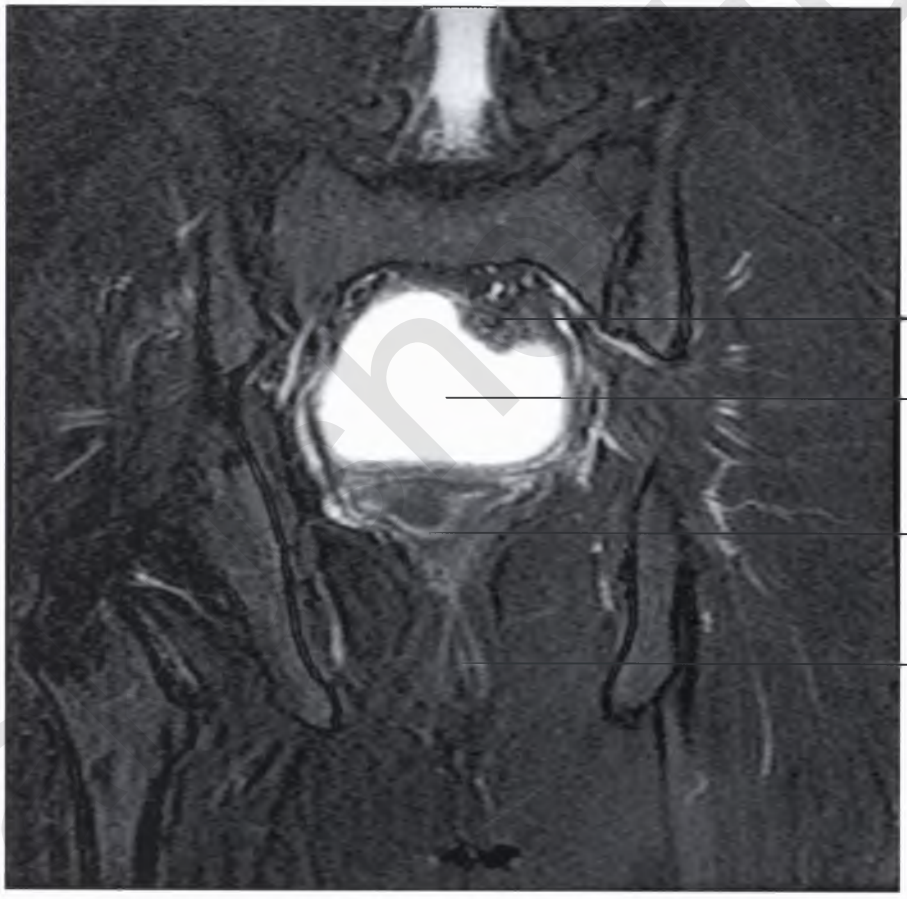
Sigmoid colon
Rectouterine space (pouch of Douglas) (aka cul-de-sac)
Posterior vaginal fornix
Rectum

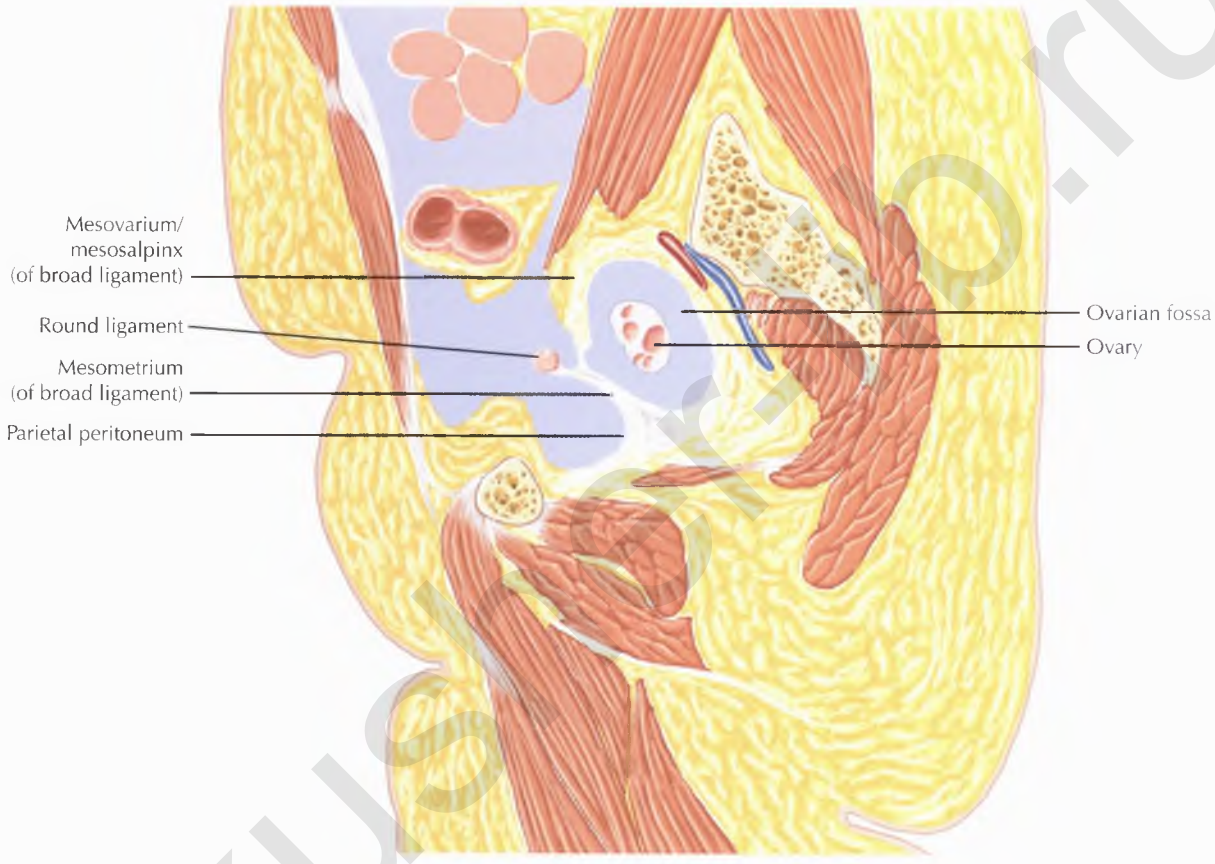

NORMAL ANATOMY

The ovarian fossa occupies the lateral aspect of the rectouterine space (pouch of Douglas or cul-de-sac), posterior to the broad ligament and anterior to the ureter and internal iliac vessels (see Pelvis Axial 4).

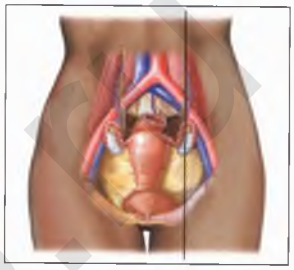

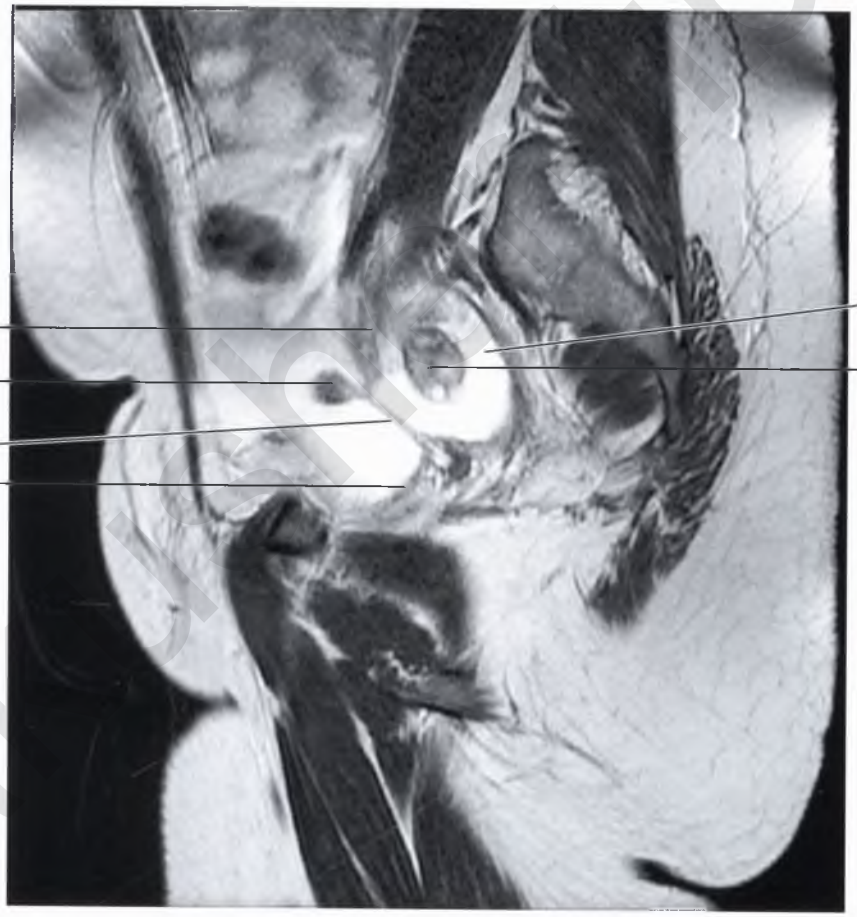
Mesovarium/
mesosalpinx
(of broad ligament)
Round ligament
Mesometrium
(of broad ligament)
Parietal peritoneum
Ovarian fossa
Ovary

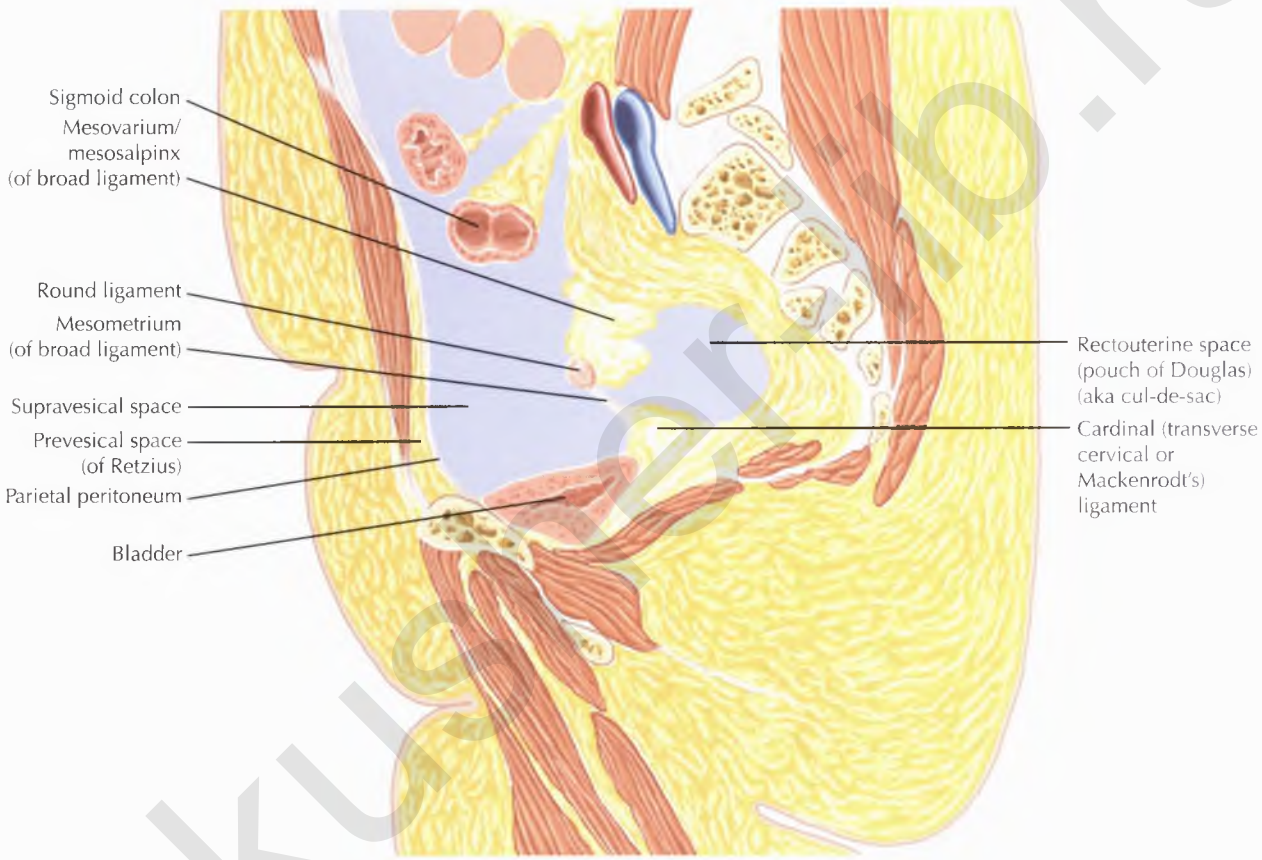

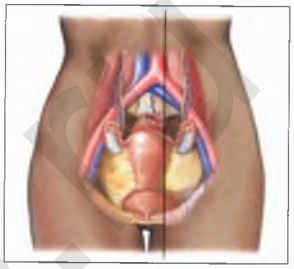

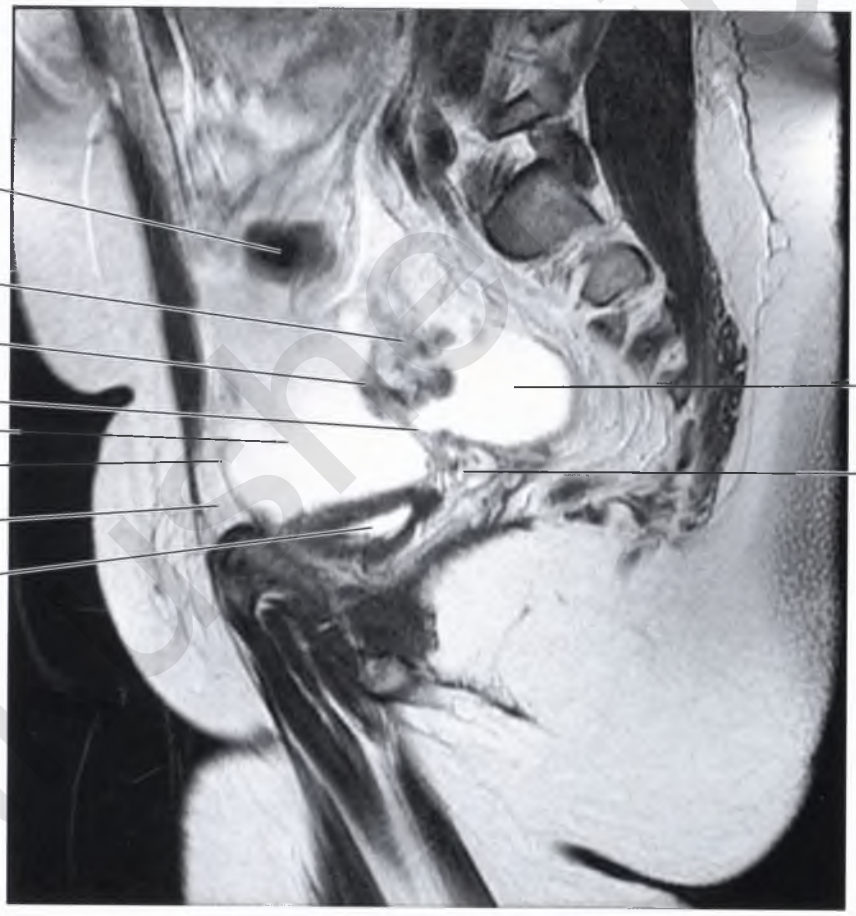
Sigmoid colon
Mesovarium/ mesosalpinx (of broad ligament)
Round ligament
Mesometrium (of broad ligament)
Supravesical space
Parietal peritoneum
Prevesical space (of Retzius)
Bladder
Rectouterine space (pouch of Douglas) (aka cul-de-sac)
Cardinal (transverse cervical or Mackenrodt's) ligament

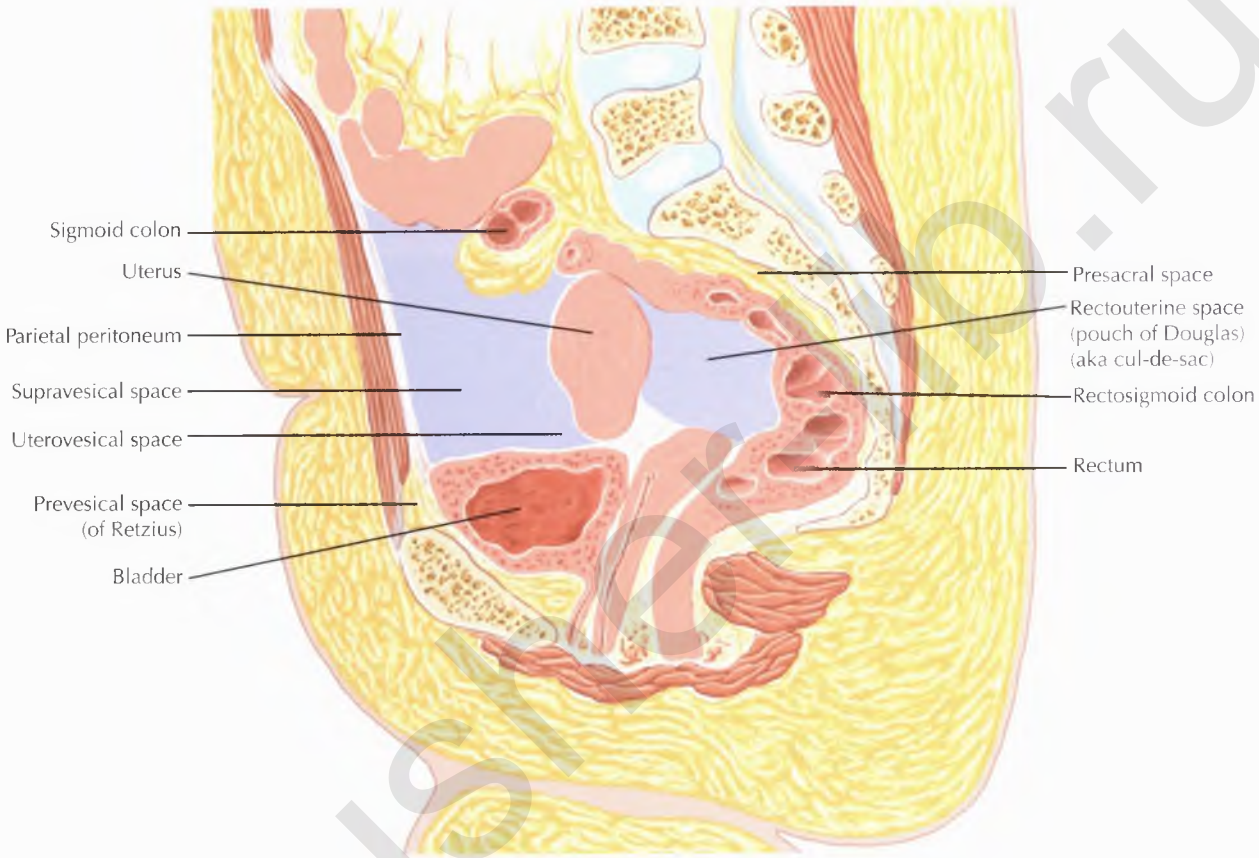

NORMAL ANATOMY

Extraperitoneal spaces in the pelvis include the *prevesical space* (of Retzius) anteriorly, a large-volume potential space located anterior and lateral to the umbilicovesical fascia and posterior to the pubic bones and rectus sheath, as well as the *presacral space* posteriorly (as shown). The other main extraperitoneal spaces of the pelvis include the *perivesical space*, a small-volume potential space bounded anteriorly by the umbilicovesical fascia, which contains the urachus, urinary bladder, and fat, as well as the *perirectal space*.

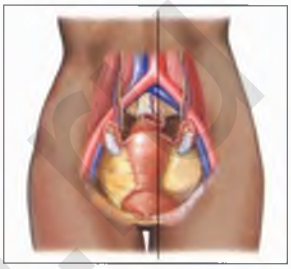

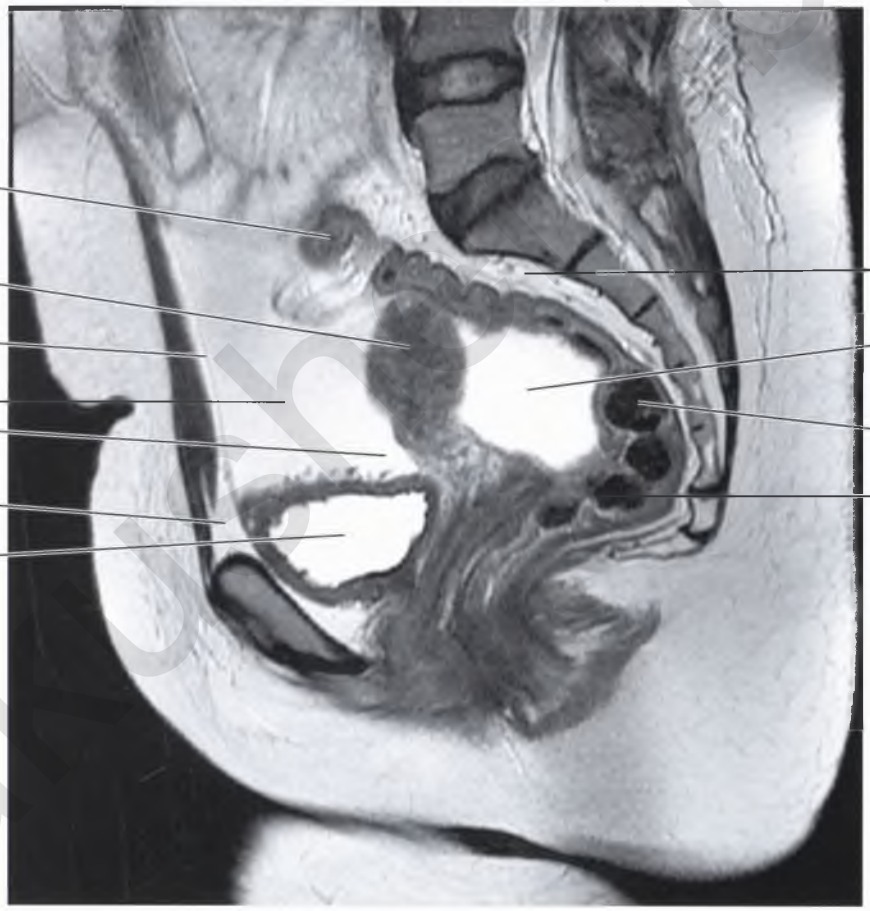
Sigmoid colon
Uterus
Parietal peritoneum
Supravesical space
Uterovesical space
Prevesical space
(of Retzius)
Bladder
Presacral space
Rectouterine space
(pouch of Douglas)
(aka cul-de-sac)
Rectosigmoid colon
Rectum

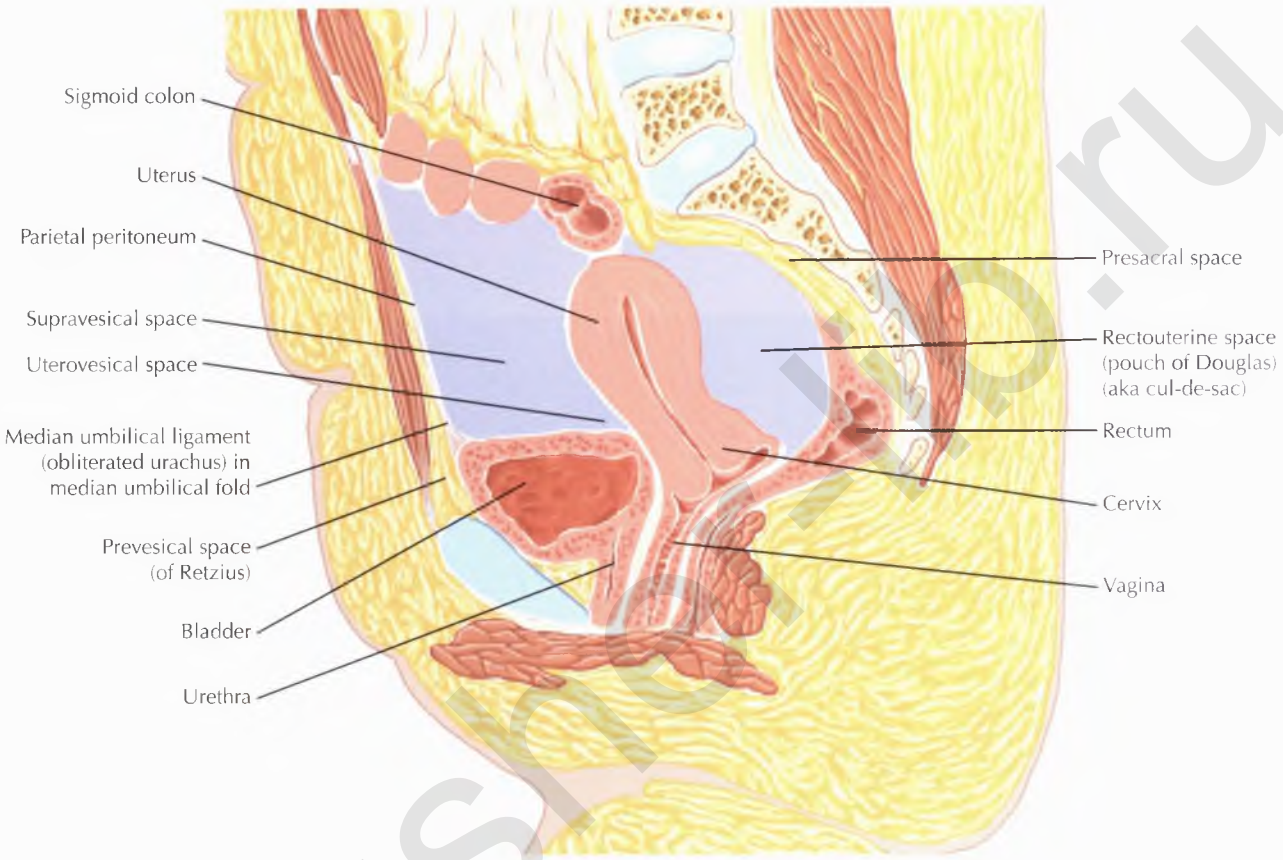

NORMAL ANATOMY

The anteriorly located pelvic peritoneal paravesical space is divided into the *supravesical space* and the medial and lateral *inguinal fossae* (best seen in Pelvis Axials 5 and 6 and Pelvis Coronal 1). More posteriorly, the peritoneum covering the bladder and rectum forms the *rectovesical space*, which in the female is subdivided into the *uterovesical space* anterior to the uterus and the *rectouterine space* (pouch of Douglas or cul-de-sac) posterior to the uterus. The rectouterine space is further subdivided into the *pararectal space* and the *ovarian fossae* by peritoneal reflections covering the vesical and uterine vessels, known as the *rectouterine folds*. The rectouterine folds extend posterolaterally from the uterine cervix to the sacrum, forming the lateral boundaries of the pararectal fossae (see Pelvis Axials 5 and 6). These folds are more prominent and easier to visualize in men and are called the *sacrogenital folds*

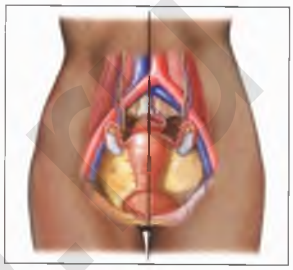

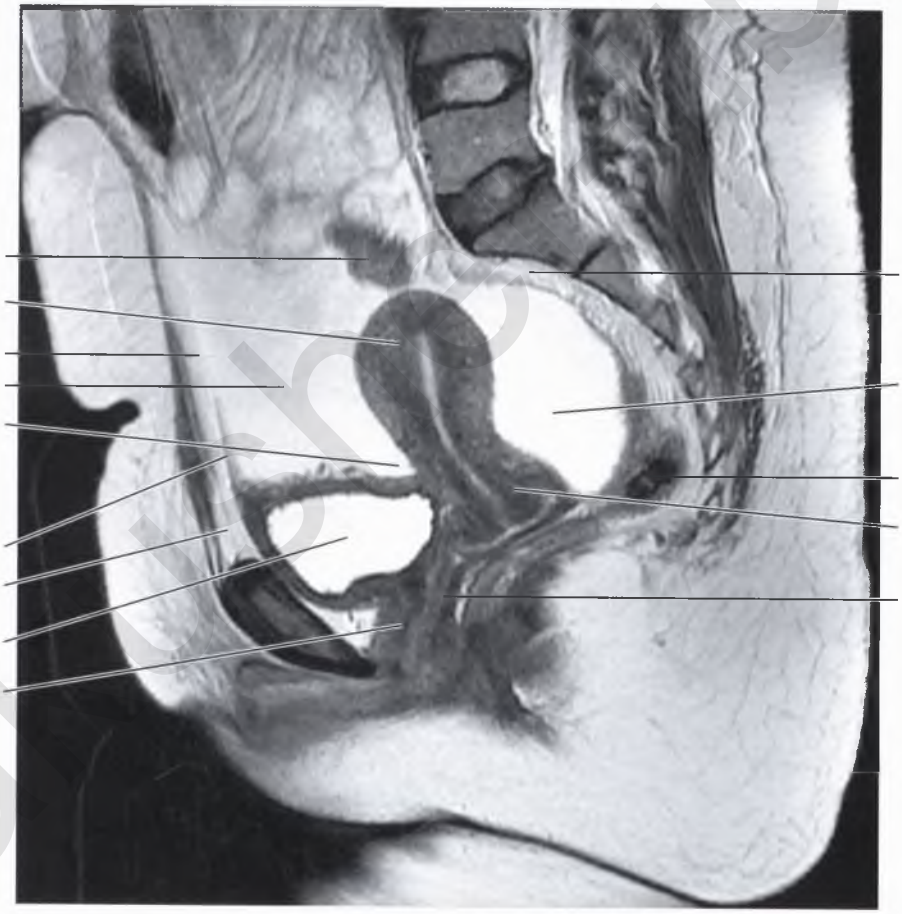
Sigmoid colon
Uterus
Parietal peritoneum
Supravesical space
Uterovesical space
Median umbilical ligament (obliterated urachus) in median umbilical fold
Prevesical space (of Retzius)
Bladder
Urethra
Presacral space
Rectouterine space (pouch of Douglas) (aka cul-de-sac)
Rectum
Cervix
Vagina

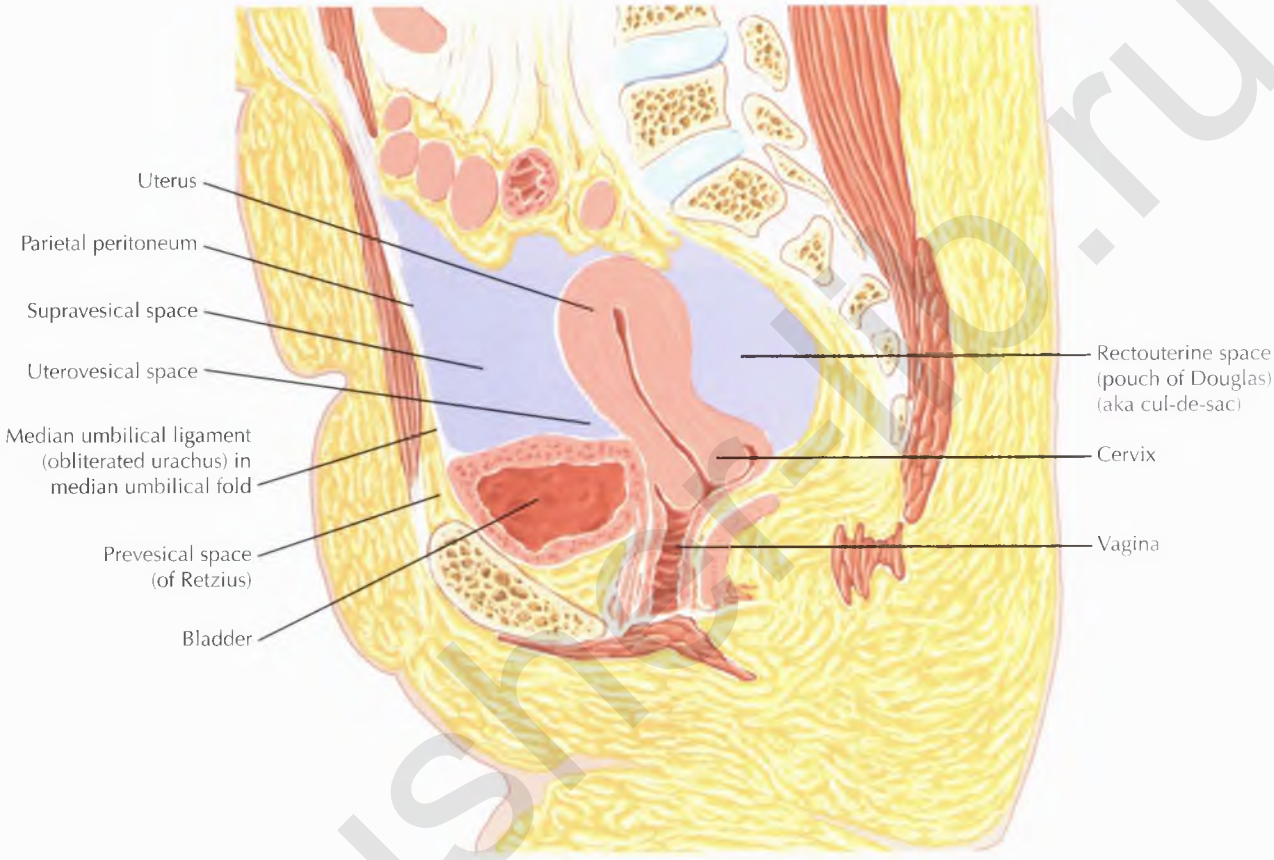

DIAGNOSTIC CONSIDERATION

Fluid collections in the anterior pelvic peritoneal space may be differentiated from collections in the extraperitoneal prevesical space by inferior (rather than posterior) displacement of the urinary bladder, visualization of the umbilical folds surrounded by fluid, and preservation of the preperitoneal fat. Extraperitoneal prevesical fluid collections surround and displace the bladder posteriorly and are often described as having a "molar tooth" configuration in the axial plane. These extraperitoneal collections do not extend into the inguinal fossae, another distinguishing characteristic.

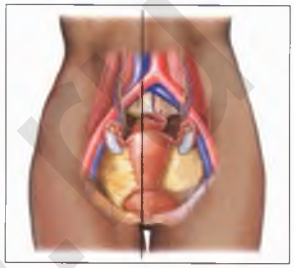

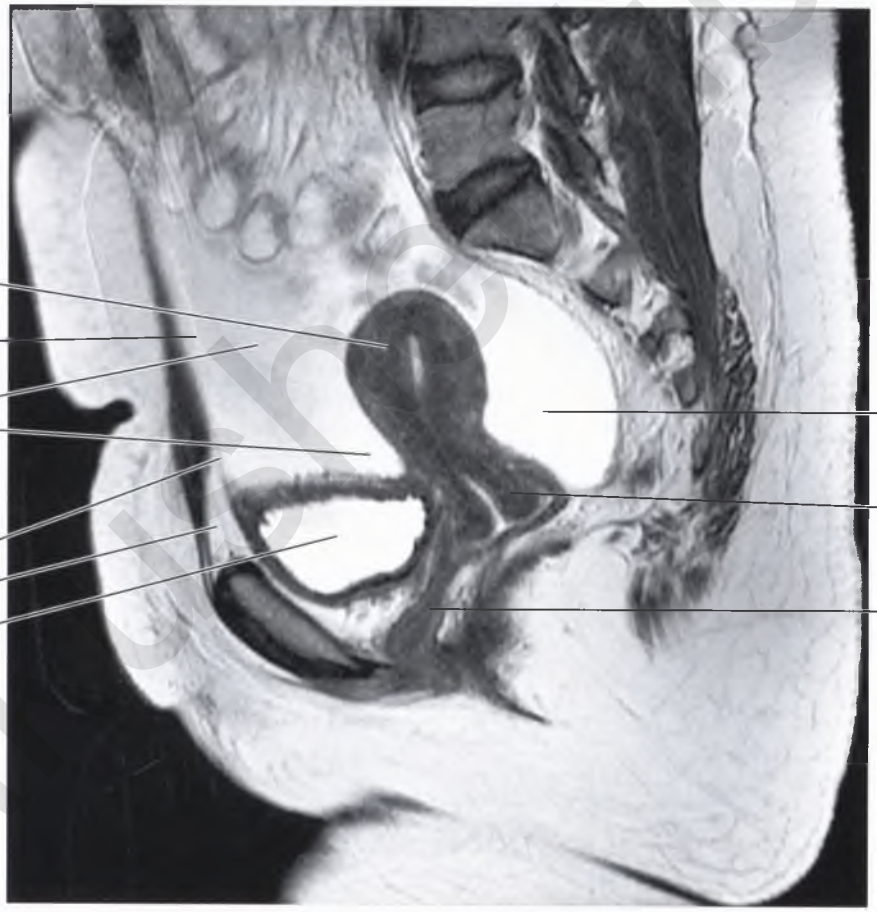
Uterus
Parietal peritoneum
Supravesical space
Uterovesical space
Median umbilical ligament (obliterated urachus) in median umbilical fold
Prevesical space
Bladder
Rectouterine space (pouch of Douglas) (aka cul-de-sac)
Cervix
Vagina

Chapter 4 BILIARY SYSTEM

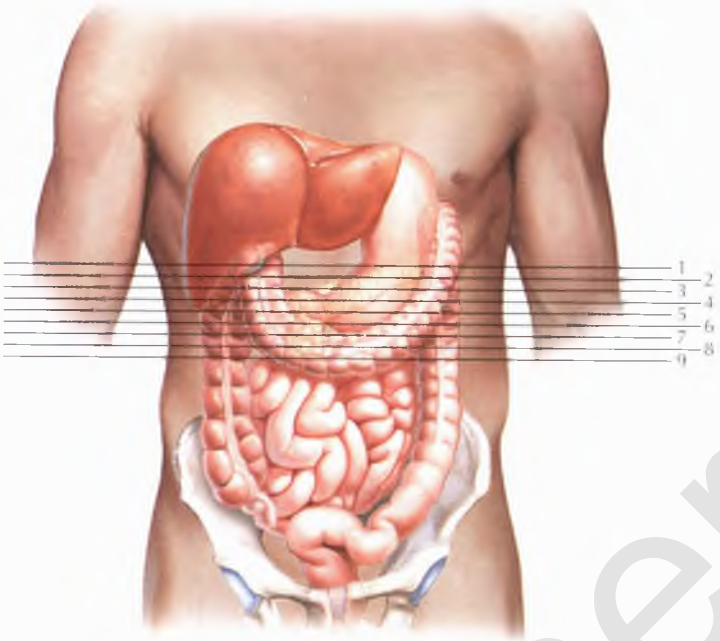

AXIAL 208

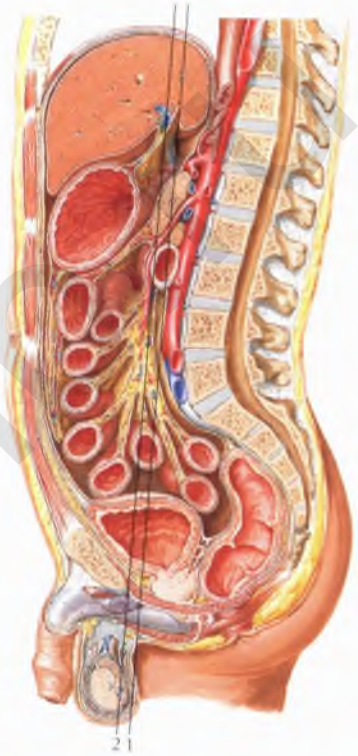

CORONAL 226

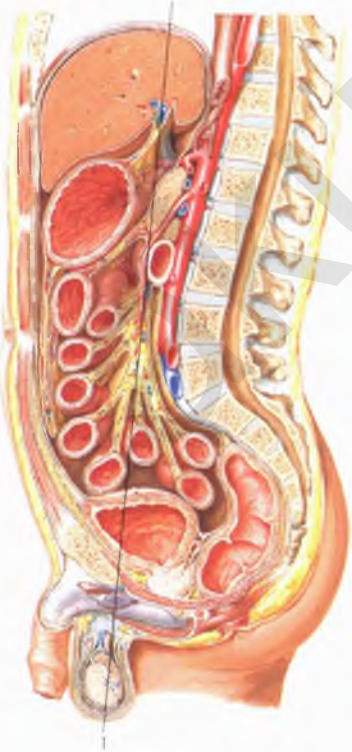

CORONAL MAXIMUM INTENSITY PROJECTION (MIP) 230

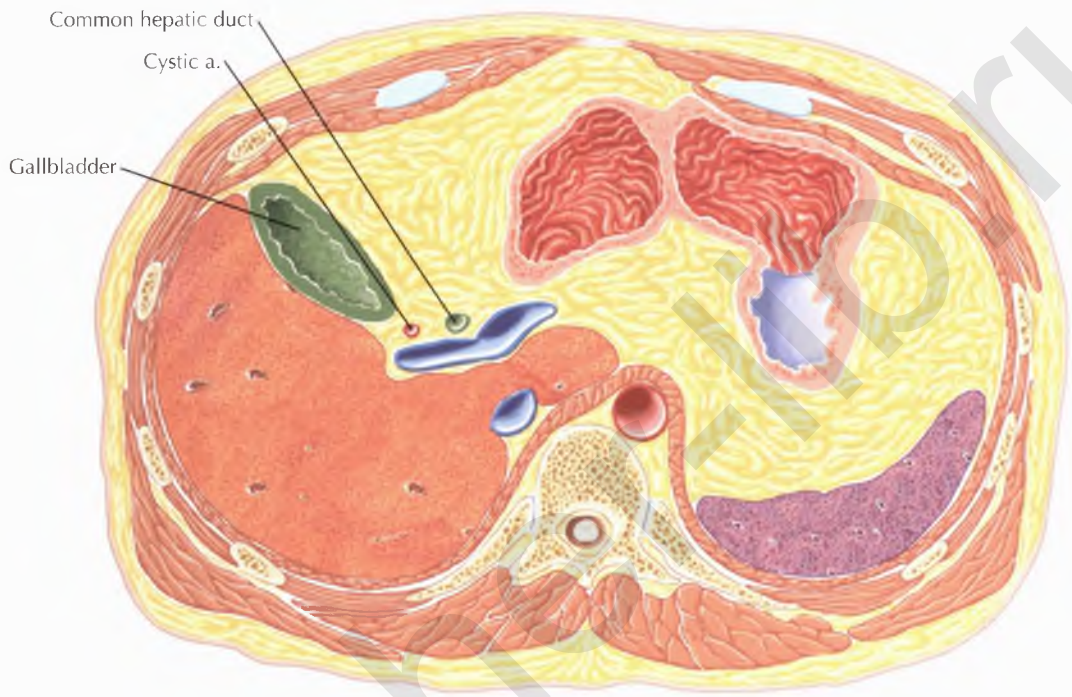

NORMAL ANATOMY

The normal gallbladder wall should be thin, measuring no more than 3 mm in thickness when well distended.

PATHOLOGIC PROCESS

Thickening of the gallbladder wall is seen in many pathologic conditions, including primary gallbladder disorders (e.g., acute and chronic cholecystitis, carcinoma, adenomyomatosis), systemic conditions (e.g., hepatic, cardiac, or renal failure; hypoproteinemia), infections, such as infectious mononucleosis or opportunistic infections in the patient with acquired immunodeficiency syndrome (AIDS), and extracholecystic inflammation such as with acute hepatitis, pancreatitis, or pyelonephritis.

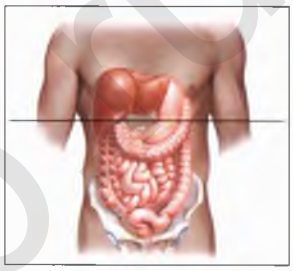

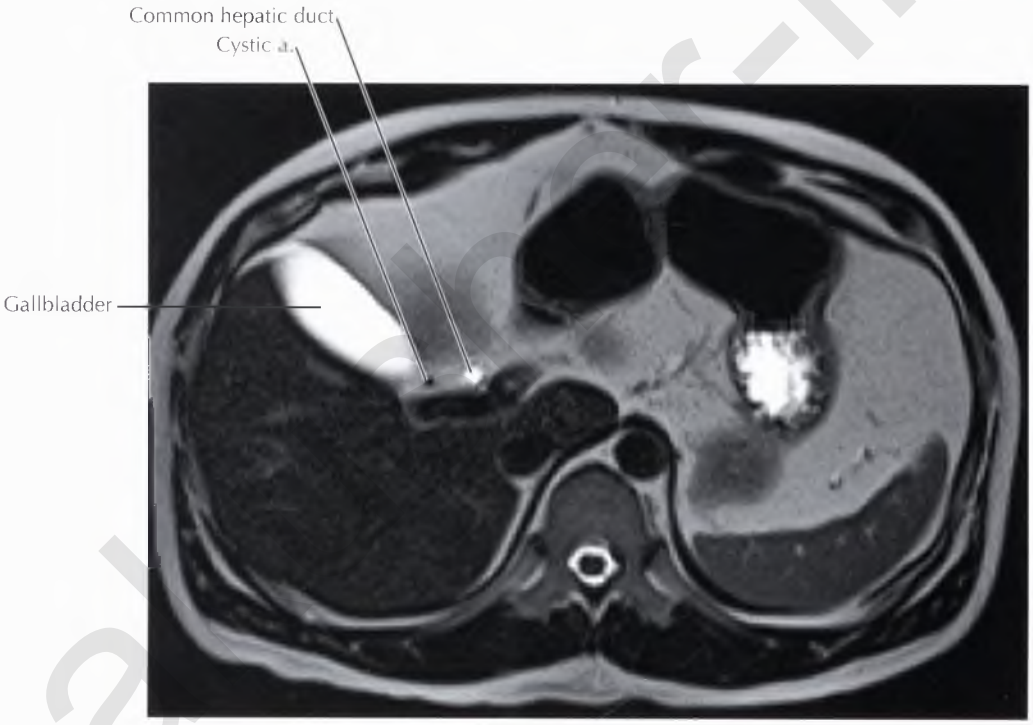
Common hepatic duct
Cystic a.
Gallbladder

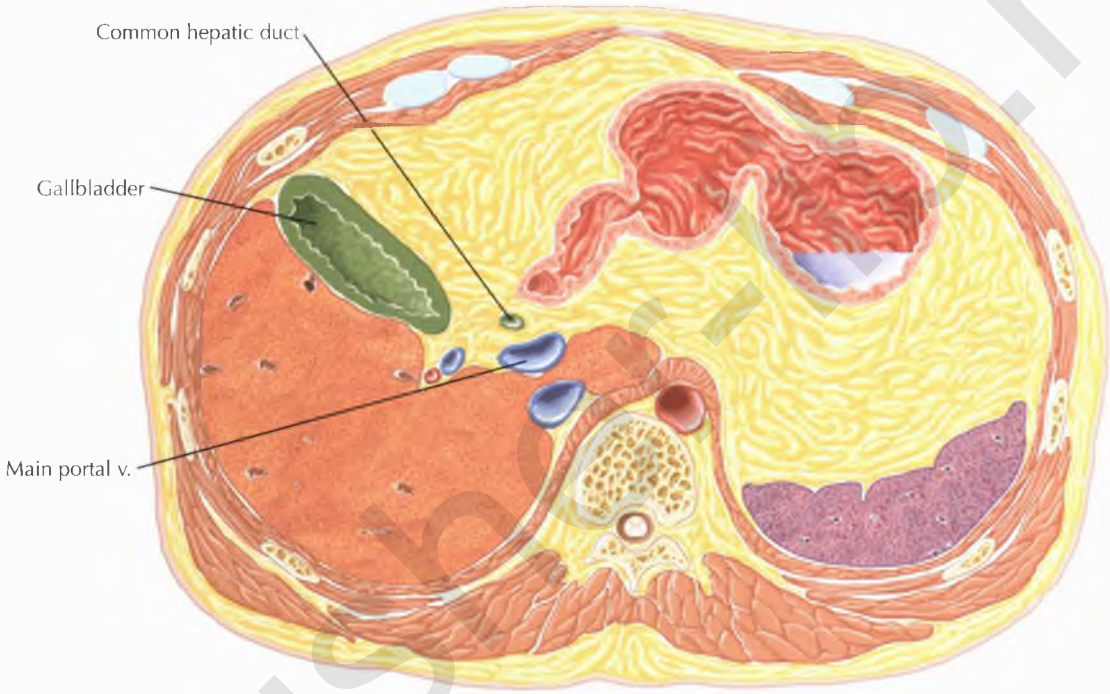

NORMAL ANATOMY

Classically, the left and right hepatic ducts merge to form the *common hepatic duct* just anterior to the extrahepatic portal vein within a sheath that is continuous with the hepatoduodenal ligament.

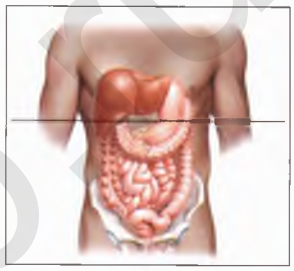

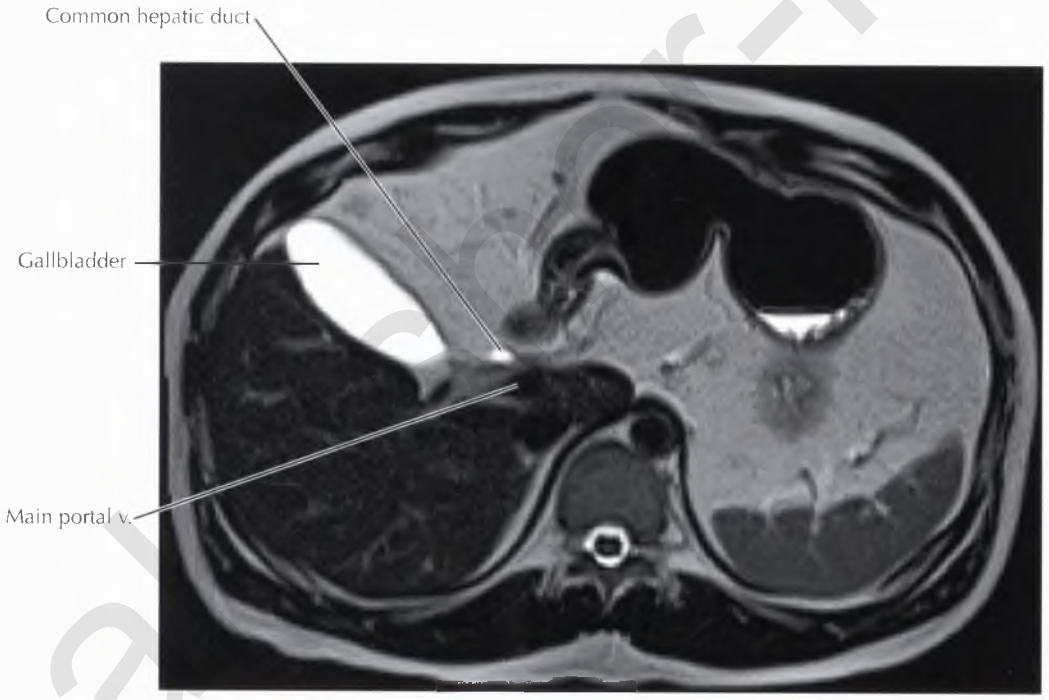
Common hepatic duct
Gallbladder
Main portal v.

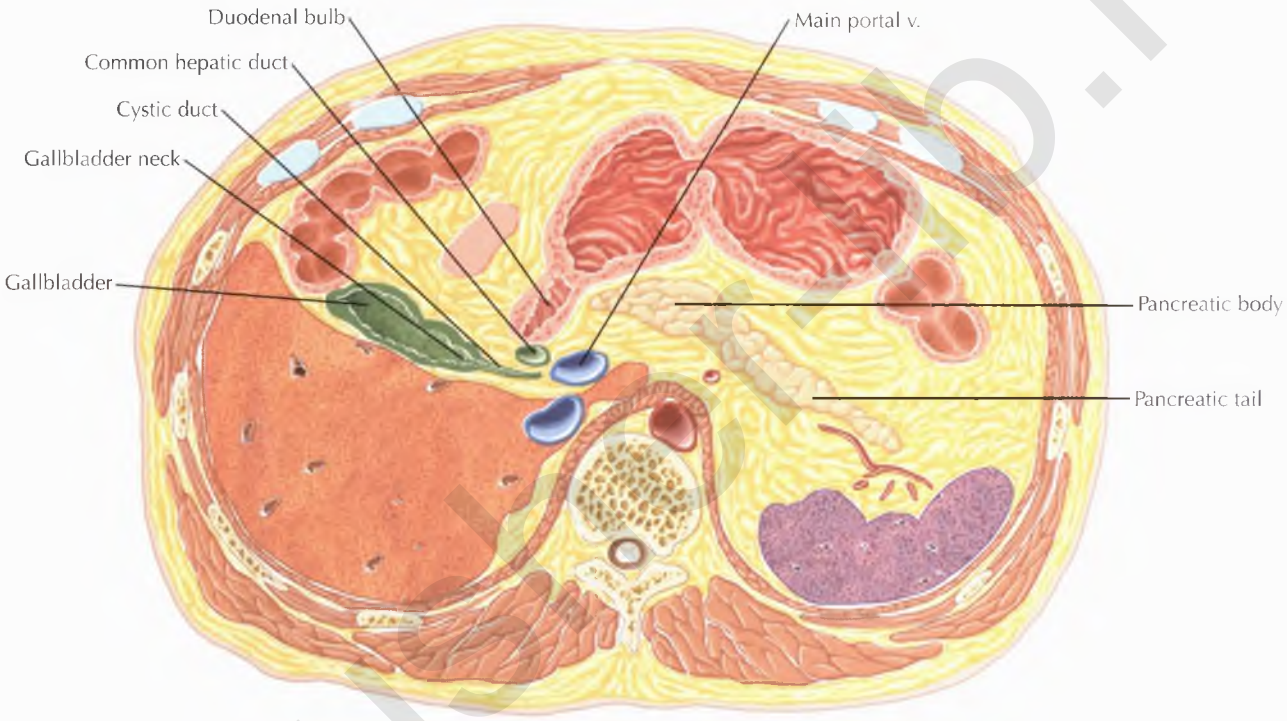

NORMAL ANATOMY

The cystic duct drains into the common hepatic duct to form the common bile duct.

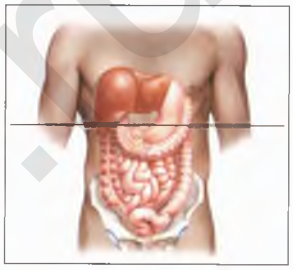

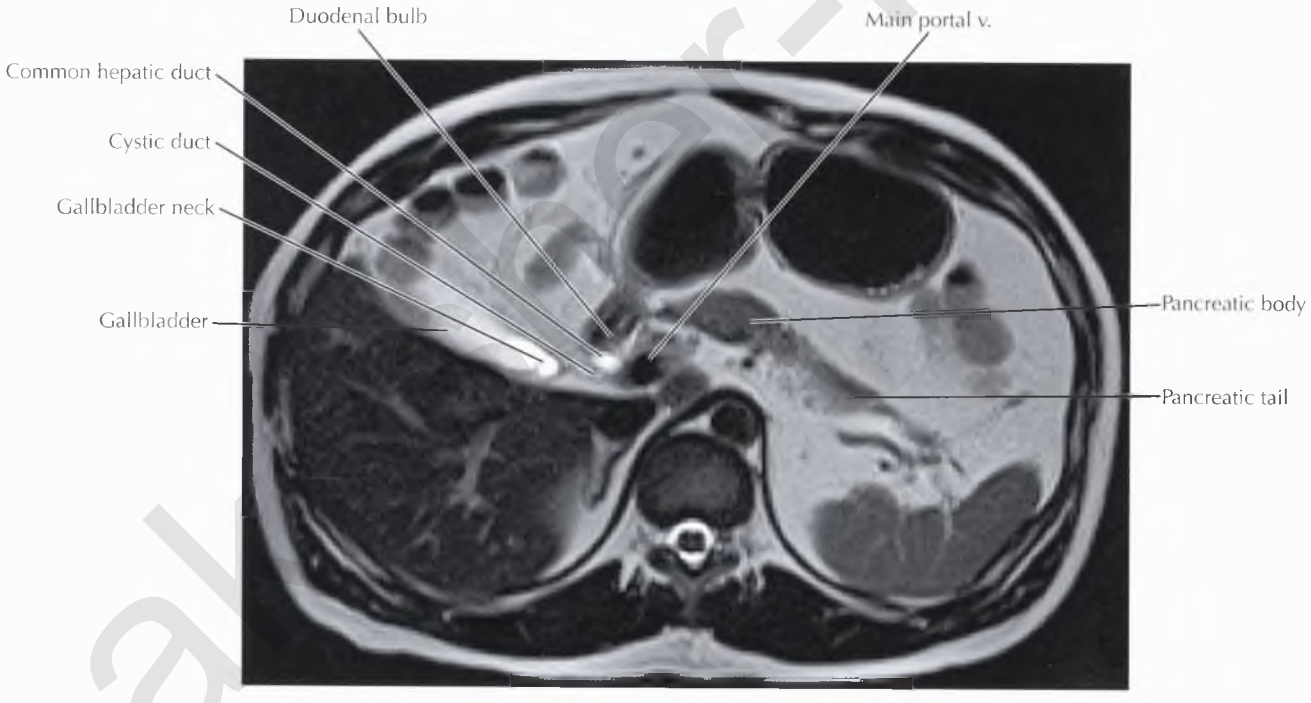

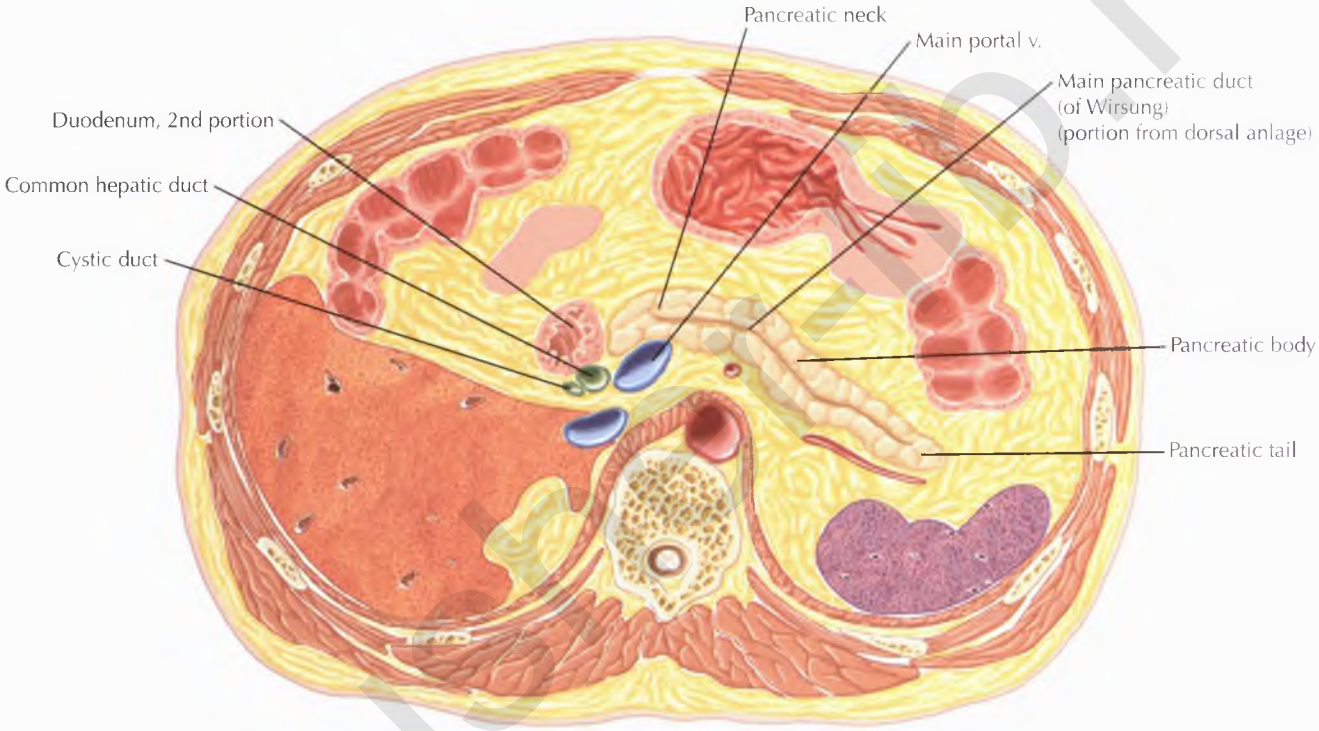

NORMAL ANATOMY

The main pancreatic duct normally measures 2 to 3 mm in diameter at ages 30 to 50, which may increase to an average 4.5 mm at 70 to 90 years.

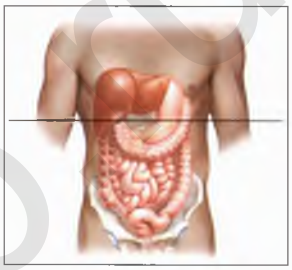

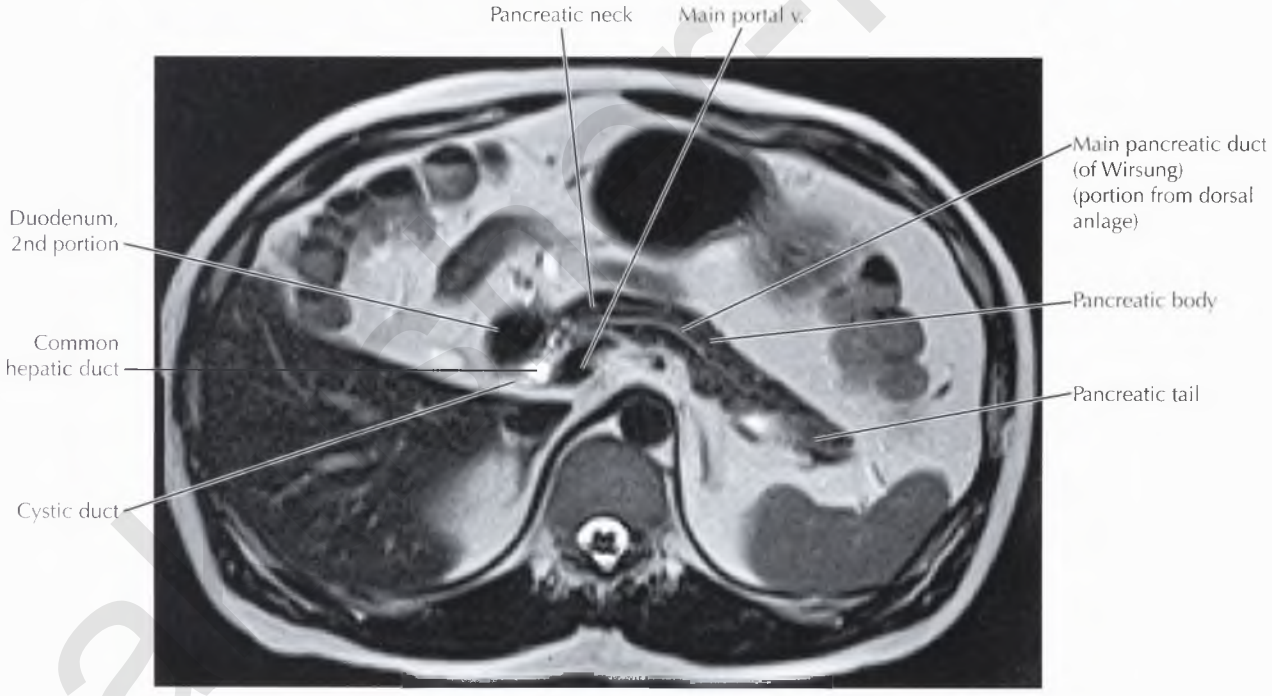
Pancreatic neck
Main portal v.
Main pancreatic duct (of Wirsung) (portion from dorsal anlage)
Duodenum, 2nd portion
Pancreatic body
Common hepatic duct
Pancreatic tail
Cystic duct

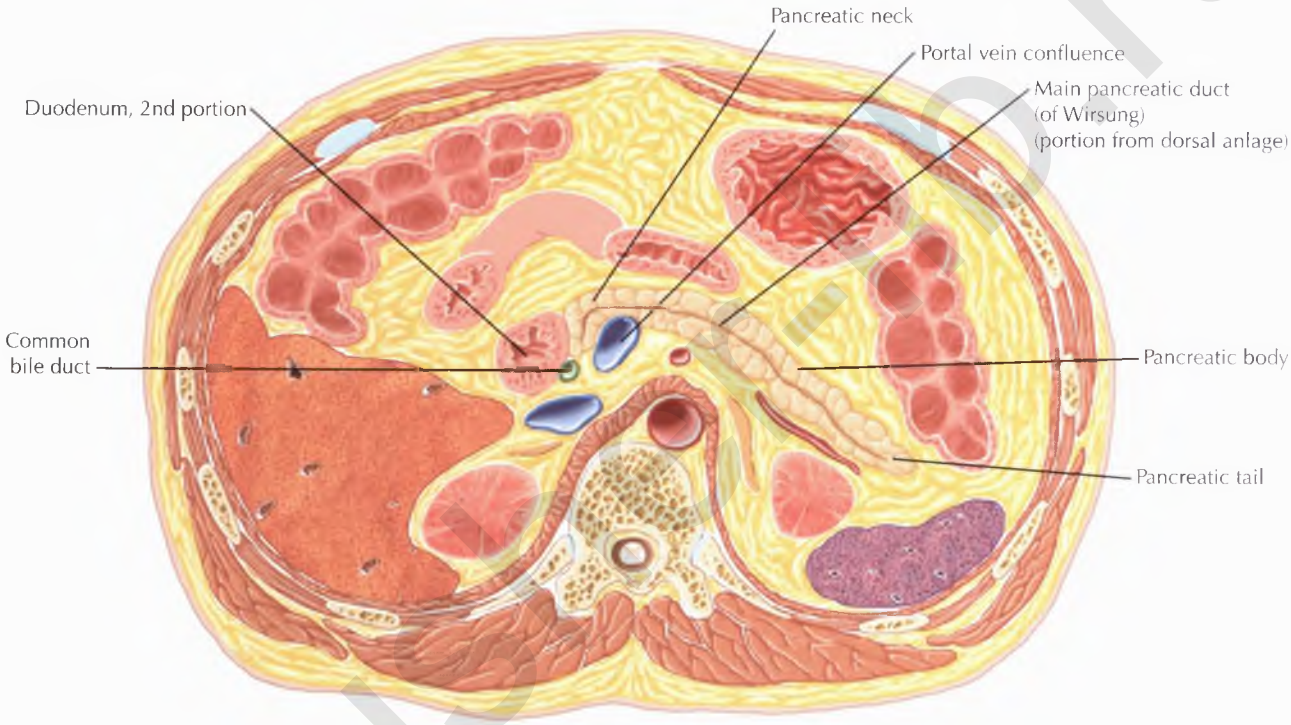

PATHOLOGIC PROCESS

In patients with pancreatic carcinoma, the portion of the pancreatic duct obstructed by the tumor typically triples in size.

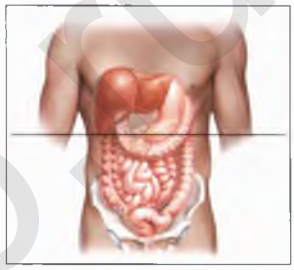


Pancreatic neck
Portal vein confluence
Main pancreatic duct (of Wirsung) (portion from dorsal anlage)
Duodenum, 2nd portion
Common bile duct
Pancreatic body
Pancreatic tail

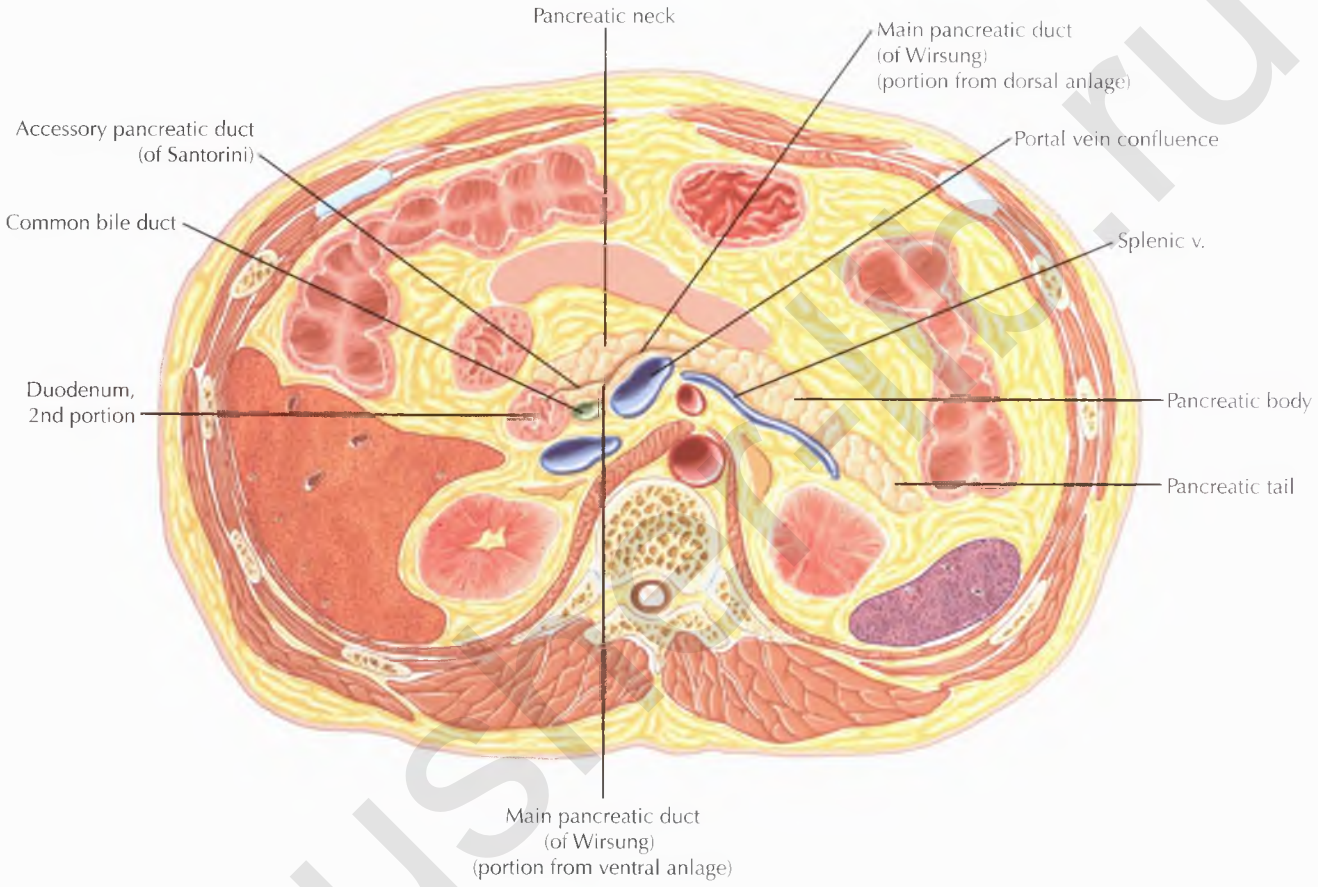

NORMAL ANATOMY AND NORMAL VARIANTS

The *main pancreatic duct* (of Wirsung), formed by fusion of the ventral and dorsal pancreatic anlagen of ductal systems during development, typically joins the common bile duct and drains into the duodenum through the major duodenal papilla (of Vater). An accessory pancreatic duct (of Santorini) can occasionally be seen more superiorly, draining more proximally into the duodenum through the minor duodenal papilla.

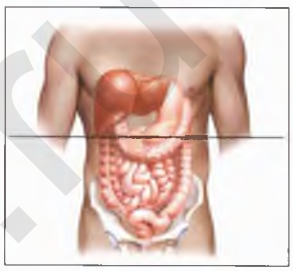

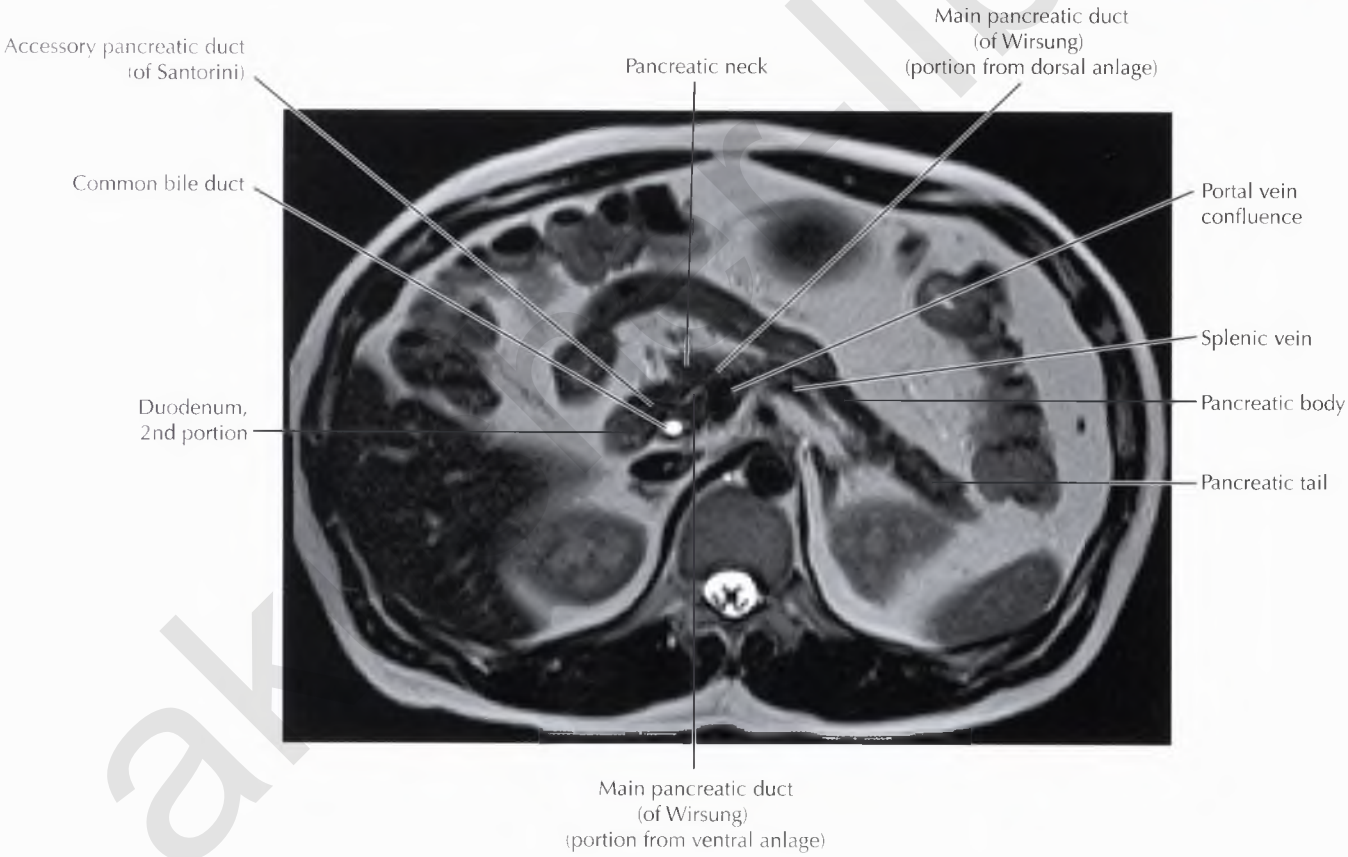

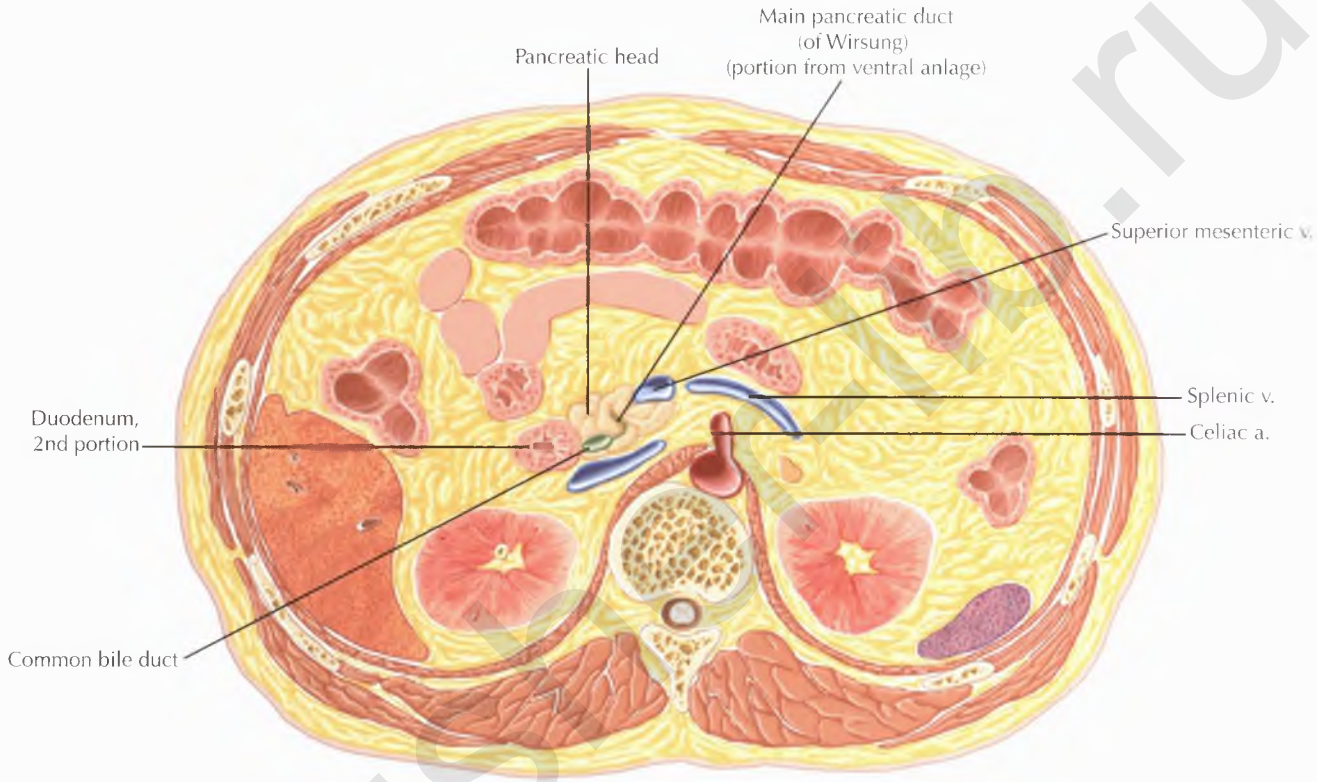

PATHOLOGIC PROCESS

Pancreas divisum, the most common congenital pancreatic variant, results from failure of the dorsal and ventral pancreatic anlagen of the ductal systems to fuse during the 6th to 8th weeks of gestation. The duct in the pancreatic body and tail, derived from the dorsal pancreatic anlage, drains into the duodenum through the accessory duct (of Santorini) and minor duodenal papilla, whereas the separate, more posteriorly and inferiorly located duct in the pancreatic head and uncinate process, derived from the ventral pancreatic anlage, joins the distal common bile duct to drain into the duodenum through the major duodenal papilla (of Vater).

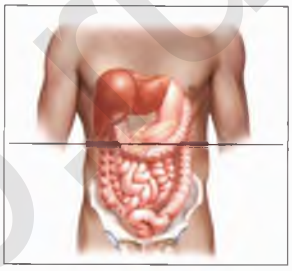

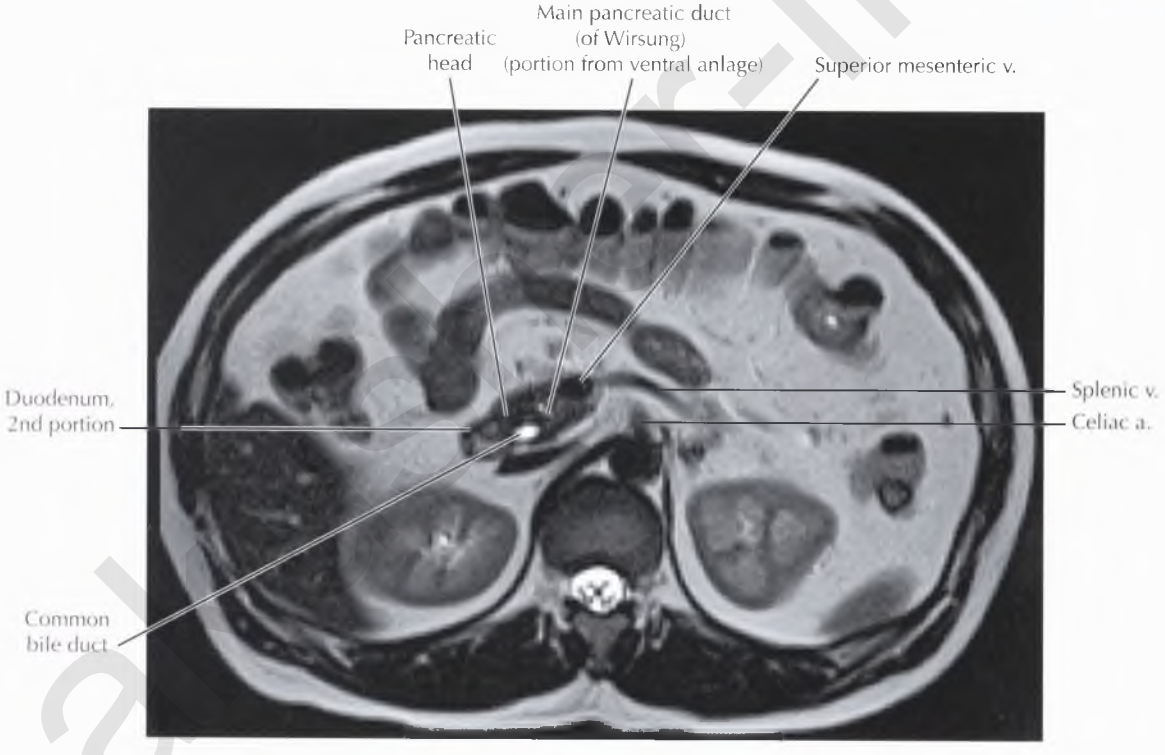

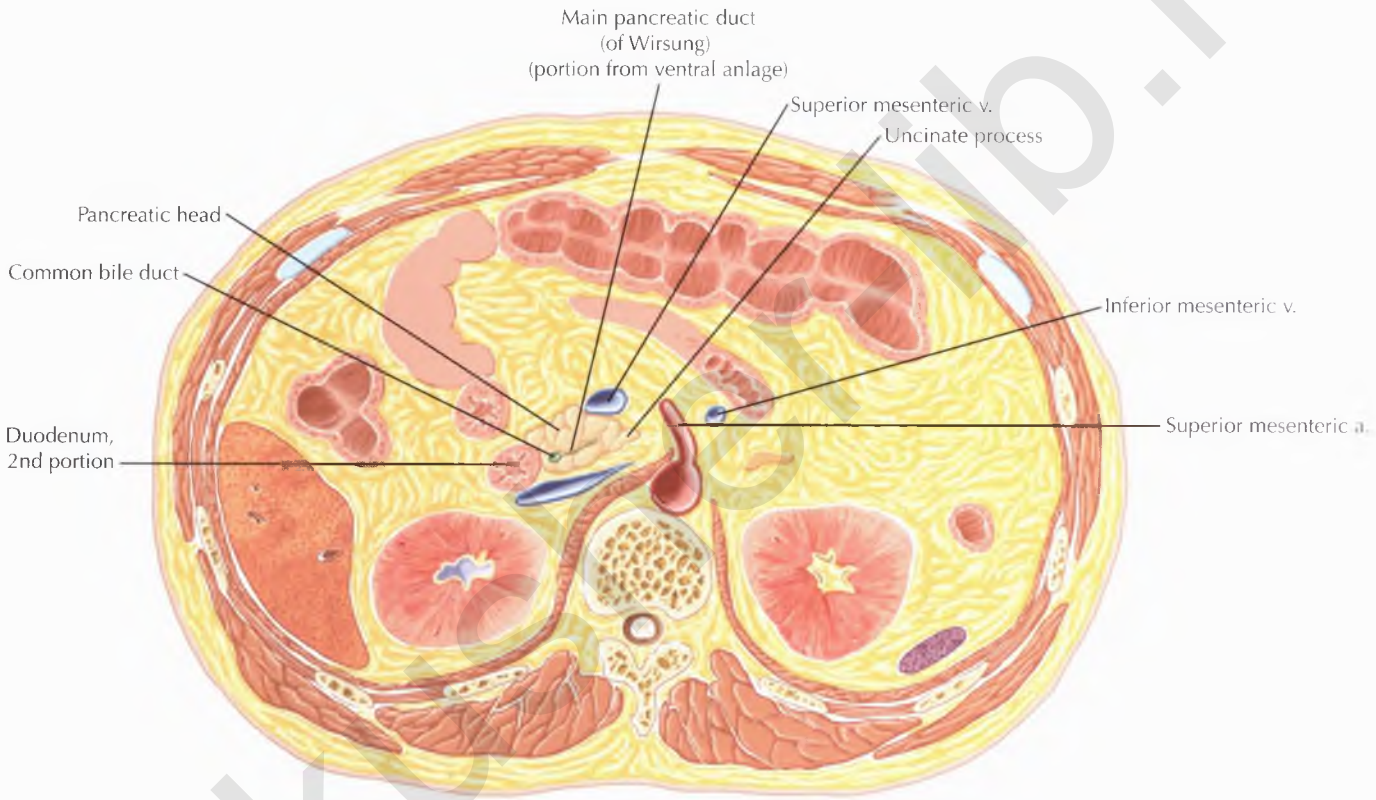

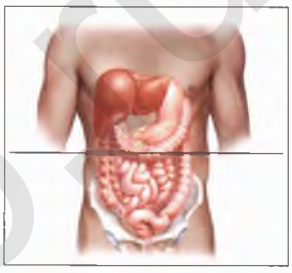

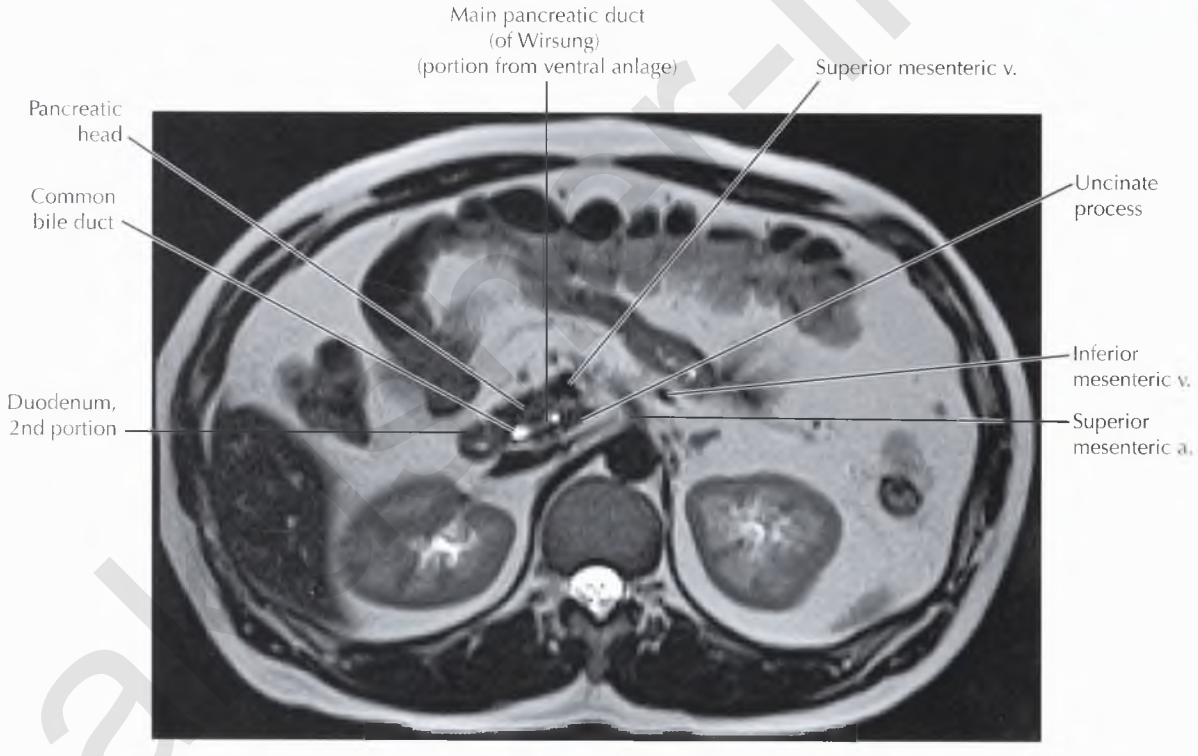
Main pancreatic duct
(of Wirsung)
(portion from ventral anlage)
Superior mesenteric v.
Pancreatic
head
Common
bile duct
Uncinate
process
Inferior
mesenteric v.
Duodenum,
2nd portion
Superior
mesenteric a.

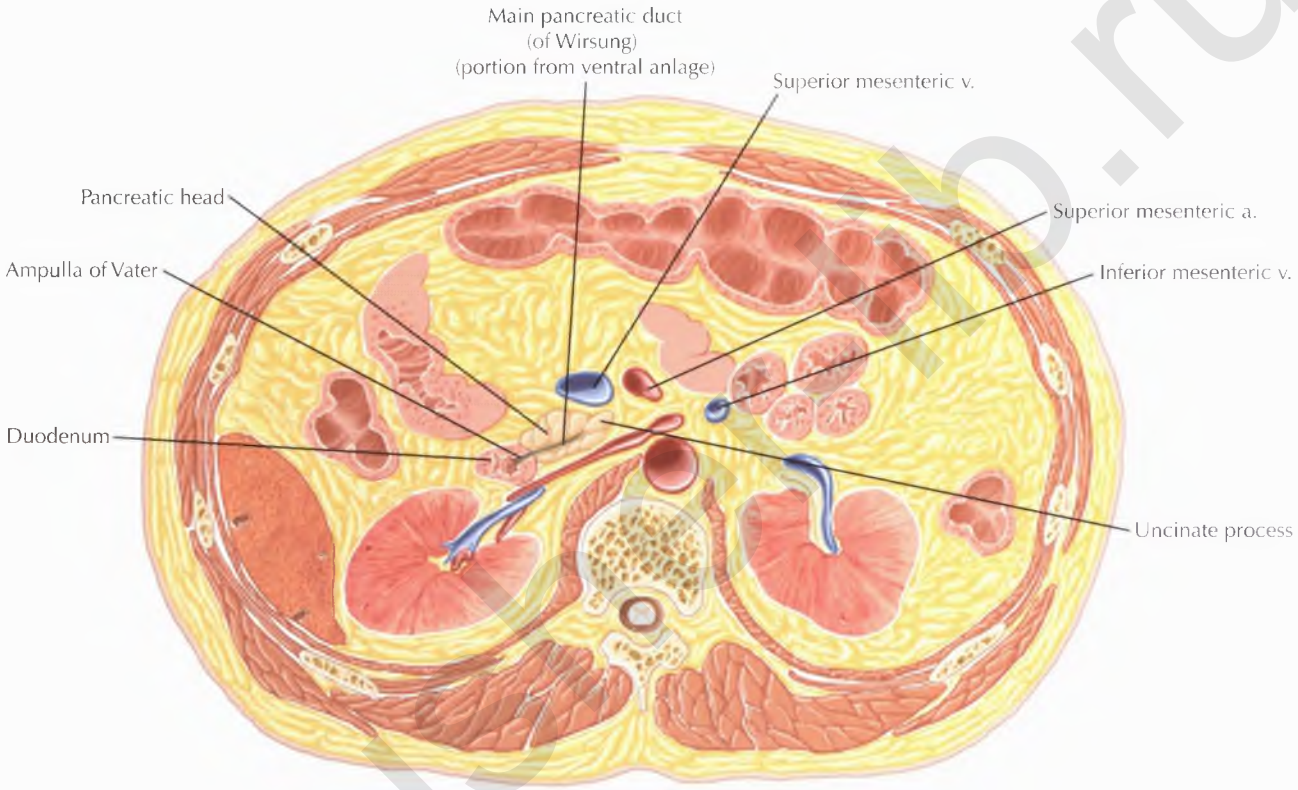

NORMAL ANATOMY

The common bile duct joins the main pancreatic duct (of Wirsung) to form the ampulla of Vater within the posteromedial wall of the 2nd portion of the duodenum. The sphincter of Oddi, a sheath of circular smooth muscle fibers, surrounds the ampulla of Vater and controls the flow of bile and pancreatic secretions into the duodenum.

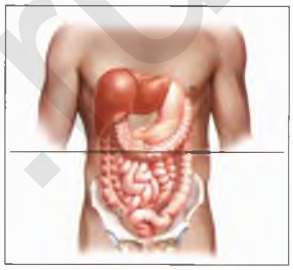

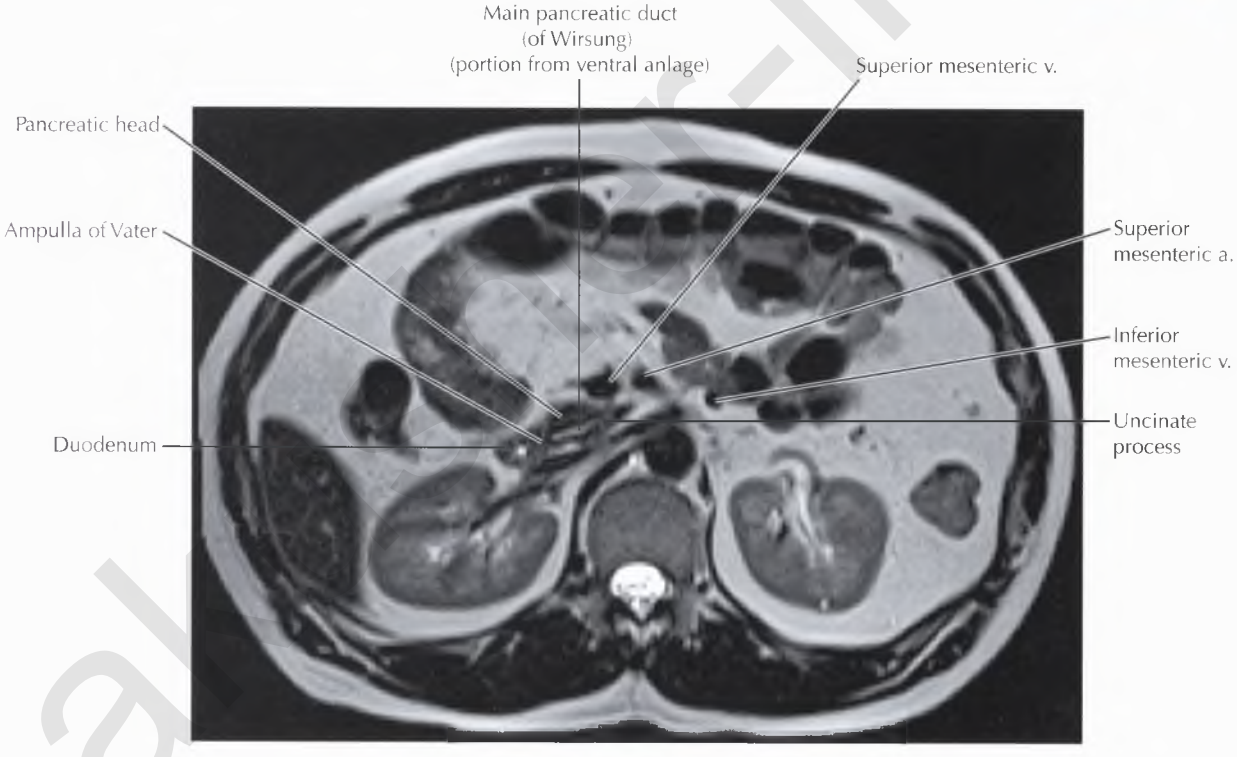
Main pancreatic duct
(of Wirsung)
(portion from ventral anlage)
Superior mesenteric v.
Pancreatic head
Ampulla of Vater
Duodenum
Superior
mesenteric a.
Inferior
mesenteric v.
Uncinate
process

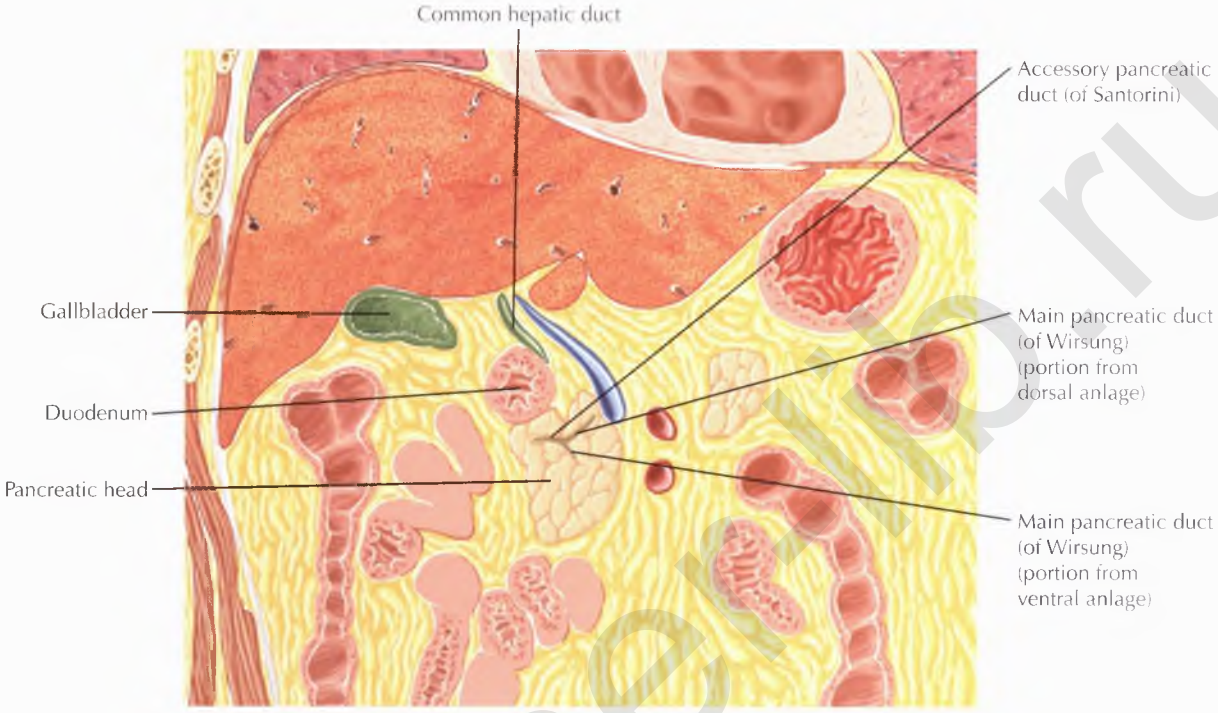

NORMAL ANATOMY

The common hepatic duct is formed by the union of the right and left (1st-order) hepatic ducts. Classically, the union of the 2nd-order biliary ducts from the posterior segments (VI and VII) and anterior segments (V and VIII) of the liver form the right hepatic duct, and biliary ducts from the lateral segments (II and III) and medial segments (IVa and IVb) of the liver join to form the left hepatic duct.

NORMAL VARIANTS

There is significant variation in normal biliary anatomy. In 15% to 20% of patients the posterior duct joins the left hepatic duct; in approximately 10% the anterior, posterior, and left hepatic ducts join to form a trifurcation, and in 5% the posterior duct joins the common hepatic duct after the anterior and left hepatic ducts have merged, which is an important anatomic variant that can result in significant morbidity after biliary surgery if not recognized preoperatively.

Biliary drainage from the caudate lobe of the liver (segment I) is also variable, although in most cases, the left part of the caudate lobe drains into the left hepatic duct. The right part of the caudate lobe drains into the left or the right hepatic duct, with approximately equal frequency.

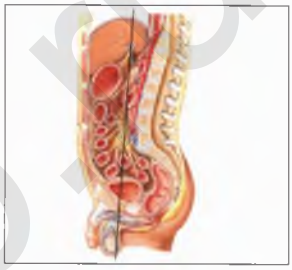

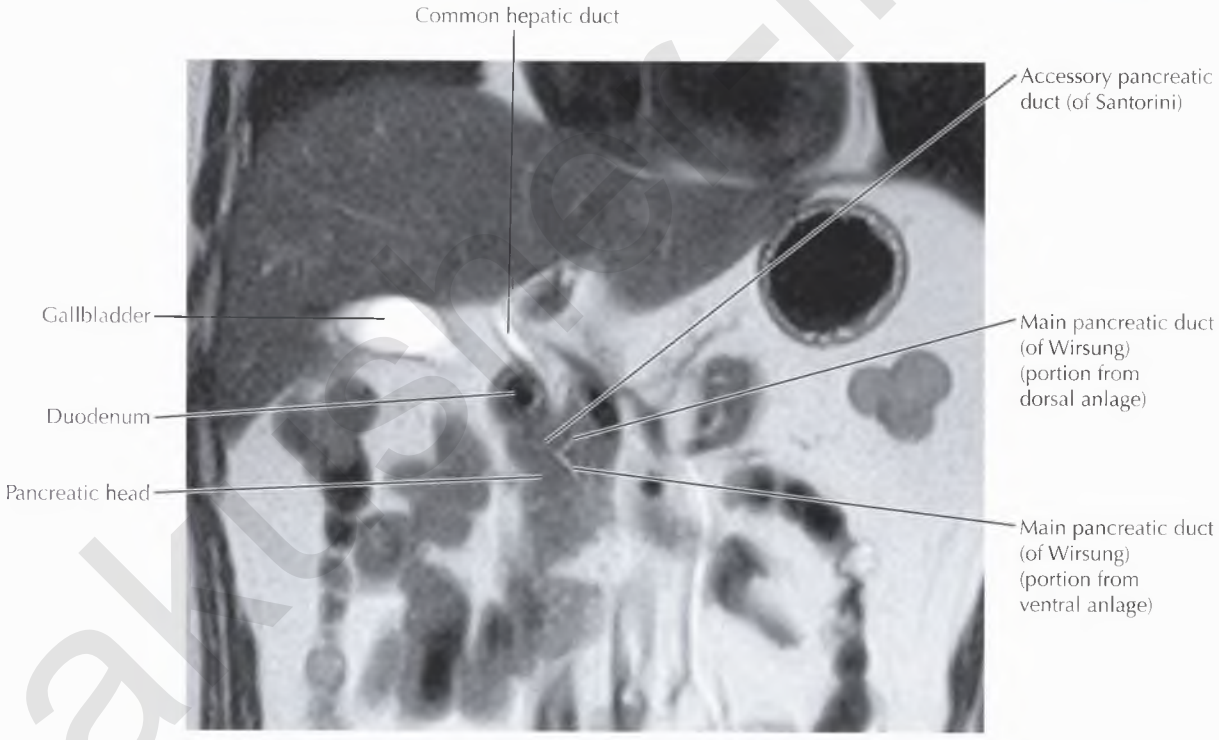
Common hepatic duct
Accessory pancreatic duct (of Santorini)
Gallbladder
Main pancreatic duct (of Wirsung) (portion from dorsal anlage)
Duodenum
Pancreatic head
Main pancreatic duct (of Wirsung) (portion from ventral anlage)

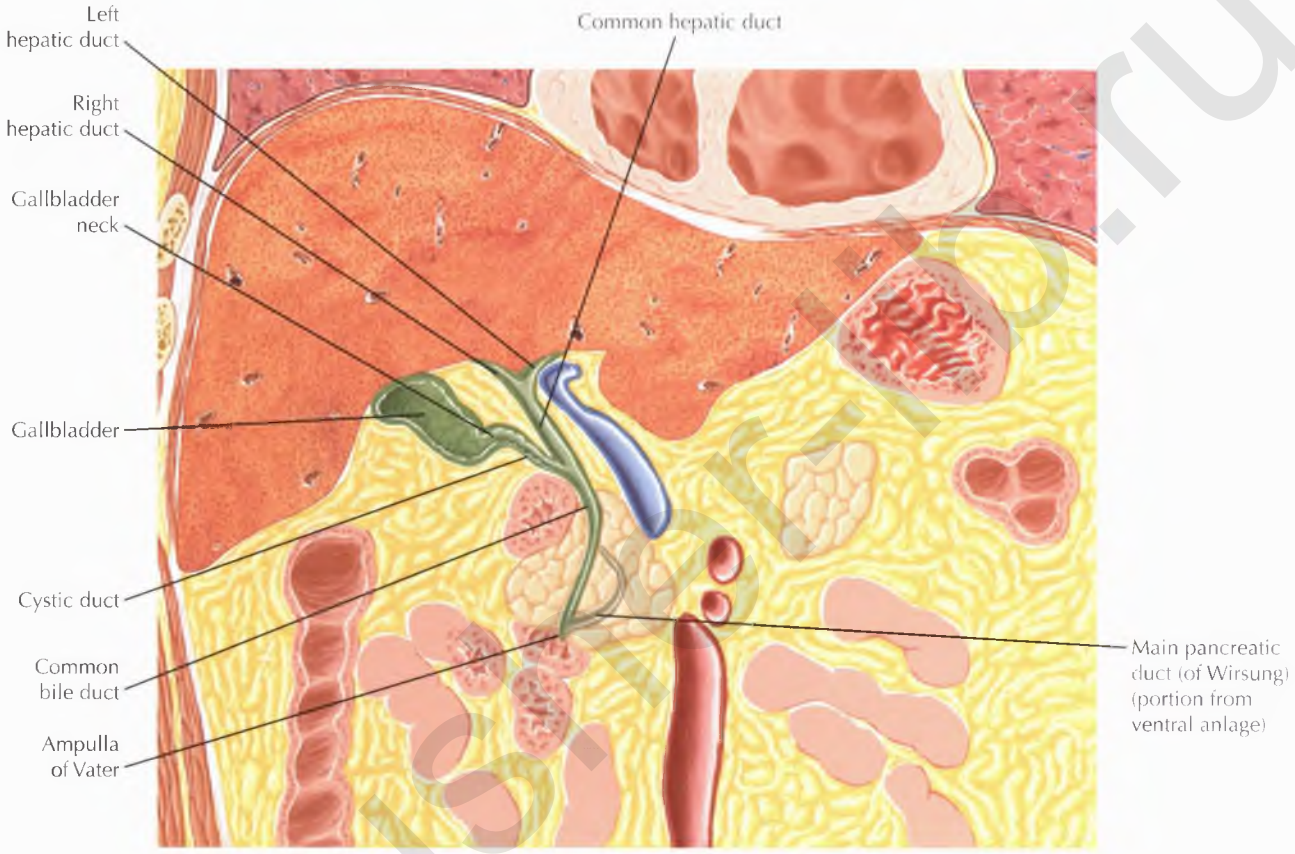

DIAGNOSTIC CONSIDERATION

Magnetic resonance cholangiopancreatography (MRCP) uses a long echo time (TE) to increase T2 weighting and a long repetition time (TR) to decrease T1 weighting, resulting in a heavily T2-weighted sequence. The sequence is not specific for bile, since any fluid-containing structure (e.g., bowel, thecal sac, collecting system, ureter, cystic or necrotic portions of lesions) will appear hyperintense. Coronal maximum intensity projection (MIP) images are useful and typically used to evaluate the biliary system.

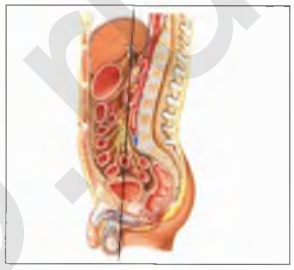

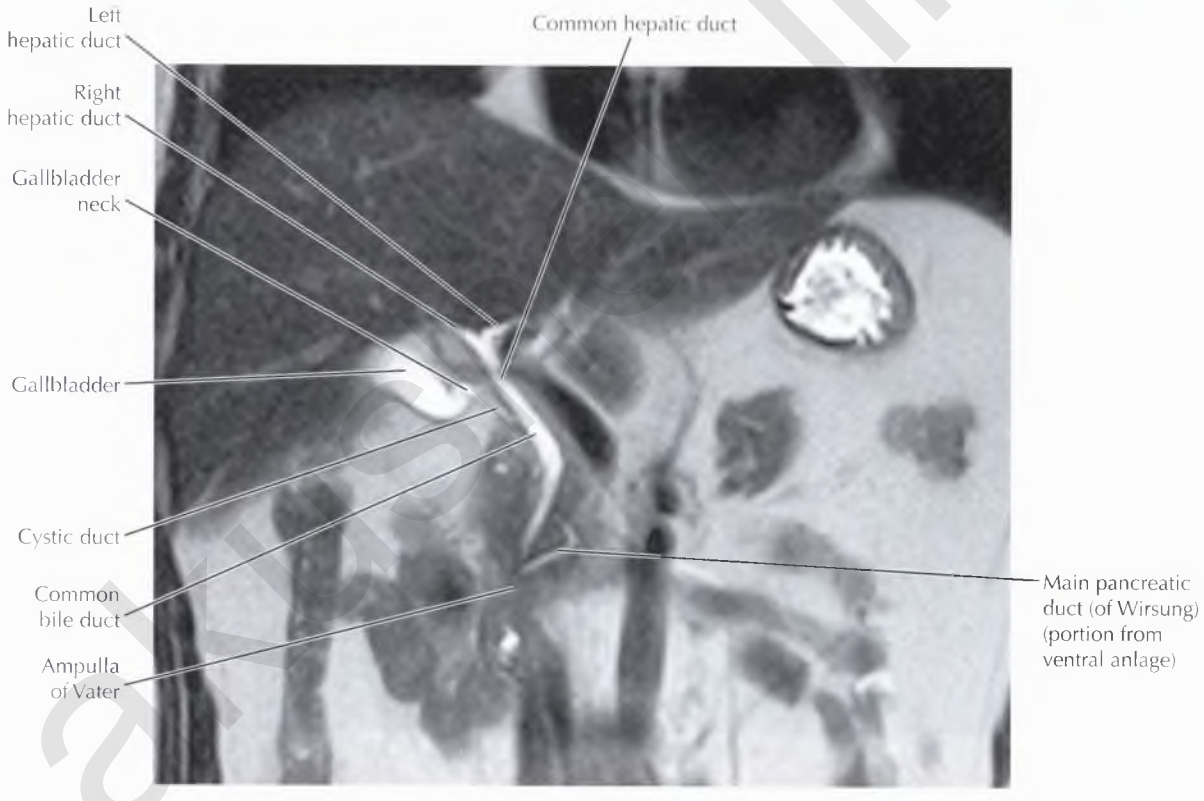
Left hepatic duct
Common hepatic duct
Right hepatic duct
Gallbladder neck
Gallbladder
Cystic duct
Common bile duct
Ampulla of Vater
Main pancreatic duct (of Wirsung) (portion from ventral anlage)

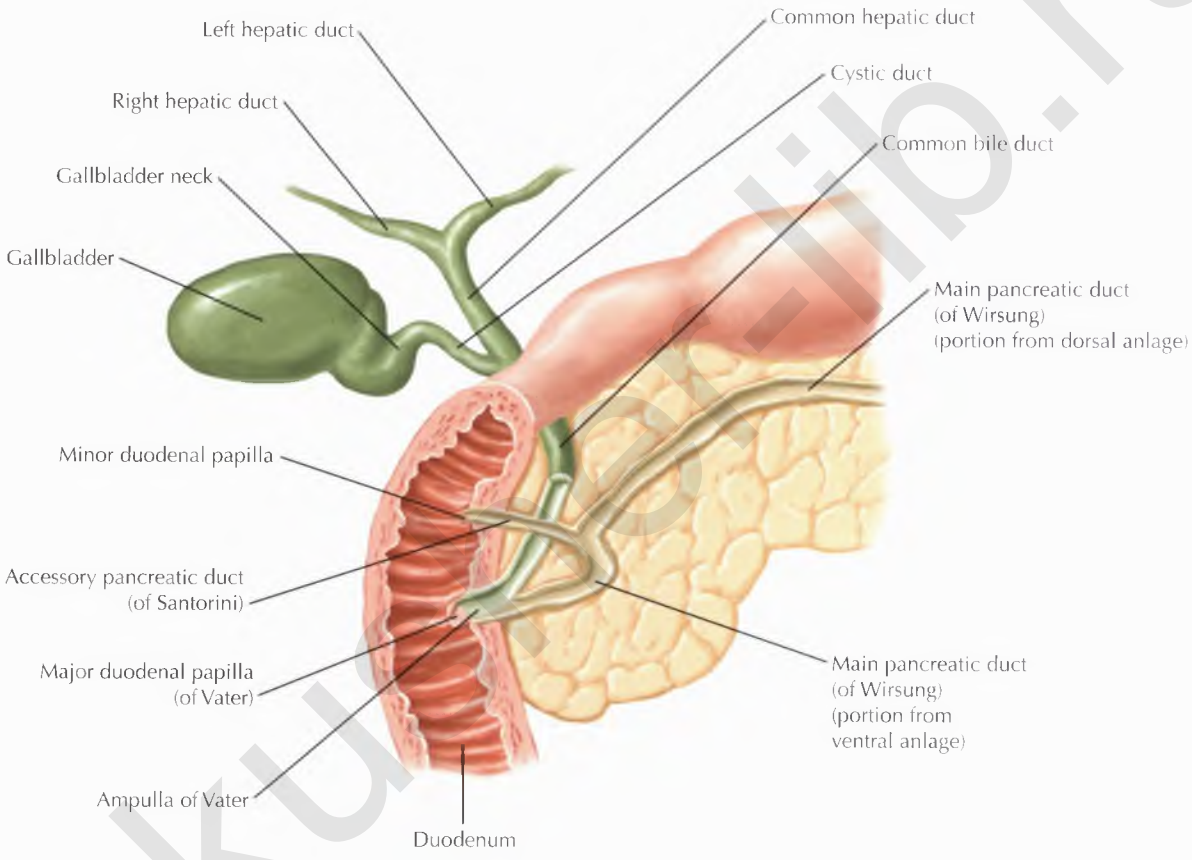
Left hepatic duct
Right hepatic duct
Gallbladder neck
Gallbladder
Common hepatic duct
Cystic duct
Common bile duct
Main pancreatic duct
(of Wirsung)
(portion from dorsal anlage)
Minor duodenal papilla
Accessory pancreatic duct
(of Santorini)
Major duodenal papilla
(of Vater)
Ampulla of Vater
Duodenum
Main pancreatic duct
(of Wirsung)
(portion from
ventral anlage)

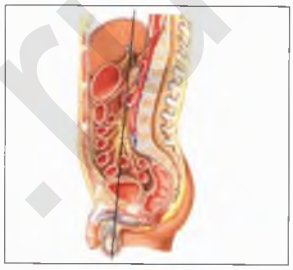

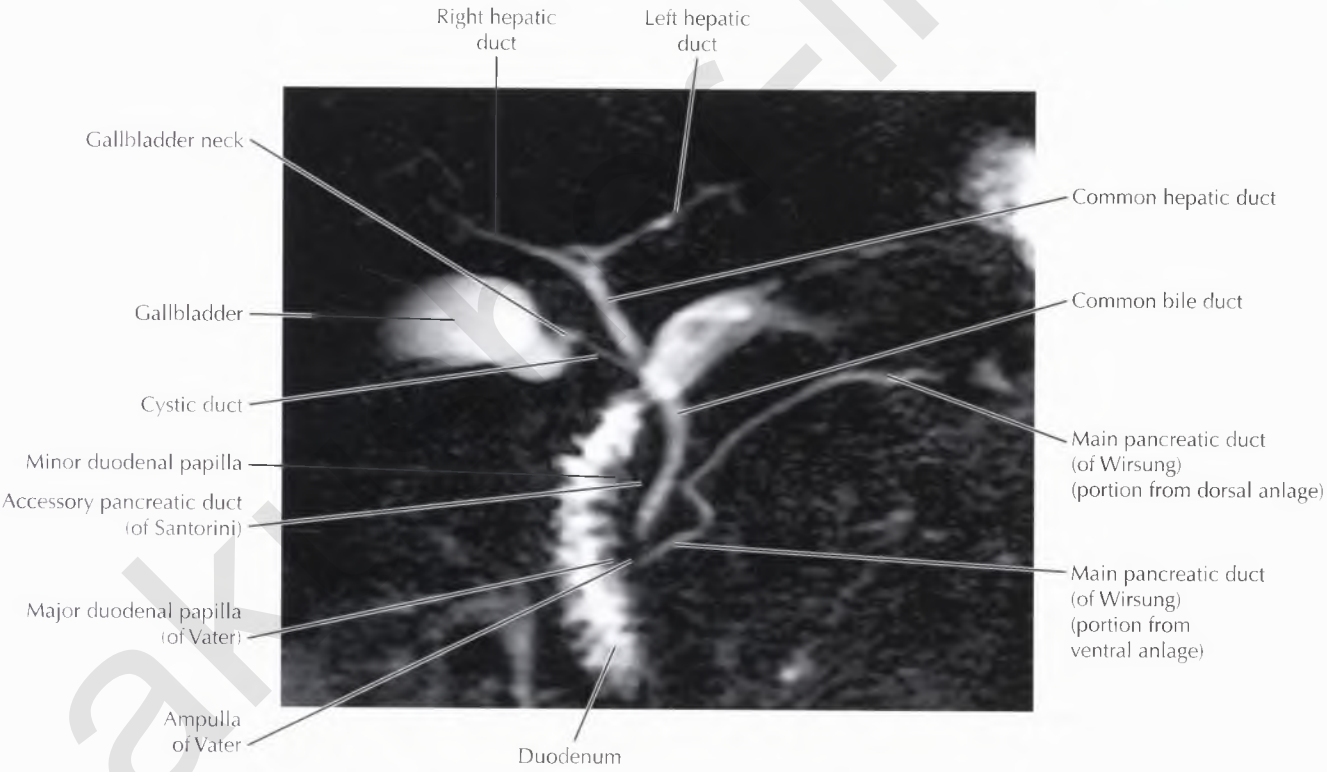

PART 2 PELVIC ANATOMY

*For Peritoneal Cavity–Pelvis, see Chapter 3, pp. 166-205.

Chapter 5 OVERVIEW OF PELVIS

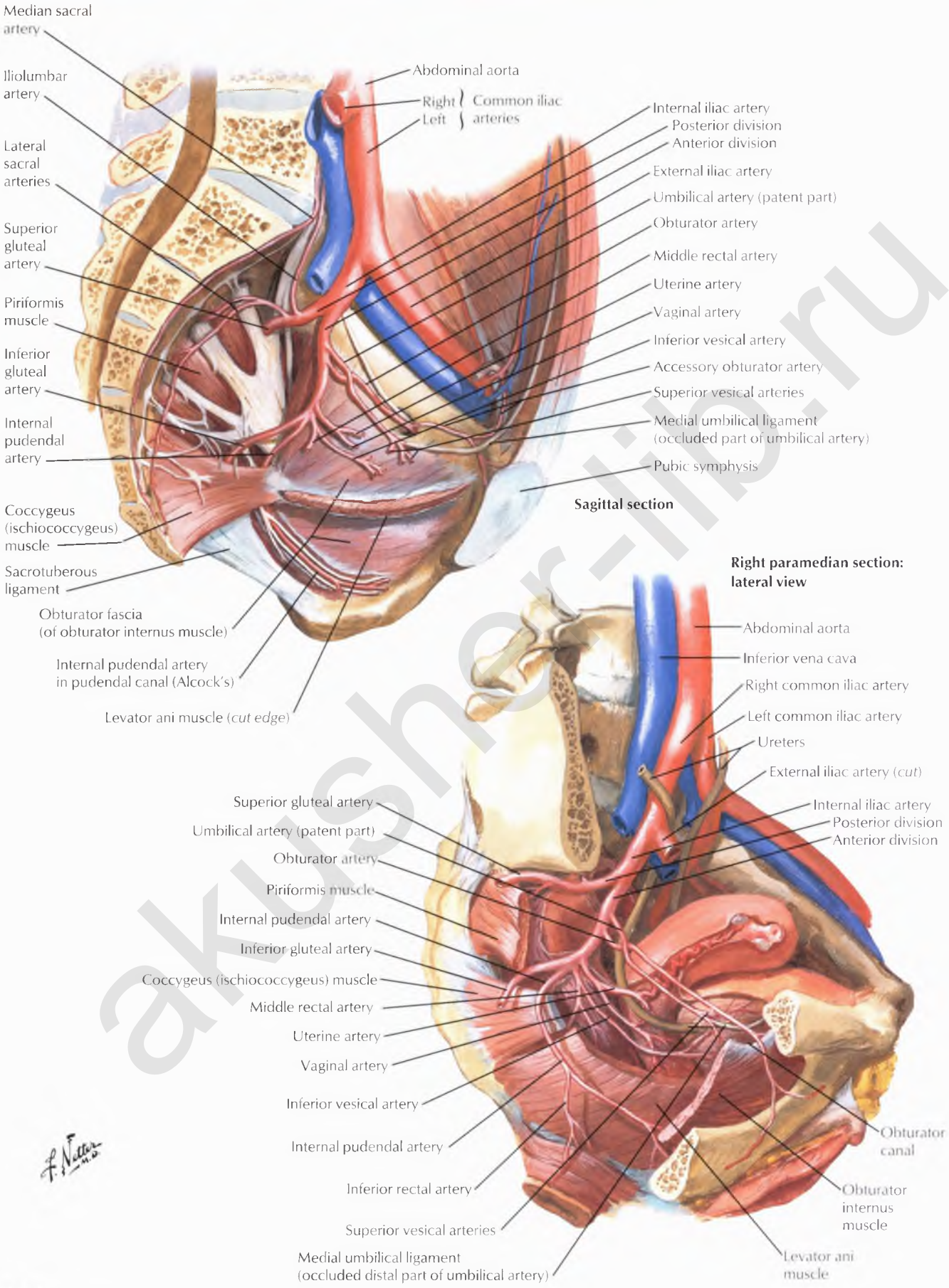

Left paramedian section: lateral view

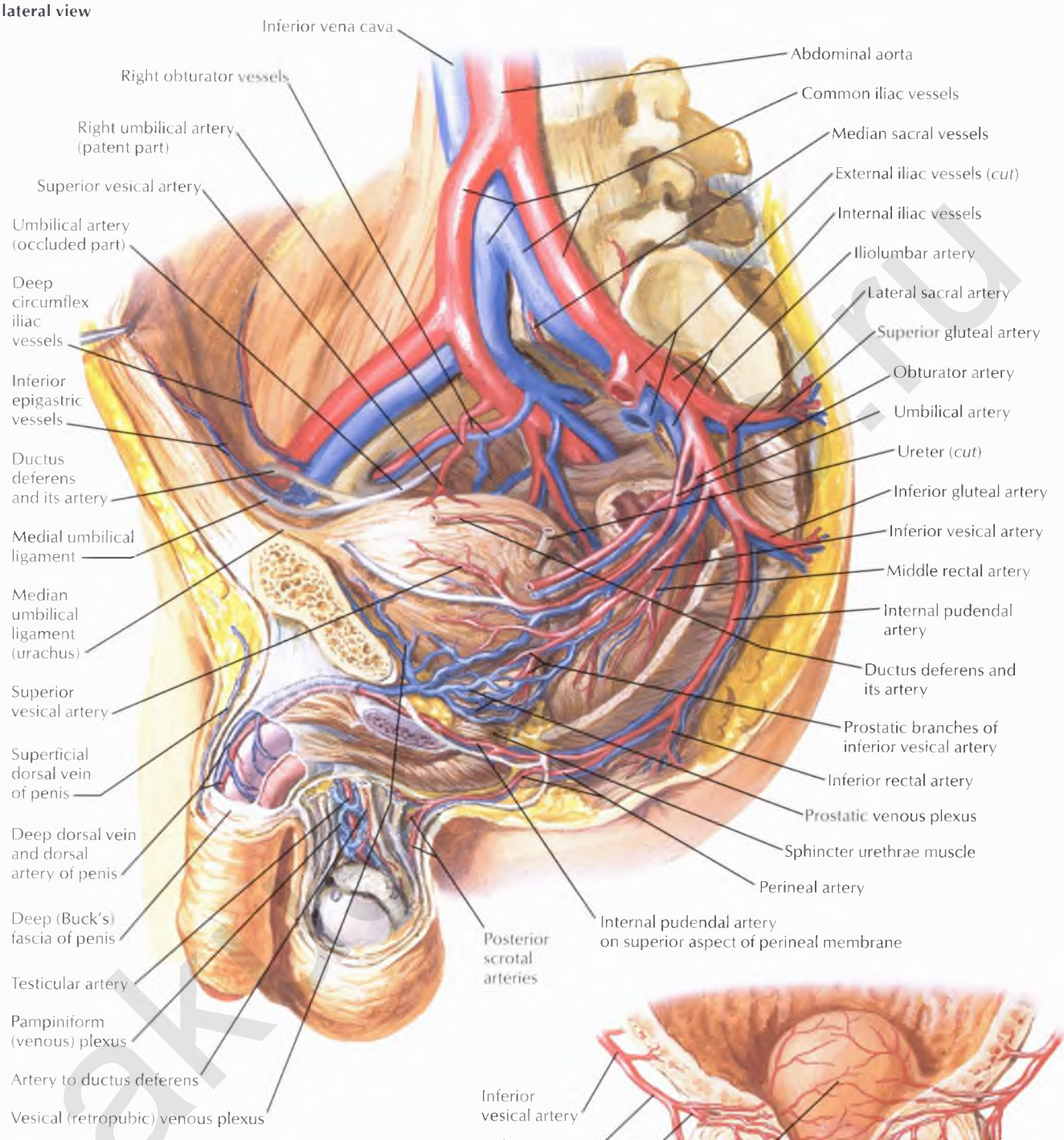

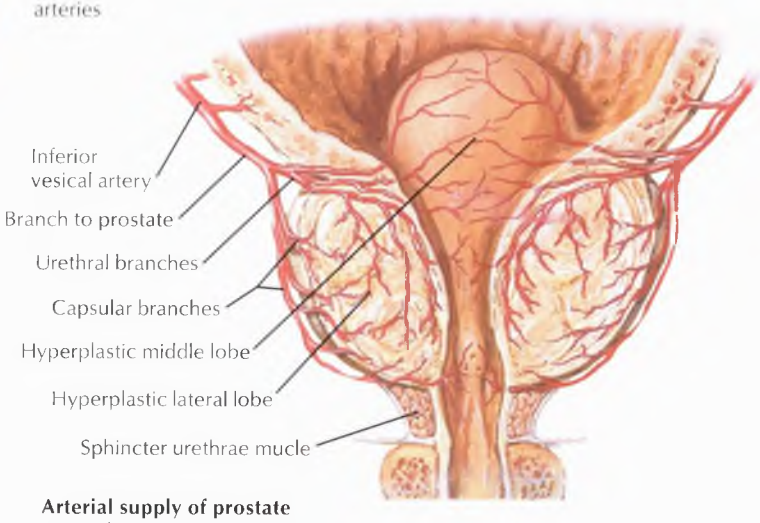

Arterial supply of prostate
(Frontal section, anterior view of specimen with benign hyperplasia)

Lymph Vessels and Nodes of Pelvis and Genitalia: Female

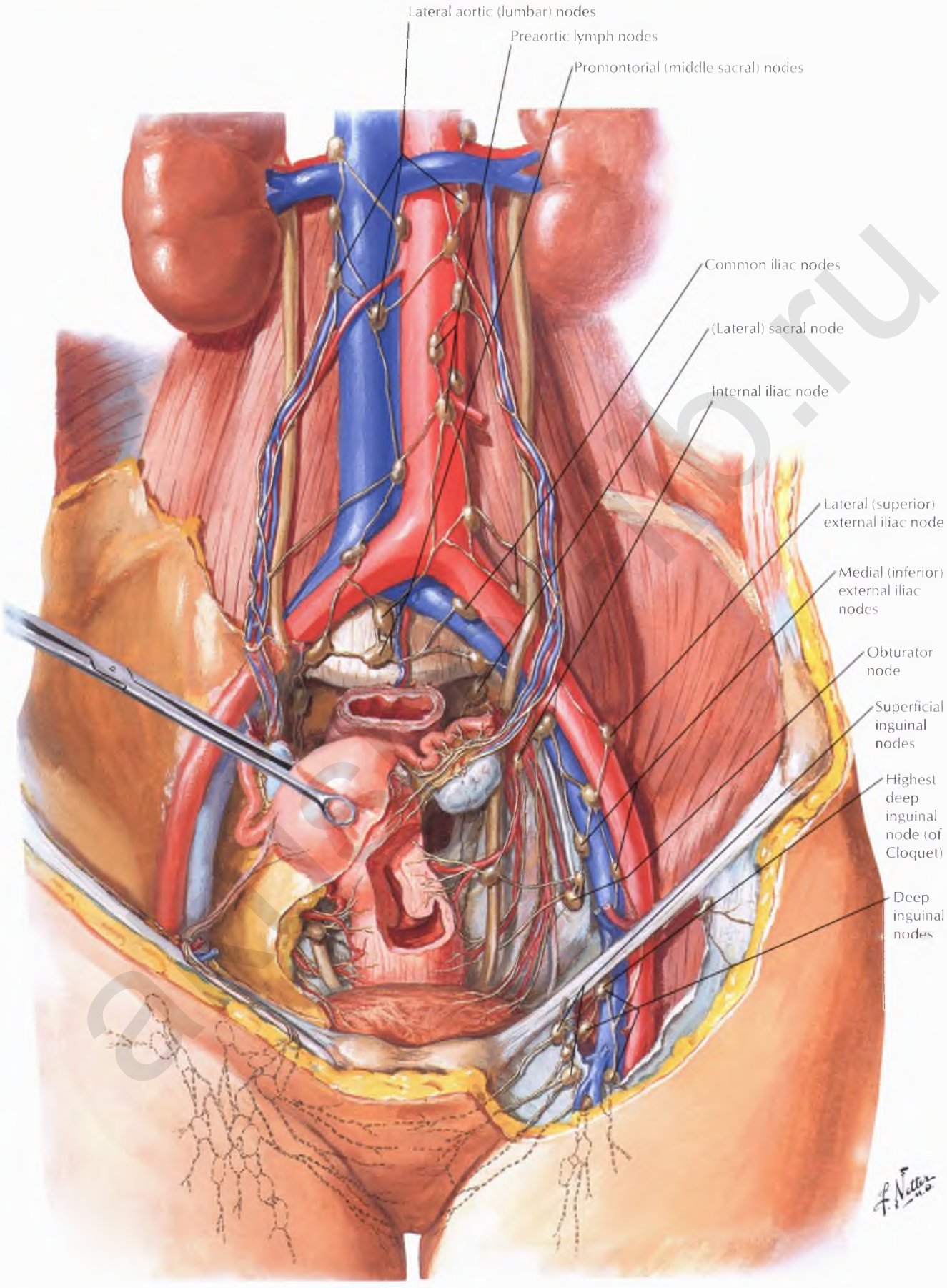

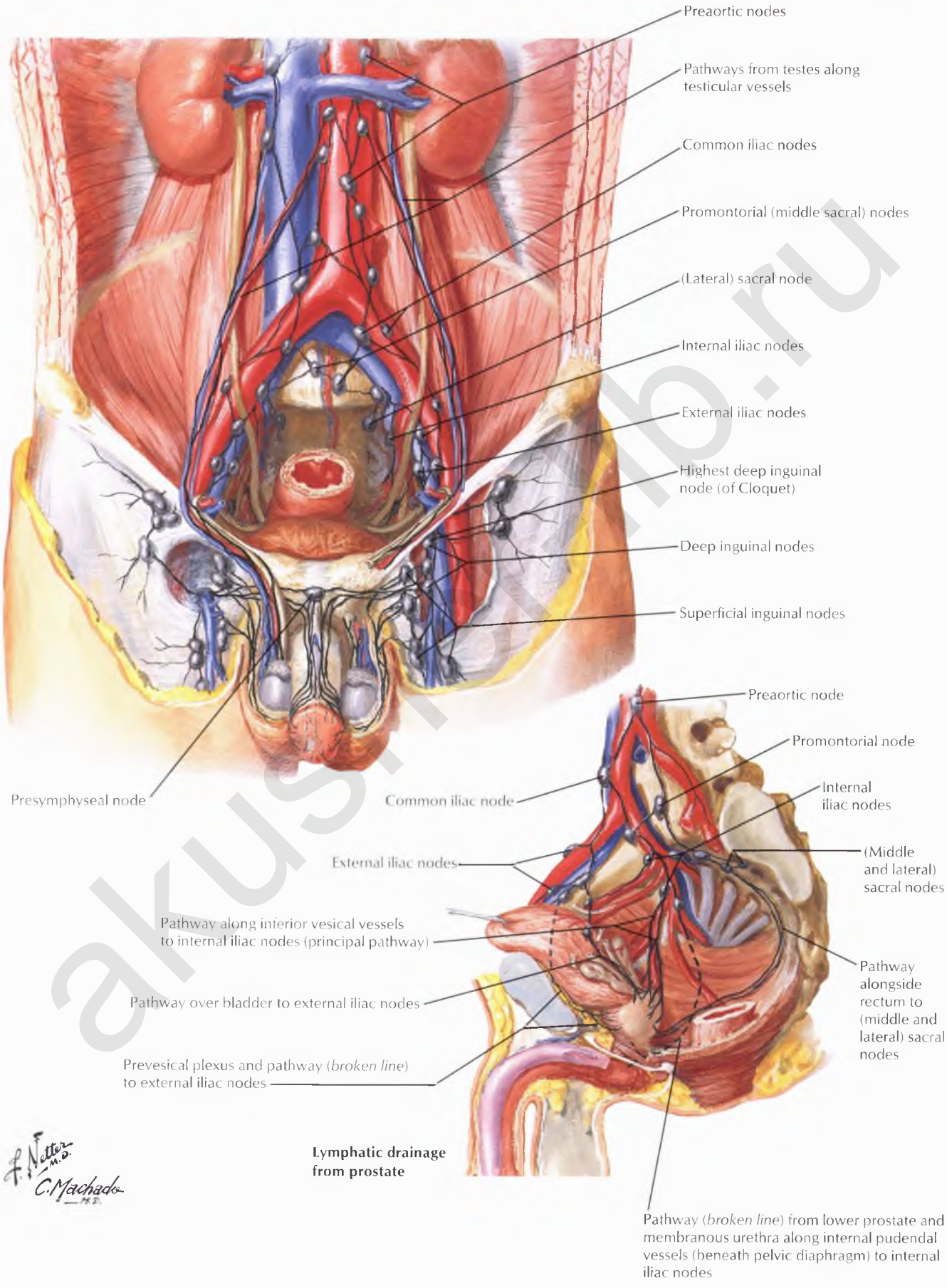

F. Netter, M.D.
C. Machado, M.D.

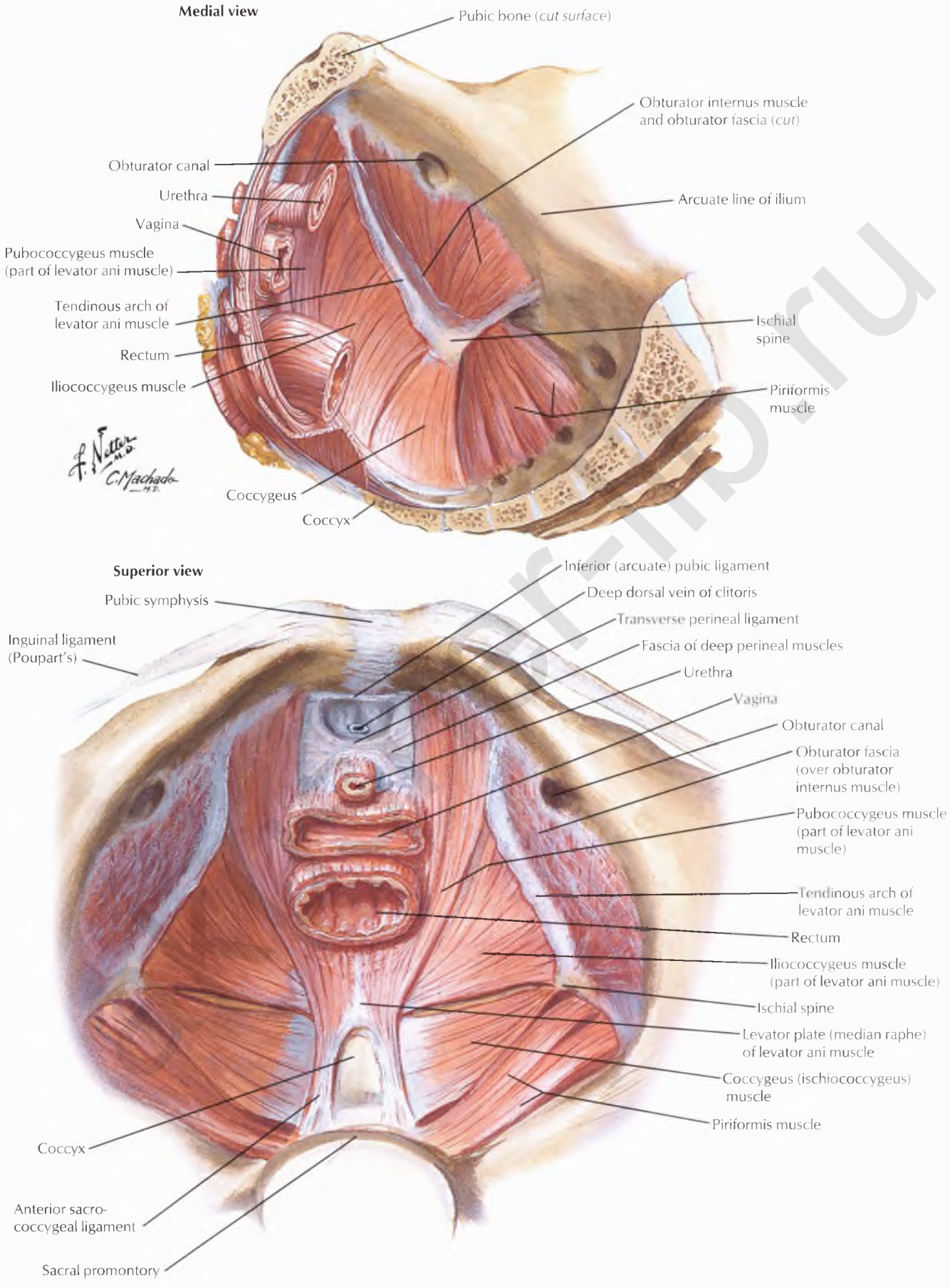
Medial view
Pubic bone (cut surface)
Obturator internus muscle and obturator fascia (cut)
Obturator canal
Urethra
Vagina
Arcuate line of ilium
Pubococcygeus muscle (part of levator ani muscle)
Tendinous arch of levator ani muscle
Ischial spine
Rectum
Iliococcygeus muscle
Piriformis muscle
Coccygeus
Coccyx
Superior view
Inferior (arcuate) pubic ligament
Pubic symphysis
Deep dorsal vein of clitoris
Transverse perineal ligament
Inguinal ligament (Poupart's)
Fascia of deep perineal muscles
Urethra
Vagina
Obturator canal
Obturator fascia (over obturator internus muscle)
Pubococcygeus muscle (part of levator ani muscle)
Tendinous arch of levator ani muscle
Rectum
Iliococcygeus muscle (part of levator ani muscle)
Ischial spine
Levator plate (median raphe) of levator ani muscle
Coccygeus (ischiococcygeus) muscle
Piriformis muscle
Coccyx
Anterior sacro-coccygeal ligament
Sacral promontory

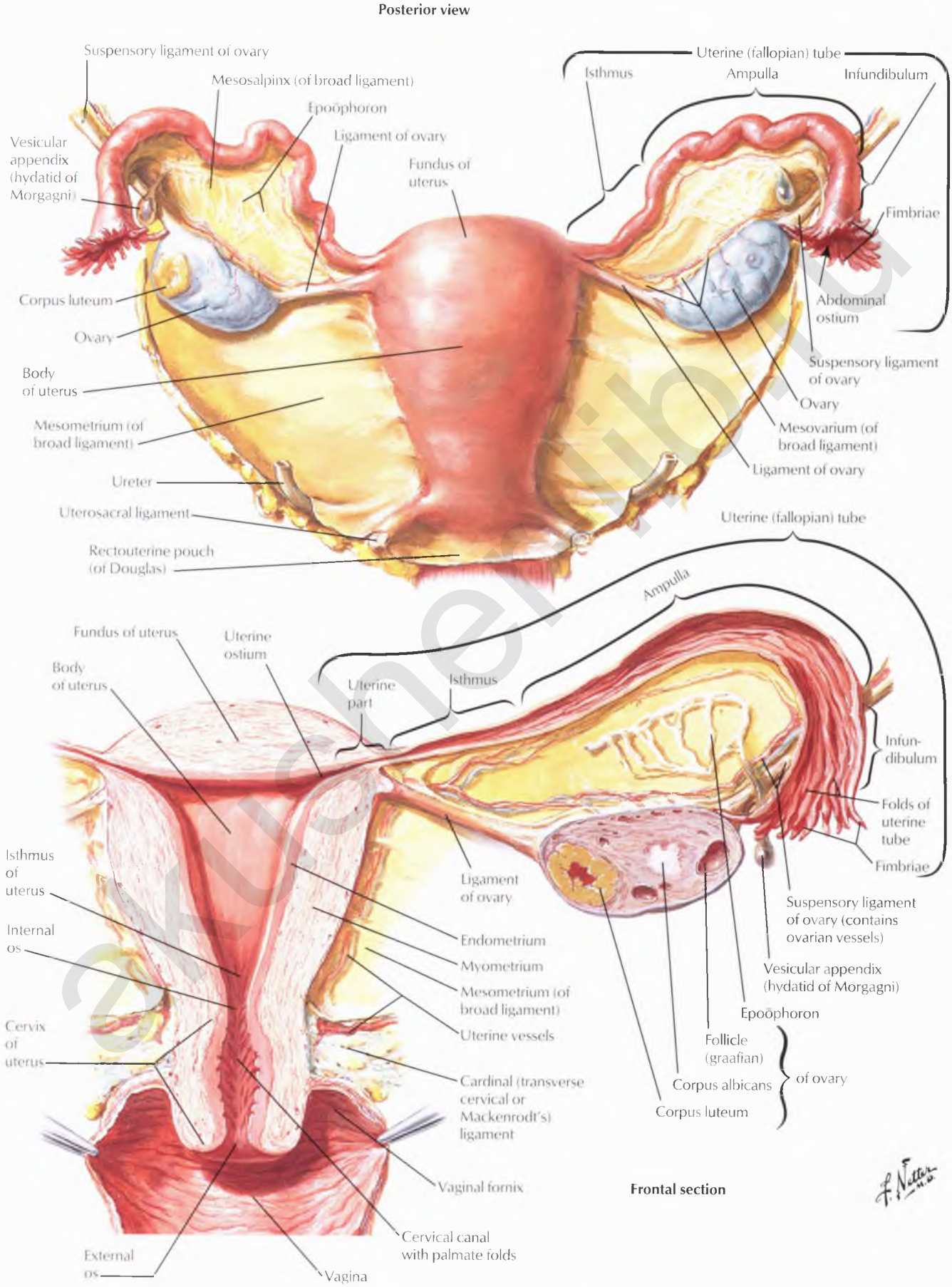

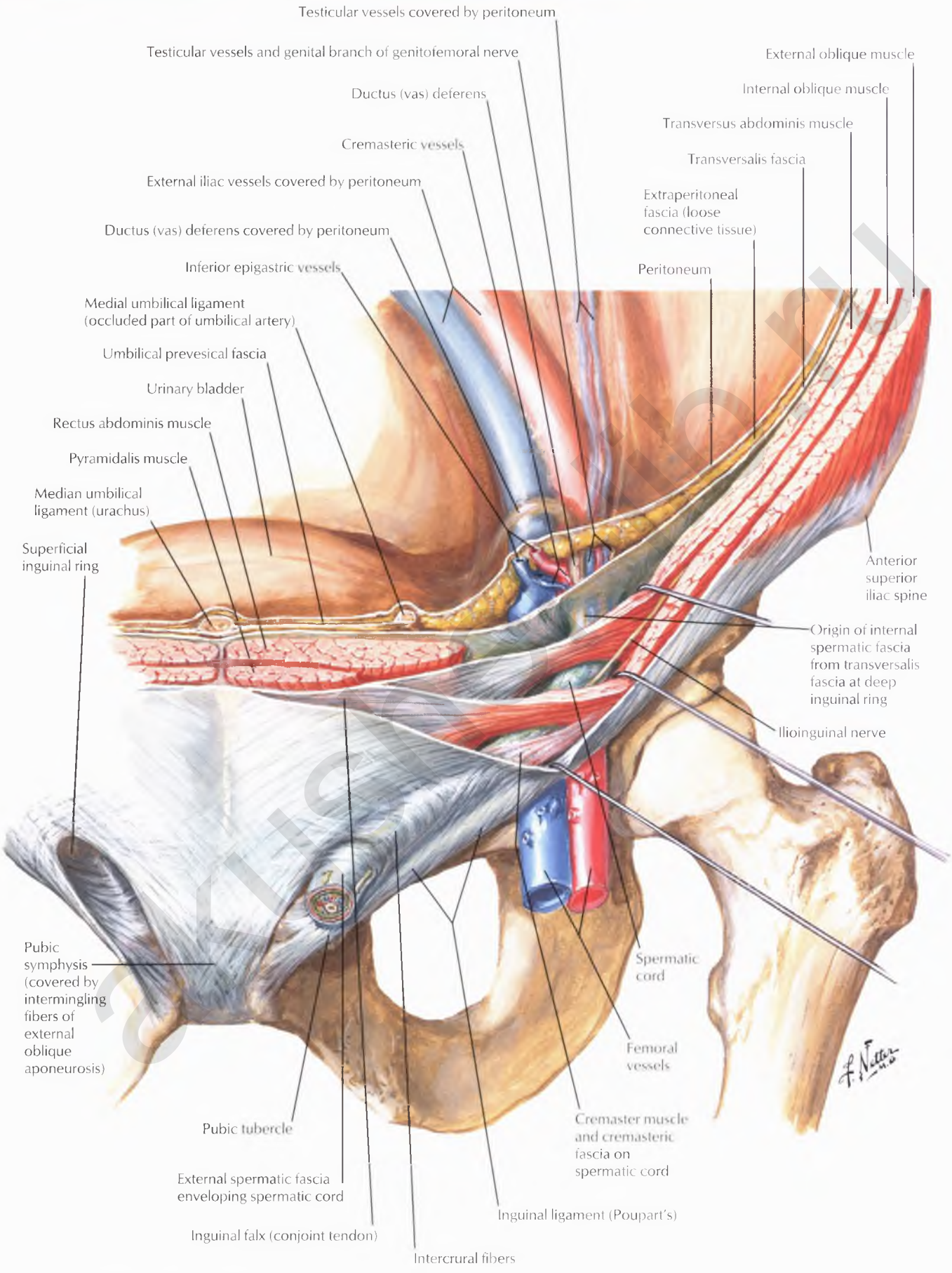
Testicular vessels covered by peritoneum
Testicular vessels and genital branch of genitofemoral nerve
Ductus (vas) deferens
Cremasteric vessels
External iliac vessels covered by peritoneum
Ductus (vas) deferens covered by peritoneum
Inferior epigastric vessels
Medial umbilical ligament (occluded part of umbilical artery)
Umbilical prevesical fascia
Urinary bladder
Rectus abdominis muscle
Pyramidalis muscle
Median umbilical ligament (urachus)
Superficial inguinal ring
External oblique muscle
Internal oblique muscle
Transversus abdominis muscle
Transversalis fascia
Extraperitoneal fascia (loose connective tissue)
Peritoneum
Anterior superior iliac spine
Origin of internal spermatic fascia from transversalis fascia at deep inguinal ring
Ilioinguinal nerve
Spermatic cord
Femoral vessels
Cremaster muscle and cremasteric fascia on spermatic cord
Inguinal ligament (Poupart's)
Intercrural fibers
Inguinal falx (conjoint tendon)
External spermatic fascia enveloping spermatic cord
Pubic tubercle
Pubic symphysis (covered by intermingling fibers of external oblique aponeurosis)

Chapter 6 MALE PELVIS*

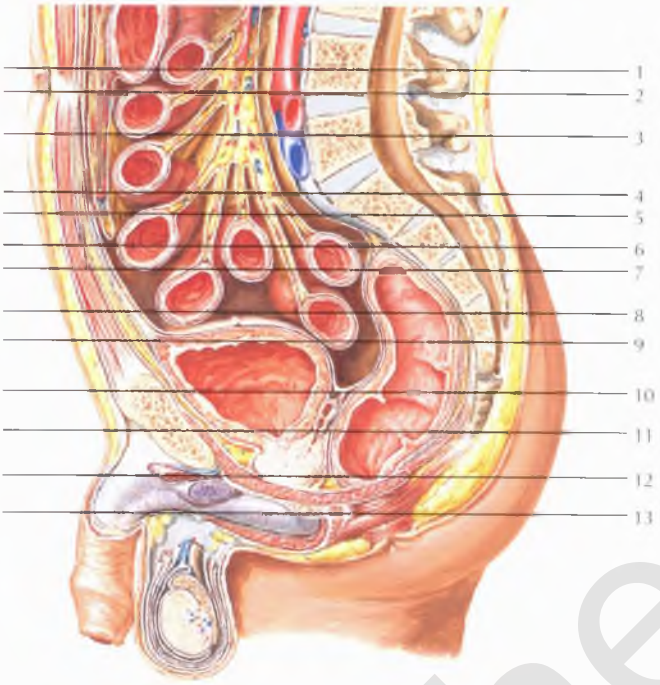

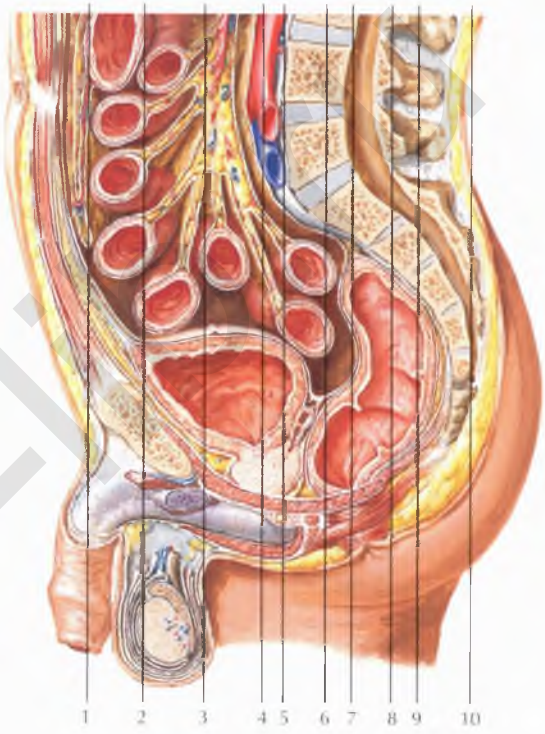

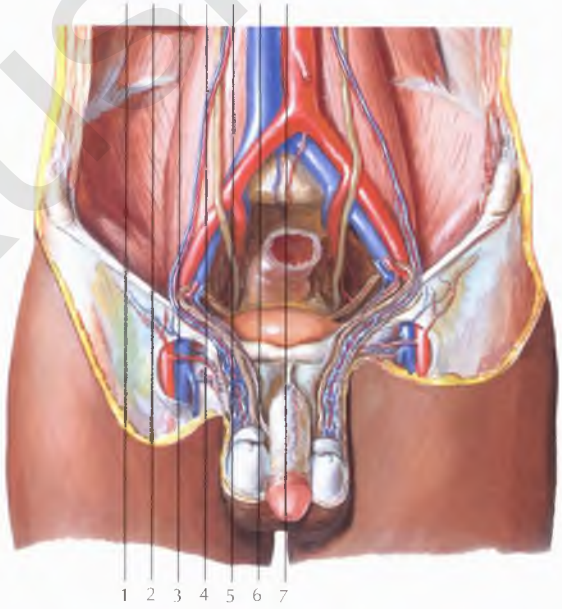

*For Peritoneal Cavity–Pelvis, see Chapter 3 (pp. 166-205).

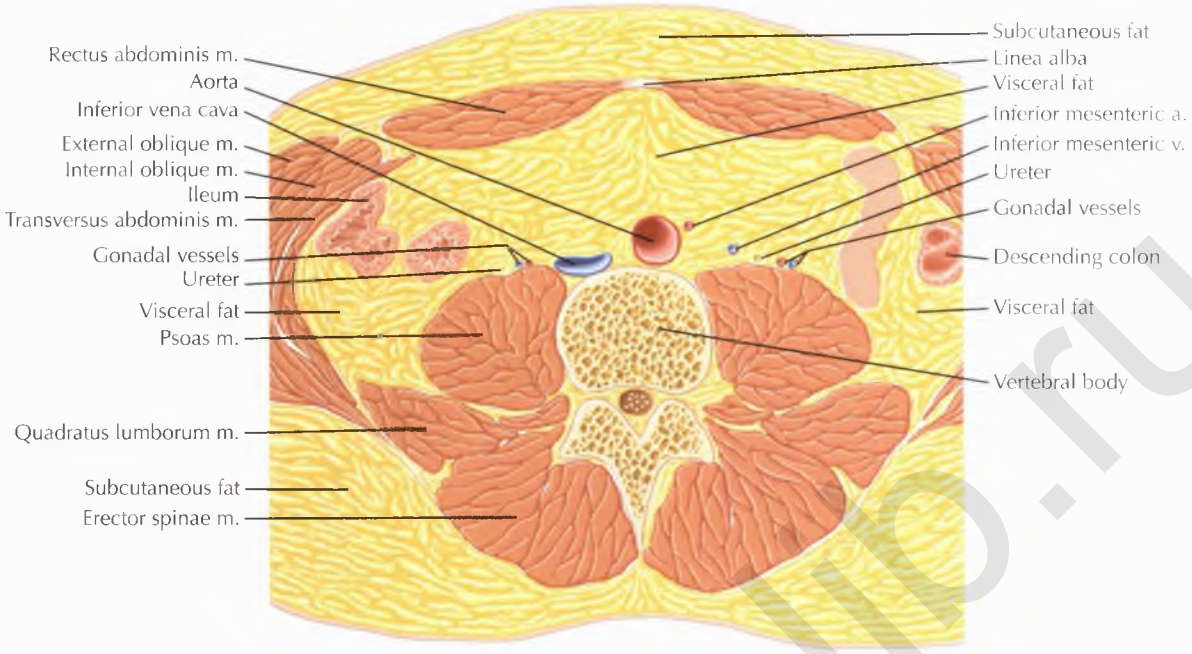

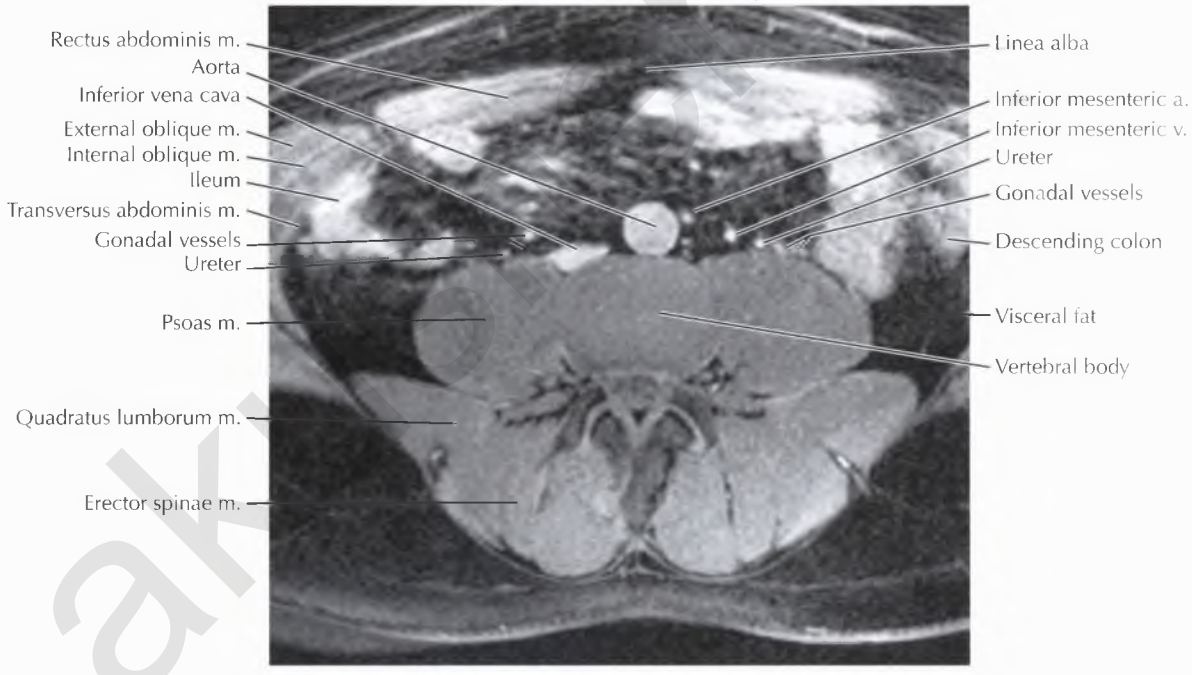

NORMAL ANATOMY

The *gonadal vessels* refer to the testicular artery and testicular vein in males and the ovarian artery and ovarian vein in females. The gonadal arteries arise directly from the aorta and carry blood to the gonads (testicles or ovaries). The right gonadal vein drains into the inferior vena cava (IVC), and the left gonadal vein drains into the left renal vein. On this image in the lower abdomen, the gonadal vessels are seen coursing anterior to the psoas muscles, adjacent to the ureters.

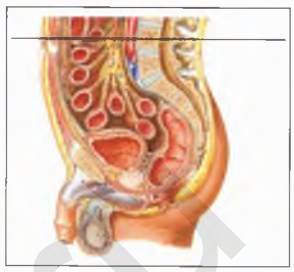

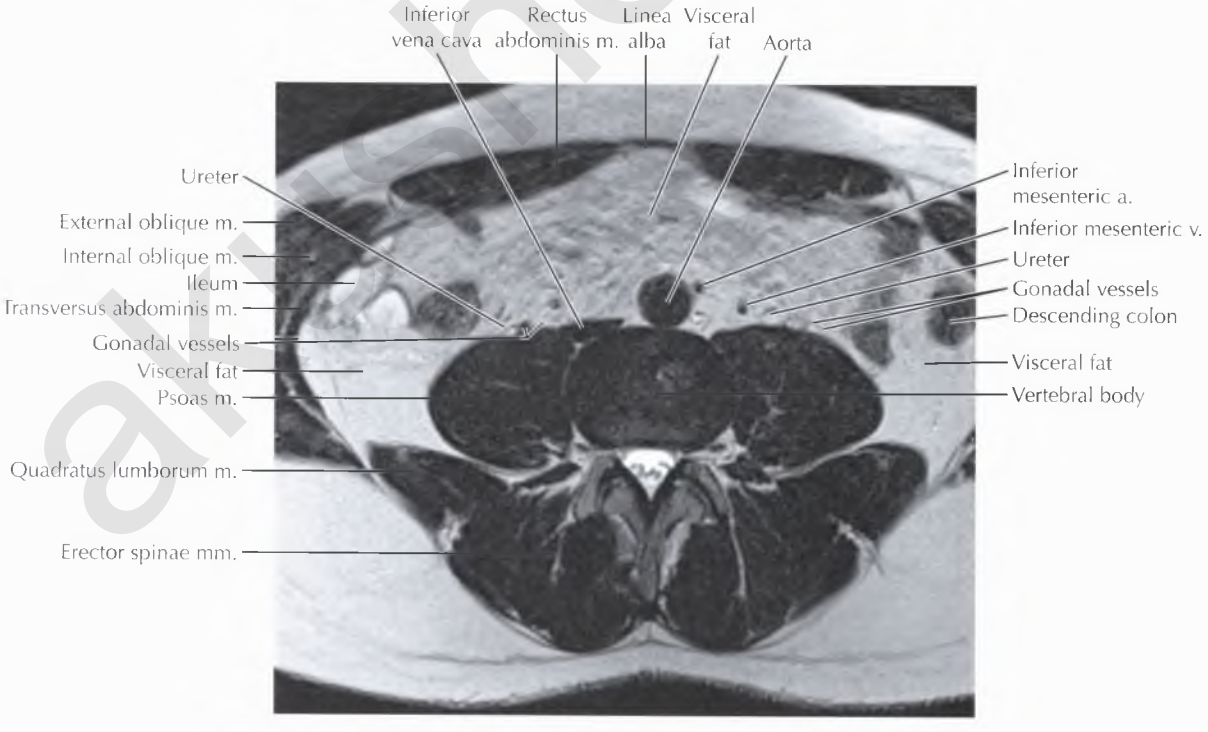

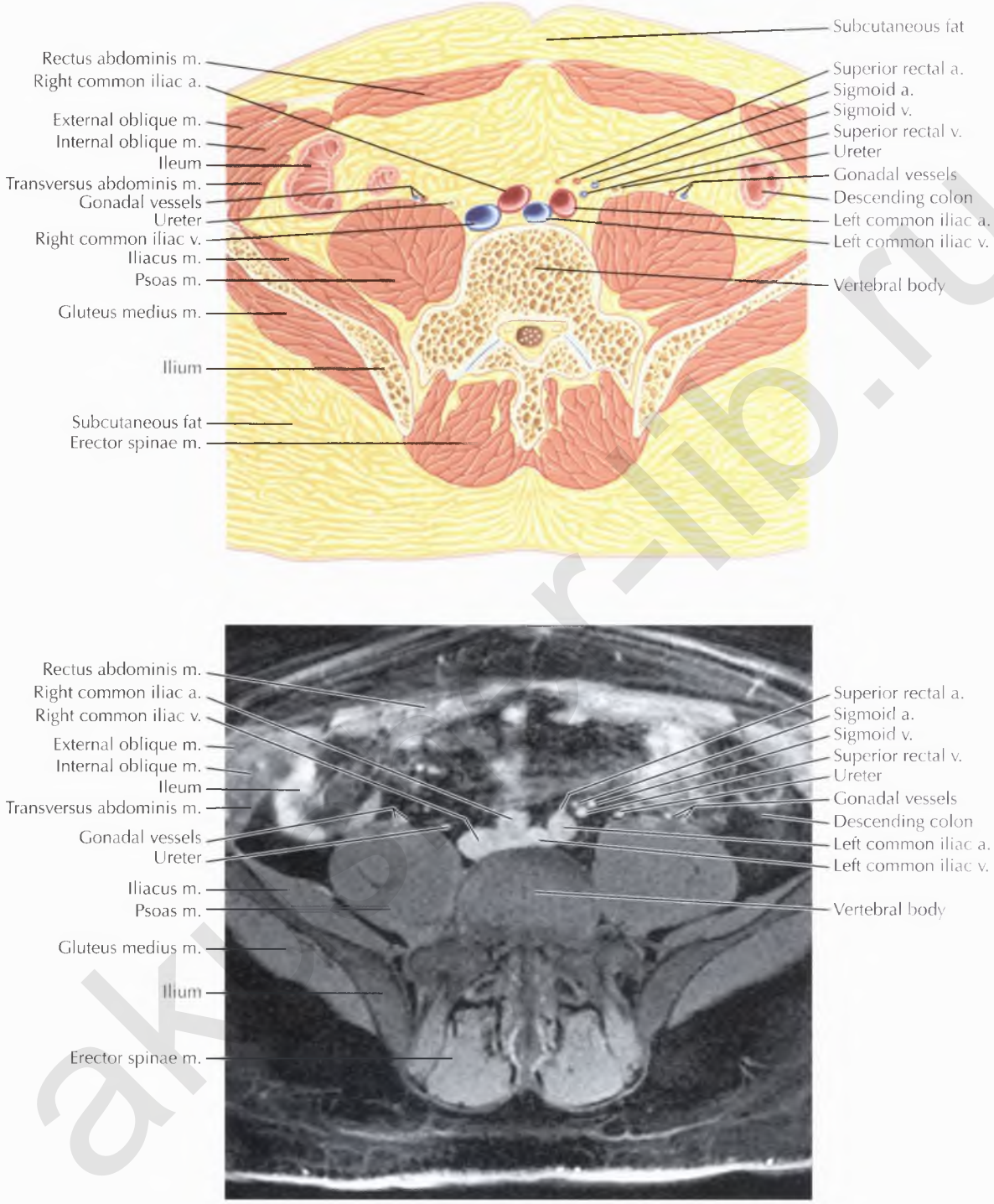

PATHOLOGIC PROCESS

May-Thurner syndrome is caused by extrinsic compression of the left common iliac vein as it passes between the right common iliac artery and spine, resulting in thrombosis and occlusion.

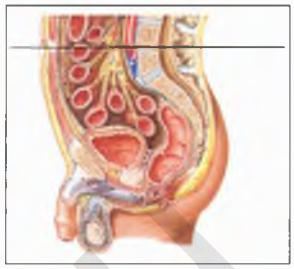

Subcutaneous fat
Superior rectal a.
Sigmoid a.
Sigmoid v.
Rectus abdominis m.
Right common iliac a.
External oblique m.
Internal oblique m.
Ileum
Transversus abdominis m.
Ureter
Right common iliac v.
Psoas m.
Iliacus m.
Gluteus medius m.
Ilium
Subcutaneous fat
Erector spinae m.
Superior rectal v.
Descending colon
Ureter
Left common iliac a.
Left common iliac v.
Vertebral body
Superior rectal a.
Sigmoid a.
Sigmoid v.
Rectus abdominis m.
Right common iliac a.
External oblique m.
Internal oblique m.
Ileum
Gonadal vessels
Transversus abdominis m.
Ureter
Right common iliac v.
Psoas m.
Iliacus m.
Gluteus medius m.
Ilium
Erector spinae m.
Superior rectal v.
Descending colon
Gonadal vessels
Ureter
Left common iliac a.
Left common iliac v.
Vertebral body

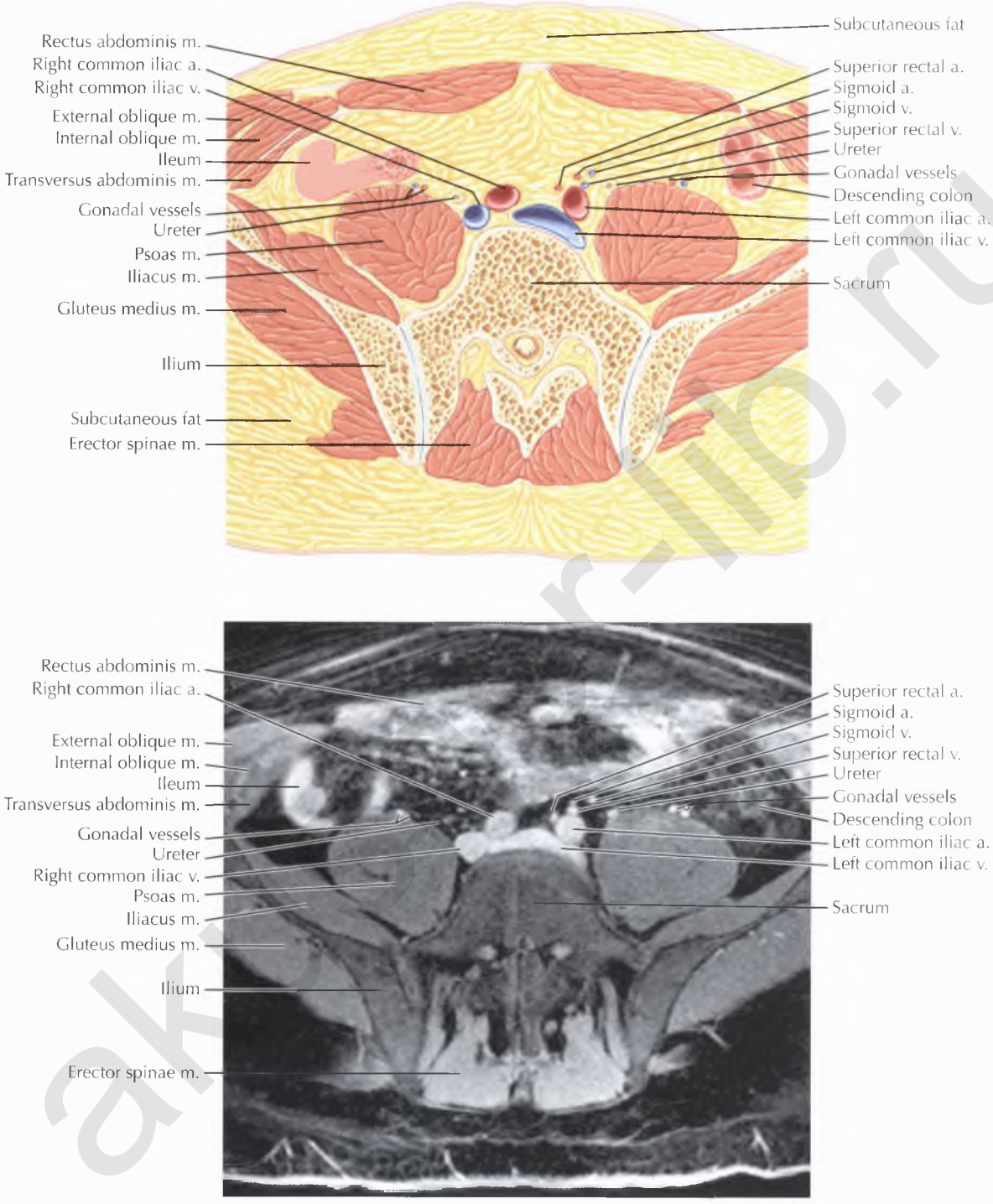

NORMAL ANATOMY

The inferior mesenteric artery gives off two or three sigmoid artery branches, then continues as the *superior rectal artery*, which descends into the pelvis between the layers of the sigmoid mesentery.

Subcutaneous fat
Rectus abdominis m.
Right common iliac a.
External oblique m.
Internal oblique m.
Ileum
Transversus abdominis m.
Ureter
Right common iliac v.
Psoas m.
Iliacus m.
Gluteus medius m.
Ilium
Subcutaneous fat
Erector spinae m.
Descending colon
Ureter
Left common iliac a.
Left common iliac v.
Sacrum

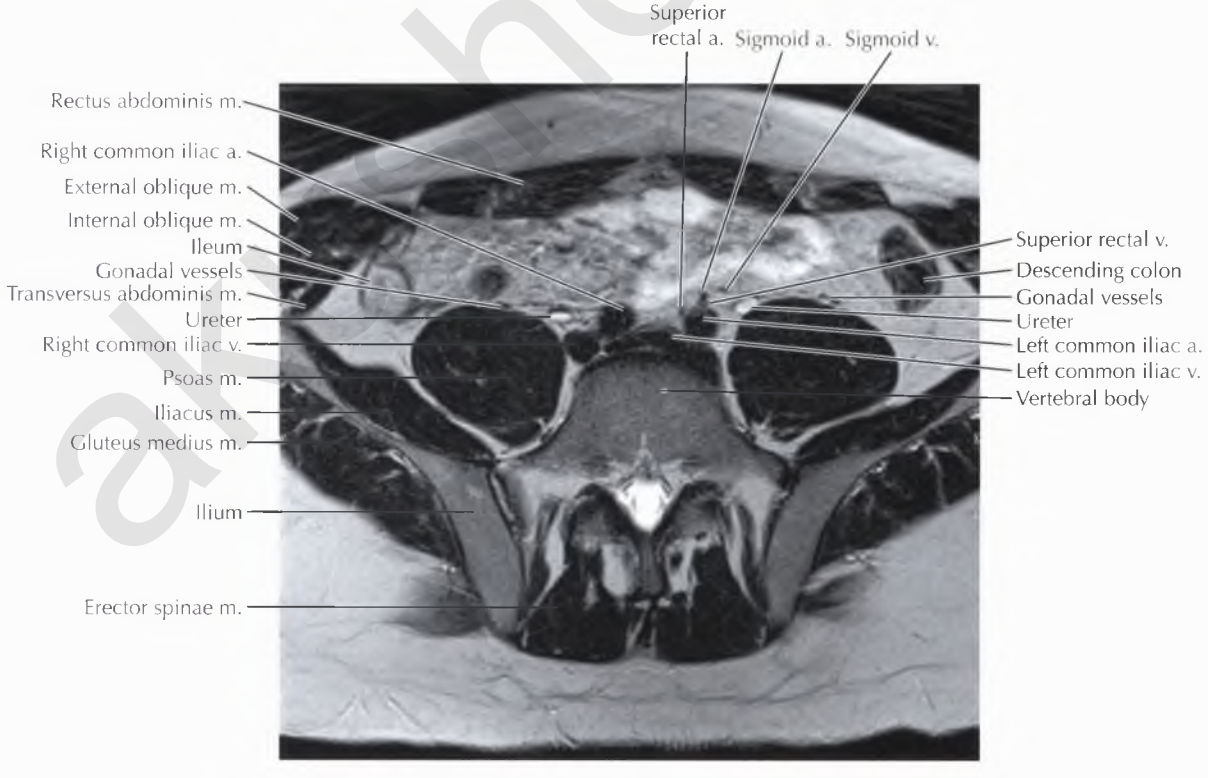
Superior rectal a.
Sigmoid a.
Sigmoid v.
Rectus abdominis m.
Right common iliac a.
External oblique m.
Internal oblique m.
Ileum
Gonadal vessels
Transversus abdominis m.
Ureter
Right common iliac v.
Psoas m.
Iliacus m.
Gluteus medius m.
Ilium
Erector spinae m.
Superior rectal v.
Descending colon
Gonadal vessels
Ureter
Left common iliac a.
Left common iliac v.
Vertebral body

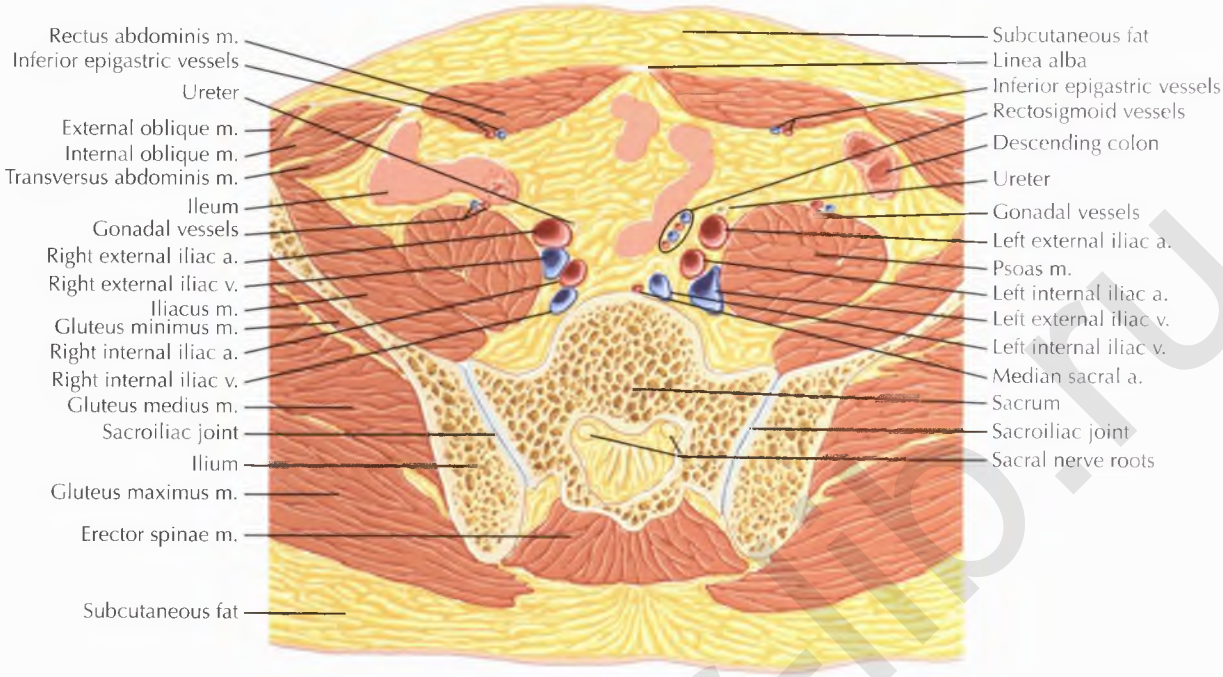

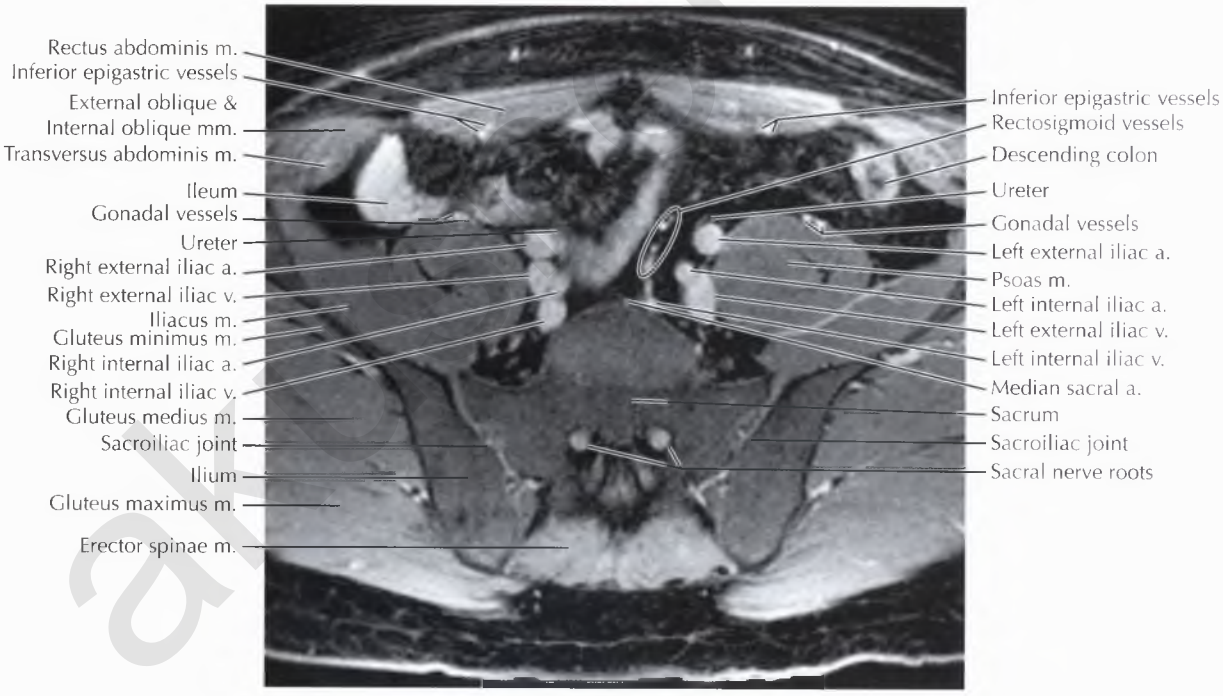

NORMAL ANATOMY

The common iliac arteries and veins divide into the external iliac arteries and veins and the internal iliac (or hypogastric) arteries and veins, respectively, in the pelvis. Note that the arteries are located anterior to the veins.

Subcutaneous fat
Linea alba
Rectus abdominis m.
External oblique & Internal oblique mm.
Right external iliac a.
Transversus abdominis m.
Ileum
Ureter
Right external iliac v.
Iliacus m.
Gluteus minimus m.
Right internal iliac a.
Gluteus medius m.
Right internal iliac v.
Sacroiliac joint
Ilium
Gluteus maximus m.
Erector spinae m.
Subcutaneous fat
Descending colon
Ureter
Left external iliac a.
Psoas m.
Left internal iliac a.
Left external iliac v.
Left internal iliac v.
Sacrum
Sacroiliac joint
Sacral nerve roots

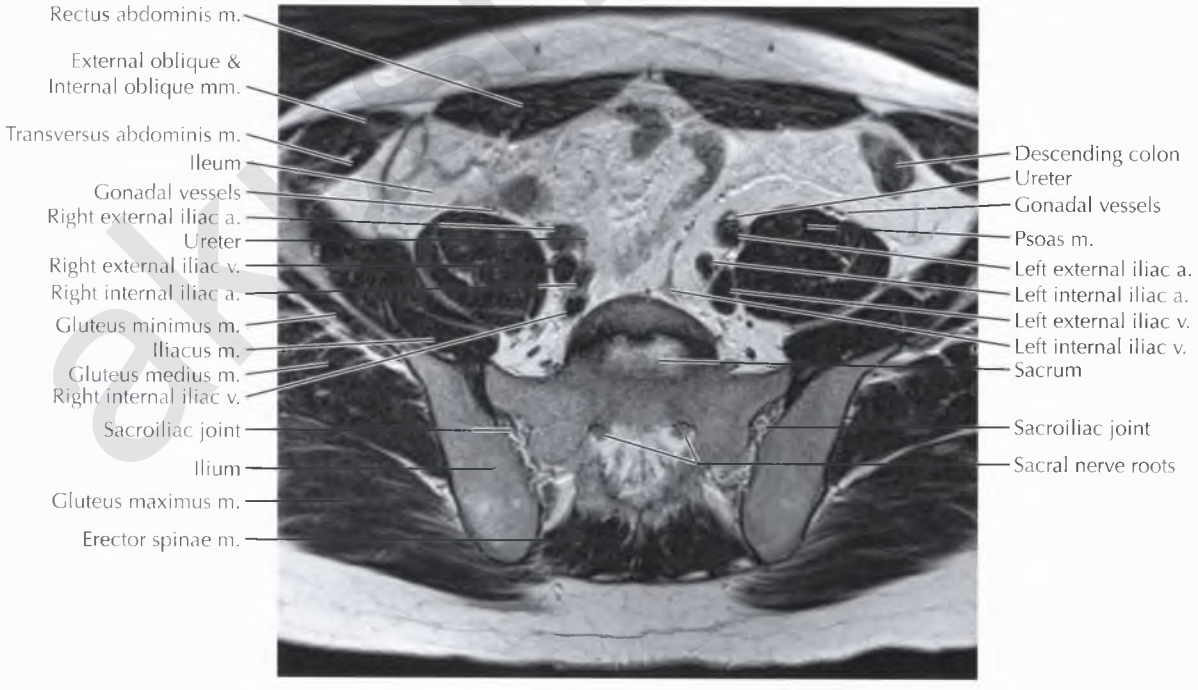
Rectus abdominis m.
External oblique & Internal oblique mm.
Transversus abdominis m.
Ileum
Gonadal vessels
Right external iliac a.
Ureter
Right external iliac v.
Right internal iliac a.
Gluteus minimus m.
Iliacus m.
Gluteus medius m.
Right internal iliac v.
Sacroiliac joint
Ilium
Gluteus maximus m.
Erector spinae m.
Descending colon
Ureter
Gonadal vessels
Psoas m.
Left external iliac a.
Left internal iliac a.
Left external iliac v.
Left internal iliac v.
Sacrum
Sacroiliac joint
Sacral nerve roots

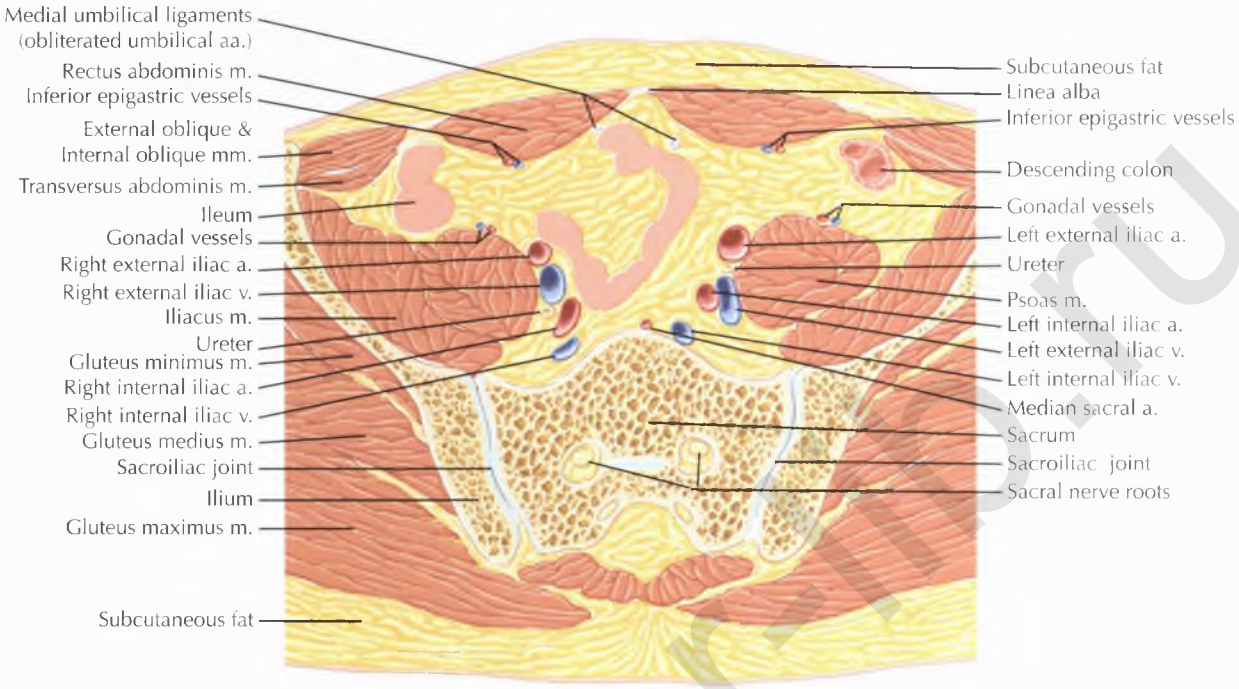
Medial umbilical ligaments (obliterated umbilical aa.)
Rectus abdominis m.
Inferior epigastric vessels
External oblique & Internal oblique mm.
Transversus abdominis m.
Ileum
Gonadal vessels
Right external iliac a.
Right external iliac v.
Iliacus m.
Ureter
Gluteus minimus m.
Right internal iliac a.
Right internal iliac v.
Gluteus medius m.
Sacroiliac joint
Ilium
Gluteus maximus m.
Subcutaneous fat
Subcutaneous fat
Linea alba
Inferior epigastric vessels
Descending colon
Gonadal vessels
Left external iliac a.
Ureter
Psoas m.
Left internal iliac a.
Left external iliac v.
Left internal iliac v.
Median sacral a.
Sacrum
Sacroiliac joint
Sacral nerve roots

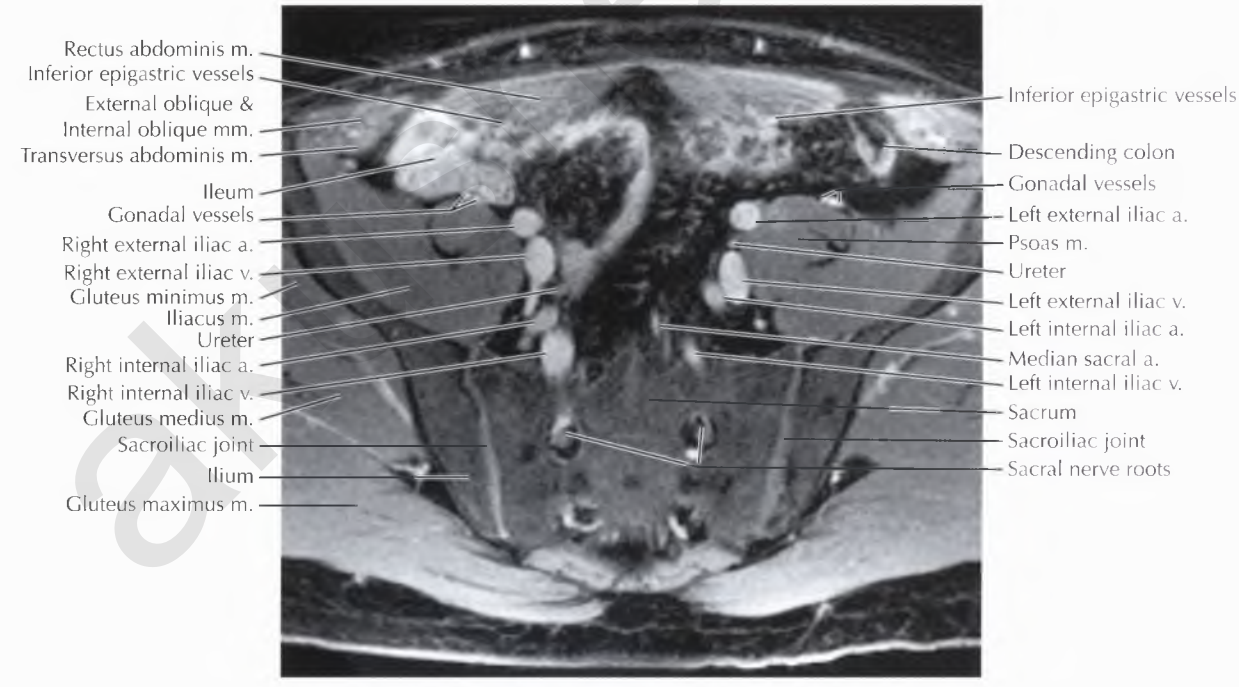
Rectus abdominis m.
Inferior epigastric vessels
External oblique & Internal oblique mm.
Transversus abdominis m.
Ileum
Gonadal vessels
Right external iliac a.
Right external iliac v.
Gluteus minimus m.
Iliacus m.
Ureter
Right internal iliac a.
Right internal iliac v.
Gluteus medius m.
Sacroiliac joint
Ilium
Gluteus maximus m.
Inferior epigastric vessels
Descending colon
Gonadal vessels
Left external iliac a.
Psoas m.
Ureter
Left external iliac v.
Left internal iliac a.
Median sacral a.
Left internal iliac v.
Sacrum
Sacroiliac joint
Sacral nerve roots

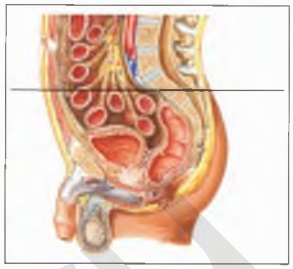

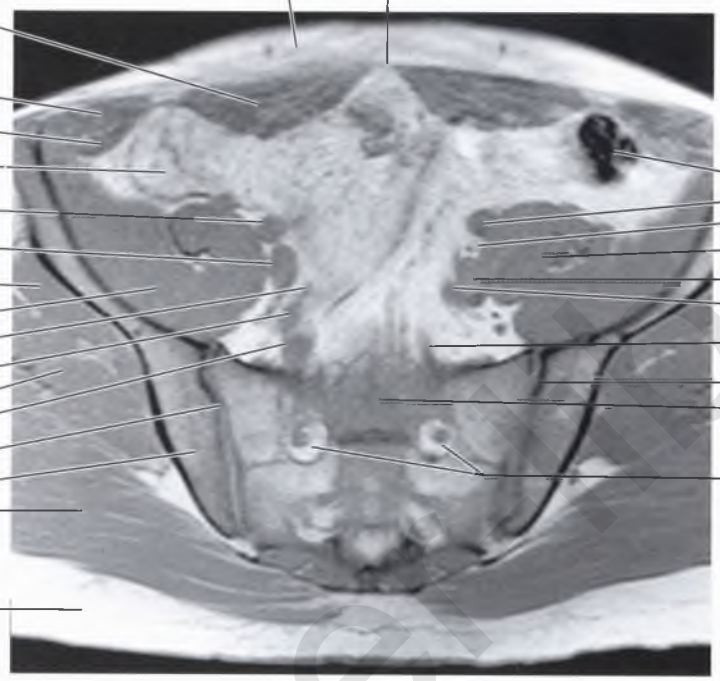
Subcutaneous fat
Linea alba
Rectus abdominis m.
External oblique & Internal oblique mm.
Transversus abdominis m.
Ileum
Right external iliac a.
Right external iliac v.
Gluteus minimus m.
Iliacus m.
Ureter
Right internal iliac a.
Gluteus medius m.
Right internal iliac v.
Sacroiliac joint
Ilium
Gluteus maximus m.
Subcutaneous fat
Descending colon
Left external iliac a.
Ureter
Psoas m.
Left external iliac v.
Left internal iliac a.
Left internal iliac v.
Sacroiliac joint
Sacrum
Sacral nerve roots

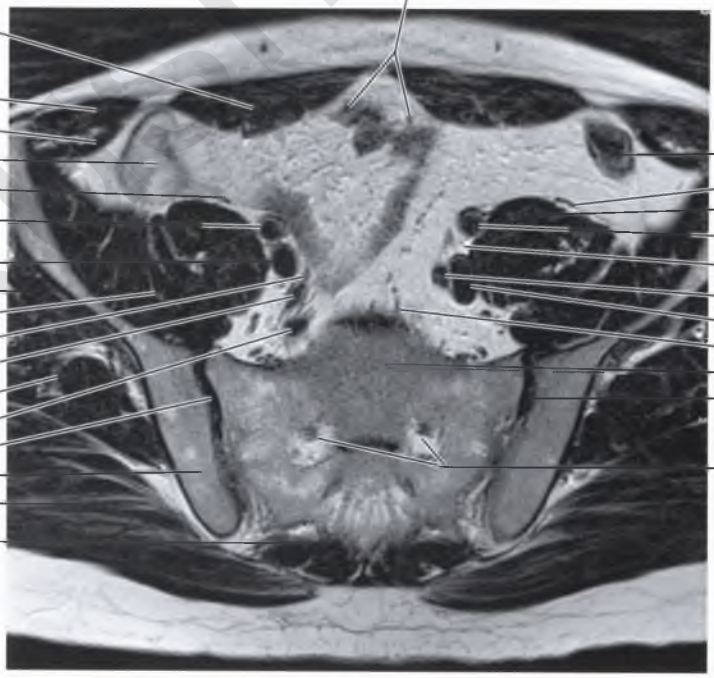
Medial umbilical ligaments (obliterated umbilical aa.)
Rectus abdominis m.
External oblique & Internal oblique mm.
Transversus abdominis m.
Ileum
Gonadal vessels
Right external iliac a.
Right external iliac v.
Gluteus minimus m.
Iliacus m.
Ureter
Right internal iliac a.
Gluteus medius m.
Right internal iliac v.
Sacroiliac joint
Ilium
Gluteus maximus m.
Erector spinae m.
Descending colon
Gonadal vessels
Psoas m.
Left external iliac a.
Ureter
Left internal iliac a.
Left external iliac v.
Left internal iliac v.
Sacrum
Sacroiliac joint
Sacral nerve roots

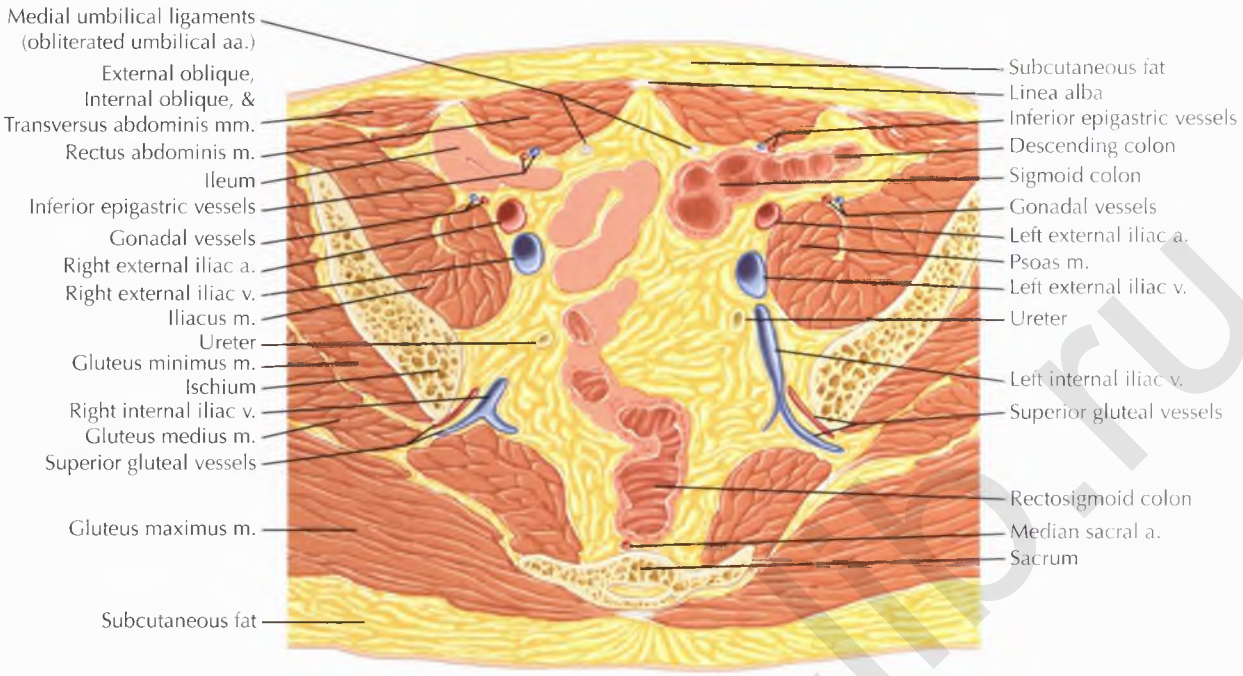

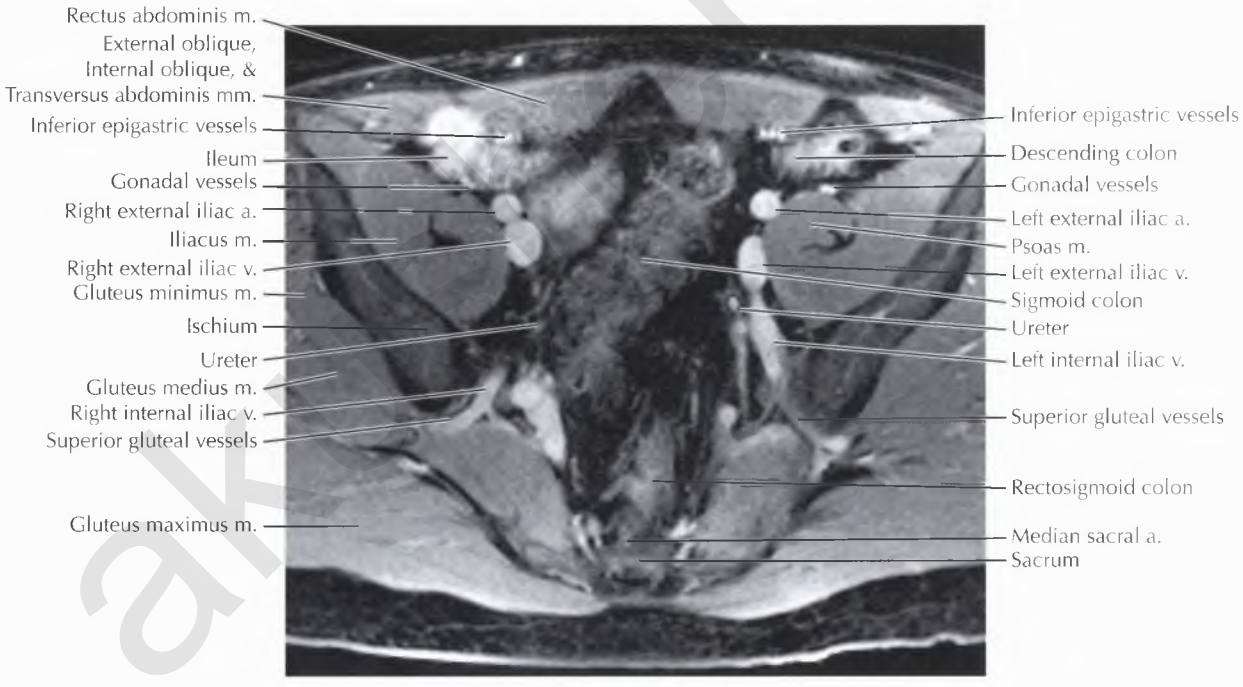

NORMAL ANATOMY

The superior gluteal artery is the largest branch of the internal iliac artery and appears as the continuation of the posterior division of the internal iliac artery. On this image, the *superior gluteal vessels* are seen traveling through the greater sciatic foramen just above the piriformis muscle. Other branches of the posterior division of the internal iliac artery include the iliolumbar and lateral sacral arteries.

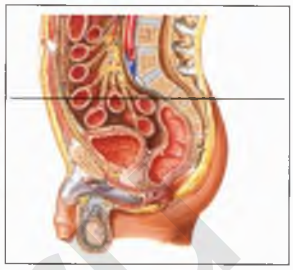

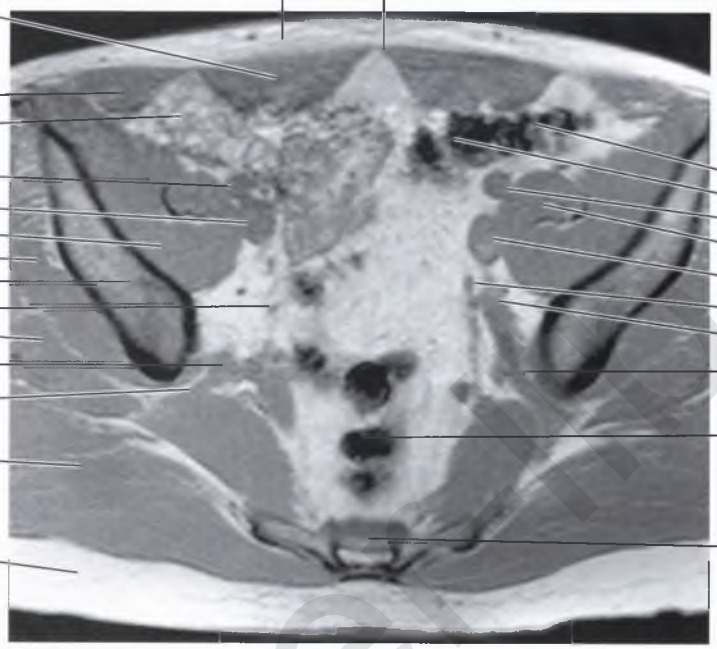
Subcutaneous fat
Linea alba
Rectus abdominis m.
External oblique, Internal oblique, & Transversus abdominis mm.
Ileum
Right external iliac a.
Right external iliac v.
Iliacus m.
Gluteus minimus m.
Ischium
Ureter
Gluteus medius m.
Right internal iliac v.
Superior gluteal vessels
Gluteus maximus m.
Subcutaneous fat
Descending colon
Sigmoid colon
Left external iliac a.
Psoas m.
Left external iliac v.
Ureter
Left internal iliac v.
Superior gluteal vessels
Rectosigmoid colon
Sacrum


Medial umbilical ligaments (obliterated umbilical aa.)
Sigmoid colon
Rectus abdominis m.
External oblique, Internal oblique, & Transversus abdominis mm.
Ileum
Gonadal vessels
Right external iliac a.
Right external iliac v.
Gluteus minimus m.
Iliacus m.
Ischium
Ureter
Gluteus medius m.
Right internal iliac v.
Superior gluteal vessels
Gluteus maximus m.
Descending colon
Gonadal vessels
Left external iliac a.
Psoas m.
Left external iliac v.
Ureter
Left internal iliac v.
Superior gluteal vessels
Rectosigmoid colon
Sacrum

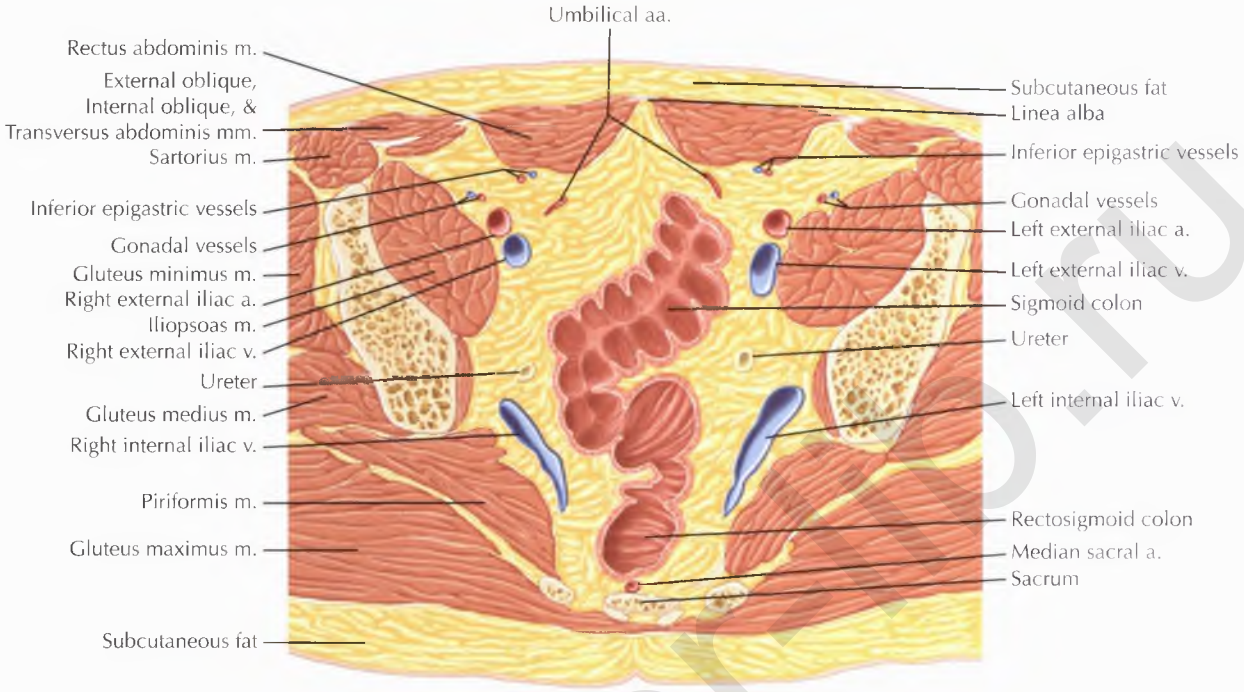

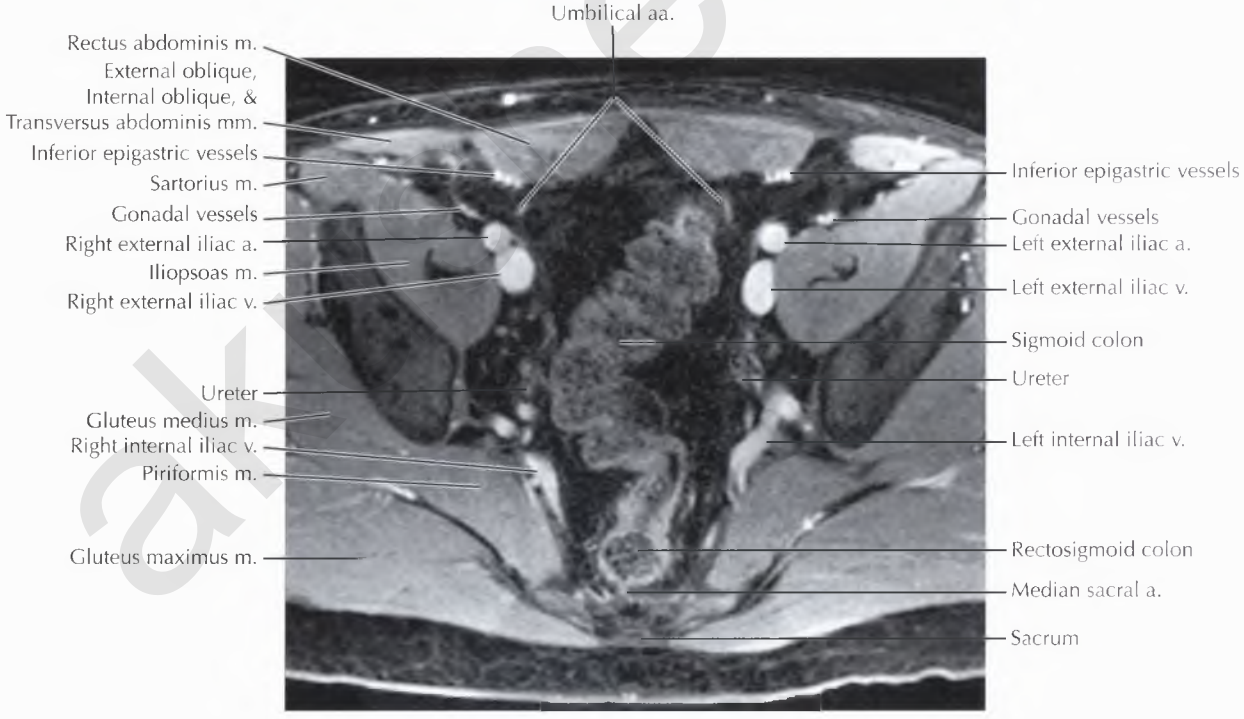

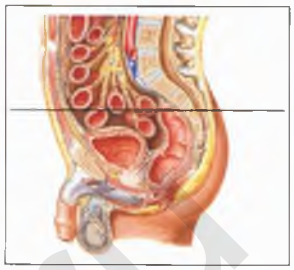

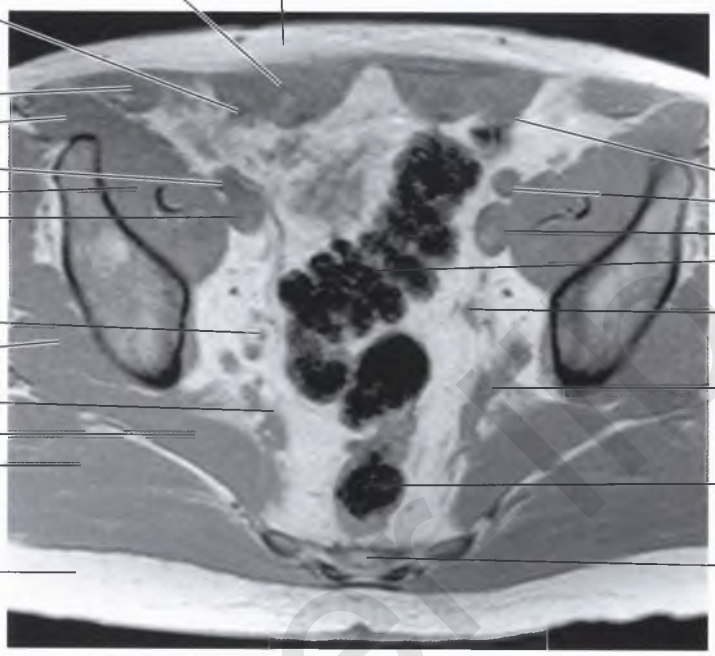
Rectus abdominis m.
Subcutaneous fat
Inferior epigastric vessels
External oblique, Internal oblique, & Transversus abdominis mm.
Sartorius m.
Right external iliac a.
Iliopsoas m.
Right external iliac v.
Ureter
Gluteus medius m.
Right internal iliac v.
Piriformis m.
Gluteus maximus m.
Subcutaneous fat
Inferior epigastric vessels
Left external iliac a.
Left external iliac v.
Sigmoid colon
Ureter
Left internal iliac v.
Rectosigmoid colon
Sacrum

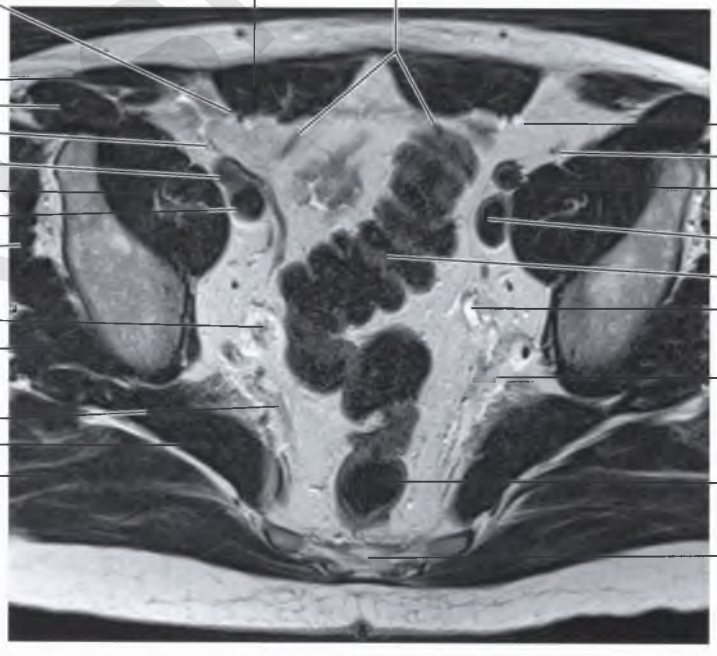
Rectus abdominis m.
Umbilical aa.
Inferior epigastric vessels
External oblique, Internal oblique, & Transversus abdominis mm.
Sartorius m.
Gonadal vessels
Right external iliac a.
Iliopsoas m.
Right external iliac v.
Gluteus minimus m.
Ureter
Gluteus medius m.
Right internal iliac v.
Piriformis m.
Gluteus maximus m.
Inferior epigastric vessels
Gonadal vessels
Left external iliac a.
Left external iliac v.
Sigmoid colon
Ureter
Left internal iliac v.
Rectosigmoid colon
Sacrum

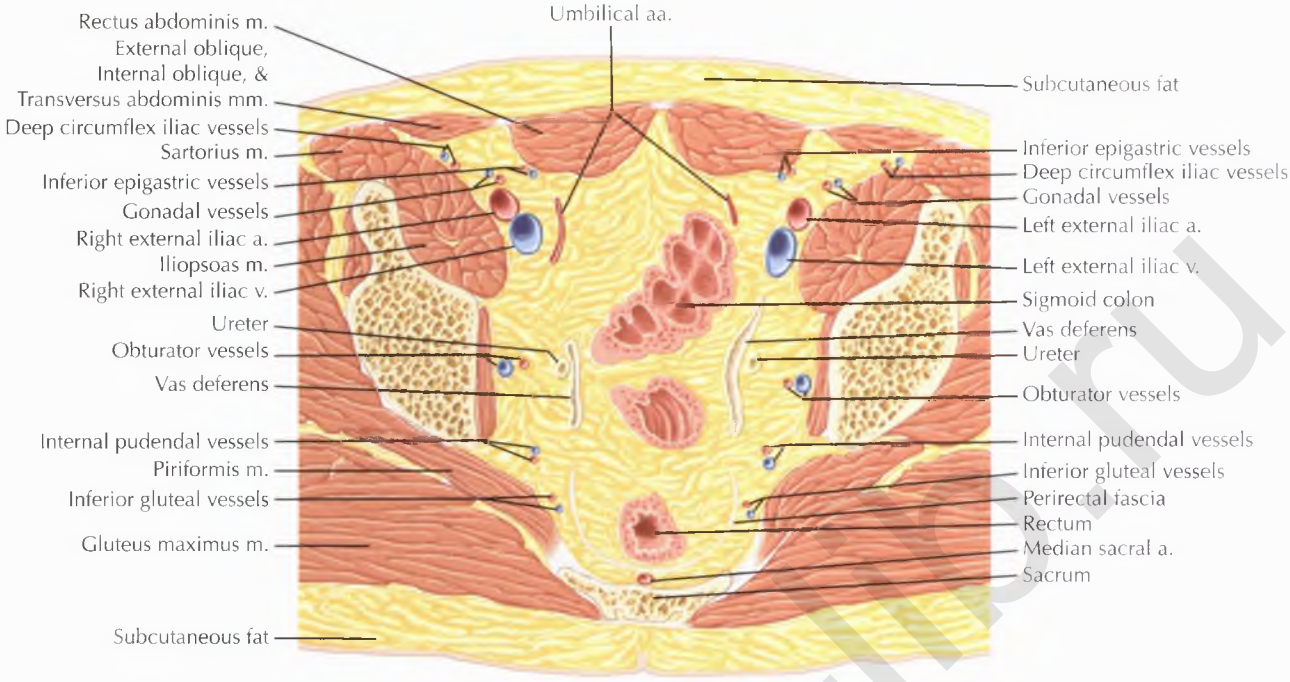

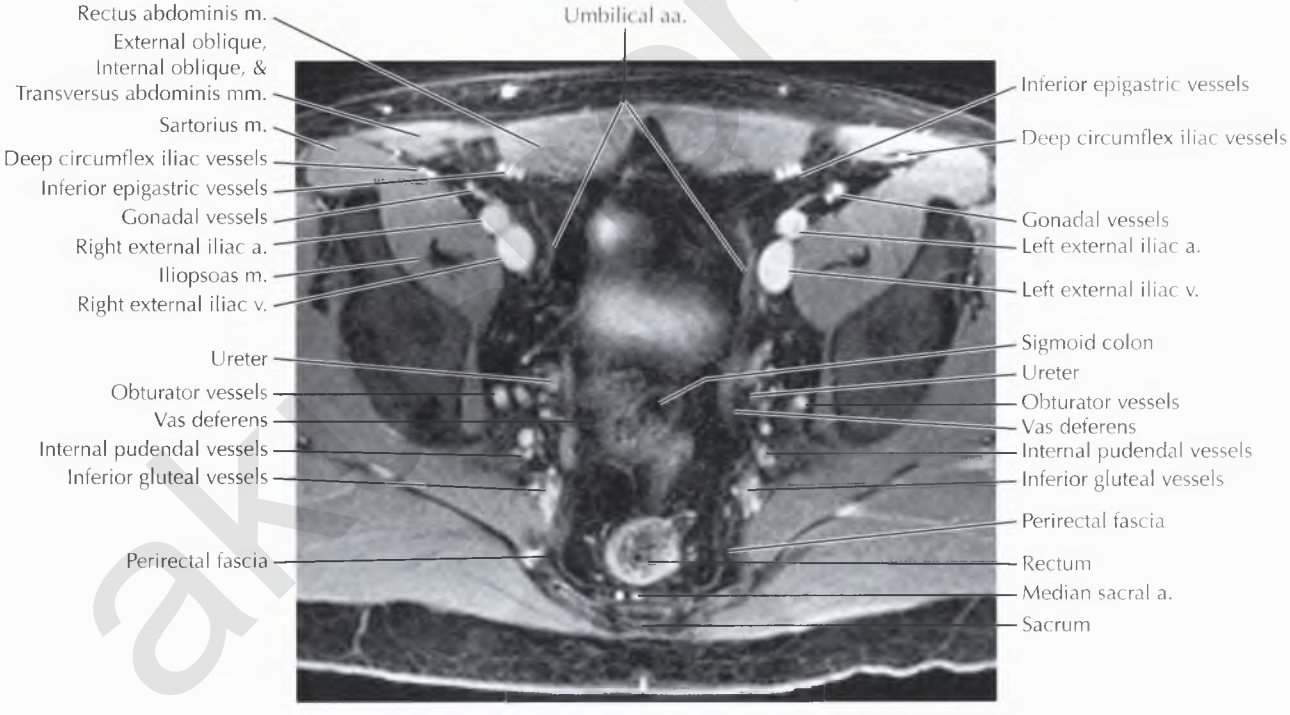

NORMAL ANATOMY

The paired vasa deferentia are continuations of the *epididymal tails* (cauda epididymidis), which ascend from the scrotum into the pelvis through the inguinal canals, course along the lateral pelvic walls, cross over (anterior and superior to) the ureters, and then curve along the superomedial surface of the seminal vesicles, where they dilate to form the ampullary portions of the vasa deferentia.

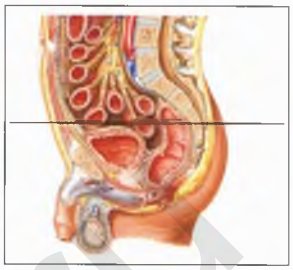

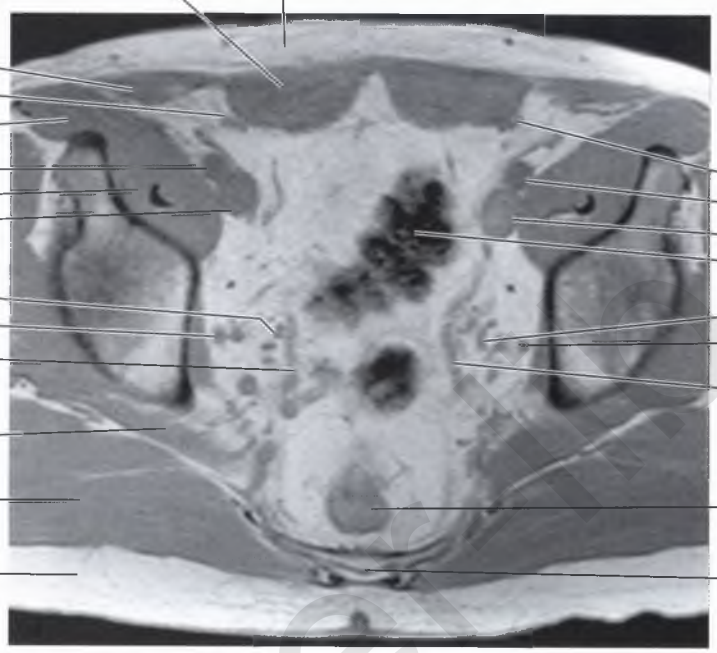
Rectus abdominis m.
Subcutaneous fat
External oblique, Internal oblique, & Transversus abdominis mm.
Inferior epigastric vessels
Sartorius m.
Right external iliac a.
Iliopsoas m.
Right external iliac v.
Ureter
Obturator vessels
Vas deferens
Piriformis m.
Gluteus maximus m.
Subcutaneous fat
Inferior epigastric vessels
Left external iliac a.
Left external iliac v.
Sigmoid colon
Ureter
Obturator vessels
Vas deferens
Rectum
Sacrum

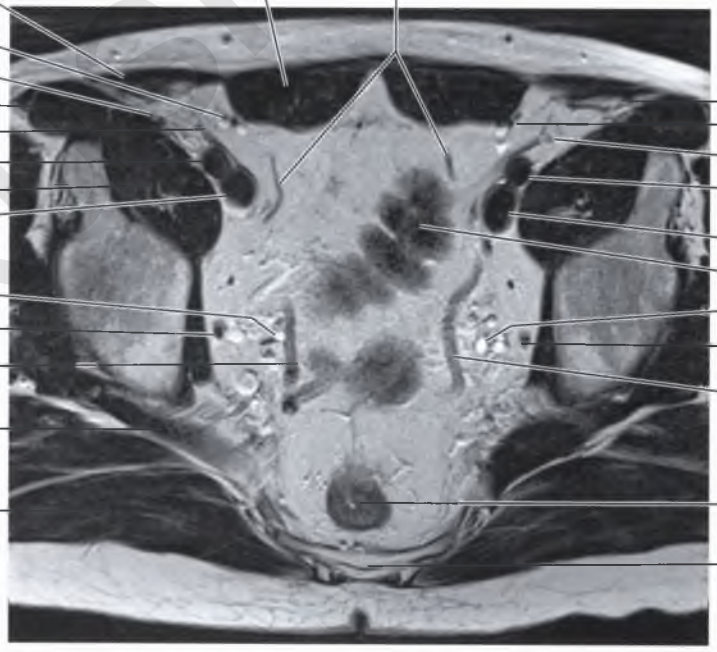
External oblique, Internal oblique, & Transversus abdominis mm.
Rectus abdominis m.
Umbilical aa.
Inferior epigastric vessels
Deep circumflex vessels
Sartorius m.
Gonadal vessels
Right external iliac a.
Iliopsoas m.
Right external iliac v.
Ureter
Obturator vessels
Vas deferens
Piriformis m.
Gluteus maximus m.
Deep circumflex vessels
Inferior epigastric vessels
Gonadal vessels
Left external iliac a.
Left external iliac v.
Sigmoid colon
Ureter
Obturator vessels
Vas deferens
Rectum
Sacrum

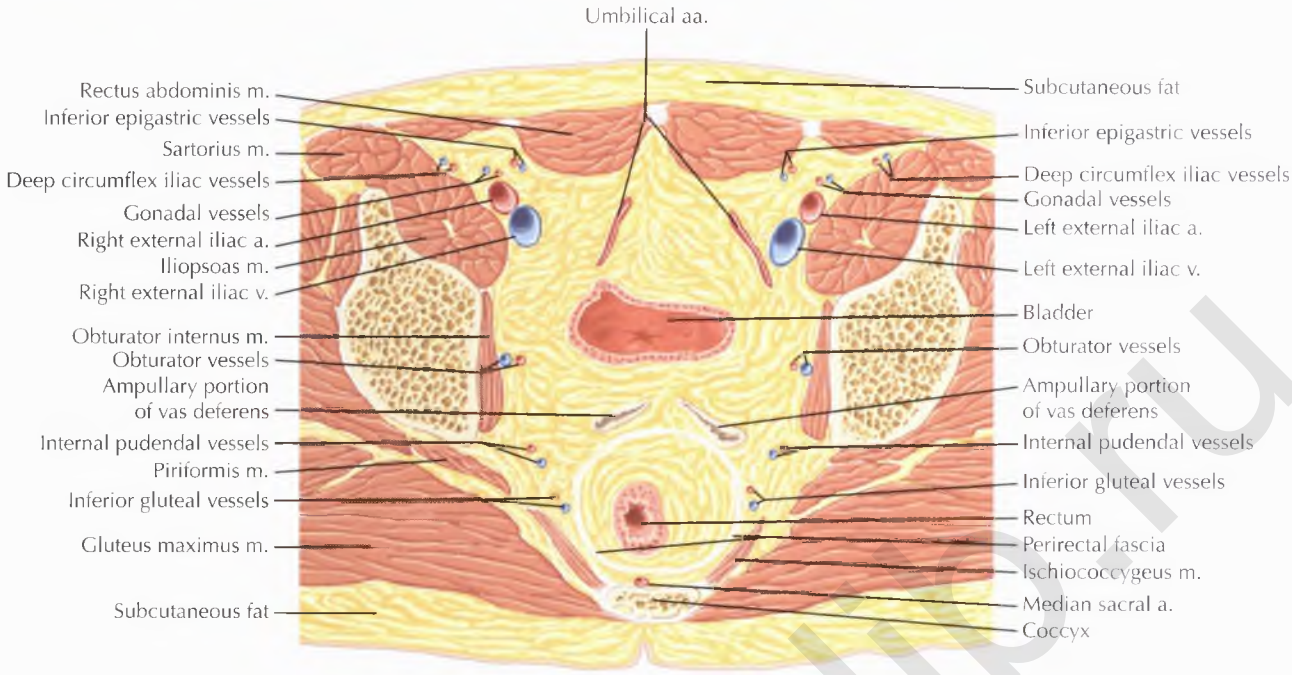

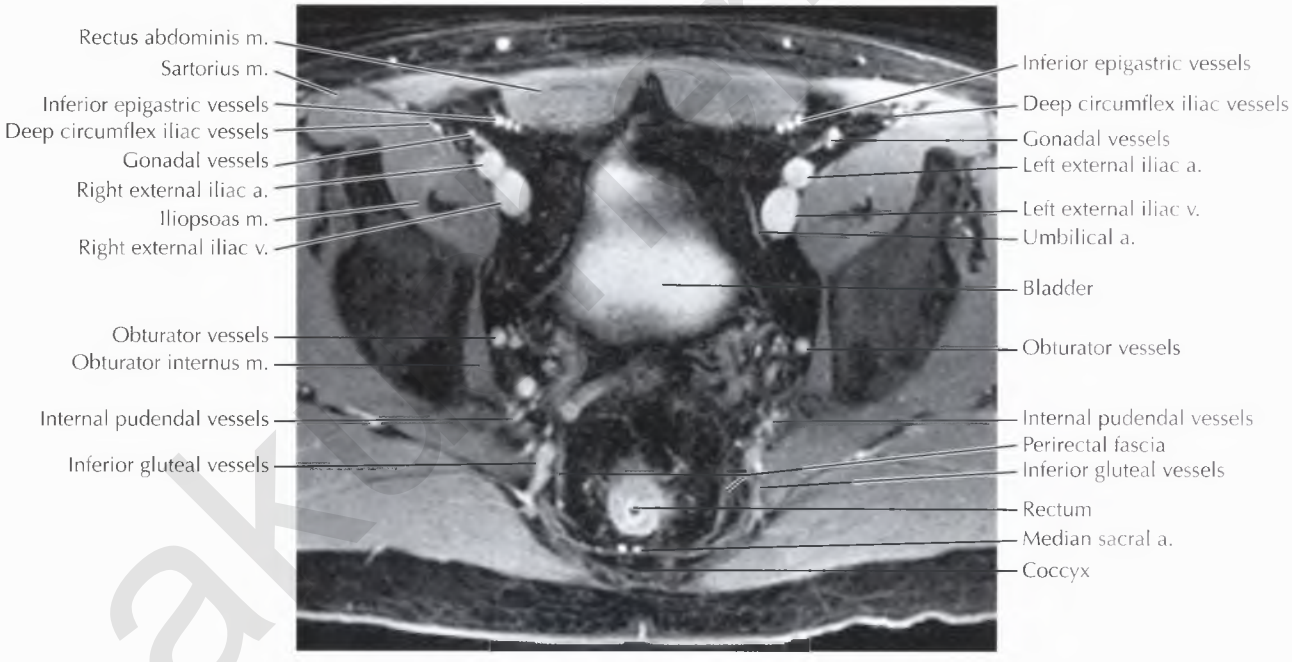

NORMAL ANATOMY

Several of the main branches of the anterior division of the internal iliac artery can be seen on this image, including the *umbilical artery*, which usually gives off the superior vesical artery; the *obturator artery*, which exits the pelvis through the obturator canal; and the *inferior gluteal* and *internal pudendal* arteries, which exit through the greater sciatic foramen, with the internal pudendal giving off the inferior rectal artery. Other branches from the anterior division of the internal iliac artery include the inferior vesical artery (whereas the middle vesical artery usually arises from the superior vesical artery), the middle rectal artery, the deferential artery in men (which more often arises from the superior vesical artery), and the uterine and vaginal arteries in women.

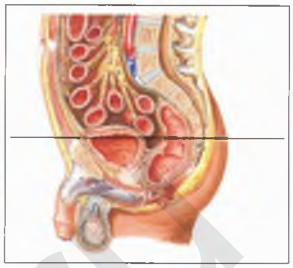

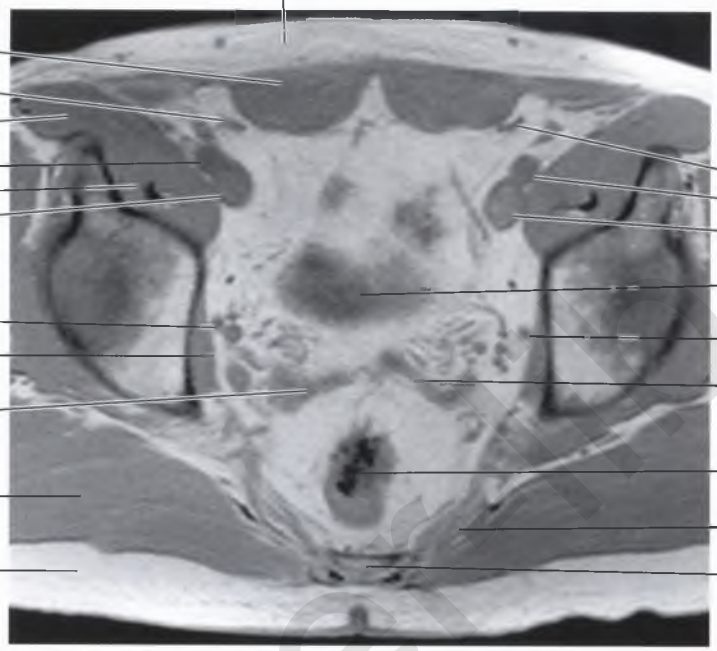
Subcutaneous fat
Rectus abdominis m.
Inferior epigastric vessels
Sartorius m.
Right external iliac a.
Iliopsoas m.
Right external iliac v.
Obturator vessels
Obturator internus m.
Ampullary portion of vas deferens
Gluteus maximus m.
Subcutaneous fat
Inferior epigastric vessels
Left external iliac a.
Left external iliac v.
Bladder
Obturator vessels
Ampullary portion of vas deferens
Rectum
Ischiococcygeus m.
Coccyx

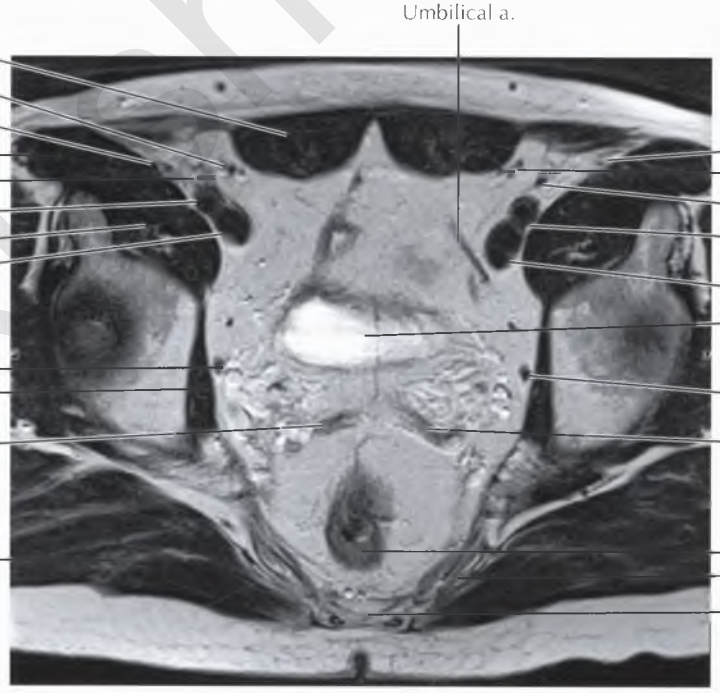
Umbilical a.
Rectus abdominis m.
Inferior epigastric vessels
Deep circumflex vessels
Sartorius m.
Gonadal vessels
Right external iliac a.
Iliopsoas m.
Right external iliac v.
Obturator vessels
Obturator internus m.
Ampullary portion of vas deferens
Gluteus maximus m.
Deep circumflex vessels
Inferior epigastric vessels
Gonadal vessels
Left external iliac a.
Left external iliac v.
Bladder
Obturator vessels
Ampullary portion of vas deferens
Rectum
Ischiococcygeus m.
Coccyx

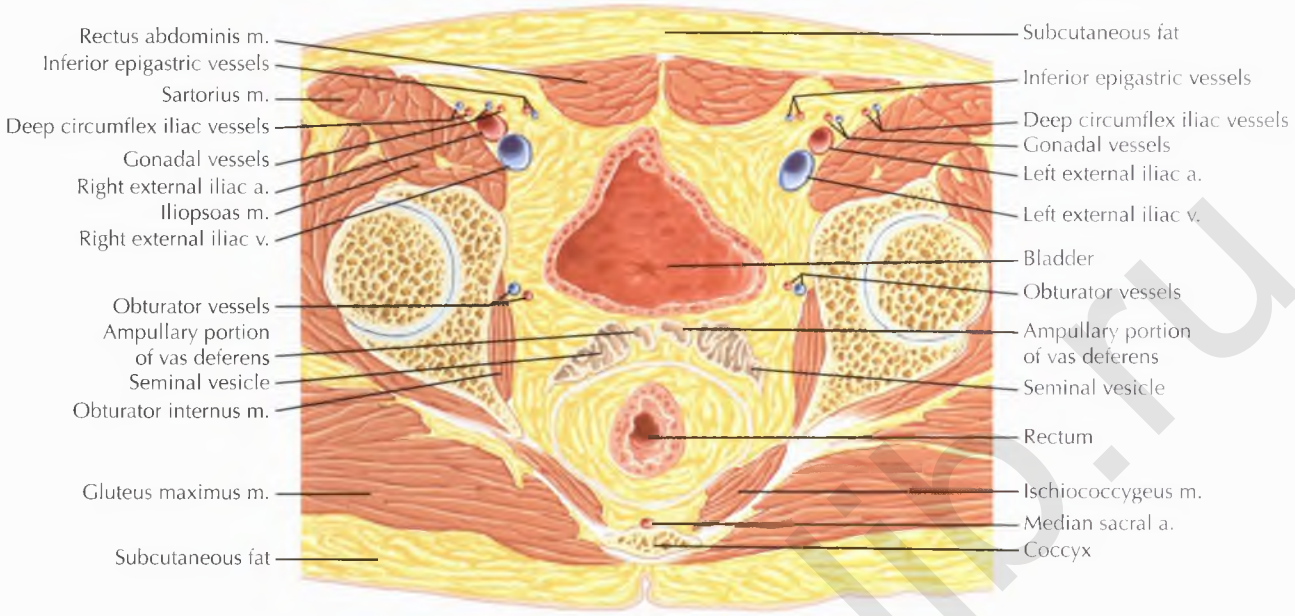

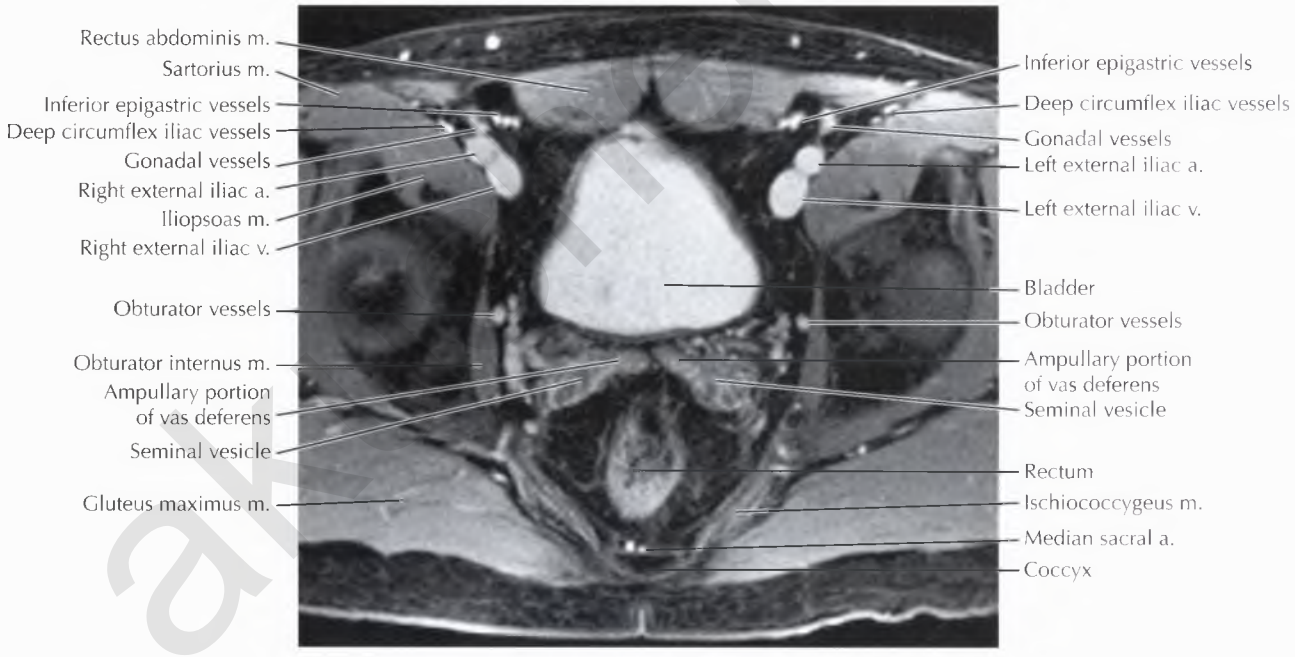

NORMAL ANATOMY

The origin of the inferior epigastric artery defines the transition from the external iliac artery to the common femoral artery. On this image, the inferior epigastric artery can be seen extending medially from the external iliac artery, whereas the deep circumflex iliac artery is seen extending laterally.

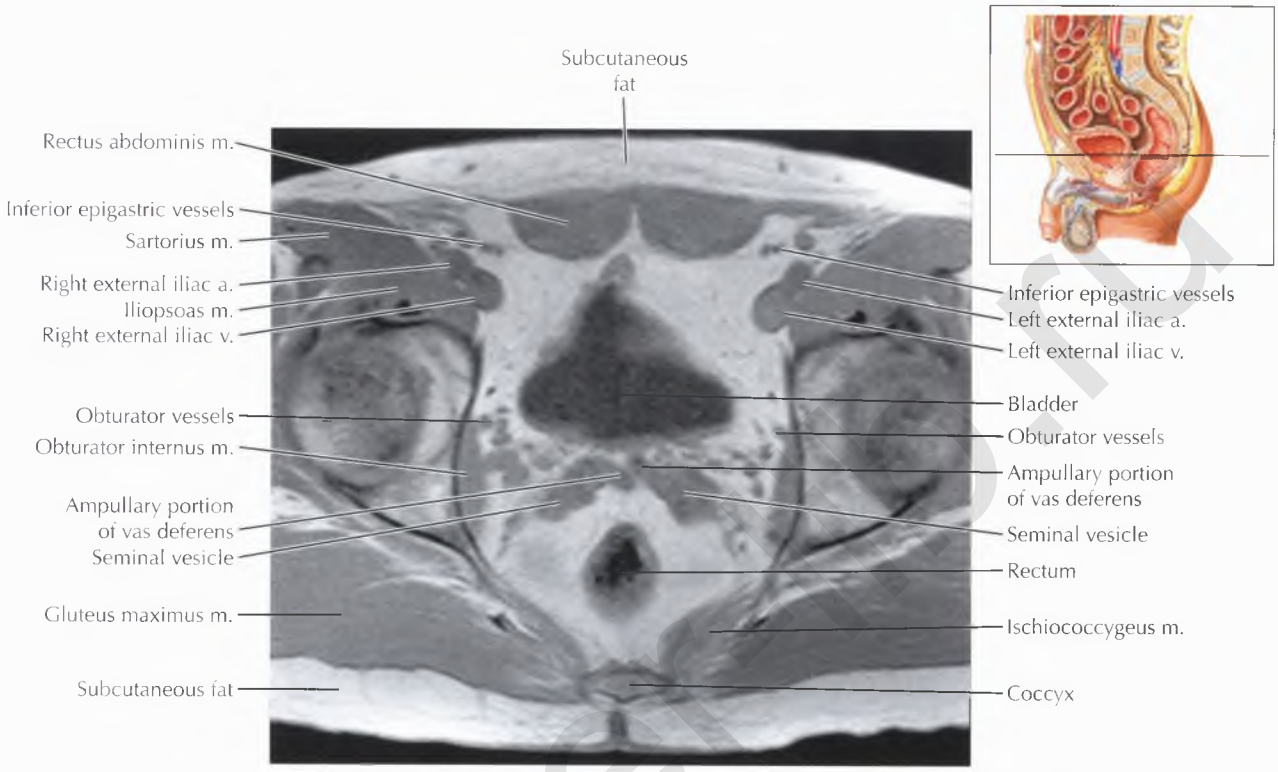
Subcutaneous fat
Rectus abdominis m.
Inferior epigastric vessels
Sartorius m.
Right external iliac a.
Iliopsoas m.
Right external iliac v.
Obturator vessels
Obturator internus m.
Ampullary portion of vas deferens
Seminal vesicle
Gluteus maximus m.
Subcutaneous fat
Inferior epigastric vessels
Left external iliac a.
Left external iliac v.
Bladder
Obturator vessels
Ampullary portion of vas deferens
Seminal vesicle
Rectum
Ischiococcygeus m.
Coccyx

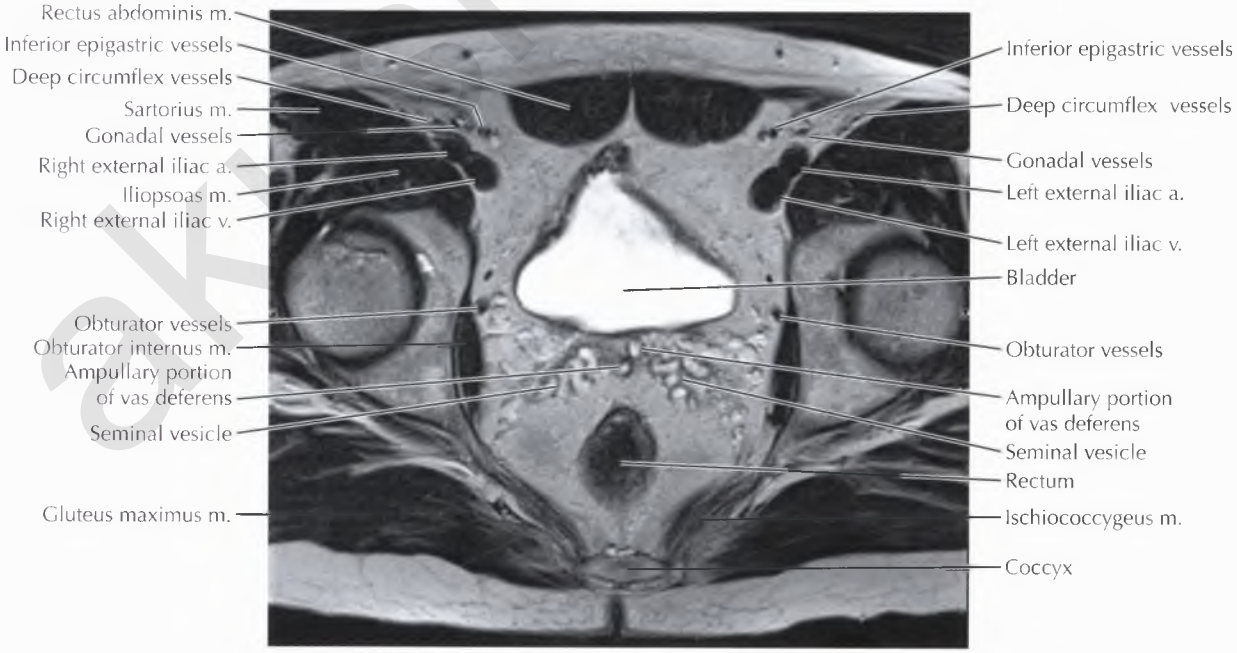
Rectus abdominis m.
Inferior epigastric vessels
Deep circumflex vessels
Sartorius m.
Gonadal vessels
Right external iliac a.
Iliopsoas m.
Right external iliac v.
Obturator vessels
Obturator internus m.
Ampullary portion of vas deferens
Seminal vesicle
Gluteus maximus m.
Inferior epigastric vessels
Deep circumflex vessels
Gonadal vessels
Left external iliac a.
Left external iliac v.
Bladder
Obturator vessels
Ampullary portion of vas deferens
Seminal vesicle
Rectum
Ischiococcygeus m.
Coccyx

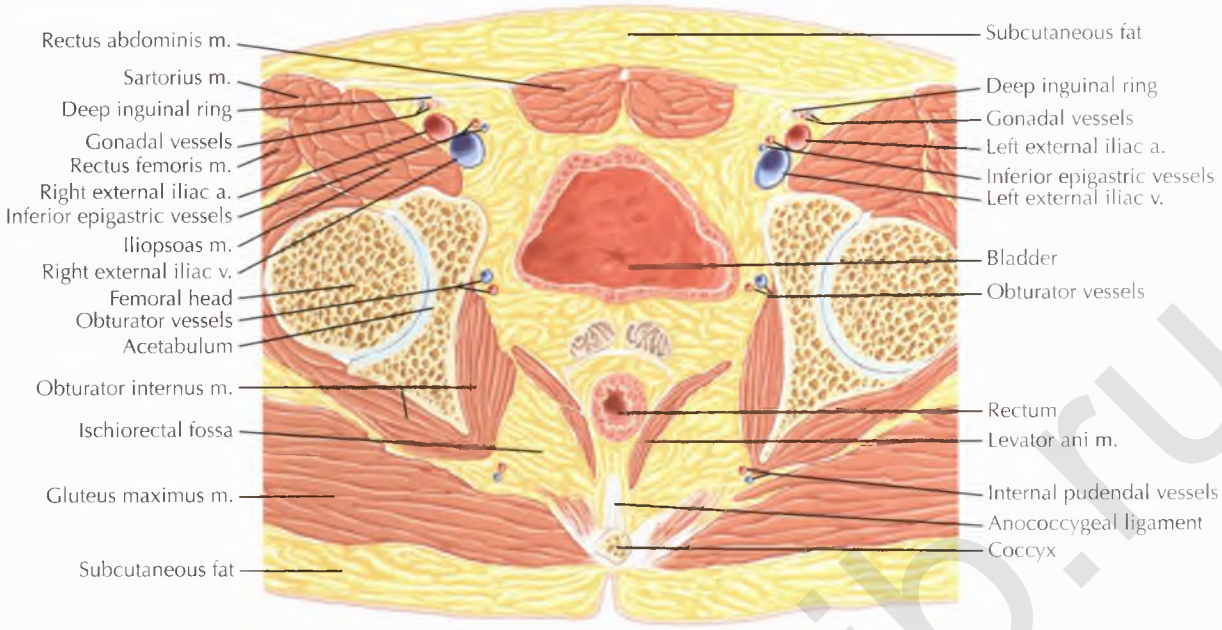

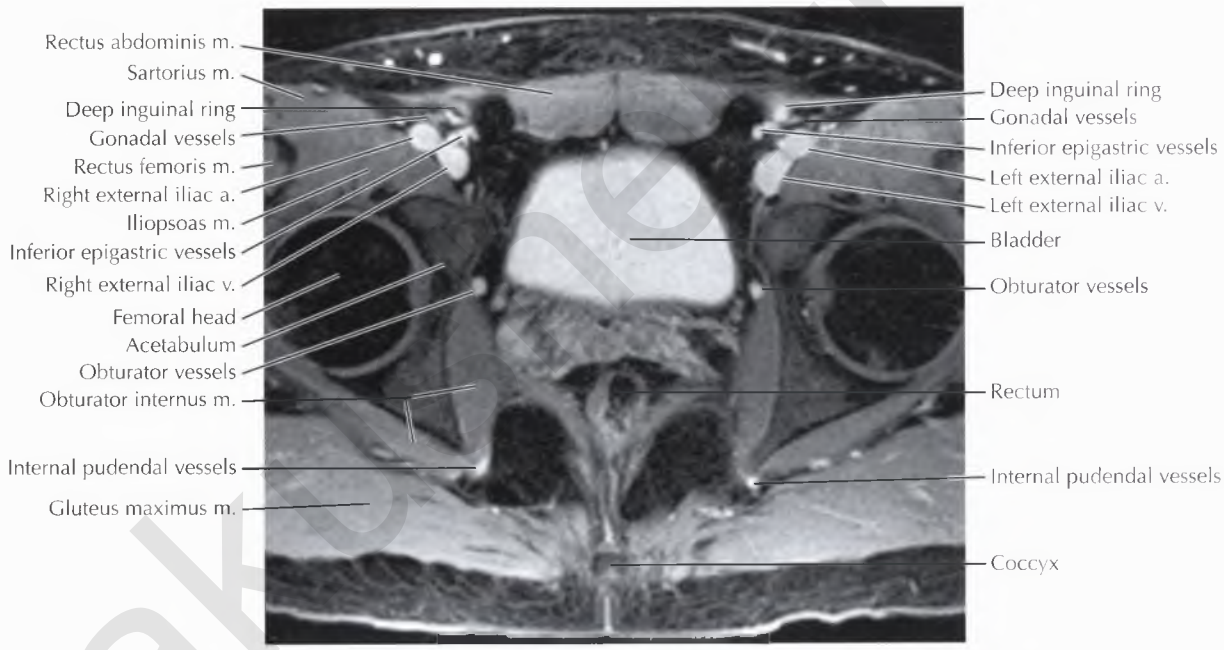

NORMAL ANATOMY

The spermatic cord begins at the deep (internal) inguinal ring (seen on this image) and exits through the superficial (external) inguinal ring into the scrotum (seen on Pelvis Axial 12). The main contents of the spermatic cord include the vas deferens, testicular artery, and pampiniform plexus of veins.

DIAGNOSTIC CONSIDERATION

Note the bilateral ureteral jets, seen as low-signal-intensity linear streams crisscrossing each other in the partially distended urinary bladder on the T2-weighted MR image, indicating bilateral ureteral patency.

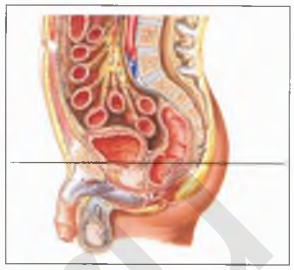

Subcutaneous fat
Rectus abdominis m.
Sartorius m.
Right external iliac a.
Rectus femoris m.
Iliopsoas m.
Right external iliac v.
Acetabulum
Femoral head
Obturator vessels
Obturator internus m.
Ischiorectal fossa
Gluteus maximus m.
Subcutaneous fat
Left external iliac a.
Left external iliac v.
Bladder
Obturator vessels
Rectum
Levator ani m.
Anococcygeal ligament
Coccyx

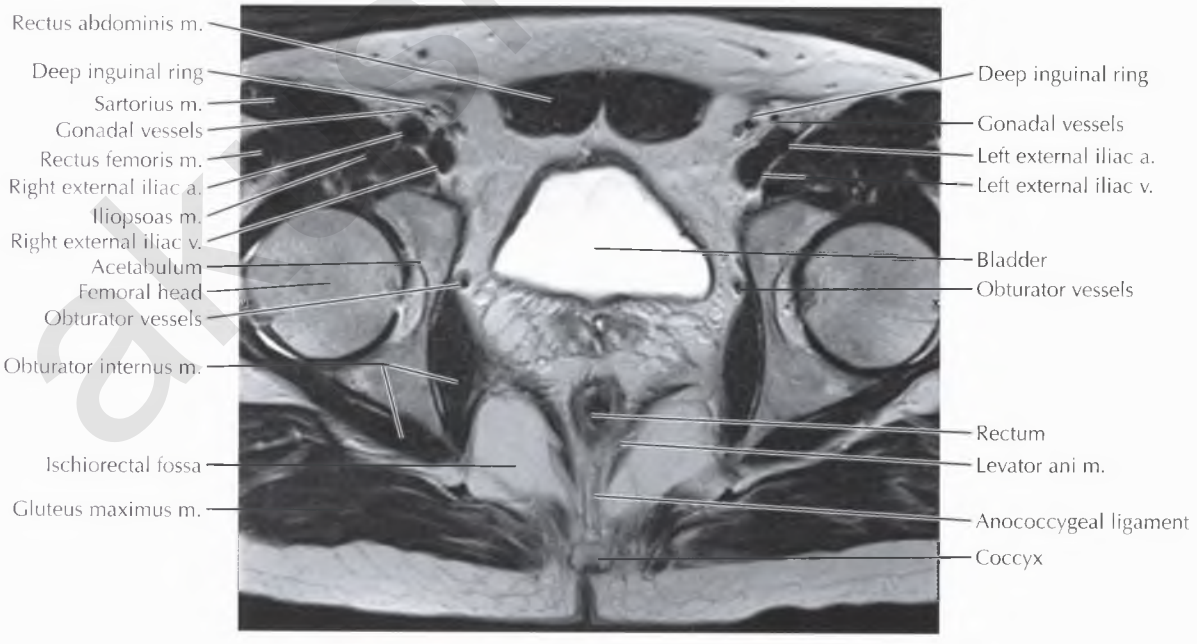
Rectus abdominis m.
Deep inguinal ring
Sartorius m.
Gonadal vessels
Rectus femoris m.
Right external iliac a.
Iliopsoas m.
Right external iliac v.
Acetabulum
Femoral head
Obturator vessels
Obturator internus m.
Ischiorectal fossa
Gluteus maximus m.
Deep inguinal ring
Gonadal vessels
Left external iliac a.
Left external iliac v.
Bladder
Obturator vessels
Rectum
Levator ani m.
Anococcygeal ligament
Coccyx

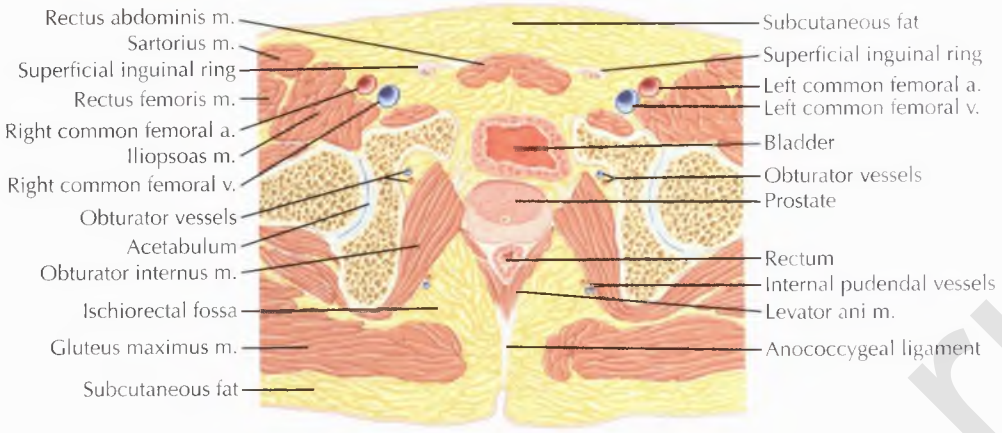

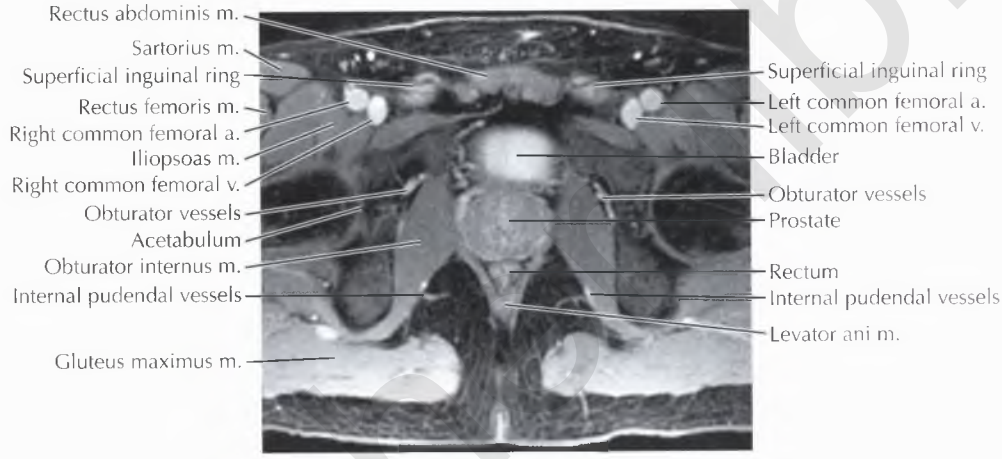

PATHOLOGIC PROCESS

Inguinal hernias are common, especially in men, and consist of two types: direct and indirect. Five times more common than direct hernias, *indirect inguinal hernias* occur when abdominal contents protrude through the deep inguinal ring, into the inguinal canal, and out through the superficial inguinal ring into the scrotum or labia majora. In contrast, *direct inguinal hernias* do not travel through the deep inguinal ring, but instead protrude into the inguinal canal directly through an area of weakness in the abdominal wall at *Hesselbach's triangle*, bordered by the rectus abdominis muscle medially, the inferior epigastric vessels superolaterally, and the inguinal ligament inferiorly. On cross-sectional imaging in the axial plane, direct inguinal hernias are seen medial to the inferior epigastric vessels, whereas indirect inguinal hernias are seen lateral to the inferior epigastric vessels.

DIAGNOSTIC CONSIDERATION

The ischiorectal fossa is a common location for anorectal fistulae and sinus tracts in patients with inflammatory bowel disease. Pelvic magnetic resonance imaging (MRI) is becomingly increasingly popular as a preoperative diagnostic study in patients with suspected perianal fistulae. MRI can clearly define the relationship of a fistula to the ischiorectal and ischioanal fossae, as well as to the levator ani musculature, which may have important surgical and prognostic implications. Involvement of the ischioanal or ischiorectal fossa may require more complex surgery, including possible colostomy, to allow time for healing.

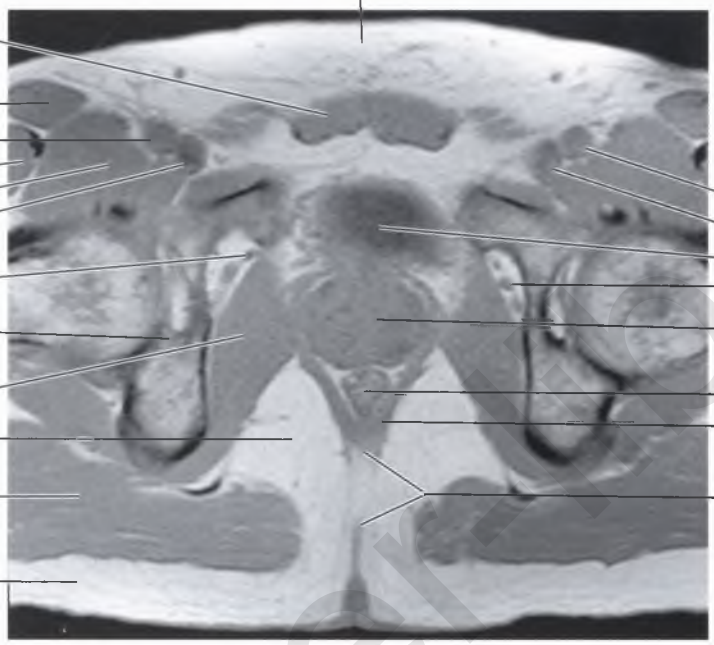
Subcutaneous fat
Rectus abdominis m.
Sartorius m.
Right common femoral a.
Rectus femoris m.
Iliopsoas m.
Right common femoral v.
Obturator vessels
Acetabulum
Obturator internus m.
Ischiorectal fossa
Gluteus maximus m.
Subcutaneous fat
Left common femoral a.
Left common femoral v.
Bladder
Obturator vessels
Prostate
Rectum
Levator ani m.
Anococcygeal ligament

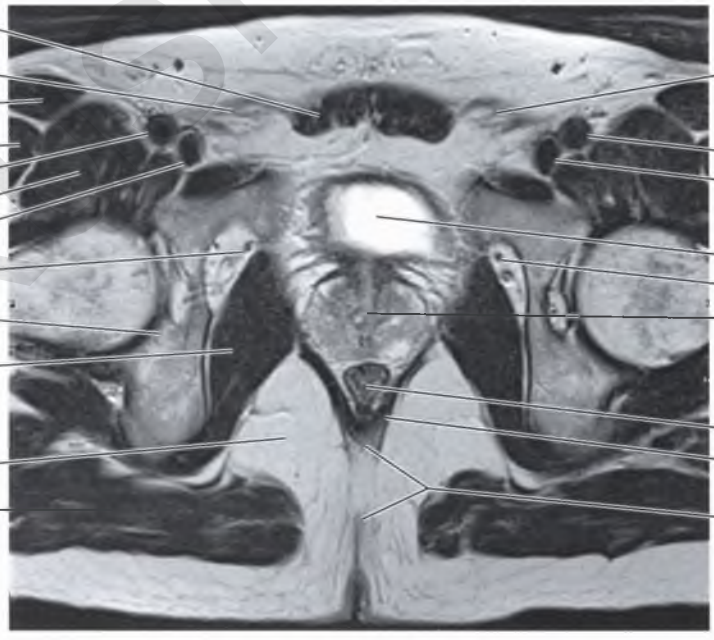
Rectus abdominis m.
Superficial inguinal ring
Sartorius m.
Rectus femoris m.
Right common femoral a.
Iliopsoas m.
Right common femoral v.
Obturator vessels
Acetabulum
Obturator internus m.
Ischiorectal fossa
Gluteus maximus m.
Superficial inguinal ring
Left common femoral a.
Left common femoral v.
Bladder
Obturator vessels
Prostate
Rectum
Levator ani m.
Anococcygeal ligament

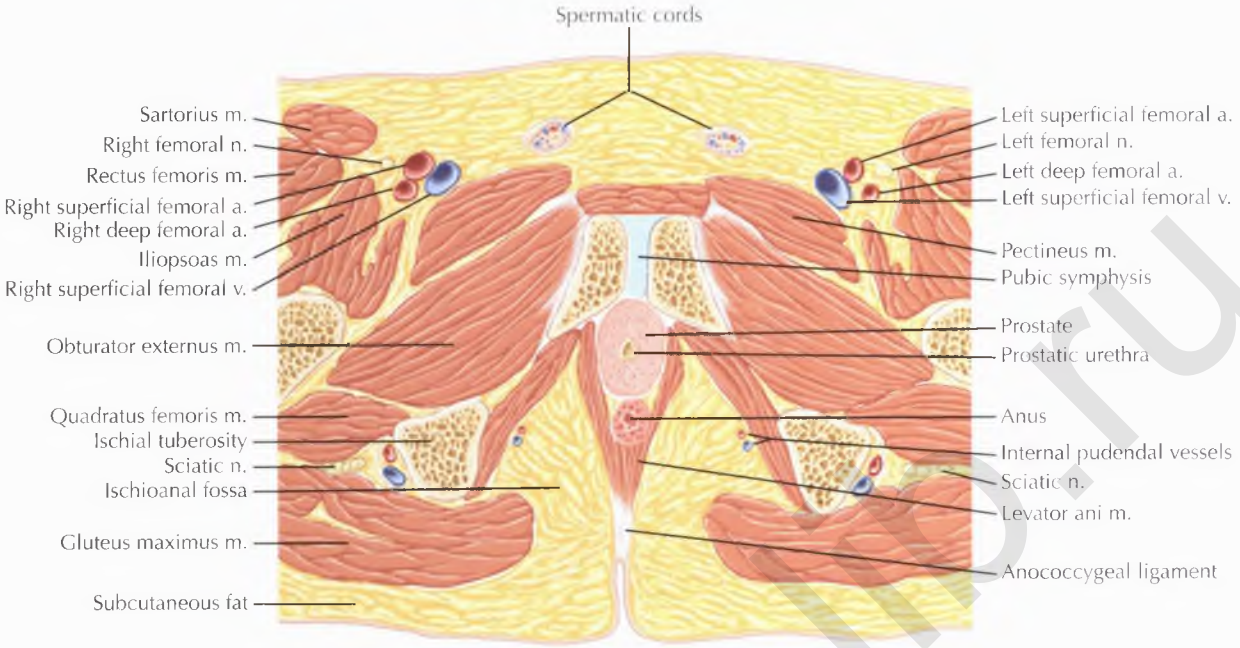

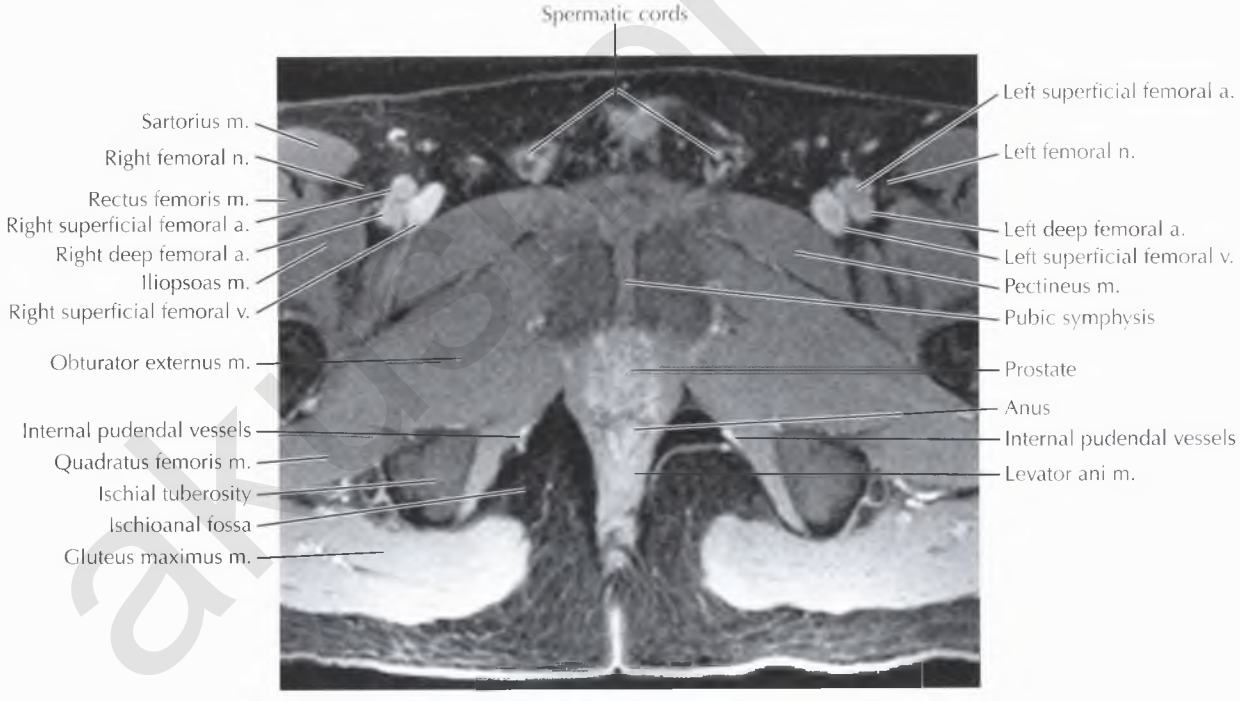

NORMAL ANATOMY

The *levator ani* musculature and fascia form the pelvic diaphragm, providing the primary support for the pelvic organs, which is critical for maintaining continence. The levator ani musculature is composed of the iliococcygeus, pubococcygeus, and puborectalis muscles. Note that the ischiococcygeus muscle is not considered as part of the levator ani musculature.

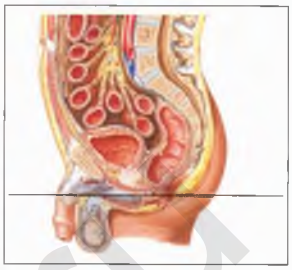

Spermatic cords
Sartorius m.
Right femoral n.
Rectus femoris m.
Right superficial femoral a.
Right deep femoral a.
Iliopsoas m.
Right superficial femoral v.
Obturator externus m.
Quadratus femoris m.
Ischioanal fossa
Sciatic n.
Ischial tuberosity
Gluteus maximus m.
Subcutaneous fat
Left femoral n.
Left superficial femoral a.
Left deep femoral a.
Left superficial femoral v.
Pectineus m.
Pubic symphysis
Prostate
Anus
Sciatic n.
Levator ani m.
Anococcygeal ligament


Spermatic cords
Sartorius m.
Right femoral n.
Rectus femoris m.
Right superficial femoral a.
Right deep femoral a.
Iliopsoas m.
Right superficial femoral v.
Obturator externus m.
Ischioanal fossa
Quadratus femoris m.
Ischial tuberosity
Sciatic n.
Gluteus maximus m.
Left superficial femoral a.
Left femoral n.
Left deep femoral a.
Left superficial femoral v.
Pectineus m.
Pubic symphysis
Prostate
Prostatic urethra
Anus
Sciatic n.
Levator ani m.
Anococcygeal ligament

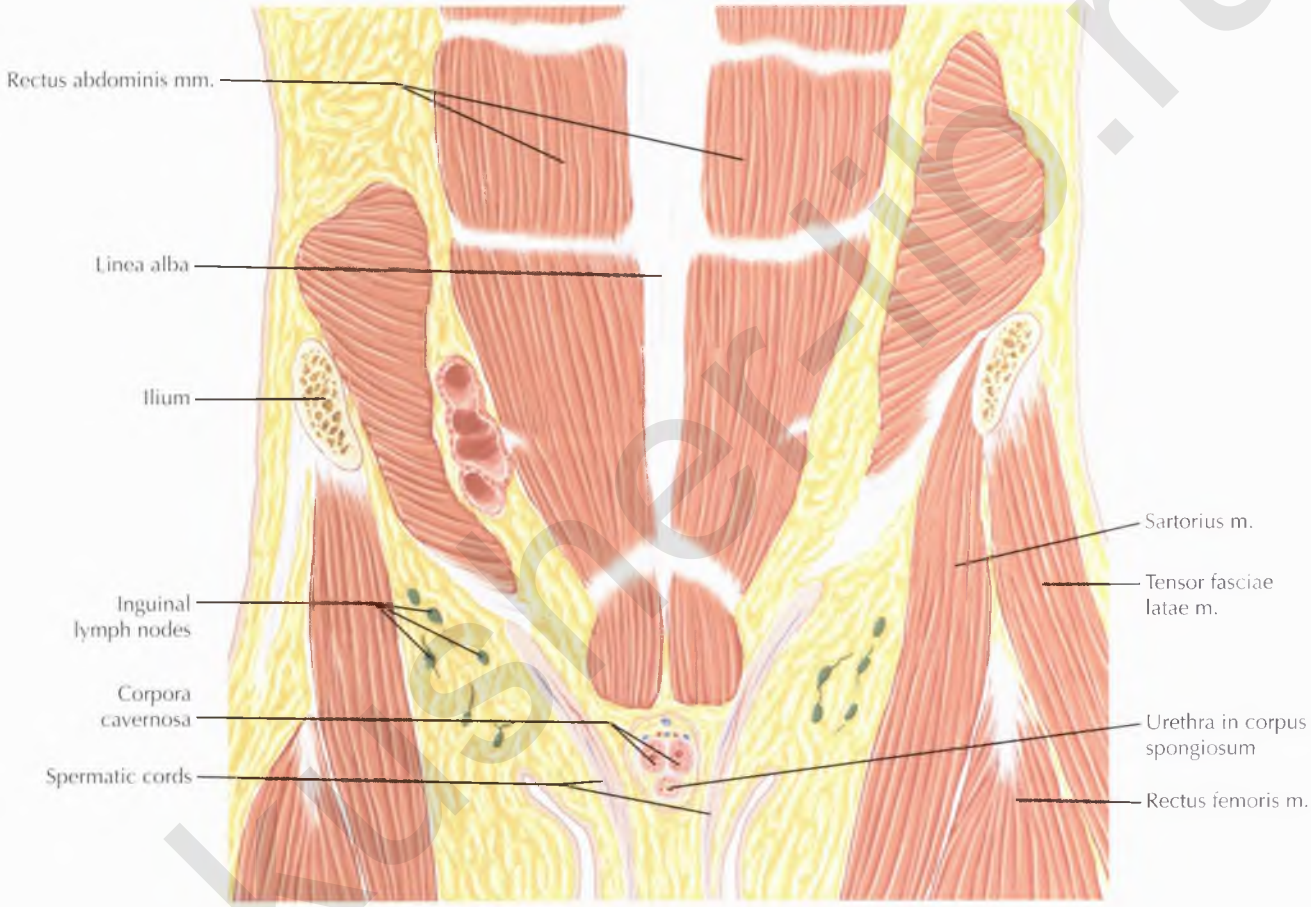
Rectus abdominis mm.
Linea alba
Ilium
Inguinal lymph nodes
Corpora cavernosa
Spermatic cords
Sartorius m.
Tensor fasciae latae m.
Urethra in corpus spongiosum
Rectus femoris m.

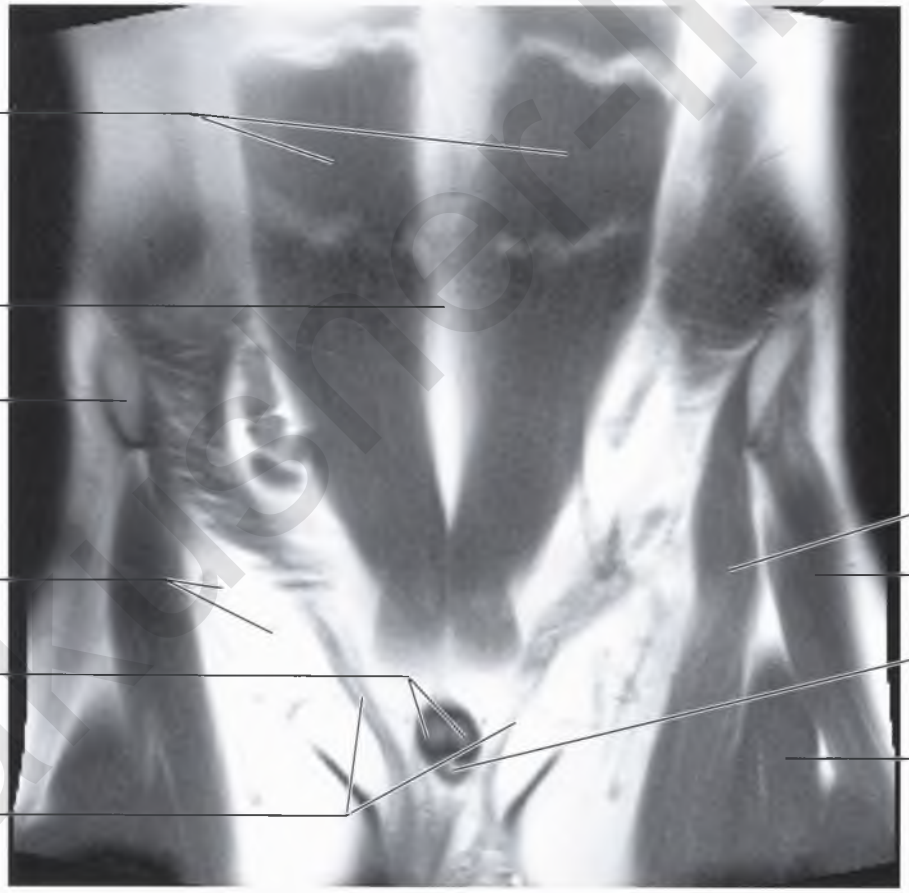

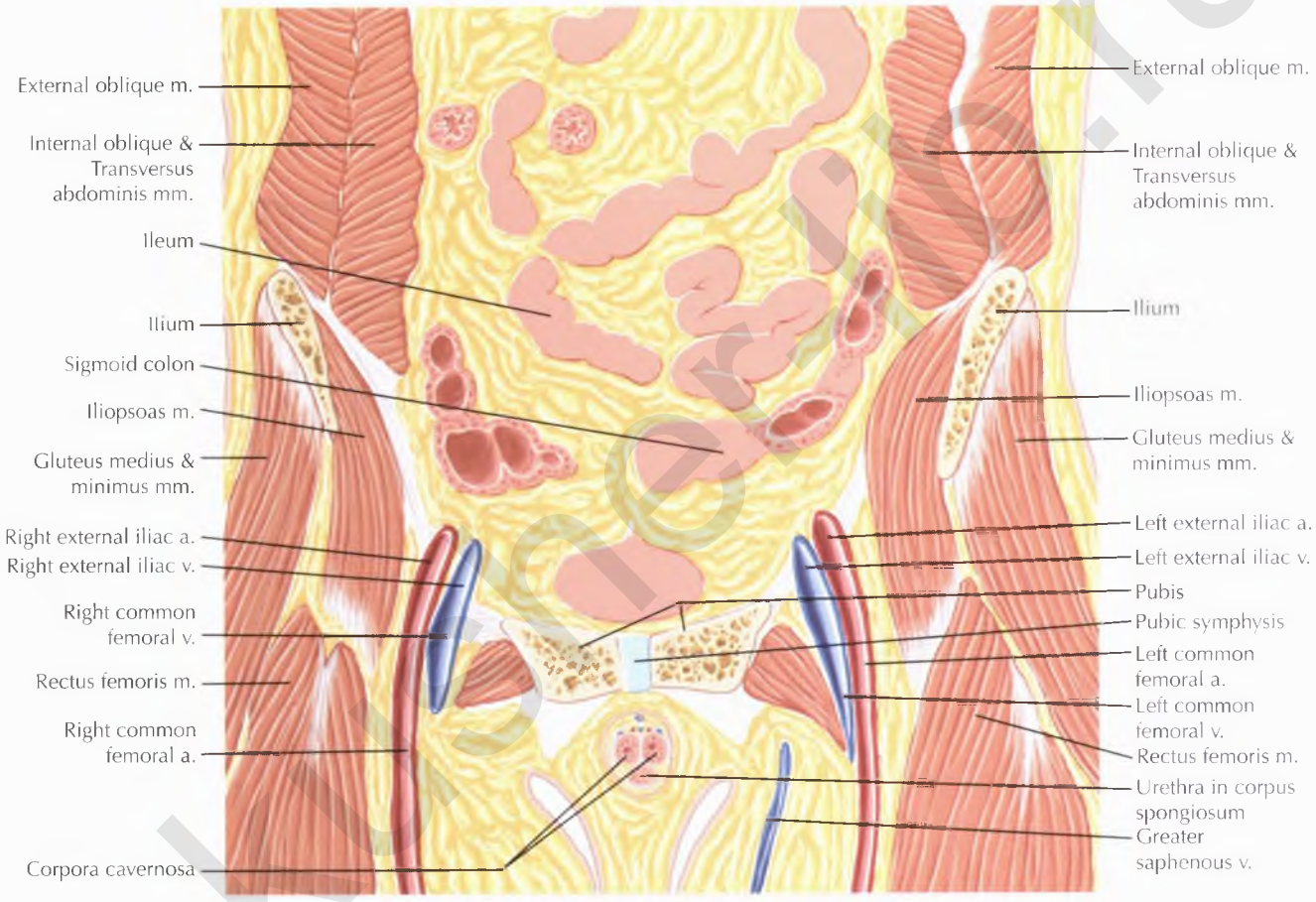
External oblique m.
Internal oblique & Transversus abdominis mm.
Ileum
Ilium
Sigmoid colon
Iliopsoas m.
Gluteus medius & minimus mm.
Right external iliac a.
Right external iliac v.
Right common femoral v.
Rectus femoris m.
Right common femoral a.
Corpora cavernosa
External oblique m.
Internal oblique & Transversus abdominis mm.
Ilium
Iliopsoas m.
Gluteus medius & minimus mm.
Left external iliac a.
Left external iliac v.
Pubis
Pubic symphysis
Left common femoral a.
Left common femoral v.
Rectus femoris m.
Urethra in corpus spongiosum
Greater saphenous v.

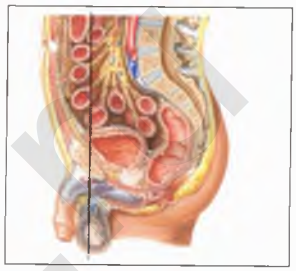

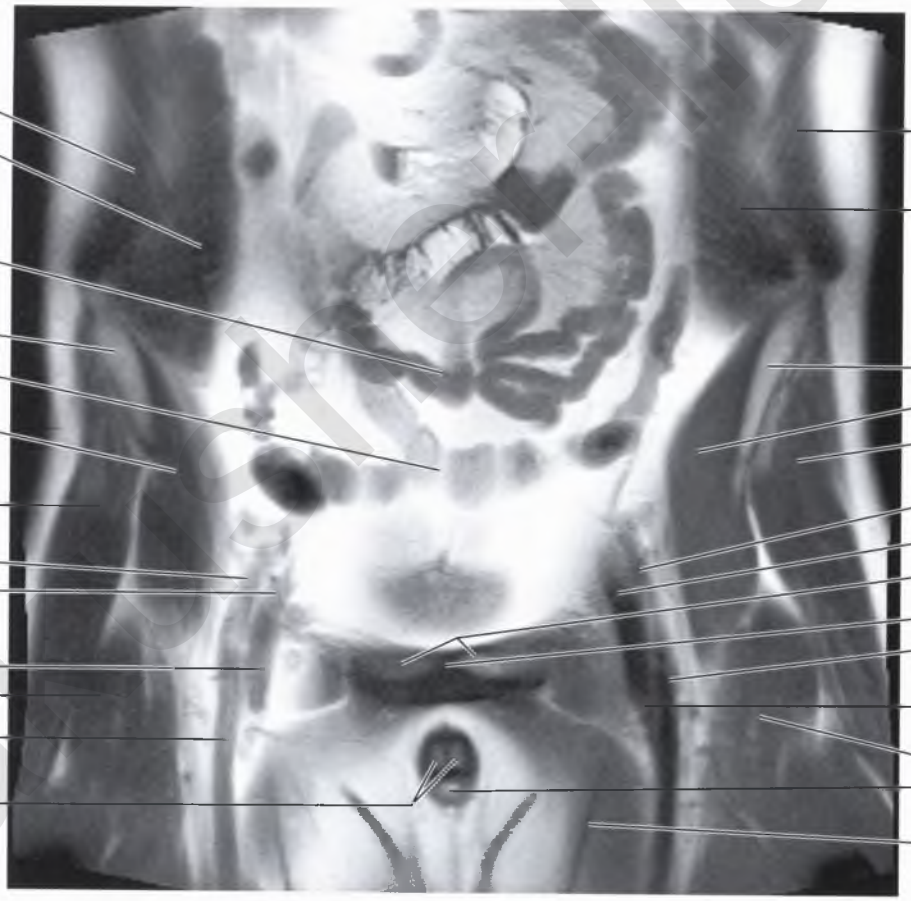
External oblique m.
Internal oblique & Transversus abdominis mm.
Ileum
Ilium
Sigmoid colon
Iliopsoas m.
Gluteus medius & minimus mm.
Right external iliac a.
Right external iliac v.
Right common femoral v.
Rectus femoris m.
Right common femoral a.
Corpora cavernosa
External oblique m.
Internal oblique & Transversus abdominis mm.
Ilium
Iliopsoas m.
Gluteus medius & minimus mm.
Left external iliac a.
Left external iliac v.
Pubis
Pubic symphysis
Left common femoral a.
Left common femoral v.
Rectus femoris m.
Urethra in corpus spongiosum
Greater saphenous v.


Ileocecal valve
External oblique m.
Internal oblique m.
Transversus abdominis m.
Cecum
Terminal ileum
Ilium
Iliopsoas m.
Pubis
Corpora cavernosa
Urethra in corpus spongiosum
Branches of superior mesenteric vessels
Descending colon
Ilium
Iliopsoas m.
Gluteus medius & minimus mm.
Bladder
Pectineus m.
Adductor mm.
Vastus mm.

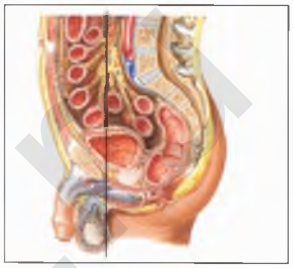

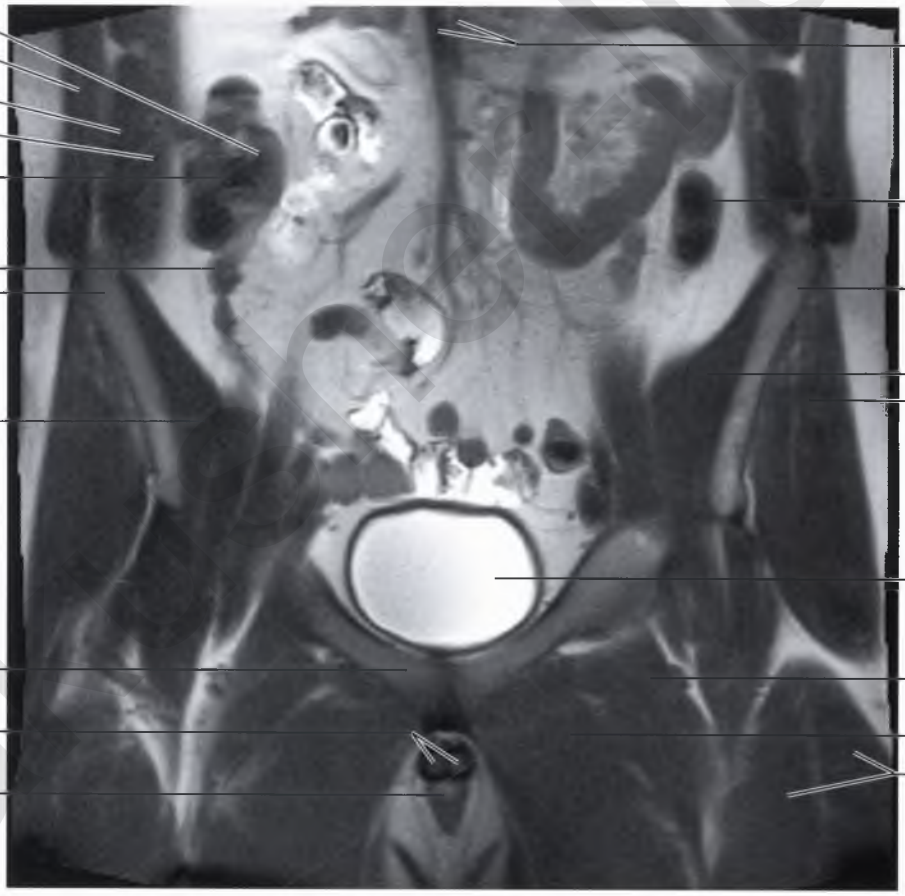
Ileocecal valve
External oblique m.
Internal oblique m.
Transversus abdominis m.
Cecum
Terminal ileum
Ilium
Iliopsoas m.
Pubis
Corpora cavernosa
Urethra in corpus spongiosum
Branches of superior mesenteric vessels
Descending colon
Ilium
Iliopsoas m.
Gluteus medius & minimus mm.
Bladder
Pectineus m.
Adductor mm.
Vastus mm.

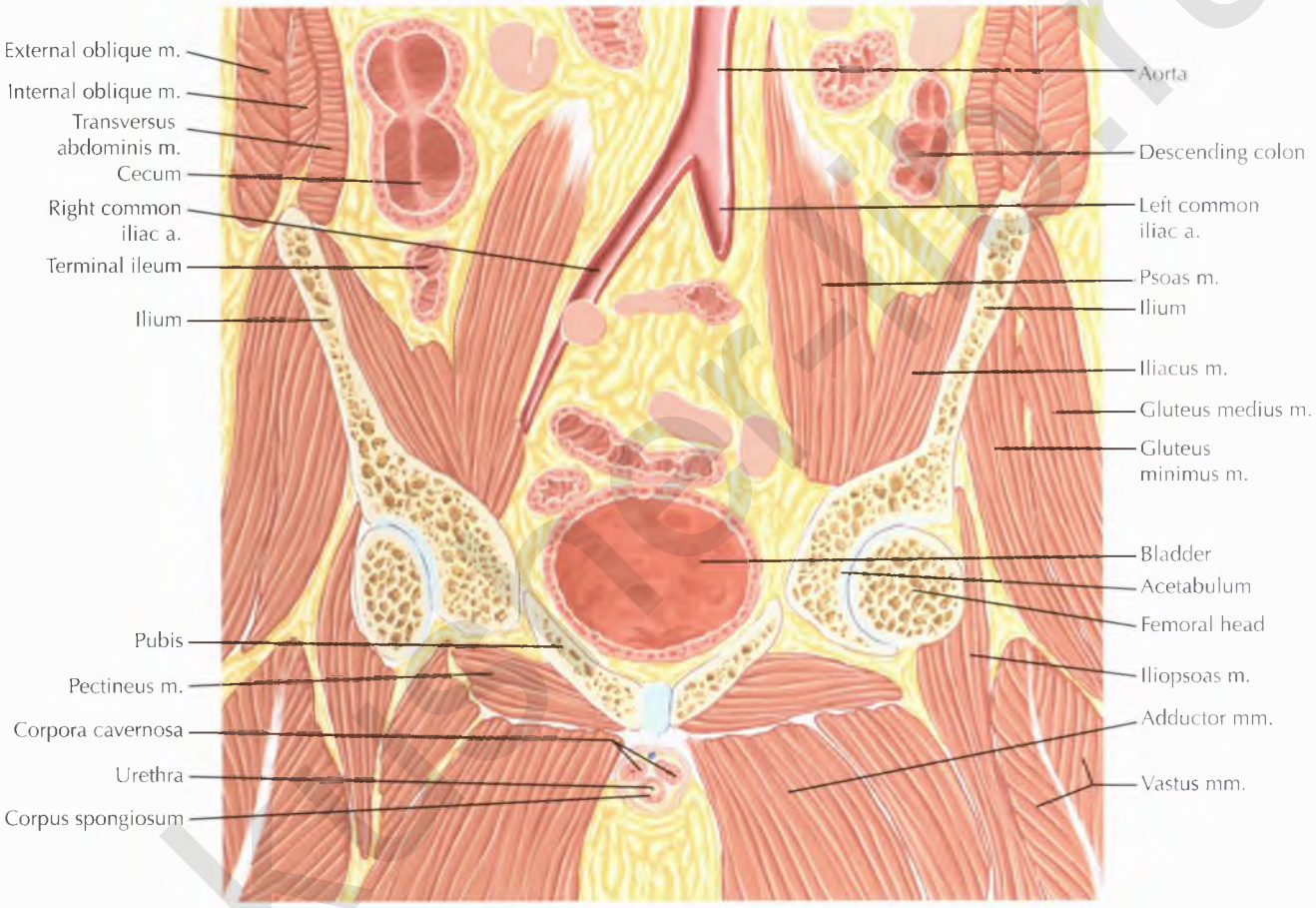

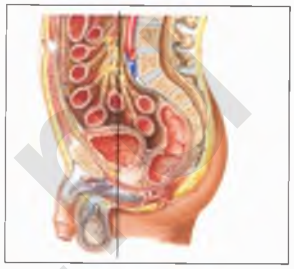

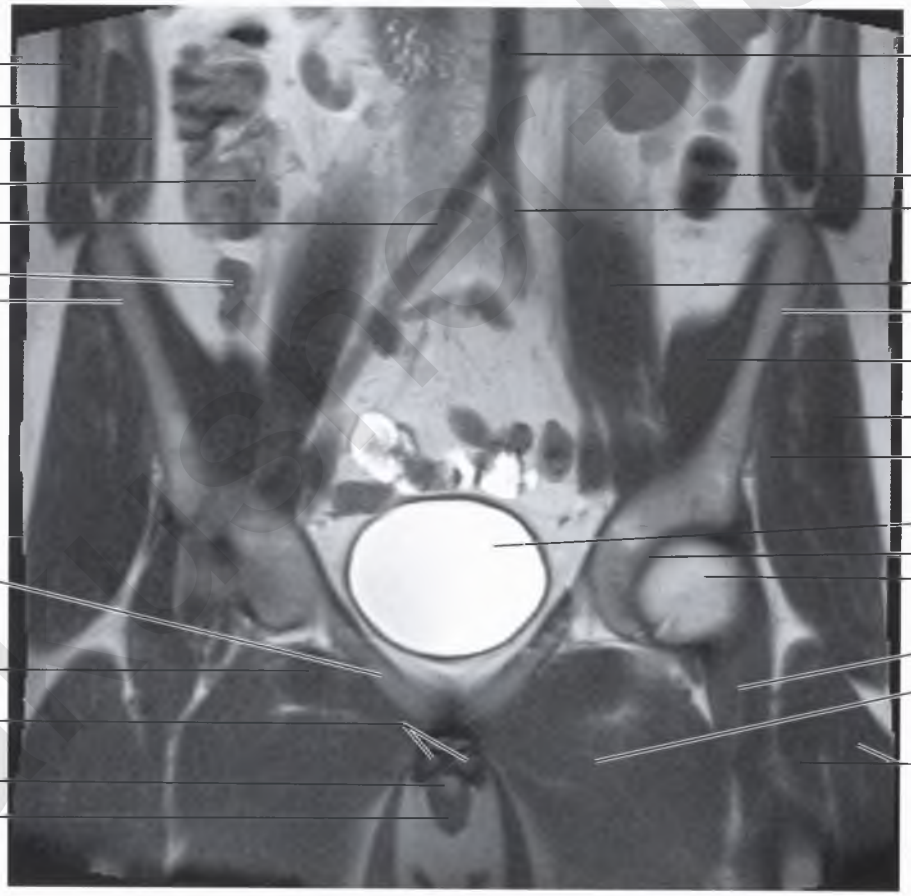
External oblique m.
Internal oblique m.
Transversus abdominis m.
Cecum
Right common iliac a.
Terminal ileum
Ilium
Pubis
Pectineus m.
Corpora cavernosa
Urethra
Corpus spongiosum
Aorta
Descending colon
Left common iliac a.
Psoas m.
Ilium
Iliacus m.
Gluteus medius m.
Gluteus minimus m.
Bladder
Acetabulum
Femoral head
Iliopsoas m.
Adductor mm.
Vastus mm.


Vertebral body
Intervertebral disc
External oblique m.
Internal oblique m.
Transversus abdominis m.
Right common iliac v.
Ilium
Right external iliac v.
Right internal iliac v.
Obturator internus m.
Obturator externus m.
Penis
Psoas m.
Ilium
Iliacus m.
Left common iliac v.
Gluteus medius m.
Gluteus minimus m.
Acetabulum
Bladder
Femoral head
Obturator internus m.
Obturator externus m.
Adductor mm.
Vastus lateralis m.

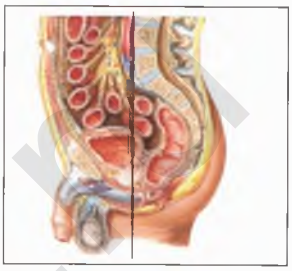

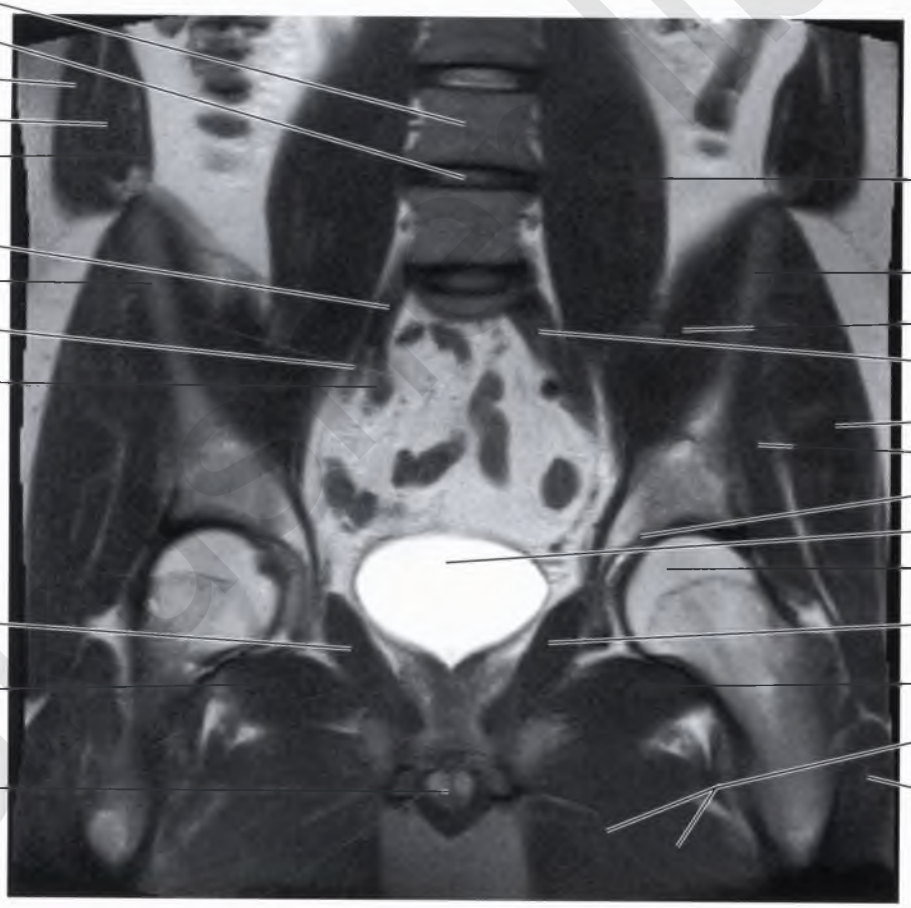

NORMAL ANATOMY

The prostate gland is an extraperitoneal fibromuscular gland surrounding the prostatic urethra at the bladder base. The seminal vesicles are paired extraperitoneal structures located superior and posterior to the prostate gland and are partially covered by the parietal peritoneum.

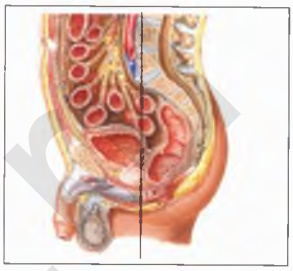

PATHOLOGIC PROCESS

Seminal vesicle cysts are usually seen laterally within the seminal vesicles. Frequent associations include autosomal dominant polycystic kidney disease (ADPCKD) and ipsilateral genitourinary anomalies, including renal agenesis, congenital absence of the vas deferens, and ectopic ureteral insertion into mesonephric duct derivatives (e.g., seminal vesicle, ejaculatory duct).

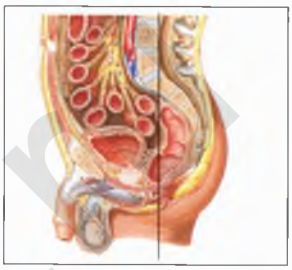

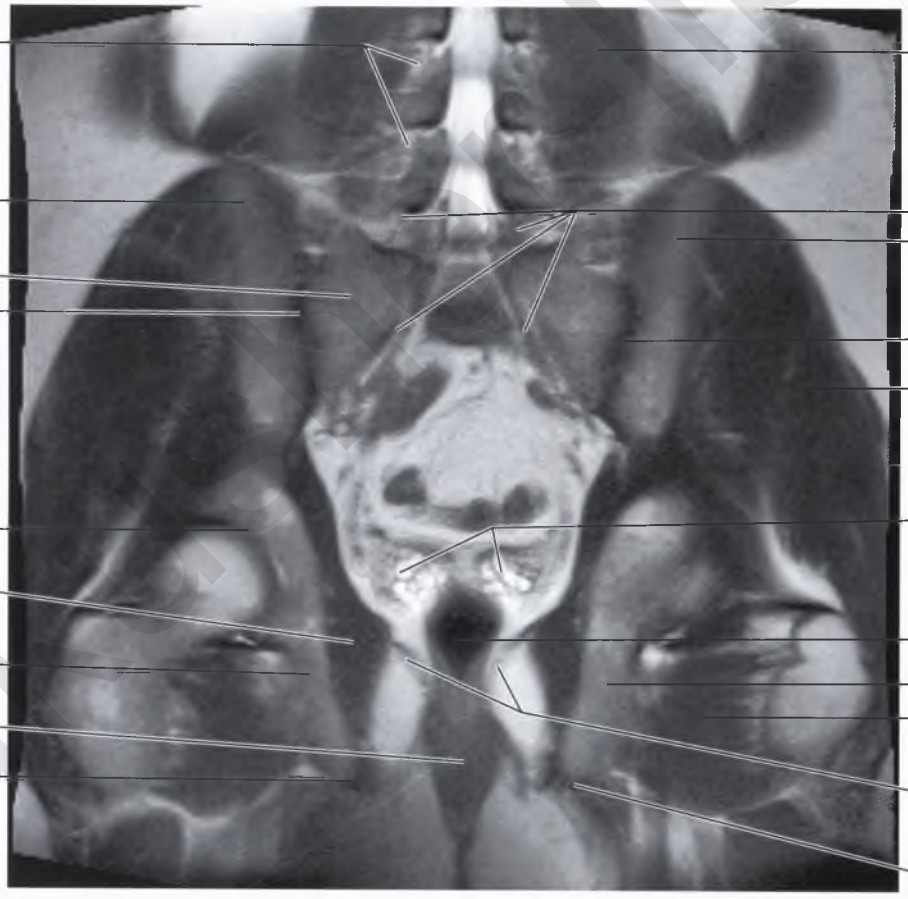
Spinal nerve roots
Ilium
Sacrum
Sacroiliac joint
Acetabulum
Obturator internus m.
Ischium
Anus
Ischial tuberosity
Psoas m.
Spinal nerve roots
Ilium
Sacroiliac joint
Gluteus minimus & medius mm.
Seminal vesicles
Rectum
Ischium
Obturator externus m.
Levator ani mm.
Ischial tuberosity


Psoas m.
Ilium
Ilium
Sacrum
Gluteus medius m.
Gluteus medius m.
Gluteus maximus m.
Seminal vesicles
Rectum
Obturator internus m.
Obturator internus m.
Ischium
Ischium
Obturator externus m.
Anus
Levator ani mm.

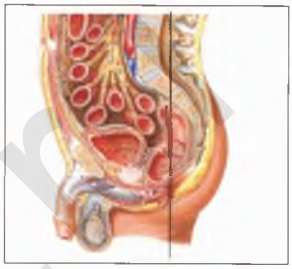

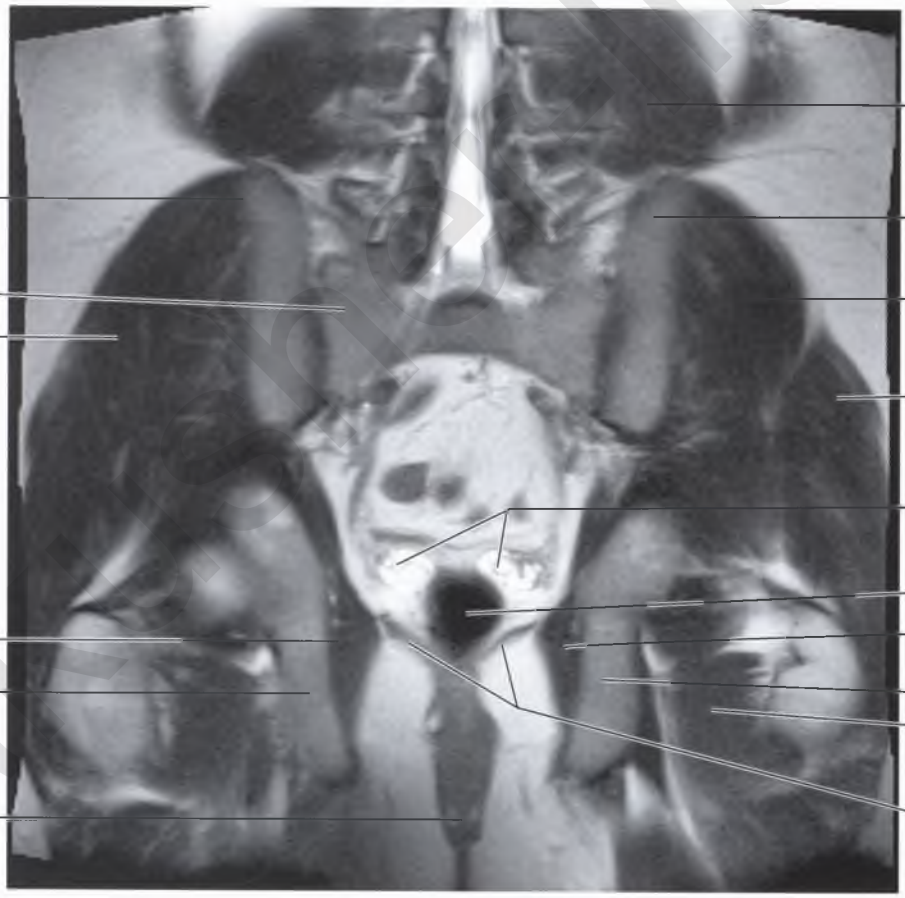
Psoas m.
Ilium
Ilium
Sacrum
Gluteus medius m.
Gluteus medius m.
Gluteus maximus m.
Seminal vesicles
Rectum
Obturator internus m.
Obturator internus m.
Ischium
Ischium
Obturator externus m.
Anus
Levator ani mm.

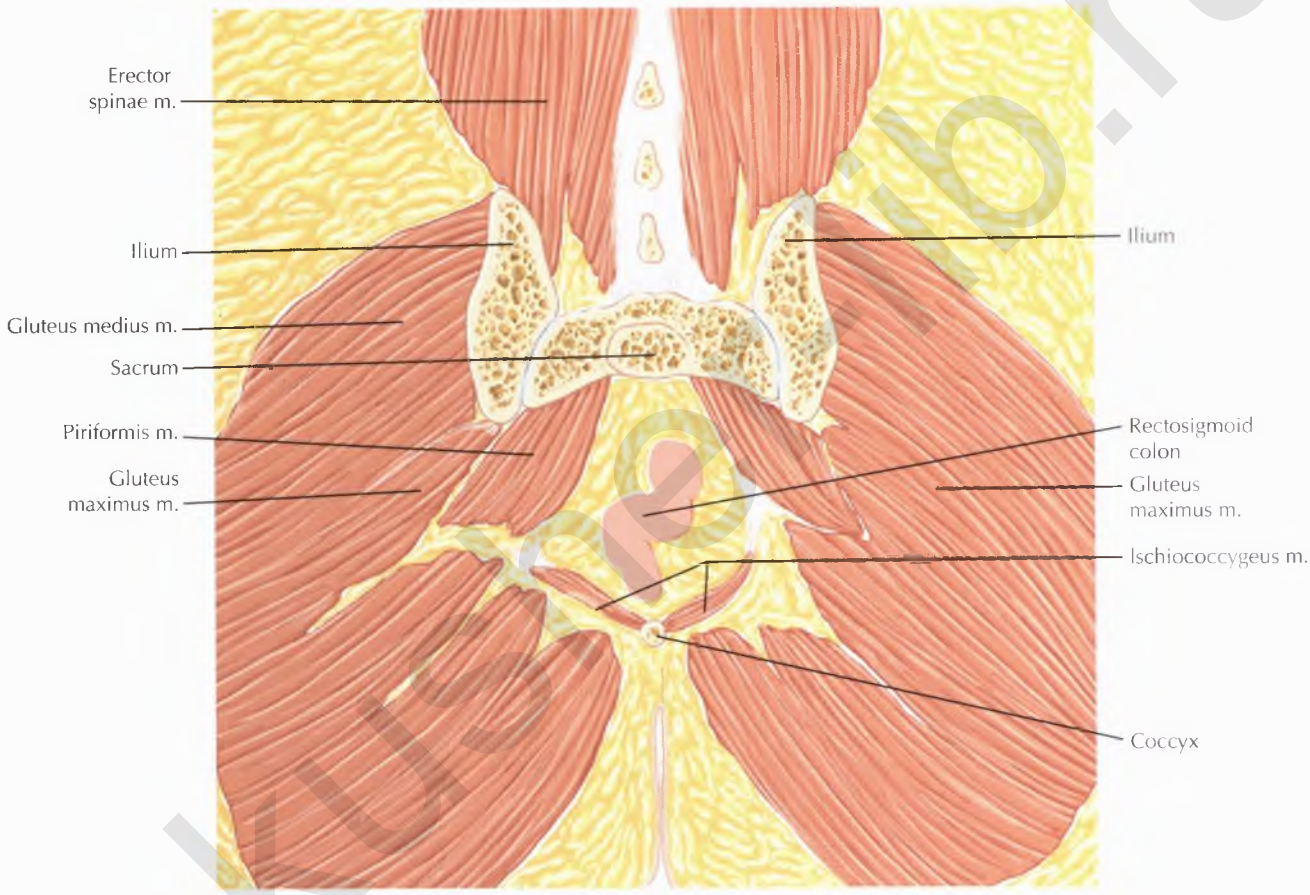
Erector spinae m.
Ilium
Gluteus medius m.
Sacrum
Piriformis m.
Gluteus maximus m.
Ilium
Rectosigmoid colon
Gluteus maximus m.
Ischiococcygeus m.
Coccyx

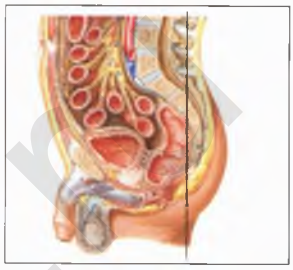

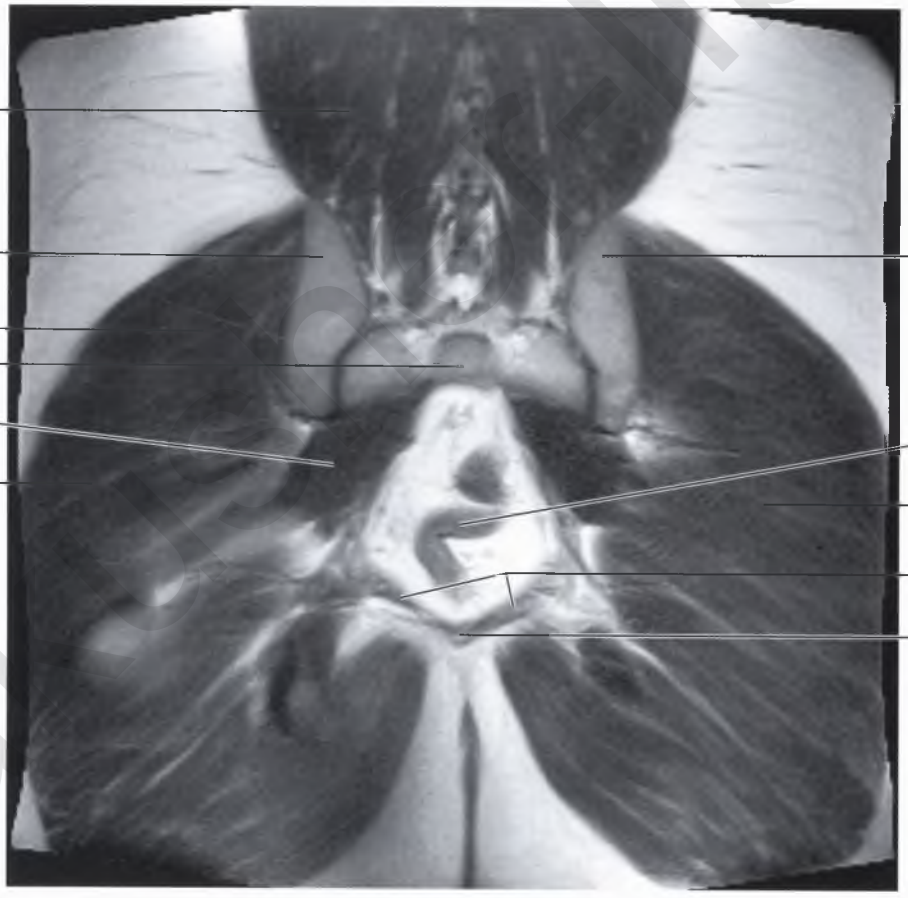
Erector spinae m.
Ilium
Gluteus medius m.
Sacrum
Piriformis m.
Gluteus maximus m.
Ilium
Rectosigmoid colon
Gluteus maximus m.
Ischiococcygeus m.
Coccyx

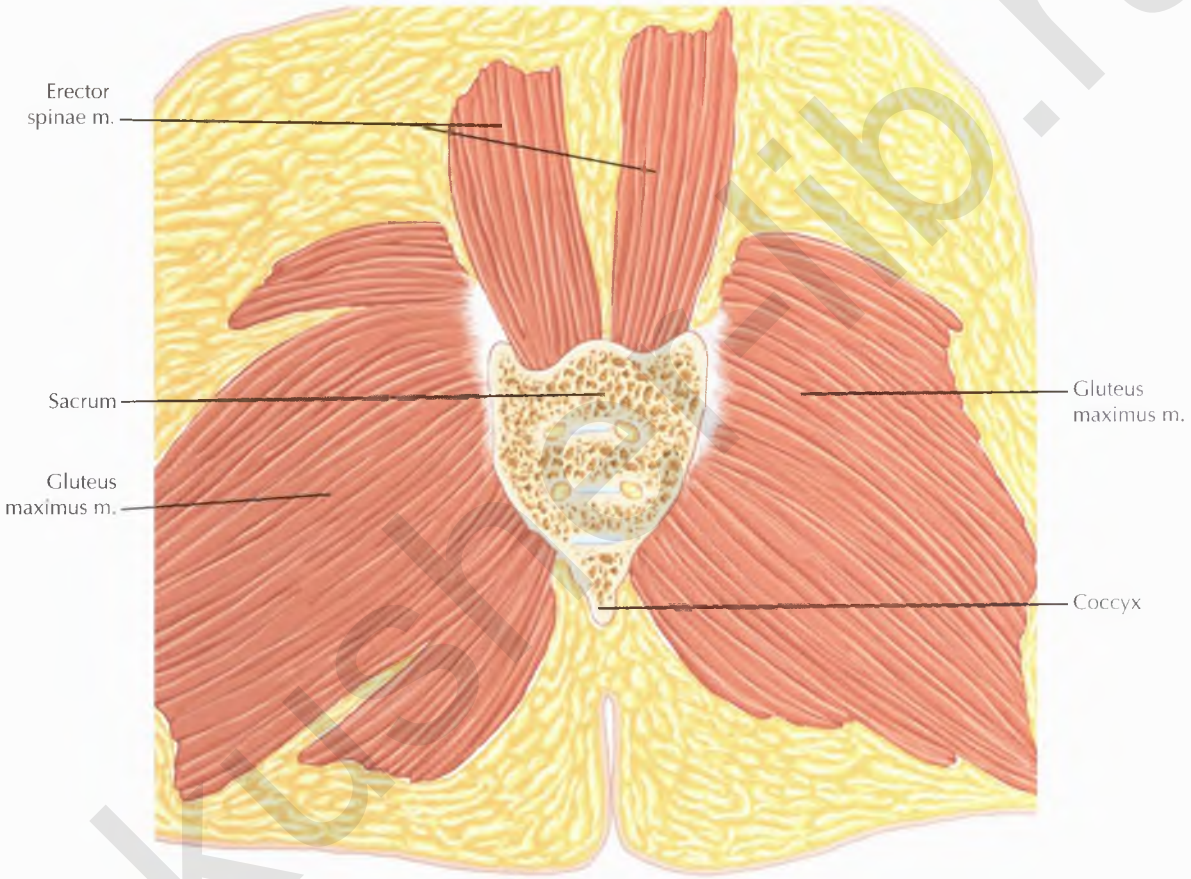
Erector spinae m.
Sacrum
Gluteus maximus m.
Gluteus maximus m.
Coccyx


Erector spinae m.
Sacrum
Gluteus maximus m.
Gluteus maximus m.
Coccyx

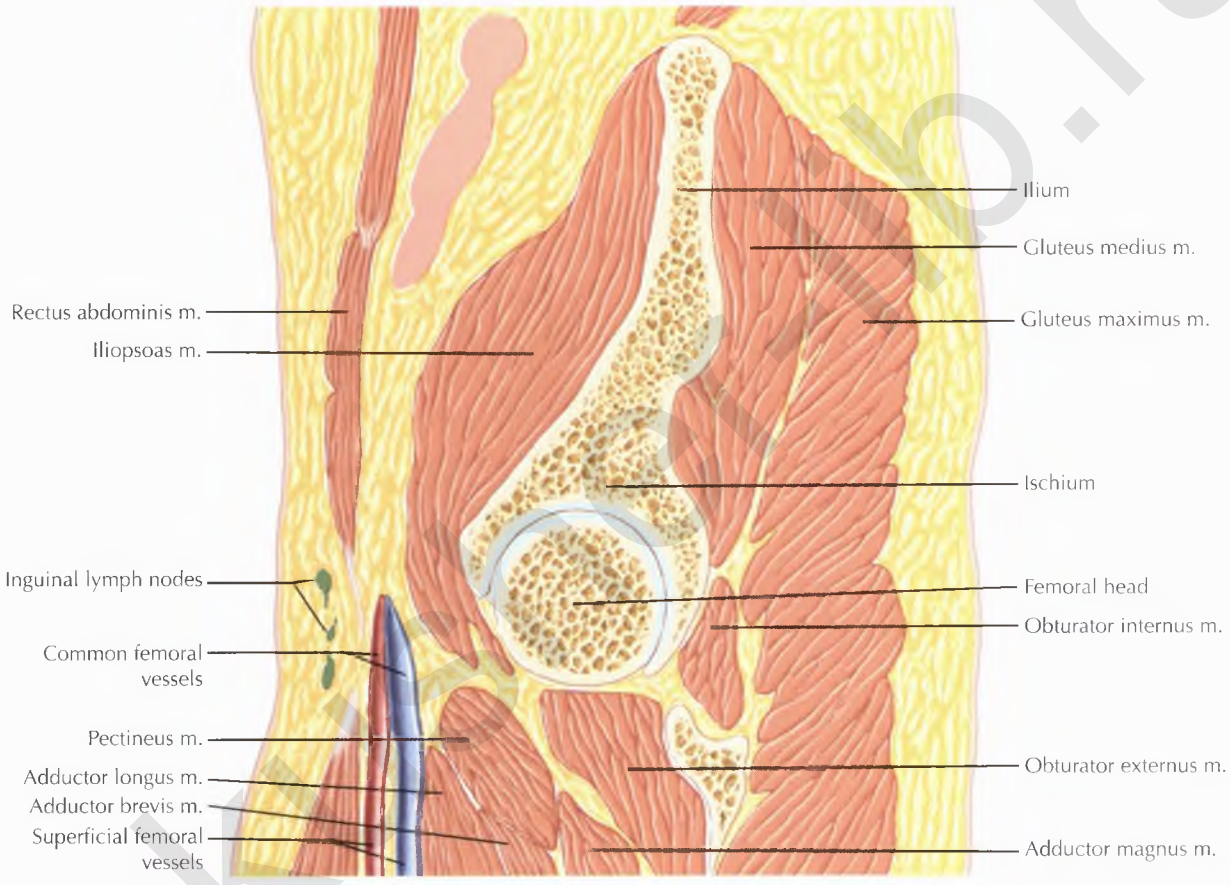
Ilium
Gluteus medius m.
Rectus abdominis m.
Gluteus maximus m.
Iliopsoas m.
Ischium
Inguinal lymph nodes
Femoral head
Obturator internus m.
Common femoral vessels
Pectineus m.
Obturator externus m.
Adductor longus m.
Adductor brevis m.
Superficial femoral vessels
Adductor magnus m.

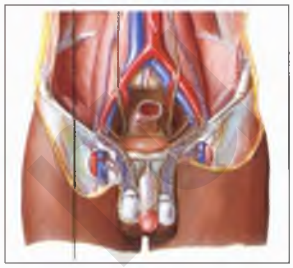


Ilium
Gluteus medius m.
Rectus abdominis m.
Gluteus maximus m.
Iliopsoas m.
Ischium
Inguinal lymph node
Femoral head
Common femoral vessels
Obturator internus m.
Pectineus m.
Obturator externus m.
Adductor longus m.
Adductor brevis m.
Adductor magnus m.
Superficial femoral vessels

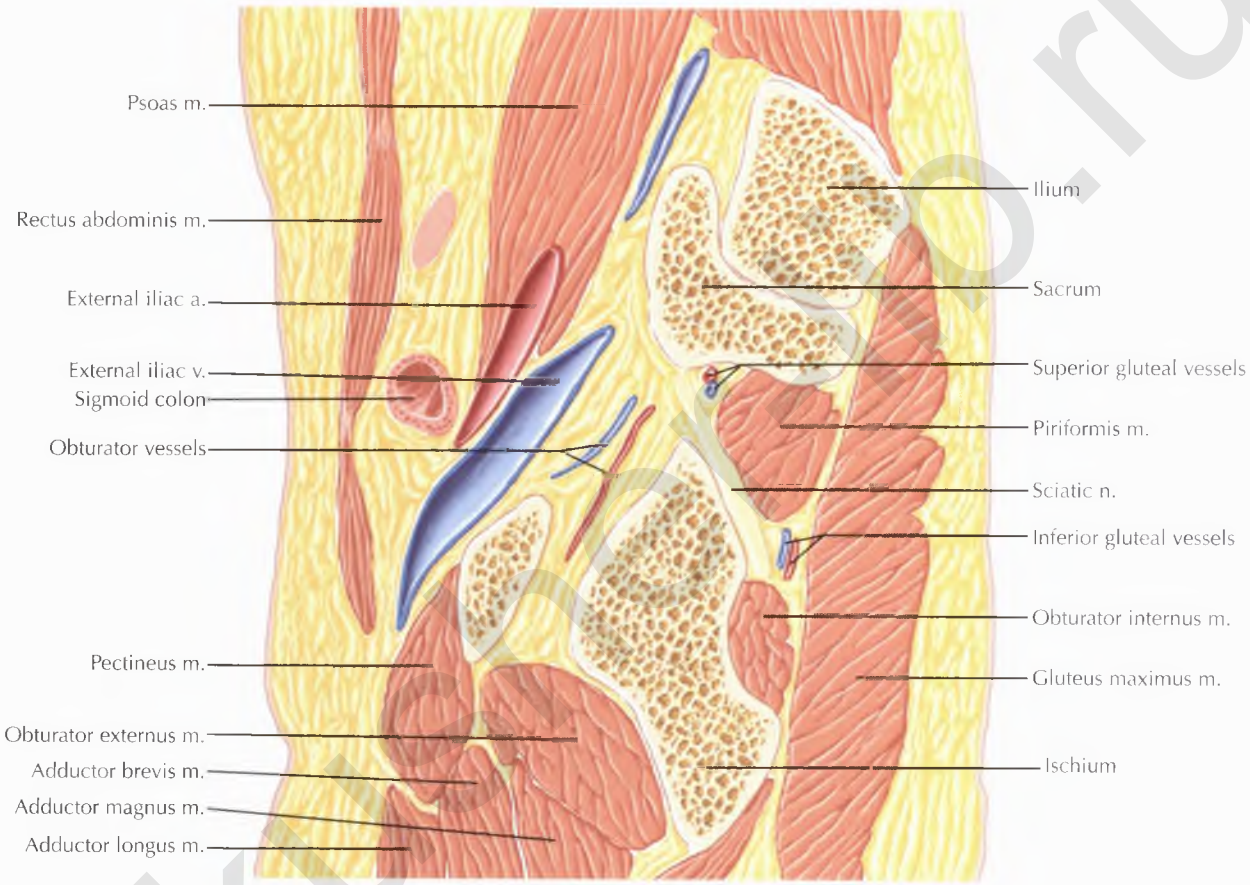

NORMAL ANATOMY

The superior gluteal vessels, piriformis muscle, inferior gluteal vessels, and sciatic nerve are seen in their course traversing the greater sciatic foramen.

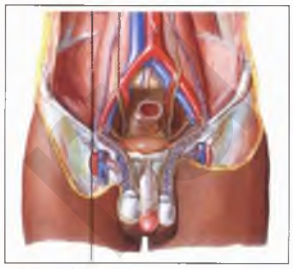

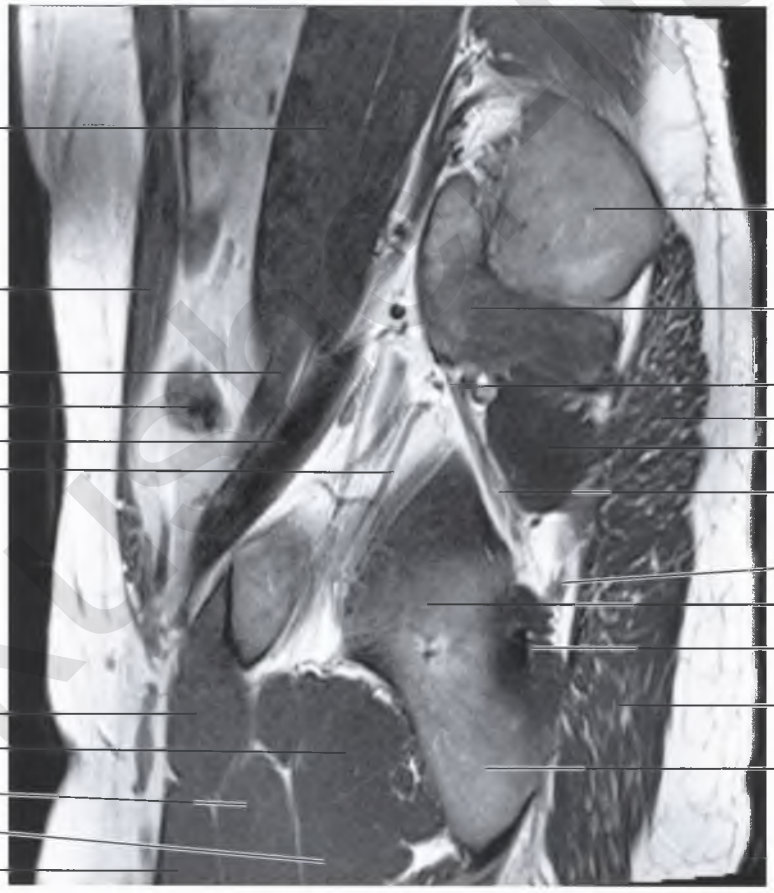
Psoas m.
Rectus abdominis m.
External iliac a.
Sigmoid colon
External iliac v.
Obturator vessels
Pectineus m.
Obturator externus m.
Adductor brevis m.
Adductor magnus m.
Adductor longus m.
Ilium
Sacrum
Superior gluteal vessels
Gluteus maximus m.
Piriformis m.
Sciatic n.
Inferior gluteal vessels
Ischium
Obturator internus m.
Gluteus maximus m.
Ischium

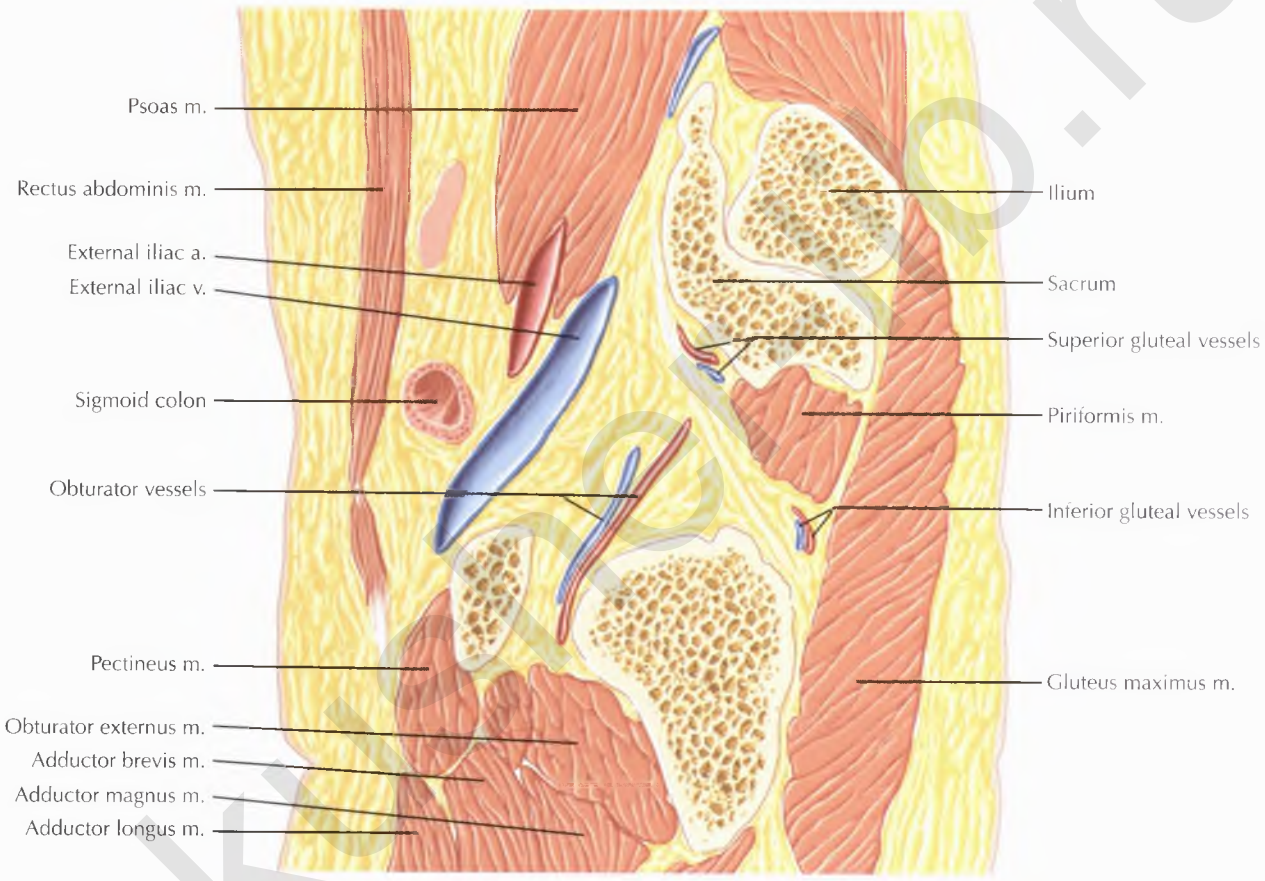

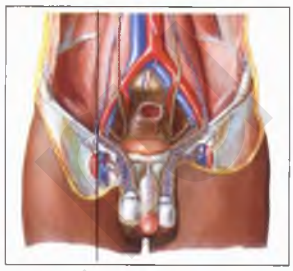

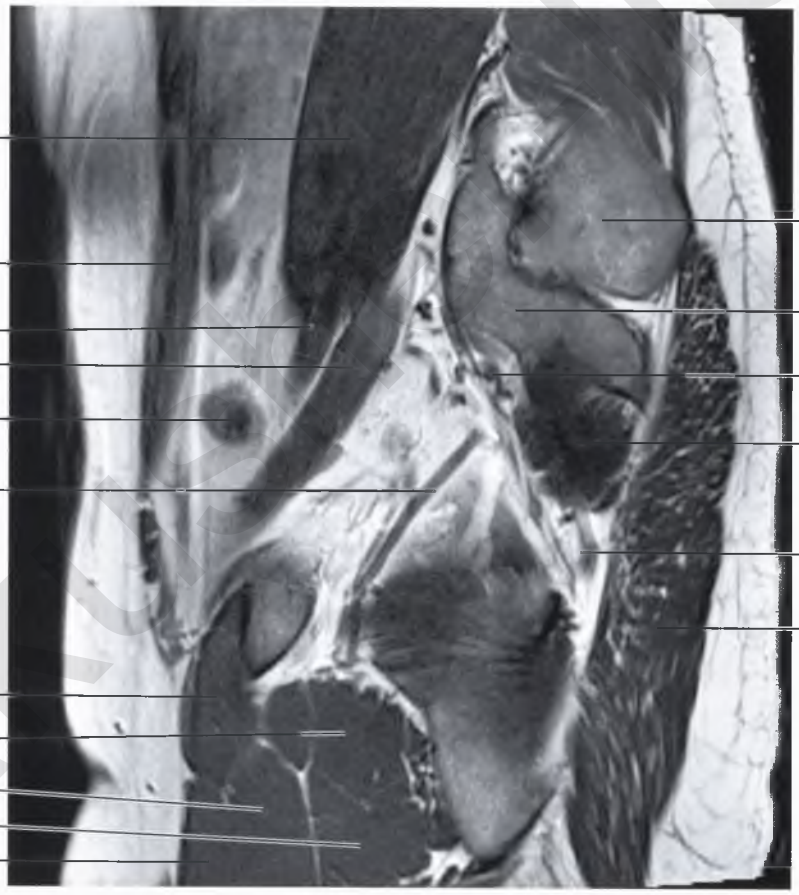
Psoas m.
Rectus abdominis m.
External iliac a.
External iliac v.
Sigmoid colon
Obturator vessels
Pectineus m.
Obturator externus m.
Adductor brevis m.
Adductor magnus m.
Adductor longus m.
Ilium
Sacrum
Superior gluteal vessels
Piriformis m.
Inferior gluteal vessels
Gluteus maximus m.

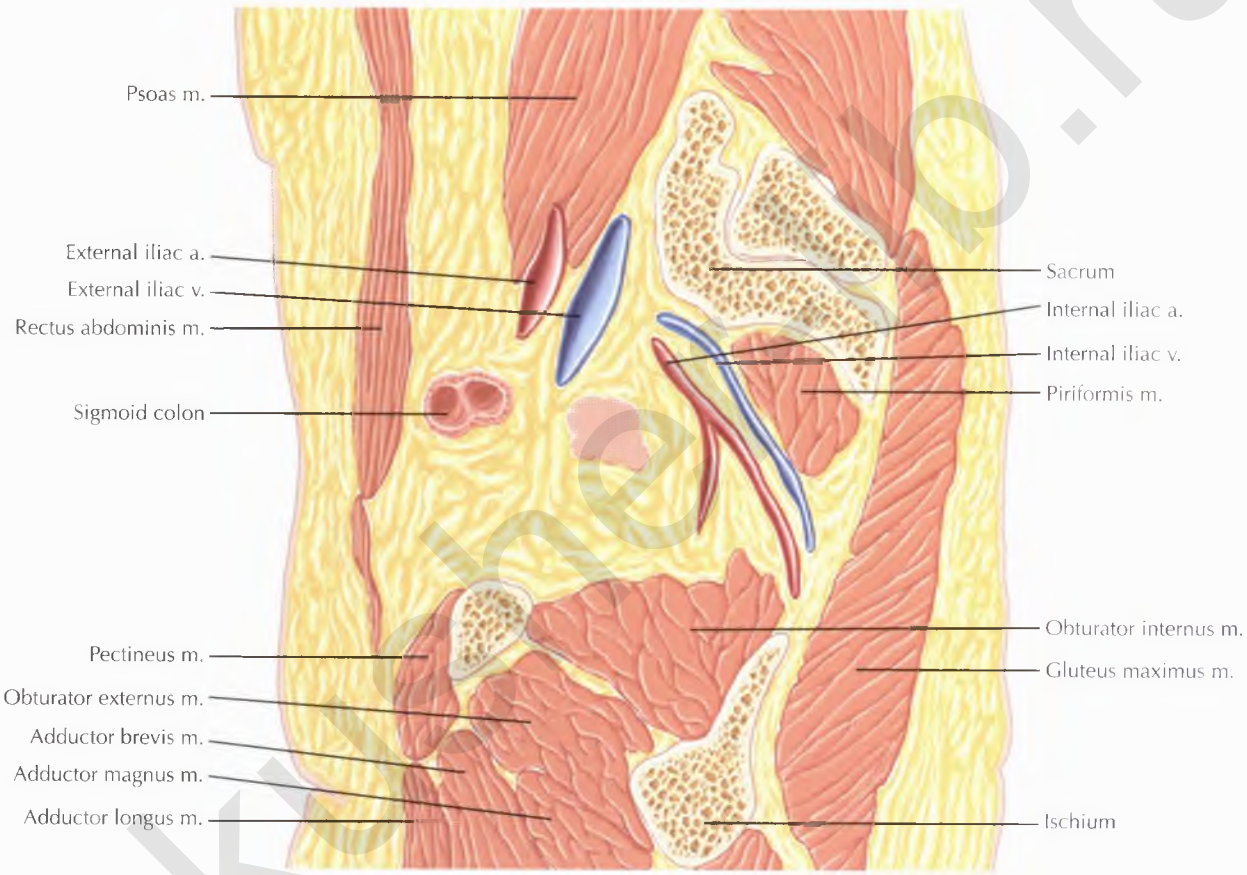
Psoas m.
External iliac a.
External iliac v.
Rectus abdominis m.
Sigmoid colon
Pectineus m.
Obturator externus m.
Adductor brevis m.
Adductor magnus m.
Adductor longus m.
Sacrum
Internal iliac a.
Internal iliac v.
Piriformis m.
Obturator internus m.
Gluteus maximus m.
Ischium

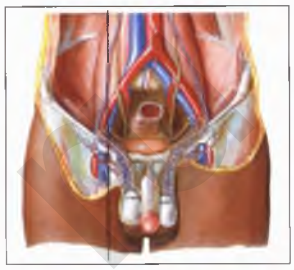

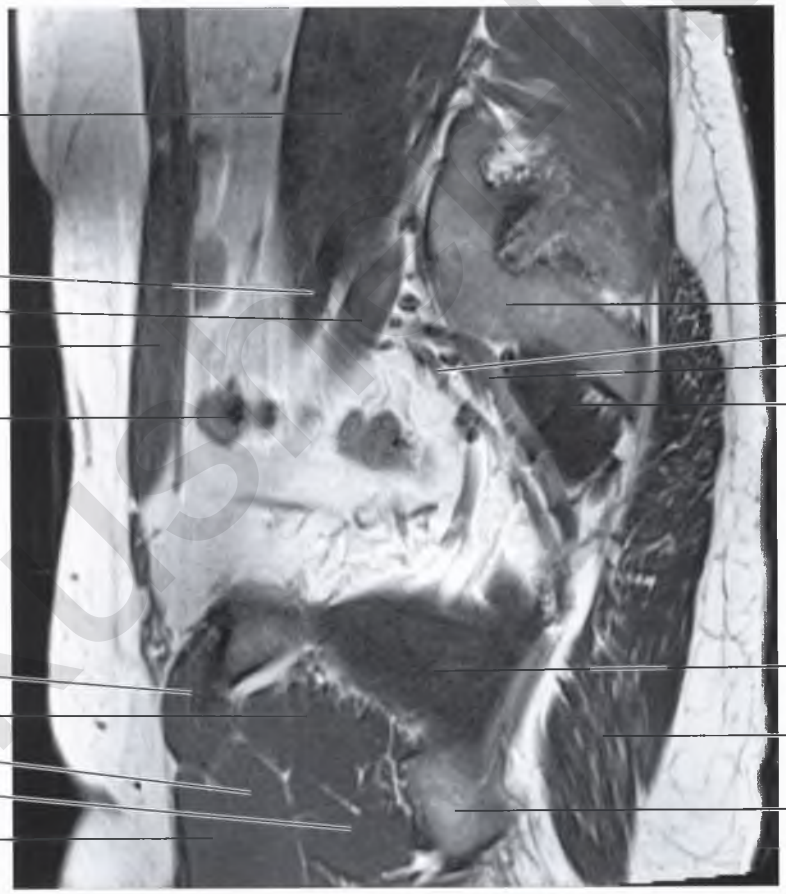

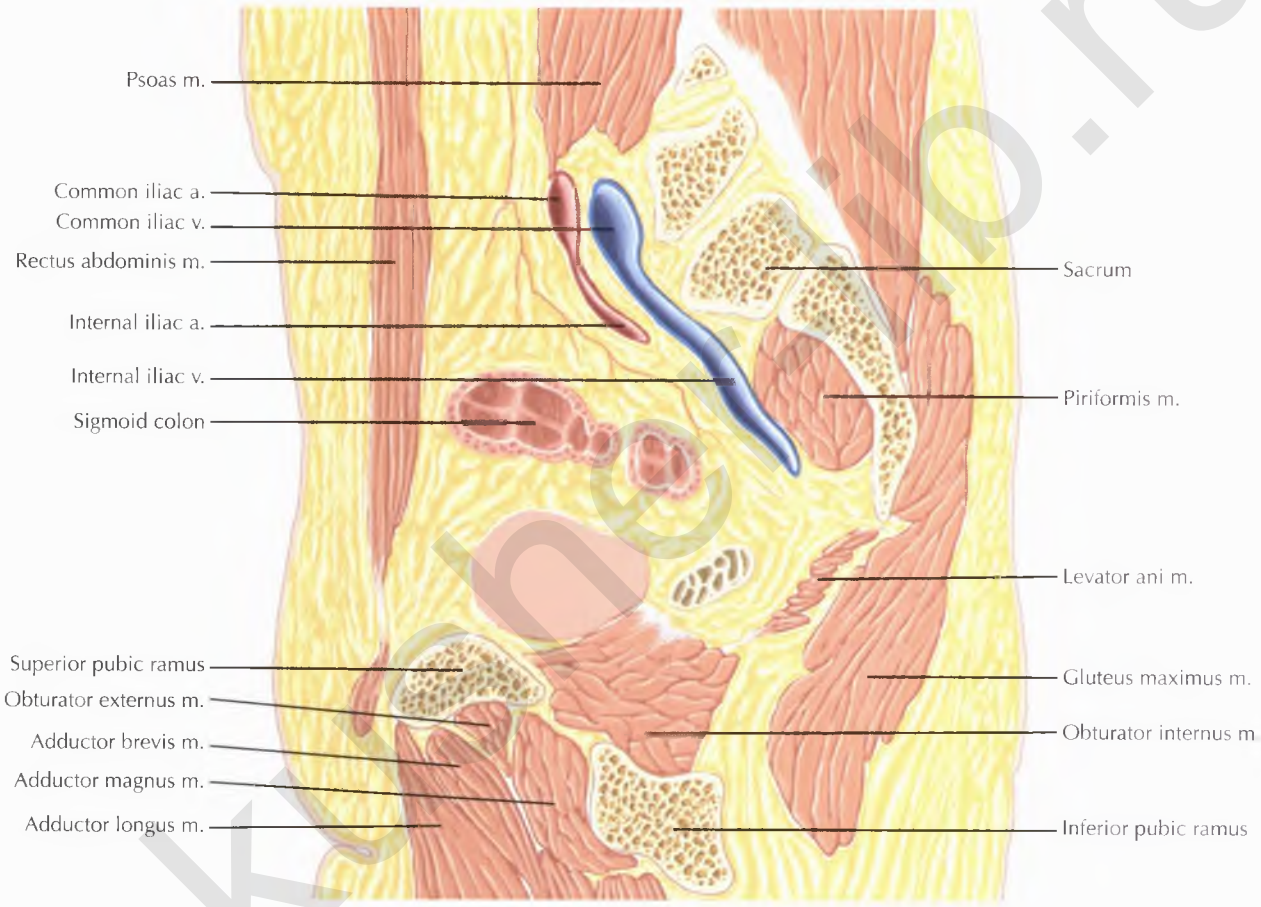
Psoas m.
Common iliac a.
Common iliac v.
Rectus abdominis m.
Internal iliac a.
Internal iliac v.
Sigmoid colon
Superior pubic ramus
Obturator externus m.
Adductor brevis m.
Adductor magnus m.
Adductor longus m.
Sacrum
Piriformis m.
Levator ani m.
Gluteus maximus m.
Obturator internus m.
Inferior pubic ramus

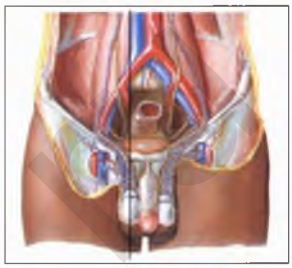

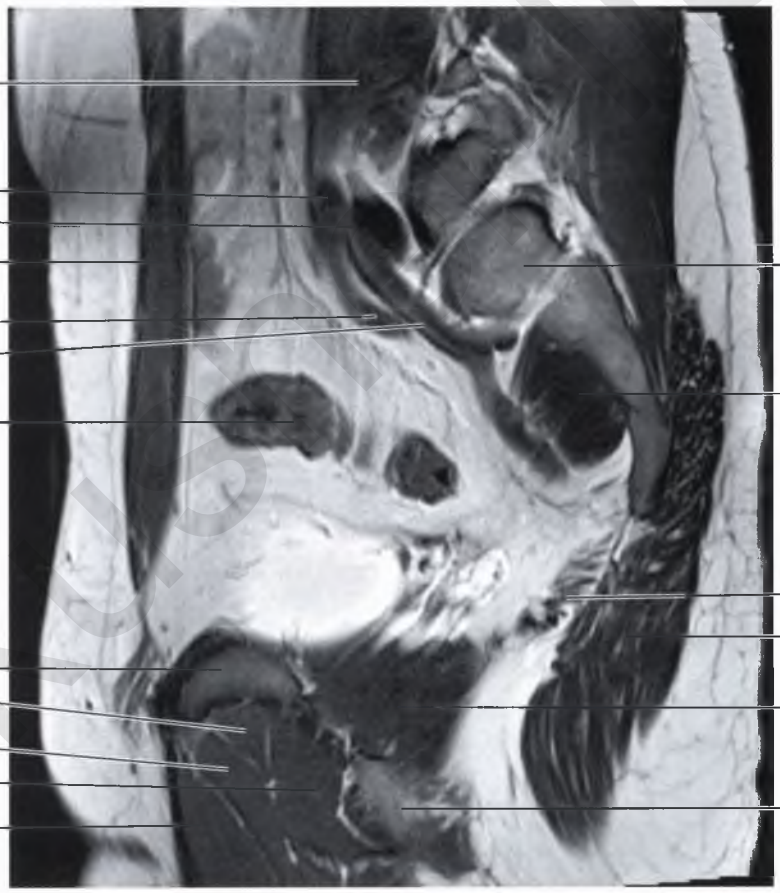
Psoas m.
Common iliac a.
Common iliac v.
Rectus abdominis m.
Internal iliac a.
Internal iliac v.
Sigmoid colon
Superior pubic ramus
Obturator externus m.
Adductor brevis m.
Adductor magnus m.
Adductor longus m.
Sacrum
Piriformis m.
Levator ani m.
Gluteus maximus m.
Obturator internus m.
Inferior pubic ramus

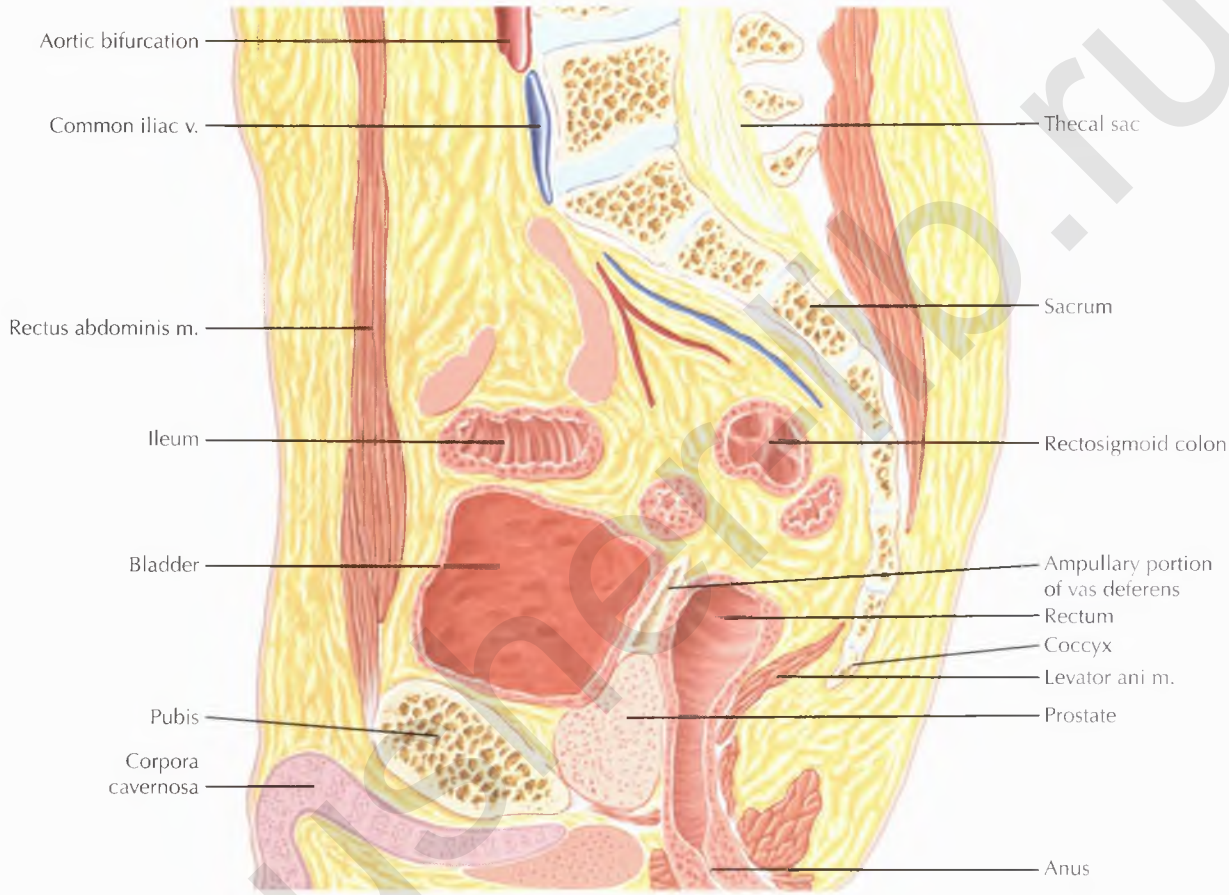

PATHOLOGIC PROCESS

The bladder is normally a distensible viscus with a strong muscular wall. Bladder outpouchings, or *diverticula*, may occur through areas of weakness in the bladder wall and often result from bladder outlet obstruction. *Hutch diverticula* are an unusual congenital type and occur near the ureterovesical junction. Urinary stasis caused by the diverticulum results in a higher incidence of infection, calculus formation, and tumor occurrence within the diverticulum.

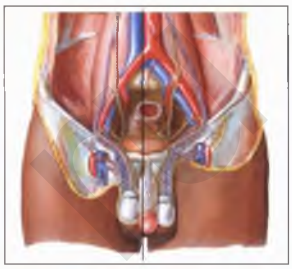

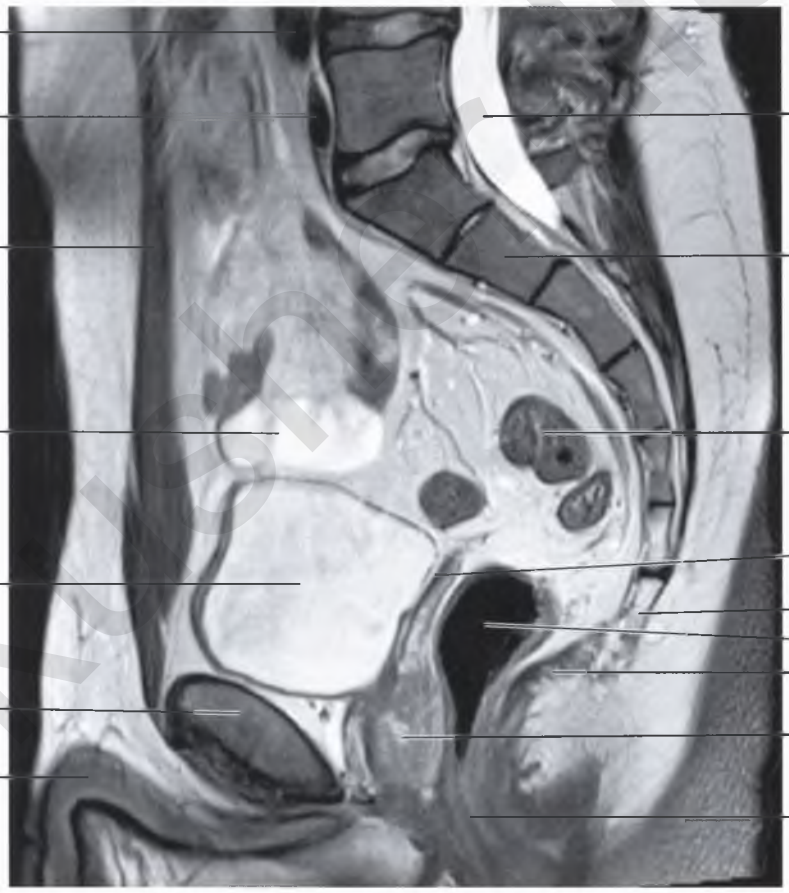
Aortic bifurcation
Common iliac v.
Rectus abdominis m.
Ileum
Bladder
Pubis
Corpora cavernosa
Thecal sac
Sacrum
Rectosigmoid colon
Ampullary portion of vas deferens
Coccyx
Rectum
Levator ani m.
Prostate
Anus

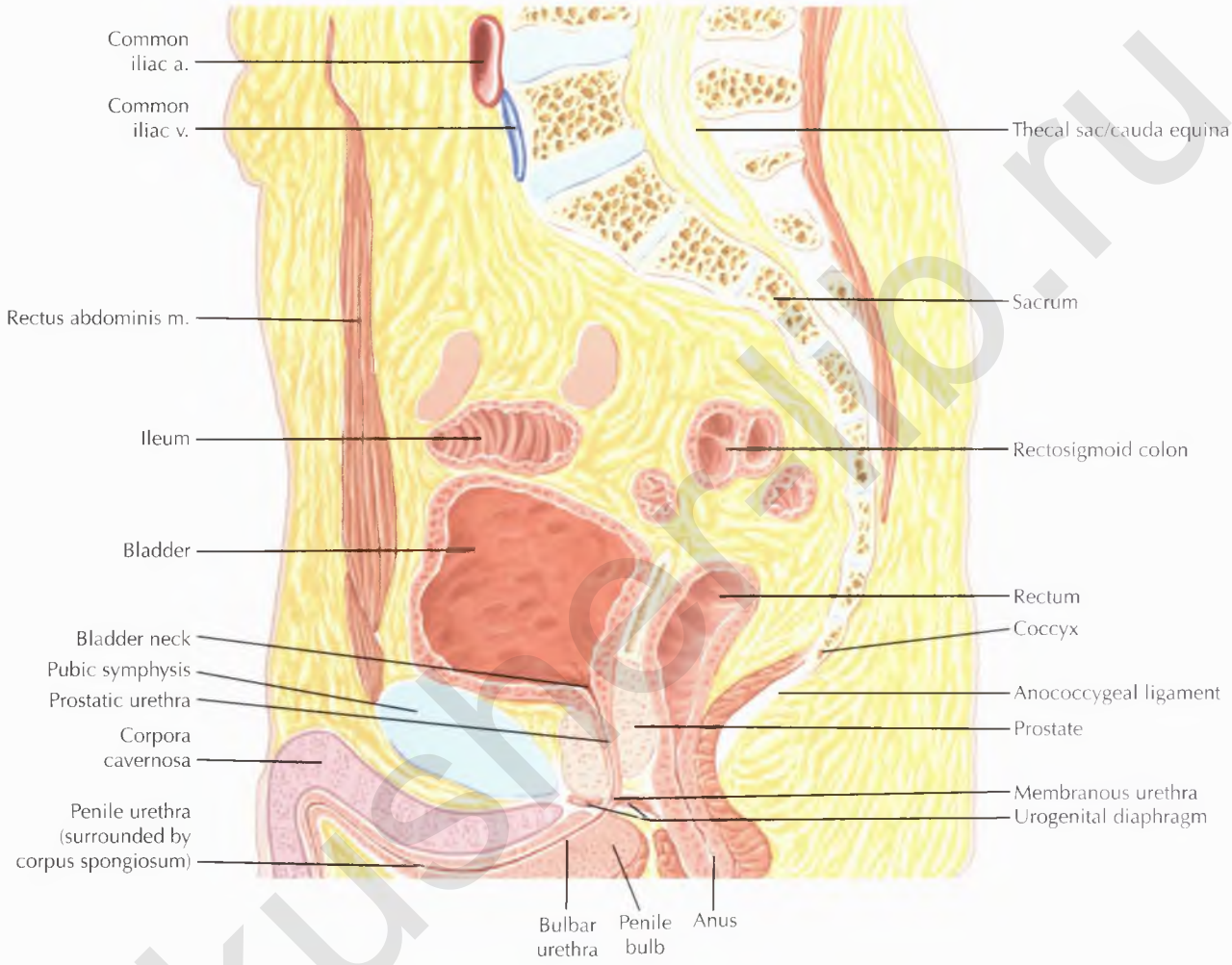

NORMAL ANATOMY

The *urachus*, which forms a conduit between the umbilicus and the urinary bladder in utero, is normally obliterated before birth, forming the median umbilical ligament. Patency of any part of the urachal remnant is abnormal, leading to a urachal sinus, cyst, or diverticulum, depending on whether the patent portion involves the umbilicus, midportion, or bladder, respectively. Patent urachal remnants may become infected and are at a higher risk for malignancy, most often with adenocarcinoma.

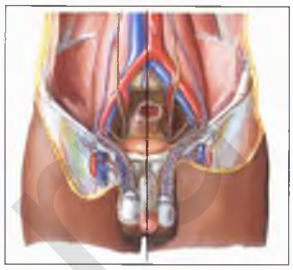

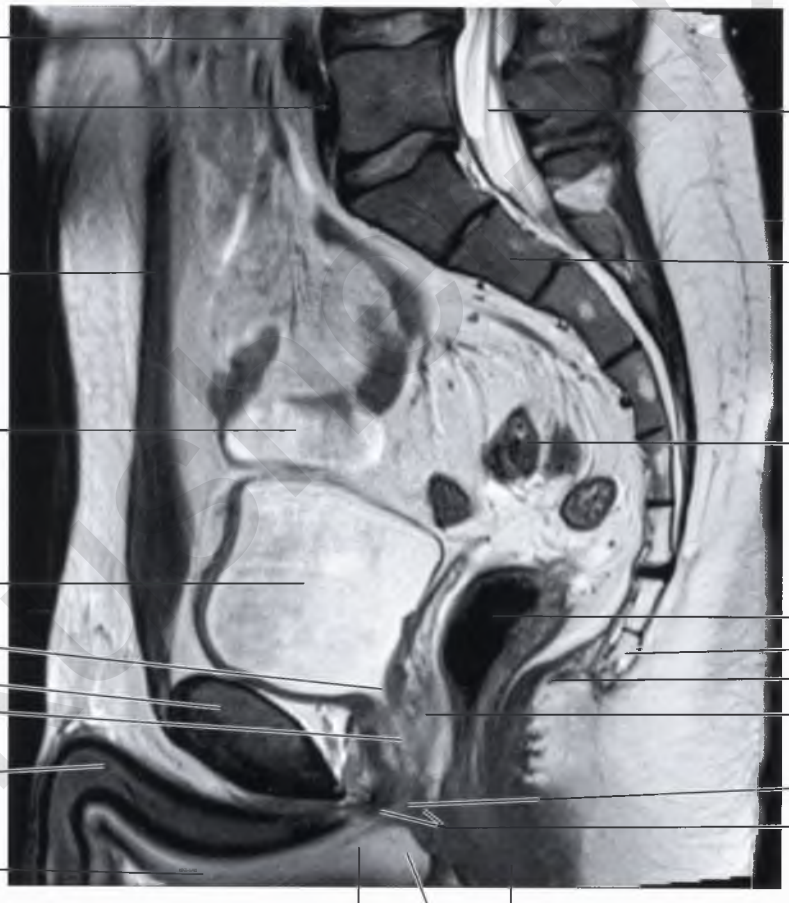
Common iliac a.
Common iliac v.
Rectus abdominis m.
Ileum
Bladder
Bladder neck
Pubic symphysis
Prostatic urethra
Corpora cavernosa
Penile urethra (surrounded by corpus spongiosum)
Thecal sac/cauda equina
Sacrum
Rectosigmoid colon
Rectum
Coccyx
Anococcygeal ligament
Prostate
Membranous urethra
Urogenital diaphragm
Bulbar urethra
Penile bulb
Anus

Chapter 7 PROSTATE AND SEMINAL TRACT

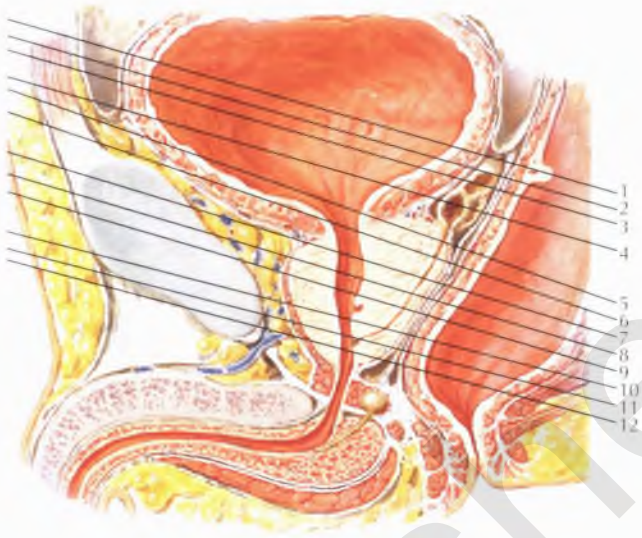

AXIAL 306

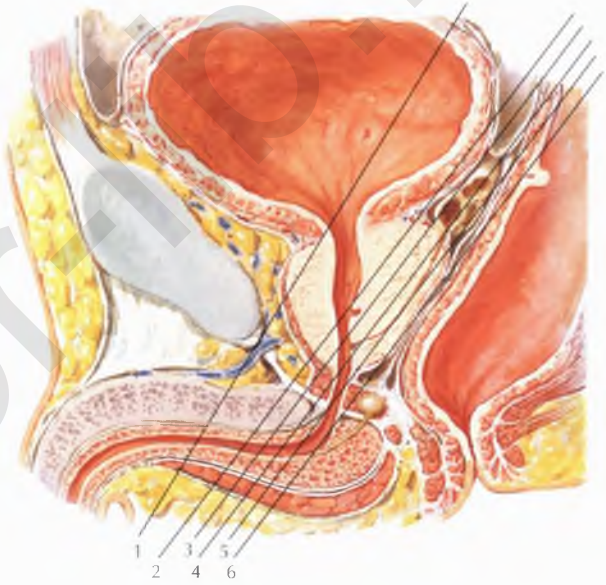

CORONAL 330

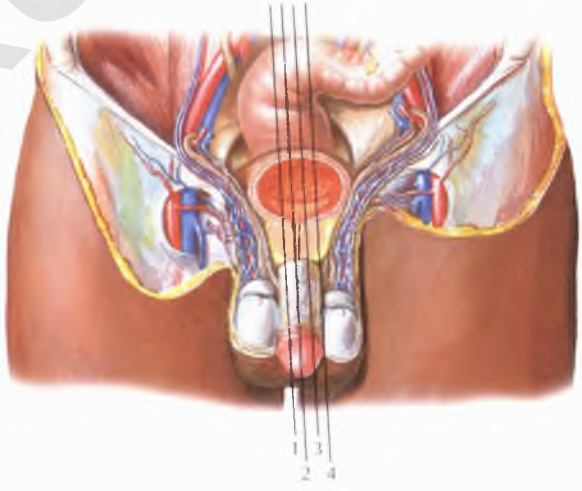

SAGITTAL 342

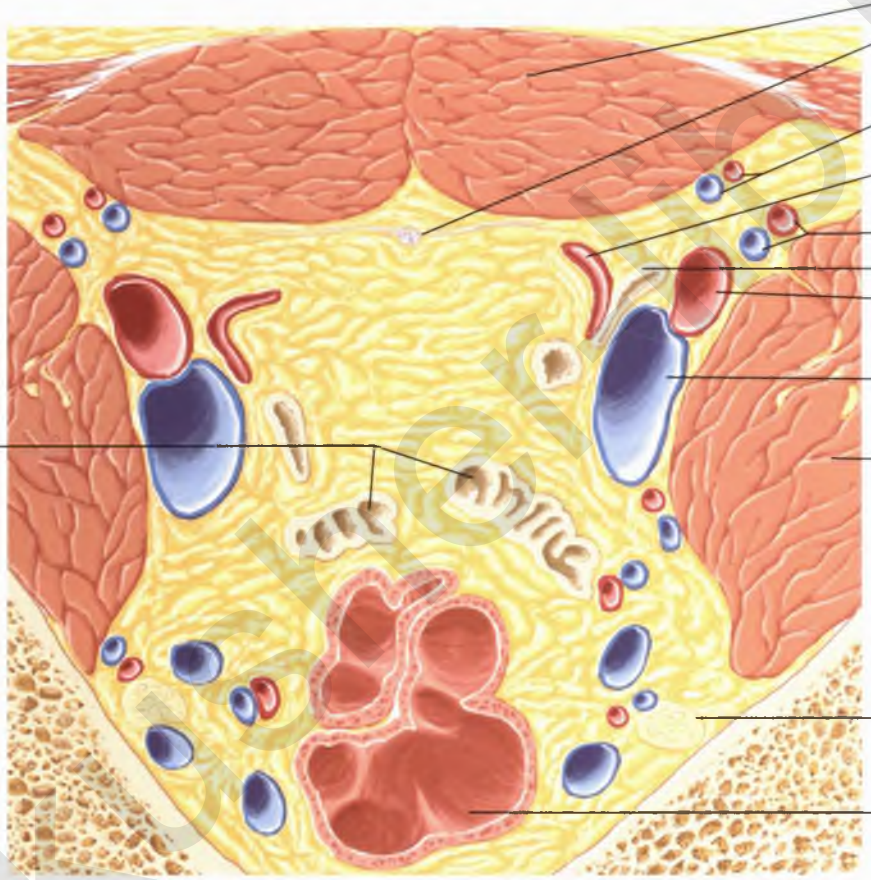
Rectus abdominis m.
Median umbilical ligament (obliterated urachus)
Inferior epigastric vessels
Umbilical a.
Gonadal vessels
Vas deferens
Left external iliac a.
Left external iliac v.
Ampullary portion of vasa deferentia
Iliopsoas m.
Sciatic nerve
Rectosigmoid colon


Rectus abdominis m.
Median umbilical ligament (obliterated urachus)
Inferior epigastric vessels
Umbilical a.
Gonadal vessels
Vas deferens
Left external iliac a.
Left external iliac v.
Ampullary portion of vasa deferentia
Iliopsoas m.
Sciatic nerve
Rectosigmoid colon

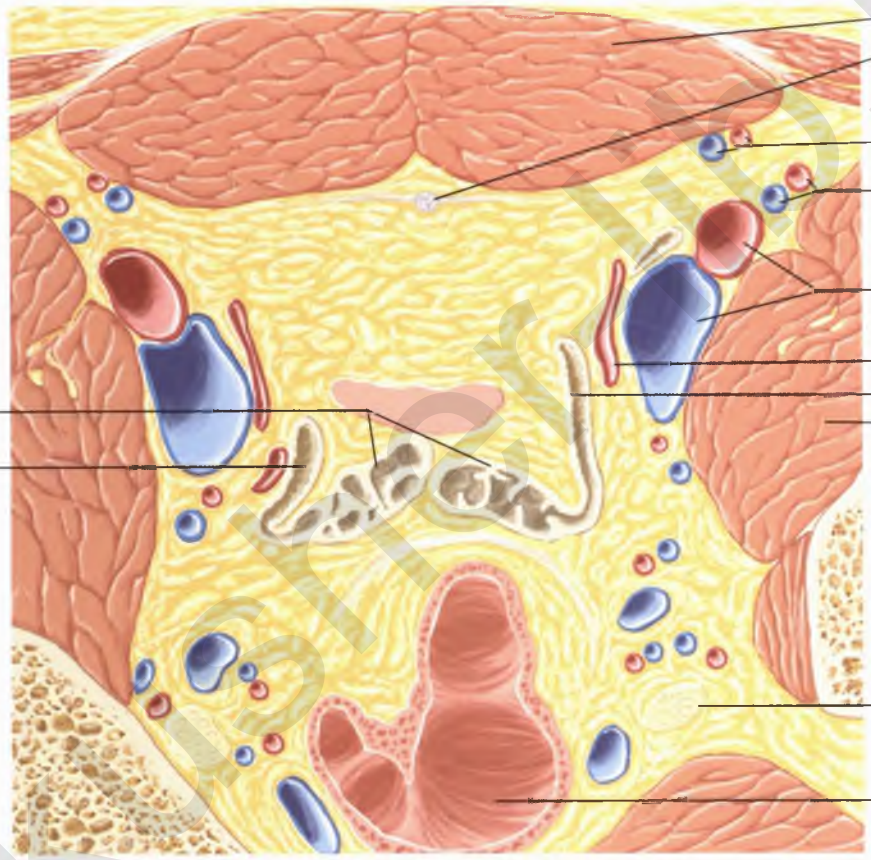
Rectus abdominis m.
Median umbilical ligament (obliterated urachus)
Inferior epigastric vessels
Gonadal vessels
Left external iliac vessels
Umbilical a.
Vas deferens
Iliopsoas m.
Ampullary portion of vasa deferentia
Vas deferens
Sciatic nerve
Rectosigmoid colon


Rectus abdominis m.
Median umbilical ligament (obliterated urachus)
Inferior epigastric vessels
Gonadal vessels
Left external iliac vessels
Ampullary portion of vasa deferentia
Vas deferens
Umbilical a.
Vas deferens
Iliopsoas m.
Sciatic nerve
Rectosigmoid colon

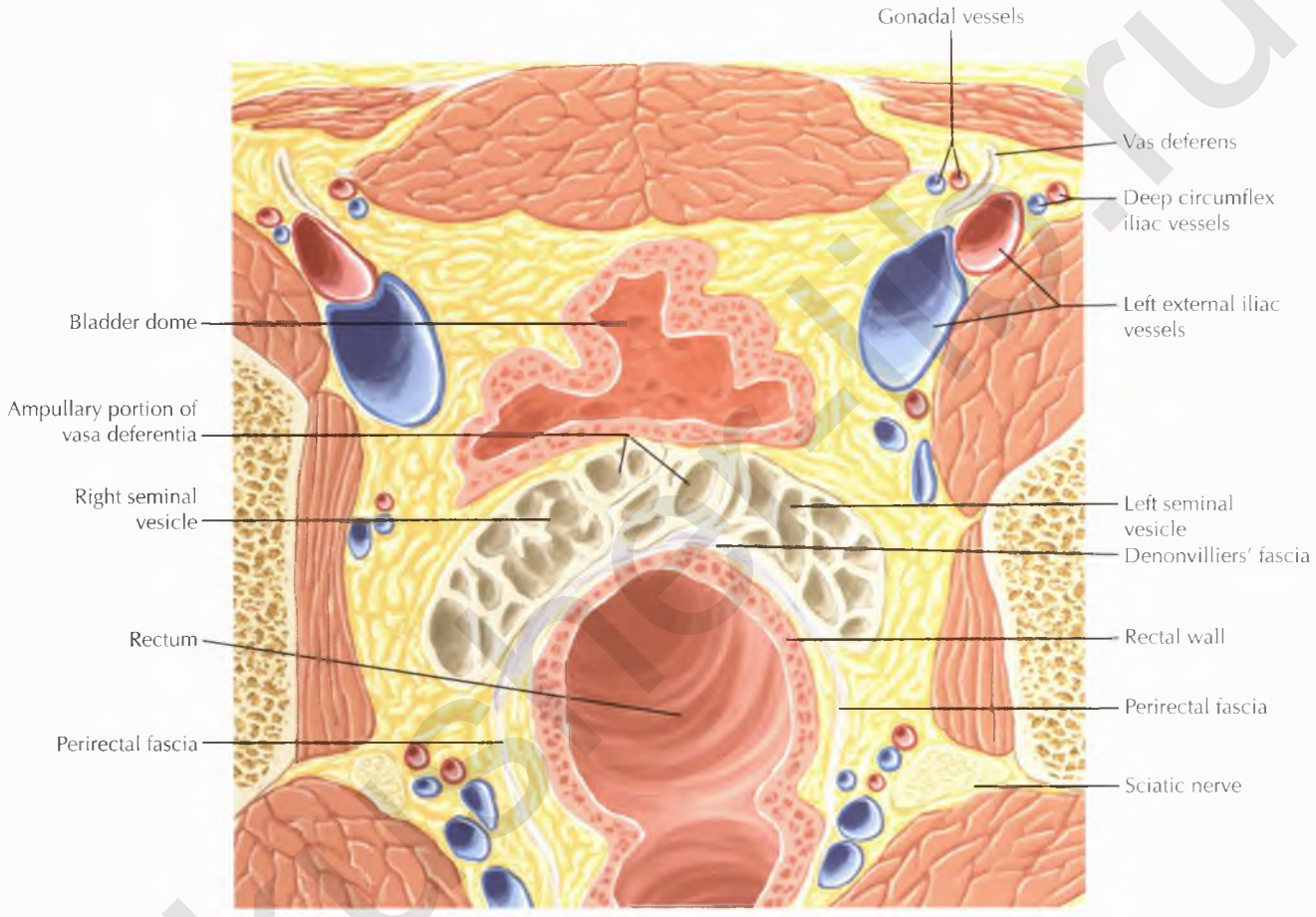

NORMAL ANATOMY

The seminal vesicles are paired accessory sex glands that produce and secrete fructose-rich seminal fluid, which is the major component of ejaculate volume. The detail of the convoluted, fluid-filled tubules that form the seminal vesicles is best depicted on T2-weighted MR images.

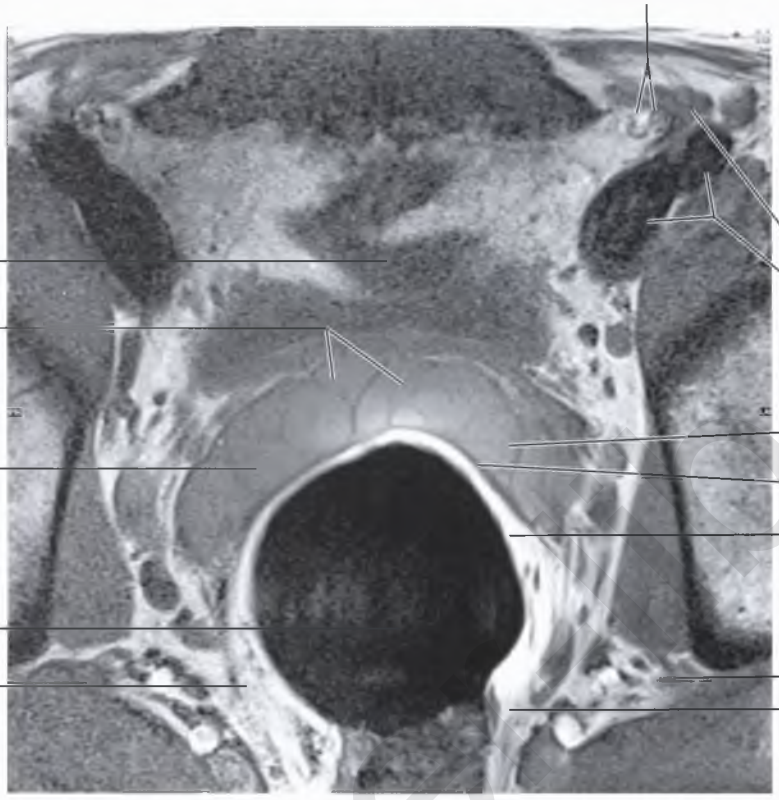
Gonadal vessels
Vas deferens
Left external iliac vessels
Bladder dome
Ampullary portion of vasa deferentia
Right seminal vesicle
Left seminal vesicle
Denonvilliers' fascia
Rectal wall
Rectum
Perirectal fascia
Sciatic nerve
Perirectal fascia

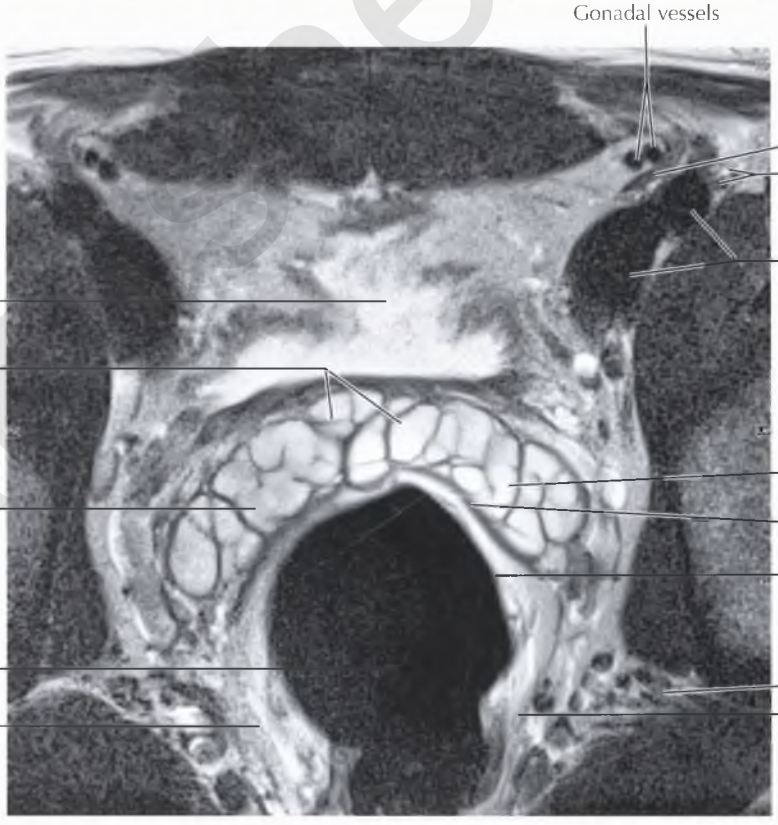
Gonadal vessels
Vas deferens
Deep circumflex iliac vessels
Left external iliac vessels
Bladder dome
Ampullary portion of vasa deferentia
Right seminal vesicle
Left seminal vesicle
Denonvilliers' fascia
Rectal wall
Rectum
Perirectal fascia
Sciatic nerve
Perirectal fascia

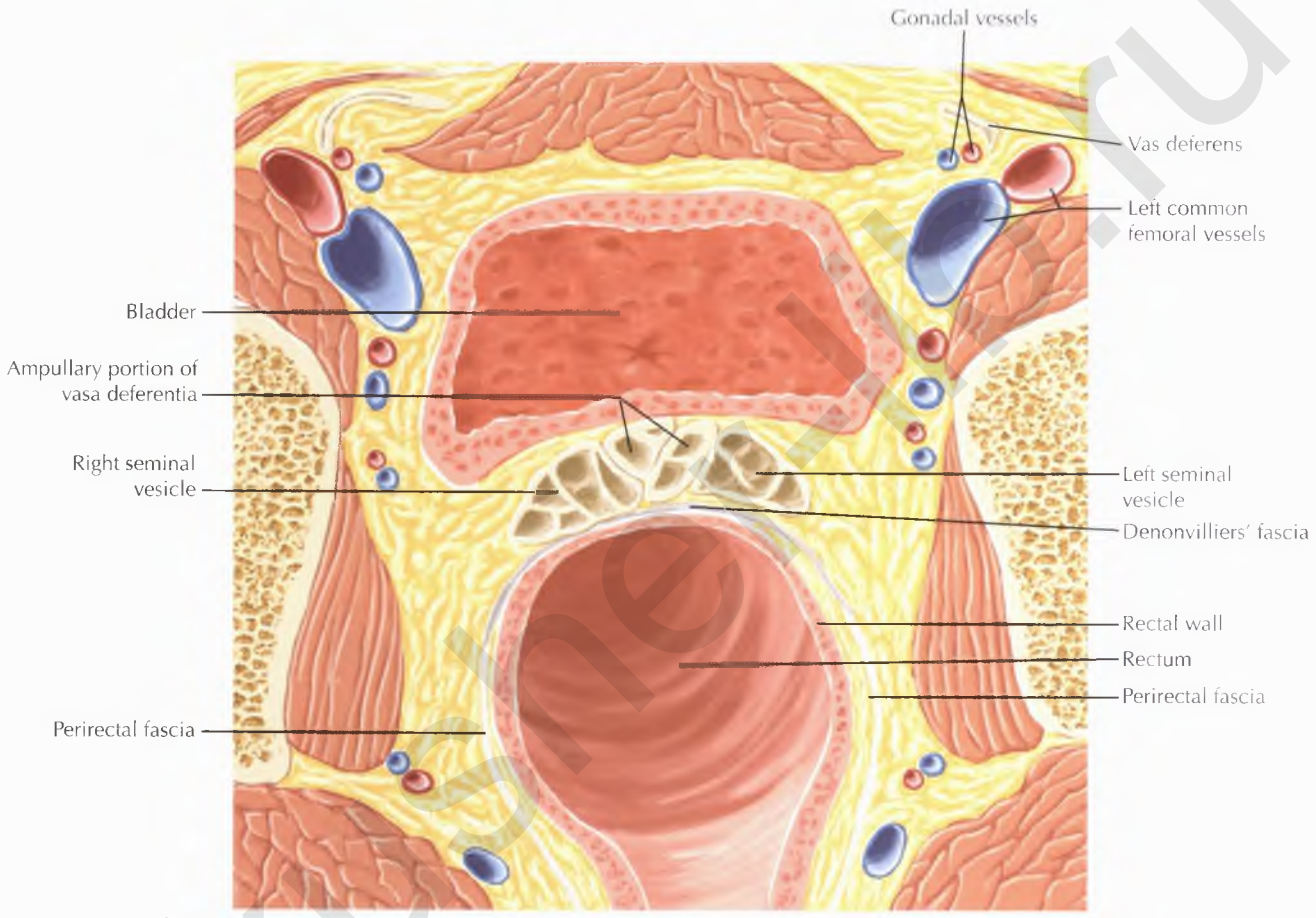

DIAGNOSTIC CONSIDERATION

Denonvilliers' fascia, also known as the *rectoprostatic fascia,* covers the seminal vesicles and the posterior aspect of the prostate gland, separating these structures from the rectum. Denonvilliers' fascia helps limit the posterior spread of prostate cancer, making direct invasion of the rectum unusual.

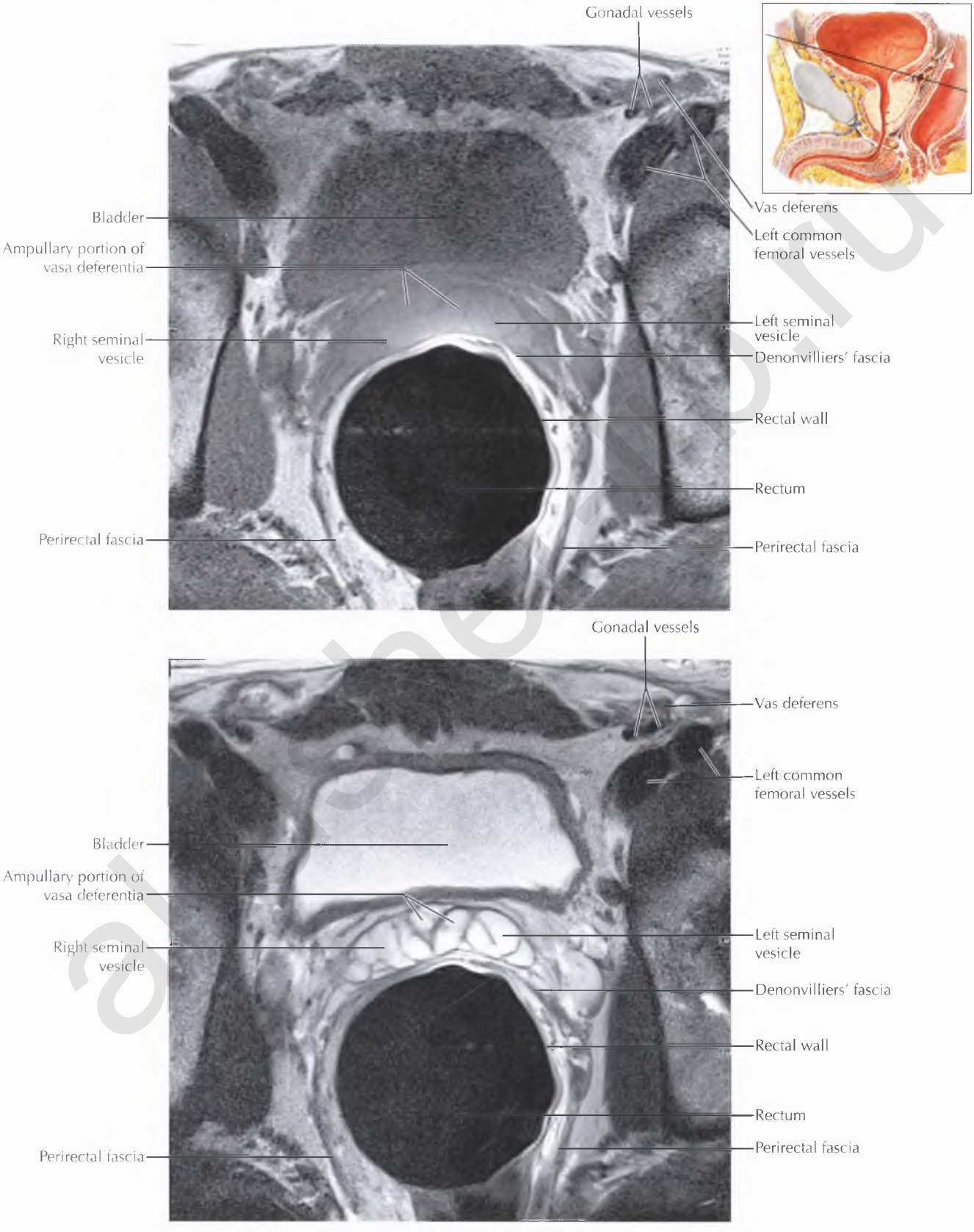
Gonadal vessels
Vas deferens
Left common femoral vessels
Bladder
Ampullary portion of vasa deferentia
Right seminal vesicle
Left seminal vesicle
Denonvilliers' fascia
Rectal wall
Rectum
Perirectal fascia
Perirectal fascia
Gonadal vessels
Vas deferens
Left common femoral vessels
Bladder
Ampullary portion of vasa deferentia
Right seminal vesicle
Left seminal vesicle
Denonvilliers' fascia
Rectal wall
Rectum
Perirectal fascia

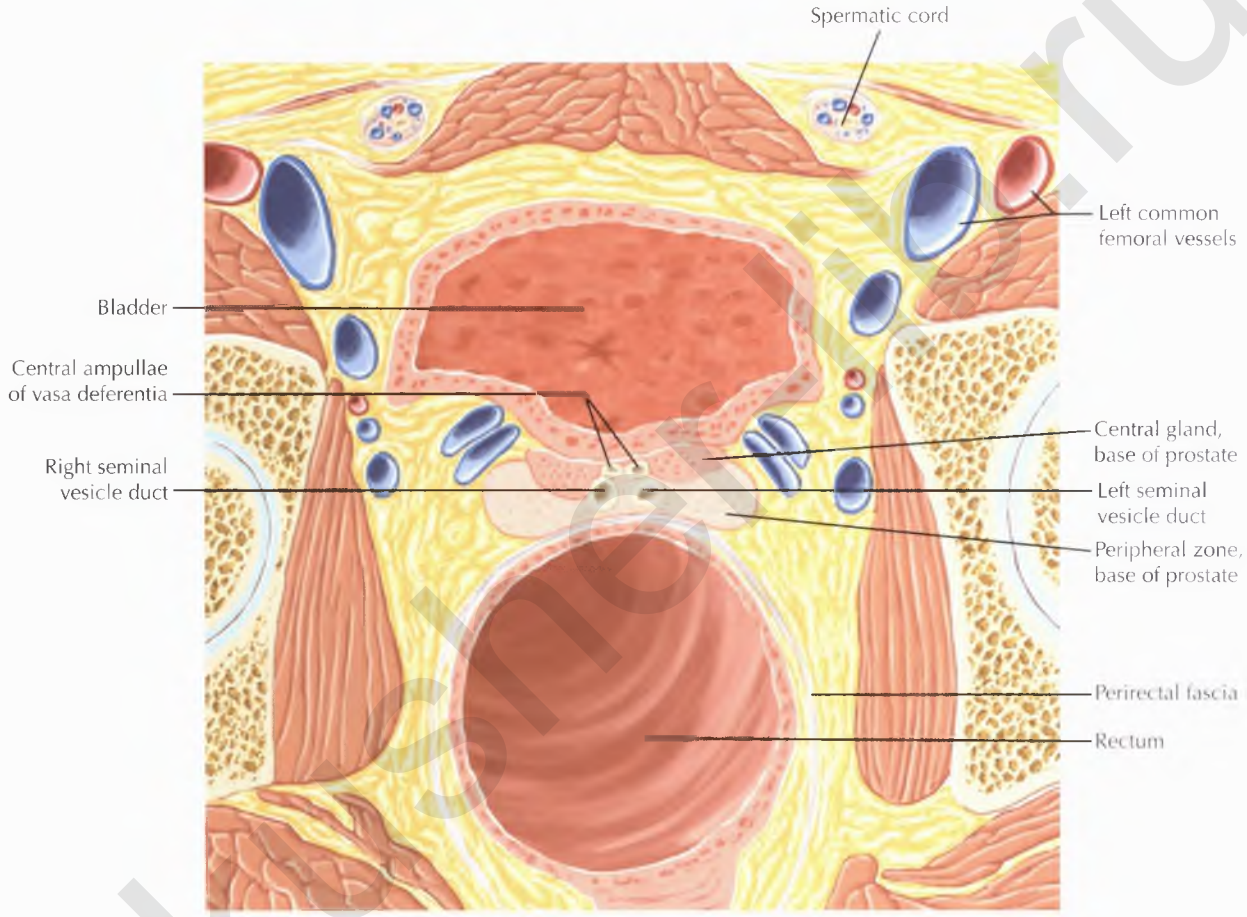

NORMAL ANATOMY

On this image, the paired ampullae of the vasa deferentia are seen just superior to their union with the paired seminal vesicle ducts, which, in combination, will form the ejaculatory ducts.

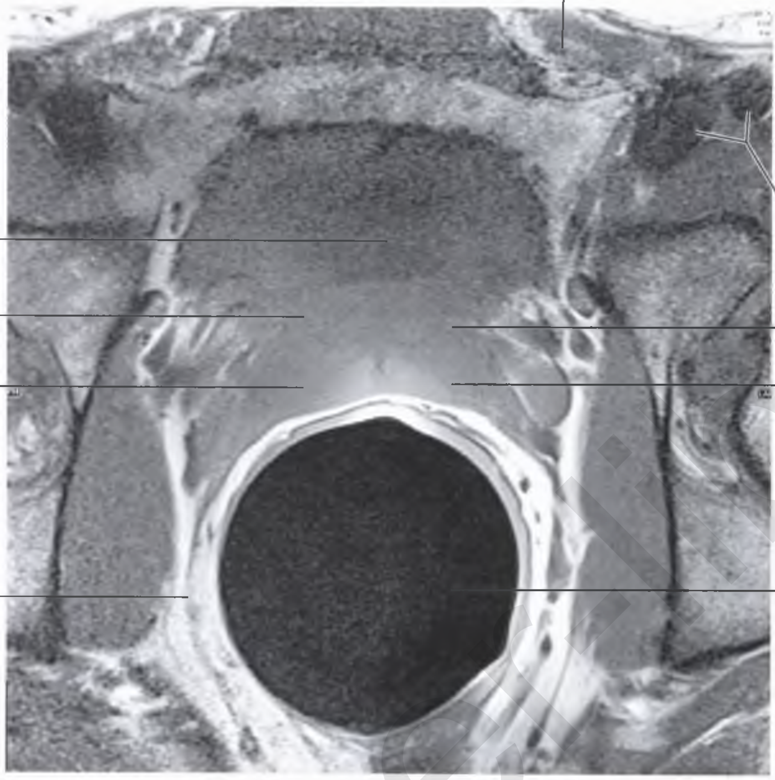
Spermatic cord
Bladder
Central gland, base of prostate
Peripheral zone, base of prostate
Perirectal fascia
Left common femoral vessels
Central gland, base of prostate
Peripheral zone, base of prostate
Rectum

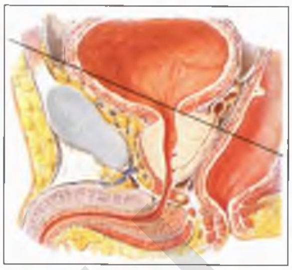

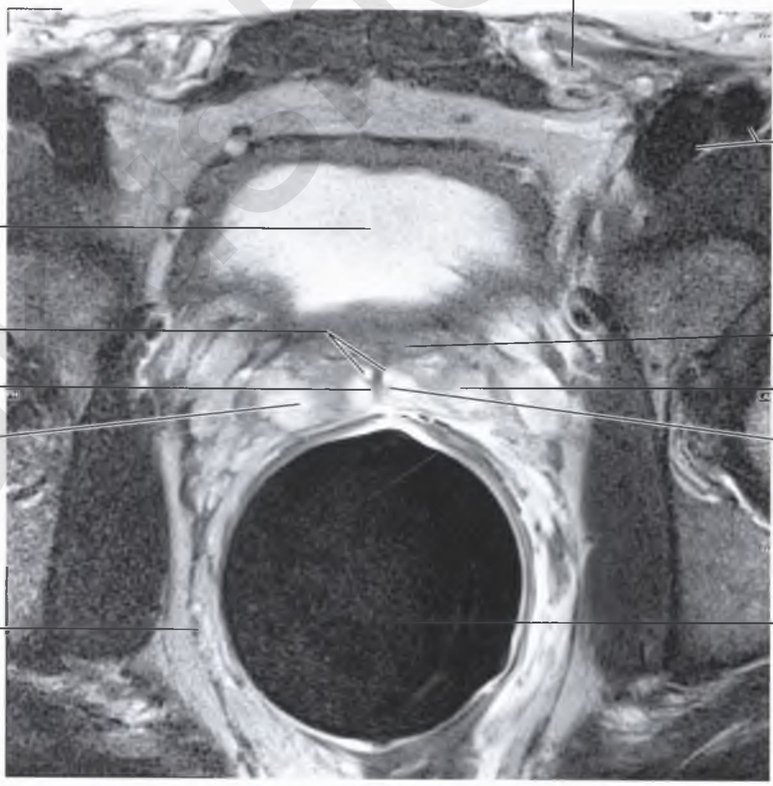
Spermatic cord
Left common femoral vessels
Bladder
Central ampullae of vasa deferentia
Right seminal vesicle duct
Peripheral zone, base of prostate
Central gland, base of prostate
Peripheral zone, base of prostate
Left seminal vesicle duct
Perirectal fascia
Rectum

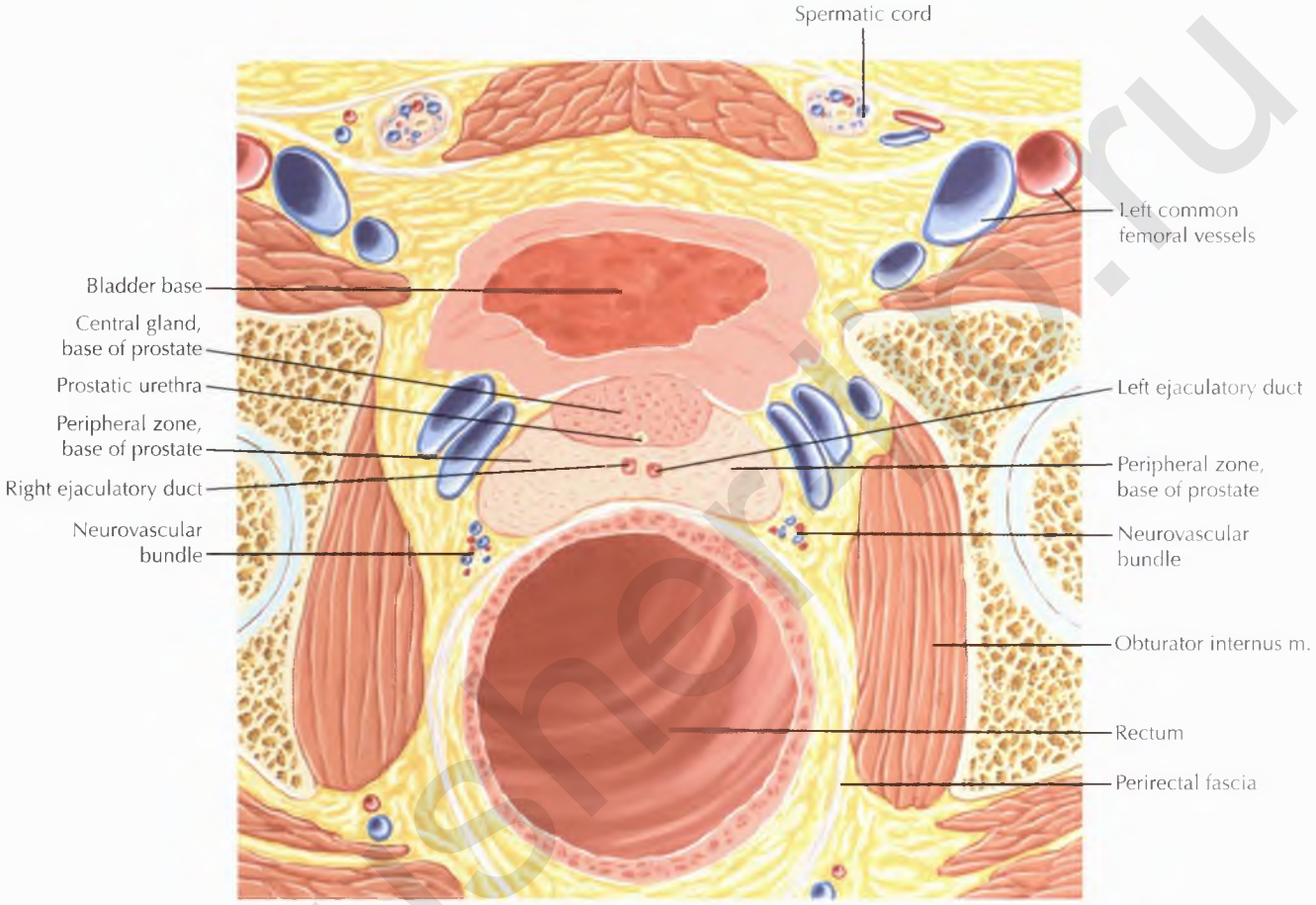

NORMAL ANATOMY

The prostate gland is separated into a peripheral zone, central zone, and transitional zone, which constitute approximately 70%, 25%, and 5% of the prostate gland, respectively. The central and transitional zones are not well delineated on MRI and are collectively referred to as the *central gland*. Differentiation between the central gland and peripheral zone of the prostate is best appreciated on T2-weighted images, which reveal the posteriorly located, homogeneous, high signal intensity peripheral zone containing thin, linear, low signal intensity fibrous septa, in contrast to the anteriorly located, more heterogeneous, low intermediate signal intensity central gland.

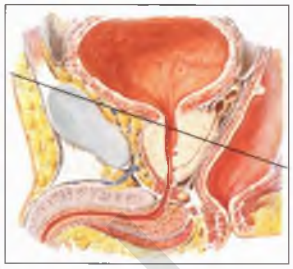

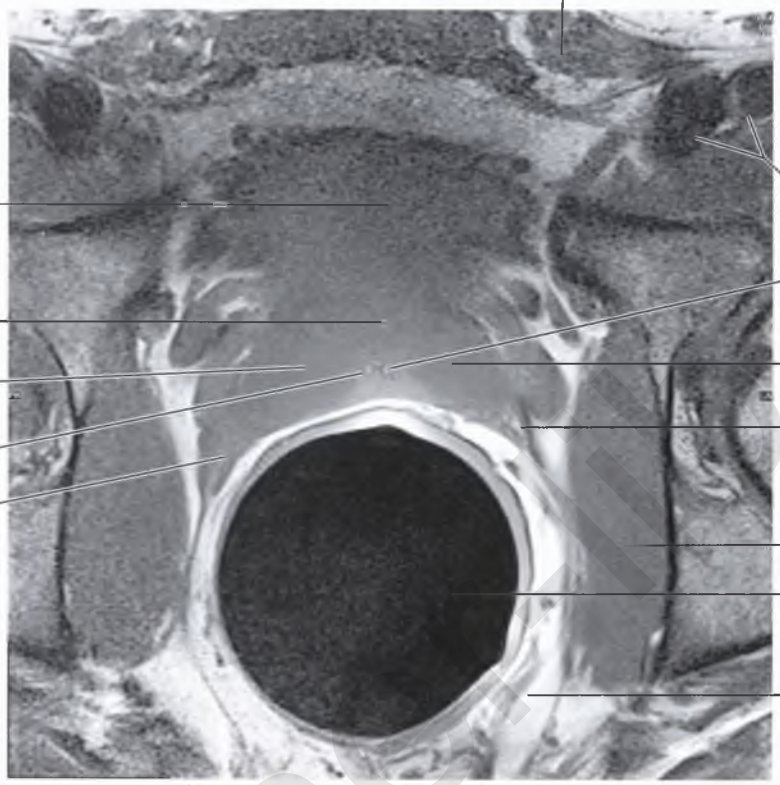
Spermatic cord
Bladder base
Central gland, base of prostate
Peripheral zone, base of prostate
Right ejaculatory duct
Neurovascular bundle
Left common femoral vessels
Left ejaculatory duct
Peripheral zone, base of prostate
Neurovascular bundle
Obturator internus m.
Rectum
Perirectal fascia

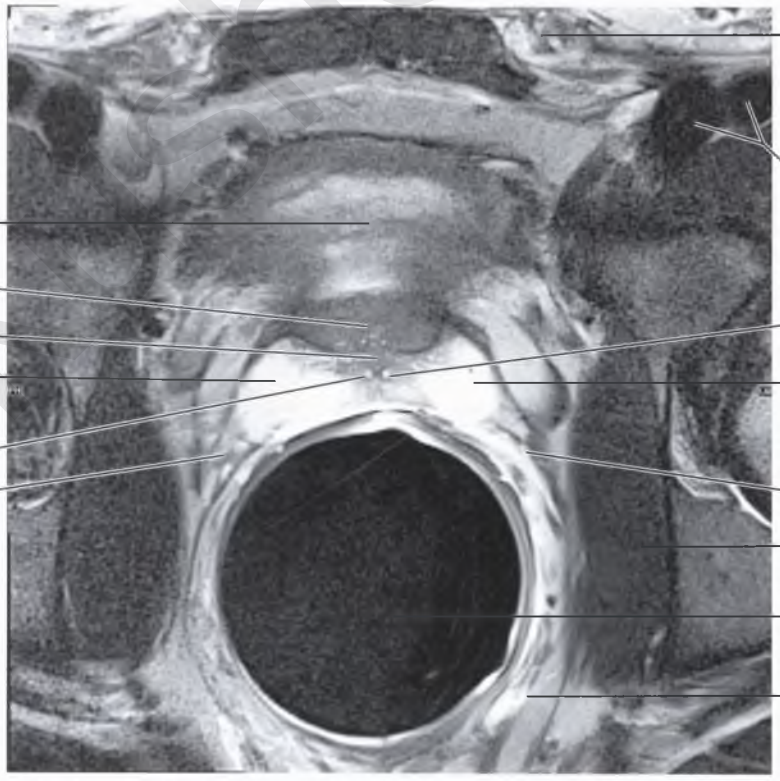
Spermatic cord
Bladder base
Central gland, base of prostate
Prostatic urethra
Peripheral zone, base of prostate
Right ejaculatory duct
Neurovascular bundle
Left common femoral vessels
Left ejaculatory duct
Peripheral zone, base of prostate
Neurovascular bundle
Obturator internus m.
Rectum
Perirectal fascia

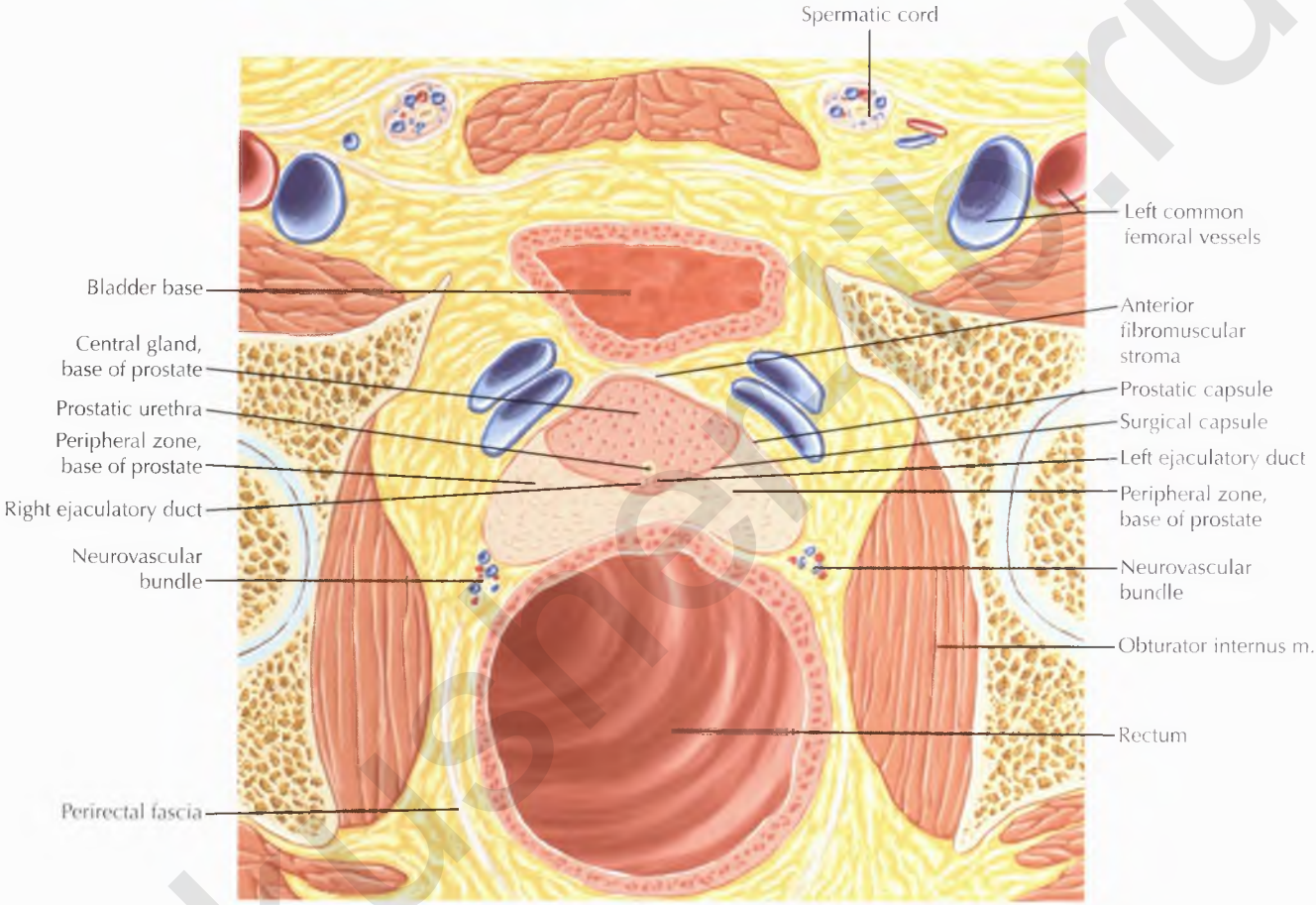

NORMAL ANATOMY

The anterior fibromuscular stroma is a thick layer of nonglandular, low signal intensity tissue that forms the anterior surface of the prostate gland.

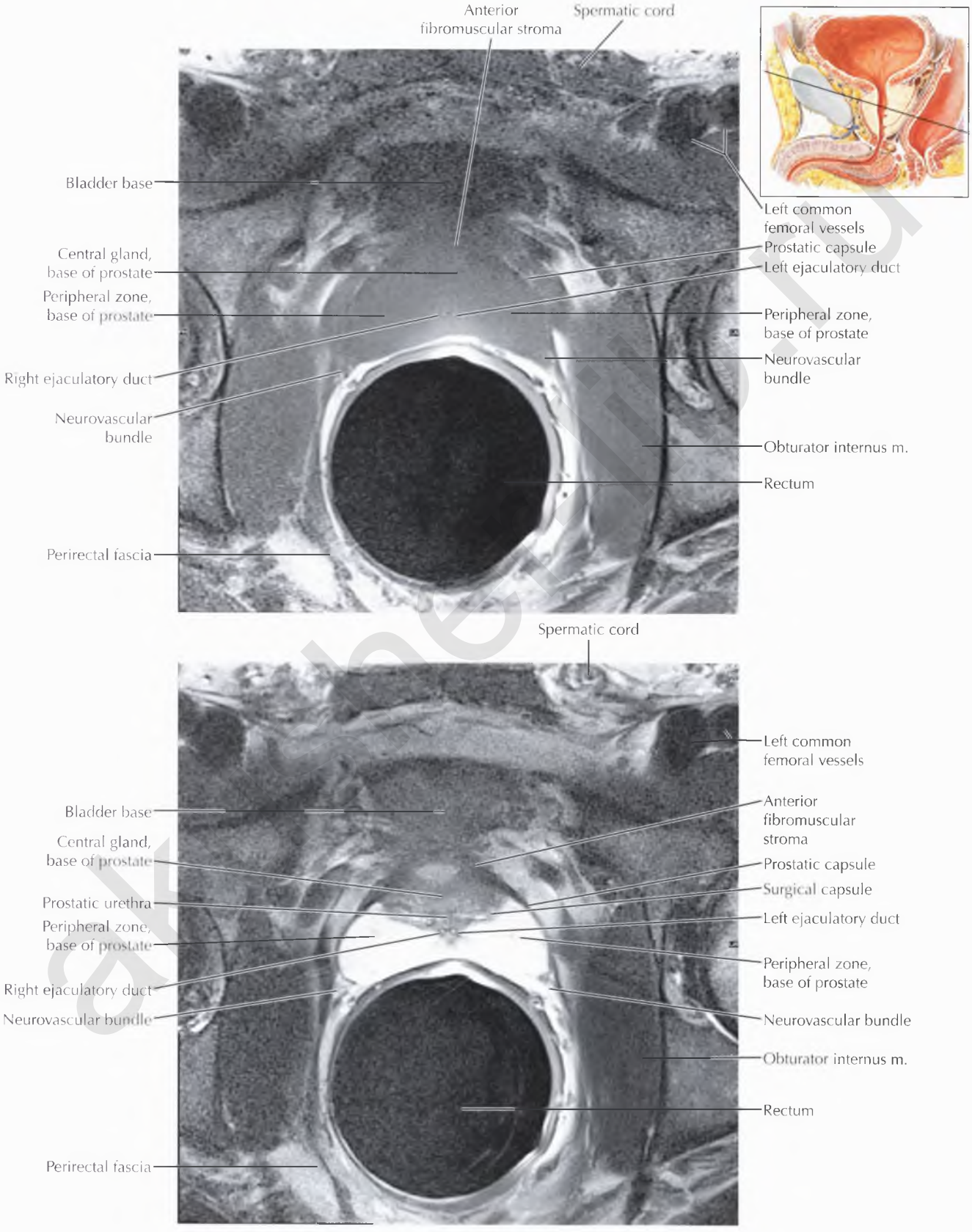
Anterior fibromuscular stroma
Spermatic cord
Bladder base
Central gland, base of prostate
Peripheral zone, base of prostate
Right ejaculatory duct
Neurovascular bundle
Perirectal fascia
Left common femoral vessels
Prostatic capsule
Left ejaculatory duct
Peripheral zone, base of prostate
Neurovascular bundle
Obturator internus m.
Rectum
Spermatic cord
Left common femoral vessels
Bladder base
Central gland, base of prostate
Prostatic urethra
Peripheral zone, base of prostate
Right ejaculatory duct
Neurovascular bundle
Perirectal fascia
Anterior fibromuscular stroma
Prostatic capsule
Surgical capsule
Left ejaculatory duct
Peripheral zone, base of prostate
Neurovascular bundle
Obturator internus m.
Rectum

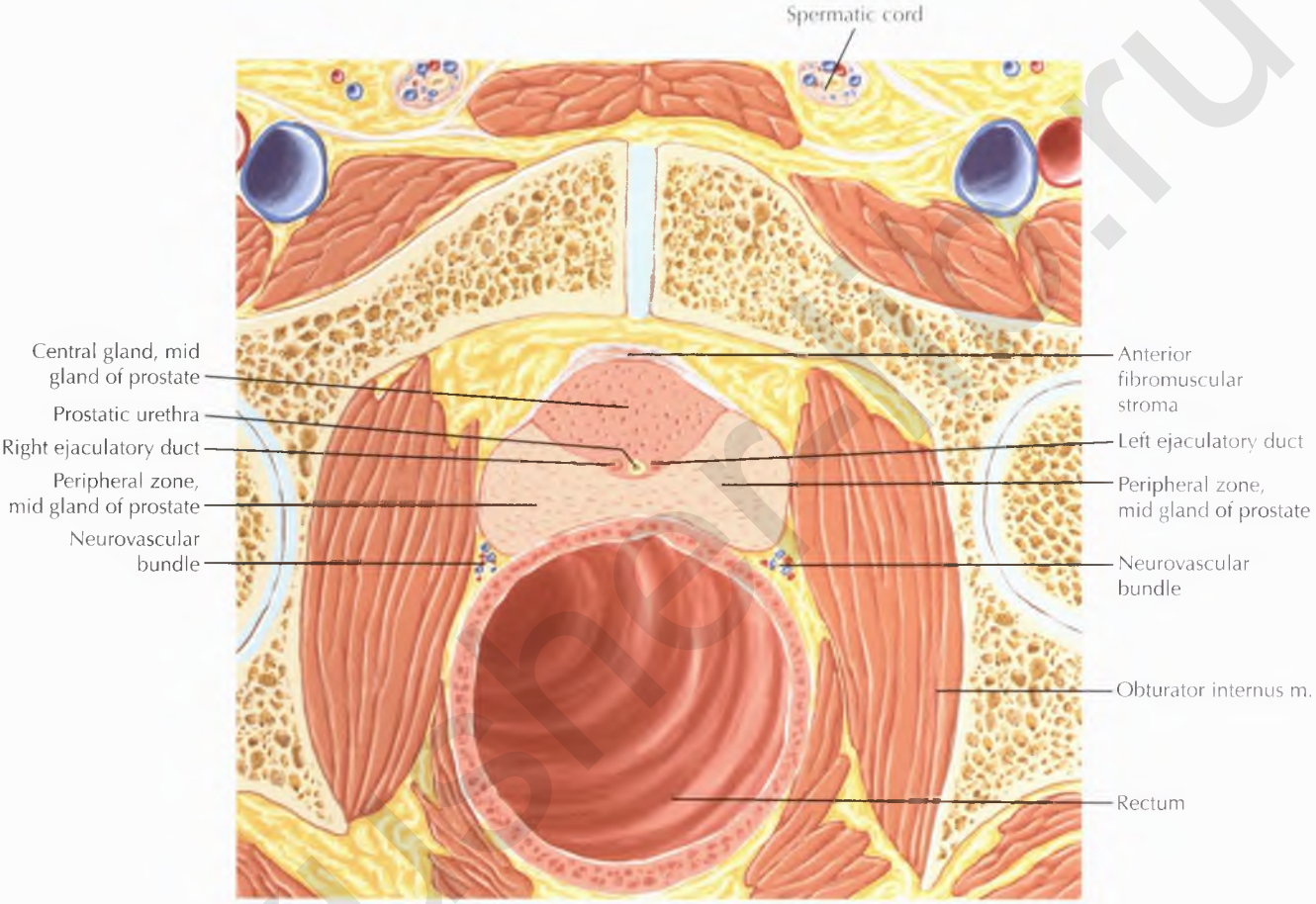

NORMAL ANATOMY

The paired neurovascular bundles are tubular structures located within the peri-prostatic fat posterolateral to the prostate gland at the 5-o'clock and 7-o'clock positions. These bundles carry *nerves*, which are low in signal intensity on T1- and T2-weighted MR images, and *vessels*, which are typically high in signal intensity because of the slow flow in veins. These nerves and vessels supply the corpora cavernosa and are critical for maintaining erectile function.

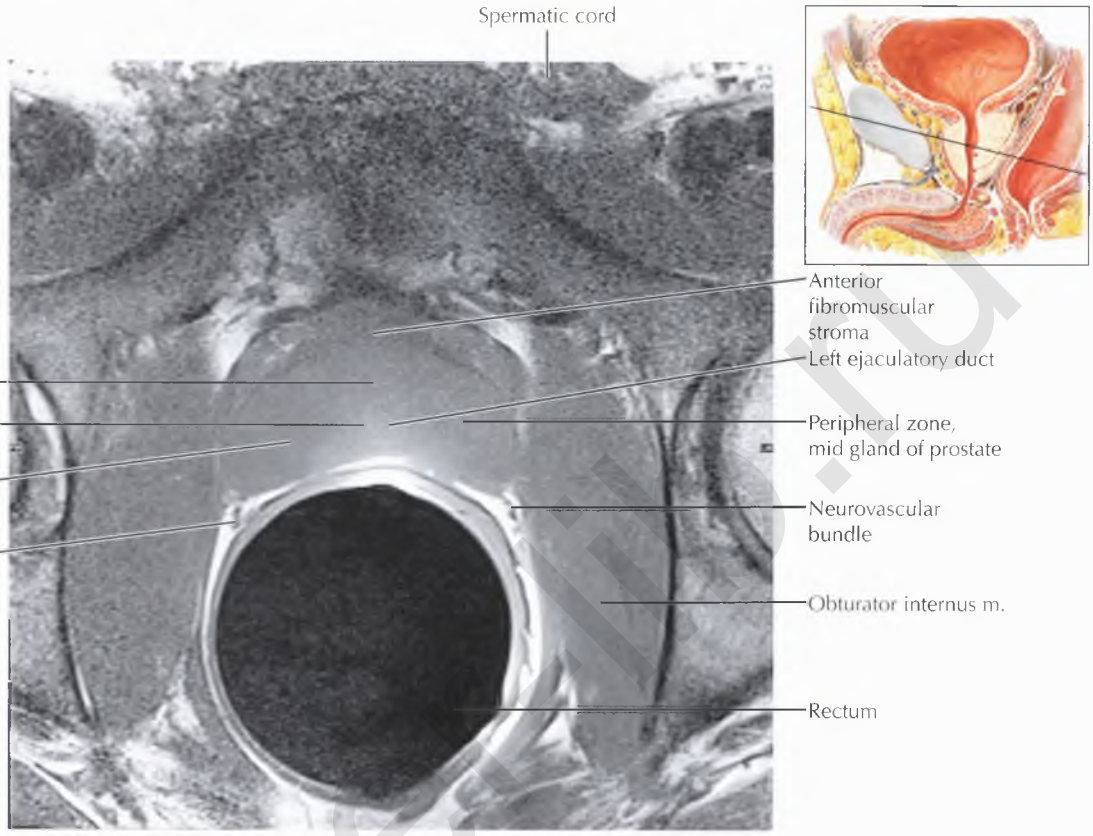
Spermatic cord
Anterior fibromuscular stroma
Central gland, base of prostate
Left ejaculatory duct
Right ejaculatory duct
Peripheral zone, mid gland of prostate
Peripheral zone, mid gland of prostate
Neurovascular bundle
Neurovascular bundle
Obturator internus m.
Rectum

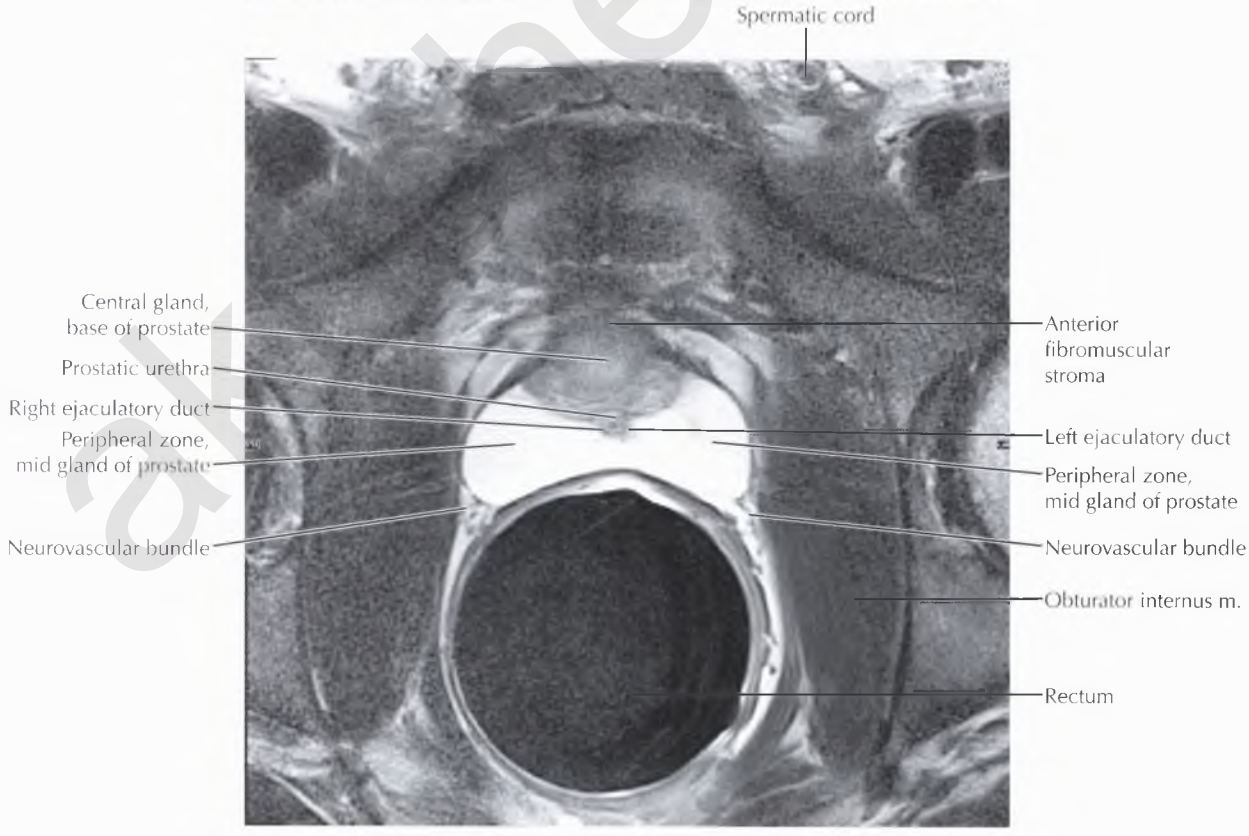
Spermatic cord
Central gland, base of prostate
Anterior fibromuscular stroma
Prostatic urethra
Right ejaculatory duct
Left ejaculatory duct
Peripheral zone, mid gland of prostate
Peripheral zone, mid gland of prostate
Neurovascular bundle
Neurovascular bundle
Obturator internus m.
Rectum

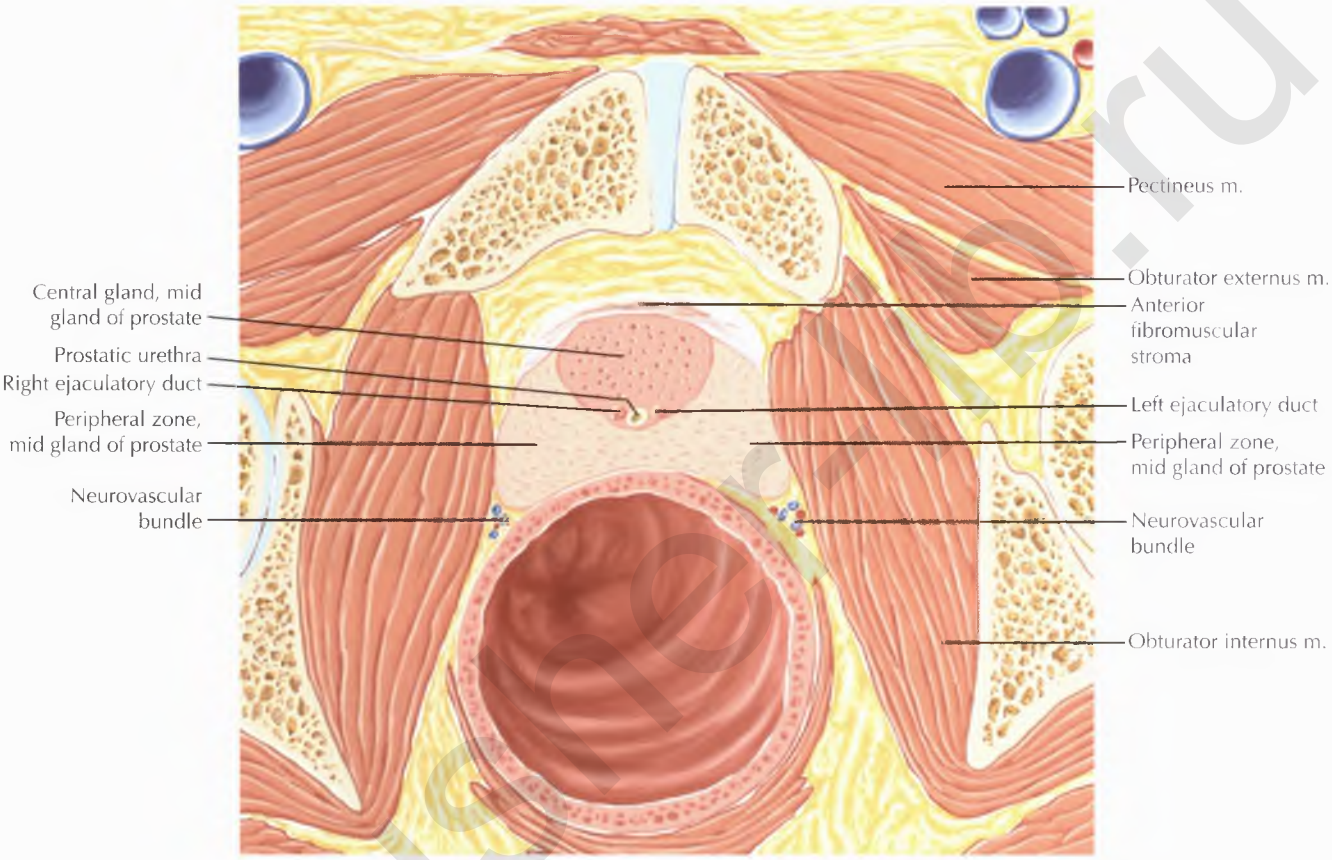

DIAGNOSTIC CONSIDERATION

The most common indication for endorectal coil MRI of the prostate gland is to evaluate for extracapsular extension of known prostate cancer. Findings of extraprostatic spread of tumor include obliteration of the rectoprostatic angle, bulging or irregularity of the true prostatic capsule, asymmetry of a neurovascular bundle, soft tissue within the peri-prostatic fat contiguous with the prostate gland, infiltration of Denonvilliers' fascia, and direct invasion of the adjacent organs (seminal vesicles, bladder, and rectum). In addition, a set of MR images with a large field of view through the pelvis is also typically acquired to evaluate for pelvic lymphadenopathy and osseous metastases.

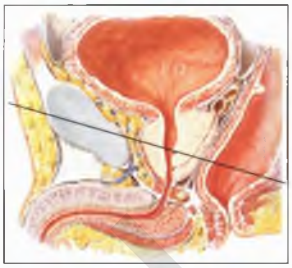

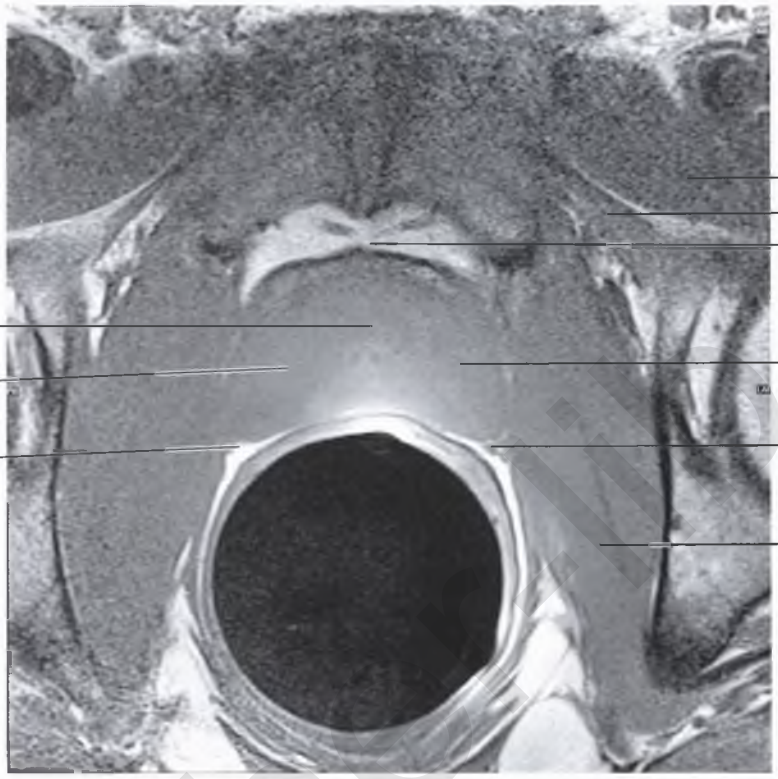

Pectineus m.
Obturator externus m.
Anterior fibromuscular stroma
Central gland, mid gland of prostate
Peripheral zone, mid gland of prostate
Peripheral zone, mid gland of prostate
Neurovascular bundle
Neurovascular bundle
Obturator internus m.

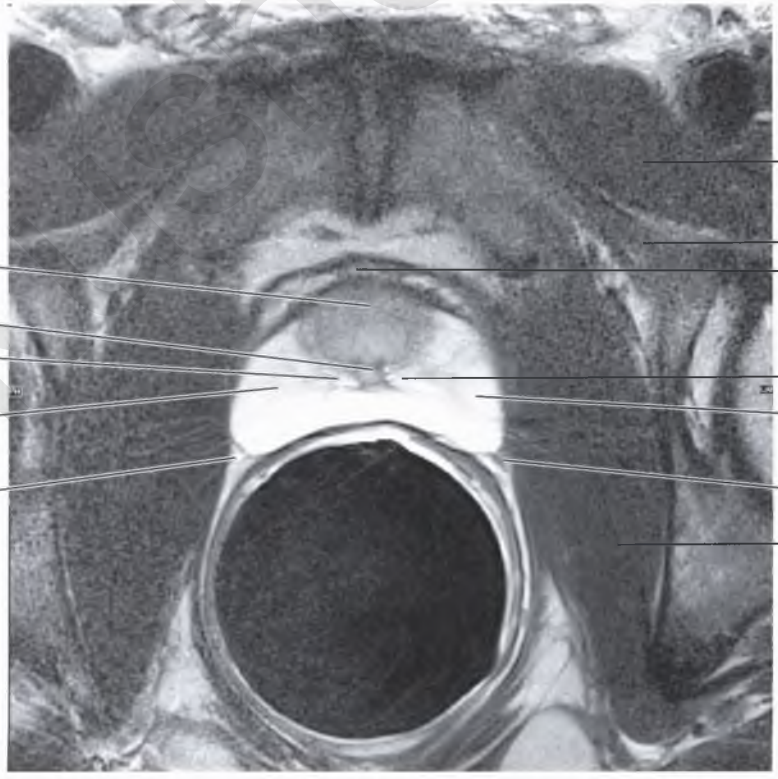

Pectineus m.
Central gland, mid gland of prostate
Obturator externus m.
Anterior fibromuscular stroma
Prostatic urethra
Right ejaculatory duct
Left ejaculatory duct
Peripheral zone, mid gland of prostate
Peripheral zone, mid gland of prostate
Neurovascular bundle
Neurovascular bundle
Obturator internus m.

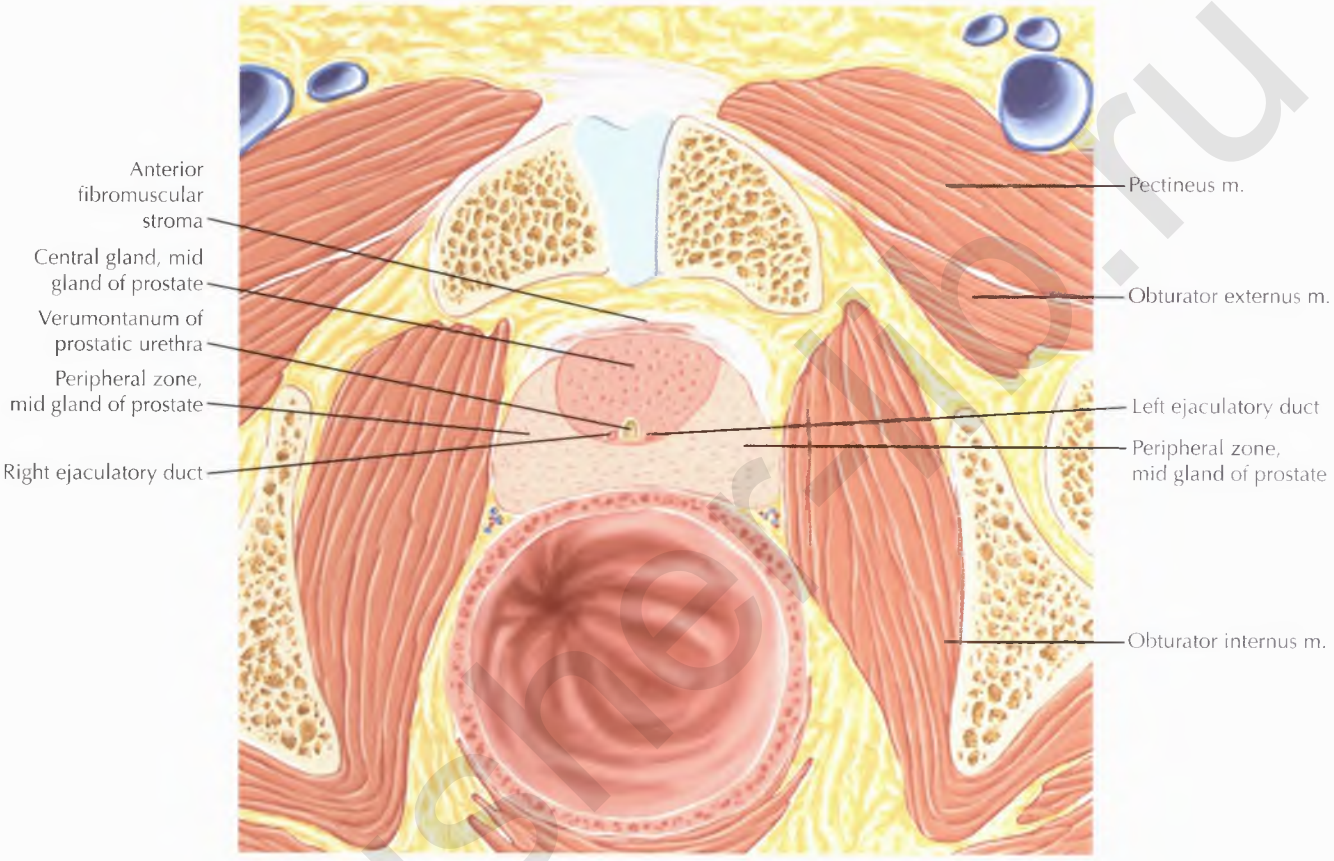

DIAGNOSTIC CONSIDERATION

Prostate adenocarcinoma most often arises from the peripheral zone of the prostate (70%), with 20% from the transitional zone and 10% from the central zone. On MRI, prostate carcinoma is typically intermediate in signal intensity on T1-weighted images and low in signal intensity on T2-weighted images, relative to the peripheral zone. Because MR studies of the prostate are often performed within a few weeks after a prostate biopsy, the presence of postbiopsy hemorrhage in the prostate parenchyma can make the tumor more apparent on T1-weighted images. Look for a T1-hypointense (and T2-hypointense) tumor nodule within a background of T1-hyperintense subacute hemorrhage. Normal peripheral-zone tissue is low in signal intensity on T1-weighted images and high in signal intensity on T2-weighted images.

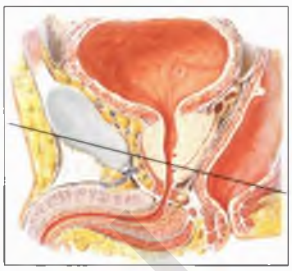

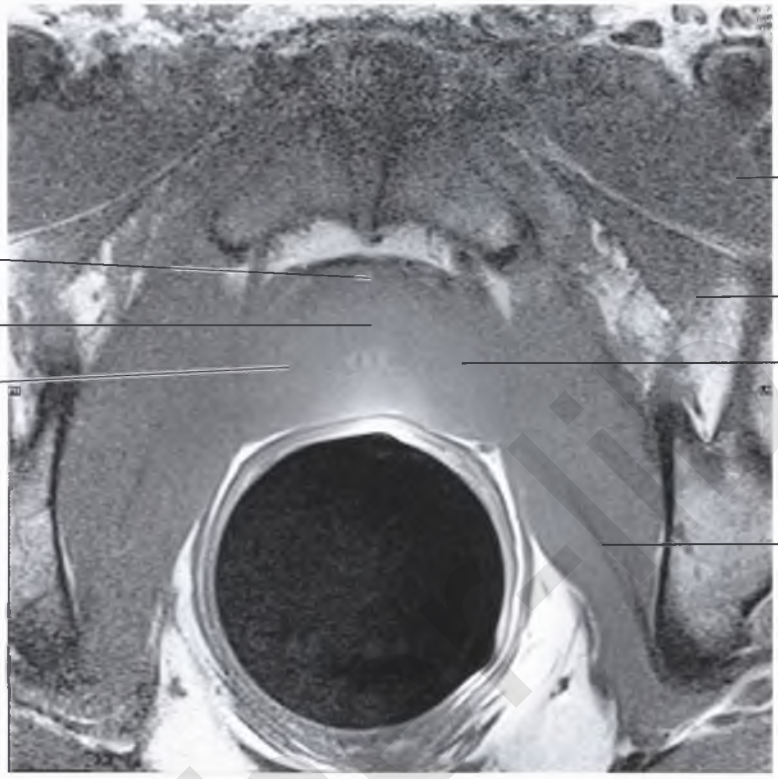
Anterior fibromuscular stroma
Central gland, mid gland of prostate
Peripheral zone, mid gland of prostate
Pectineus m.
Obturator externus m.
Peripheral zone, mid gland of prostate
Obturator internus m.

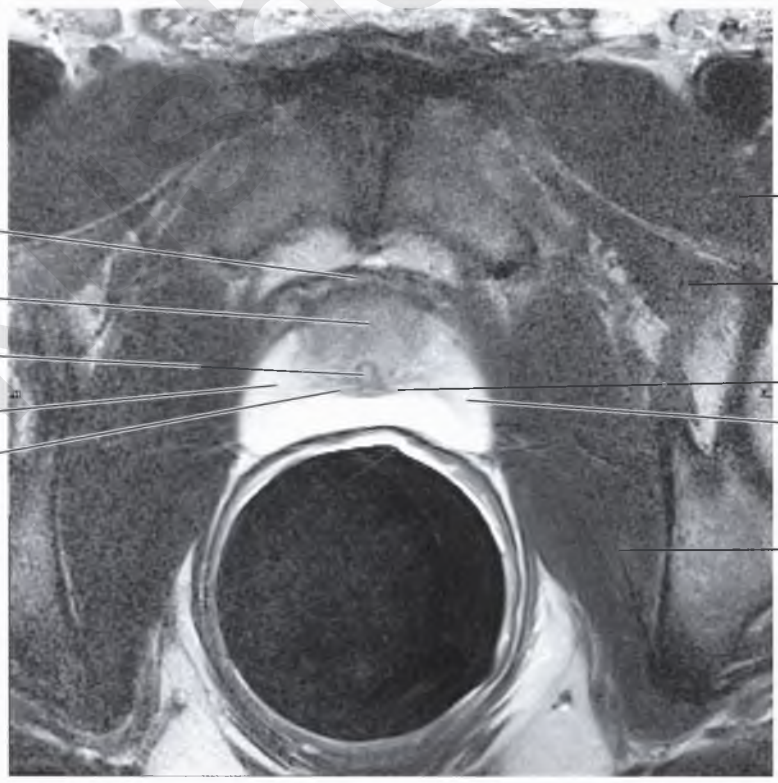
Anterior fibromuscular stroma
Central gland, mid gland of prostate
Verumontanum of prostatic urethra
Peripheral zone, mid gland of prostate
Right ejaculatory duct
Pectineus m.
Obturator externus m.
Left ejaculatory duct
Peripheral zone, mid gland of prostate
Obturator internus m.

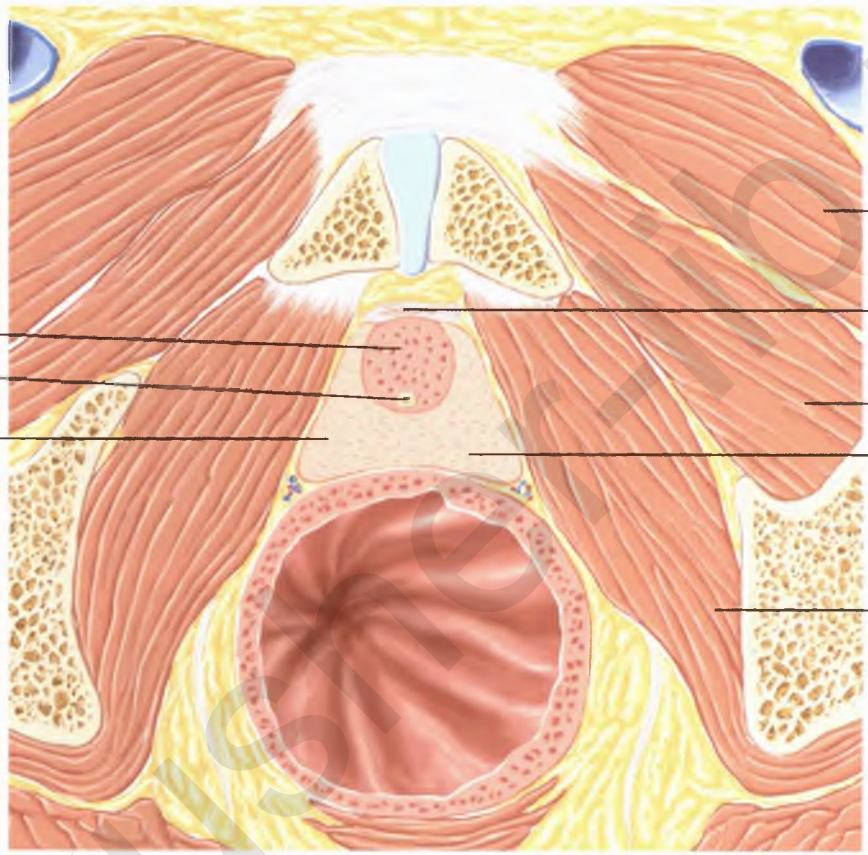

PATHOLOGIC PROCESS

Benign prostatic hypertrophy (BPH), caused by enlargement of the transitional zone, is a common finding that increases with age. On MRI, hypertrophy of T2-hyperintense glandular-rich foci and T2-hypointense stromal-dominant foci within the central gland create a heterogeneous nodular appearance on T2-weighted images.

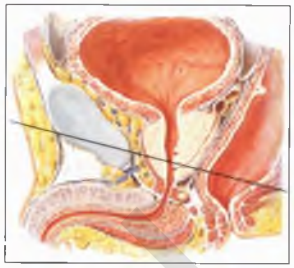

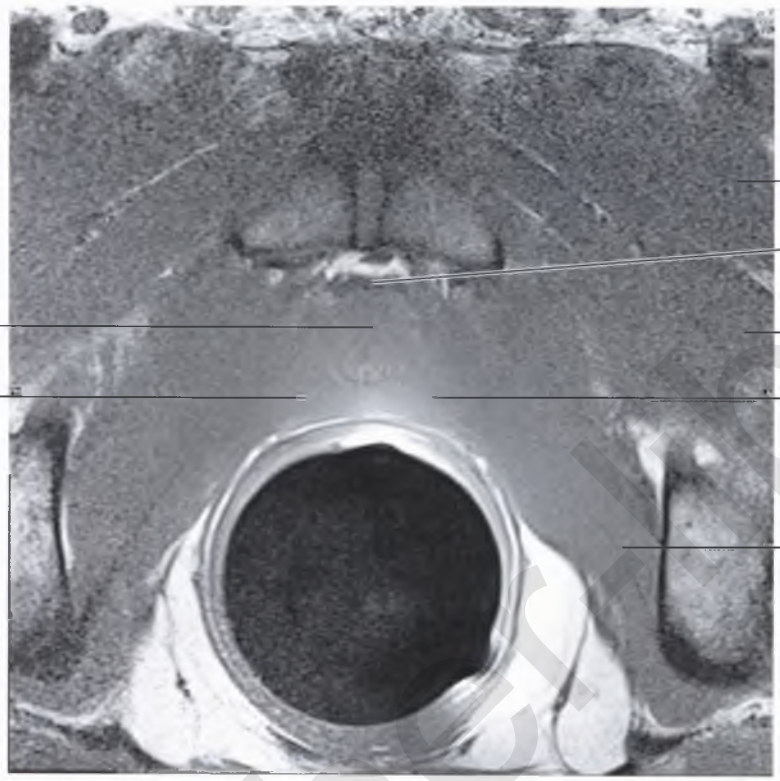

Pectineus m.
Anterior fibromuscular stroma
Central gland, apex of prostate
Obturator externus m.
Peripheral zone, apex of prostate
Peripheral zone, apex of prostate
Obturator internus m.

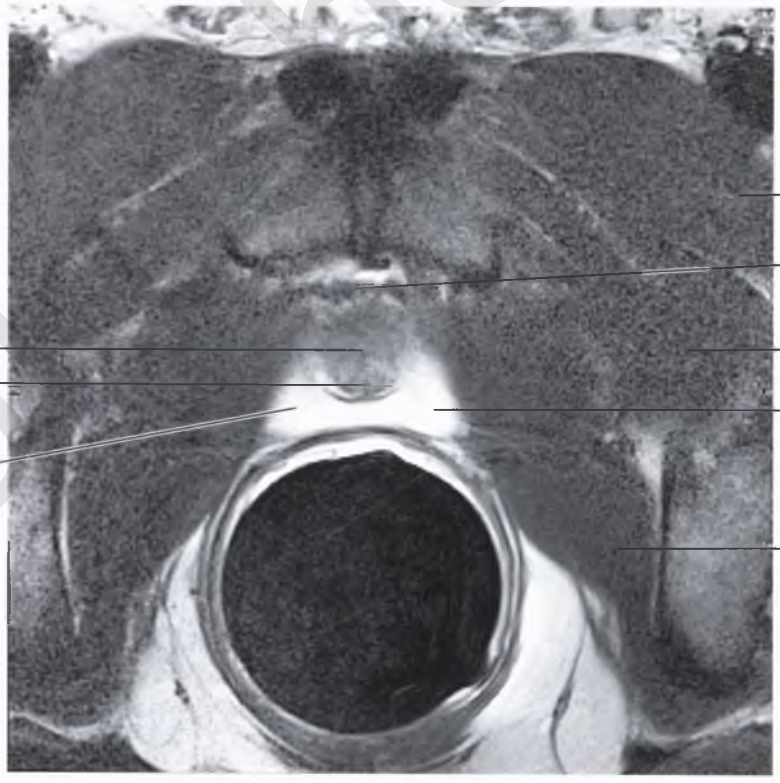

Pectineus m.
Anterior fibromuscular stroma
Central gland, apex of prostate
Obturator externus m.
Prostatic urethra
Peripheral zone, apex of prostate
Peripheral zone, apex of prostate
Obturator internus m.

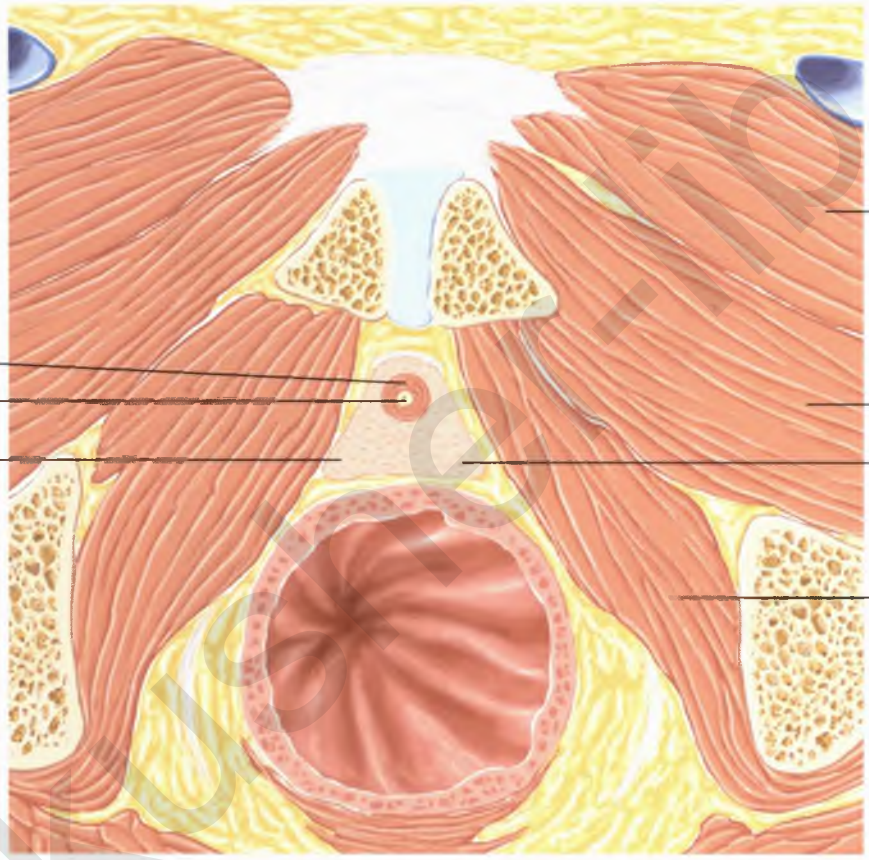
Pectineus m.
Sphincter urethrae m.
Prostatic urethra
Peripheral zone, apex of prostate
Obturator externus m.
Peripheral zone, apex of prostate
Obturator internus m.

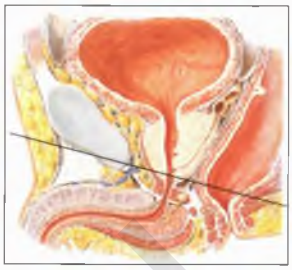

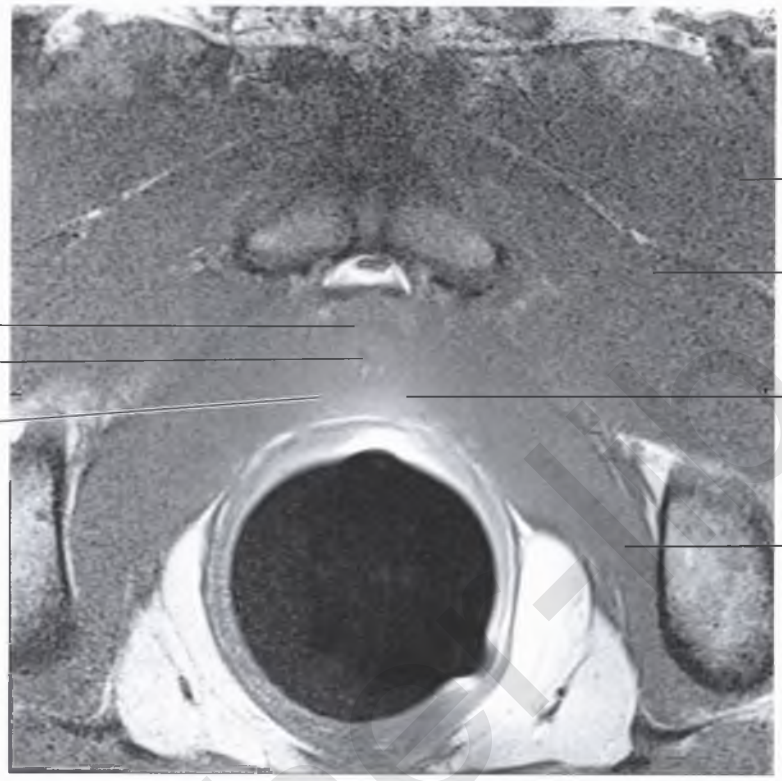

Pectineus m.

Obturator externus m.

Sphincter urethrae m.

Prostatic urethra

Peripheral zone, apex of prostate

Peripheral zone, apex of prostate

Obturator internus m.

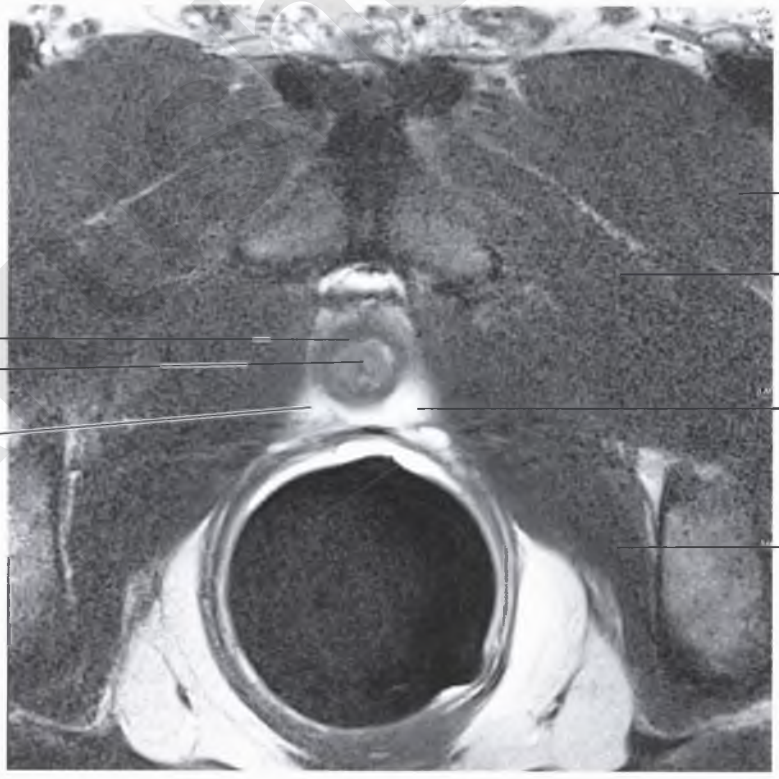

Pectineus m.

Obturator externus m.

Sphincter urethrae m.

Prostatic urethra

Peripheral zone, apex of prostate

Peripheral zone, apex of prostate

Obturator internus m.

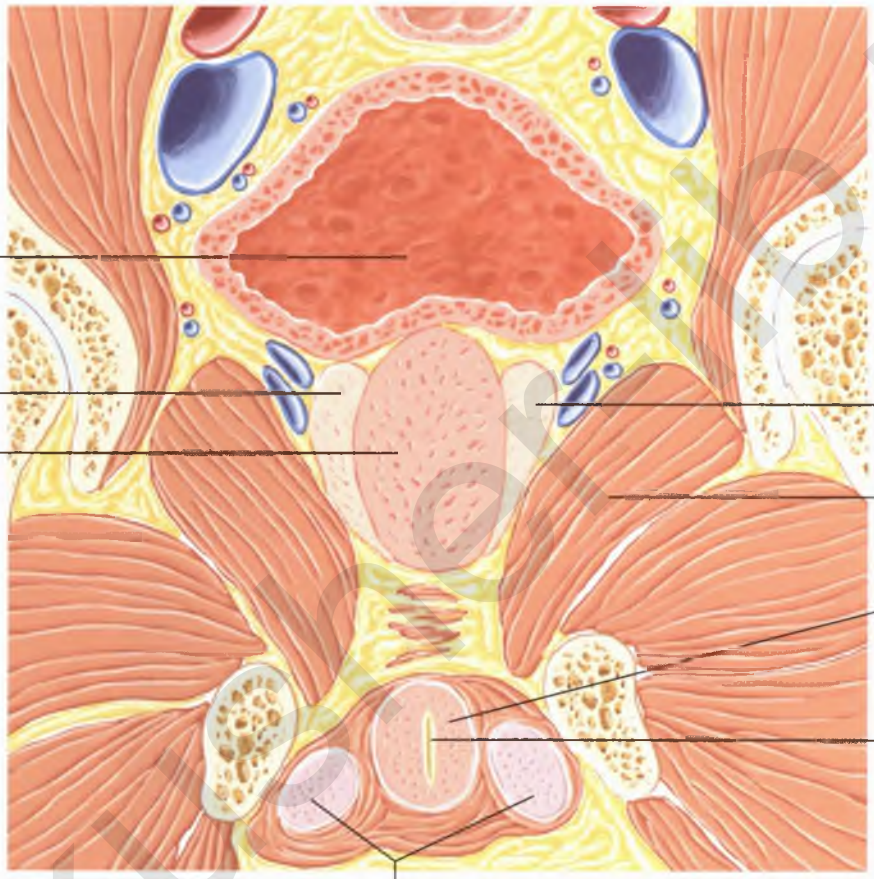
Bladder
Peripheral zone, prostate
Central gland, prostate
Peripheral zone, prostate
Obturator internus m.
Corpus spongiosum in penile bulb, surrounded by bulbospongiosus m.
Bulbar urethra
Crura of corpora cavernosa, surrounded by ischiocavernosus mm.

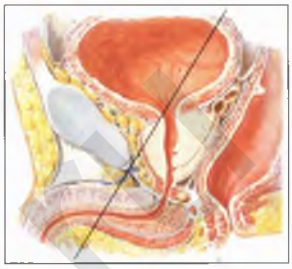

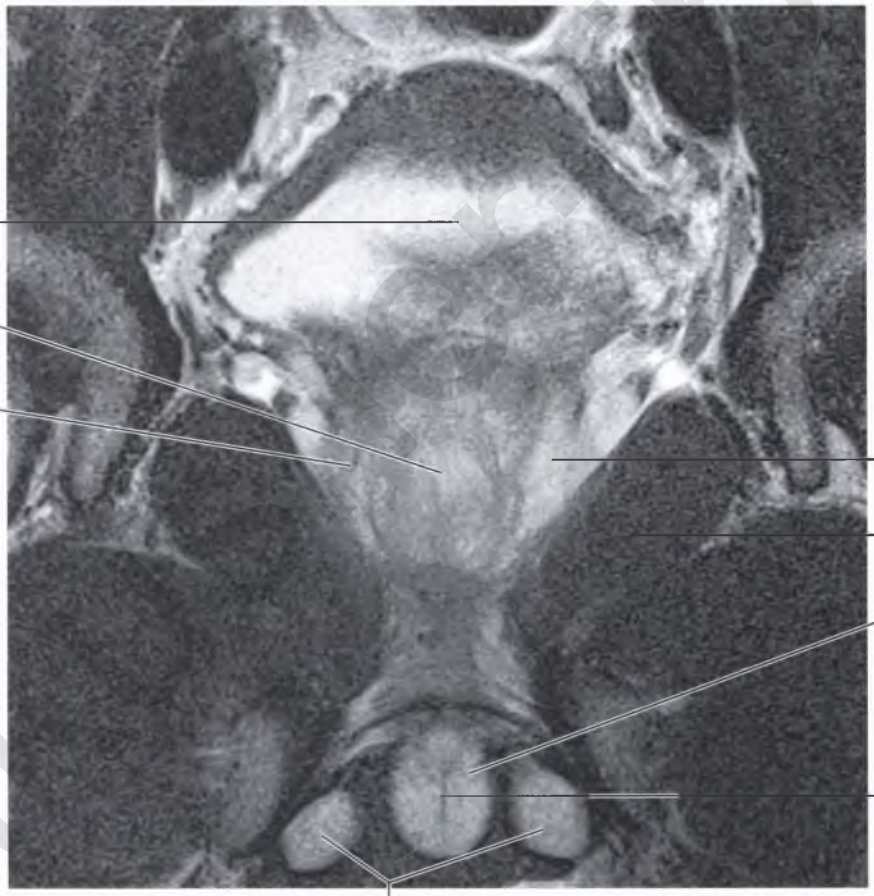
Bladder
Central gland, prostate
Peripheral zone, prostate
Peripheral zone, prostate
Obturator internus m.
Corpus spongiosum in penile bulb, surrounded by bulbospongiosus m.
Bulbar urethra
Crura of corpora cavernosa, surrounded by ischiocavernosus mm.

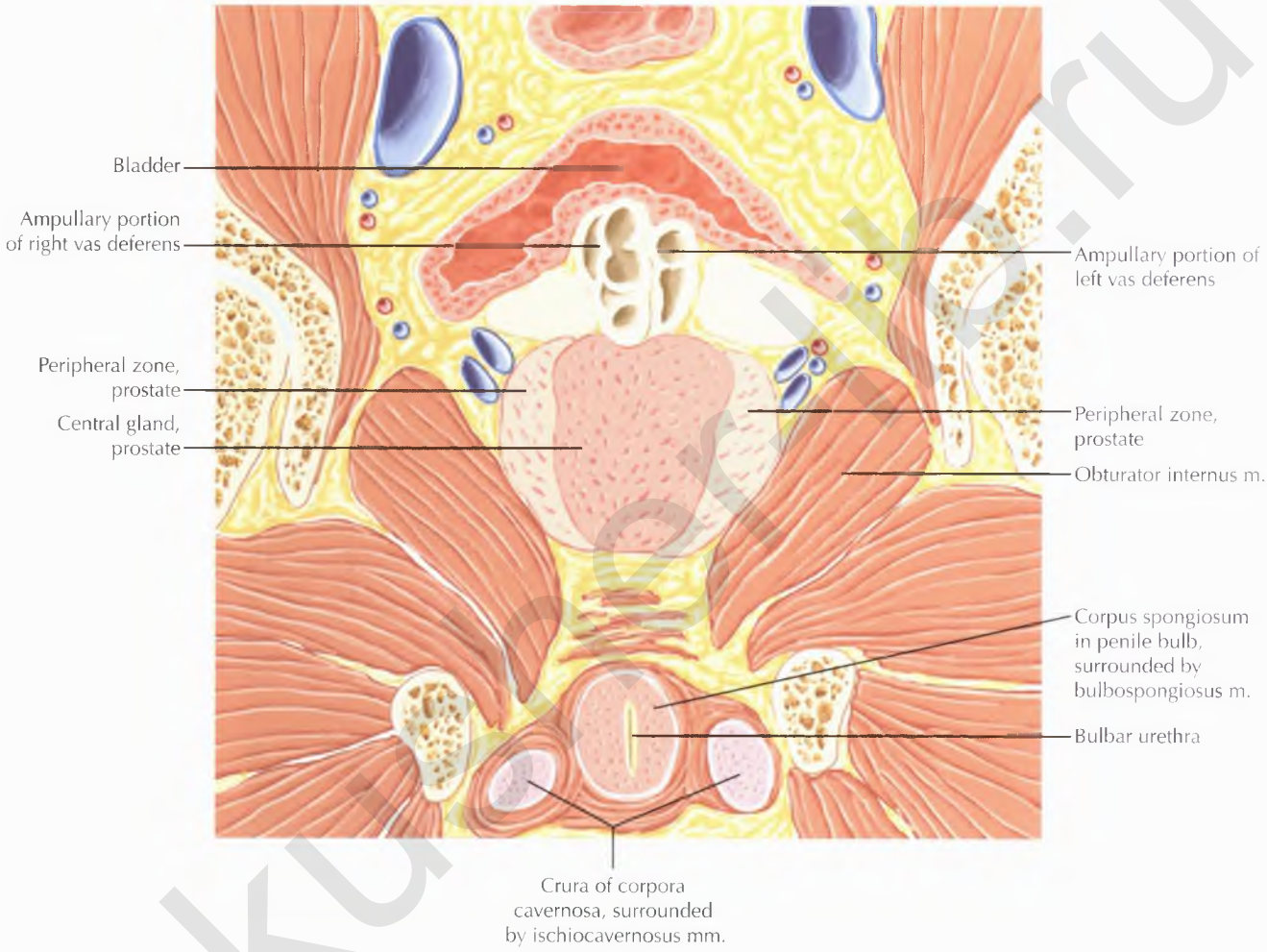

NORMAL ANATOMY

The thick-walled ampullary portion of each vas deferens is located medial and superior to the associated ipsilateral seminal vesicle.

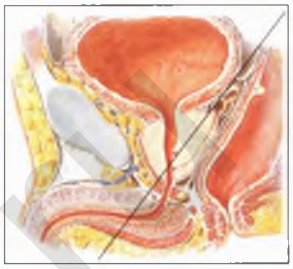

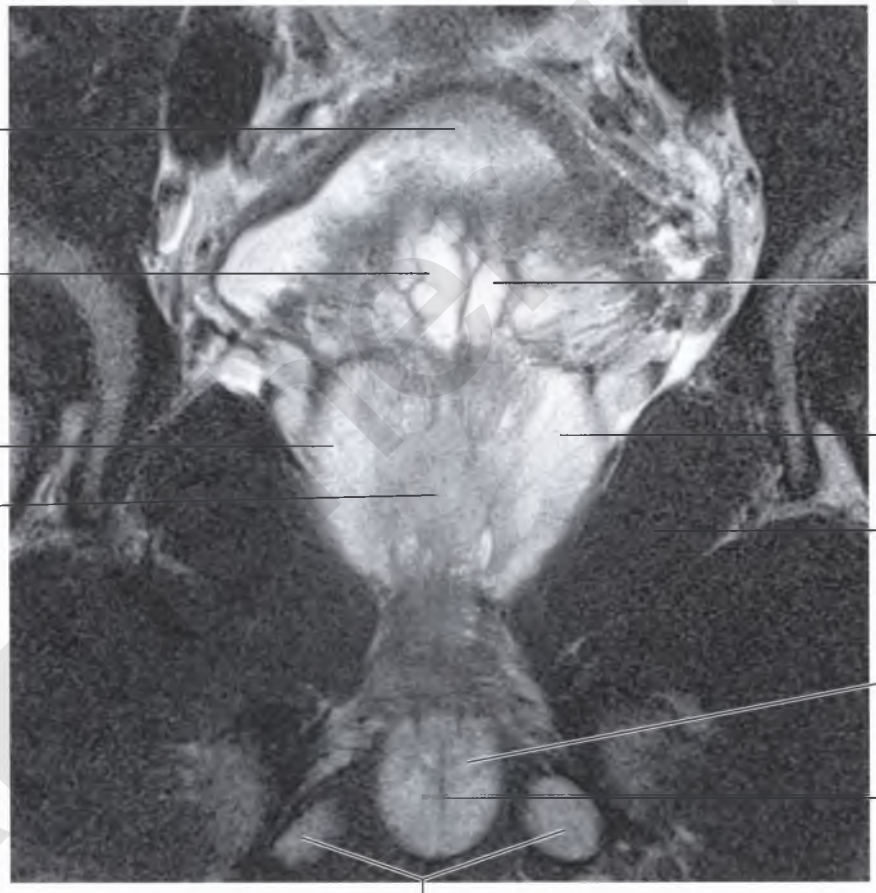
Bladder
Ampullary portion of right vas deferens
Peripheral zone, prostate
Central gland, prostate
Ampullary portion of left vas deferens
Peripheral zone, prostate
Obturator internus m.
Corpus spongiosum in penile bulb, surrounded by bulbospongiosus m.
Bulbar urethra
Crura of corpora cavernosa, surrounded by ischiocavernosus mm.

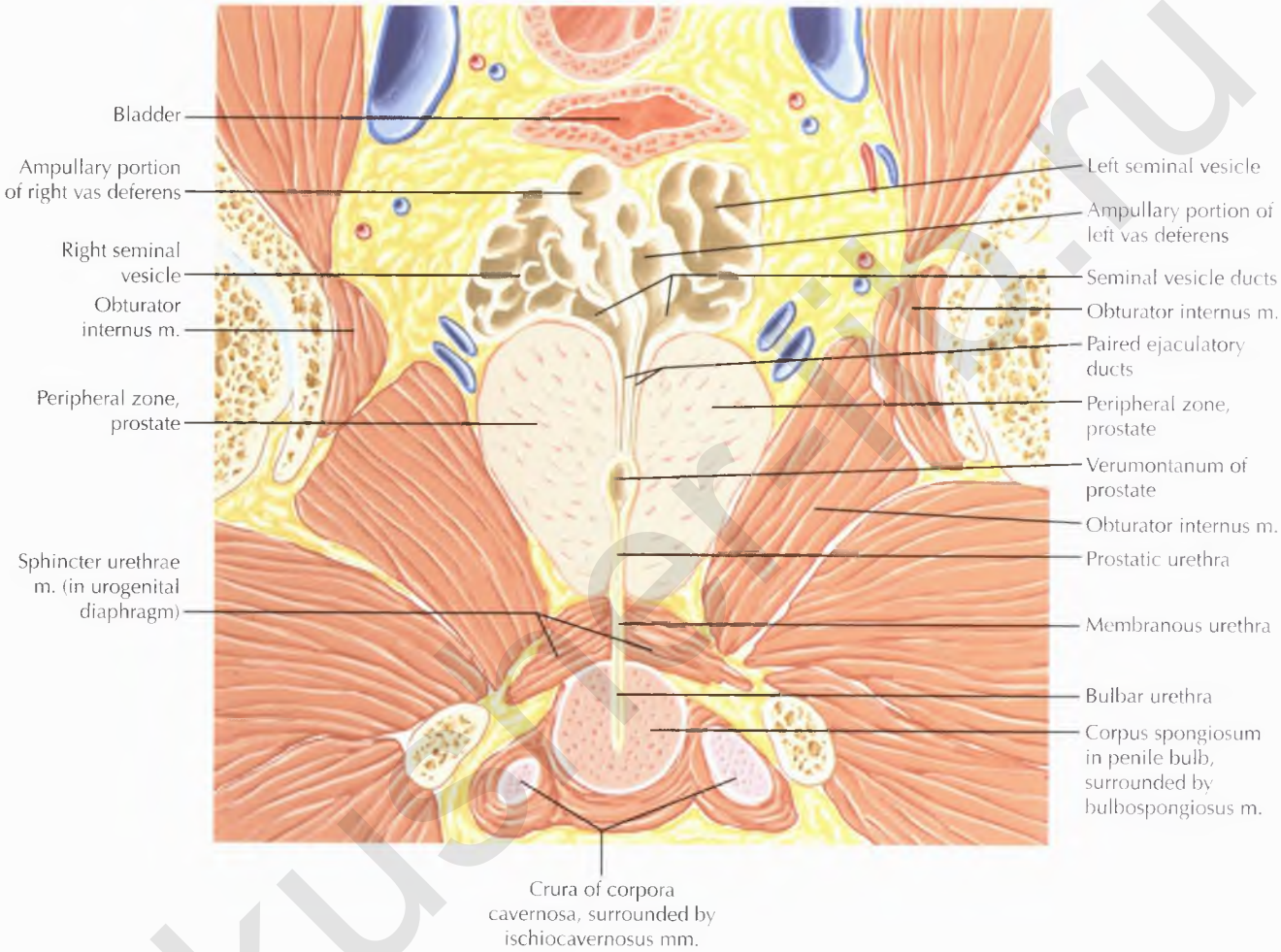

NORMAL ANATOMY

The prostatic, membranous, and bulbar segments of the male urethra are shown at this level. The paired ejaculatory ducts are also seen to traverse the prostate gland and drain into the prostatic urethra on either side of the verumontanum. The membranous urethra is surrounded by the sphincter urethrae muscle in the urogenital diaphragm.

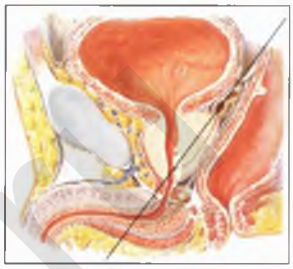

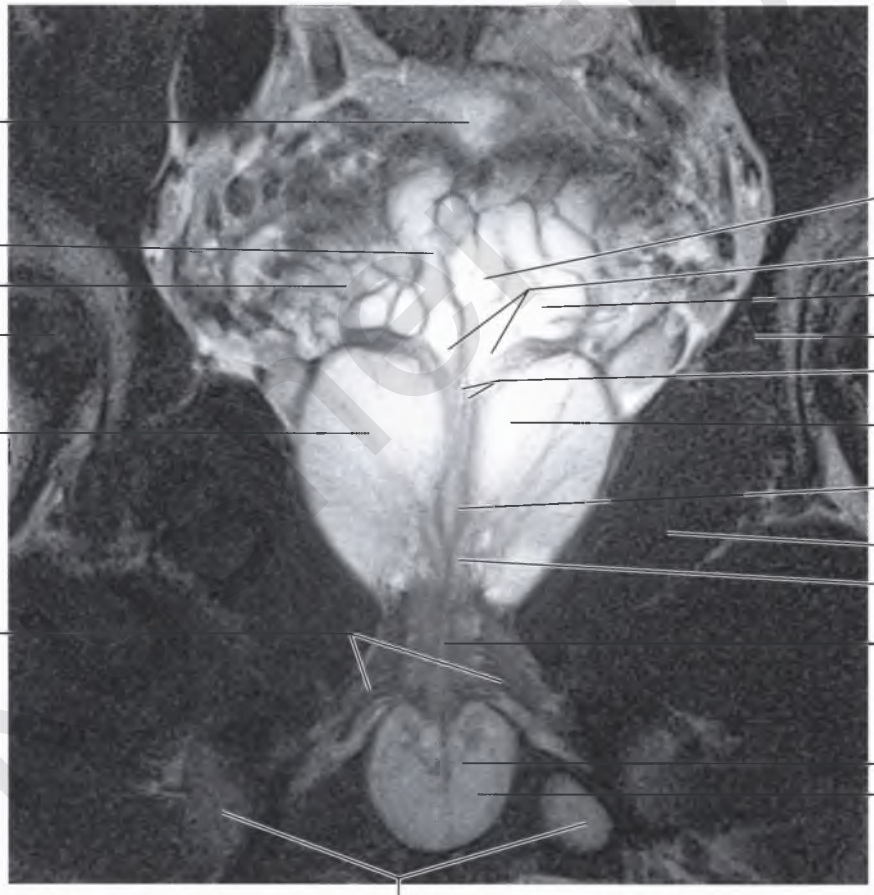
Bladder
Ampullary portion of right vas deferens
Right seminal vesicle
Obturator internus m.
Peripheral zone, prostate
Sphincter urethrae m. (in urogenital diaphragm)
Ampullary portion of left vas deferens
Seminal vesicle ducts
Left seminal vesicle
Obturator internus m.
Paired ejaculatory ducts
Peripheral zone, prostate
Verumontanum of prostate
Obturator internus m.
Prostatic urethra
Membranous urethra
Bulbar urethra
Corpus spongiosum in penile bulb, surrounded by bulbospongiosus m.
Crura of corpora cavernosa, surrounded by ischiocavernosus mm.

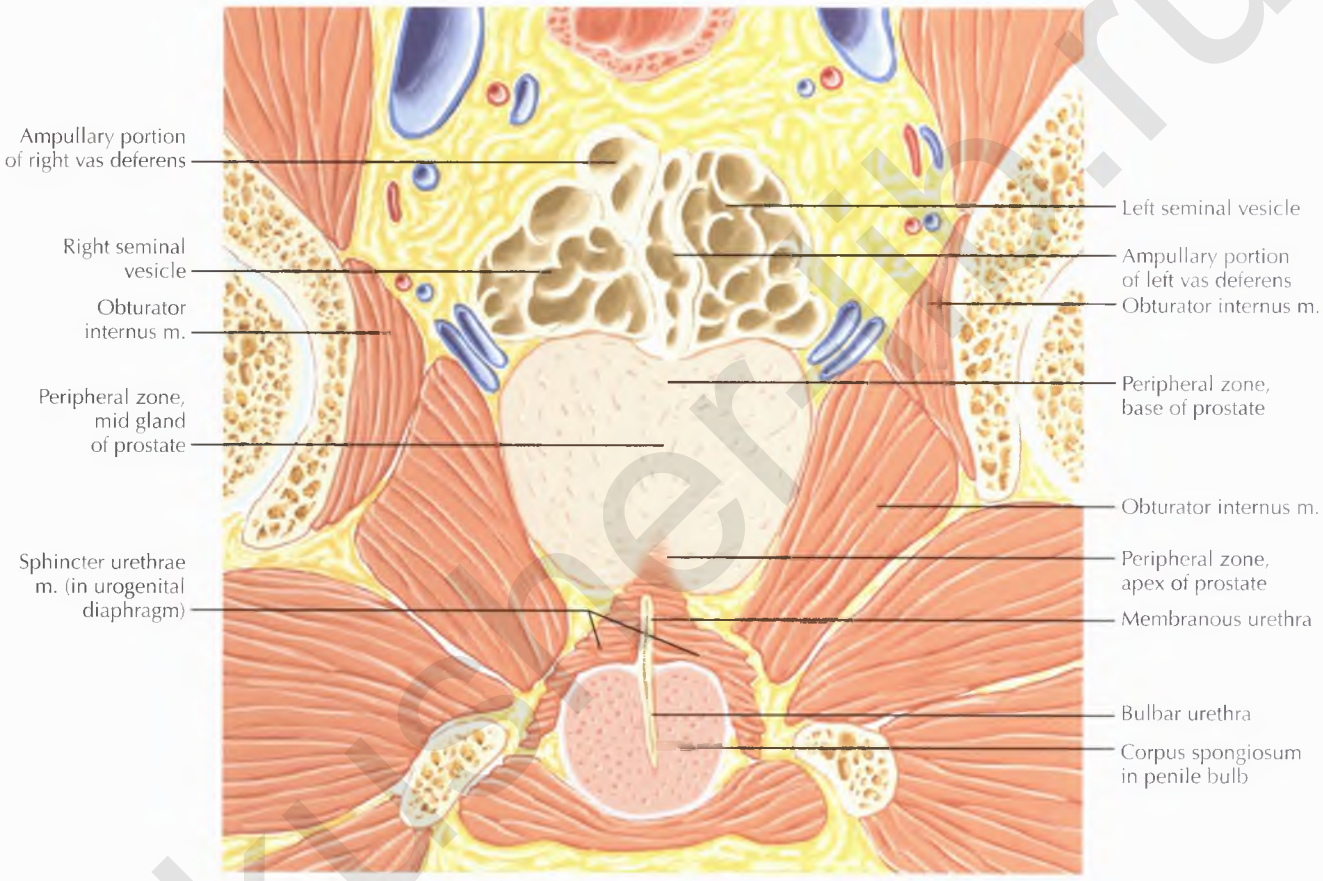

NORMAL ANATOMY

The prostate gland is divided into the base (superiorly), mid gland, and apex (inferiorly).

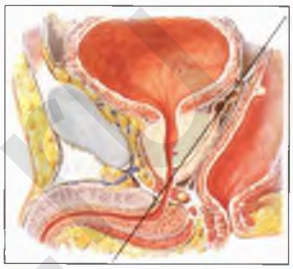

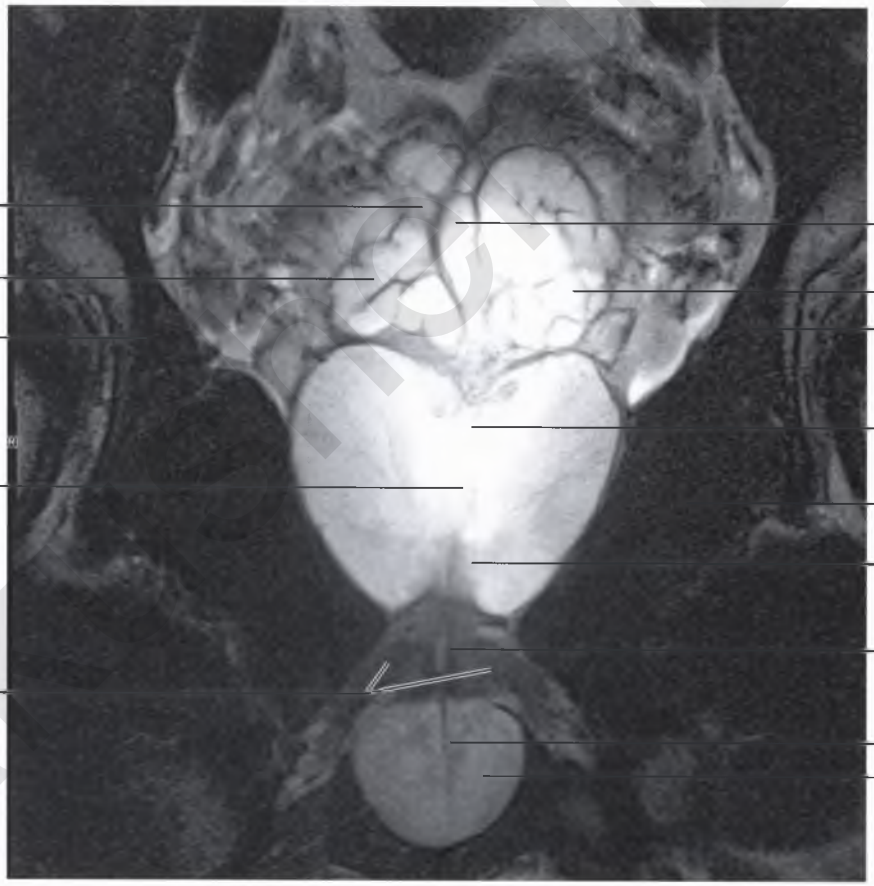


Ampullary portion of right vas deferens
Right seminal vesicle
Obturator internus m.
Peripheral zone, mid gland of prostate
Sphincter urethrae m. (in urogenital diaphragm)
Ampullary portion of left vas deferens
Left seminal vesicle
Obturator internus m.
Peripheral zone, base of prostate
Obturator internus m.
Peripheral zone, apex of prostate
Bulbar urethra
Corpus spongiosum in penile bulb

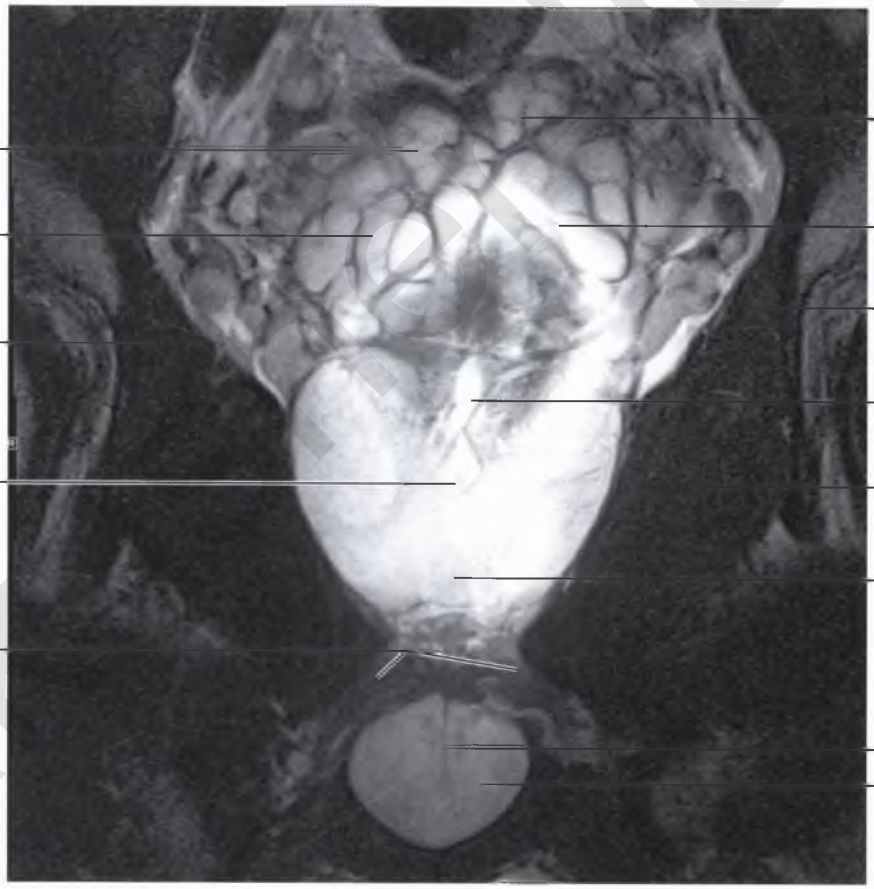

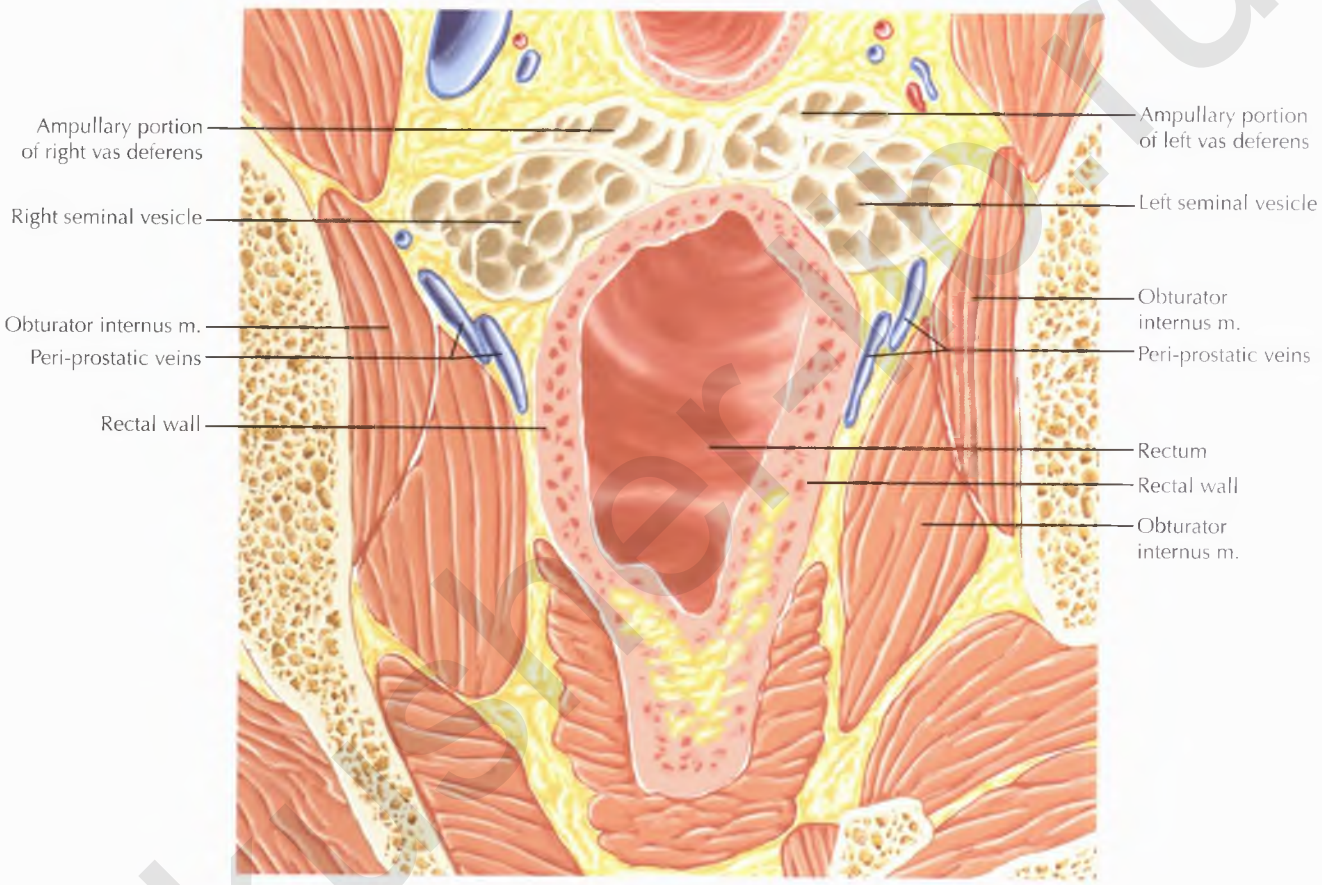

NORMAL ANATOMY

The peri-prostatic veins are usually hyperintense as a result of slow blood flow.

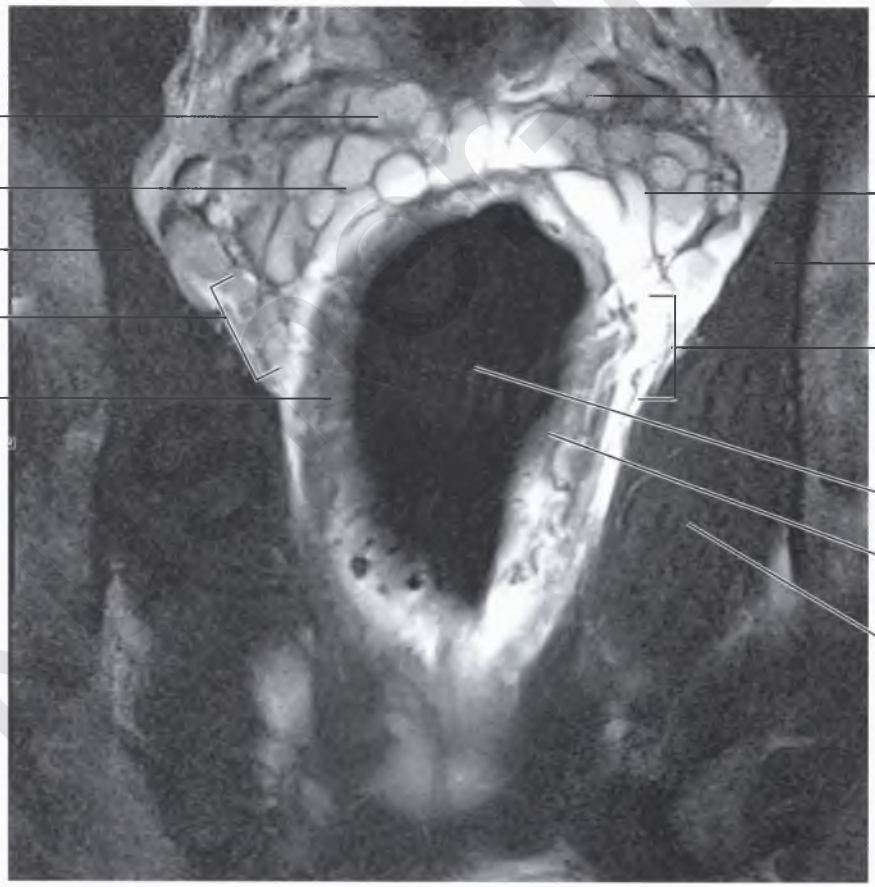
Ampullary portion of right vas deferens
Right seminal vesicle
Obturator internus m.
Peri-prostatic veins
Rectal wall
Ampullary portion of left vas deferens
Left seminal vesicle
Obturator internus m.
Peri-prostatic veins
Rectum
Rectal wall
Obturator internus m.


Seminal vesicle
Bladder
Peripheral zone, mid gland of prostate
Superior pubic ramus
Inferior pubic ramus
Rectal wall
Rectum
Peripheral zone, base of prostate
Peripheral zone, apex of prostate
Obturator internus m.

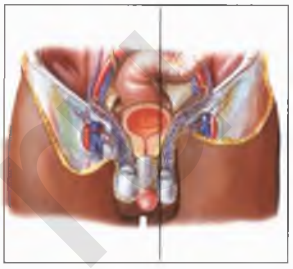

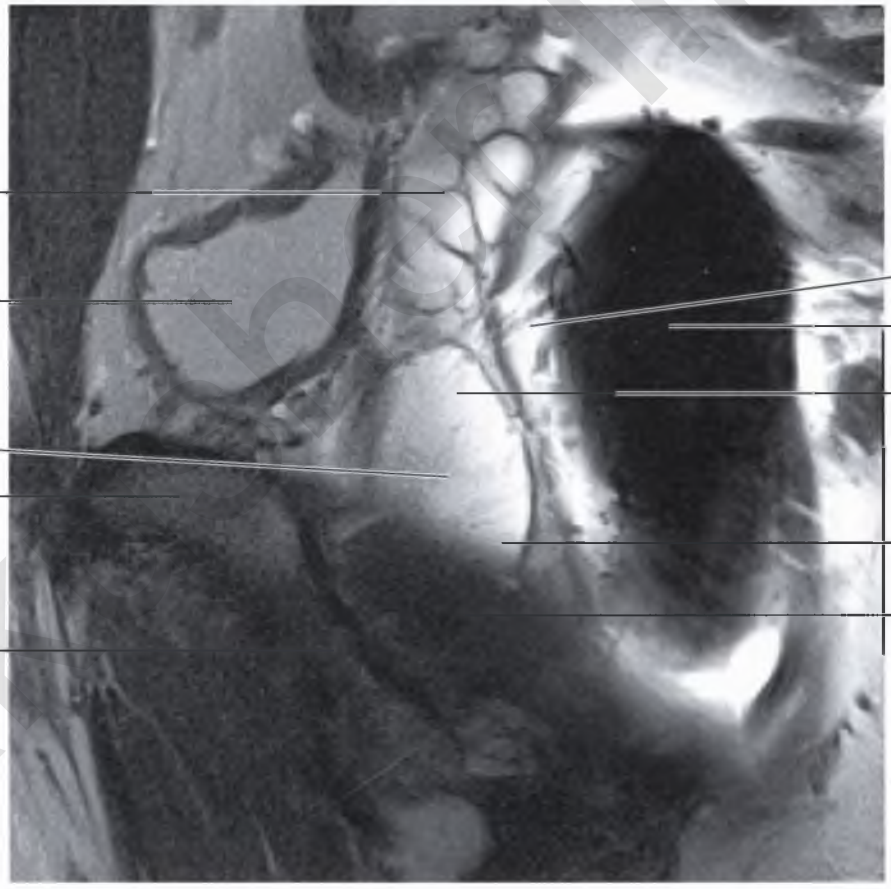


Seminal vesicle
Bladder
Anterior fibromuscular stroma
Peripheral zone, mid gland of prostate
Denonvilliers' fascia
Rectal wall
Rectum
Peripheral zone, base of prostate
Peripheral zone, apex of prostate

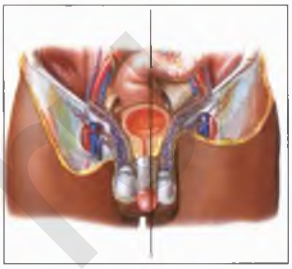

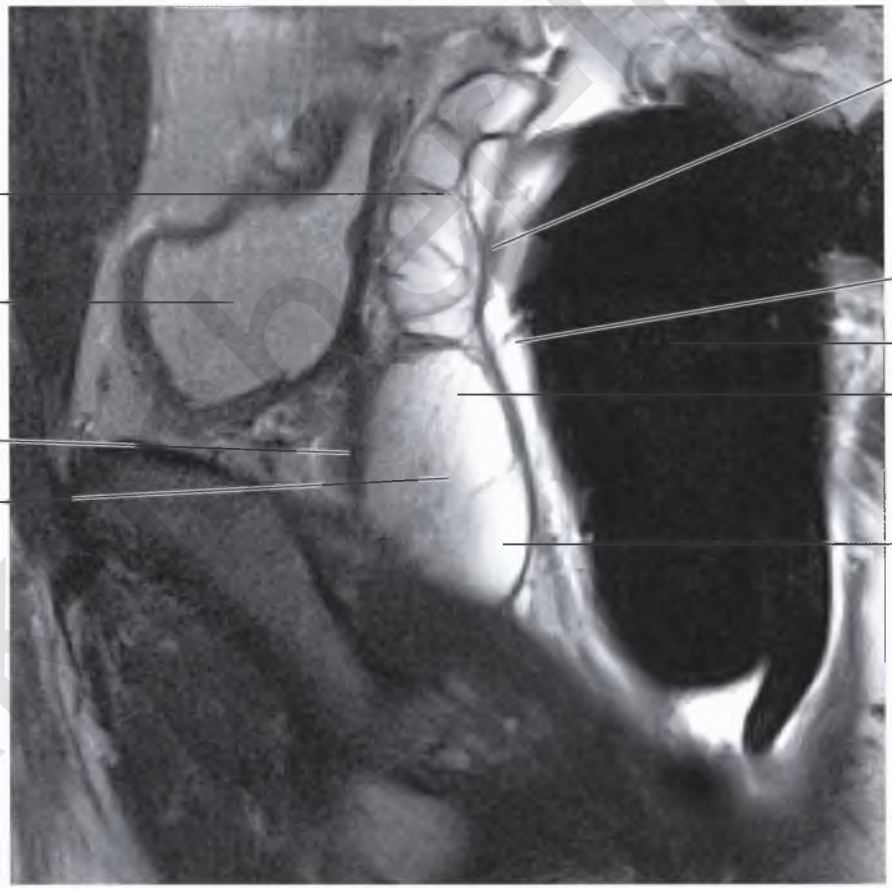
Denonvilliers' fascia
Seminal vesicle
Rectal wall
Bladder
Rectum
Anterior fibromuscular stroma
Peripheral zone, base of prostate
Peripheral zone, mid gland of prostate
Peripheral zone, apex of prostate

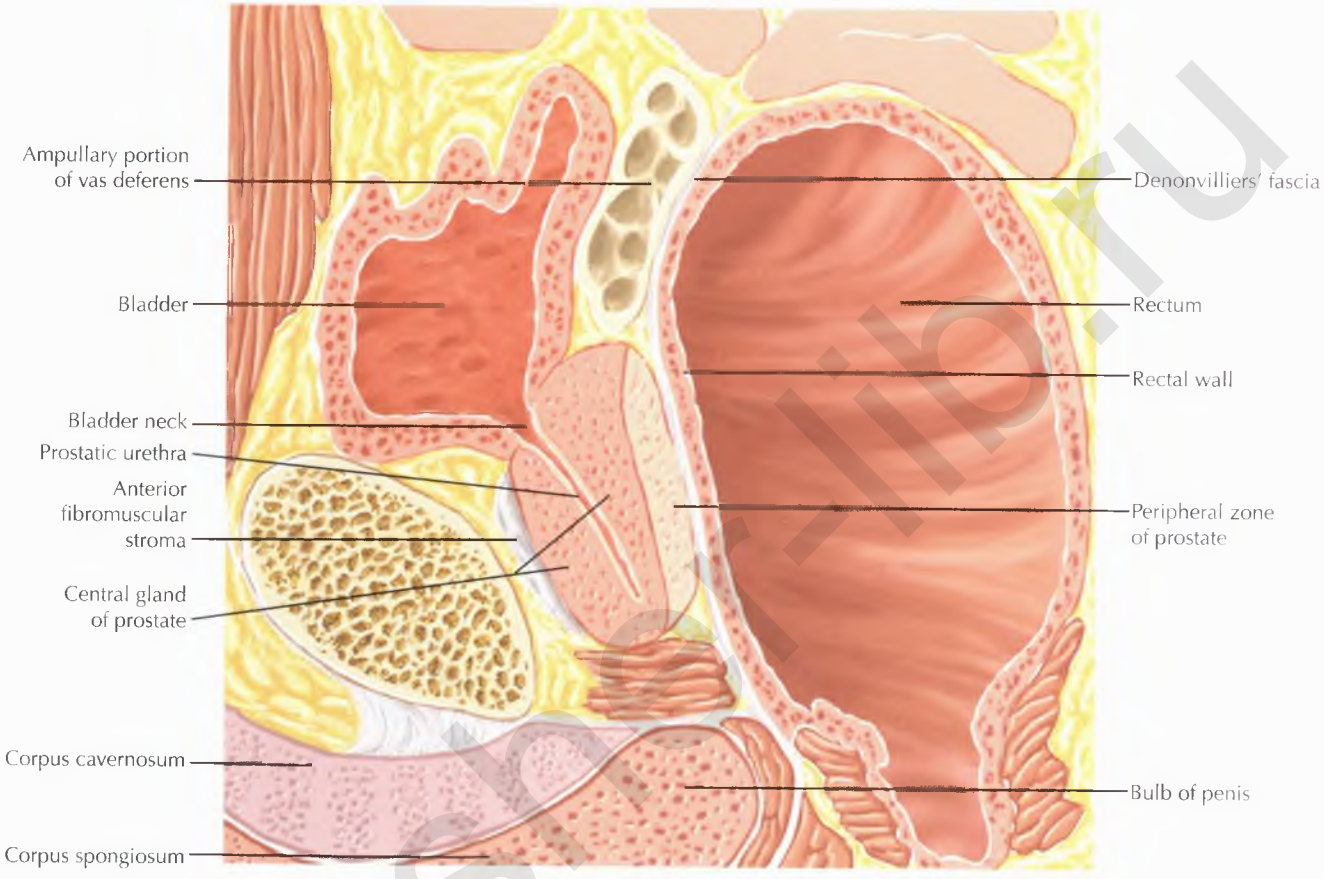

PATHOLOGIC PROCESS

Utricular and müllerian duct cysts are midline cystic structures that are often incidentally detected in the prostate gland. If symptomatic, these cysts may cause irritative or obstructive lower urinary tract symptoms as a result of compression of the prostatic urethra or ejaculatory ducts. On MRI, *müllerian duct cysts* often have a teardrop shape and may extend above the superior aspect of the prostate gland, but do not communicate with the urethra or ejaculatory duct. In contrast, *utricular cysts* do not extend above the superior aspect of the prostate gland, but may communicate with the posterior urethra or ejaculatory duct. Therefore, utricular cysts may opacify during retrograde urethrography, voiding cystourethrography, or seminal vesiculography.

Ejaculatory duct cysts are usually found in a paramedian location along the course of the ejaculatory duct and are thought to result from partial obstruction of the ejaculatory duct.

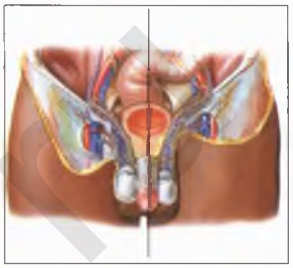

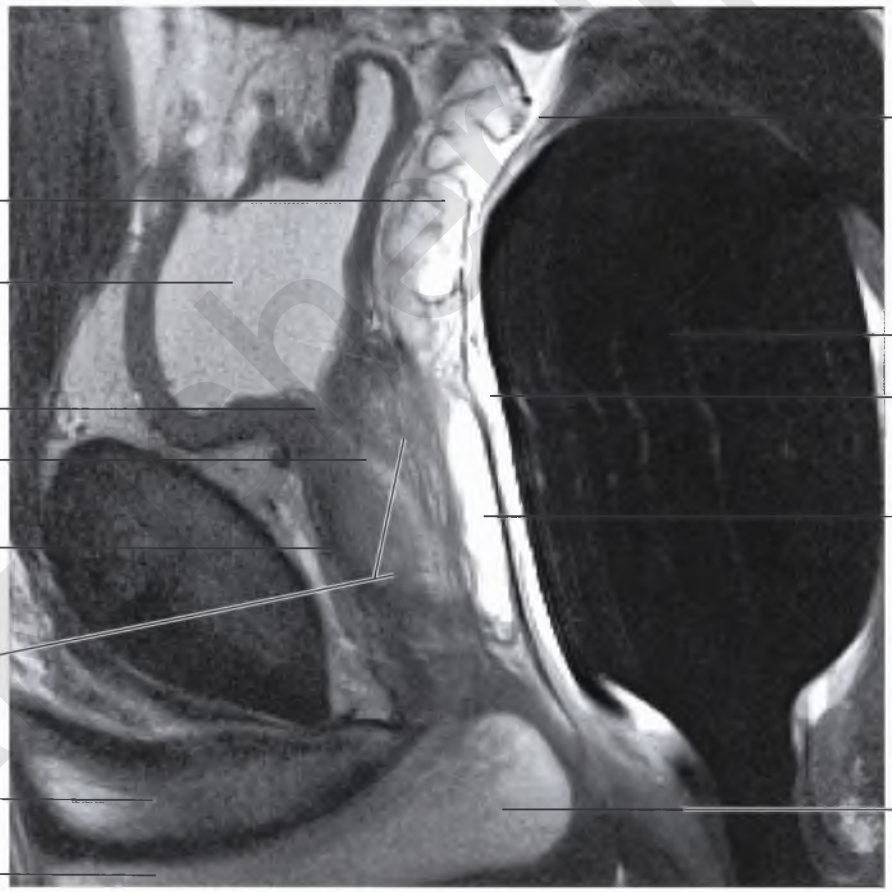
Ampullary portion of vas deferens
Bladder
Bladder neck
Prostatic urethra
Anterior fibromuscular stroma
Central gland of prostate
Corpus cavernosum
Corpus spongiosum
Denonvilliers' fascia
Rectum
Rectal wall
Peripheral zone of prostate
Bulb of penis

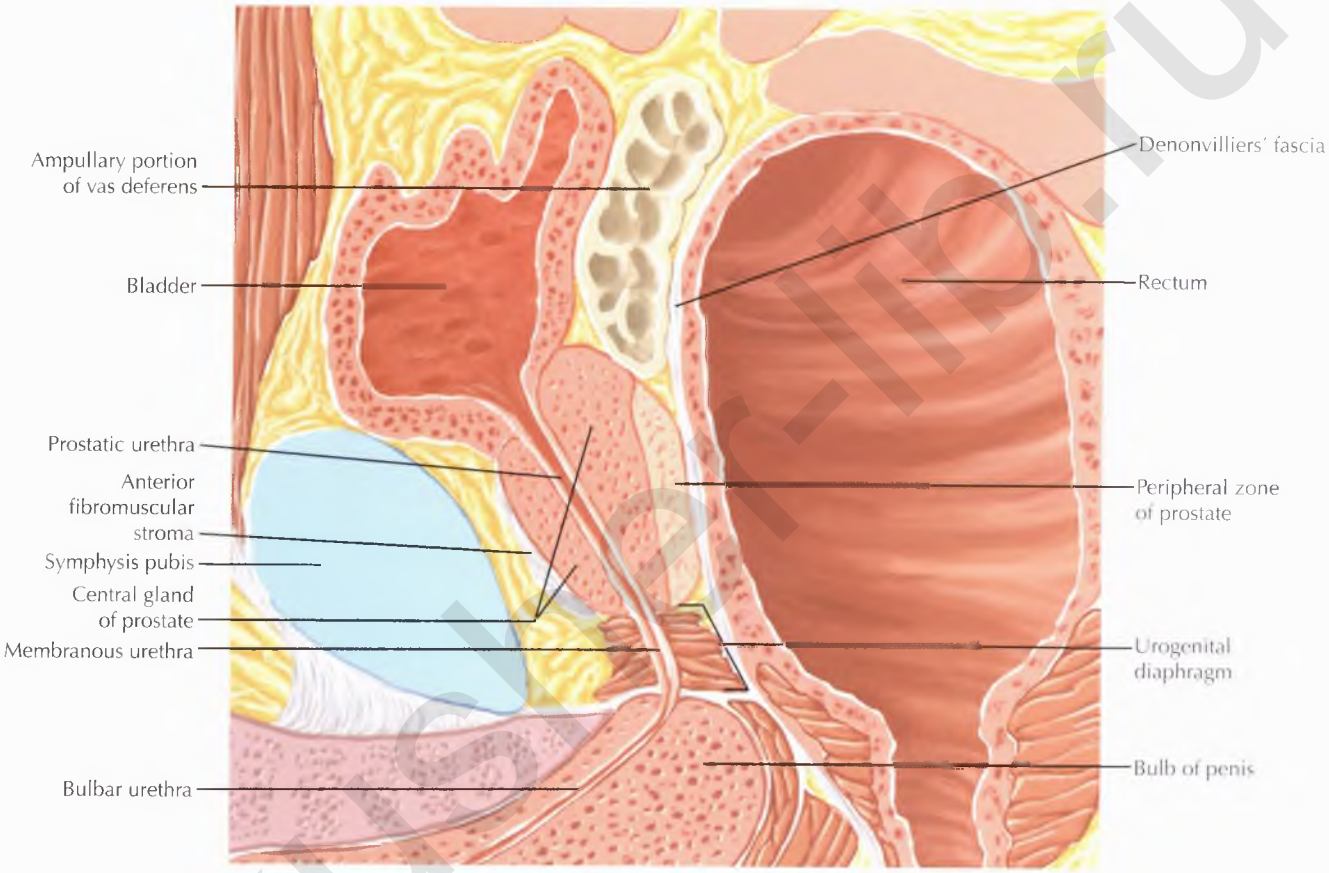

DIAGNOSTIC CONSIDERATION

Sagittal localizer sequences are initially obtained during endorectal coil MRI of the prostate gland to confirm optimal placement of the endorectal coil before acquisition of additional images. The use of an endorectal coil improves image quality and accuracy in the evaluation of prostate cancer.

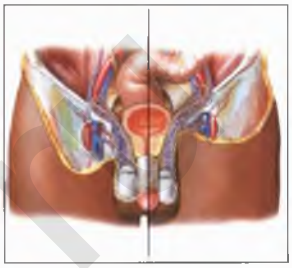

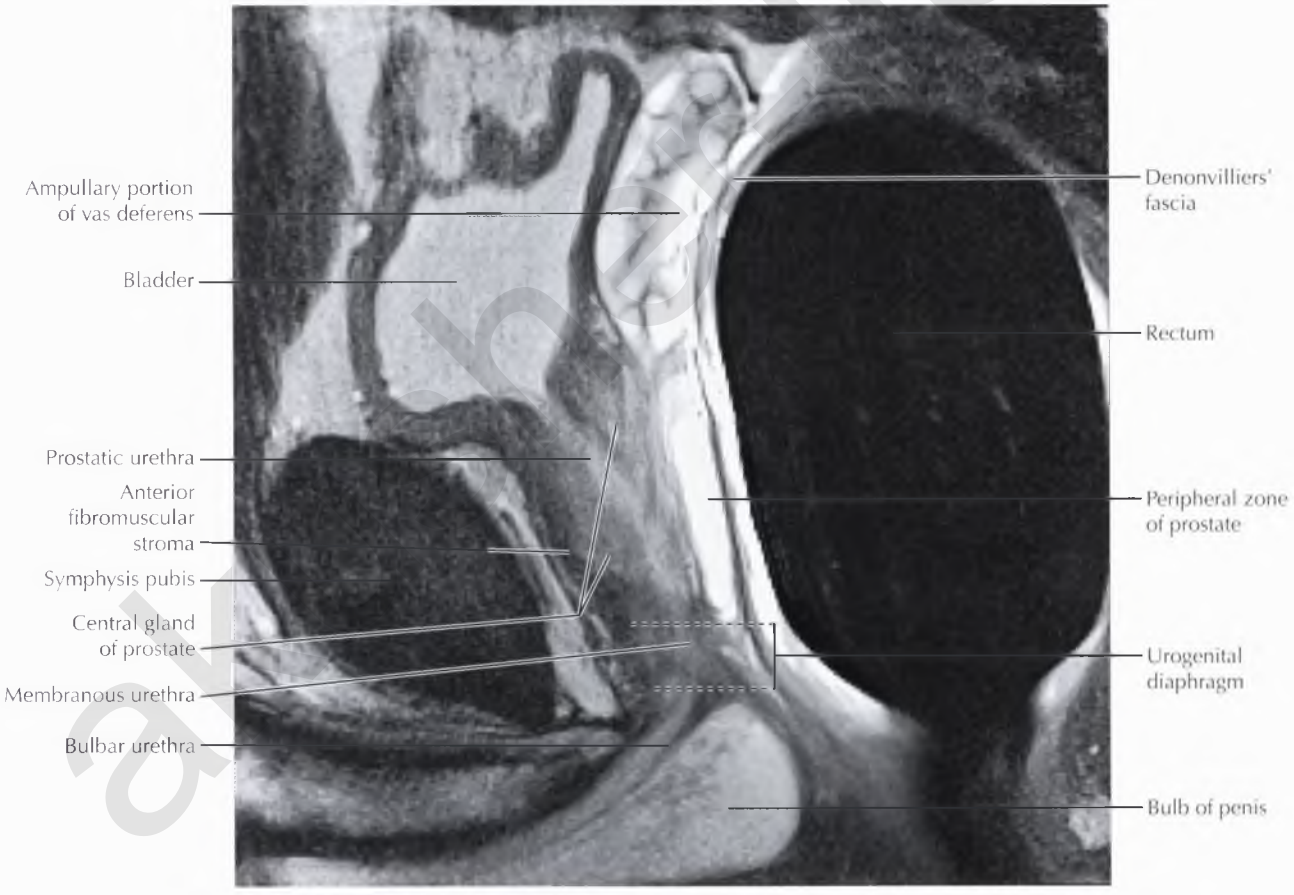
Ampullary portion of vas deferens
Bladder
Prostatic urethra
Anterior fibromuscular stroma
Symphysis pubis
Central gland of prostate
Membranous urethra
Bulbar urethra
Denonvilliers' fascia
Rectum
Peripheral zone of prostate
Urogenital diaphragm
Bulb of penis

Chapter 8 SCROTUM AND TESTES

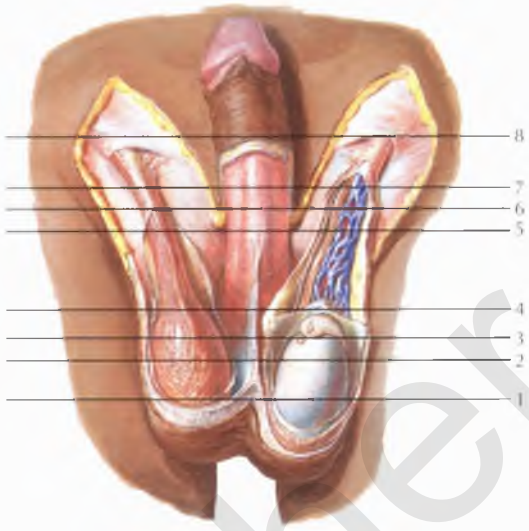

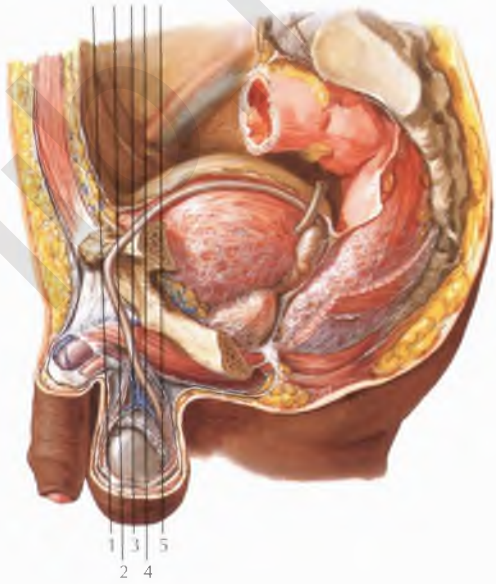

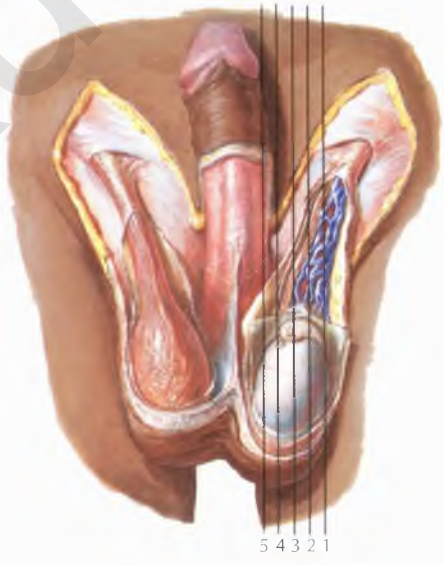

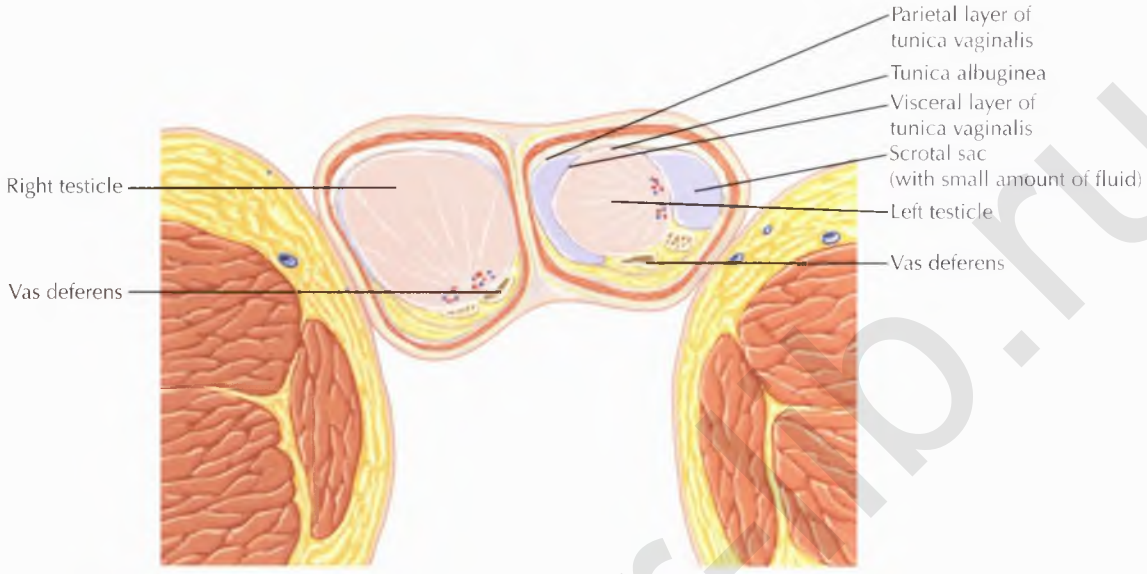

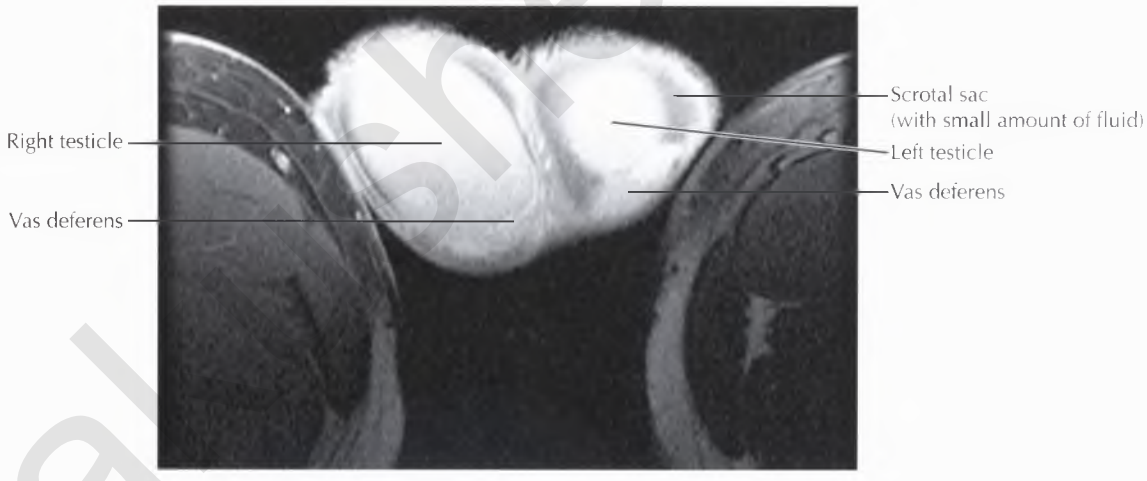

NORMAL ANATOMY

On magnetic resonance imaging (MRI), the testicles (testes) are of uniform intermediate signal intensity on T1-weighted images, moderately high signal intensity on T2-weighted images, and enhance homogenously after intravenous contrast administration.

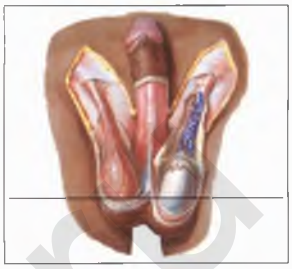

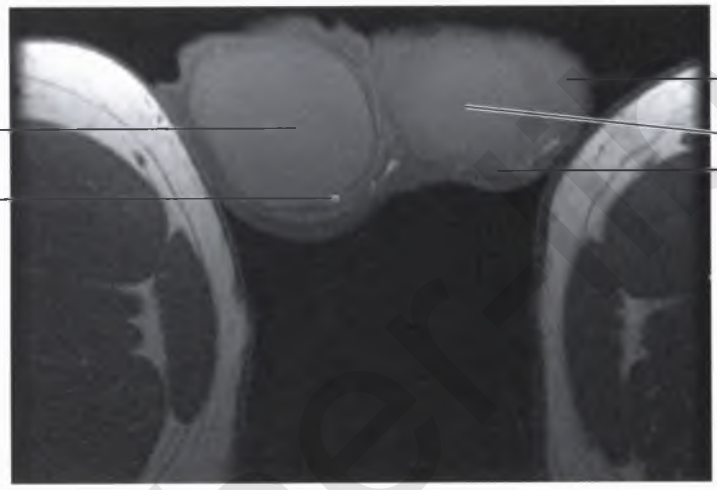
Right testicle
Vas deferens
Scrotal sac
(with small amount of fluid)
Left testicle
Vas deferens

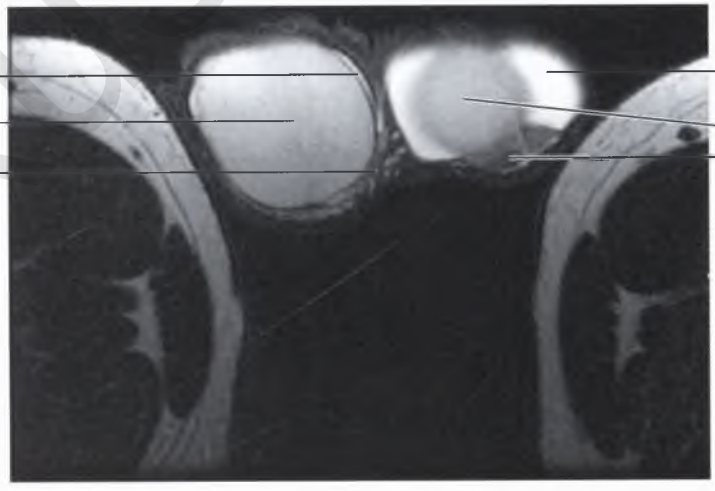
Visceral layer of tunica vaginalis
Right testicle
Vas deferens
Scrotal sac
(with small amount of fluid)
Left testicle
Vas deferens

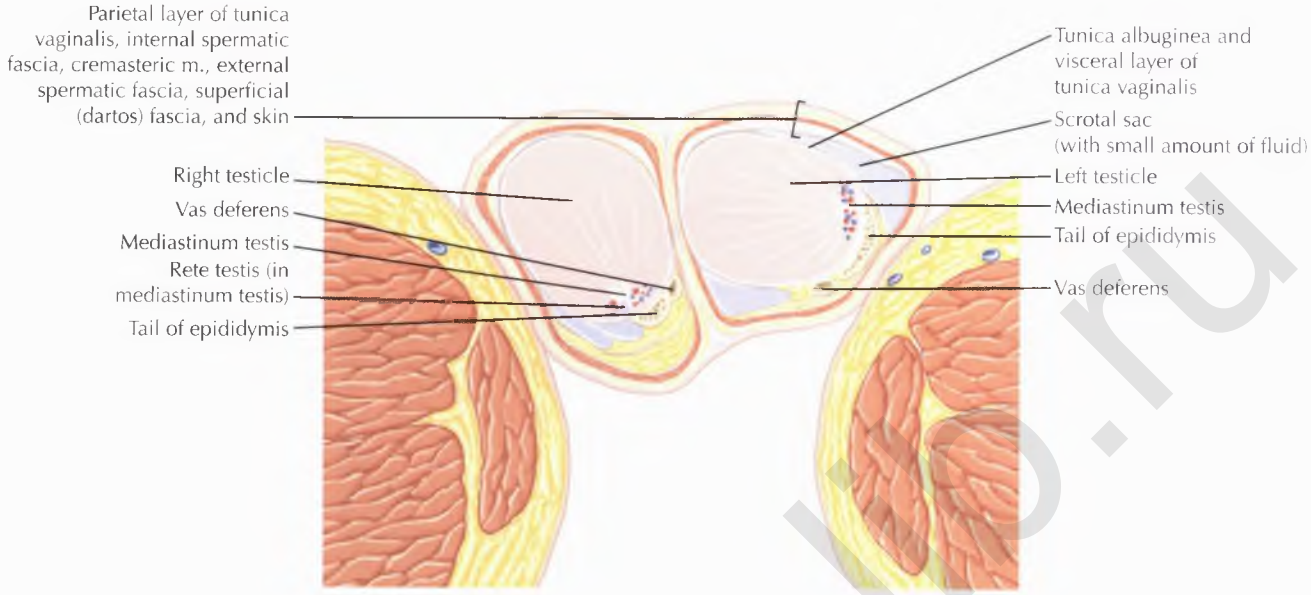

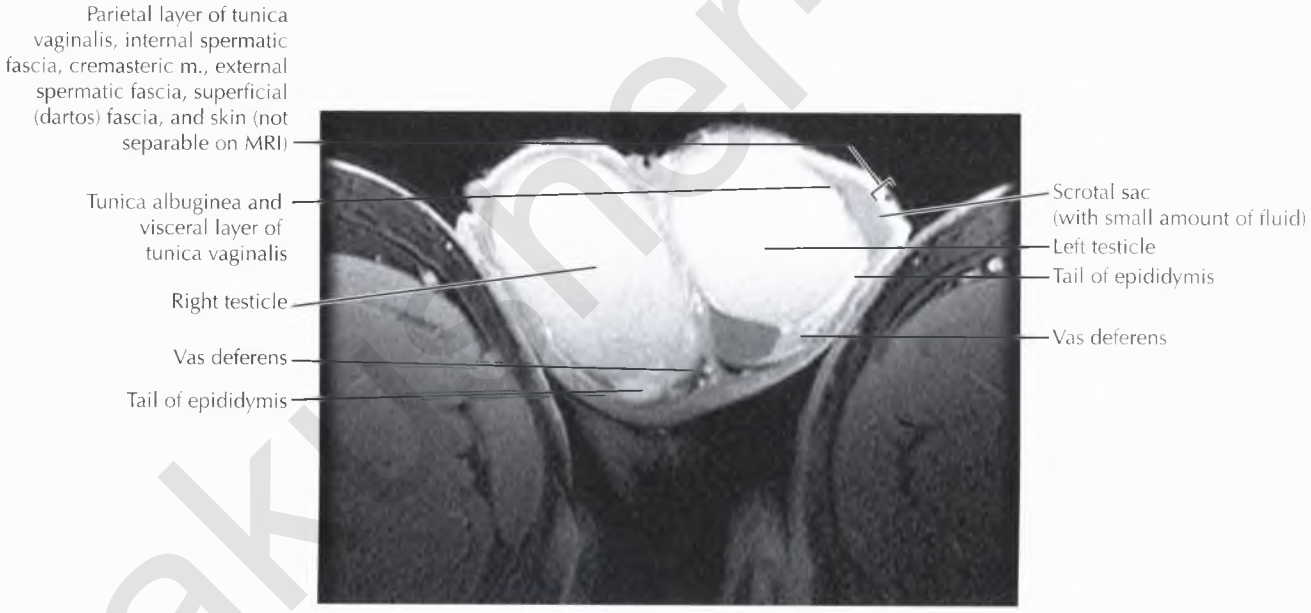

NORMAL ANATOMY

The testicles are composed of densely packed seminiferous tubules that converge posteriorly into larger ducts and drain into the rete testis at the testicular hilum. The *mediastinum testis* appears as a linear band of low signal intensity at the testicular hilum, where the ducts, nerves, and vessels enter and exit the testicle, while the *rete testis* has high signal intensity on T2-weighted MR images. It is important to be aware of the normal appearance and location of the mediastinum testis and rete testis so that these structures are not mistaken for pathology.

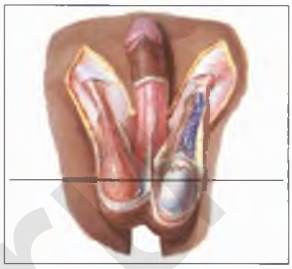

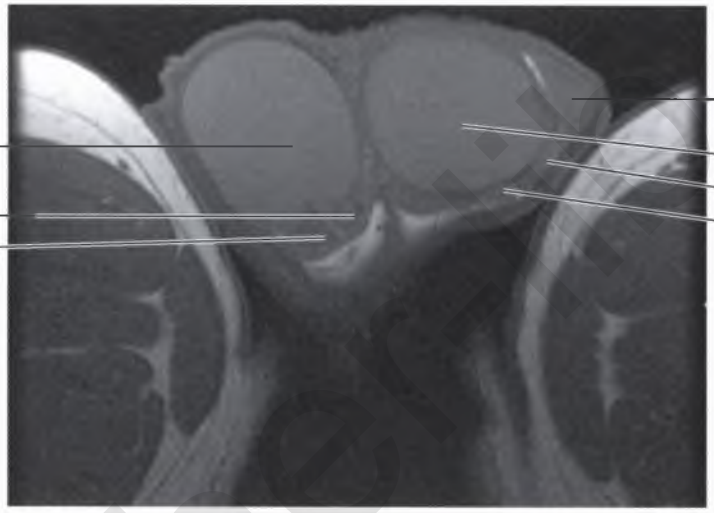
Right testicle
Vas deferens
Tail of epididymis
Scrotal sac
(with small amount of fluid)
Left testicle
Tail of epididymis
Vas deferens

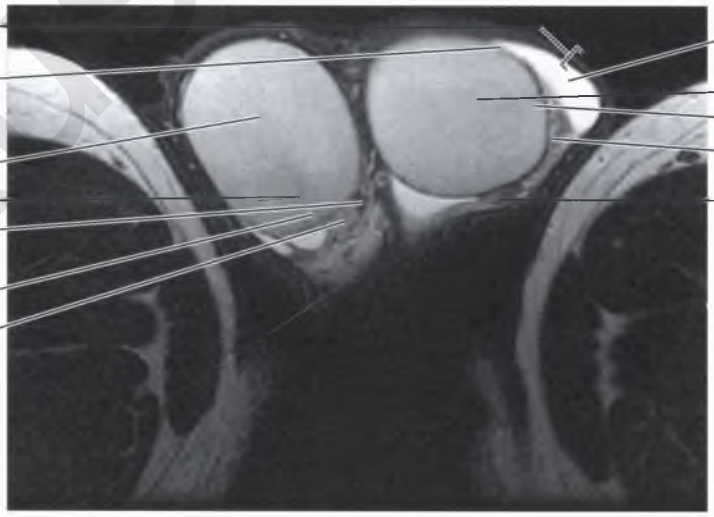
Parietal layer of tunica vaginalis, internal spermatic fascia, cremasteric m., external spermatic fascia, superficial (dartos) fascia, and skin (not separable on MRI)
Tunica albuginea and visceral layer of tunica vaginalis
Right testicle
Mediastinum testis
Vas deferens
Rete testis (in mediastinum testis)
Tail of epididymis
Scrotal sac
(with small amount of fluid)
Left testicle
Mediastinum testis
Tail of epididymis
Vas deferens

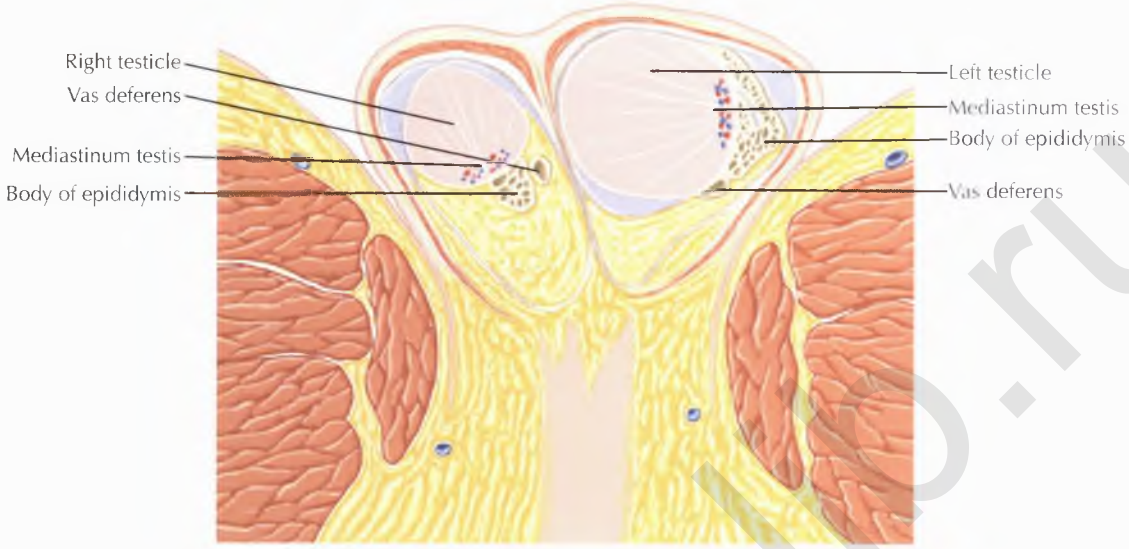

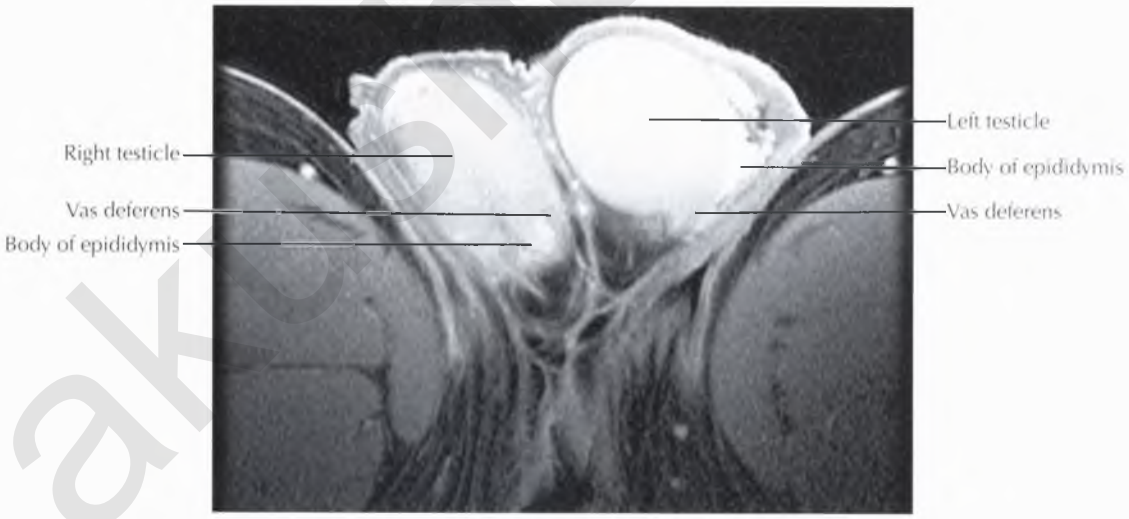

NORMAL ANATOMY

The epididymides are isointense to slightly hypointense in signal intensity relative to the testicles on T1-weighted images, and hypointense to the testicles on T2-weighted MR images.

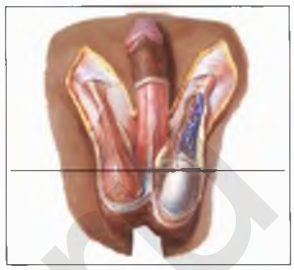

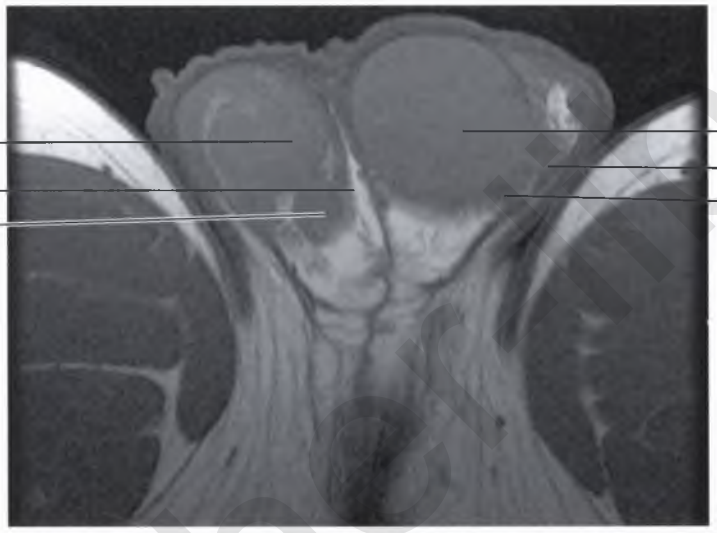

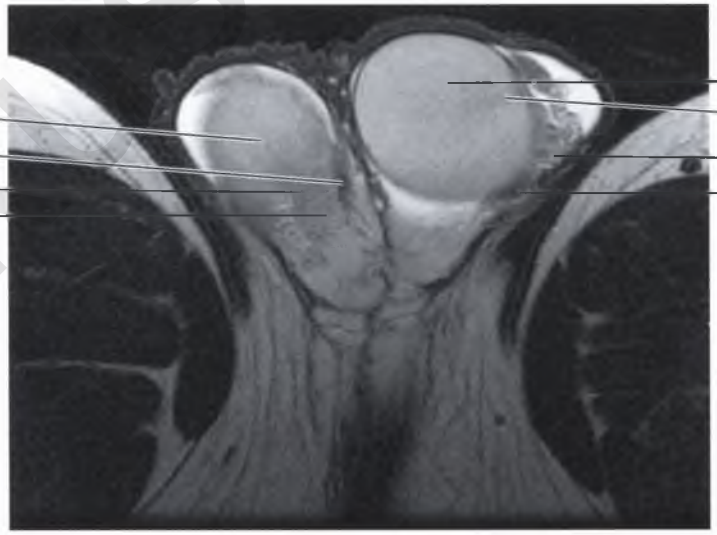

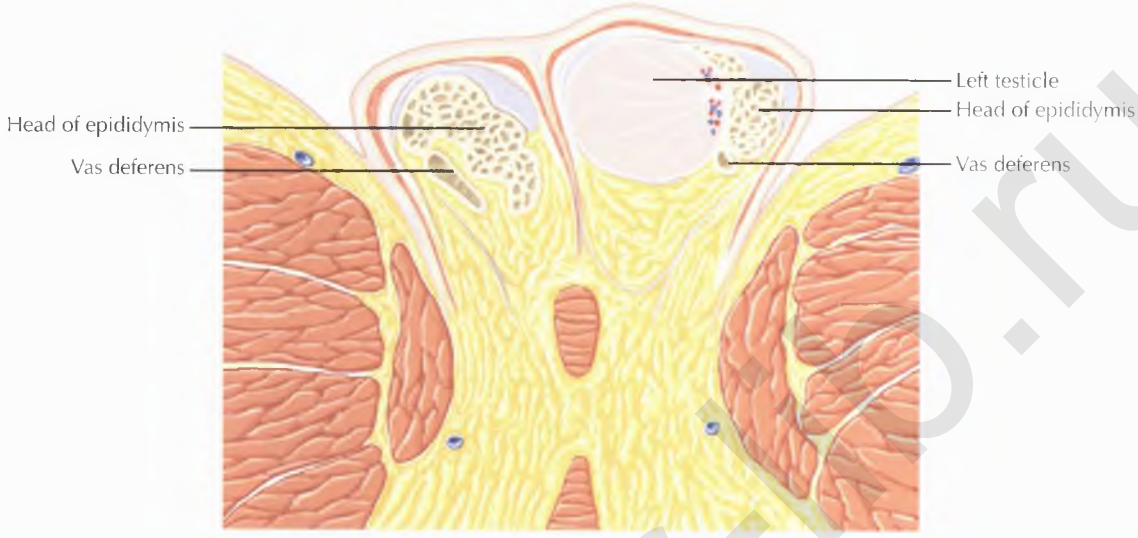

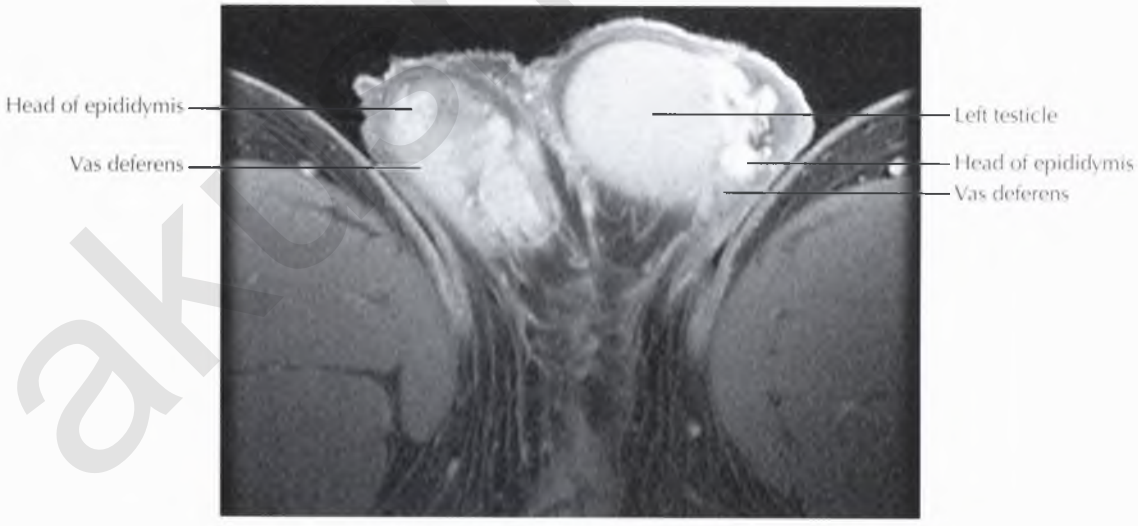

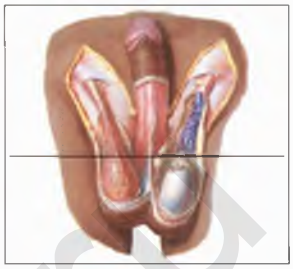

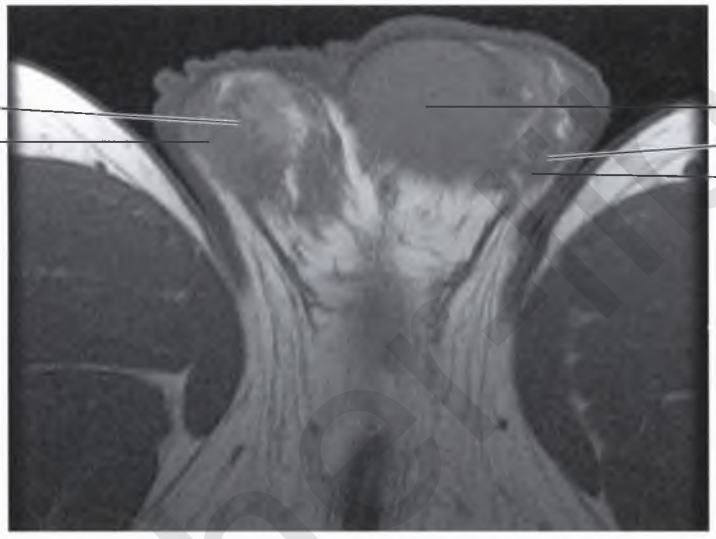
Head of epididymis
Vas deferens
Left testicle
Head of epididymis
Vas deferens

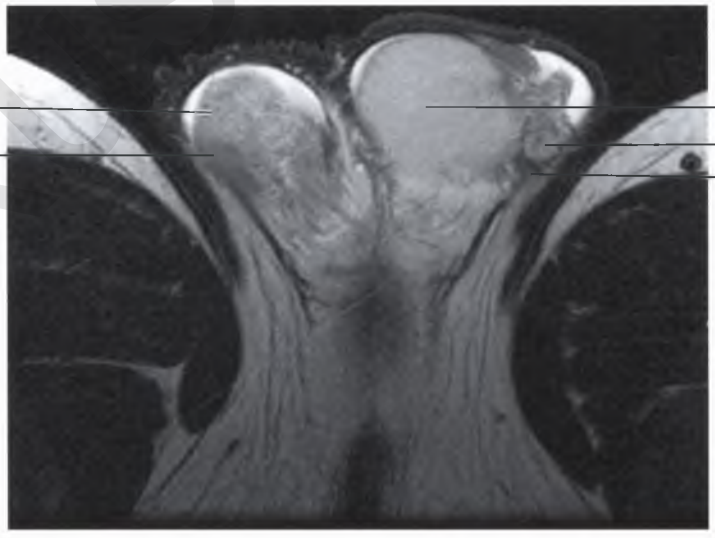
Head of epididymis
Vas deferens
Left testicle
Head of epididymis
Vas deferens

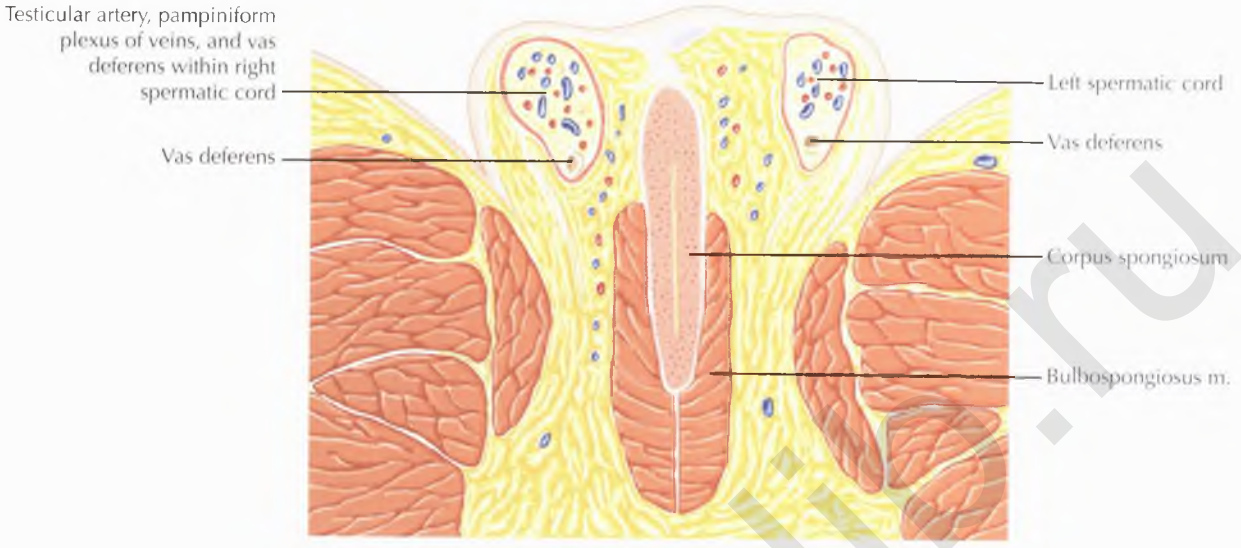

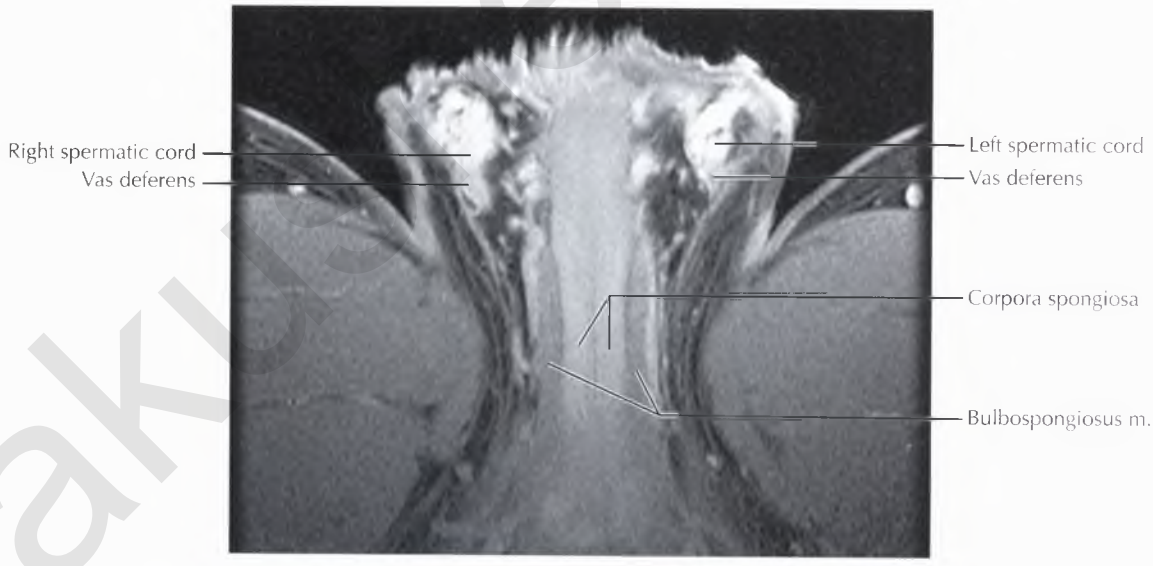

NORMAL ANATOMY

In men, the inguinal canal transfers the *spermatic cord*, which includes the vas deferens, testicular artery, pampiniform plexus of veins, and genital branch of the genitofemoral nerve, from the pelvic cavity to the scrotum.

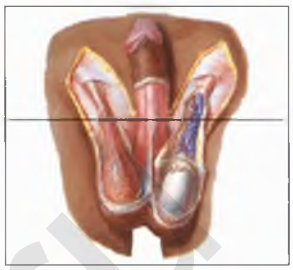

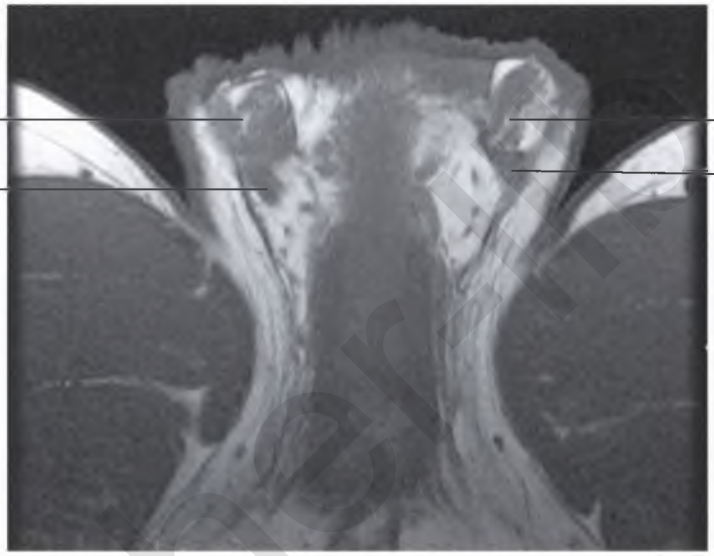

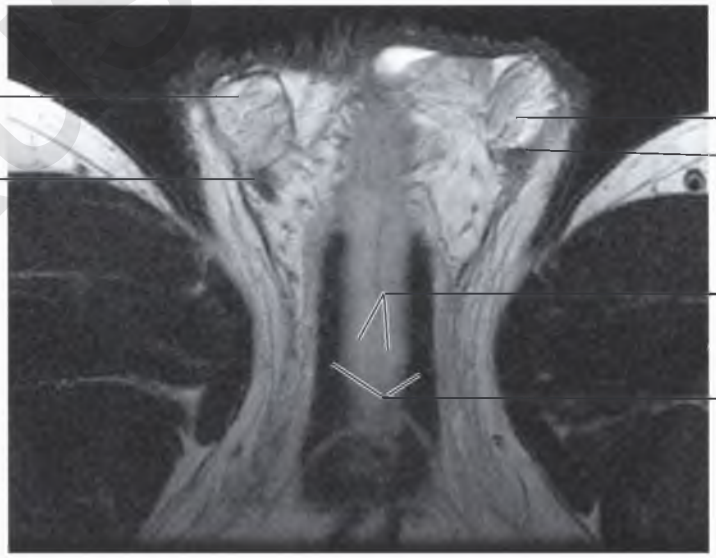

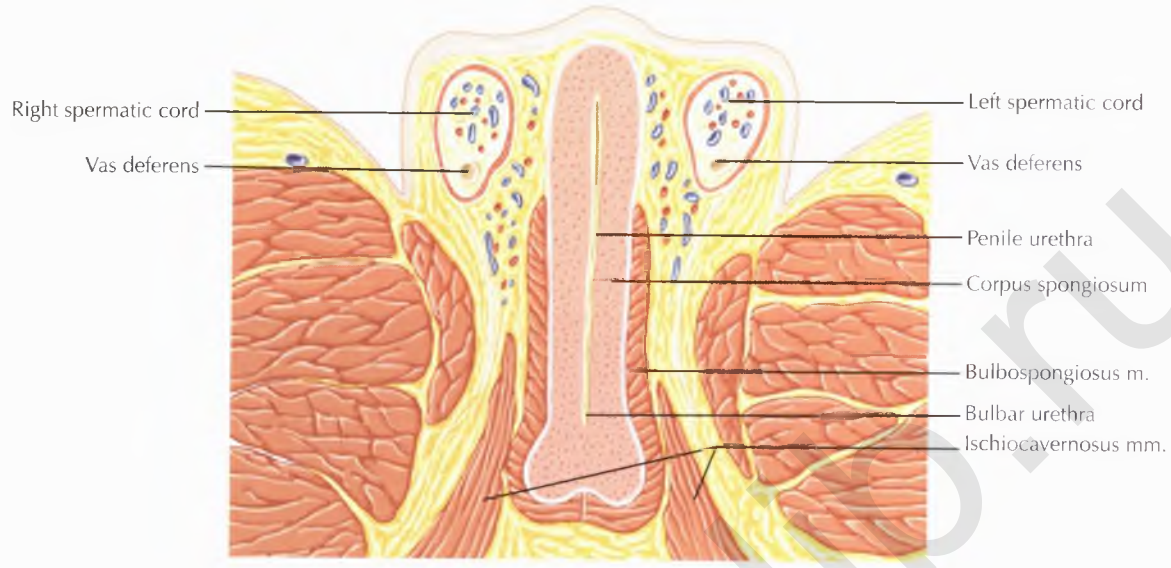

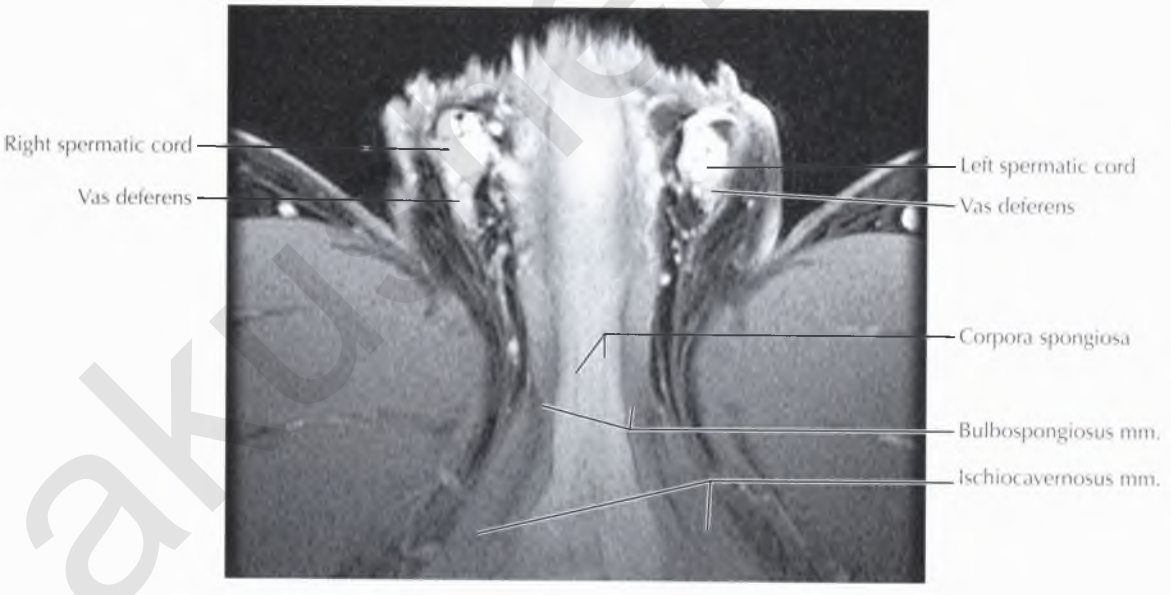

DIAGNOSTIC CONSIDERATION

Lymphatic drainage of the testicles and epididymides follows venous drainage, with the left side draining to the left para-aortic nodes near the renal hilum and the right side draining to the aortocaval nodes. Epididymal drainage may also go to the external iliac nodes. Lymphatic drainage from the skin of the scrotum is typically to the inguinal nodes.

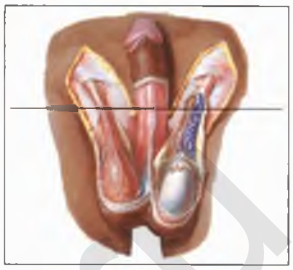

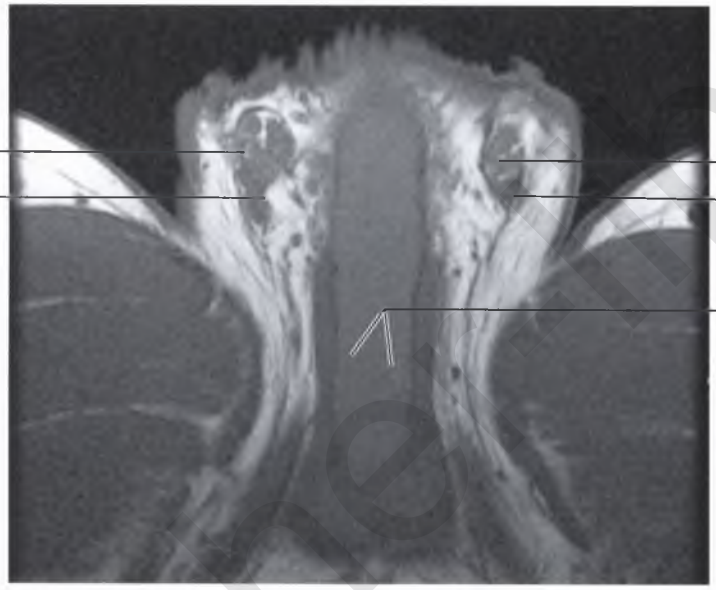
Right spermatic cord
Vas deferens
Left spermatic cord
Vas deferens
Corpora spongiosa

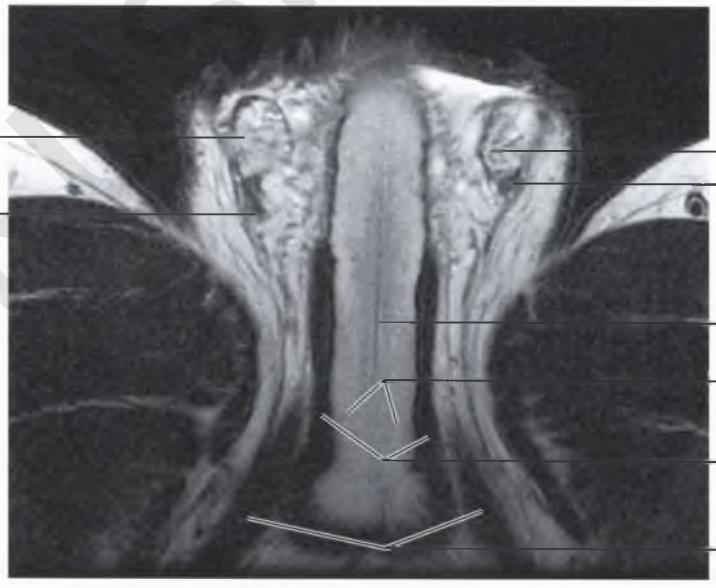
Right spermatic cord
Vas deferens
Left spermatic cord
Vas deferens
Penile urethra
Corpora spongiosa
Bulbospongiosus mm.
Ischiocavernosus mm.

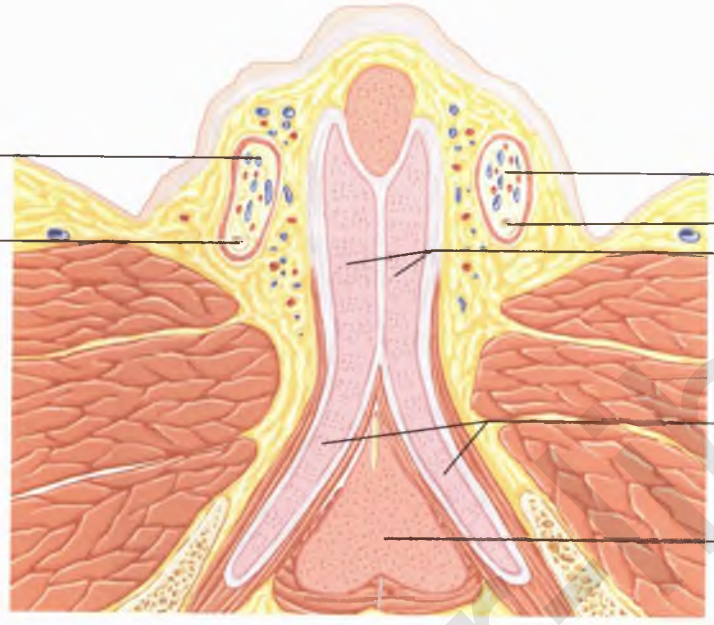
Right spermatic cord
Vas deferens
Left spermatic cord
Vas deferens
Corpora cavernosa (surrounded by tunica albuginea)
Crura of corpora cavernosa (covered by ischiocavernosus mm.)
Bulb of penis (covered by bulbospongiosus m.)

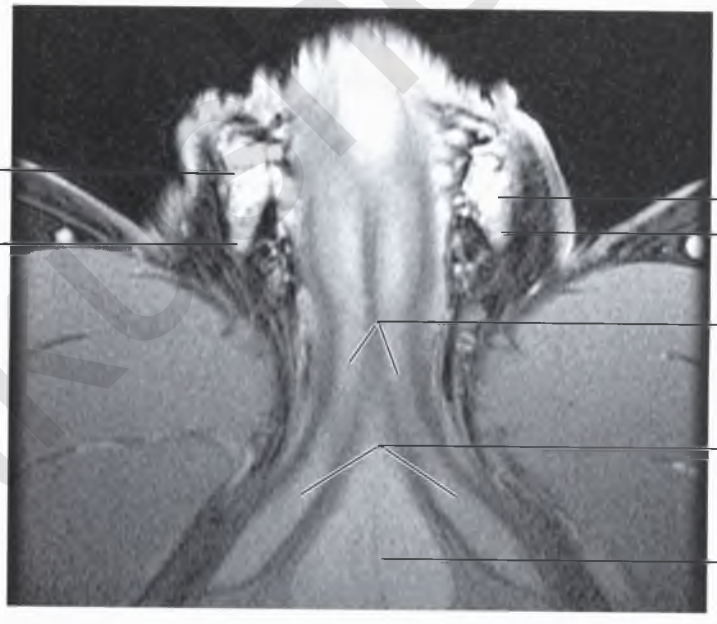
Right spermatic cord
Vas deferens
Left spermatic cord
Vas deferens
Corpora cavernosa (surrounded by tunica albuginea)
Crura of corpora cavernosa (covered by ischiocavernosus mm.)
Bulb of penis (covered by bulbospongiosus m.)

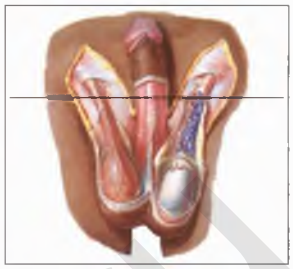

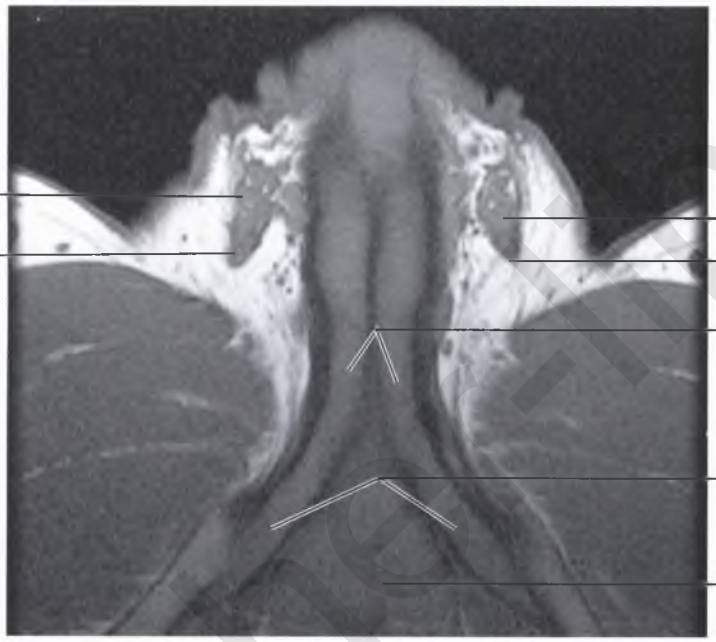
Right spermatic cord
Vas deferens
Left spermatic cord
Vas deferens
Corpora cavernosa (surrounded by tunica albuginea)
Crura of corpora cavernosa (covered by ischiocavernosus mm.)
Bulb of penis (covered by bulbospongiosus m.)

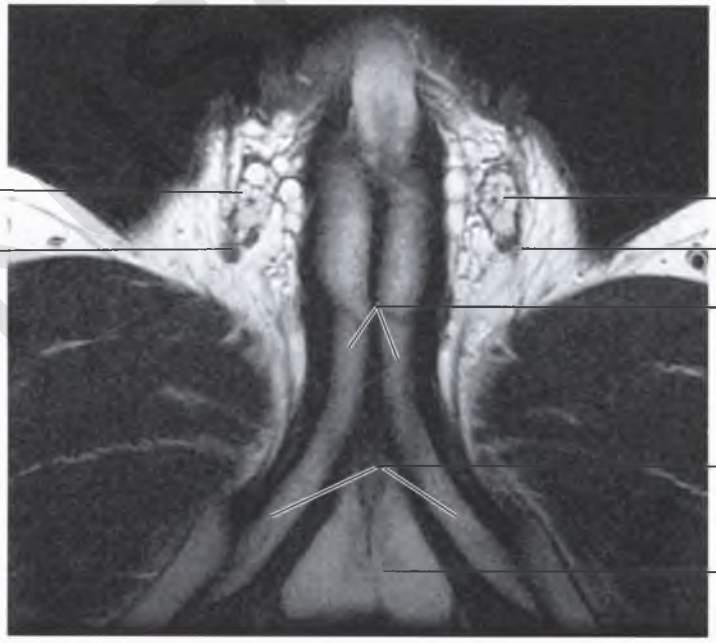
Right spermatic cord
Vas deferens
Left spermatic cord
Vas deferens
Corpora cavernosa (surrounded by tunica albuginea)
Crura of corpora cavernosa (covered by ischiocavernosus mm.)
Bulb of penis (covered by bulbospongiosus m.)

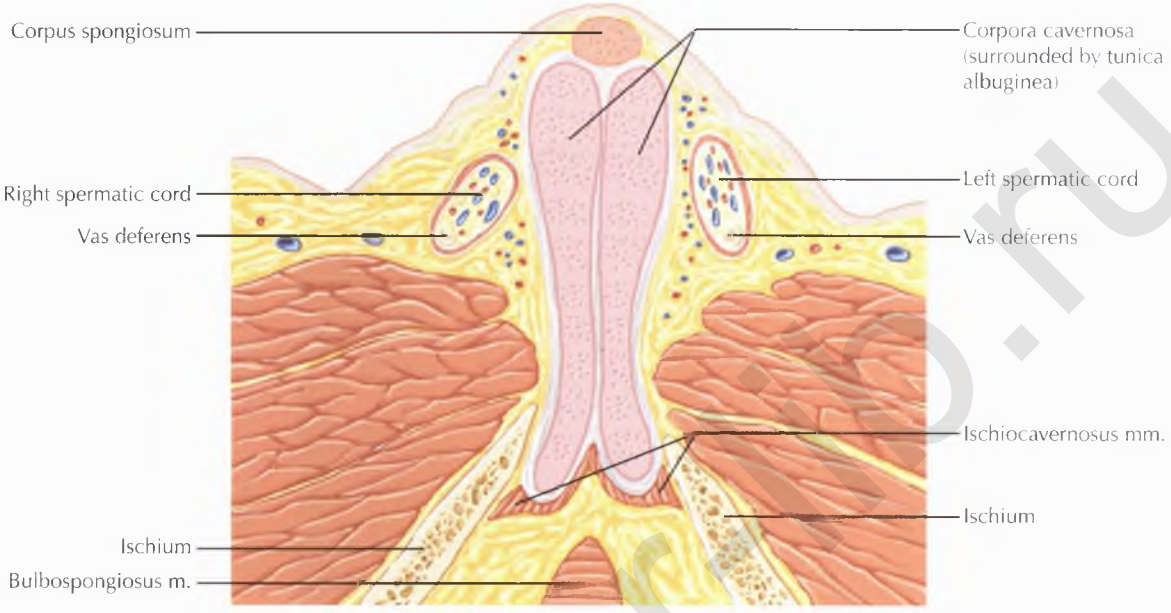

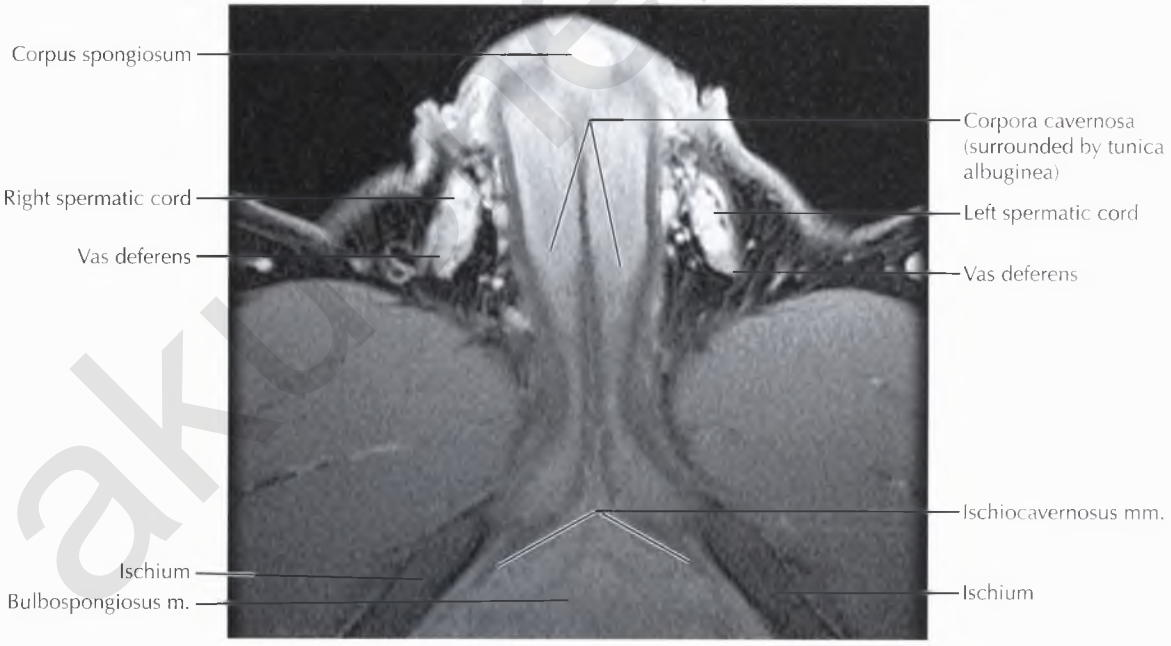

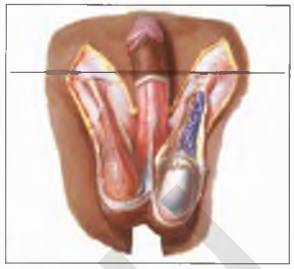

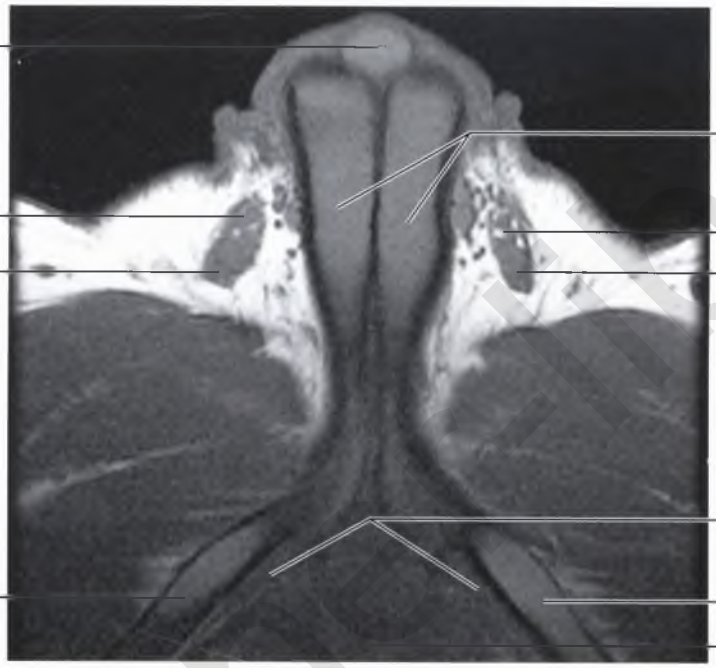
Corpus spongiosum
Right spermatic cord
Vas deferens
Ischium
Corpora cavernosa (surrounded by tunica albuginea)
Left spermatic cord
Vas deferens
Ischiocavernosus mm.
Ischium
Bulbospongiosus m.

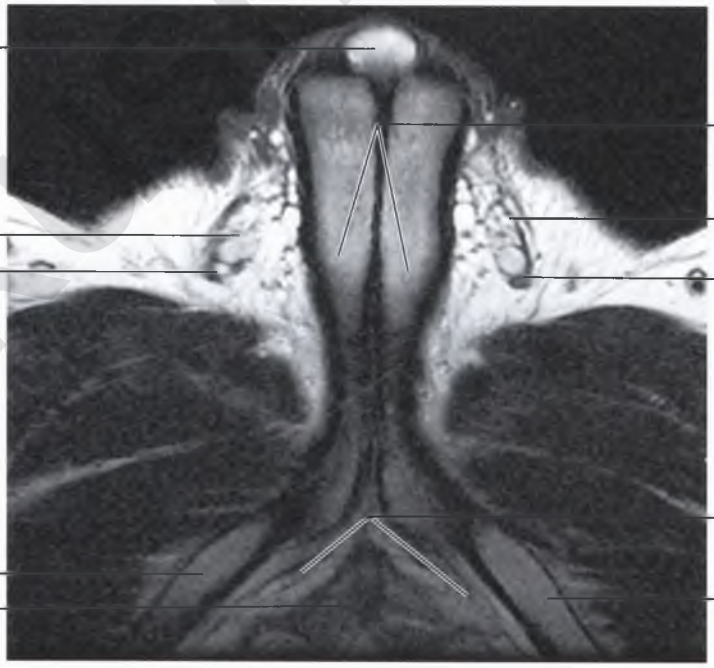
Corpus spongiosum
Right spermatic cord
Vas deferens
Ischium
Bulbospongiosus m.
Corpora cavernosa (surrounded by tunica albuginea)
Left spermatic cord
Vas deferens
Ischiocavernosus mm.
Ischium

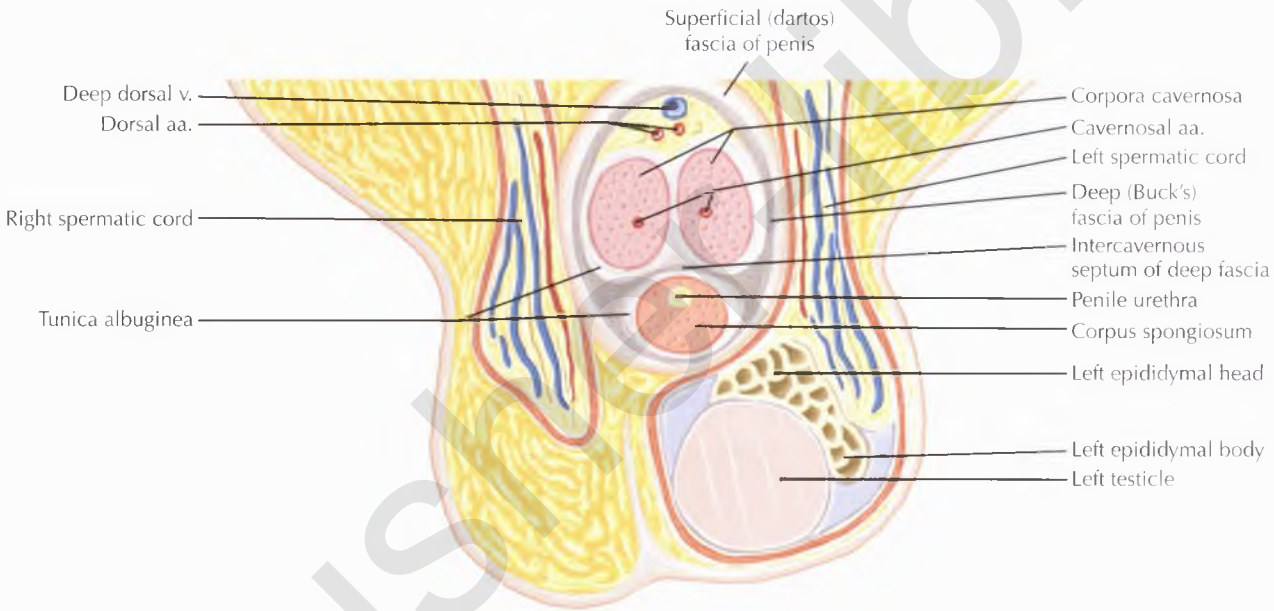
Superficial (dartos) fascia of penis
Deep dorsal v.
Dorsal aa.
Right spermatic cord
Tunica albuginea
Corpora cavernosa
Cavernosal aa.
Left spermatic cord
Deep (Buck's) fascia of penis
Intercavernous septum of deep fascia
Penile urethra
Corpus spongiosum
Left epididymal head
Left epididymal body
Left testicle

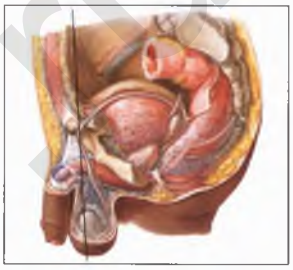

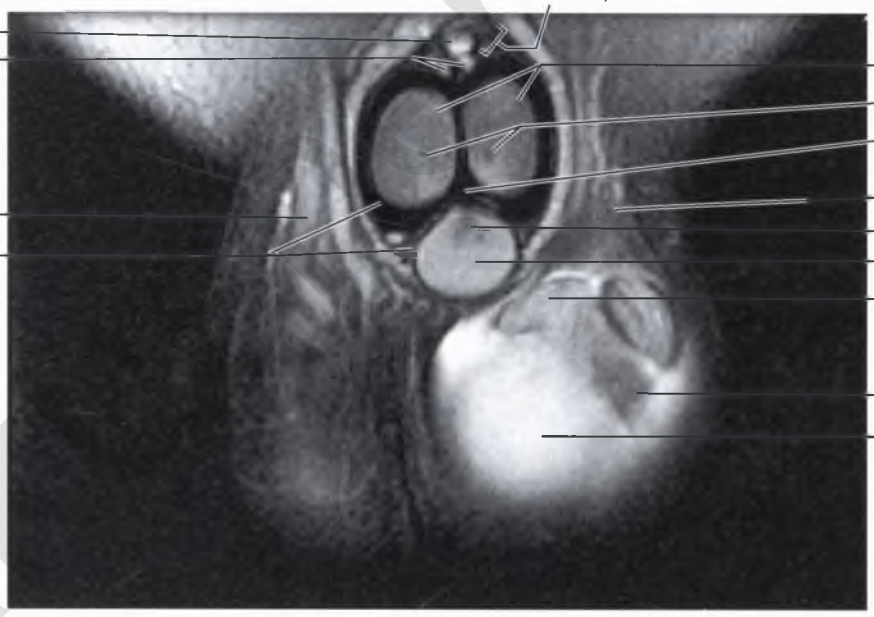
Superficial (dartos) and deep (Buck's) fascia of penis
Deep dorsal v.
Dorsal aa.
Right spermatic cord
Tunica albuginea and deep (Buck's) fascia
Corpora cavernosa
Cavernosal aa.
Intercavernous septum of deep fascia
Left spermatic cord
Penile urethra
Corpus spongiosum
Left epididymal head
Left epididymal body
Left testicle

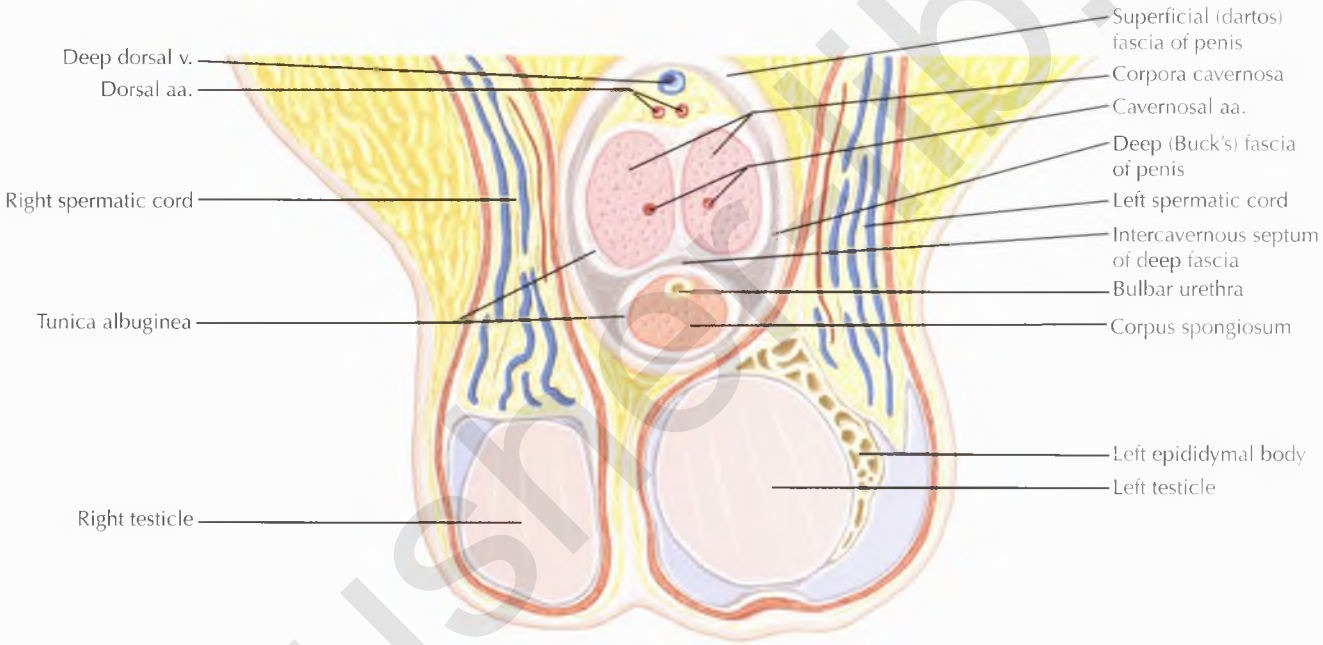

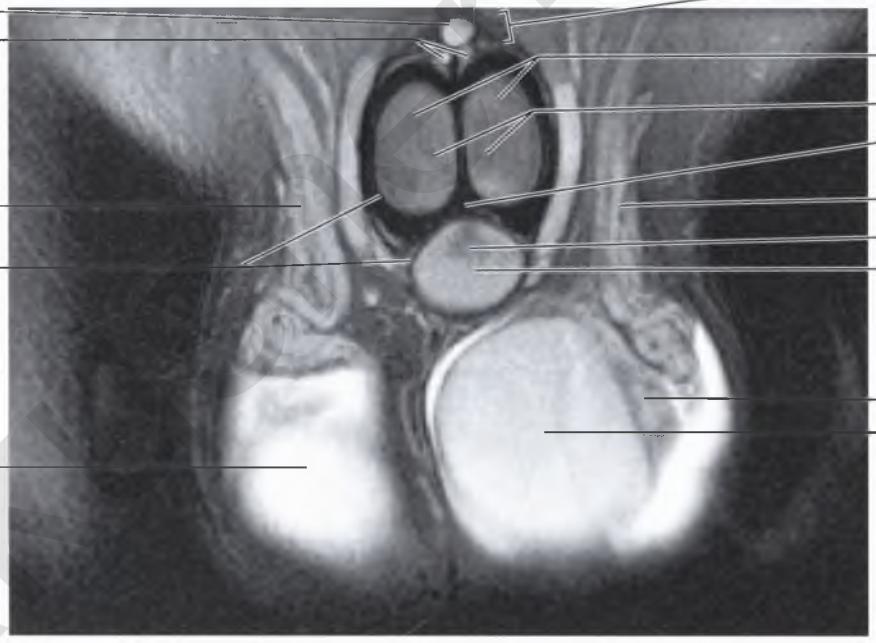
Deep dorsal v.
Dorsal aa.
Right spermatic cord
Tunica albuginea and deep (Buck's) fascia
Right testicle
Superficial (dartos) and deep (Buck's) fascia of penis
Corpora cavernosa
Cavernosal aa.
Intercavernous septum of deep fascia
Left spermatic cord
Bulbar urethra
Corpus spongiosum
Left epididymal body
Left testicle

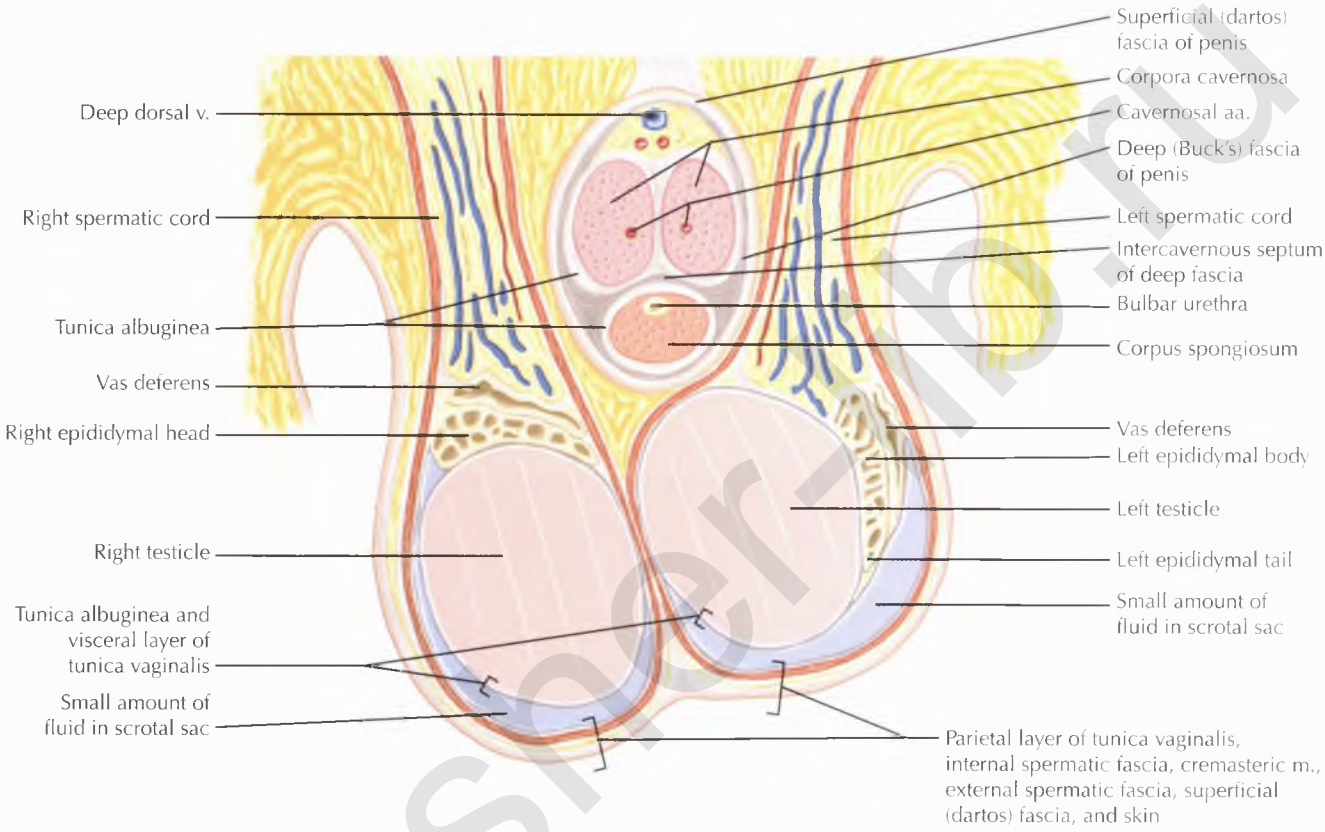

NORMAL ANATOMY

The abdominal wall layers are continuous with the layers of the spermatic cord and scrotum, with the transversalis fascia continuing into the scrotum as the internal spermatic fascia, the internal oblique muscle continuing as the cremasteric muscle and fascia, and the external oblique muscle continuing as the external spermatic fascia. The parietal layer of the tunica vaginalis, internal spermatic fascia, cremasteric muscle, external spermatic fascia, superficial (dartos) fascia, and skin (from internal to external direction) are not separable on MRI and appear as a single, hypointense scrotal lining. The visceral layer of the tunica vaginalis also blends imperceptibly with the tunica albuginea of the testicle, forming a single, hypointense layer around the testicle. It is normal to see a small amount of scrotal fluid between the visceral and parietal layers of the tunica vaginalis, which acts as a lubricant.

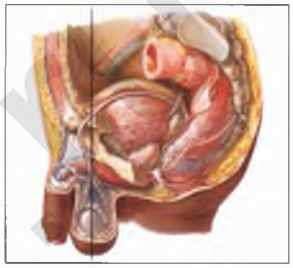

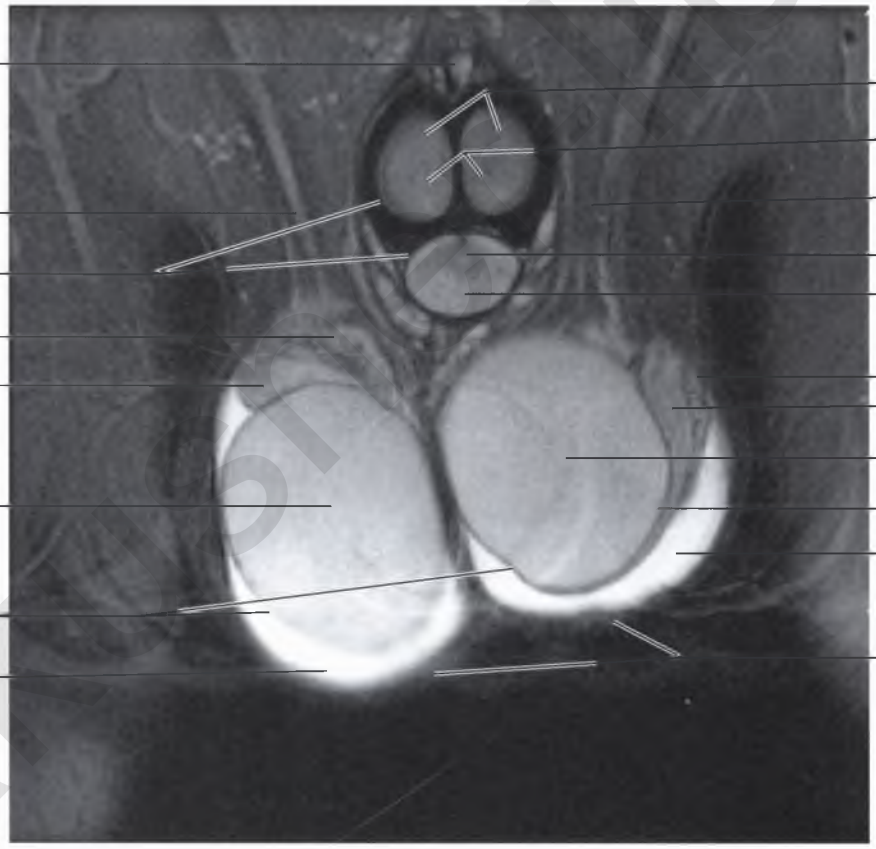
Deep dorsal v.
Right spermatic cord
Tunica albuginea and deep (Buck's) fascia
Vas deferens
Right epididymal head
Right testicle
Tunica albuginea and visceral layer of tunica vaginalis
Small amount of fluid in scrotal sac
Corpora cavernosa
Cavernosal aa.
Left spermatic cord
Bulbar urethra
Corpus spongiosum
Vas deferens
Left epididymal body
Left testicle
Left epididymal tail
Small amount of fluid in scrotal sac
Parietal layer of tunica vaginalis, internal spermatic fascia, cremasteric m., external spermatic fascia, superficial (dartos) fascia, and skin

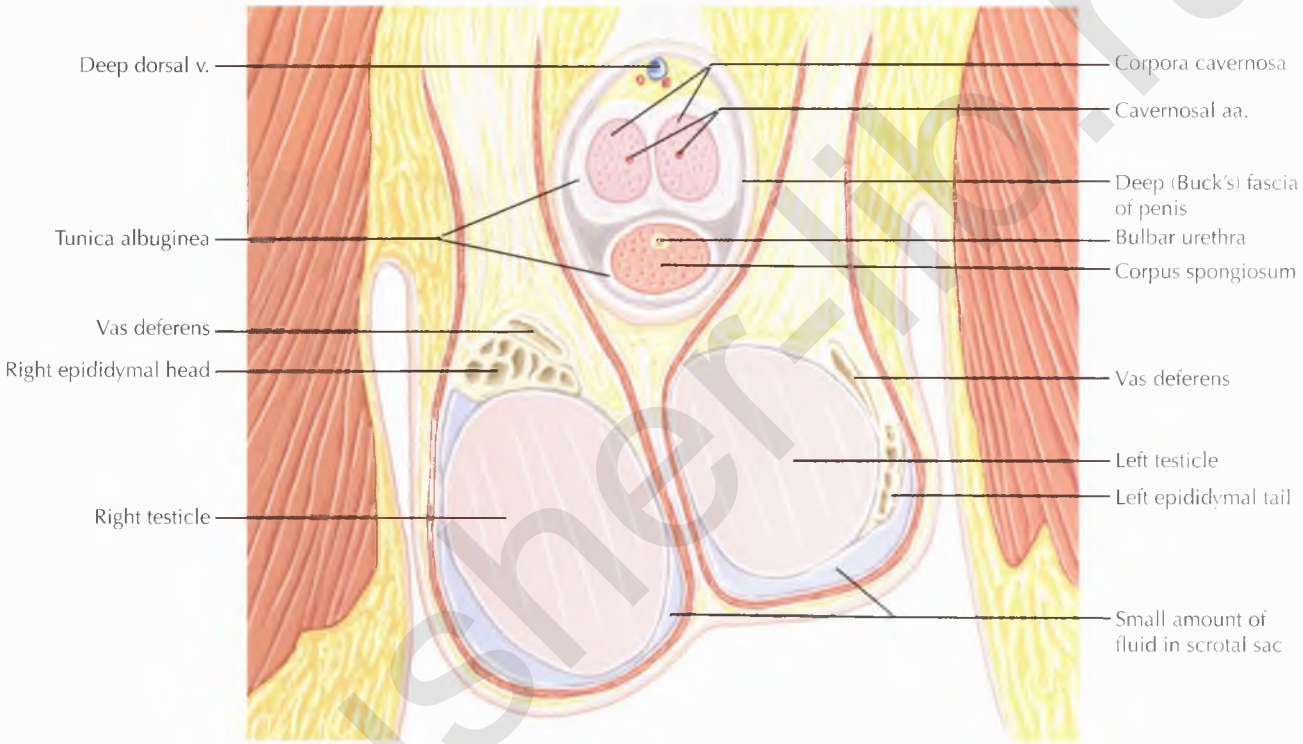

PATHOLOGIC PROCESS

A pathologic collection of fluid between the visceral and parietal layers of the tunica vaginalis is called a *hydrocele*, which may be congenital (caused by patent processus vaginalis peritonei) or acquired.

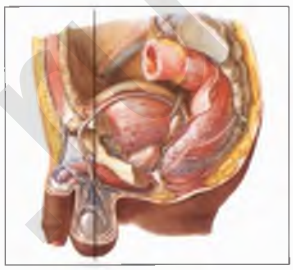

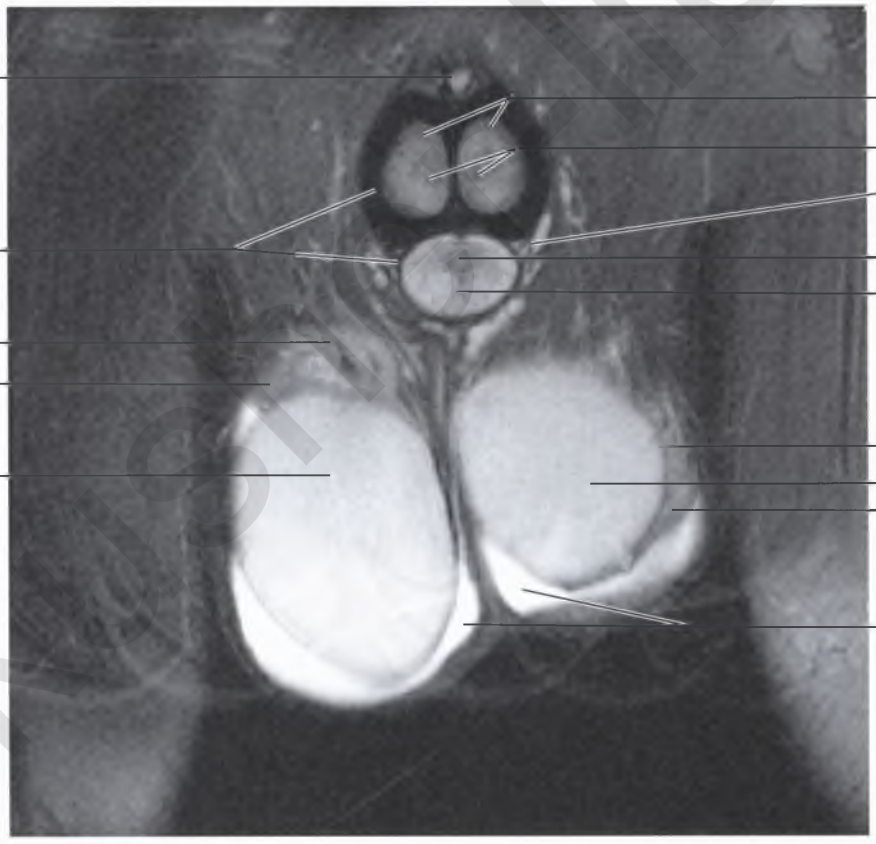
Deep dorsal v.
Tunica albuginea and deep (Buck's) fascia
Vas deferens
Right epididymal head
Right testicle
Corpora cavernosa
Cavernosal aa.
Deep (Buck's) fascia of penis
Bulbar urethra
Corpus spongiosum
Vas deferens
Left testicle
Left epididymal tail
Small amount of fluid in scrotal sac

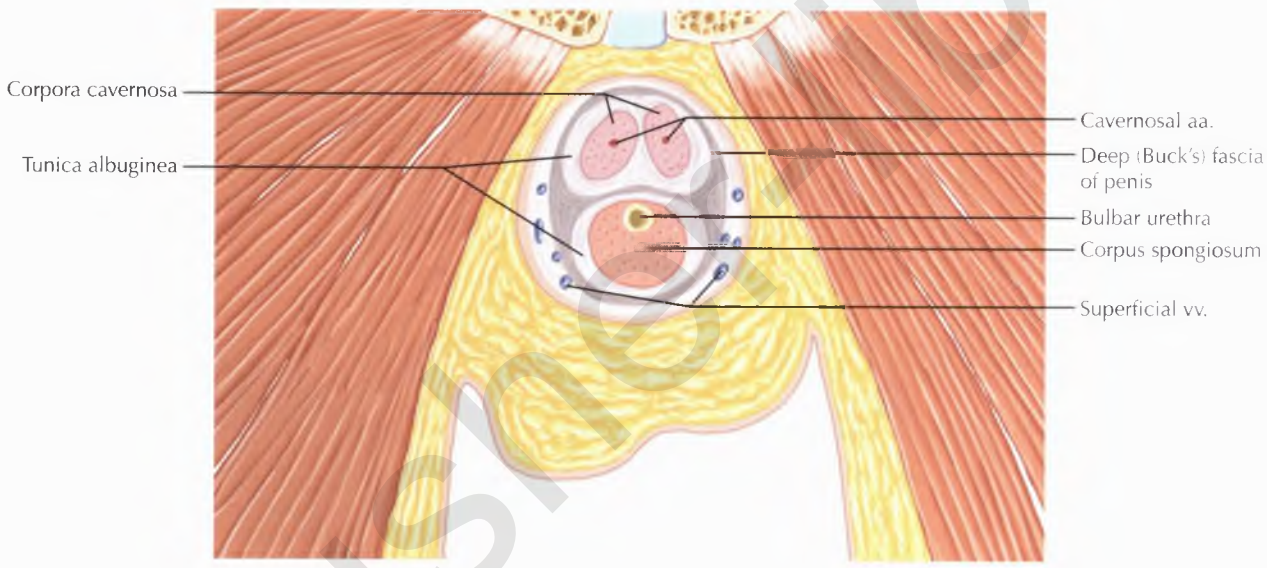
Corpora cavernosa
Tunica albuginea
Cavernosal aa.
Deep (Buck's) fascia of penis
Bulbar urethra
Corpus spongiosum
Superficial vv.

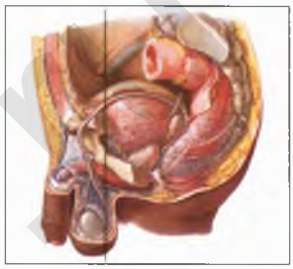

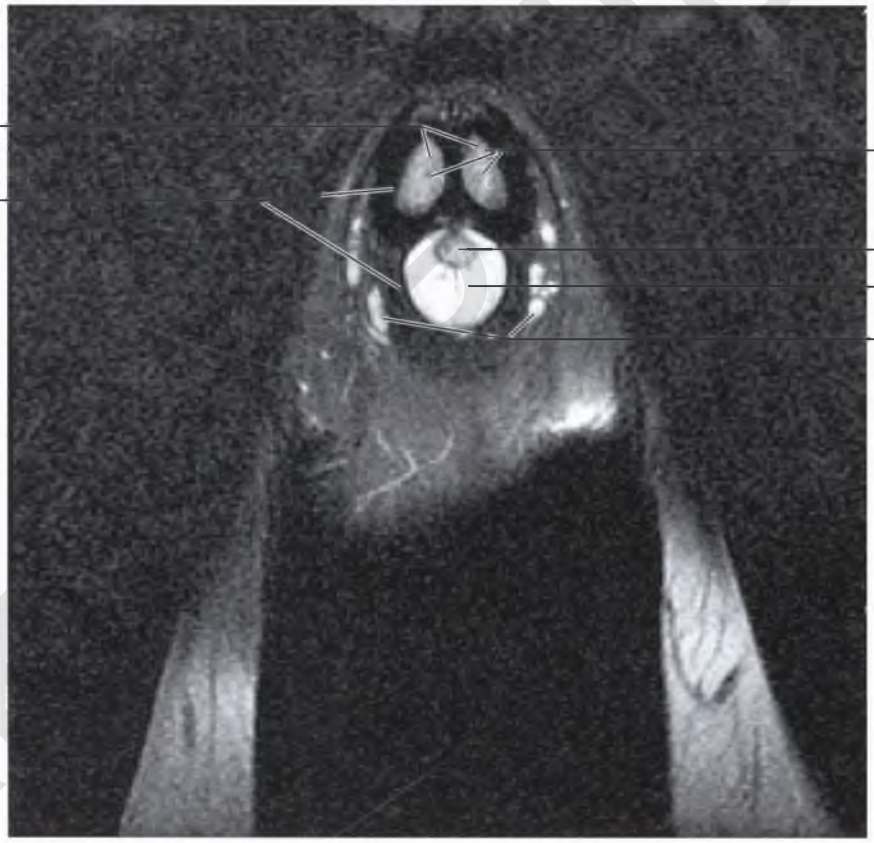
Corpora cavernosa
Tunica albuginea and deep (Buck's) fascia of penis
Cavernosal aa.
Bulbar urethra
Corpus spongiosum
Superficial vv.

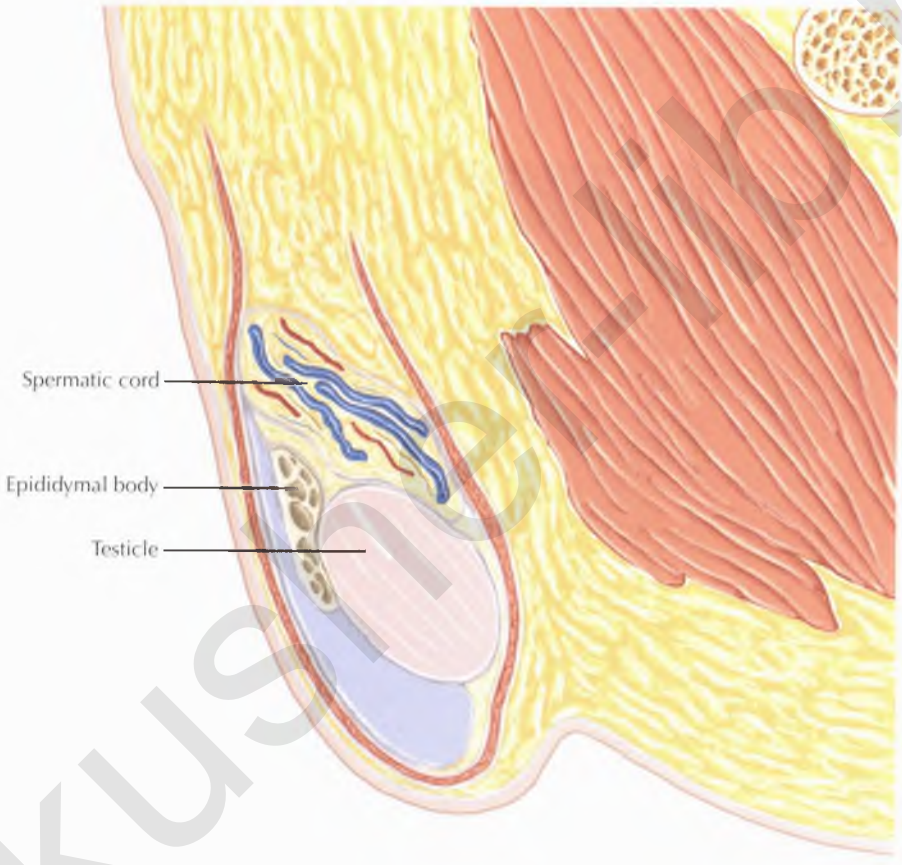

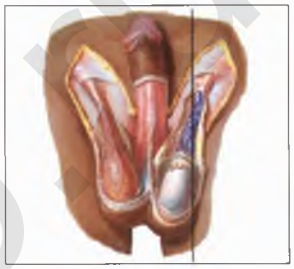

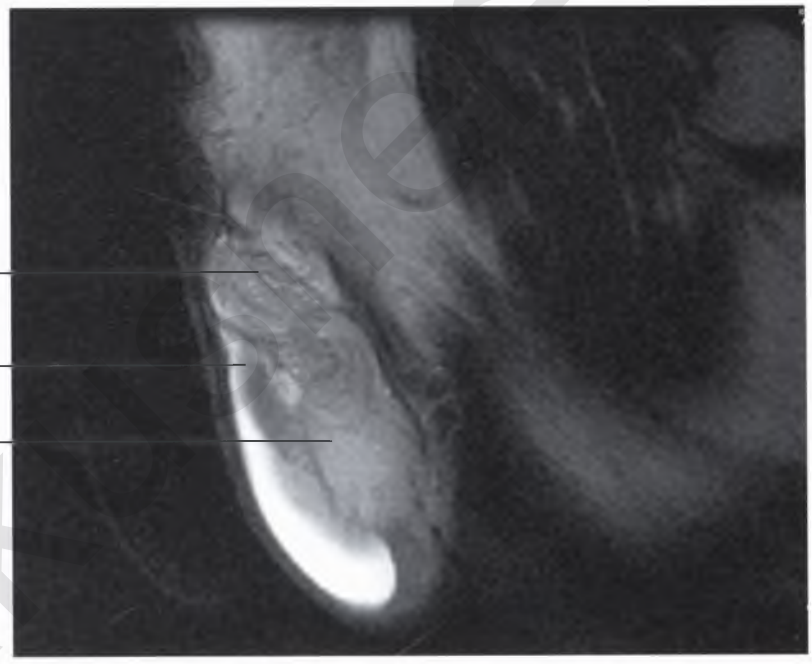

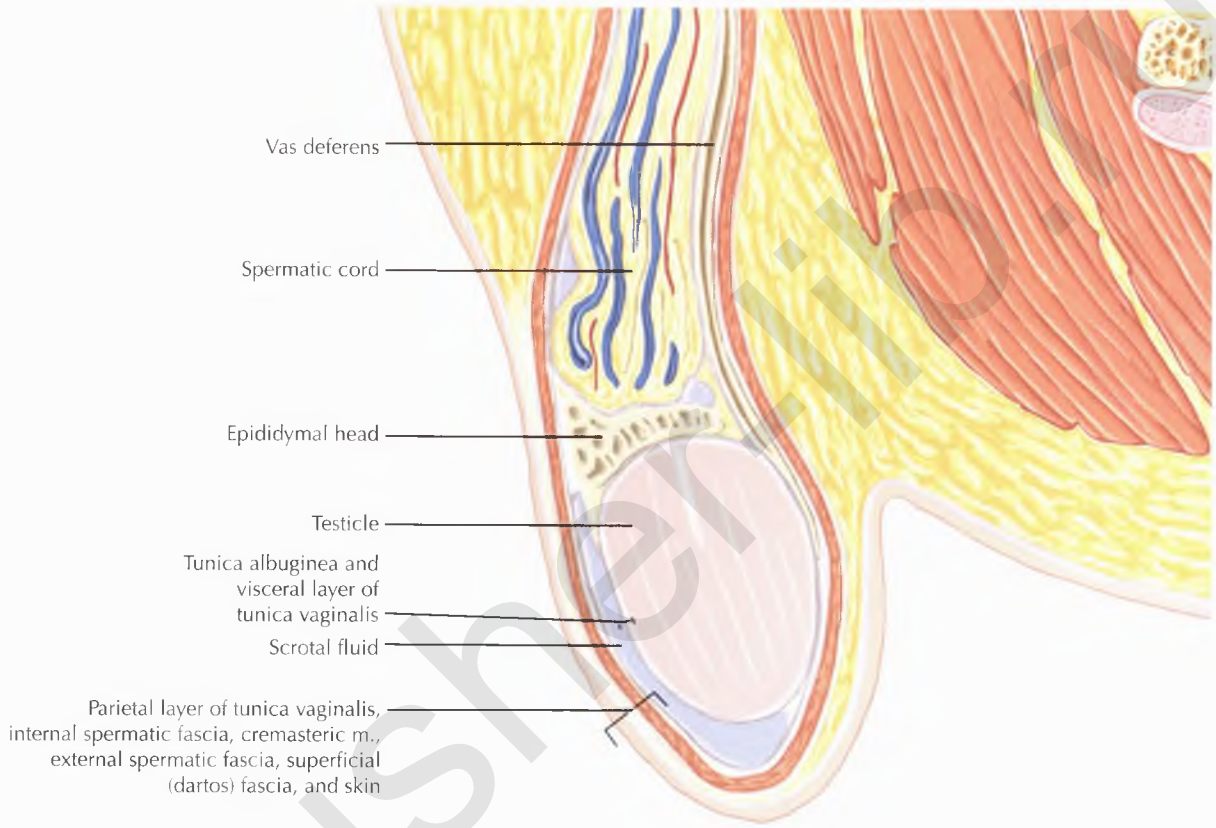

NORMAL ANATOMY

The *epididymis* is a crescent-shaped structure draped over the posterior testicle. The rete testis converges to form 15 to 20 efferent ductules, which form the head of the epididymis superiorly and then converge into a single, convoluted tubule in the body and tail of the epididymis inferiorly. The tubules emerge at an acute angle from the tail of the epididymis, forming the *vas deferens*, which continues cephalad in the spermatic cord, eventually merging with the seminal vesicle duct to form the ejaculatory duct.

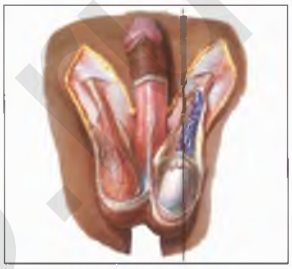

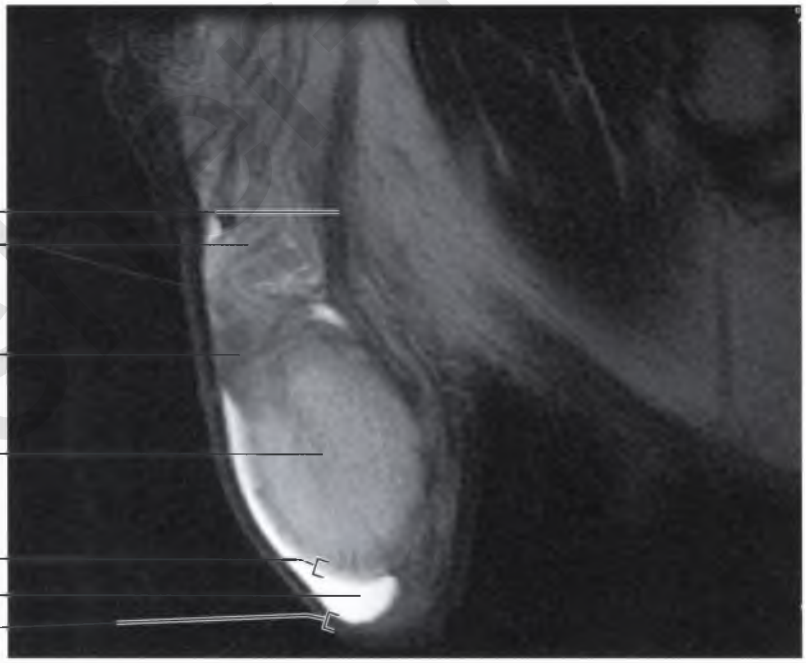

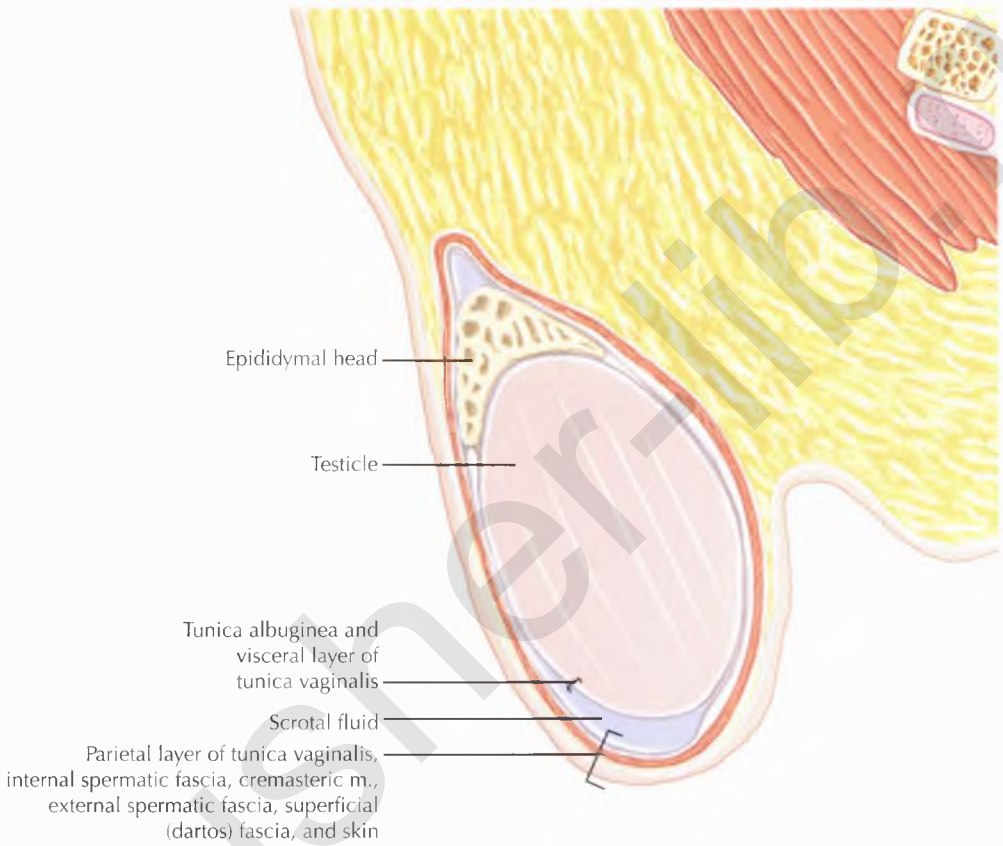

PATHOLOGIC PROCESS

Embryologically, the *processus vaginalis peritonei* is a socklike evagination of the peritoneum that descends through the inguinal canal into the scrotal sac at about the 28th week of gestation. It gradually closes around the anterior and lateral sides of the testicle, allowing the testicle to remain fixed to the scrotal wall posteriorly. If the tunica vaginalis completely surrounds the testicle and epididymis ("bell clapper" deformity), the testicle is not anchored posteriorly and is at risk for testicular torsion.

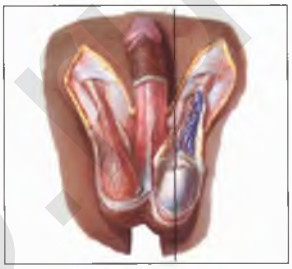

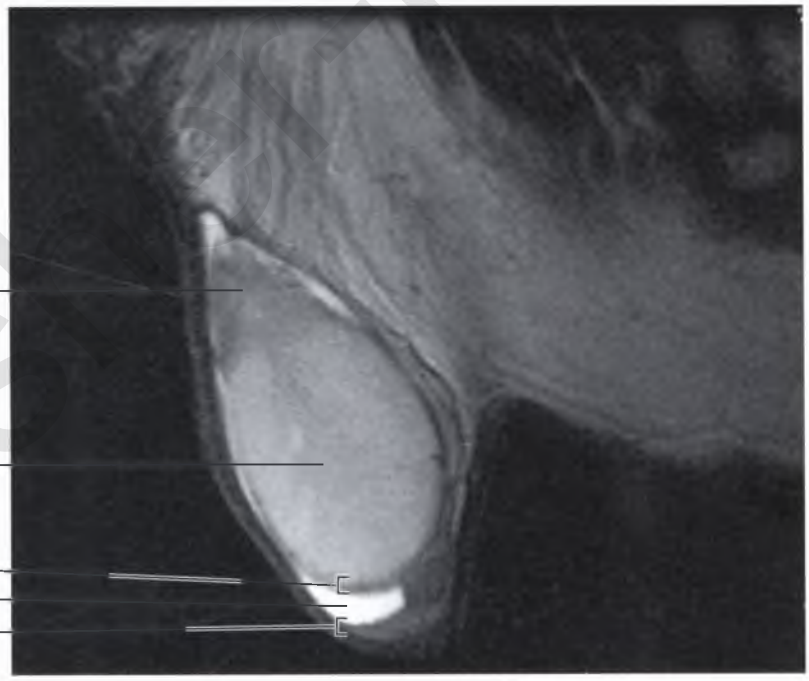

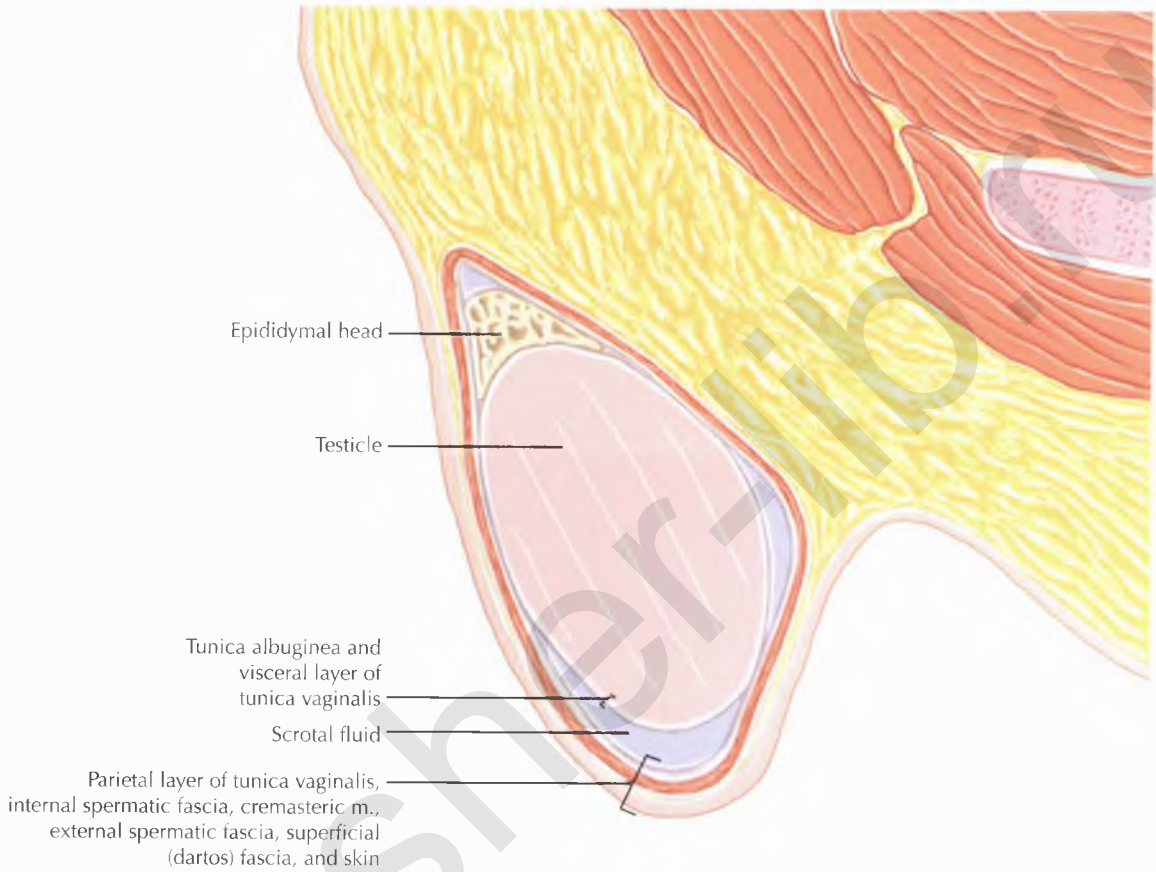

DIAGNOSTIC CONSIDERATION

The differentiation between an intratesticular and an extratesticular location of a scrotal mass is important because most extratesticular masses are benign and most intratesticular masses are malignant. *Germ cell tumors* account for 95% of the testicular malignancies in young men. Mixed germ cell tumors are the most common type overall, followed by pure seminomas. Embryonal carcinoma, yolk sac tumor, choriocarcinoma, and teratoma are less common. Sex cord (Sertoli cell) tumors and stromal (Leydig cell) tumors are much less common. In older men, lymphoma, leukemia, and metastasis should also be considered in the differential diagnosis of an intratesticular mass.

The most common extratesticular neoplasms are *lipomas*, usually arising from the spermatic cord, and adenomatoid tumors, usually arising from the epididymis.

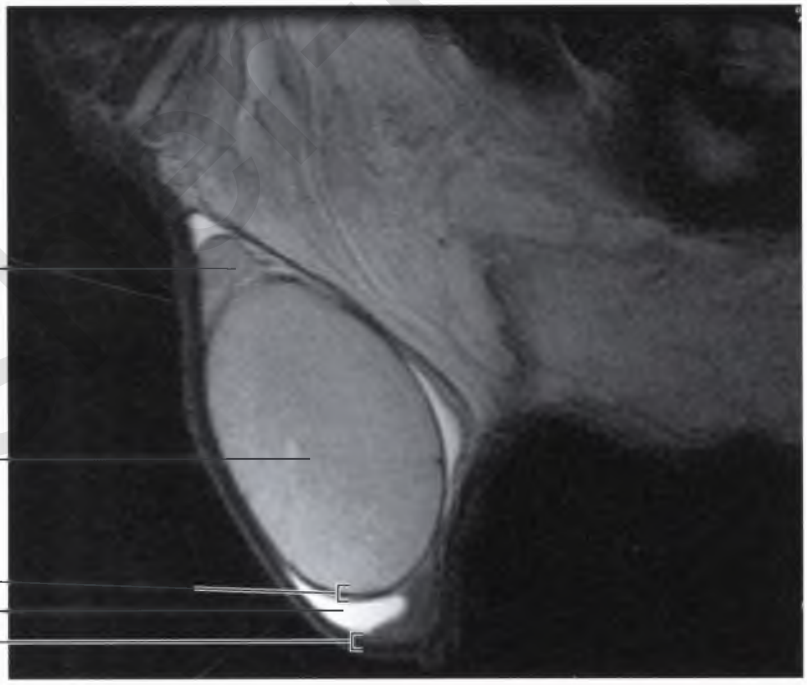

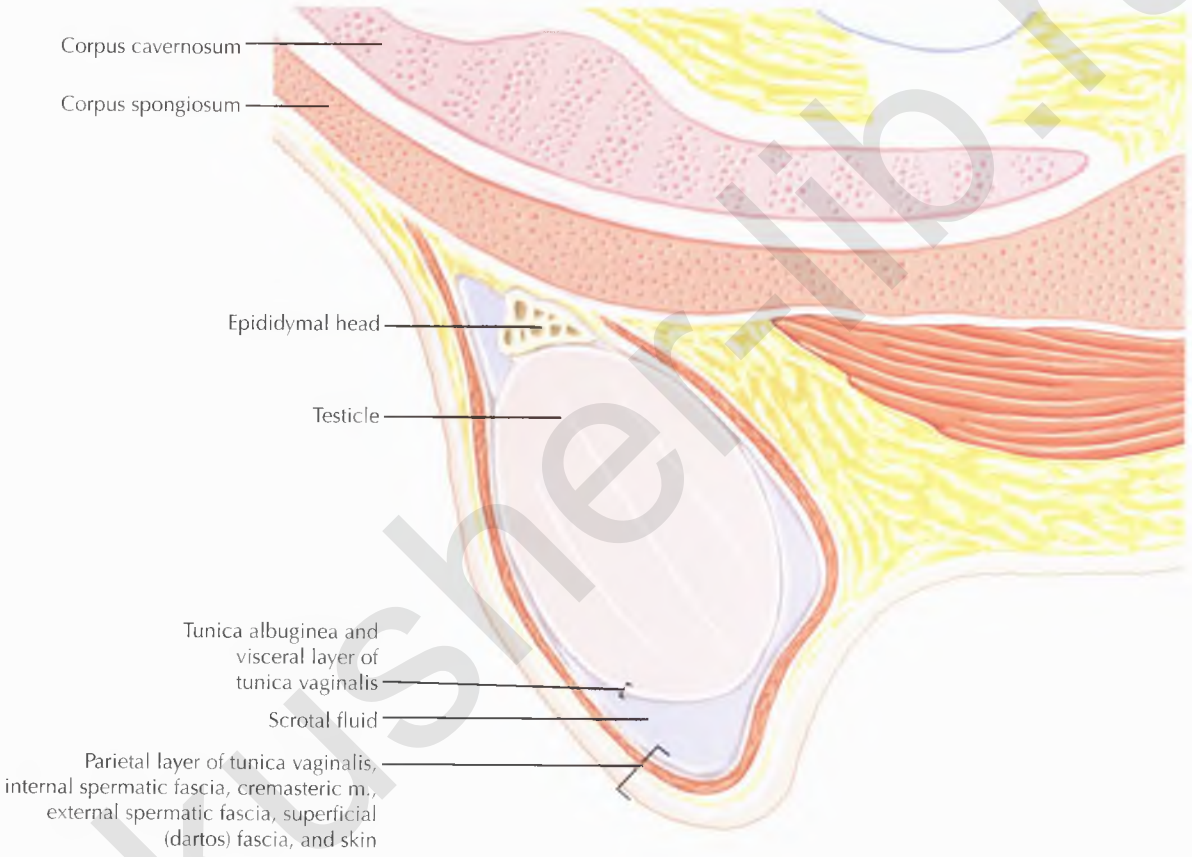

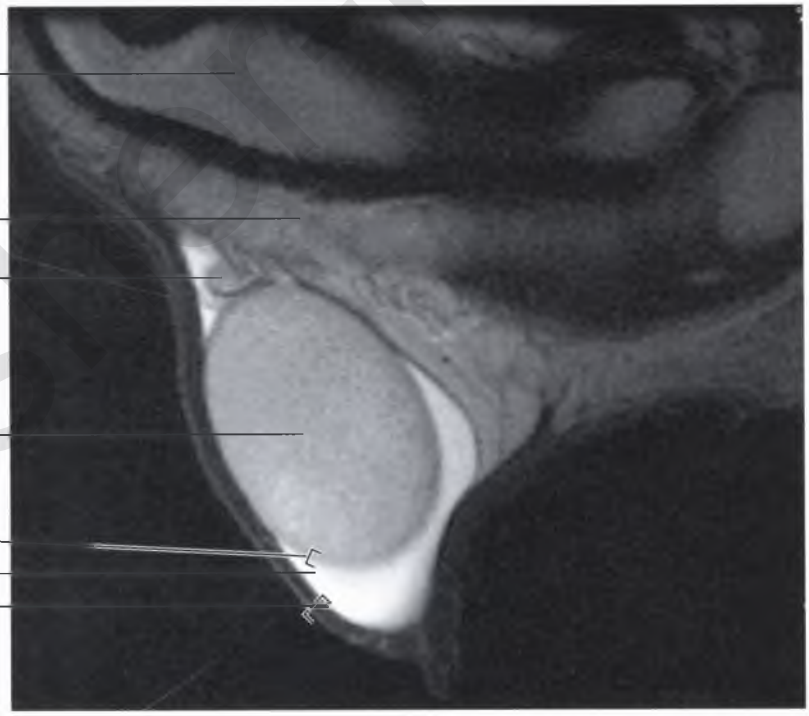
Corpus cavernosum
Corpus spongiosum
Epididymal head
Testicle
Tunica albuginea and visceral layer of tunica vaginalis
Scrotal fluid
Parietal layer of tunica vaginalis, internal spermatic fascia, cremasteric m., external spermatic fascia, superficial (dartos) fascia, and skin

Chapter 9 PENIS AND MALE URETHRA

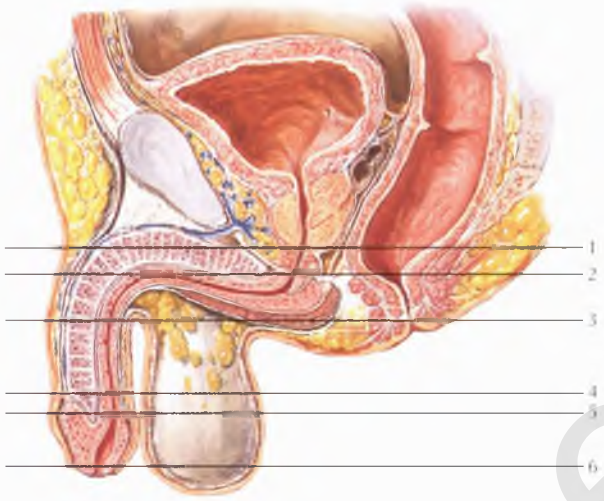

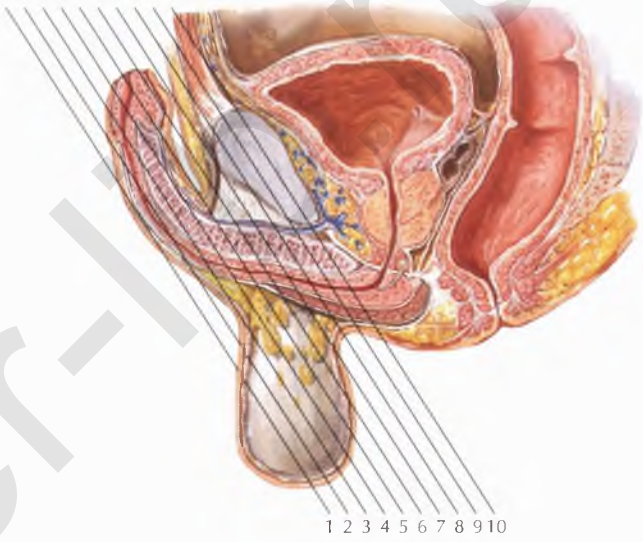

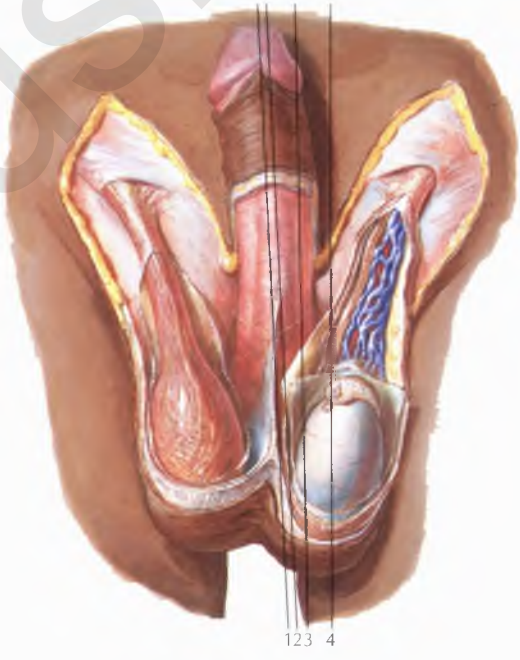

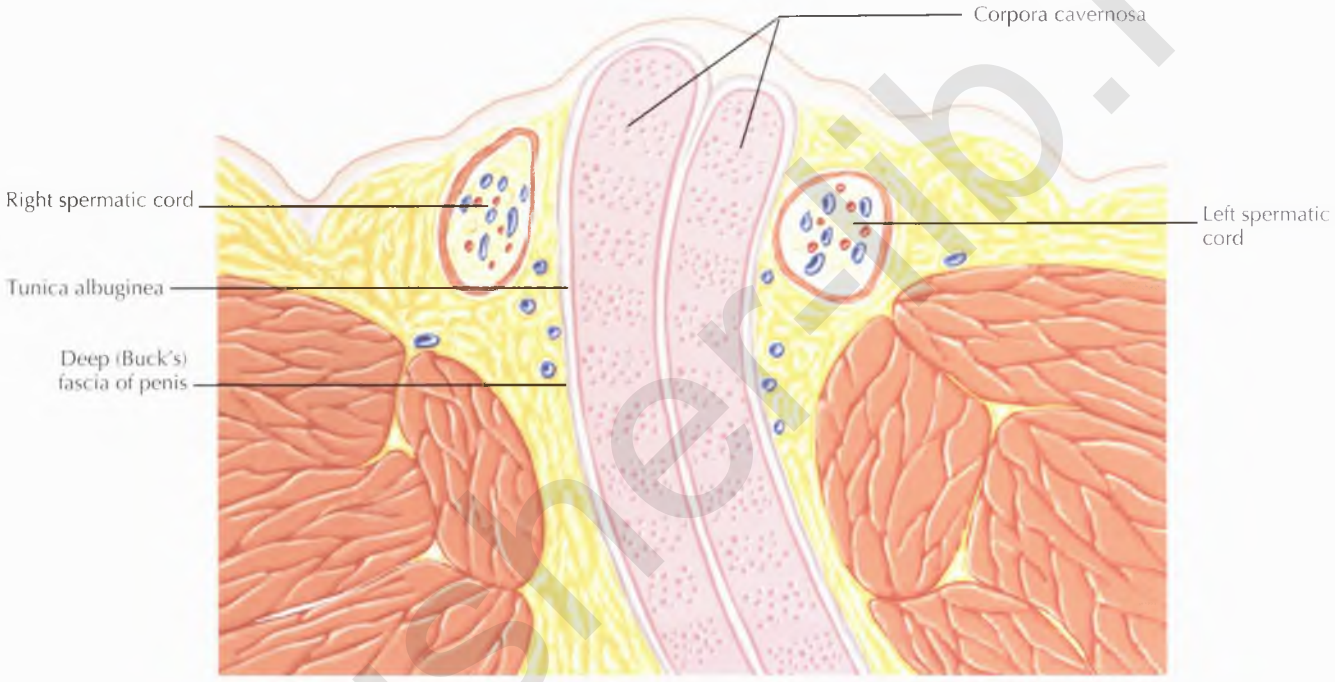

DIAGNOSTIC CONSIDERATION

Common indications for magnetic resonance imaging (MRI) of the penis include detection and staging of penile and urethral malignancies, evaluation of penile prostheses, and detection of penile fractures, Peyronie's disease, and periurethral abscesses.

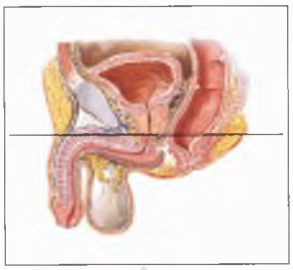

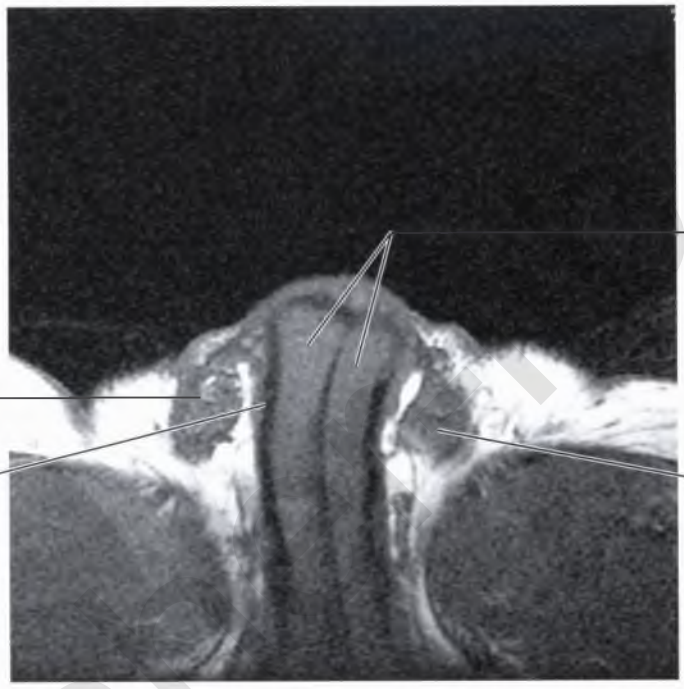
Corpora cavernosa
Right spermatic cord
Deep (Buck's) fascia of penis and tunica albuginea
Left spermatic cord

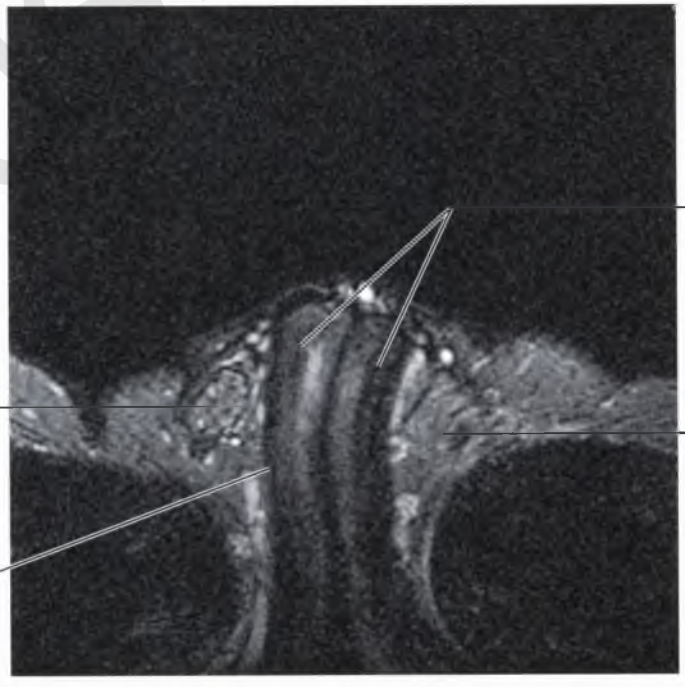
Corpora cavernosa
Right spermatic cord
Left spermatic cord
Deep (Buck's) fascia of penis and tunica albuginea

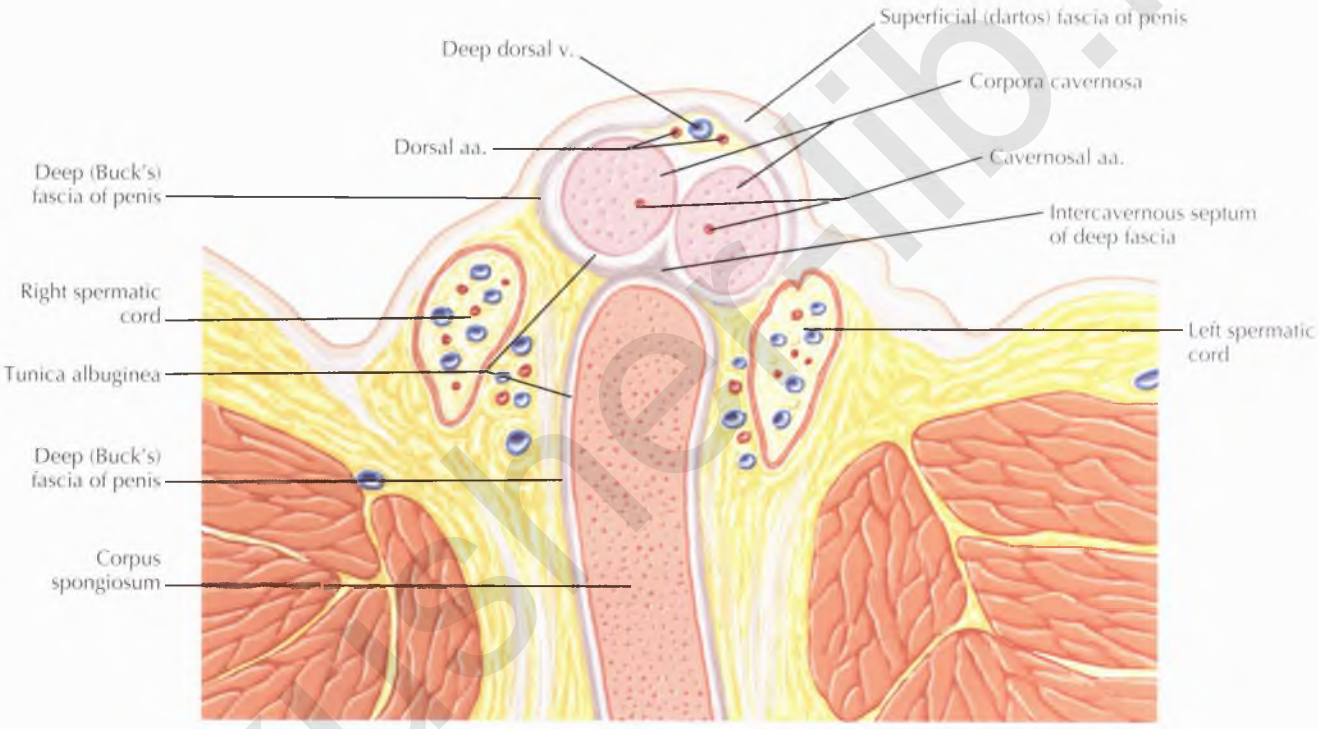

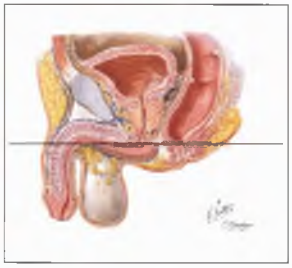

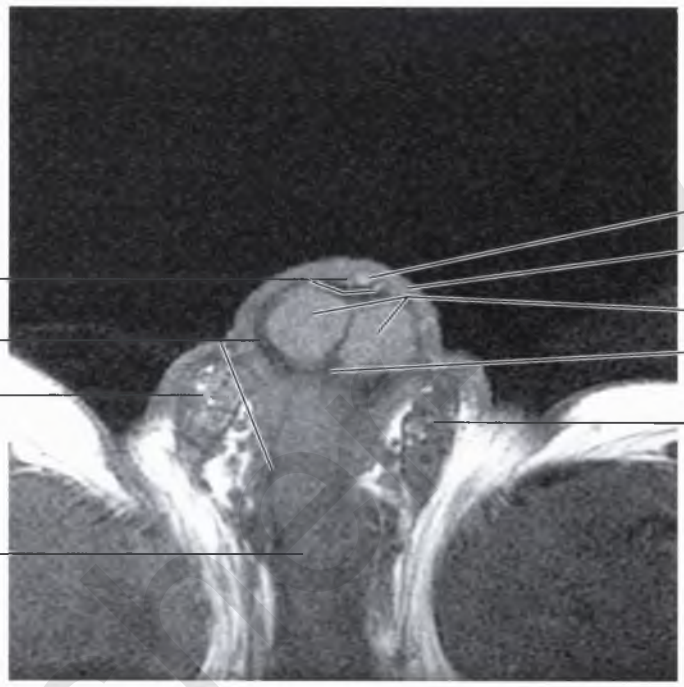
Deep dorsal v.
Superficial (dartos) fascia of penis
Dorsal aa.
Corpora cavernosa
Deep (Buck's) fascia of penis and tunica albuginea
Intercavernous septum of deep fascia
Right spermatic cord
Left spermatic cord
Corpus spongiosum

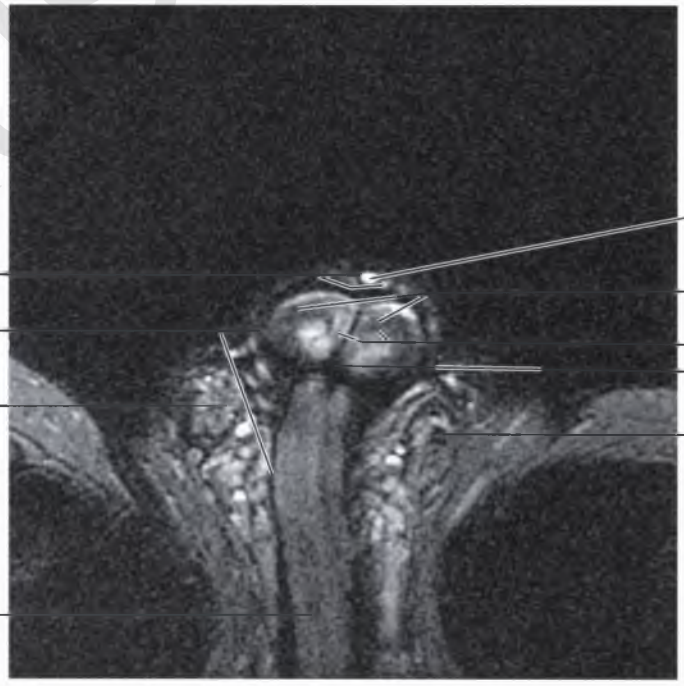
Deep dorsal v.
Dorsal aa.
Corpora cavernosa
Deep (Buck's) fascia of penis and tunica albuginea
Cavernosal aa.
Intercavernous septum of deep fascia
Right spermatic cord
Left spermatic cord
Corpus spongiosum

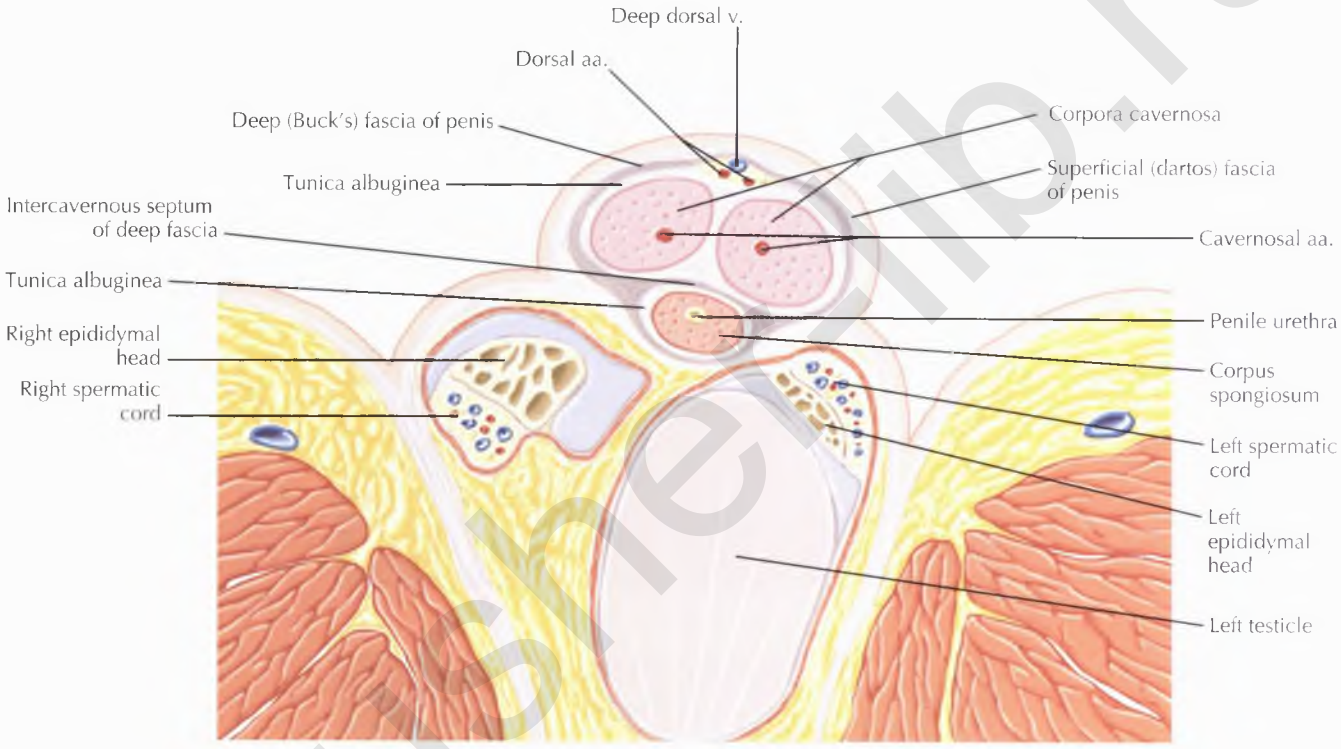

NORMAL ANATOMY

The penis is composed of three cylindrical cavernous spaces: the paired dorsal corpora cavernosa and the single ventral corpus spongiosum.

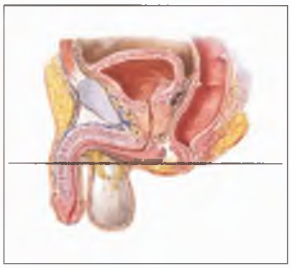


Deep (Buck's) fascia of penis and tunica albuginea
Corpora cavernosa
Superficial (dartos) fascia of penis and skin
Intercavernous septum of deep fascia
Corpus spongiosum
Right epididymal head
Left spermatic cord
Right spermatic cord
Left testicle

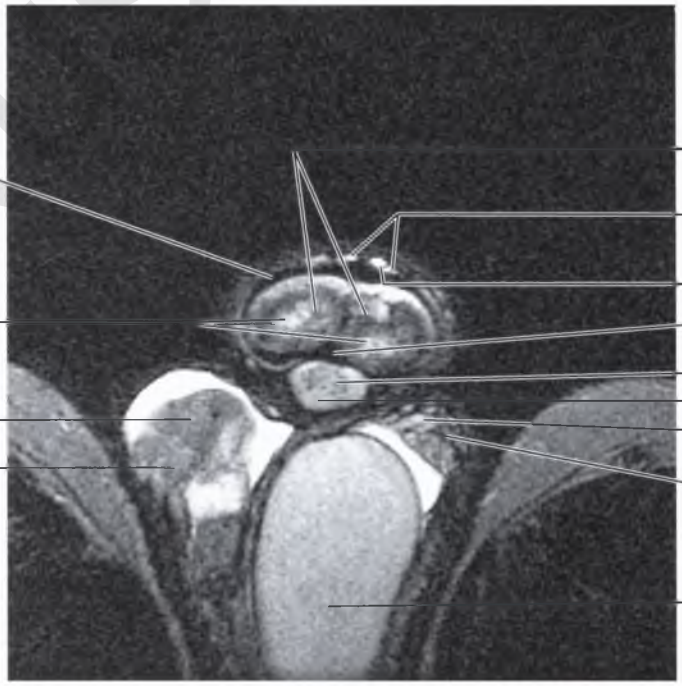
Deep (Buck's) fascia of penis and tunica albuginea
Cavernosal aa.
Dorsal aa.
Deep dorsal v.
Corpora cavernosa
Intercavernous septum of deep fascia
Penile urethra
Corpus spongiosum
Right epididymal head
Left epididymal head
Right spermatic cord
Left spermatic cord
Left testicle

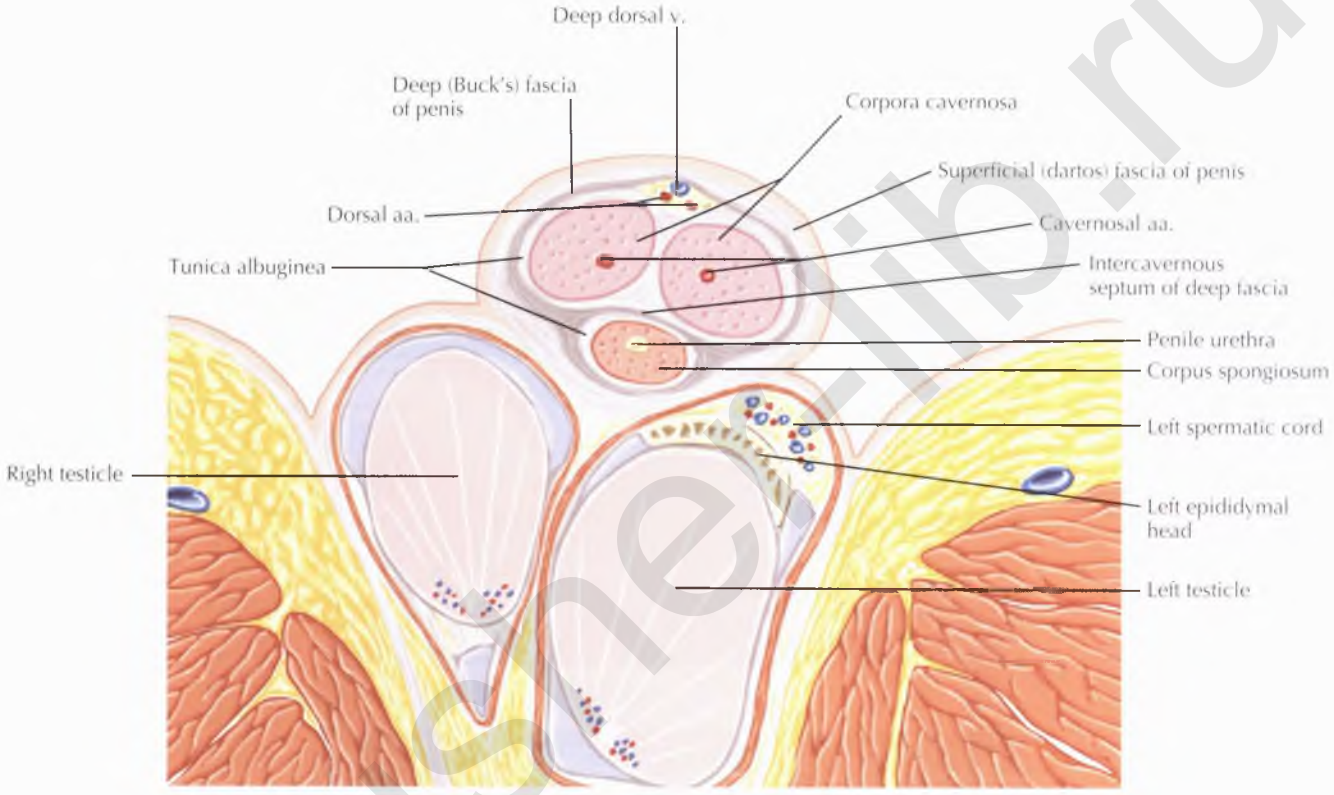

NORMAL ANATOMY

The *tunica albuginea* is a thin layer of fibrous tissue that surrounds each of the corpora cavernosa and the corpus spongiosum. The deep (Buck's) fascia is just superficial to the tunica albuginea and surrounds the corpora cavernosa in a dorsal compartment and the corpus spongiosum in a separate, ventral compartment. The tunica albuginea and deep (Buck's) fascia are inseparable on MRI and appear as a single, hypointense border surrounding the corpora. The superficial (dartos) fascia is seen more superficially, just beneath the skin and subcutaneous fat.

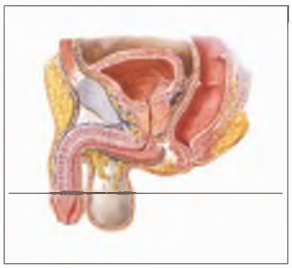

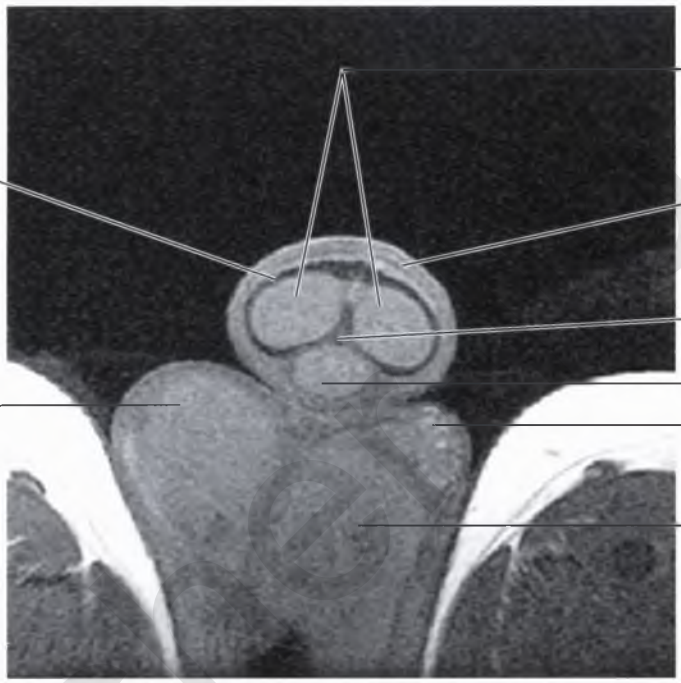
Corpora cavernosa
Deep (Buck's) fascia of penis and tunica albuginea
Superficial (dartos) fascia of penis and skin
Intercavernous septum of deep fascia
Corpus spongiosum
Right testicle
Left spermatic cord
Left testicle

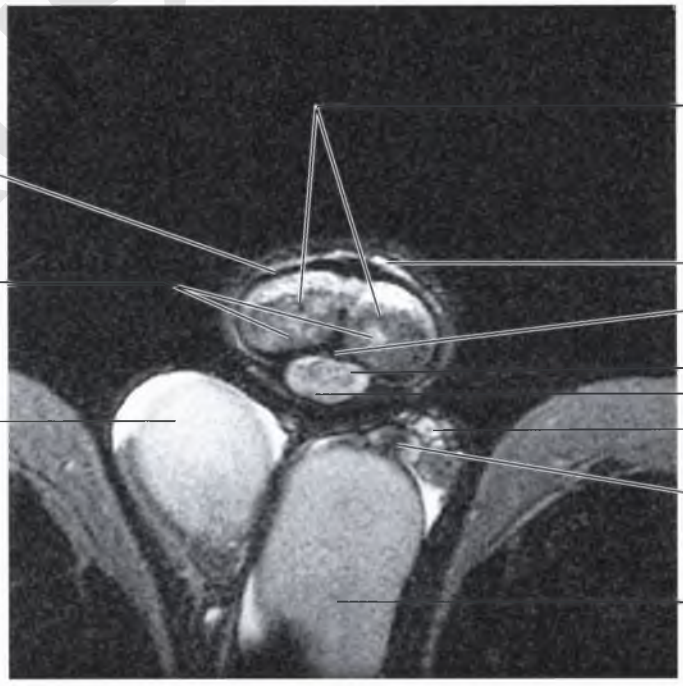
Cavernosal aa.
Deep (Buck's) fascia of penis and tunica albuginea
Deep dorsal v.
Corpora cavernosa
Intercavernous septum of deep fascia
Penile urethra
Corpus spongiosum
Right testicle
Left spermatic cord
Left epididymal head
Left testicle

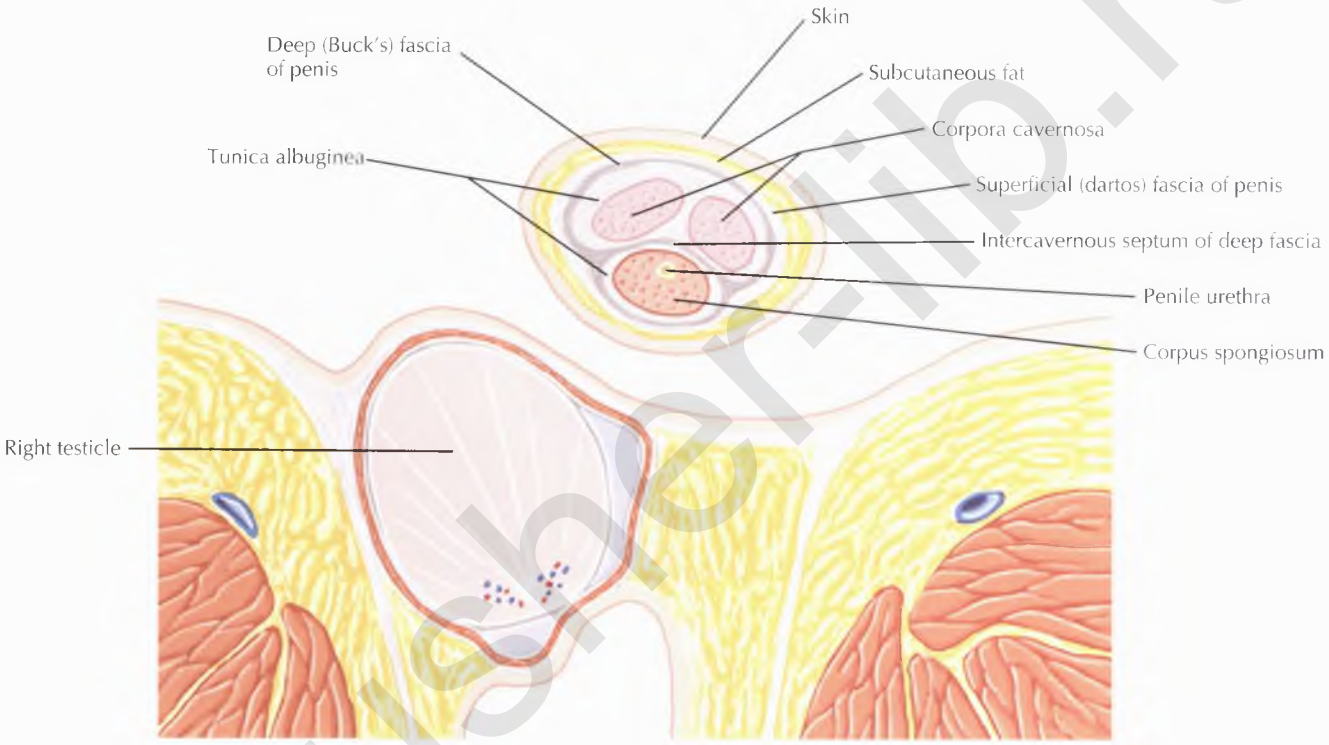

PATHOLOGIC PROCESS

Peyronie's disease results from plaque formation on the tunica albuginea, causing painful erections with shortening and curvature of the penis.

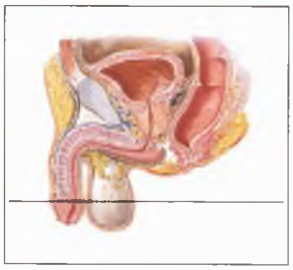

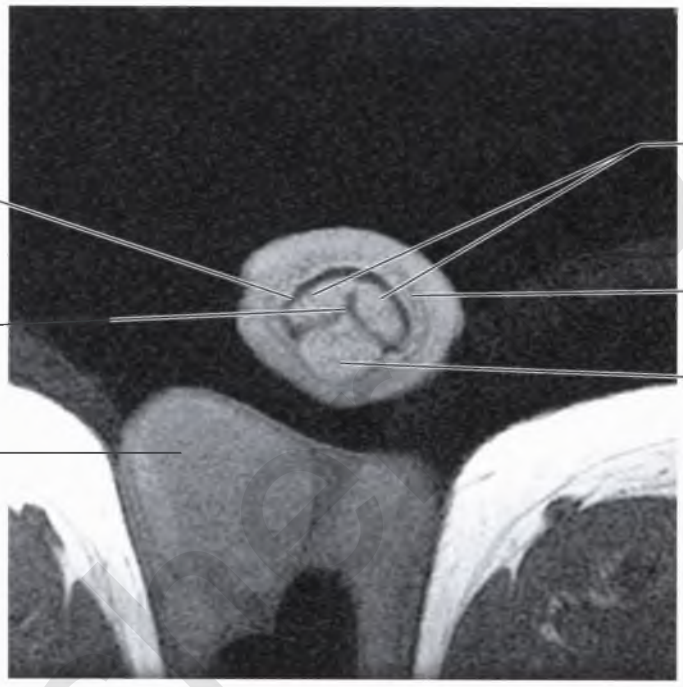
Deep (Buck's) fascia of penis and tunica albuginea
Intercavernous septum of deep fascia
Right testicle
Corpora cavernosa
Superficial (dartos) fascia of penis and skin
Corpus spongiosum

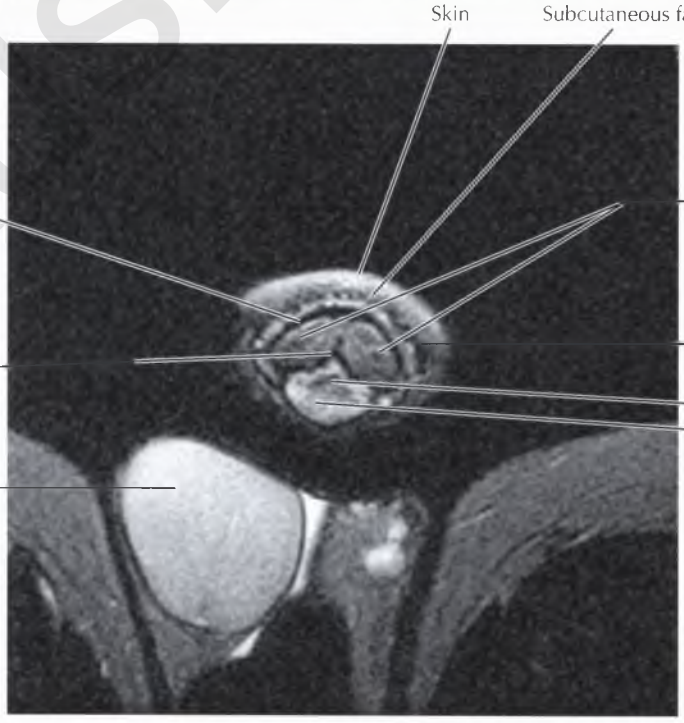
Skin
Subcutaneous fat
Deep (Buck's) fascia of penis and tunica albuginea
Intercavernous septum of deep fascia
Right testicle
Corpora cavernosa
Superficial (dartos) fascia of penis
Penile urethra
Corpus spongiosum

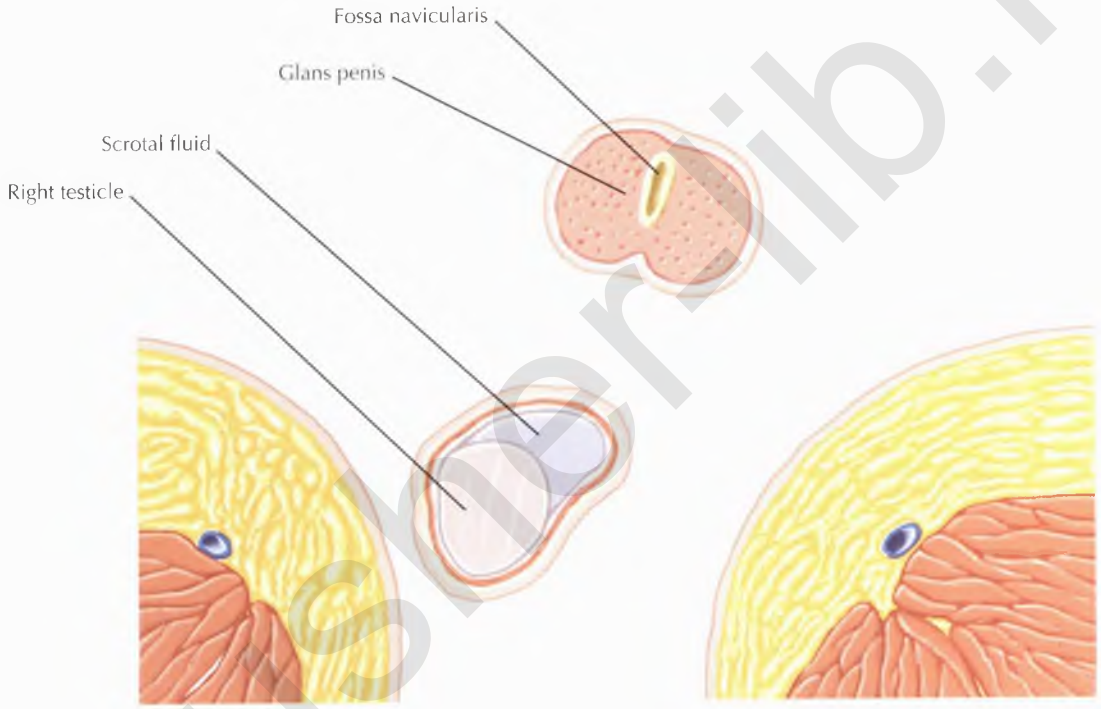

NORMAL ANATOMY

The corpus spongiosum extends and enlarges distally to form the glans penis.

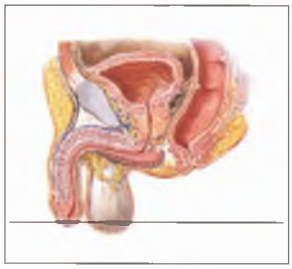

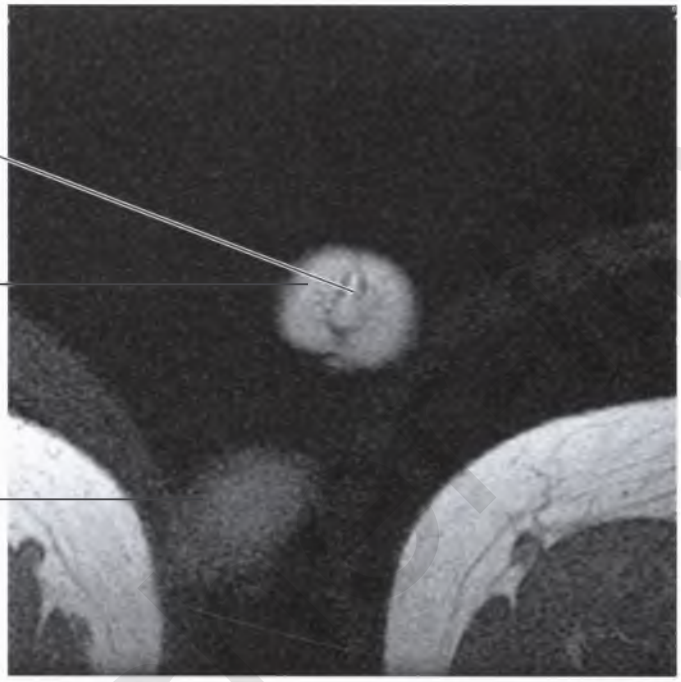

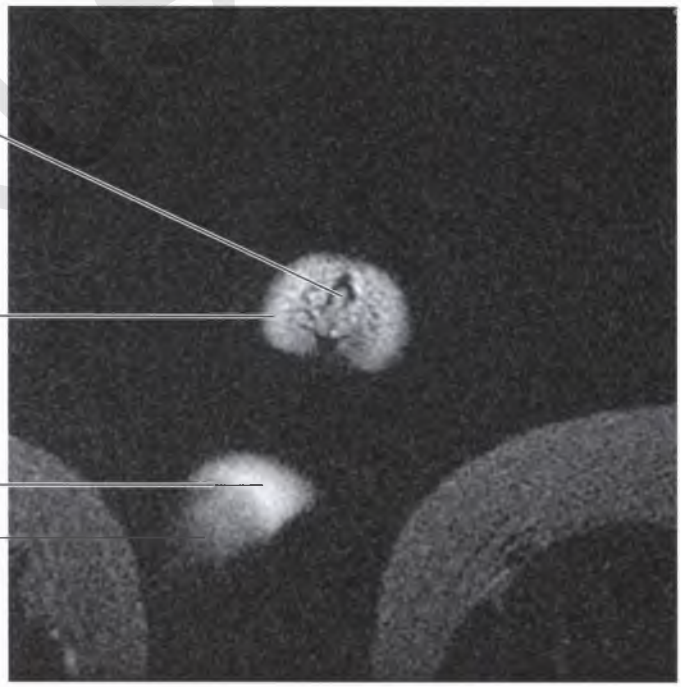

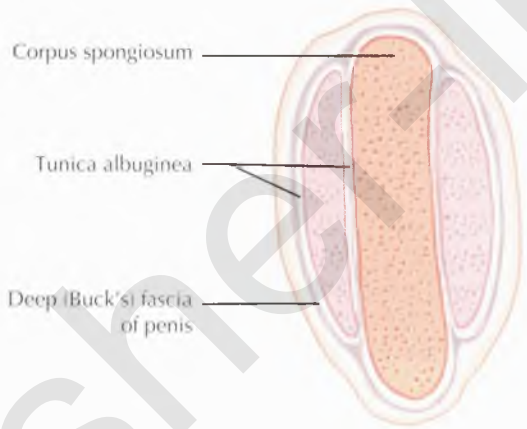

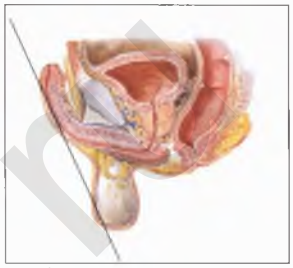


Corpus spongiosum
Deep (Buck's) fascia
and tunica albuginea

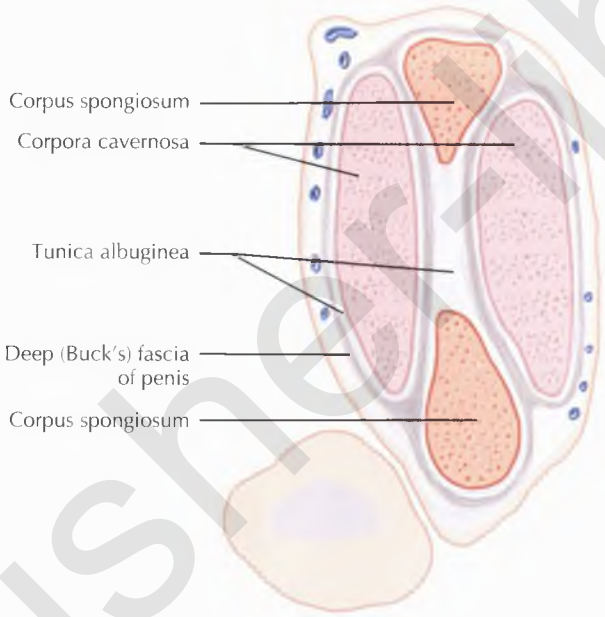

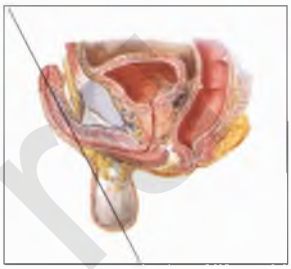


Corpus spongiosum
Corpora cavernosa
Deep (Buck's) fascia and tunica albuginea
Corpus spongiosum

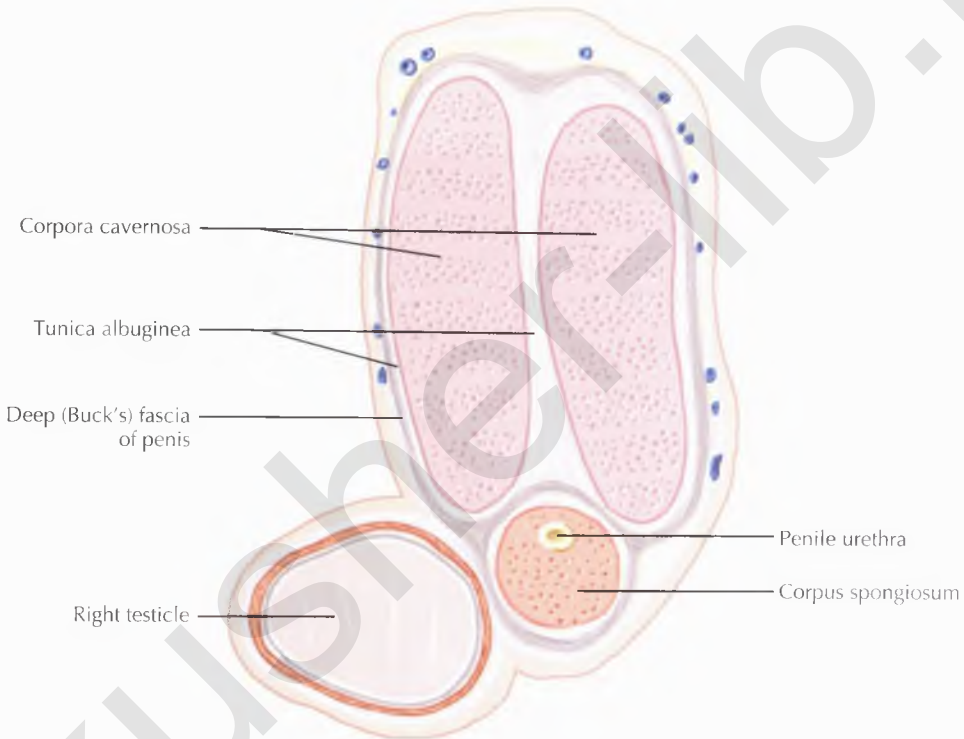

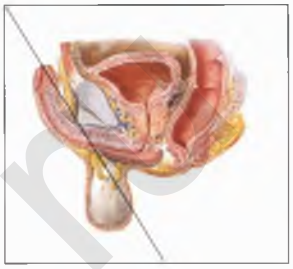


Corpora cavernosa
Deep (Buck's) fascia and tunica albuginea
Penile urethra
Corpus spongiosum
Right testicle

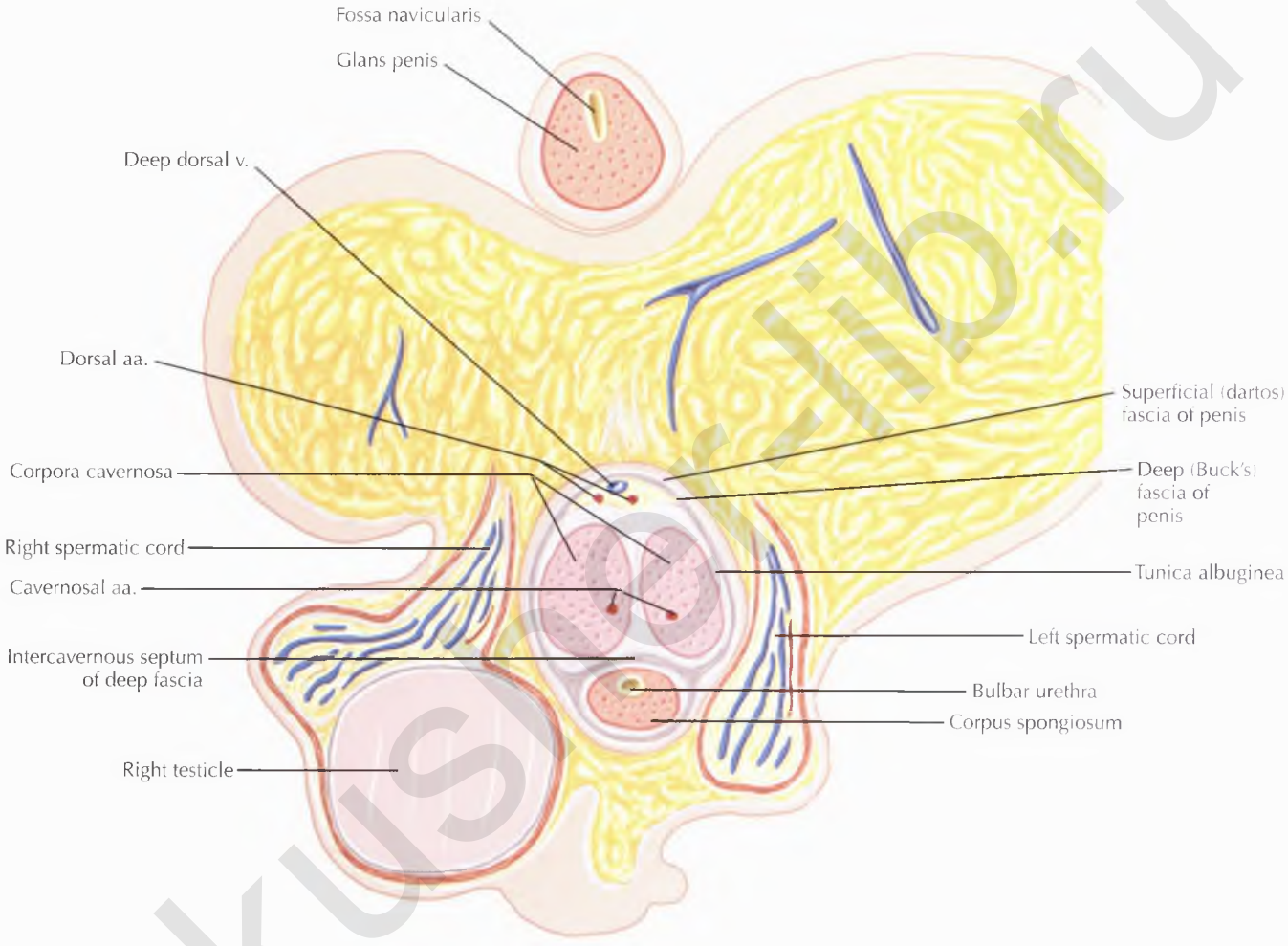

NORMAL ANATOMY

The cavernosal arteries are seen as small, round flow voids in cross section within the paired corpora cavernosa. These arteries give off the *helicine arteries*, which provide the primary source of blood for erectile function.

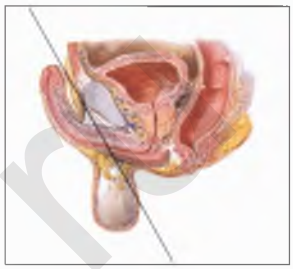

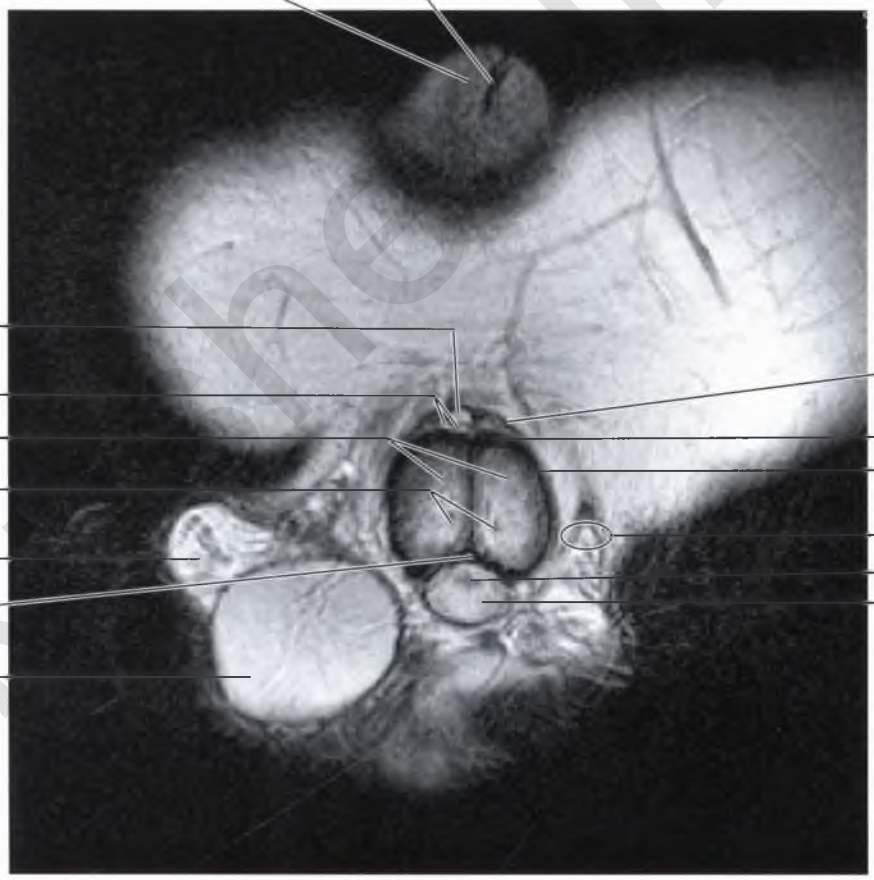
Glans penis
Fossa navicularis
Deep dorsal v.
Dorsal aa.
Corpora cavernosa
Cavernosal aa.
Right spermatic cord
Intercavernous septum of deep fascia
Right testicle
Deep (Buck's) fascia of penis
Tunica albuginea
Deep (Buck's) fascia and tunica albuginea
Left spermatic cord
Bulbar urethra
Corpus spongiosum

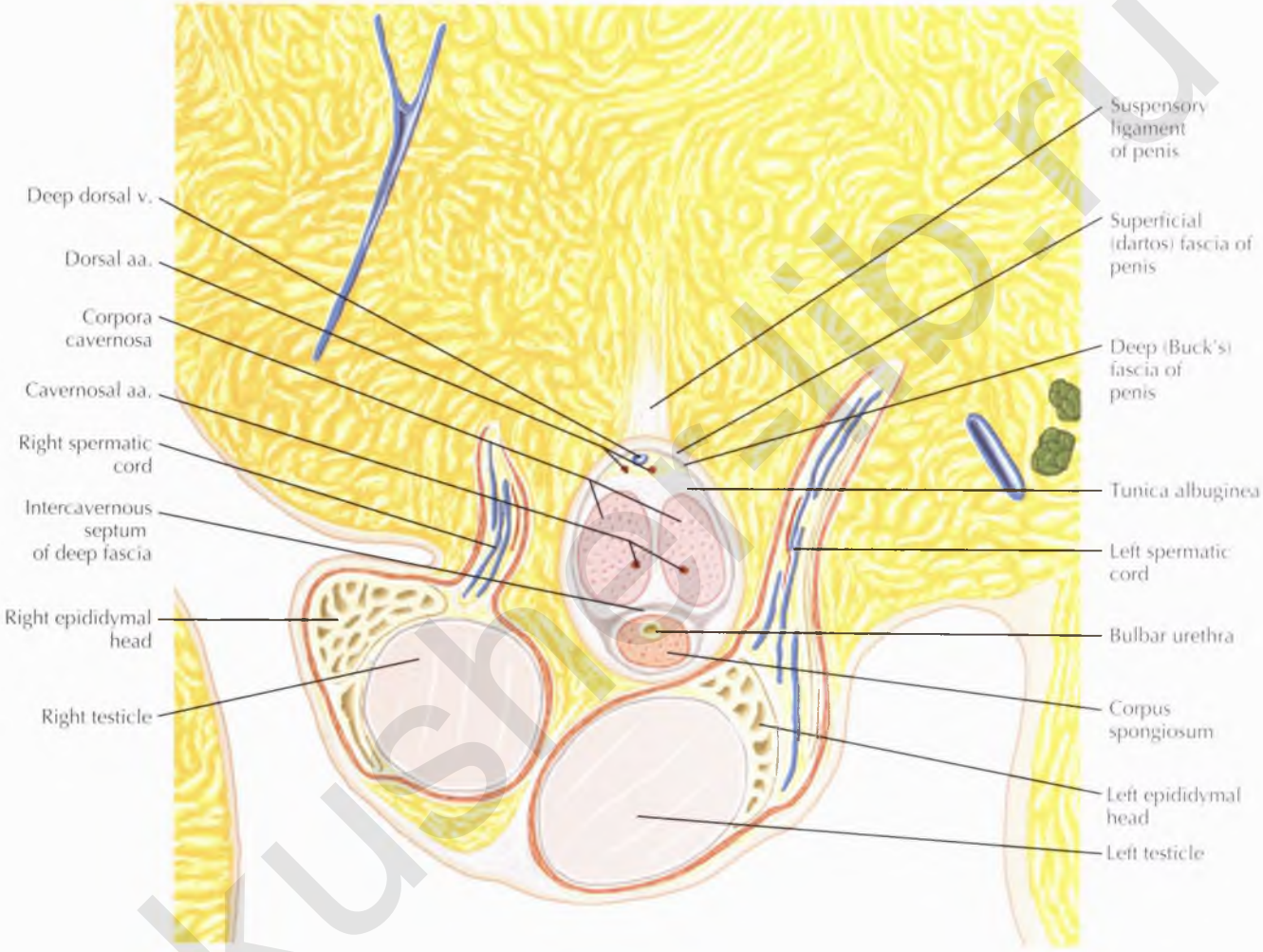

NORMAL ANATOMY

The deep dorsal vein and paired dorsal arteries lie deep to the deep (Buck's) fascia and superficial to the tunica albuginea. The paired dorsal arteries supply blood flow to the glans penis and skin. The deep dorsal vein provides the primary venous drainage for the corpora cavernosa.

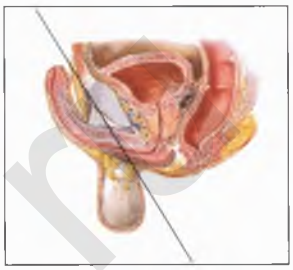

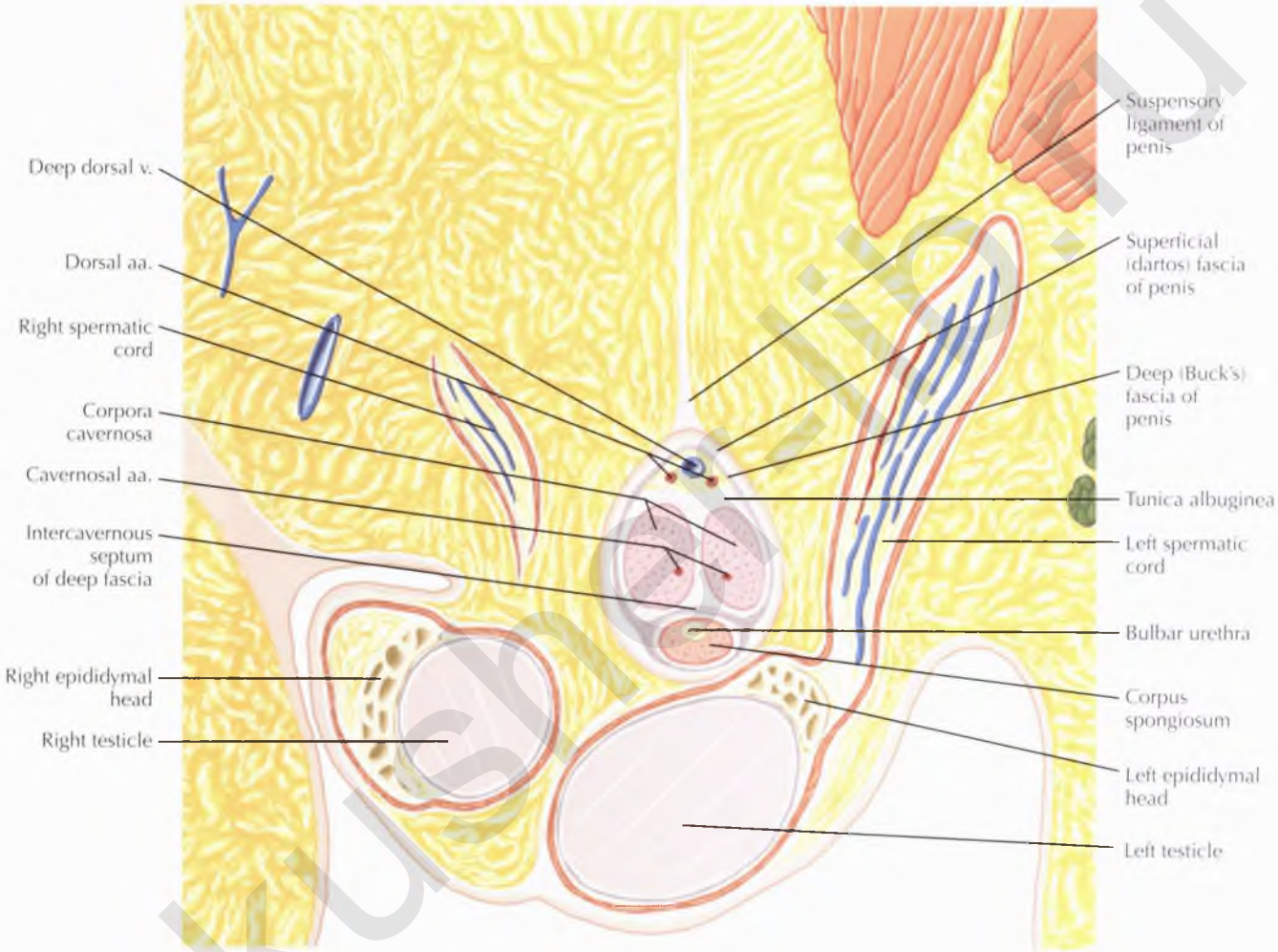

NORMAL ANATOMY

The suspensory ligament of the penis is an inferior extension of the abdominal rectus sheath that is attached to the pubic bone and supports the penis when erect. Surgical release of this ligament is performed in penile-lengthening procedures.

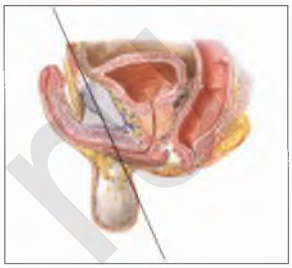

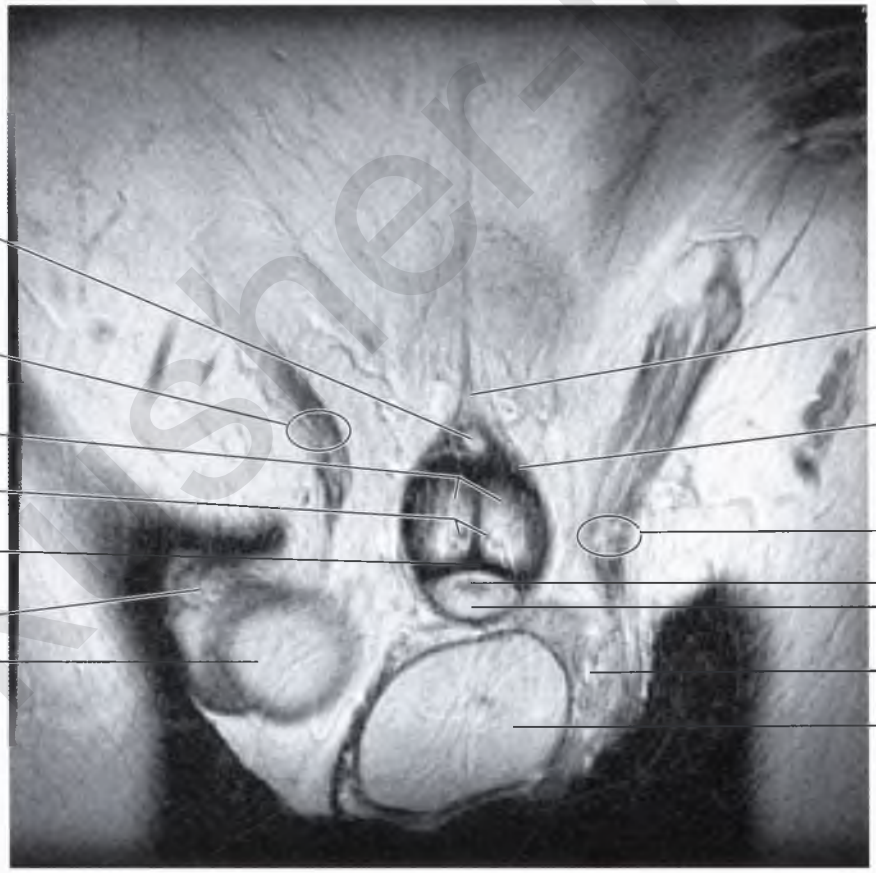

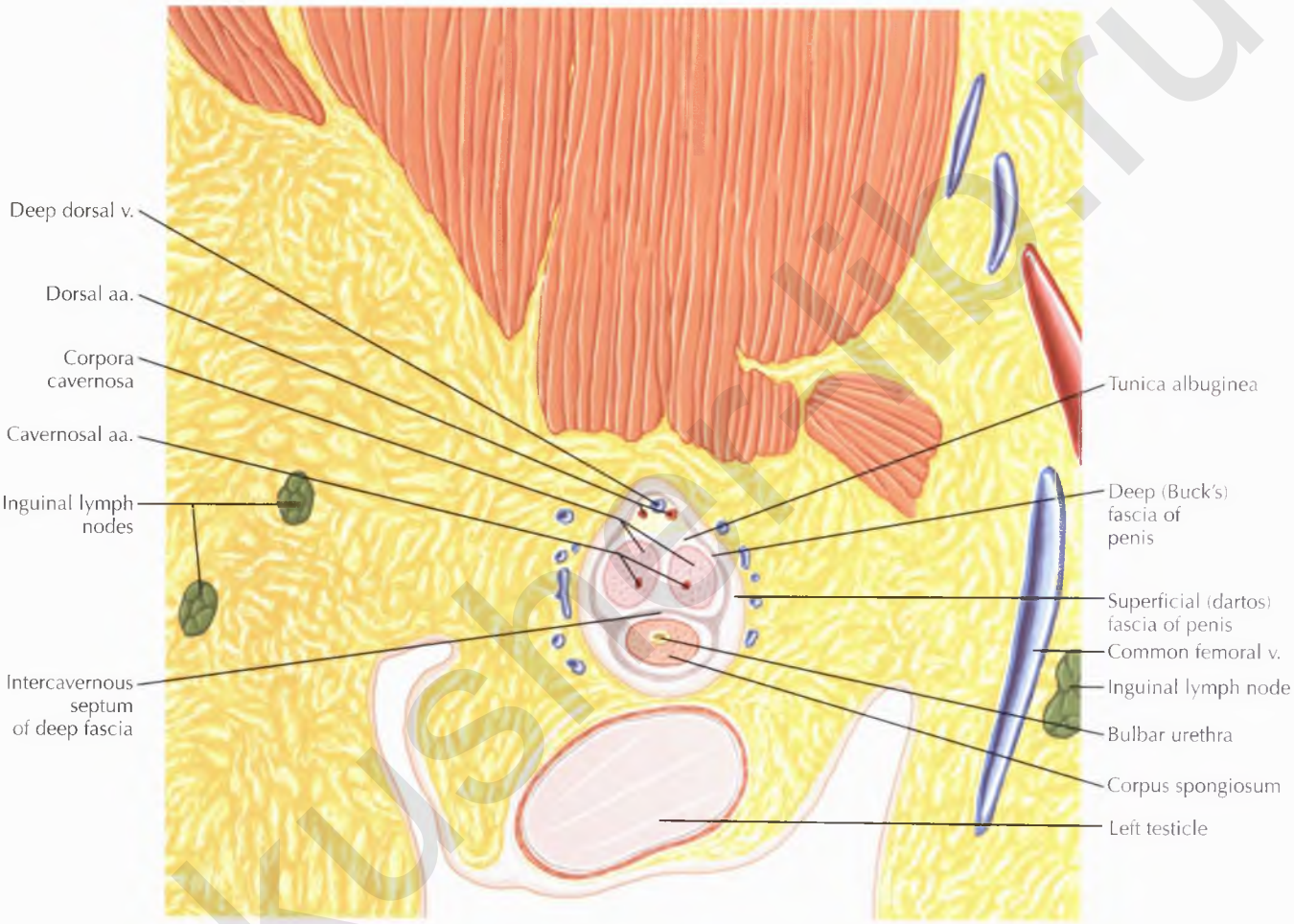

NORMAL ANATOMY

The flat, nondistended penile urethra is seen within the corpus spongiosum.

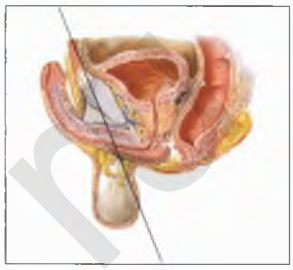

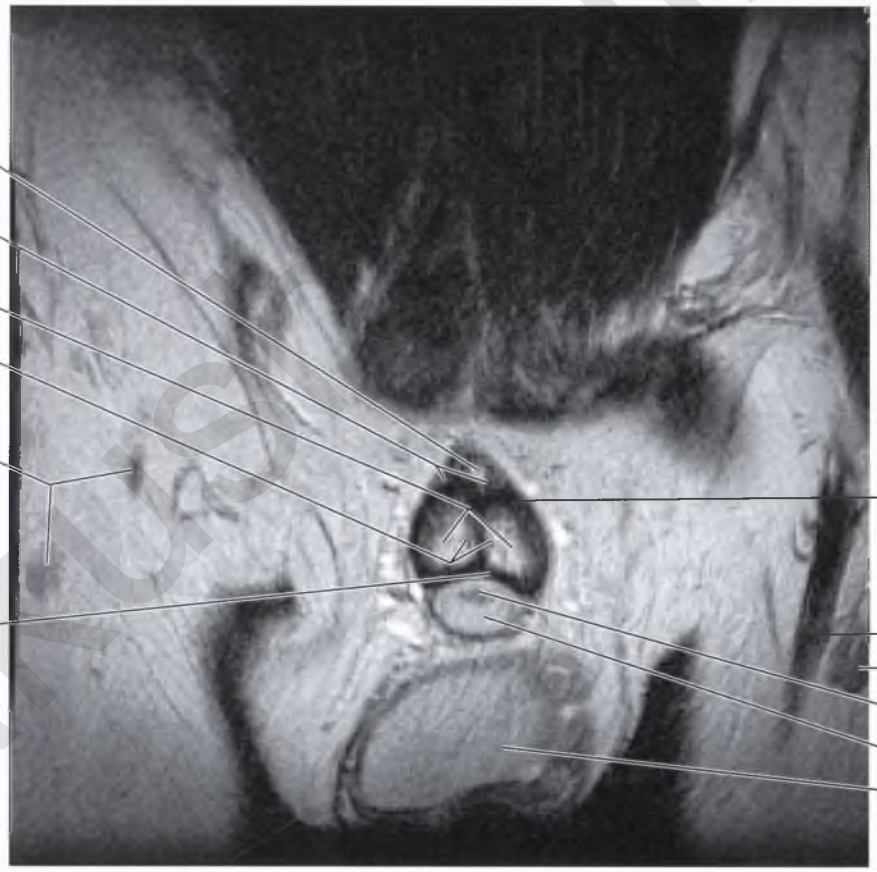
Deep dorsal v.
Dorsal aa.
Corpora cavernosa
Cavernosal aa.
Inguinal lymph nodes
Intercavernous septum of deep fascia
Deep (Buck's) fascia and tunica albuginea
Common femoral v.
Inguinal lymph node
Bulbar urethra
Corpus spongiosum
Left testicle

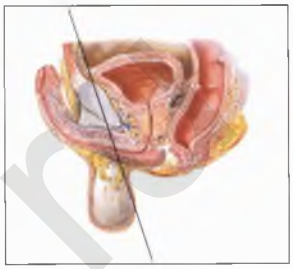

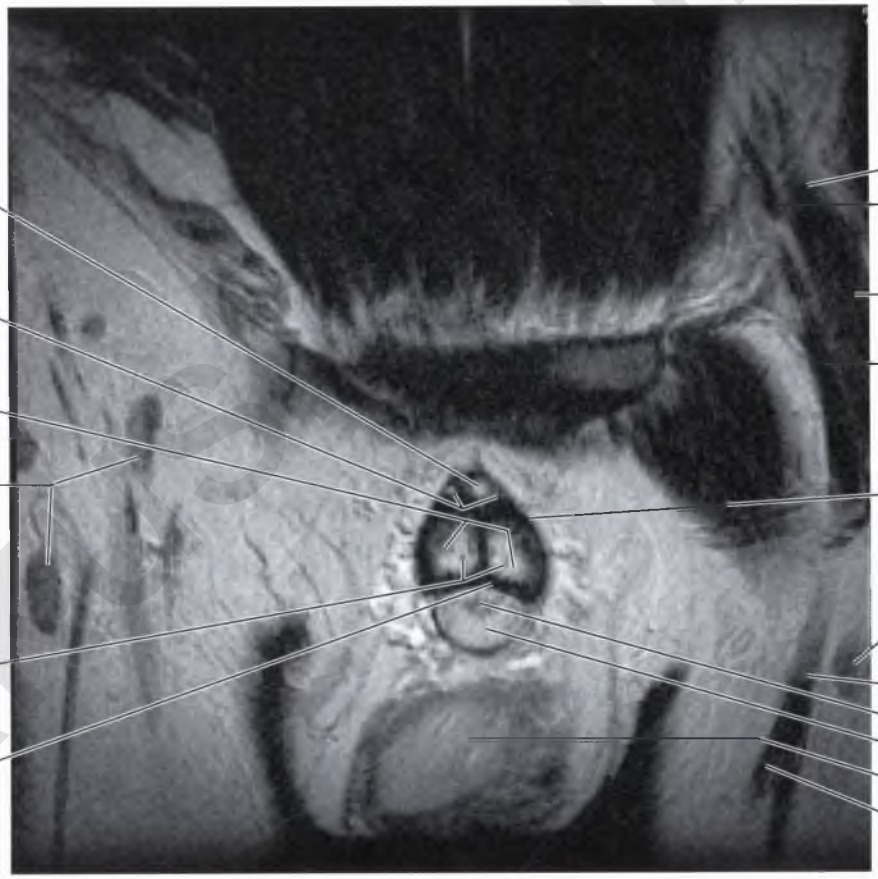
Deep dorsal v.
Dorsal aa.
Corpora cavernosa
Inguinal lymph nodes
Cavernosal aa.
Intercavernous septum of deep fascia
External iliac a.
External iliac v.
Common femoral a.
Common femoral v.
Deep (Buck's) fascia and tunica albuginea
Inguinal lymph node
Common femoral v.
Bulbar urethra
Corpus spongiosum
Left testicle
Greater saphenous v.

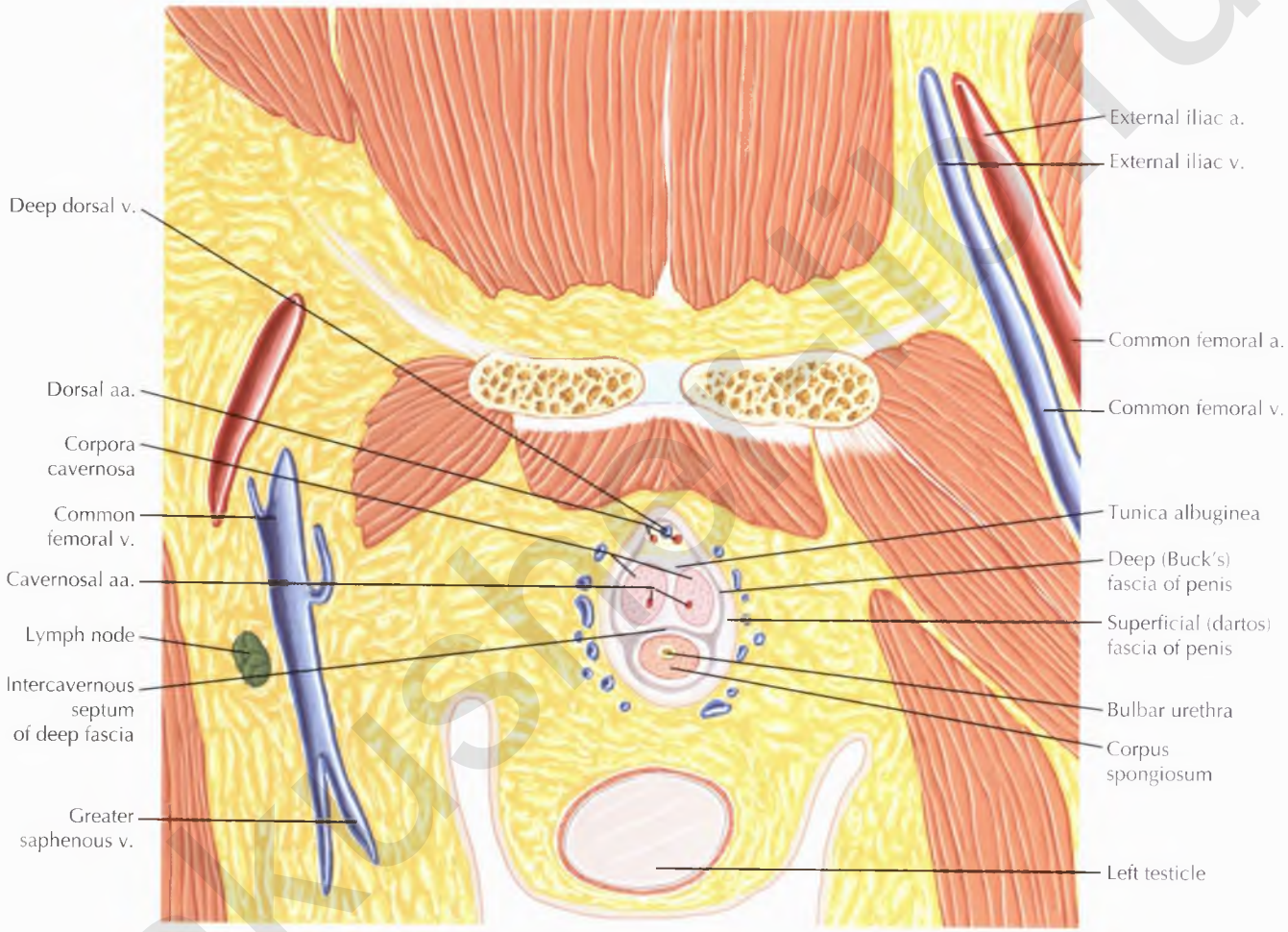
External iliac a.
External iliac v.
Deep dorsal v.
Common femoral a.
Dorsal aa.
Common femoral v.
Corpora cavernosa
Common femoral v.
Tunica albuginea
Cavernosal aa.
Deep (Buck's) fascia of penis
Lymph node
Superficial (dartos) fascia of penis
Intercavernous septum of deep fascia
Bulbar urethra
Corpus spongiosum
Greater saphenous v.
Left testicle

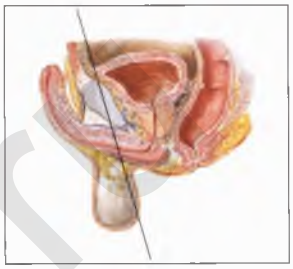

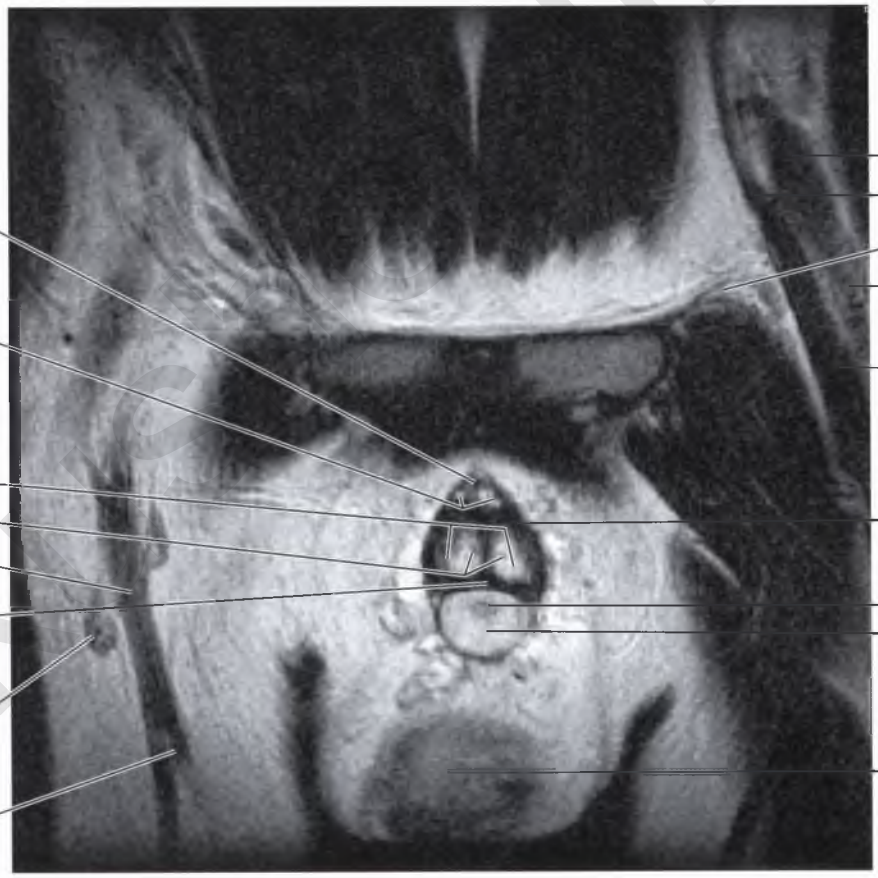
Deep dorsal v.
Dorsal aa.
Corpora cavernosa
Cavernosal aa.
Common femoral v.
Intercavernous septum of deep fascia
Inguinal lymph node
Greater saphenous v.
External iliac a.
External iliac v.
Inguinal ligament
Common femoral a.
Common femoral v.
Deep (Buck's) fascia and tunica albuginea
Bulbar urethra
Corpus spongiosum
Left testicle

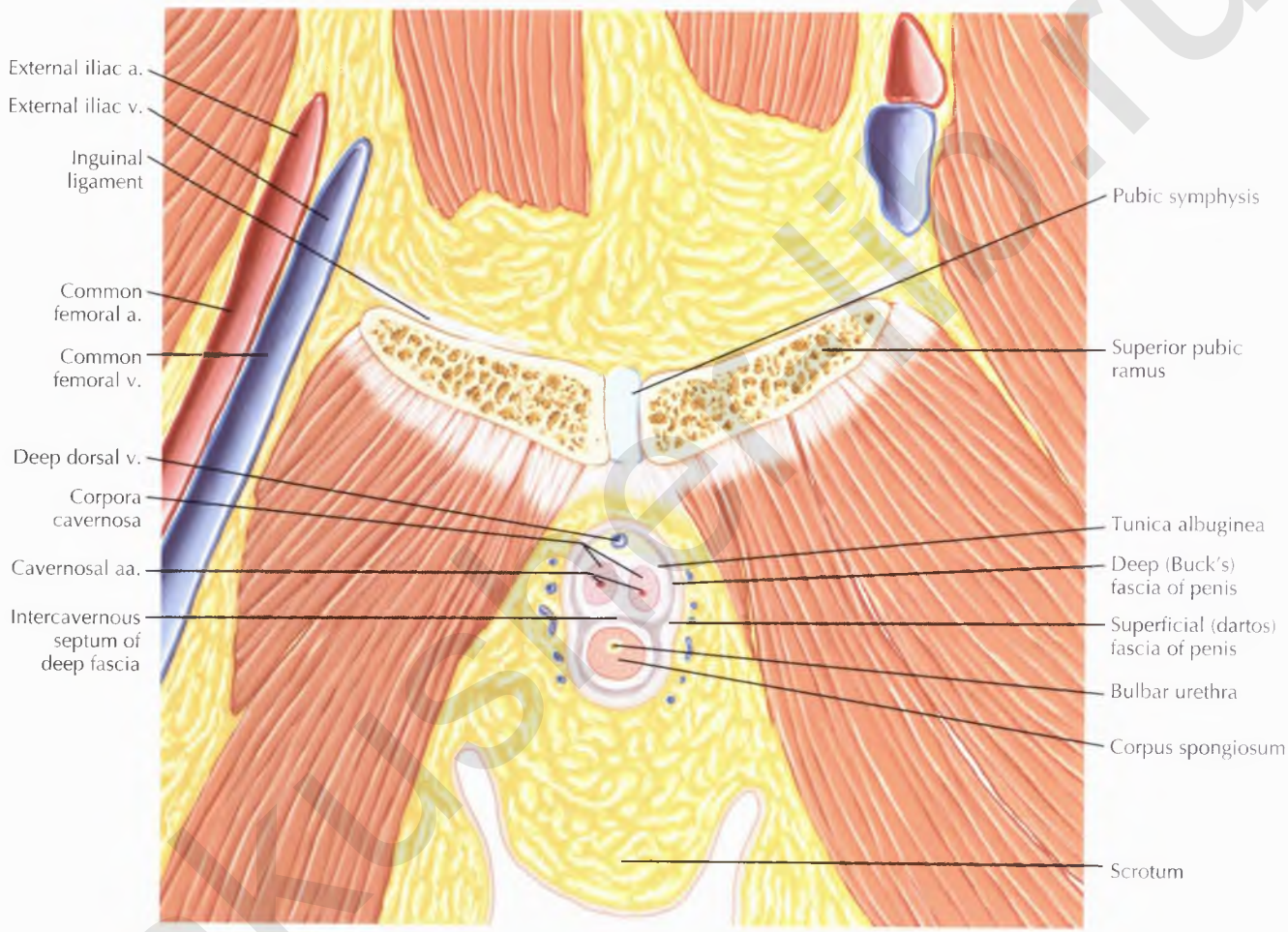
External iliac a.
External iliac v.
Inguinal ligament
Common femoral a.
Common femoral v.
Deep dorsal v.
Corpora cavernosa
Cavernosal aa.
Intercavernous septum of deep fascia
Pubic symphysis
Superior pubic ramus
Tunica albuginea
Deep (Buck's) fascia of penis
Superficial (dartos) fascia of penis
Bulbar urethra
Corpus spongiosum
Scrotum

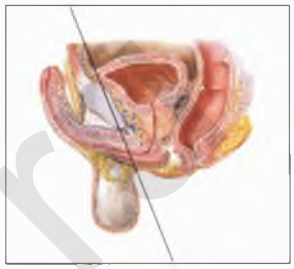

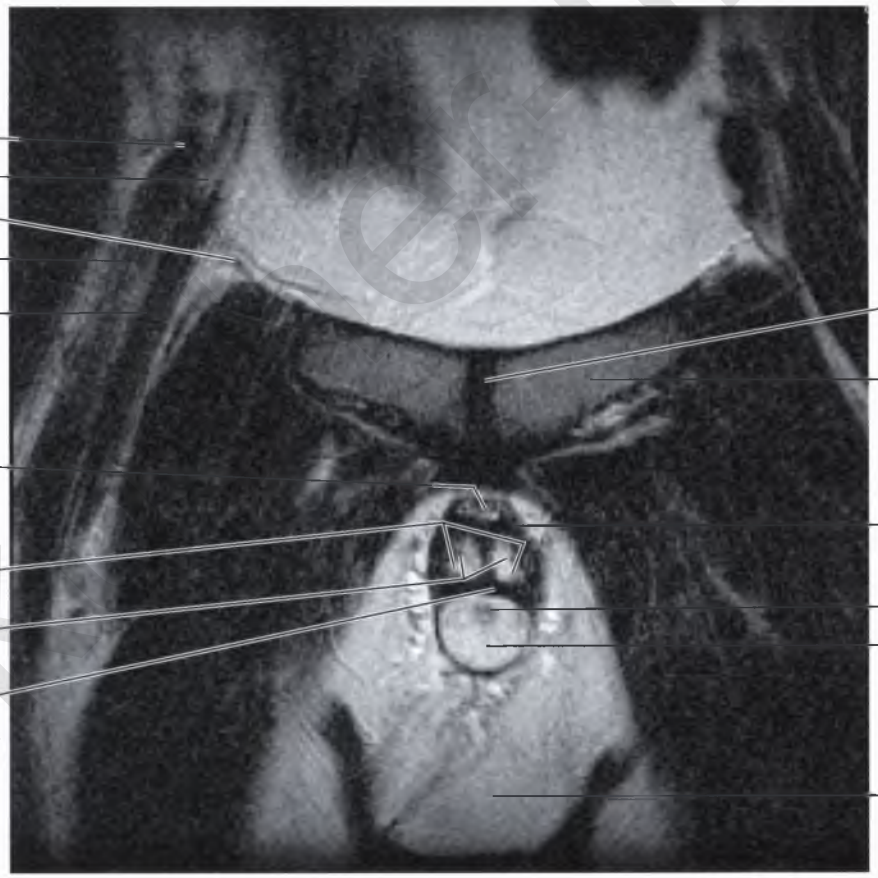
External iliac a.
External iliac v.
Inguinal ligament
Common femoral a.
Common femoral v.
Deep dorsal v.
Corpora cavernosa
Cavernosal aa.
Intercavernous septum of deep fascia
Pubic symphysis
Superior pubic ramus
Deep (Buck's) fascia and tunica albuginea
Bulbar urethra
Corpus spongiosum
Scrotum

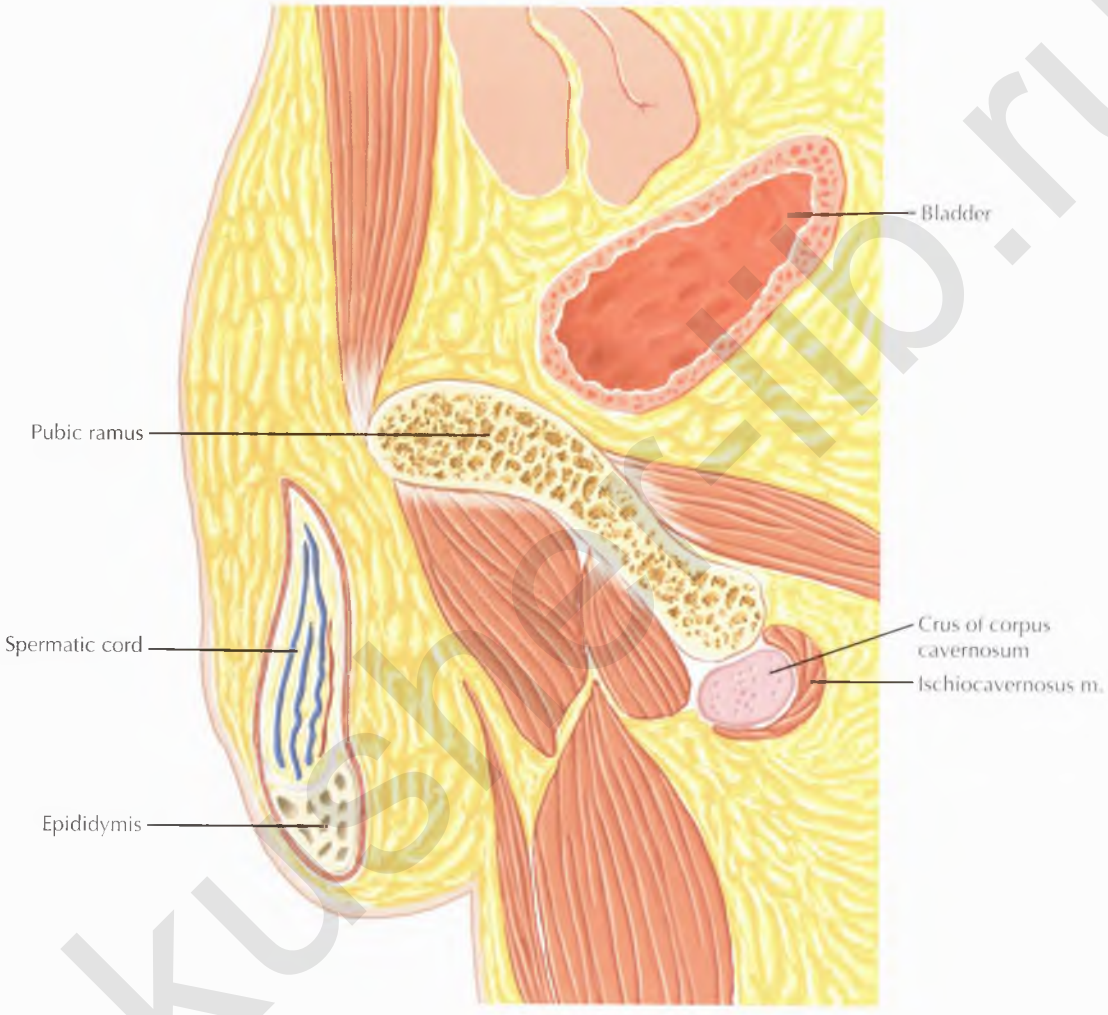

NORMAL ANATOMY

The crura of the corpora cavernosa are the most posterior portions, which flare laterally to attach to the ischiopubic rami, and are invested by the ischiocavernosus muscles.

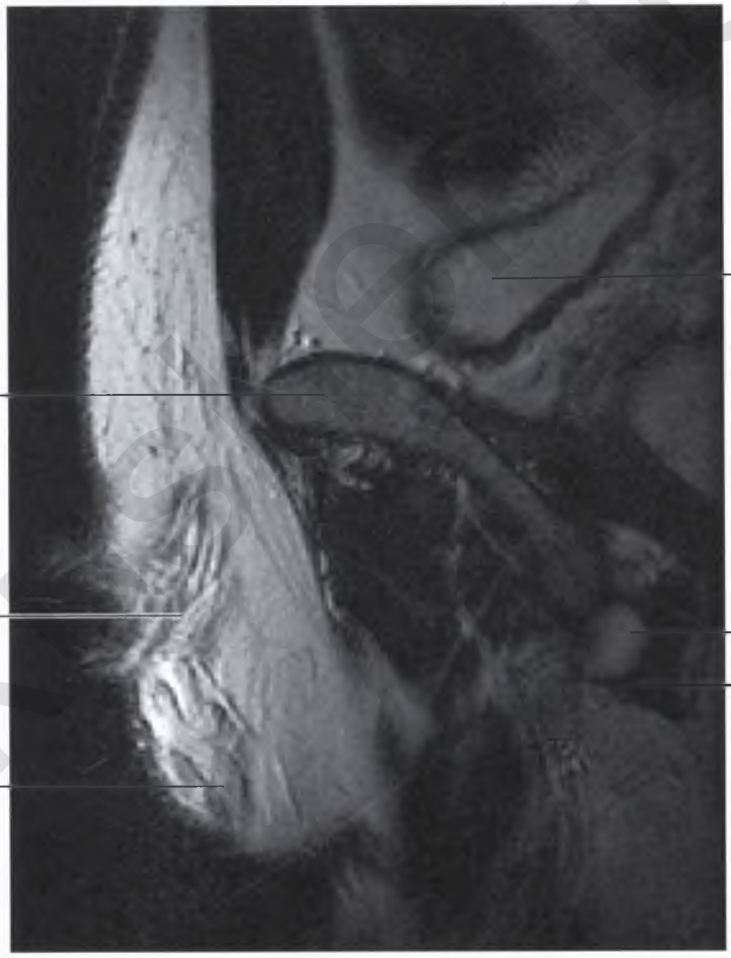

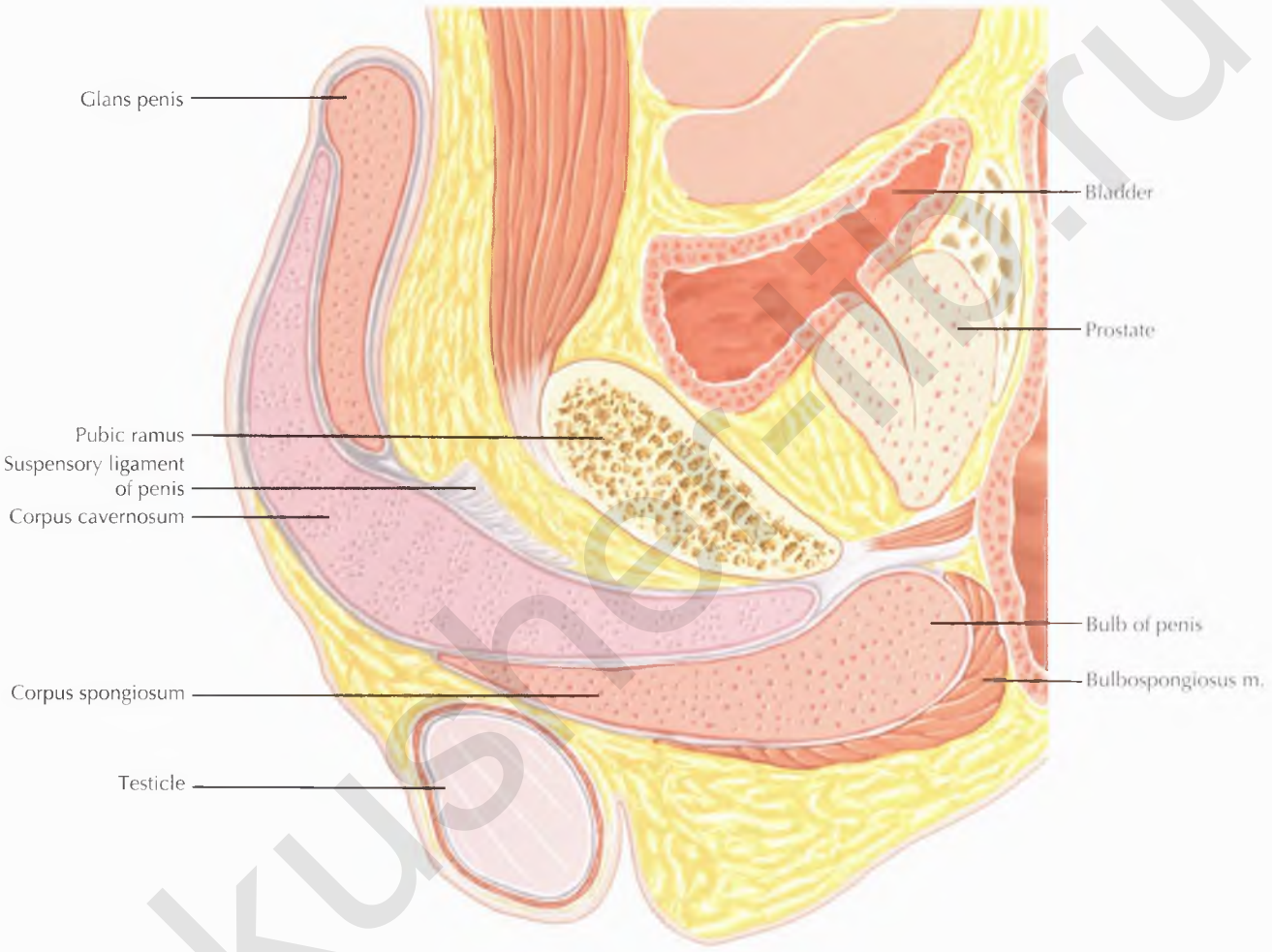

NORMAL ANATOMY

The corpus spongiosum becomes the bulb of the penis at its root and is invested by the bulbospongiosus muscle.

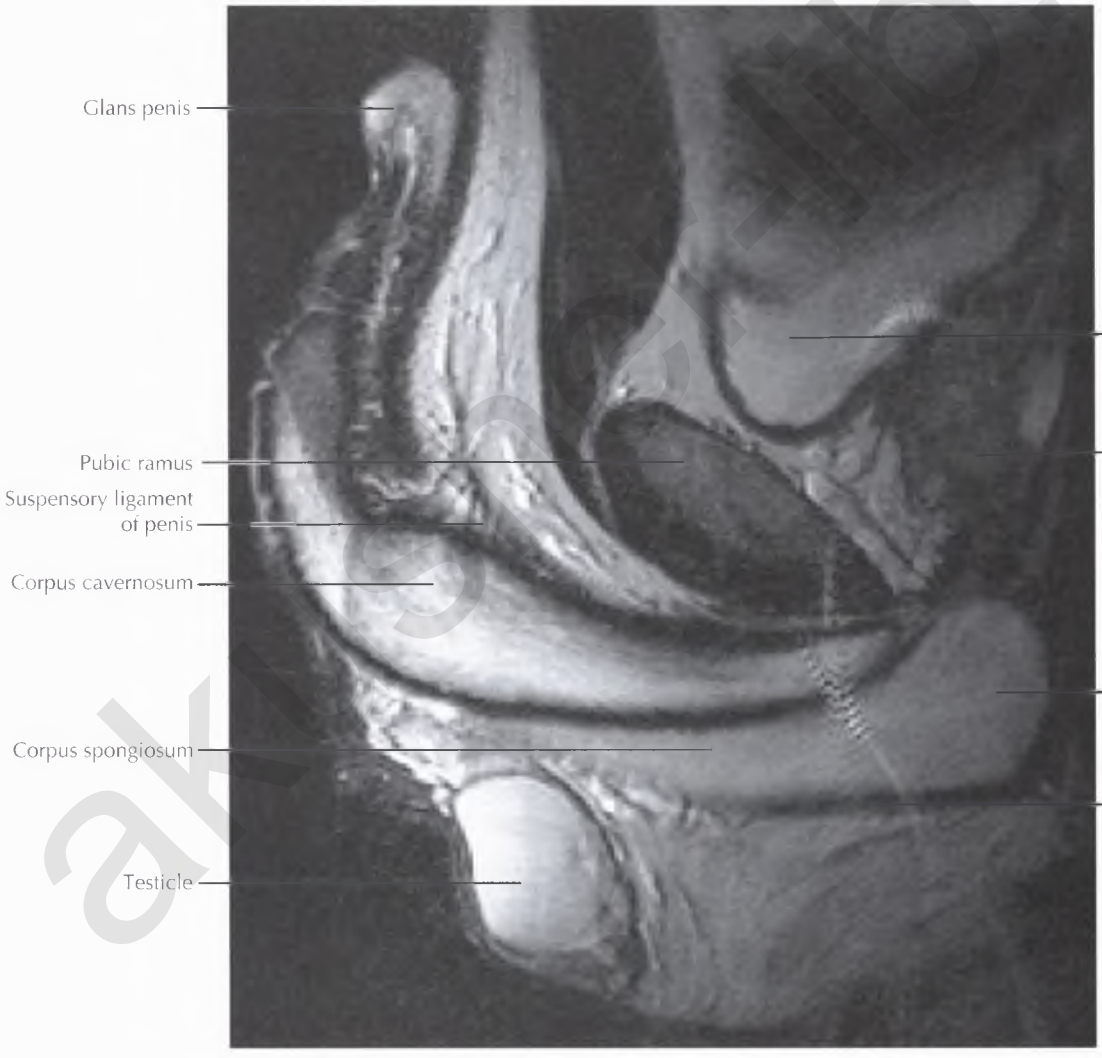
Glans penis
Bladder
Pubic ramus
Prostate
Suspensory ligament of penis
Corpus cavernosum
Bulb of penis
Corpus spongiosum
Bulbospongiosus m.
Testicle

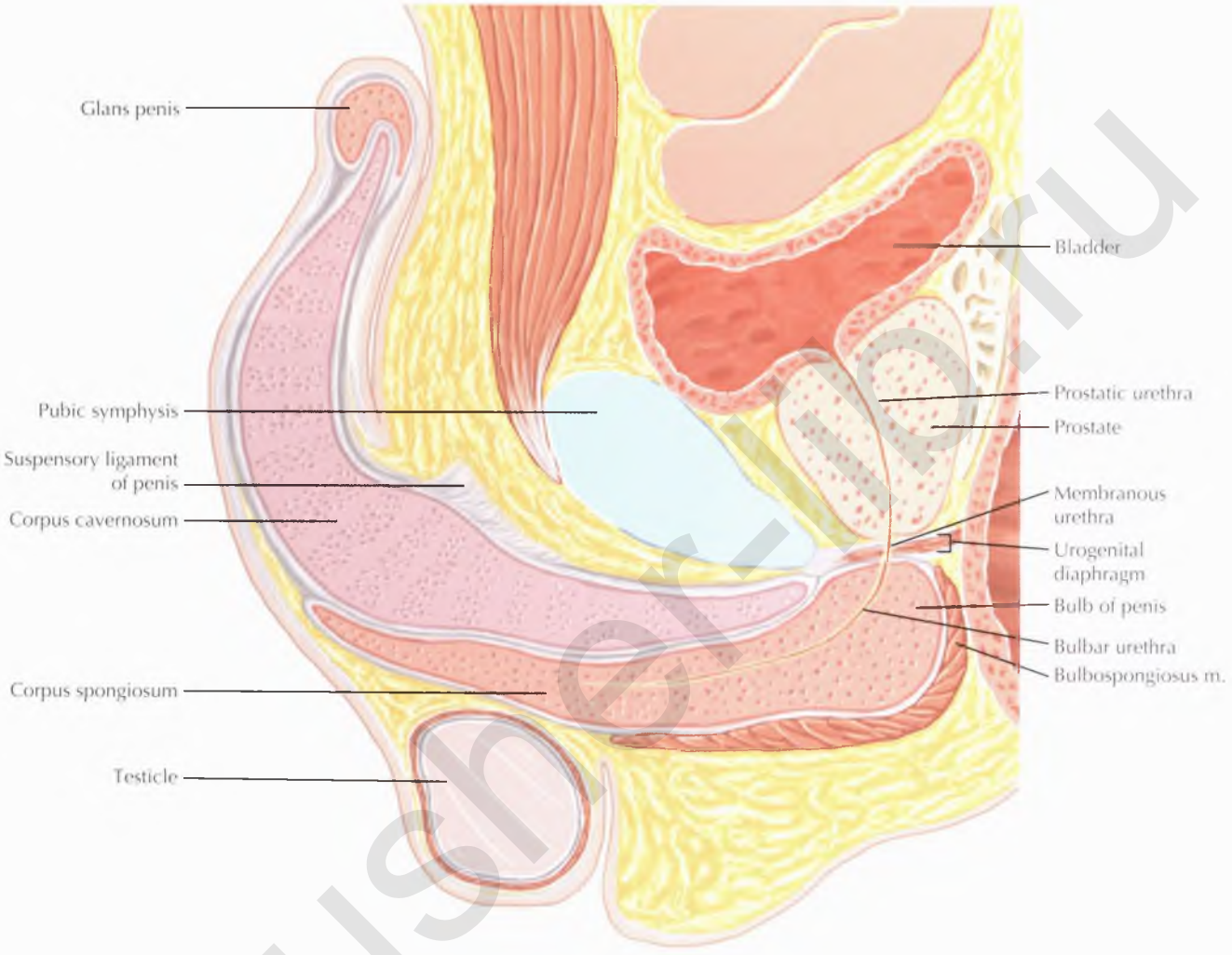

NORMAL ANATOMY

The male urethra is divided into four segments: the prostatic and membranous segments, which form the posterior urethra, and the bulbar and penile segments, which form the anterior urethra. The *prostatic* urethra traverses the prostate gland and contains openings for the prostatic utricle, prostatic ducts, and ejaculatory ducts. The *membranous* urethra courses through the urogenital diaphragm at the level of the external urethral sphincter and bulbourethral (Cowper's) glands. The bulbourethral gland ducts drain into the *bulbar* urethra, which begins inferior to the urogenital diaphragm and continues to the suspensory ligament of the penis at the penoscrotal junction. The *penile* urethra begins distal to the suspensory ligament, forming the main pendulous portion of the urethra and the *fossa navicularis*, a urethral widening at the glans penis. The nondistended anterior urethra is difficult to see on MR images, generally appearing as a flat band of hypointensity surrounded by the hyperintense tissue of the corpus spongiosum.


Glans penis
Bladder
Prostatic urethra
Prostate
Pubic symphysis
Membranous urethra
Suspensory ligament of penis
Urogenital diaphragm
Corpus cavernosum
Bulbar urethra
Bulb of penis
Corpus spongiosum
Bulbospongiosus m.
Testicle

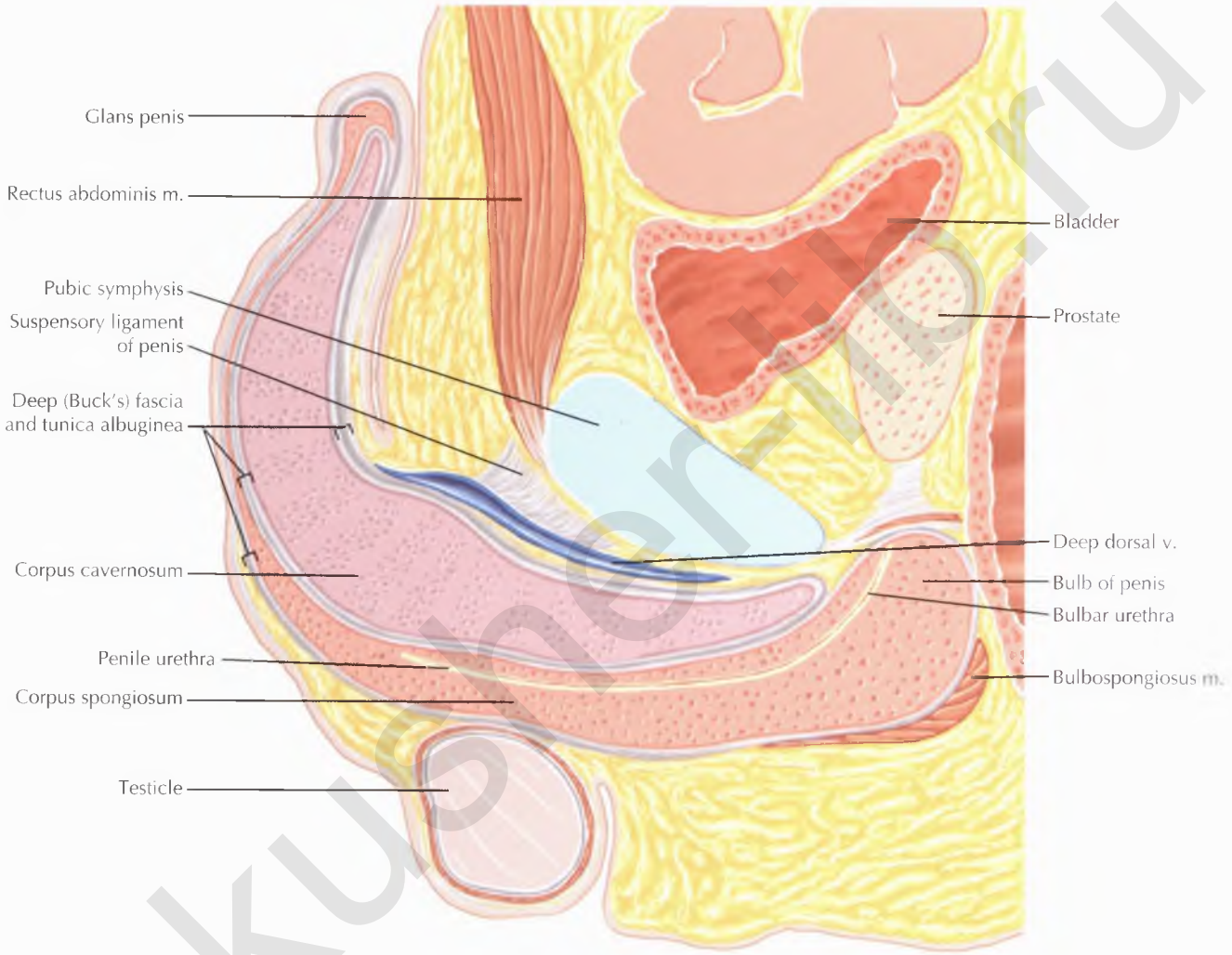

DIAGNOSTIC CONSIDERATION

Urethral injury resulting from pelvic fractures most frequently involves the membranous urethra, whereas "straddle" injuries more often involve the bulbar urethra because of compression against the inferior pubic symphysis.

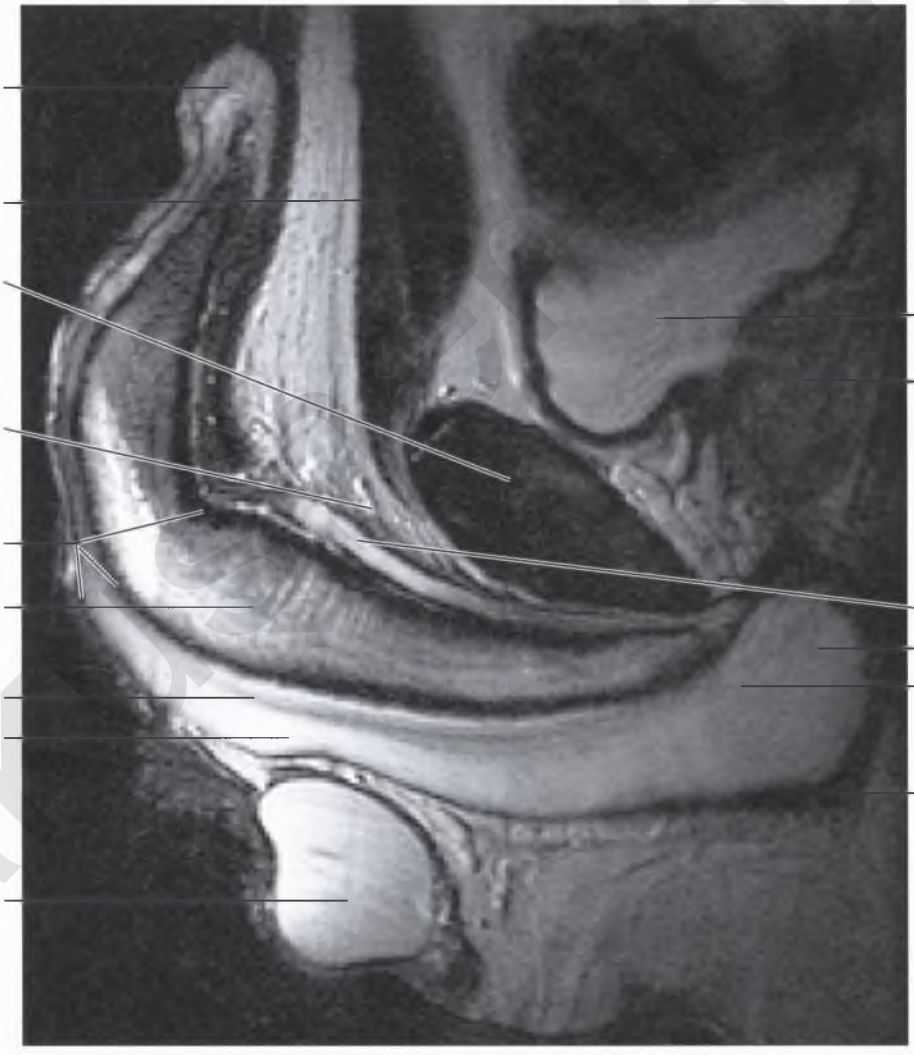
Glans penis
Rectus abdominis m.
Pubic symphysis
Suspensory ligament of penis
Deep (Buck's) fascia and tunica albuginea
Corpus cavernosum
Penile urethra
Corpus spongiosum
Testicle
Bladder
Prostate
Deep dorsal v.
Bulb of penis
Bulbar urethra
Bulbospongiosus m.

Chapter 10 FEMALE PELVIS

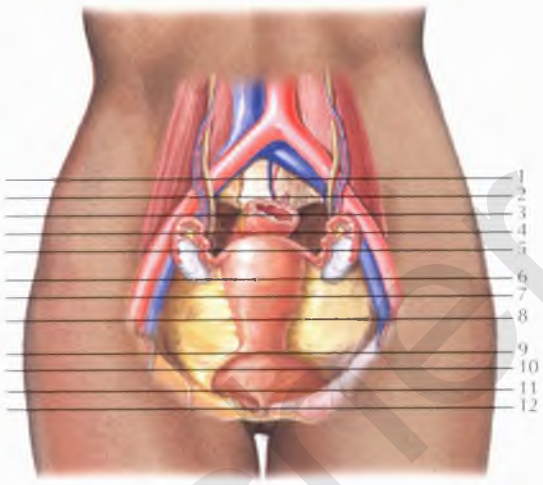

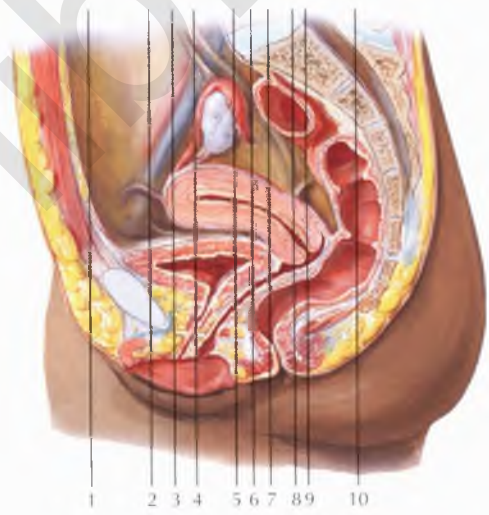

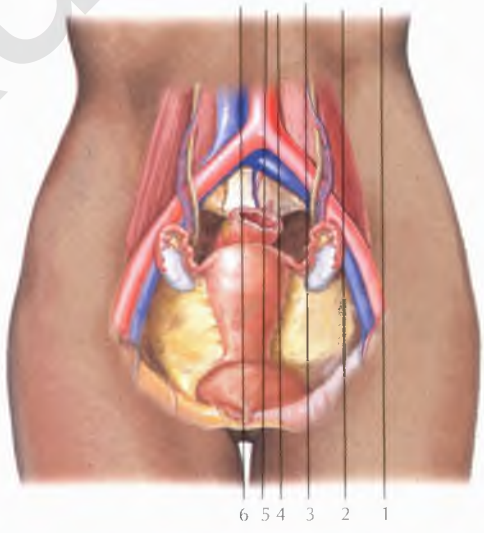

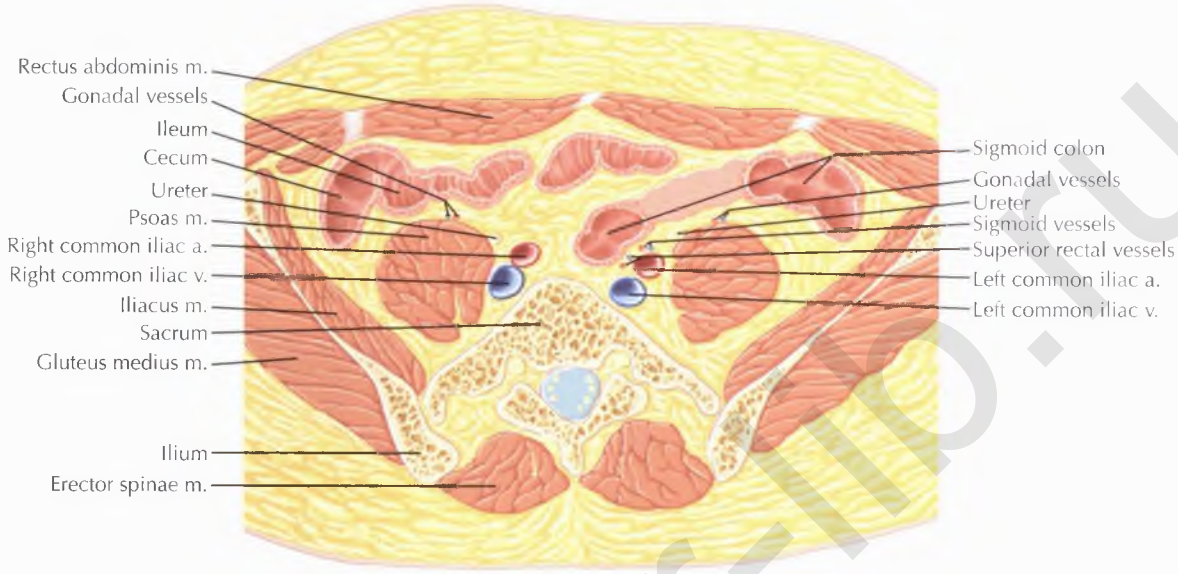
Rectus abdominis m.
Gonadal vessels
Ileum
Cecum
Ureter
Psoas m.
Right common iliac a.
Right common iliac v.
Iliacus m.
Sacrum
Gluteus medius m.
Ilium
Erector spinae m.
Sigmoid colon
Gonadal vessels
Ureter
Sigmoid vessels
Superior rectal vessels
Left common iliac a.
Left common iliac v.

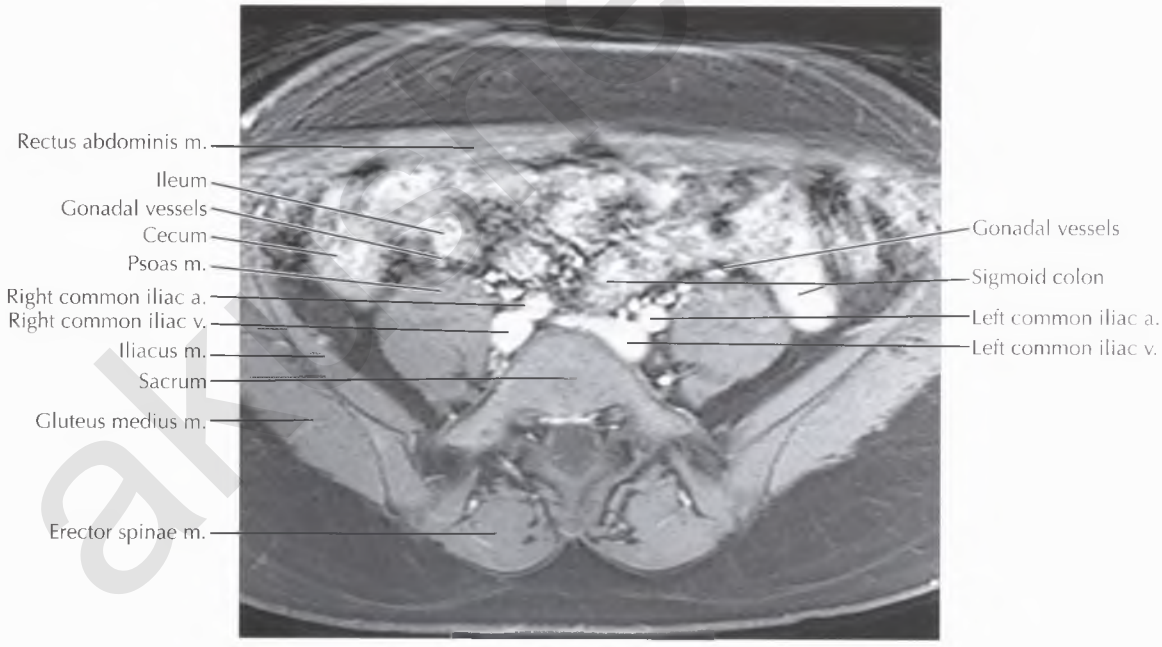
Rectus abdominis m.
Ileum
Gonadal vessels
Cecum
Psoas m.
Right common iliac a.
Right common iliac v.
Iliacus m.
Sacrum
Gluteus medius m.
Erector spinae m.
Gonadal vessels
Sigmoid colon
Left common iliac a.
Left common iliac v.

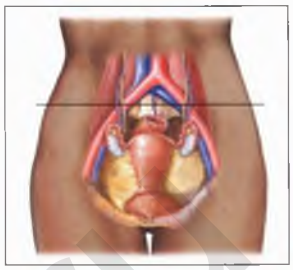

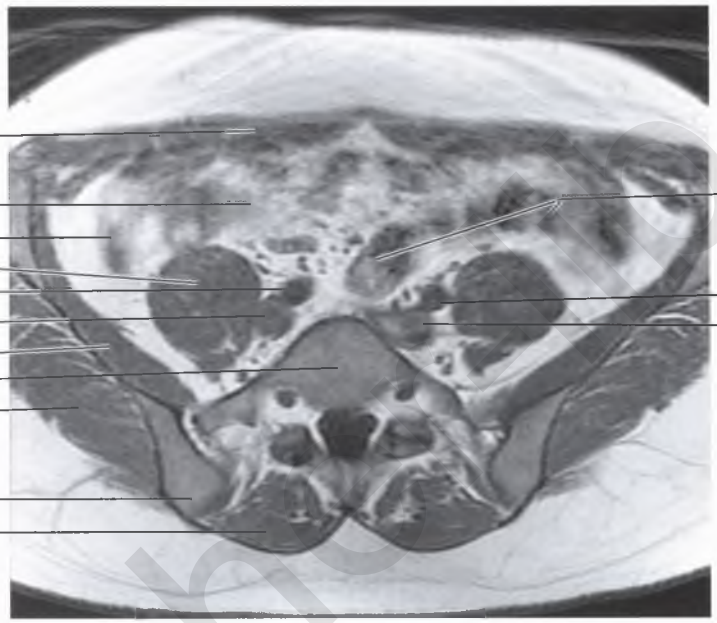
Rectus abdominis m.
Ileum
Cecum
Psoas m.
Right common iliac a.
Right common iliac v.
Iliacus m.
Sacrum
Gluteus medius m.
Ilium
Erector spinae m.
Sigmoid colon
Left common iliac a.
Left common iliac v.

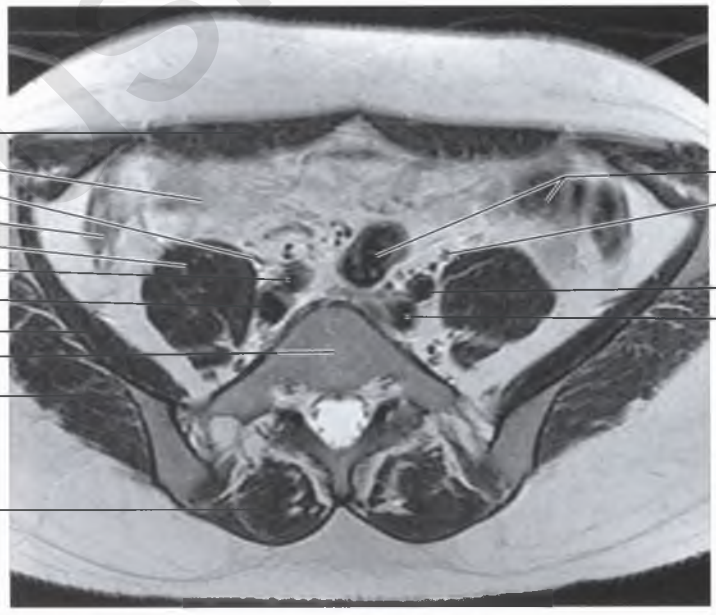
Rectus abdominis m.
Ileum
Ureter
Cecum
Psoas m.
Right common iliac a.
Right common iliac v.
Iliacus m.
Sacrum
Gluteus medius m.
Erector spinae m.
Sigmoid colon
Ureter
Left common iliac a.
Left common iliac v.

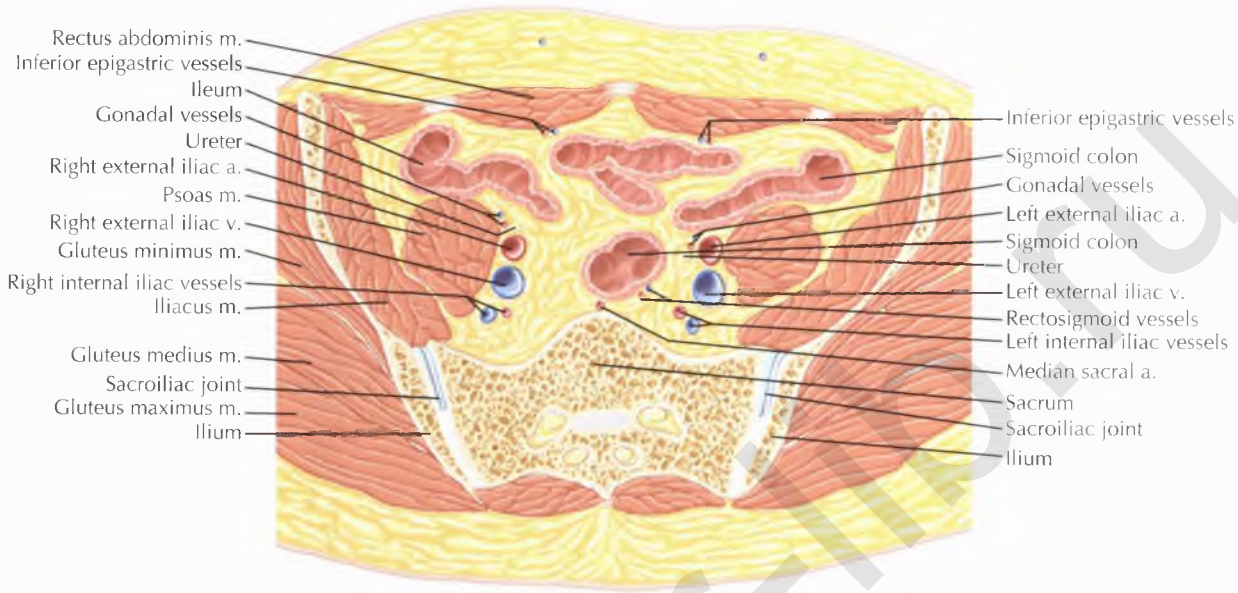
Rectus abdominis m.
Inferior epigastric vessels
Ileum
Gonadal vessels
Ureter
Right external iliac a.
Psoas m.
Right external iliac v.
Gluteus minimus m.
Right internal iliac vessels
Iliacus m.
Gluteus medius m.
Sacroiliac joint
Gluteus maximus m.
Ilium
Inferior epigastric vessels
Sigmoid colon
Gonadal vessels
Left external iliac a.
Sigmoid colon
Ureter
Left external iliac v.
Rectosigmoid vessels
Left internal iliac vessels
Median sacral a.
Sacrum
Sacroiliac joint
Ilium

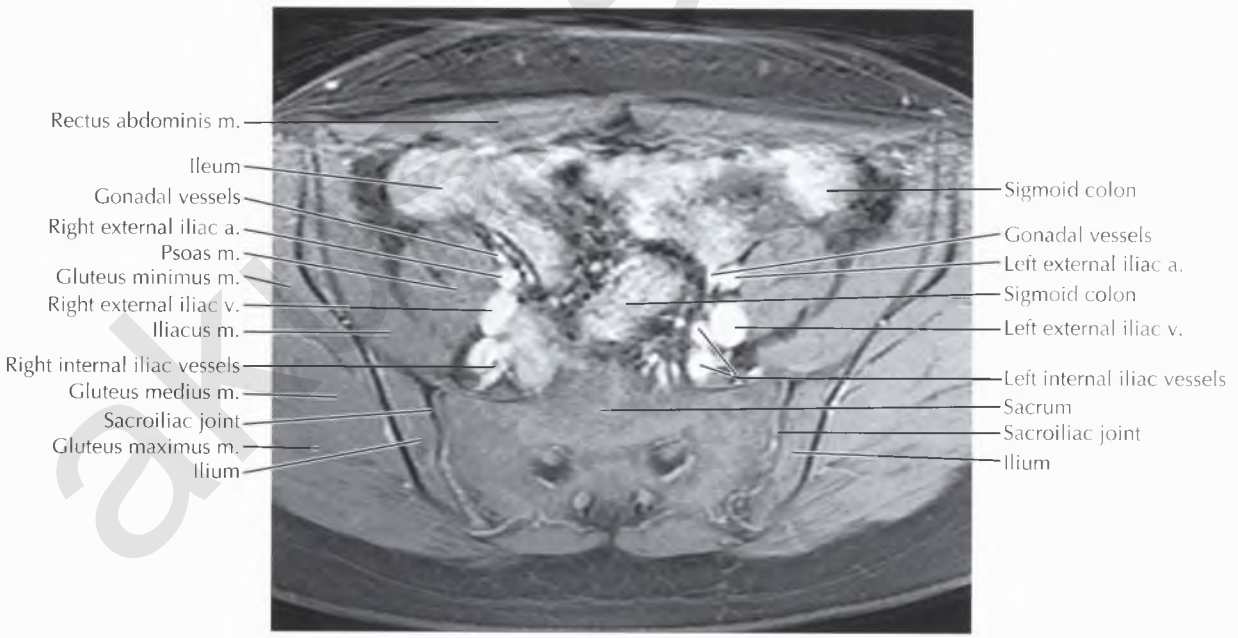
Rectus abdominis m.
Ileum
Gonadal vessels
Right external iliac a.
Psoas m.
Gluteus minimus m.
Right external iliac v.
Iliacus m.
Right internal iliac vessels
Gluteus medius m.
Sacroiliac joint
Gluteus maximus m.
Ilium
Sigmoid colon
Gonadal vessels
Left external iliac a.
Sigmoid colon
Left external iliac v.
Left internal iliac vessels
Sacrum
Sacroiliac joint
Ilium

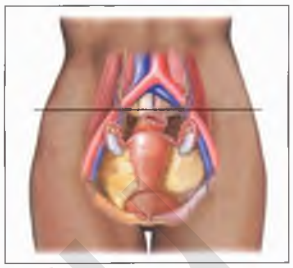

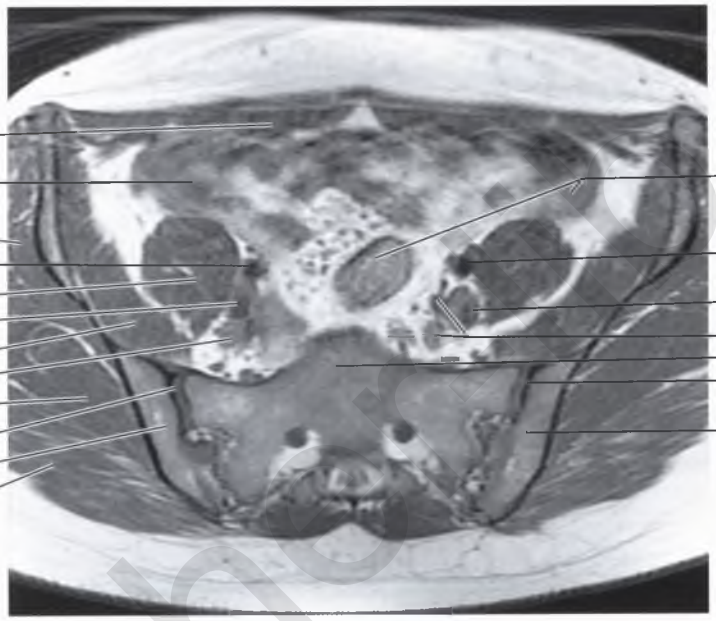

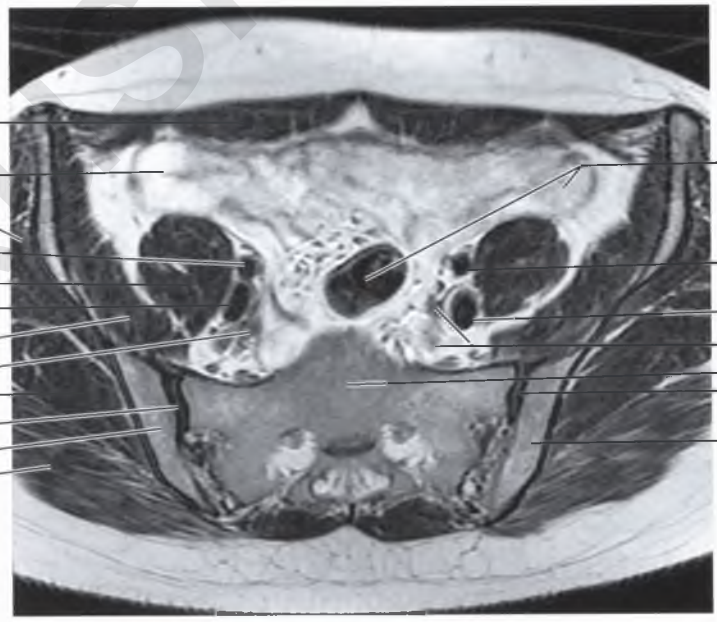

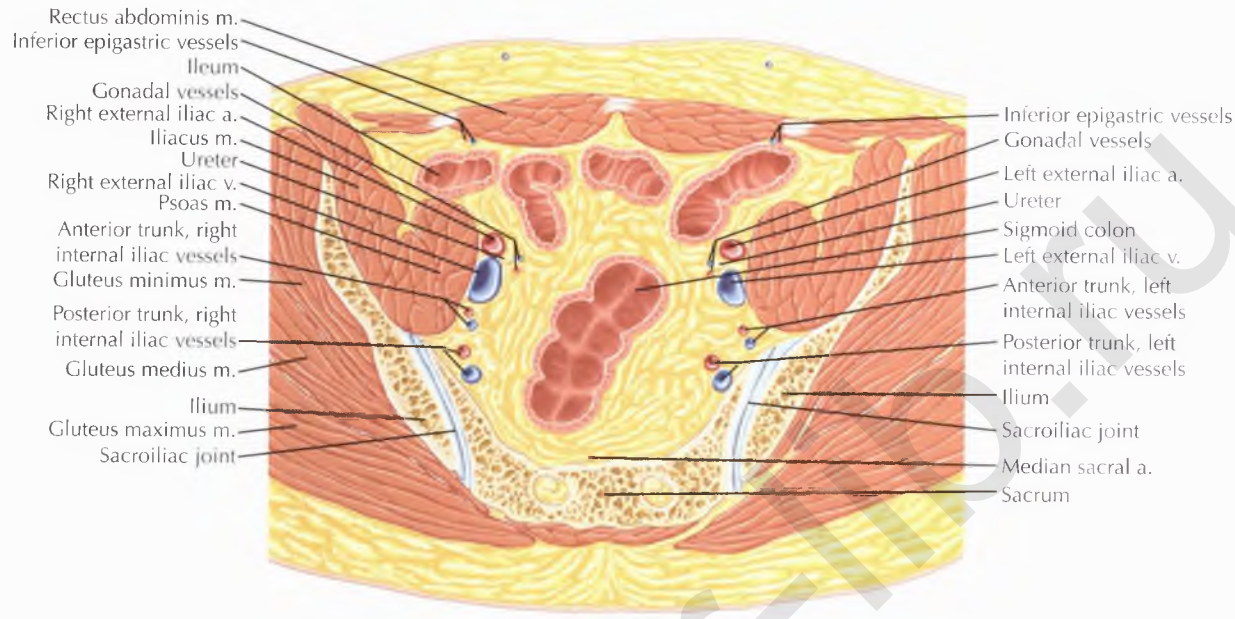

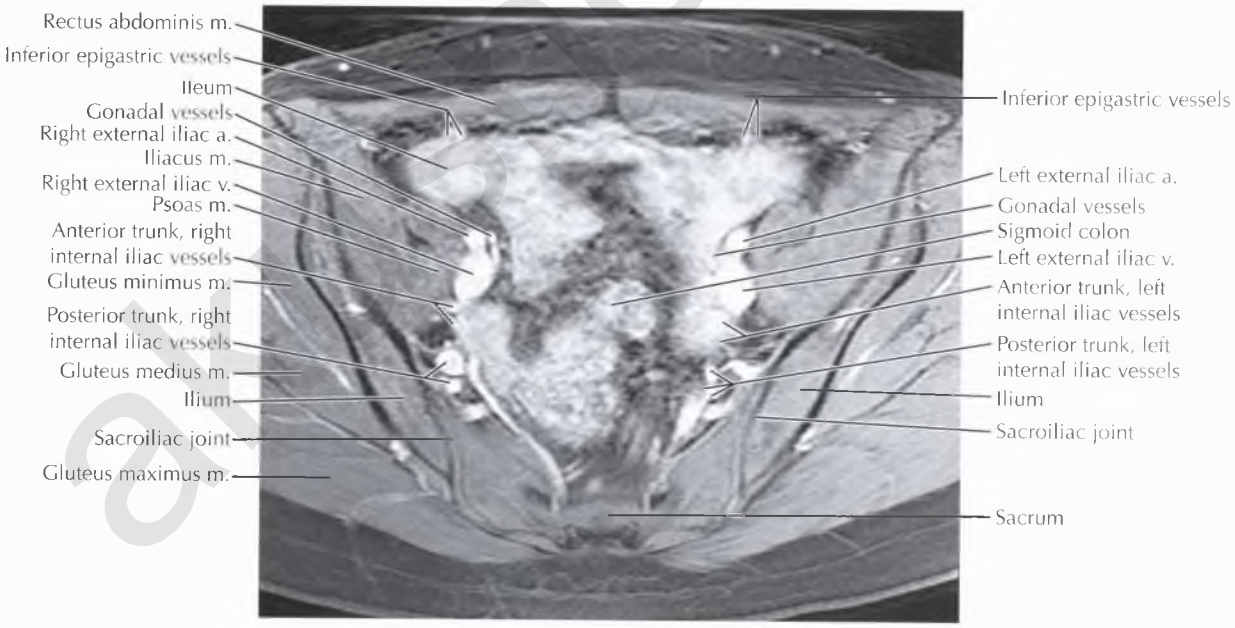

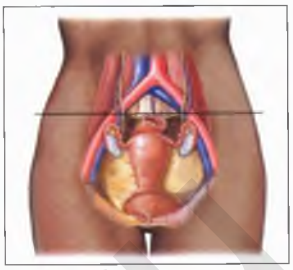

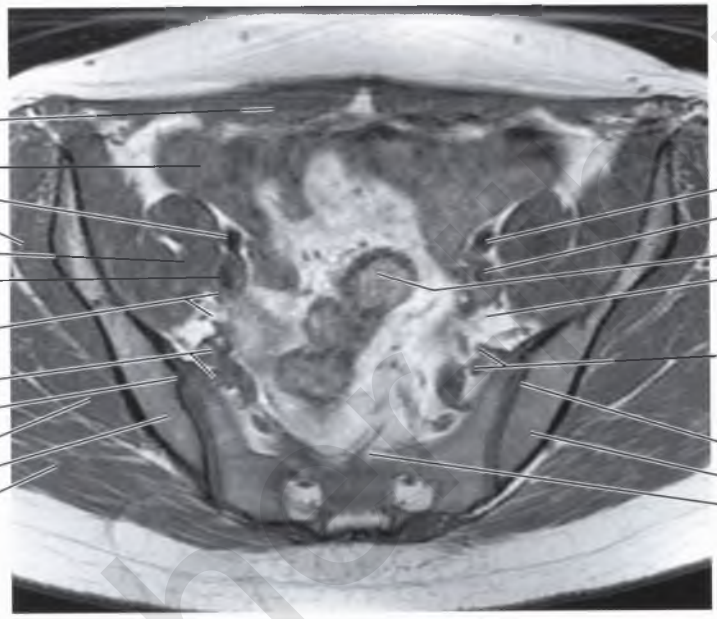
Rectus abdominis m.
Ileum
Right external iliac a.
Gluteus minimus m.
Psoas m.
Right external iliac v.
Anterior trunk, right internal iliac vessels
Posterior trunk, right internal iliac vessels
Sacroiliac joint
Gluteus medius m.
Ilium
Gluteus maximus m.
Left external iliac a.
Left external iliac v.
Sigmoid colon
Anterior trunk, left internal iliac vessels
Posterior trunk, left internal iliac vessels
Sacroiliac joint
Ilium
Sacrum

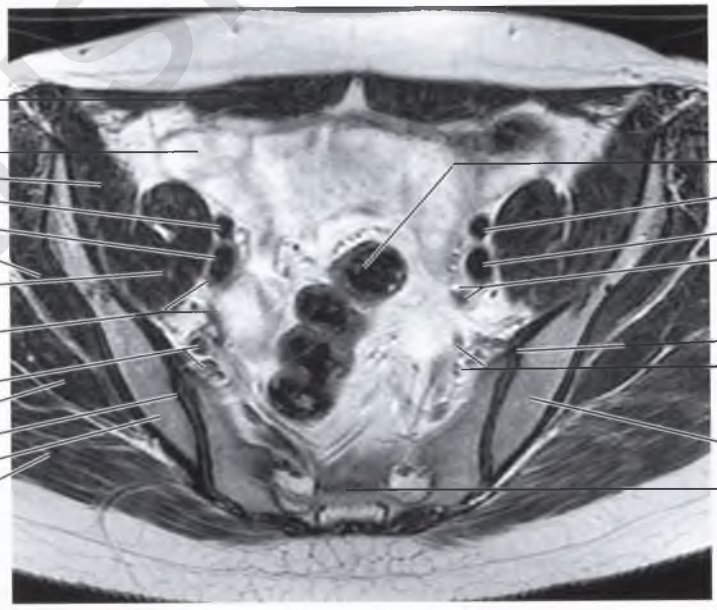
Rectus abdominis m.
Ileum
Iliacus m.
Right external iliac a.
Right external iliac v.
Gluteus minimus m.
Psoas m.
Anterior trunk, right internal iliac vessels
Posterior trunk, right internal iliac vessels
Gluteus medius m.
Sacroiliac joint
Ilium
Gluteus maximus m.
Sigmoid colon
Left external iliac a.
Left external iliac v.
Anterior trunk, left internal iliac vessels
Sacroiliac joint
Posterior trunk, left internal iliac vessels
Ilium
Sacrum

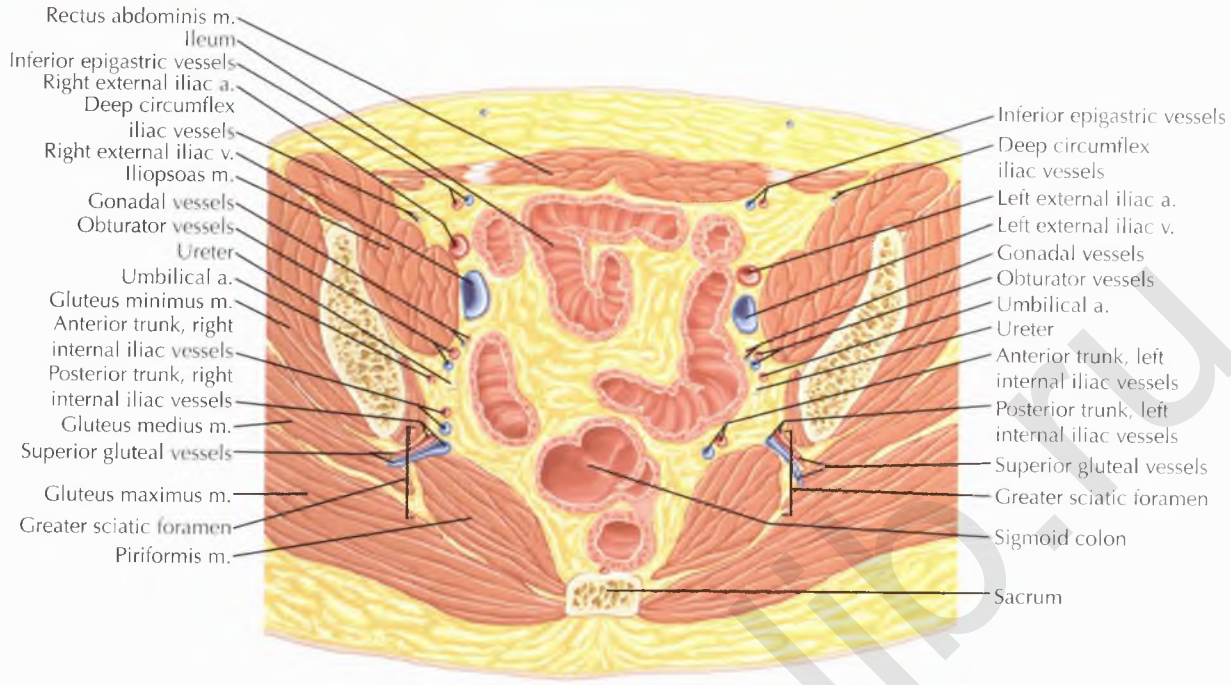

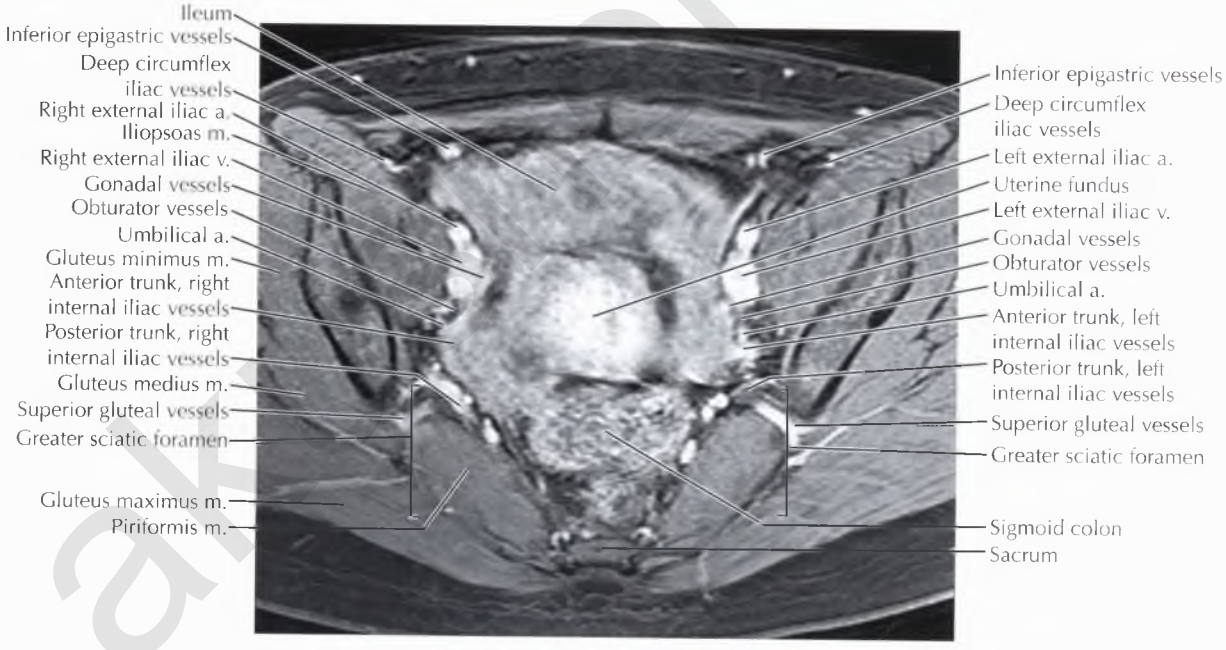

NORMAL ANATOMY

The *piriformis muscle* occupies most of the greater sciatic foramen. On this image, the superior gluteal vessels are seen exiting the pelvic through the greater sciatic foramen just superior to the piriformis muscle. The inferior gluteal vessels, internal pudendal vessels, and sciatic nerve also traverse the greater sciatic foramen just inferior to the piriformis muscle (see Female Pelvis Axials 6 and 7 and Sagittals 1 and 2).

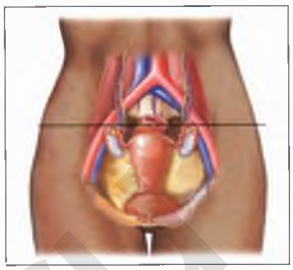

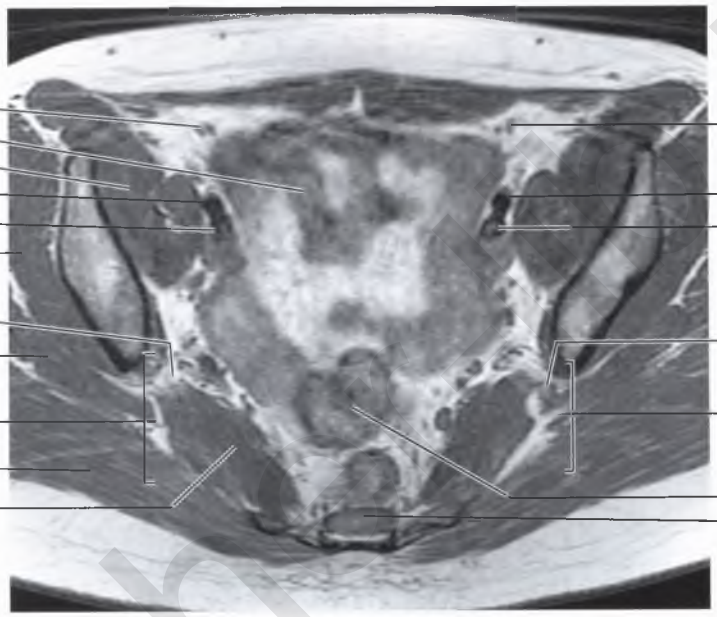
Inferior epigastric vessels
Ileum
Iliopsoas m.
Right external iliac a.
Right external iliac v.
Gluteus minimus m.
Superior gluteal vessels
Gluteus medius m.
Greater sciatic foramen
Gluteus maximus m.
Piriformis m.
Inferior epigastric vessels
Left external iliac a.
Left external iliac v.
Superior gluteal vessels
Greater sciatic foramen
Sigmoid colon
Sacrum

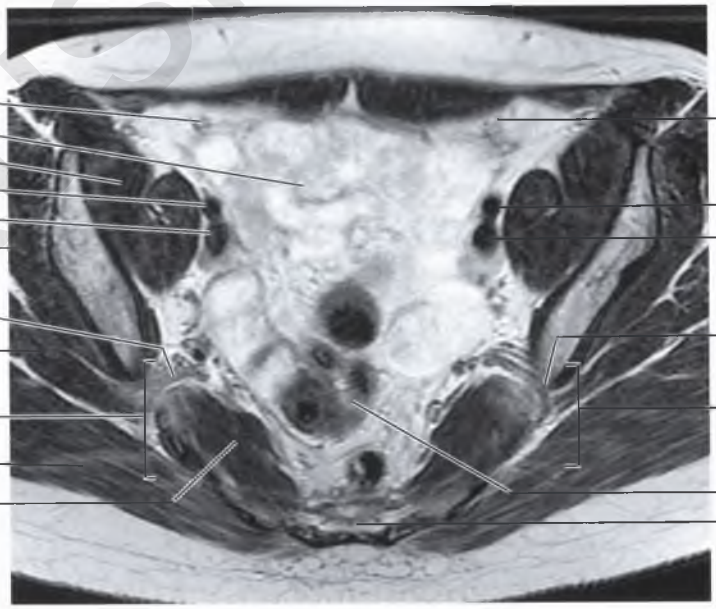
Inferior epigastric vessels
Ileum
Iliopsoas m.
Right external iliac a.
Right external iliac v.
Gluteus minimus m.
Superior gluteal vessels
Gluteus medius m.
Greater sciatic foramen
Gluteus maximus m.
Piriformis m.
Inferior epigastric vessels
Left external iliac a.
Left external iliac v.
Superior gluteal vessels
Greater sciatic foramen
Sigmoid colon
Sacrum

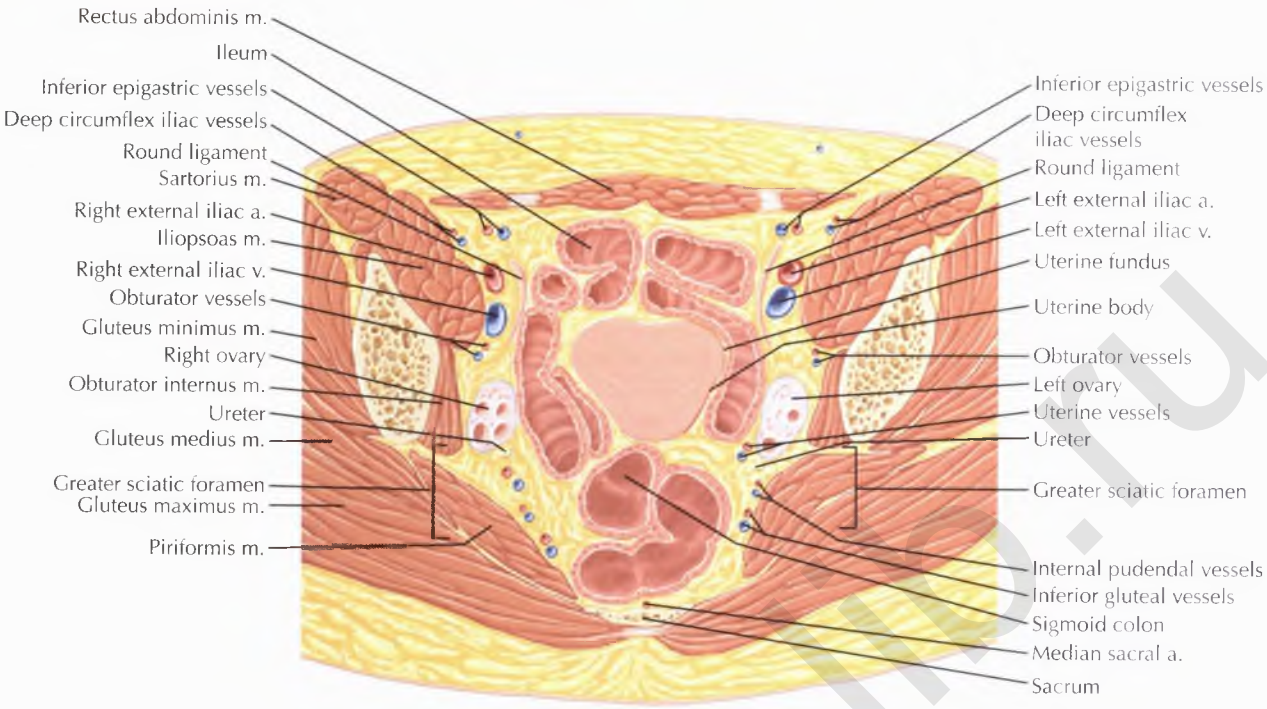

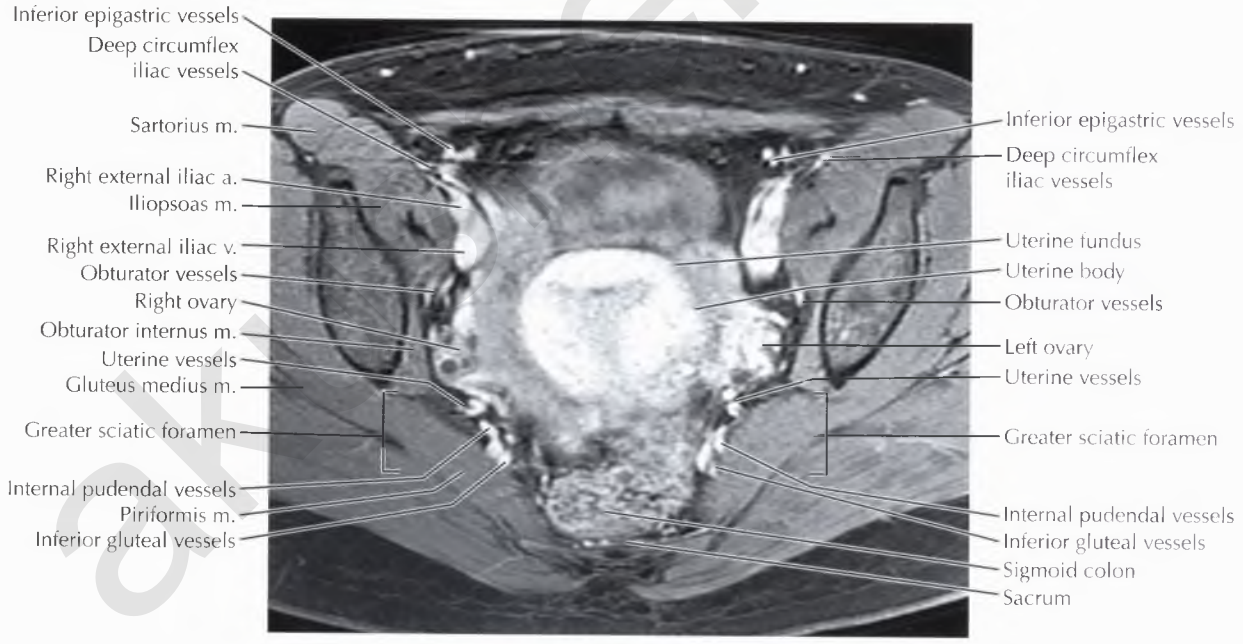

NORMAL ANATOMY

The paired *round ligaments* extend from the anterior uterine fundus, traverse the broad ligament, course anterolaterally along the pelvic wall, and travel through the inguinal canal to insert on the labia majora. The round ligament is the embryologic homologue to the gubernaculum in males.

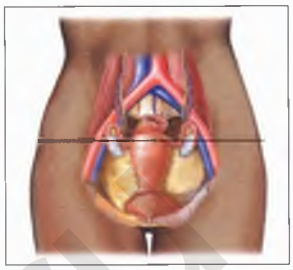

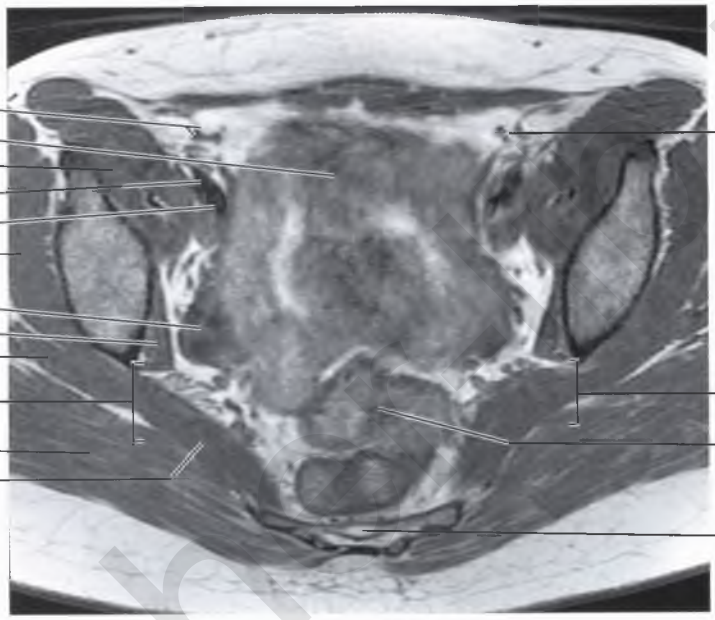
Inferior epigastric vessels
Ileum
Iliopsoas m.
Right external iliac a.
Right external iliac v.
Gluteus minimus m.
Right ovary
Obturator internus m.
Gluteus medius m.
Greater sciatic foramen
Gluteus maximus m.
Piriformis m.
Inferior epigastric vessels
Greater sciatic foramen
Sigmoid colon
Sacrum

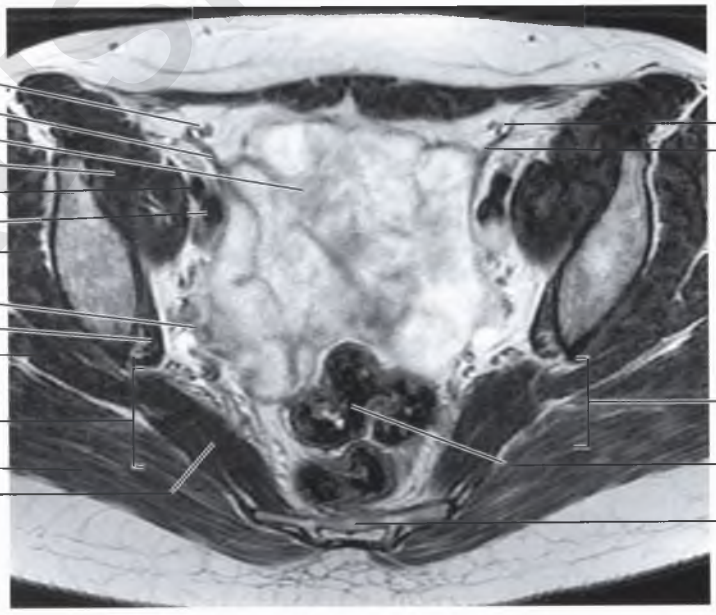
Inferior epigastric vessels
Round ligament
Ileum
Iliopsoas m.
Right external iliac a.
Right external iliac v.
Gluteus minimus m.
Right ovary
Obturator internus m.
Gluteus medius m.
Greater sciatic foramen
Gluteus maximus m.
Piriformis m.
Inferior epigastric vessels
Round ligament
Greater sciatic foramen
Sigmoid colon
Sacrum

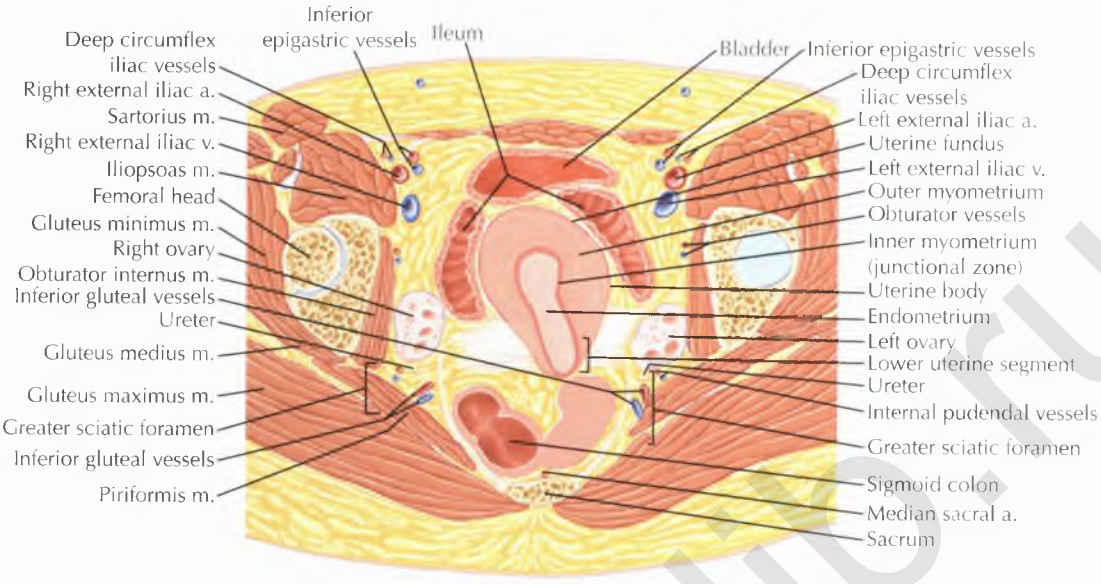

NORMAL ANATOMY

Magnetic resonance T2-weighted images clearly delineate the three uterine zones: a high signal intensity *endometrium*, a low signal intensity *inner myometrium* (also known as the junctional zone), and an intermediate–slightly high signal intensity *outer myometrium*. In some cases a very-high signal intensity endometrial canal can also be seen.

DIAGNOSTIC CONSIDERATION

Note the change in positioning of the pelvic organs as the bladder fills with urine throughout the examination. The postcontrast axial sequence was the last obtained in this MR study, and thus the urinary bladder is most distended on this sequence.

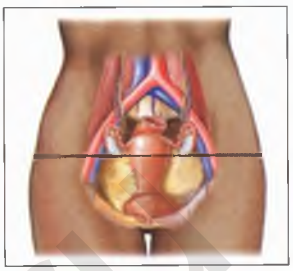

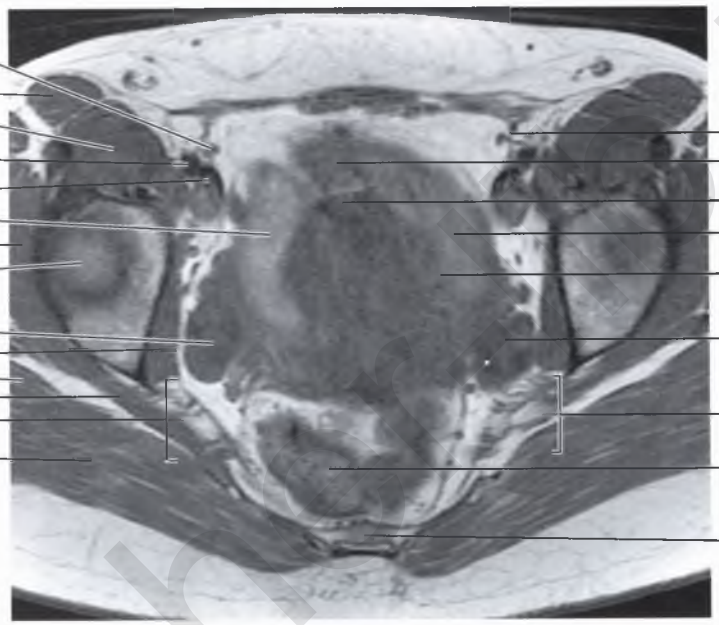
Inferior epigastric vessels
Sartorius m.
Iliopsoas m.
Right external iliac a.
Right external iliac v.
Ileum
Gluteus minimus m.
Femoral head
Right ovary
Obturator internus m.
Gluteus medius m.
Piriformis m.
Greater sciatic foramen
Gluteus maximus m.
Inferior epigastric vessels
Bladder
Uterine fundus
Ileum
Uterine body
Left ovary
Greater sciatic foramen
Sigmoid colon
Sacrum

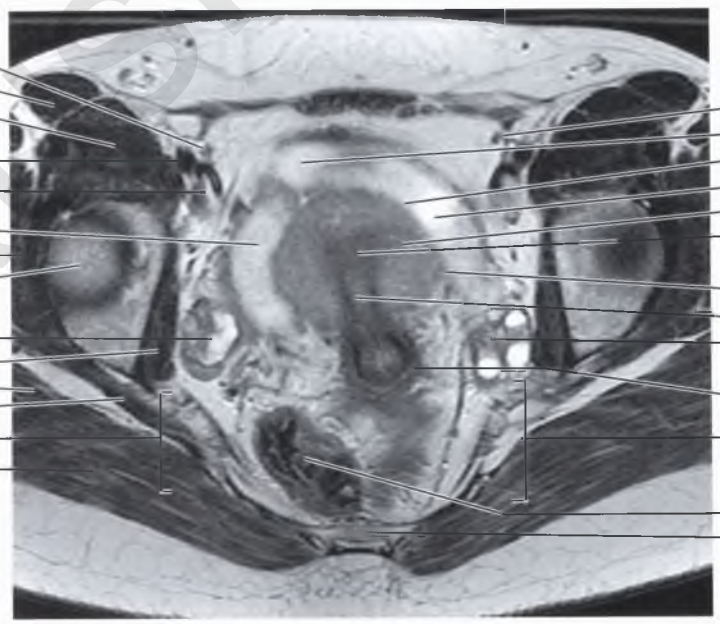
Inferior epigastric vessels
Sartorius m.
Iliopsoas m.
Right external iliac a.
Right external iliac v.
Ileum
Gluteus minimus m.
Femoral head
Right ovary
Obturator internus m.
Gluteus medius m.
Piriformis m.
Greater sciatic foramen
Gluteus maximus m.
Inferior epigastric vessels
Bladder
Uterine fundus
Ileum
Outer myometrium
Inner myometrium
(junctional zone)
Uterine body
Endometrium
Left ovary
Lower uterine segment
Greater sciatic foramen
Sigmoid colon
Sacrum

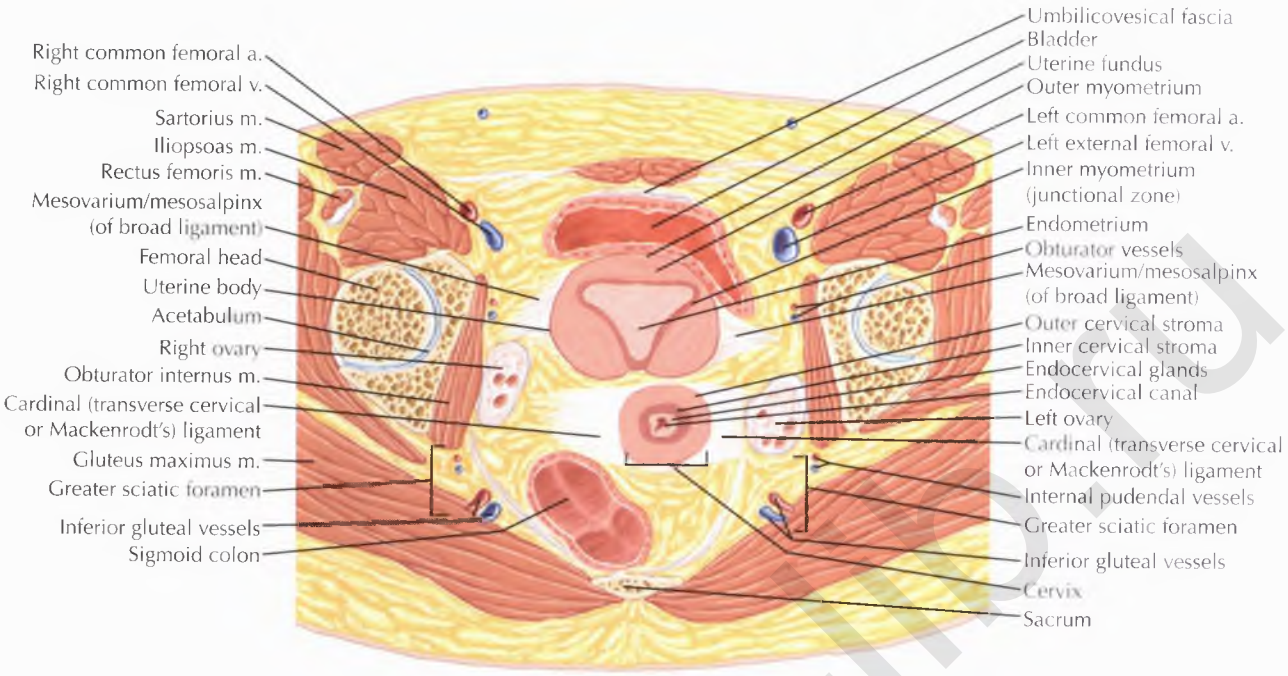

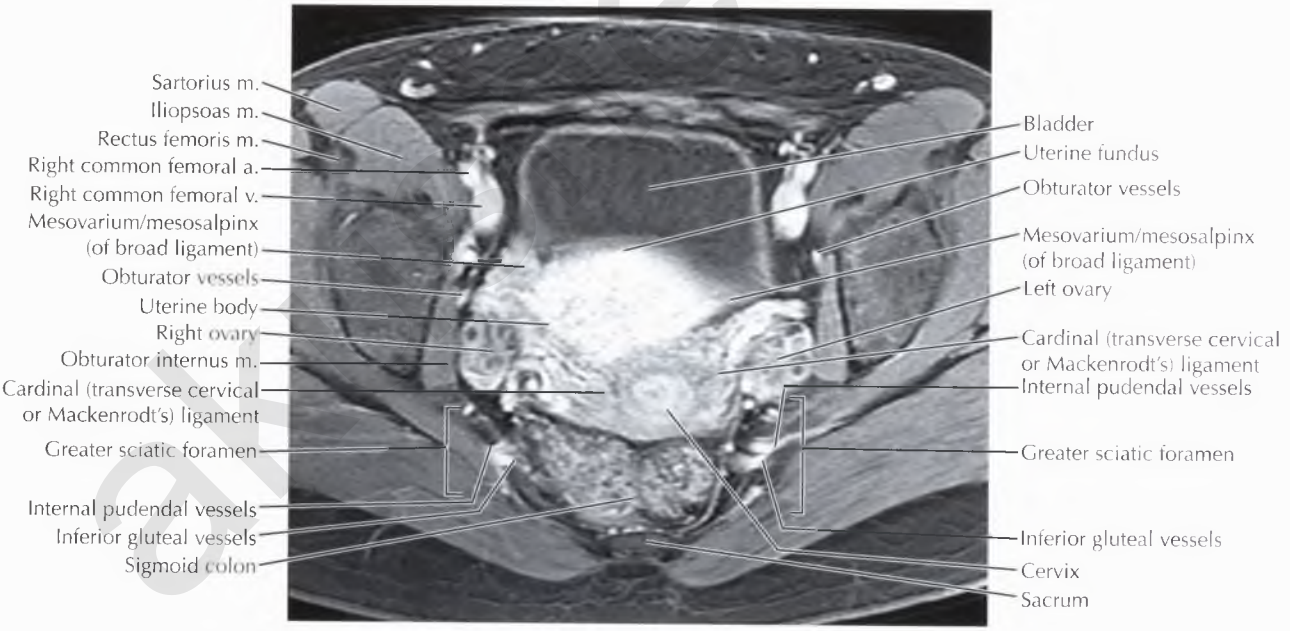

NORMAL ANATOMY

Cervical zonal anatomy is also well-demonstrated on T2-weighted MR images: the very high signal intensity fluid-filled endocervical canal is surrounded by the intermediate–slightly high signal intensity endocervical glands, followed by the low signal intensity inner cervical stroma, then the intermediate–slightly high signal intensity outer cervical stroma.

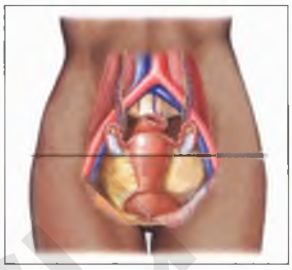

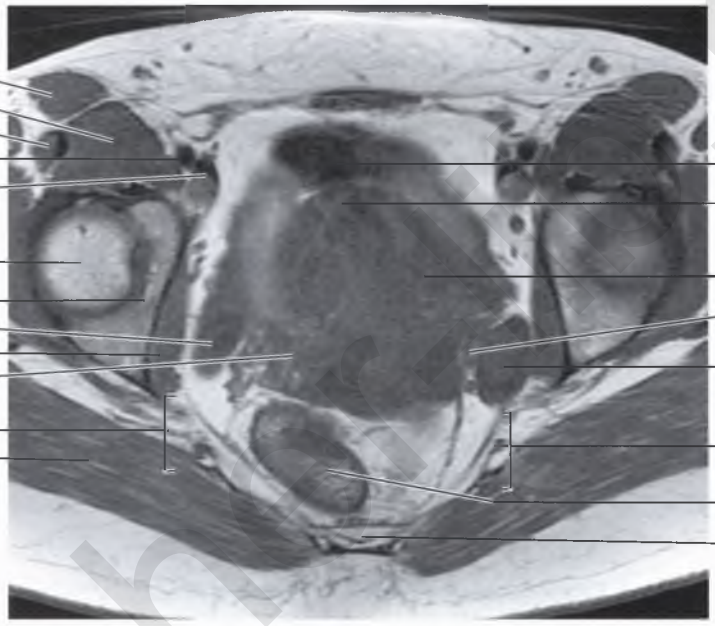

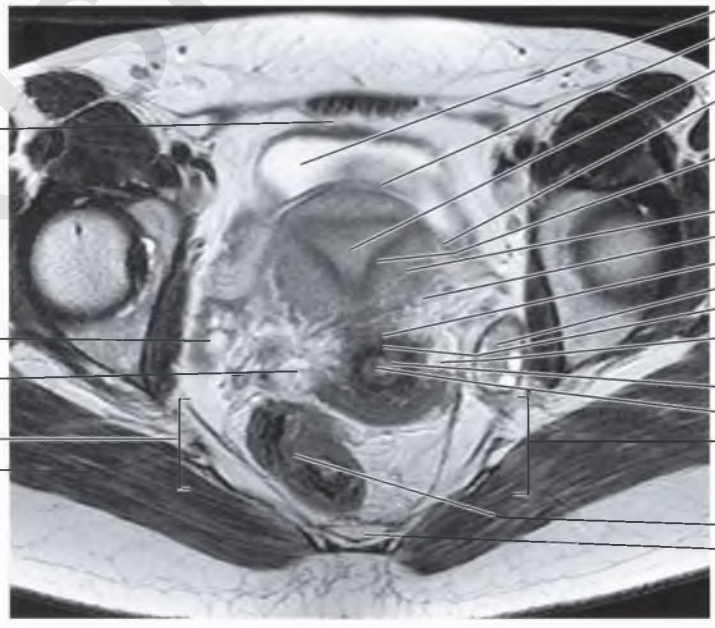

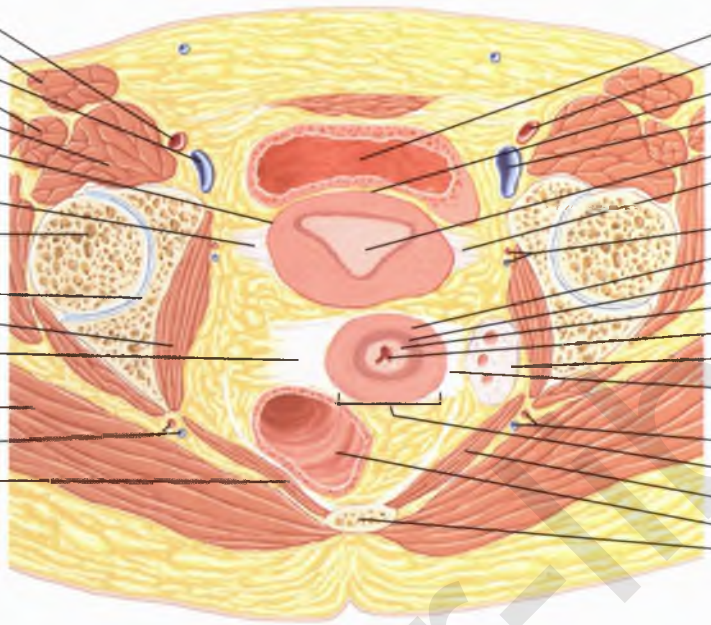
Right common femoral a.
Sartorius m.
Right common femoral v.
Rectus femoris m.
Iliopsoas m.
Uterine body
Mesometrium
(of broad ligament)
Femoral head
Acetabulum
Obturator internus m.
Cardinal (transverse cervical
or Mackenrodt's) ligament
Gluteus maximus m.
Internal pudendal vessels
Ischiococcygeus m.
Bladder
Left common femoral a.
Uterine fundus
Left common femoral v.
Endometrium
Mesometrium
(of broad ligament)
Obturator vessels
Outer cervical stroma
Inner cervical stroma
Endocervical glands
Endocervical canal
Left ovary
Cardinal (transverse cervical
or Mackenrodt's) ligament
Internal pudendal vessels
Cervix
Ischiococcygeus m.
Sigmoid colon
Coccyx

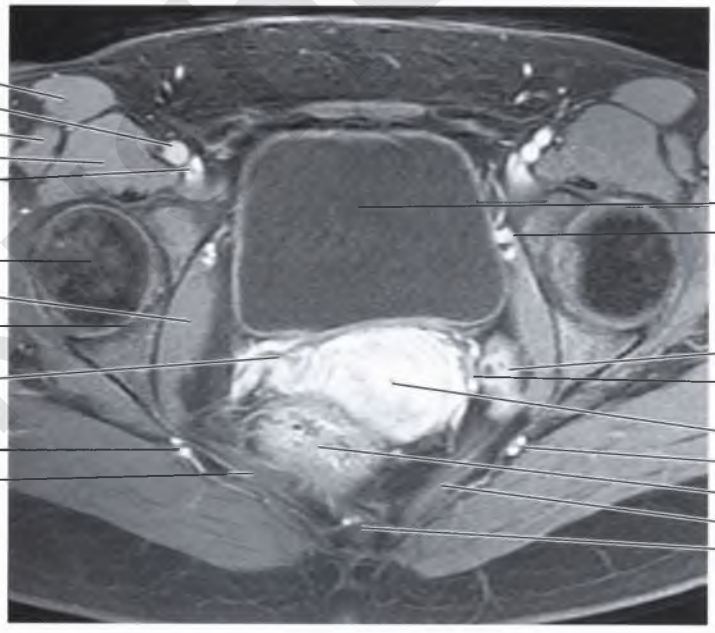
Sartorius m.
Right common femoral a.
Rectus femoris m.
Iliopsoas m.
Right common femoral v.
Femoral head
Obturator internus m.
Acetabulum
Cardinal (transverse cervical
or Mackenrodt's) ligament
Internal pudendal vessels
Ischiococcygeus m.
Bladder
Obturator vessels
Left ovary
Cardinal (transverse cervical
or Mackenrodt's) ligament
Cervix
Internal pudendal vessels
Sigmoid colon
Ischiococcygeus m.
Sacrum

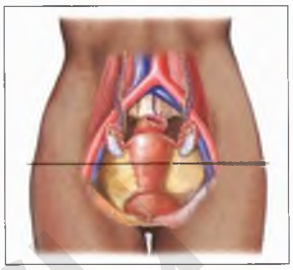

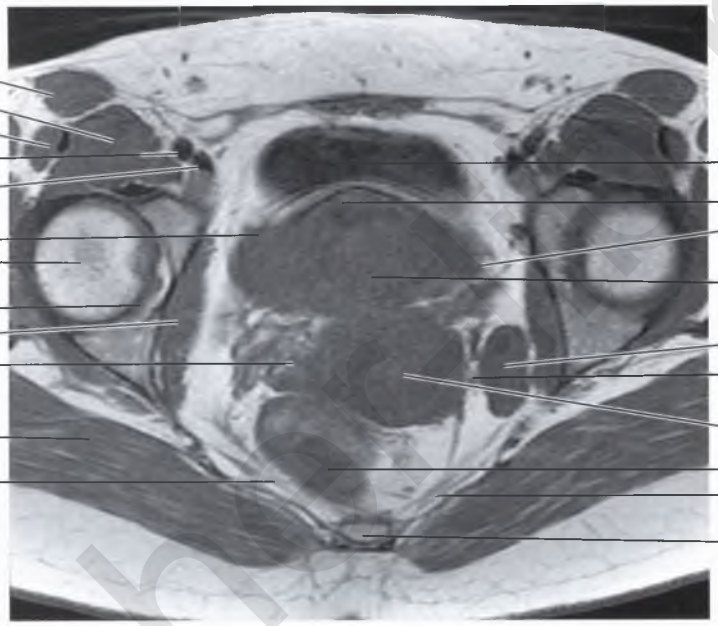
Sartorius m.
Iliopsoas m.
Rectus femoris m.
Right common femoral a.
Right common femoral v.
Mesometrium (of broad ligament)
Femoral head
Acetabulum
Obturator internus m.
Cardinal (transverse cervical or Mackenrodt's) ligament
Gluteus maximus m.
Ischiococcygeus m.
Bladder
Uterine fundus
Mesometrium (of broad ligament)
Uterine body
Left ovary
Cardinal (transverse cervical or Mackenrodt's) ligament
Cervix
Sigmoid colon
Ischiococcygeus m.
Sacrum

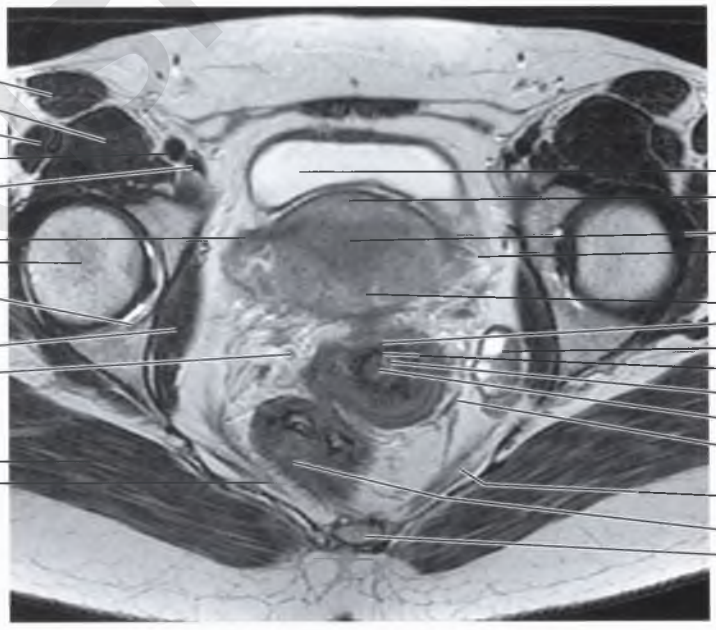
Sartorius m.
Iliopsoas m.
Rectus femoris m.
Right common femoral a.
Right common femoral v.
Mesometrium (of broad ligament)
Femoral head
Acetabulum
Obturator internus m.
Cardinal (transverse cervical or Mackenrodt's) ligament
Gluteus maximus m.
Ischiococcygeus m.
Bladder
Uterine fundus
Endometrium
Mesometrium (of broad ligament)
Uterine body
Outer cervical stroma
Left ovary
Inner cervical stroma
Endocervical glands
Endocervical canal
Cardinal (transverse cervical or Mackenrodt's) ligament
Ischiococcygeus m.
Sigmoid colon
Sacrum

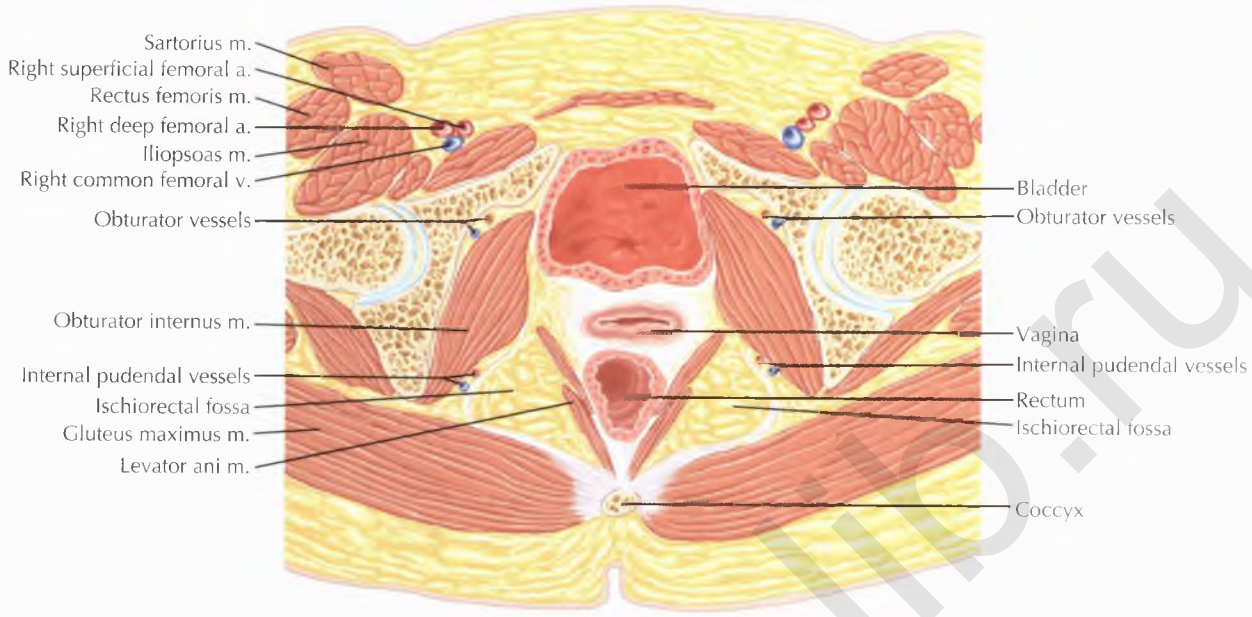

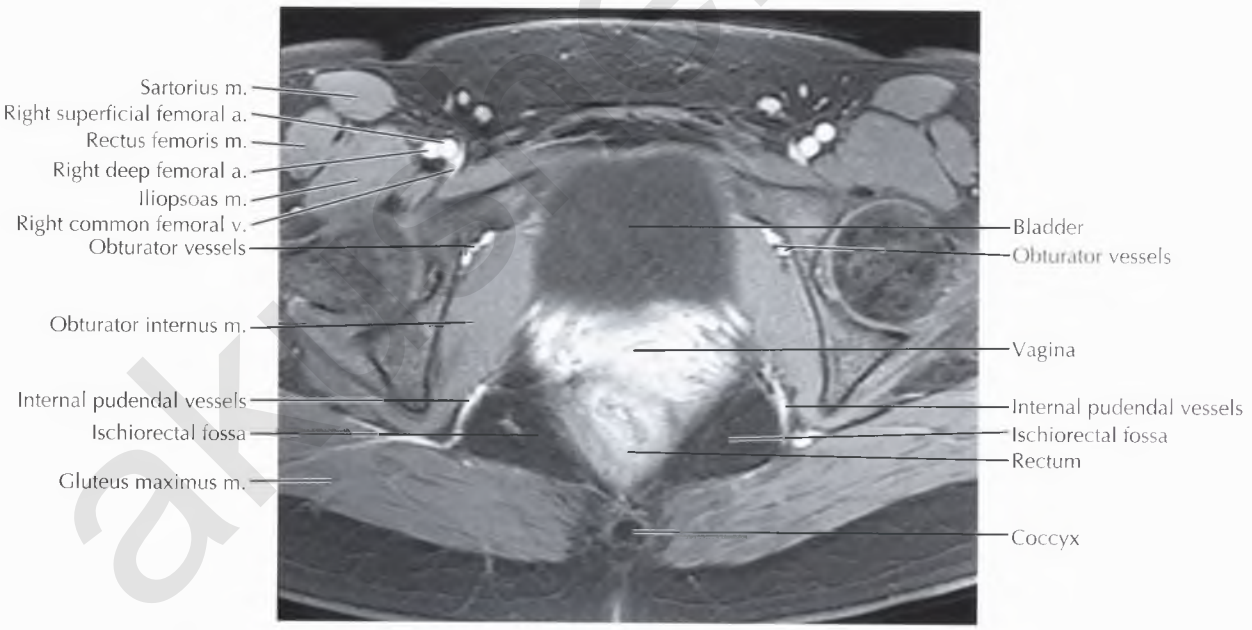

NORMAL ANATOMY

The iliococcygeus, puborectalis, and pubococcygeus muscles are components of the *levator ani* musculature. Note that the ischiococcygeus muscle is not considered a component of the levator ani musculature.

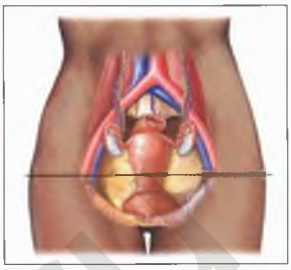

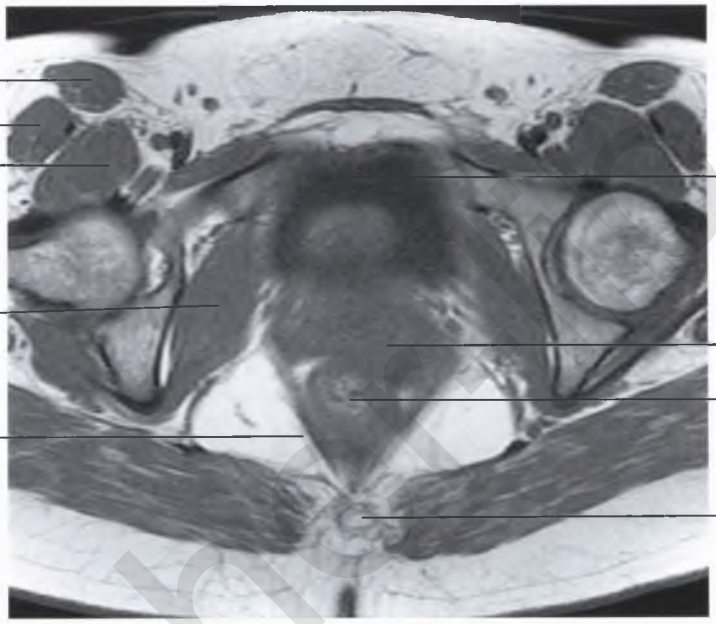

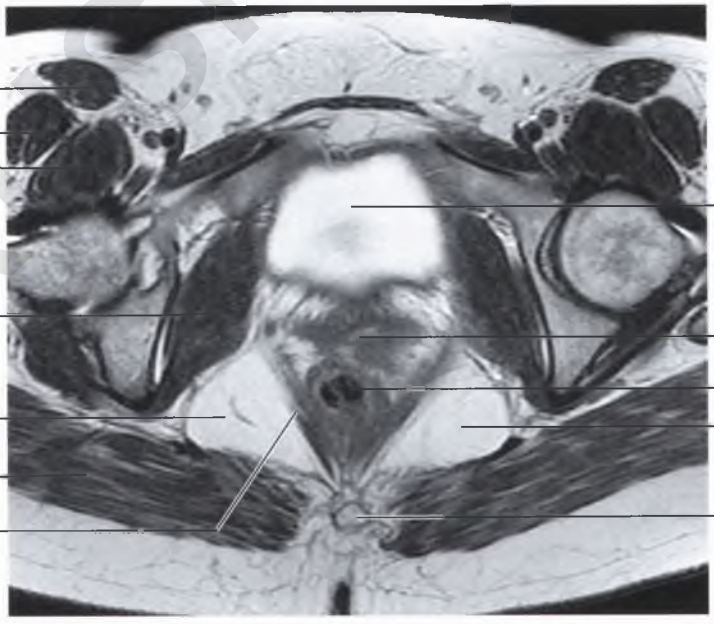

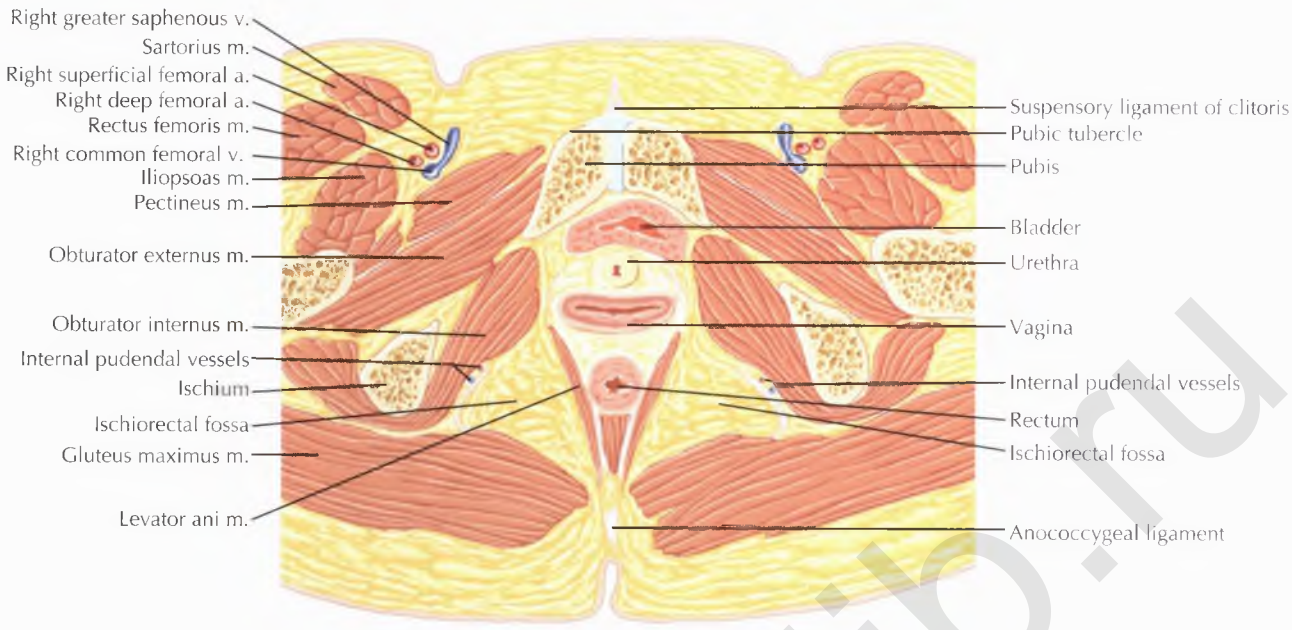

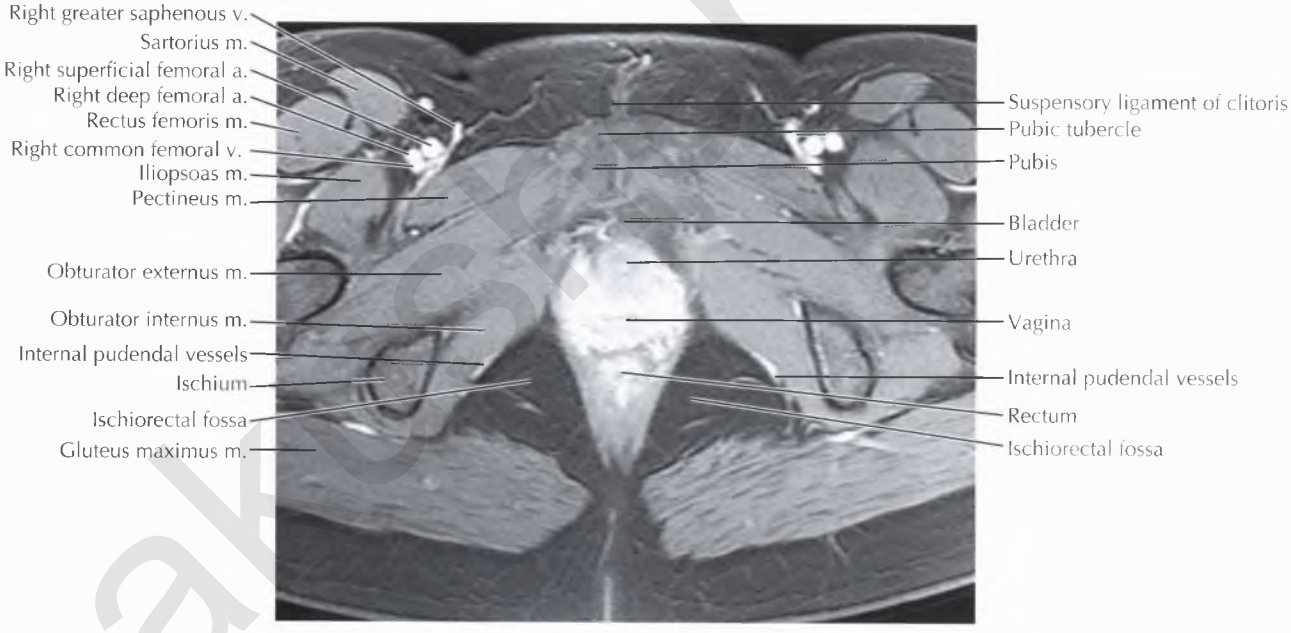

PATHOLOGIC PROCESS

Femoral and obturator hernias are less common than inguinal hernias and are usually seen in adult women. *Femoral hernias* occur when abdominopelvic contents protrude through a natural defect in the pelvic wall fascia called the femoral canal. On cross-sectional MRI, herniated contents are seen lateral to the pubic tubercle and medial to the femoral vessels. Femoral hernias can be distinguished from inguinal hernias by drawing a transverse line through the pubic tubercle; femoral hernias classically occur posterior to this line, whereas inguinal hernias tend to be located anterior to this line. In *obturator hernias*, herniation occurs through the obturator canal to a location between the pectineus and obturator externus muscles.

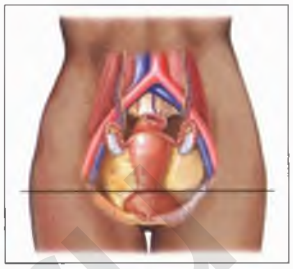

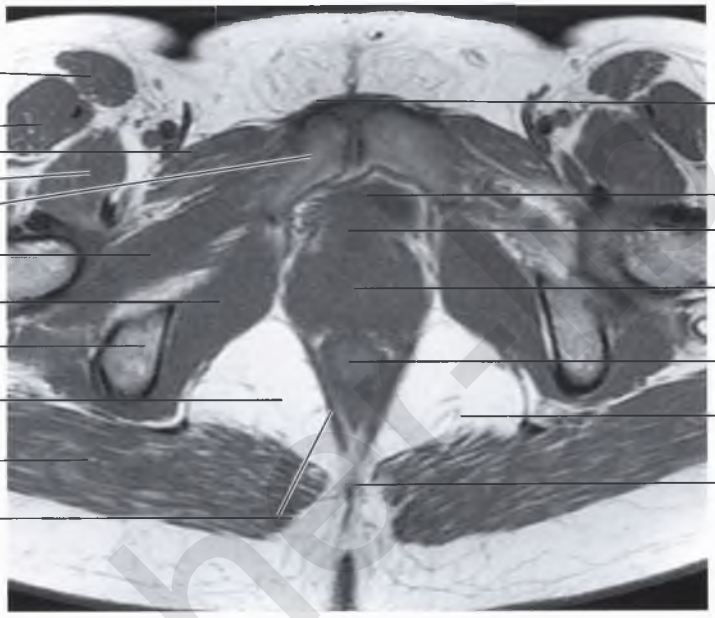
Sartorius m.
Rectus femoris m.
Pectineus m.
Iliopsoas m.
Pubis
Obturator externus m.
Obturator internus m.
Ischium
Ischiorectal fossa
Gluteus maximus m.
Levator ani m.
Pubic tubercle
Bladder
Urethra
Vagina
Rectum
Ischiorectal fossa
Anococcygeal ligament

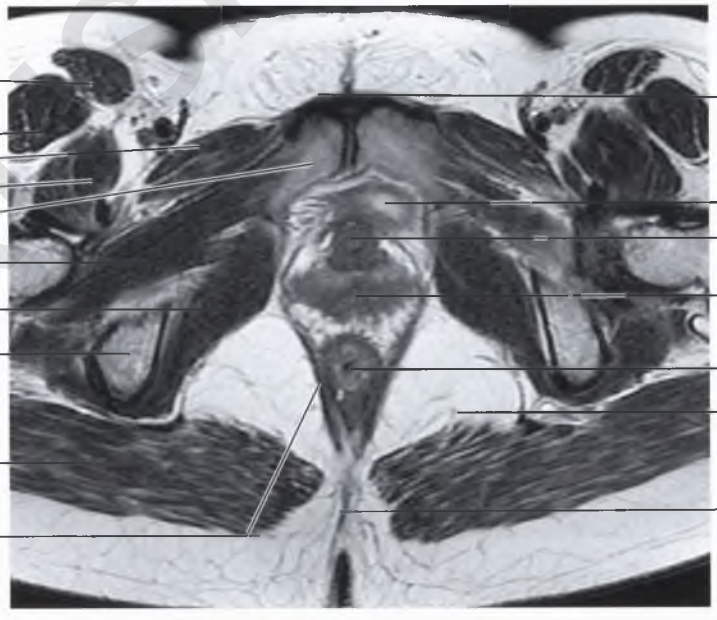
Sartorius m.
Rectus femoris m.
Pectineus m.
Iliopsoas m.
Pubis
Obturator externus m.
Obturator internus m.
Ischium
Gluteus maximus m.
Levator ani m.
Pubic tubercle
Bladder
Urethra
Vagina
Rectum
Ischiorectal fossa
Anococcygeal ligament

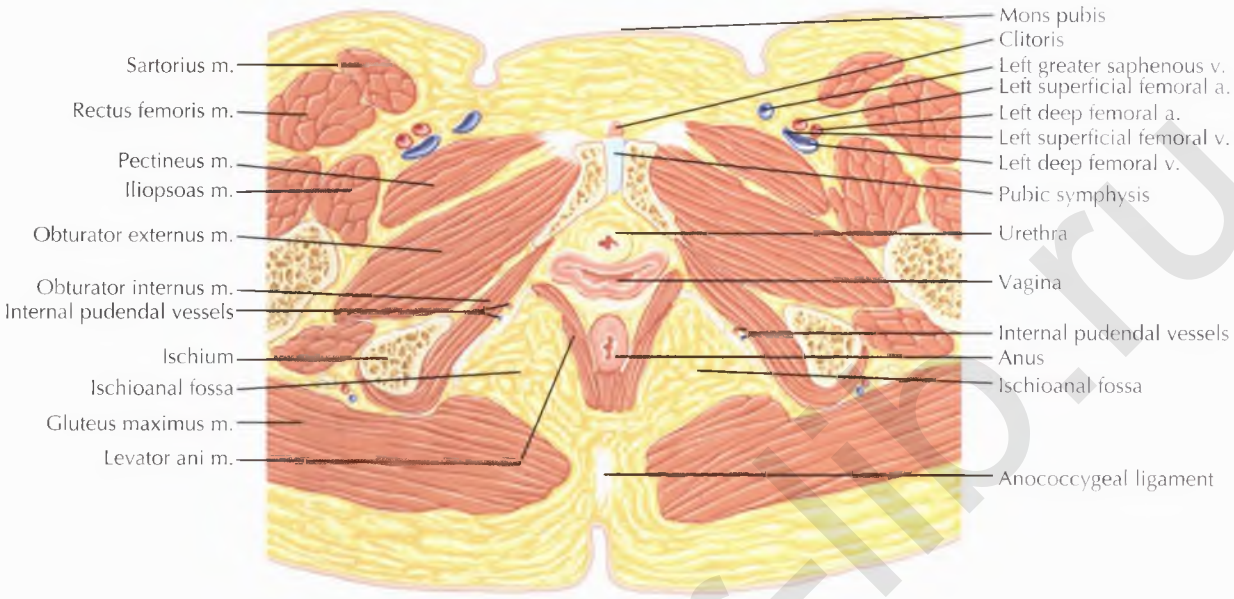

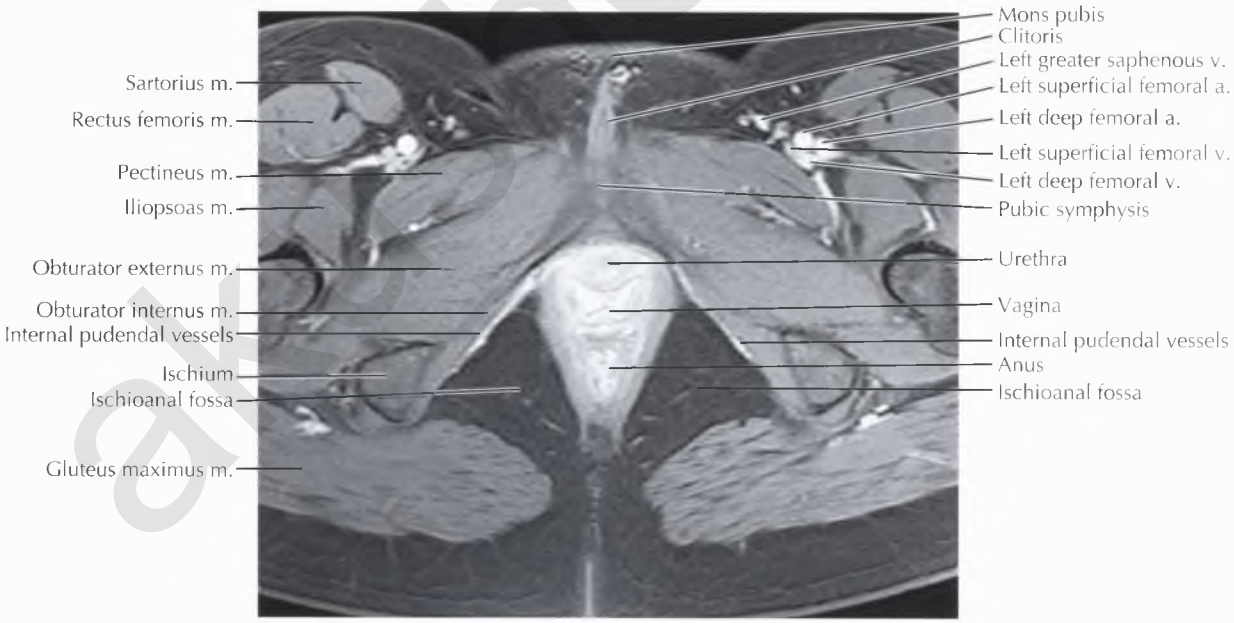

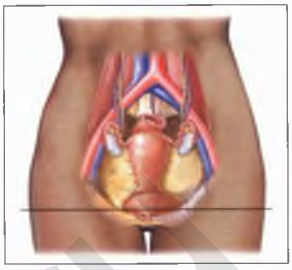

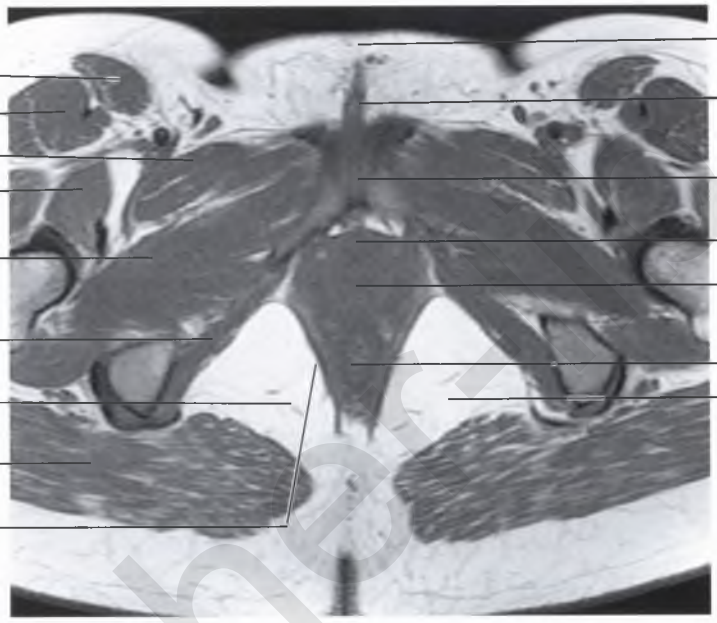
Sartorius m.
Rectus femoris m.
Pectineus m.
Iliopsoas m.
Obturator externus m.
Obturator internus m.
Ischioanal fossa.
Gluteus maximus m.
Levator ani m.
Mons pubis
Clitoris
Pubic symphysis
Urethra
Vagina
Anus
Ischioanal fossa

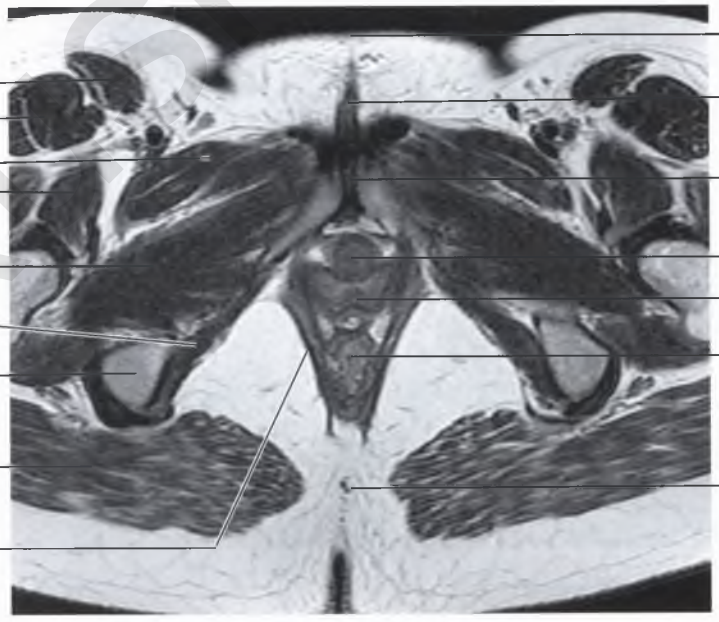
Sartorius m.
Rectus femoris m.
Pectineus m.
Iliopsoas m.
Obturator externus m.
Obturator internus m.
Ischium
Gluteus maximus m.
Levator ani m.
Mons pubis
Clitoris
Pubic symphysis
Urethra
Vagina
Anus
Anococcygeal ligament

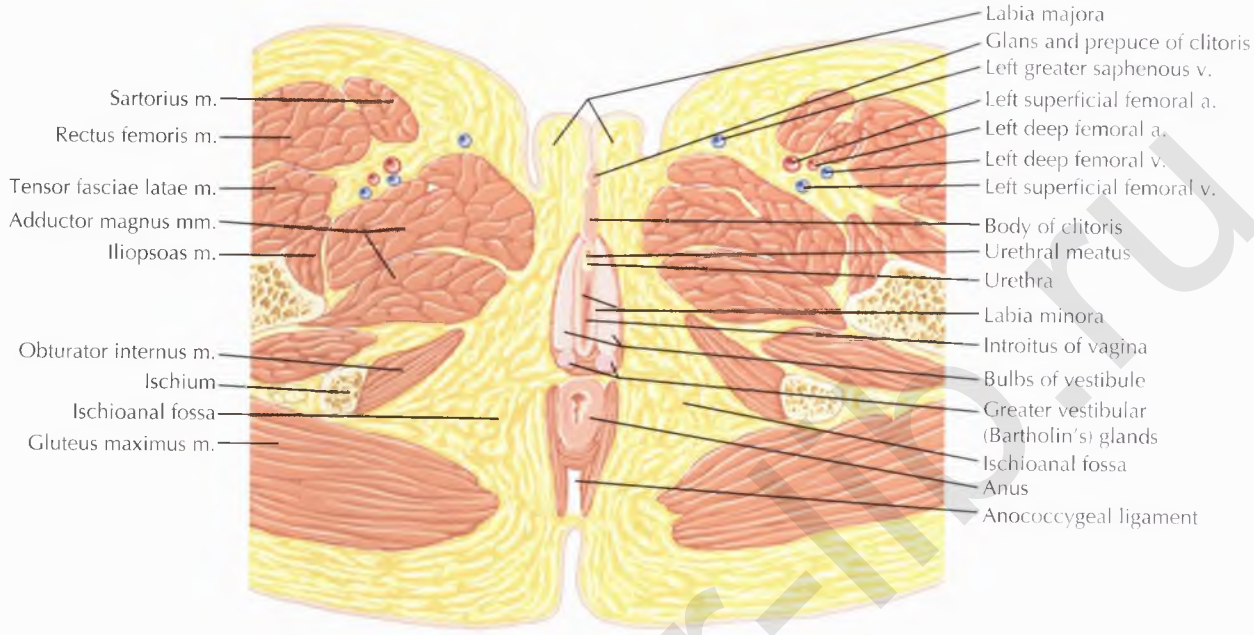
Sartorius m.
Rectus femoris m.
Tensor fasciae latae m.
Adductor magnus mm.
Iliopsoas m.
Obturator internus m.
Ischium
Ischioanal fossa
Gluteus maximus m.
Labia majora
Glans and prepuce of clitoris
Left greater saphenous v.
Left superficial femoral a.
Left deep femoral a.
Left deep femoral v.
Left superficial femoral v.
Body of clitoris
Urethral meatus
Urethra
Labia minora
Introitus of vagina
Bulbs of vestibule
Greater vestibular (Bartholin's) glands
Ischioanal fossa
Anus
Anococcygeal ligament

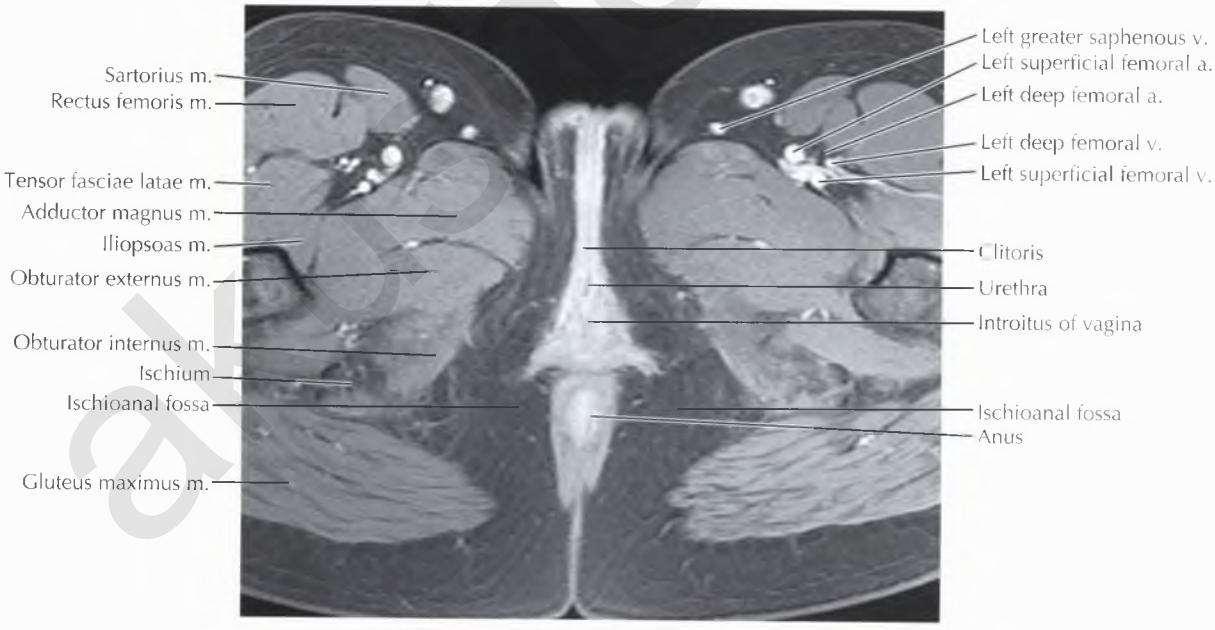
Sartorius m.
Rectus femoris m.
Tensor fasciae latae m.
Adductor magnus m.
Iliopsoas m.
Obturator externus m.
Obturator internus m.
Ischium
Ischioanal fossa
Gluteus maximus m.
Left greater saphenous v.
Left superficial femoral a.
Left deep femoral a.
Left deep femoral v.
Left superficial femoral v.
Clitoris
Urethra
Introitus of vagina
Ischioanal fossa
Anus

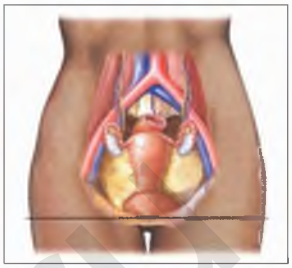

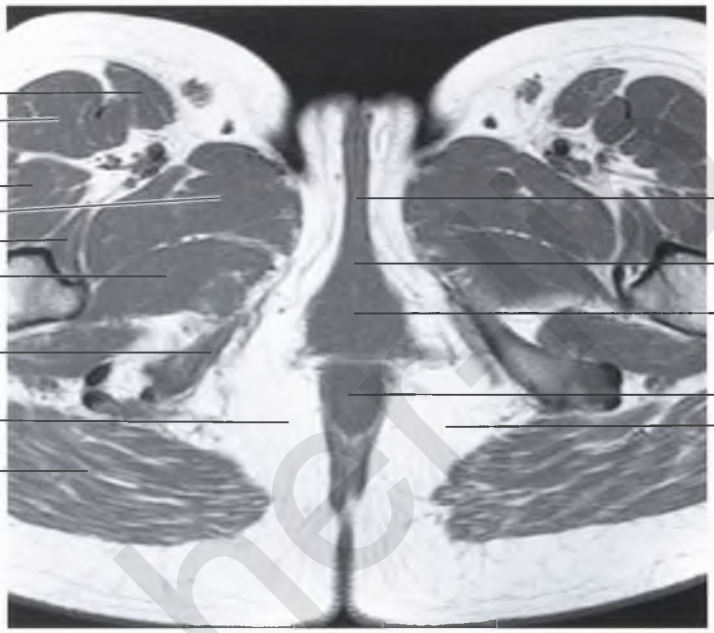
Sartorius m.
Rectus femoris m.
Tensor fasciae latae m.
Adductor magnus m.
Iliopsoas m.
Obturator externus m.
Obturator internus m.
Ischioanal fossa
Gluteus maximus m.
Clitoris
Urethra
Introitus of vagina
Anus
Ischioanal fossa

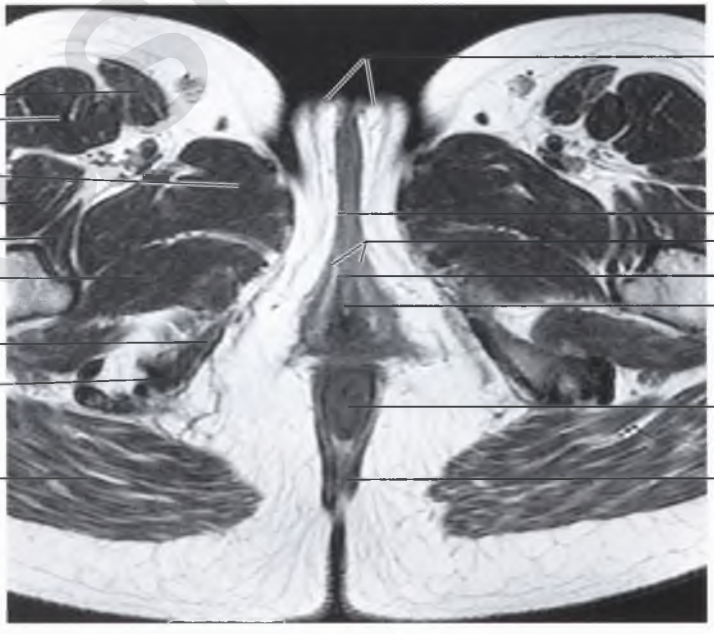
Sartorius m.
Rectus femoris m.
Adductor magnus m.
Tensor fasciae latae m.
Iliopsoas m.
Obturator externus m.
Obturator internus m.
Ischium
Gluteus maximus m.
Labia majora
Clitoris
Labia minora
Urethra
Introitus of vagina
Anus
Anococcygeal ligament

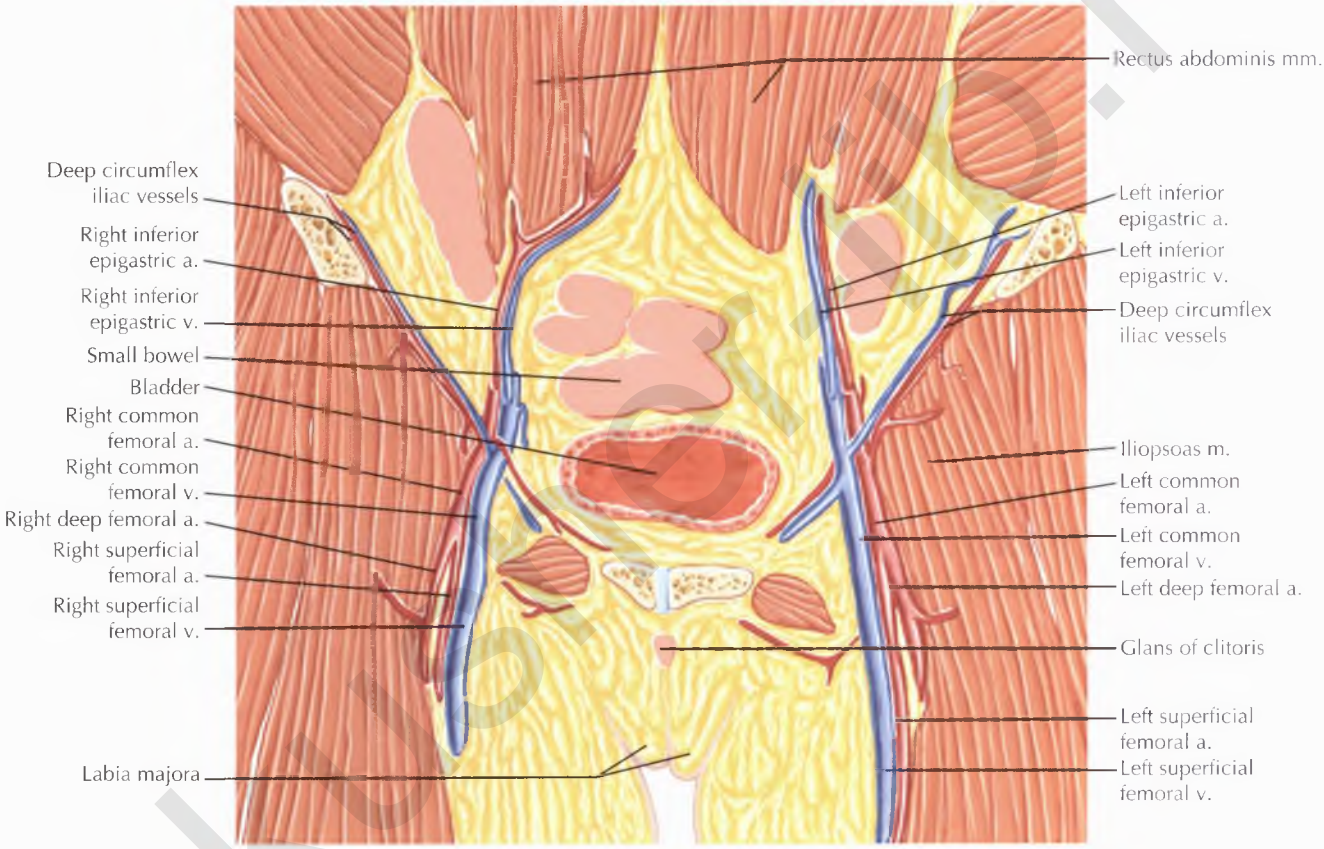

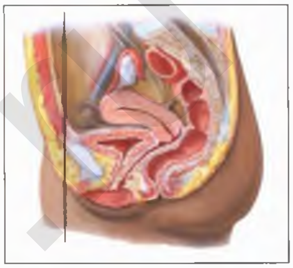


Right inferior epigastric a.
Deep circumflex iliac vessel
Right inferior epigastric v.
Small bowel
Bladder
Right common femoral v.
Right common femoral a.
Right superficial femoral a.
Right deep femoral a.
Right superficial femoral v.
Left inferior epigastric a.
Left inferior epigastric v.
Deep circumflex iliac vessels
Left common femoral a.
Left common femoral v.

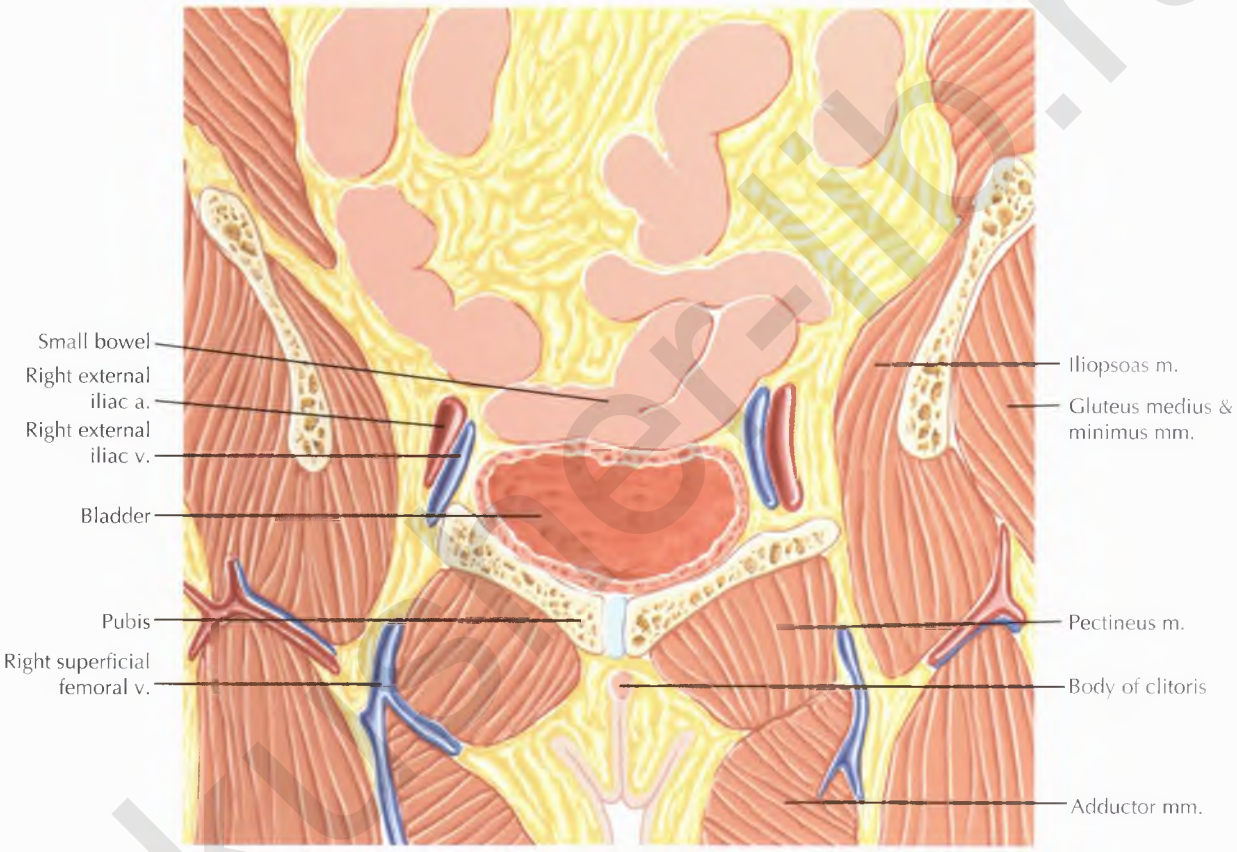

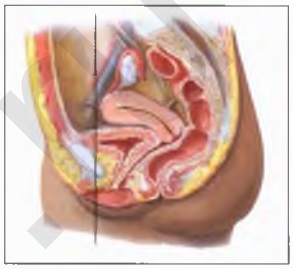

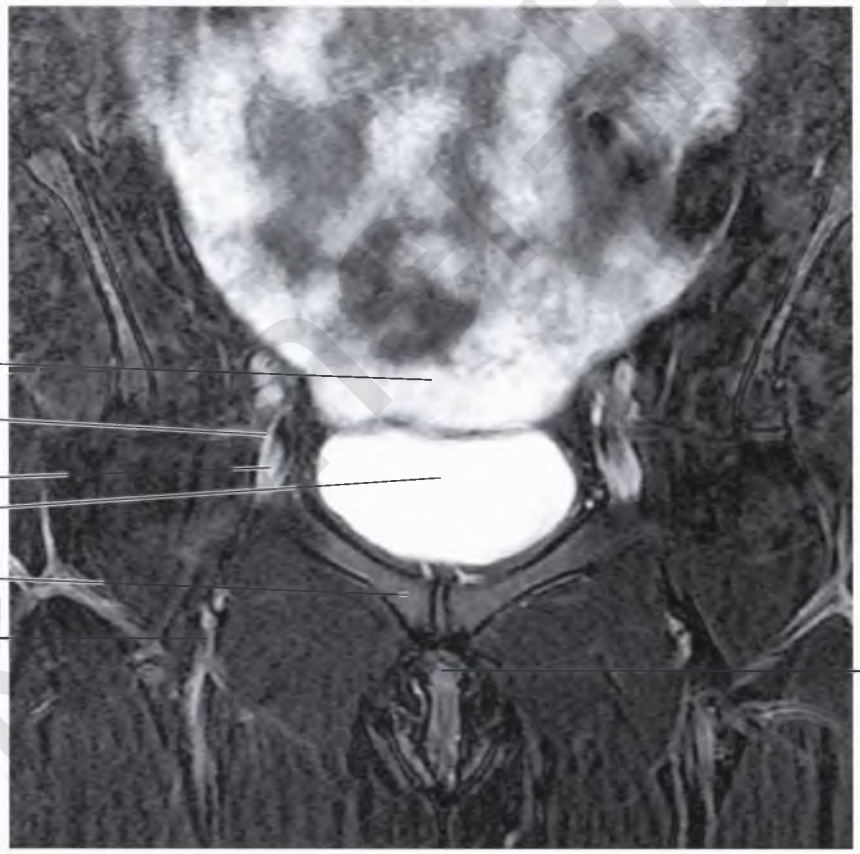
Small bowel
Right external iliac a.
Right external iliac v.
Bladder
Pubis
Right superficial femoral v.
Body of clitoris


Ilium
Small bowel
Uterine fundus
Acetabulum
Femoral head
Bladder
Bladder neck
Psoas m.
Iliopsoas m.
Gluteus medius & minimus mm.
Obturator internus m.
Obturator externus m.
Vastus mm.
Adductor mm.

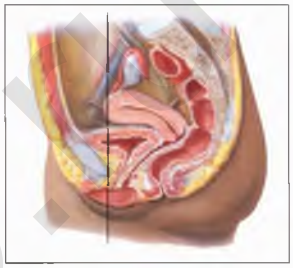

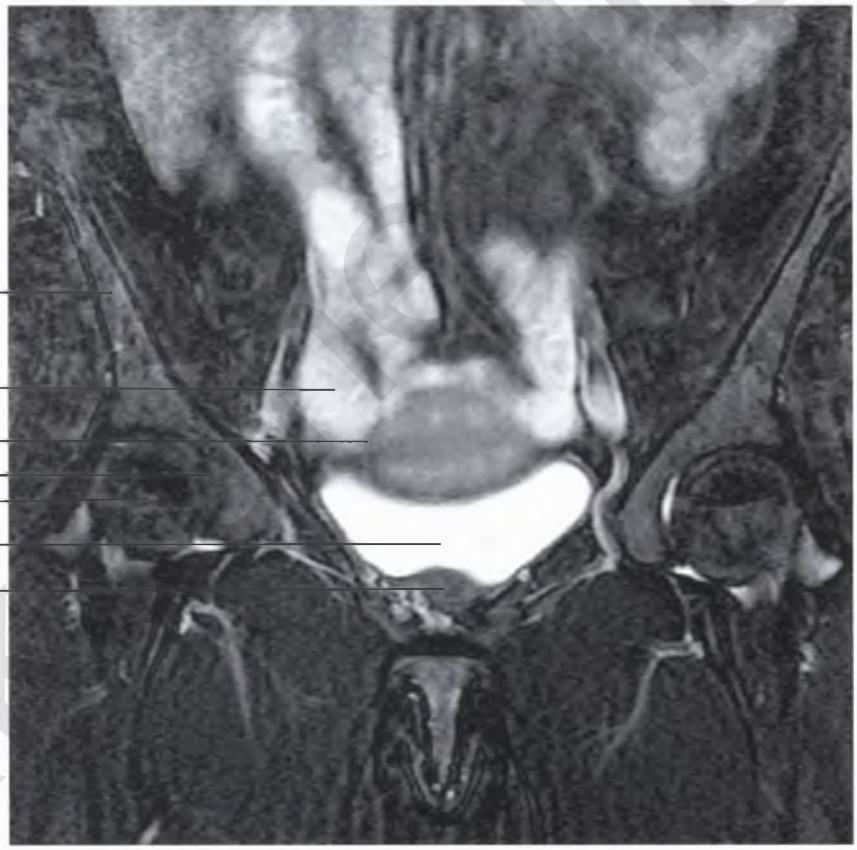
Ilium
Small bowel
Uterine fundus
Acetabulum
Femoral head
Bladder
Bladder neck

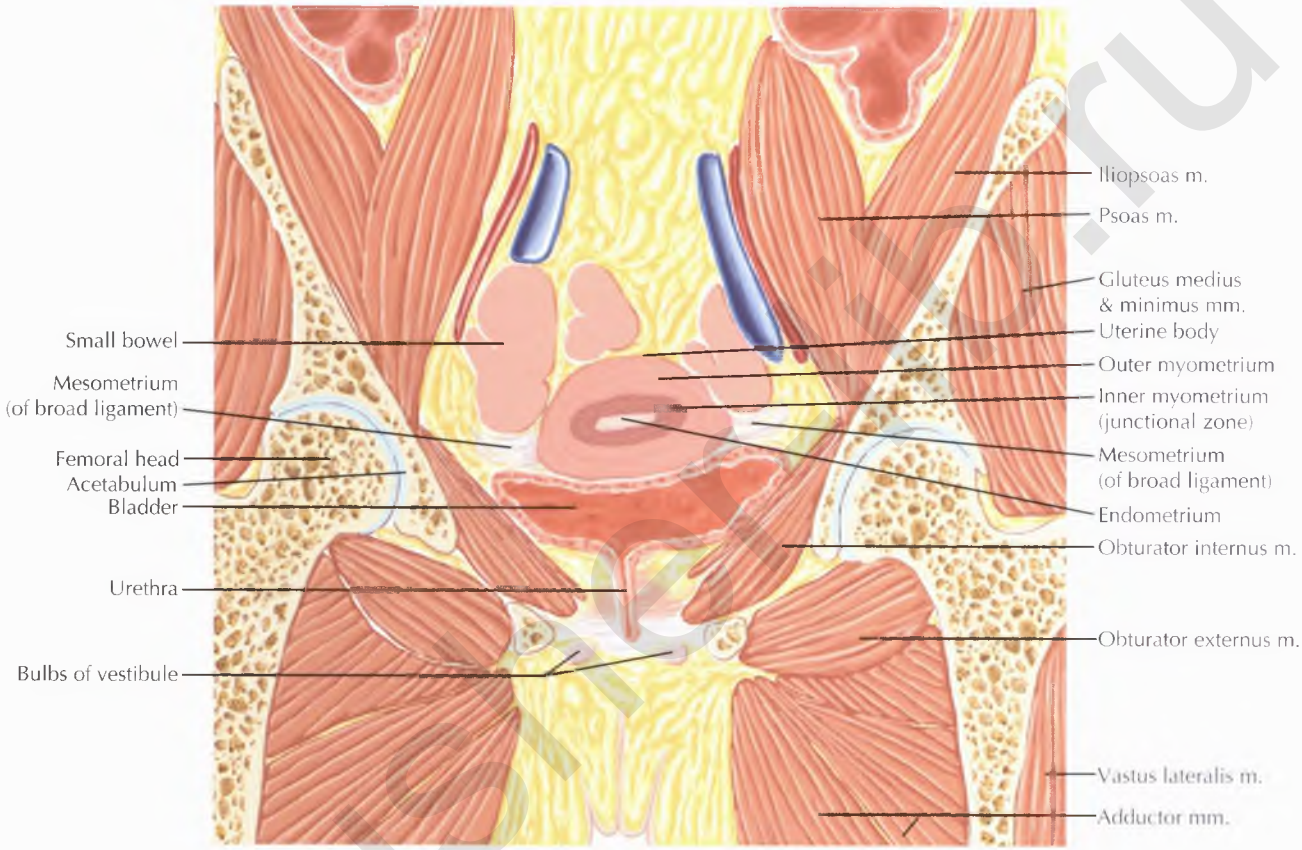

PATHOLOGIC PROCESS

Uterine leiomyomas, benign tumors of smooth muscle, are exceedingly common findings on MRI. A *leiomyoma* typically appears as a well-circumscribed mass in the outer myometrium with low-intermediate T1-weighted and low T2-weighted signal intensity, although both the signal intensity and enhancement characteristics may vary because of the variable presence of hemorrhage, cystic change, or necrosis. MRI of the uterus is usually performed for assessment of the location and viability of uterine leiomyomas before uterine artery embolization or myomectomy.

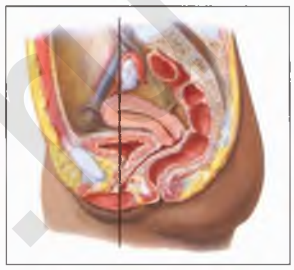

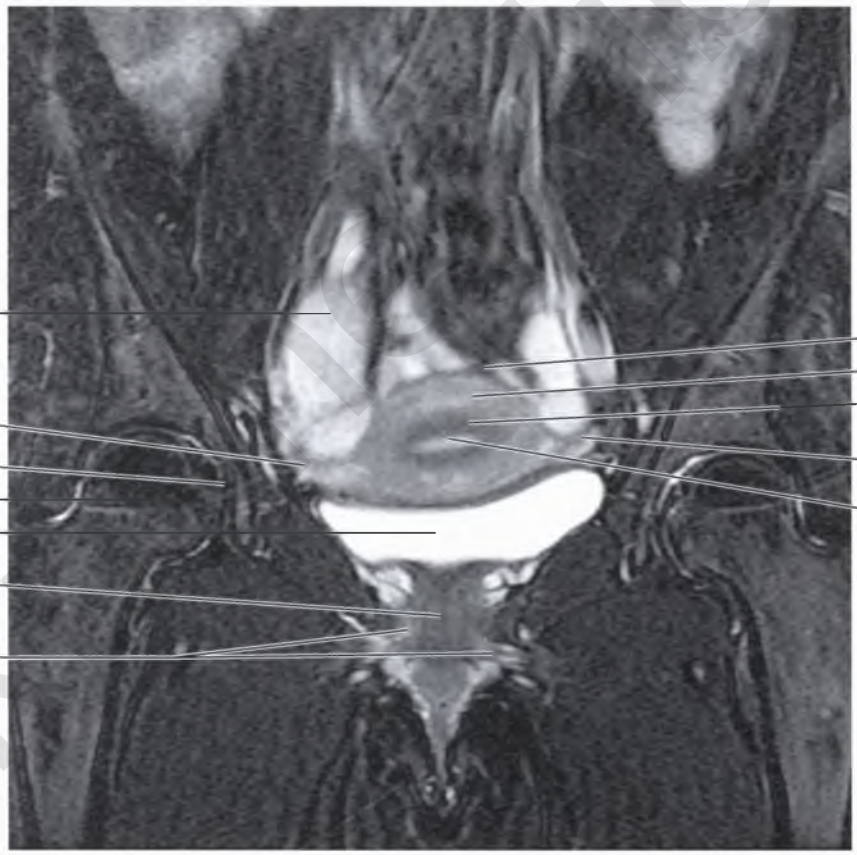
Small bowel
Mesometrium (of broad ligament)
Acetabulum
Femoral head
Bladder
Urethra
Bulbs of vestibule
Uterine body
Outer myometrium
Inner myometrium (junctional zone)
Mesometrium (of broad ligament)
Endometrium

NORMAL VARIANT

Uterine contractions, which cause low signal intensity bulges in the uterine contour, may occasionally be seen on MRI and can mimic uterine leiomyomas. However, uterine contractions may be distinguished by their transient appearance and subsequent change in appearance or resolution during the course of an MRI examination.

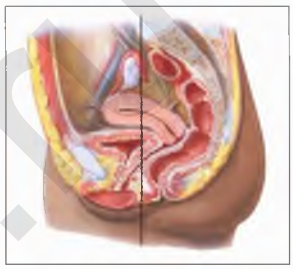

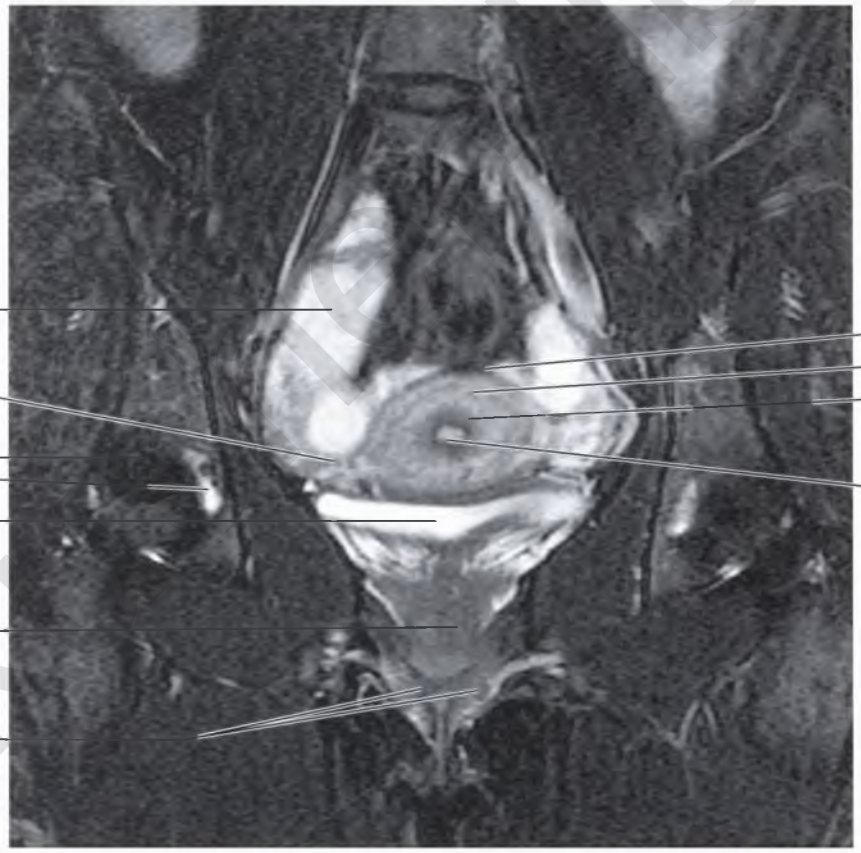

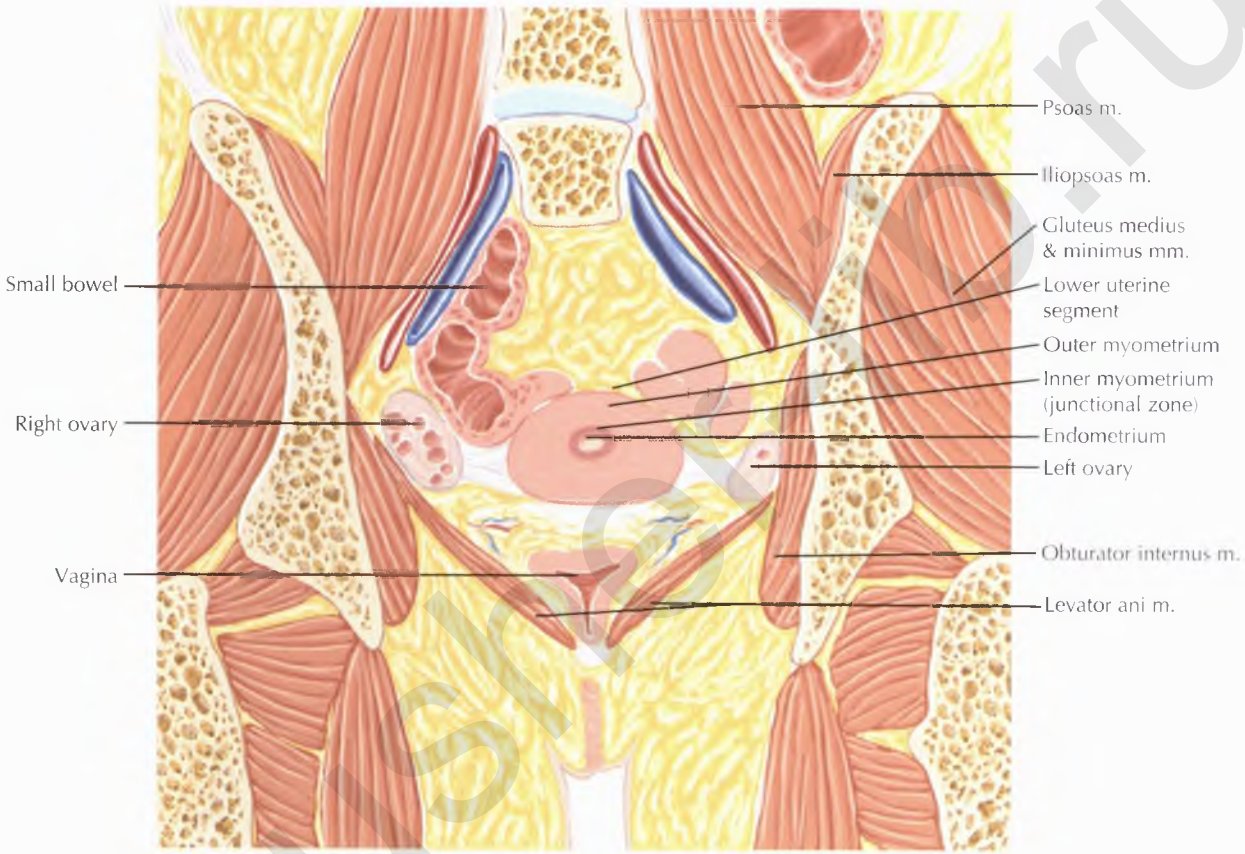

NORMAL ANATOMY

Multiple hyperintense follicles of varying sizes are typically seen within the ovaries in premenopausal women on T2-weighted MR images. Postmenopausal ovaries usually are of homogeneous, low signal intensity on T1-weighted and T2-weighted images and may not be well visualized because of their decreased size and volume in association with increasing age.

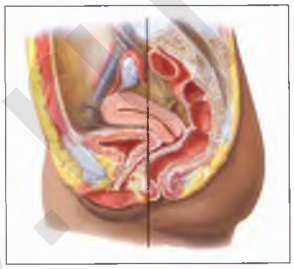

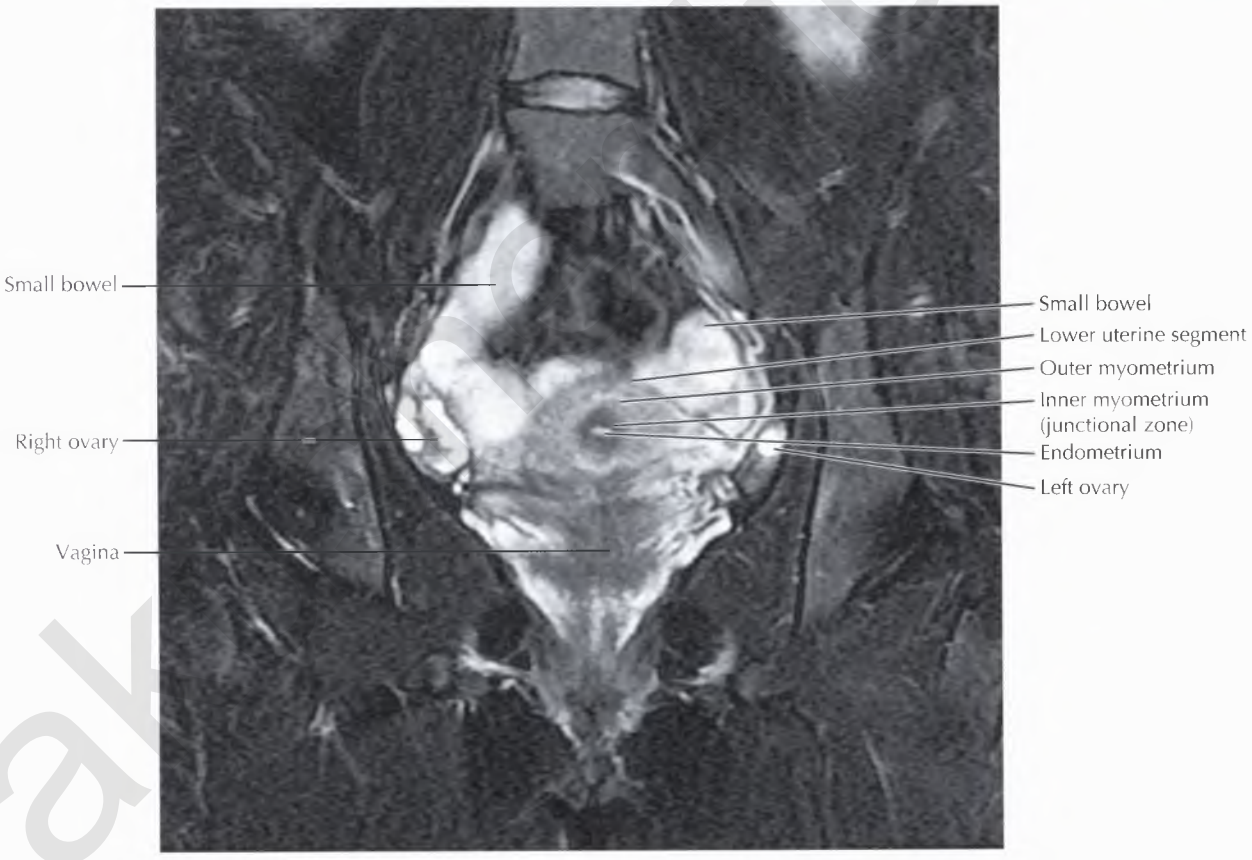
Small bowel
Right ovary
Vagina
Small bowel
Lower uterine segment
Outer myometrium
Inner myometrium
(junctional zone)
Endometrium
Left ovary

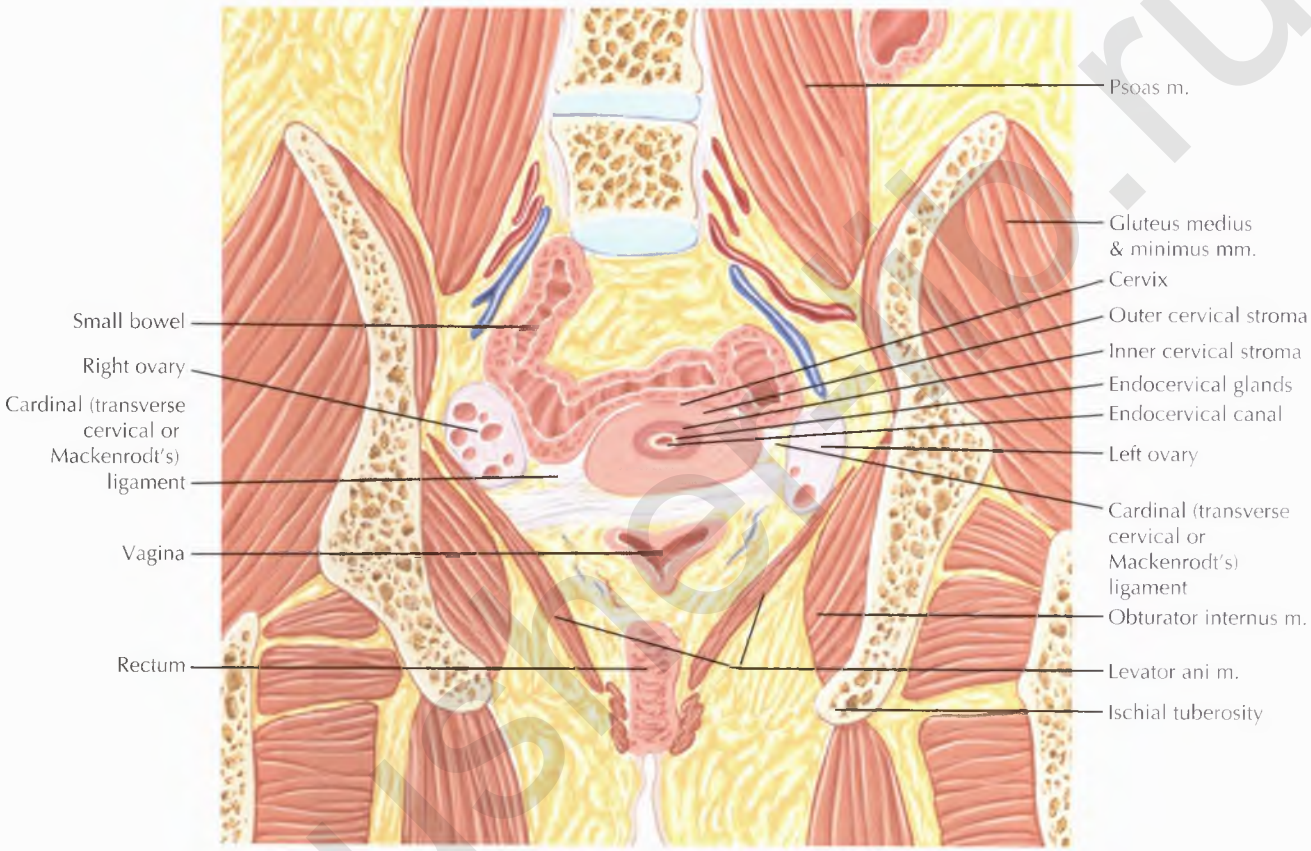

NORMAL ANATOMY

The *cardinal ligament*, also known as the transverse cervical ligament or Mackenrodt's ligament, extends laterally from the cervix and upper vagina, forming the base of the broad ligament and providing the primary ligamentous support for the uterus and upper vagina. The uterine artery runs along its superior aspect.

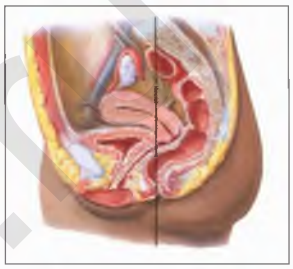

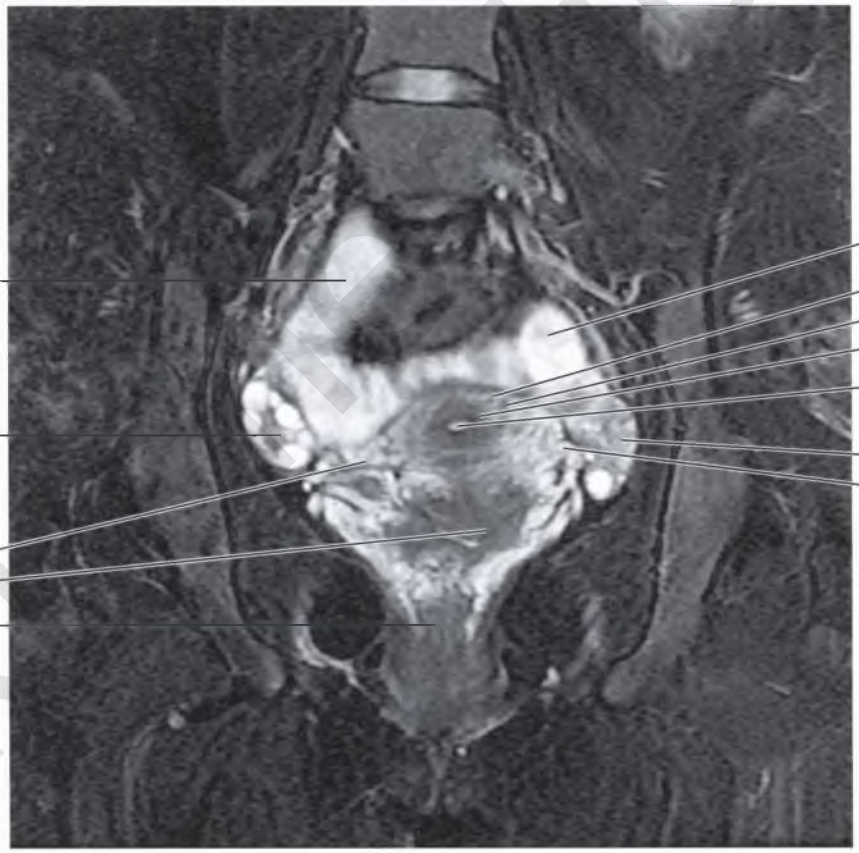
Small bowel
Right ovary
Cardinal (transverse cervical or Mackenrodt's) ligament
Vagina
Rectum
Small bowel
Cervix
Outer cervical stroma
Inner cervical stroma
Endocervical glands and canal
Left ovary
Cardinal (transverse cervical or Mackenrodt's) ligament

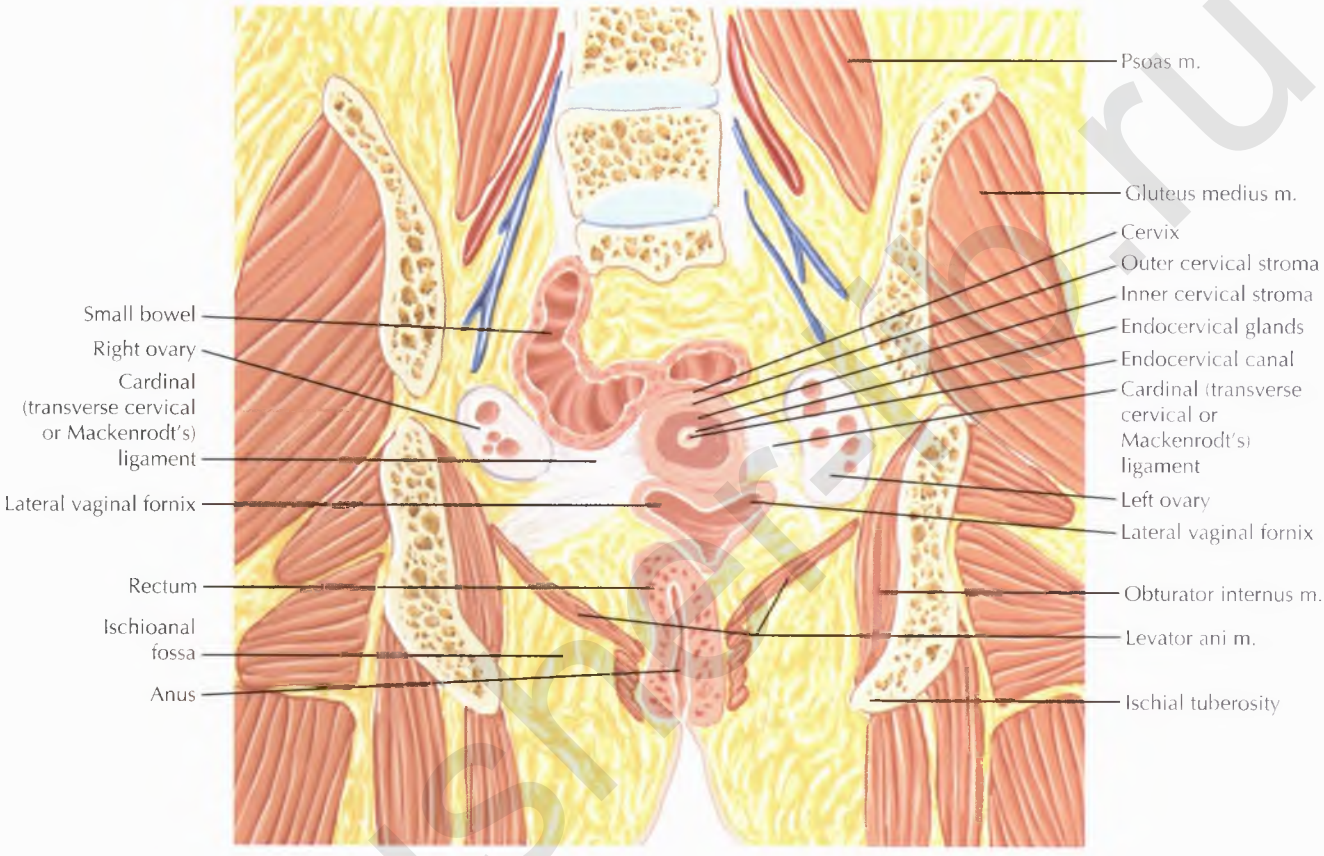

PATHOLOGIC PROCESS

Cervical carcinoma typically appears as a lesion of intermediate-high signal intensity that can disrupt the normal low signal intensity inner cervical stroma on T2-weighted MR images, and that often demonstrates early enhancement on postcontrast images. Morphologically, the tumor may appear as an exophytic mass originating at the squamocolumnar junction (especially in younger women), an infiltrative lesion, or a barrel-shaped endocervical mass expanding the endocervical canal (especially in older women). Evaluation for the presence of parametrial invasion is particularly important, because parametrial invasion generally indicates unresectable disease.

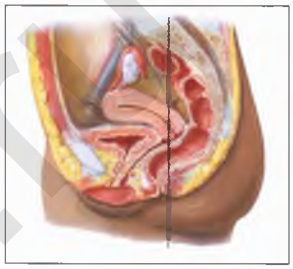

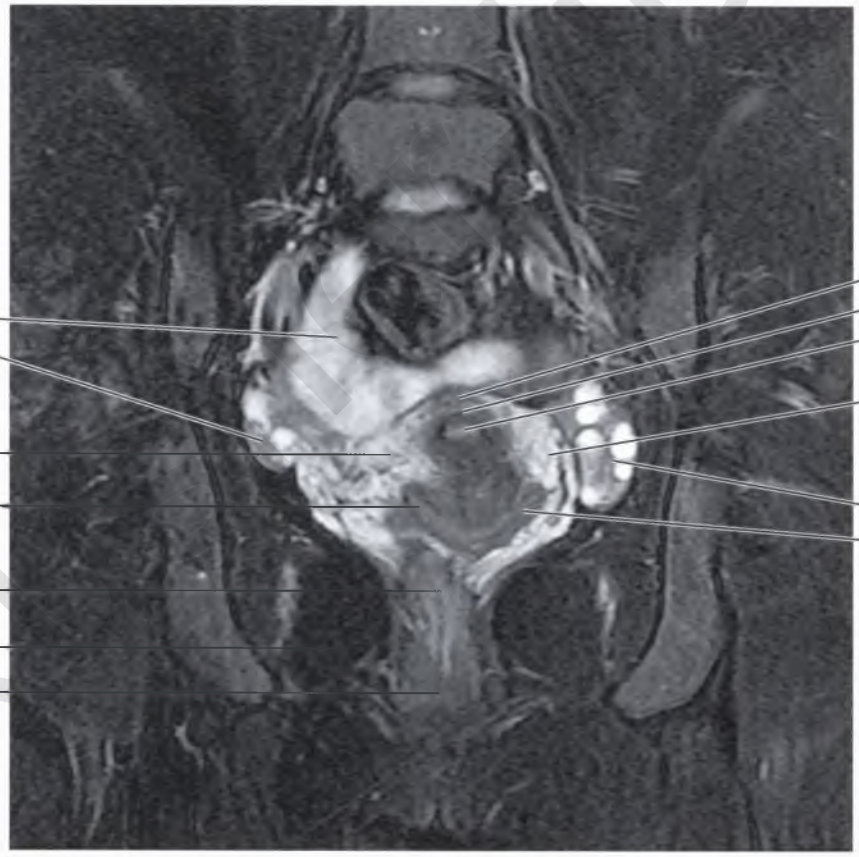
Small bowel
Right ovary
Cardinal (transverse cervical or Mackenrodt's) ligament
Lateral vaginal fornix
Rectum
Ischioanal fossa
Anus
Outer cervical stroma
Inner cervical stroma
Endocervical glands and canal
Cardinal (transverse cervical or Mackenrodt's) ligament
Left ovary
Lateral vaginal fornix

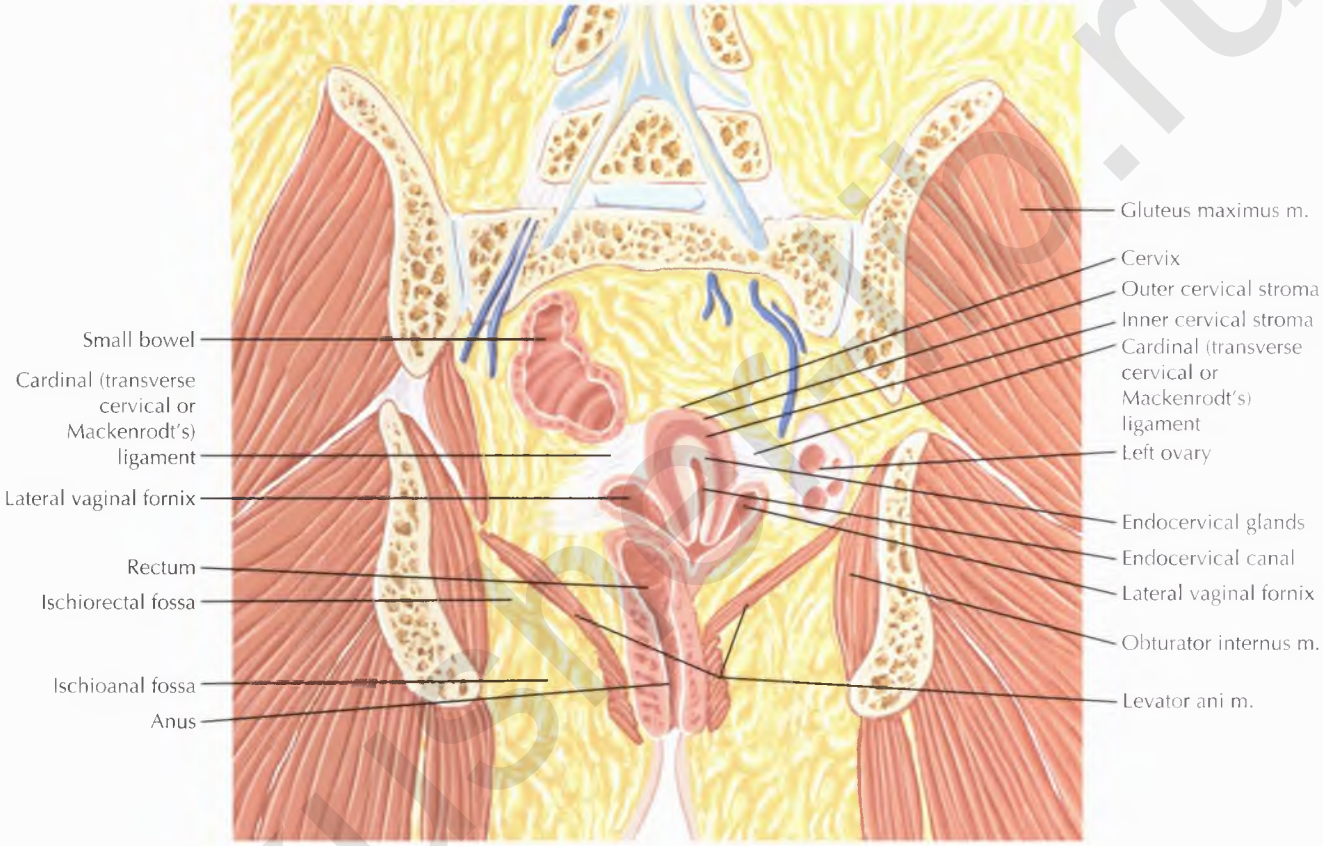

PATHOLOGIC PROCESS

Nabothian cysts represent obstructed mucus-secreting glands and are exceedingly common incidental findings on pelvic MRI.

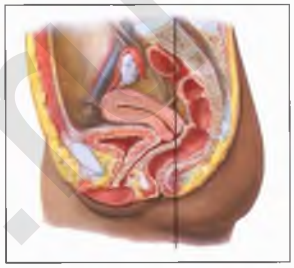

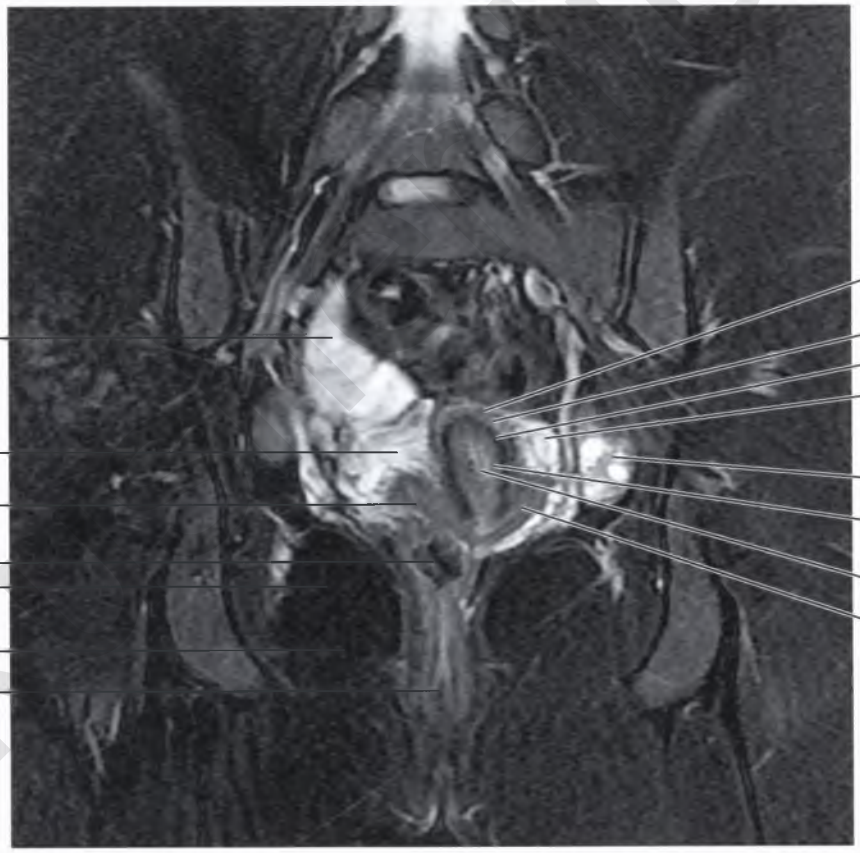
Small bowel
Cardinal (transverse cervical or Mackenrodt's) ligament
Lateral vaginal fornix
Rectum
Ischiorectal fossa
Ischioanal fossa
Anus
Cervix
Outer cervical stroma
Inner cervical stroma
Cardinal (transverse cervical or Mackenrodt's) ligament
Left ovary
Endocervical glands
Endocervical canal
Lateral vaginal fornix

PATHOLOGIC PROCESS

The general location of hematogenous metastases from rectal carcinoma depends on the location of the primary tumor. A tumor located in the upper third of the rectum tends to spread to the liver by way of the inferior mesenteric vein, through the *portal* venous system, whereas a tumor located in the lower two thirds of the rectum tends to spread to the lungs by way of the internal iliac veins, through the *systemic* venous system).

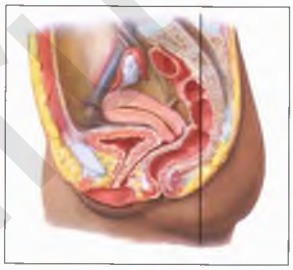

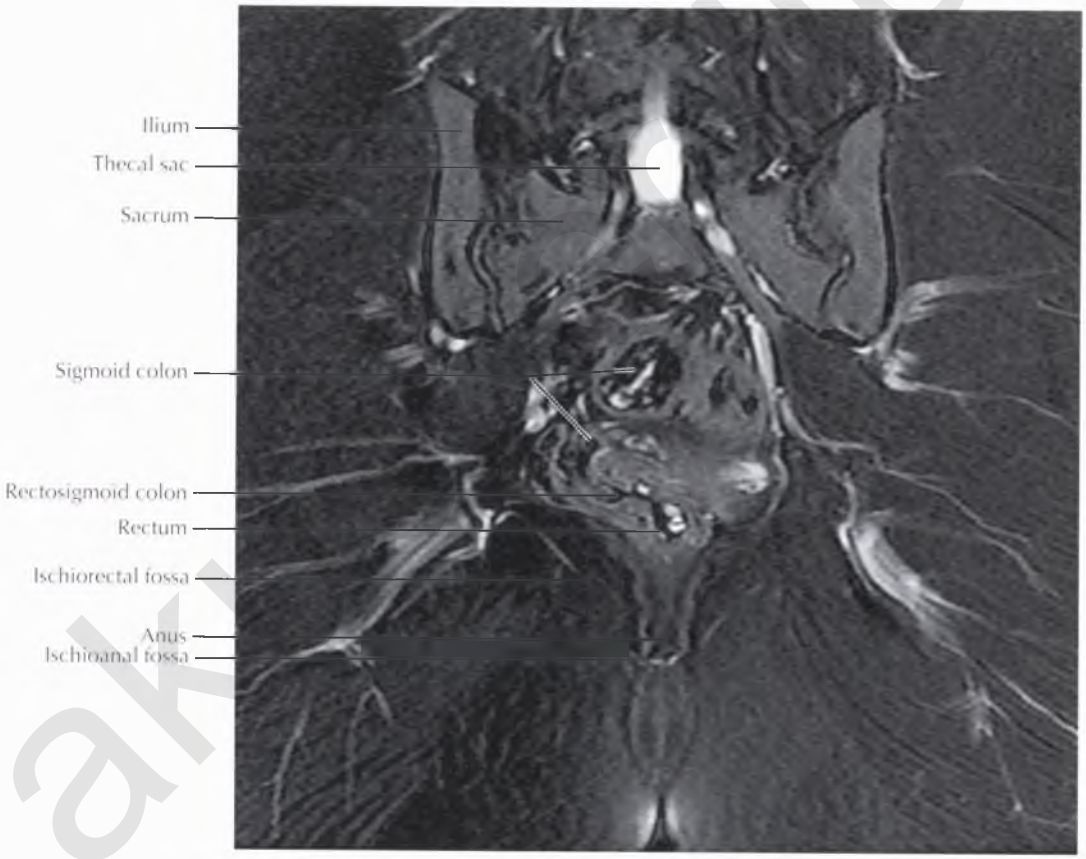
Ilium
Thecal sac
Sacrum
Sigmoid colon
Rectosigmoid colon
Rectum
Ischiorectal fossa
Anus
Ischioanal fossa

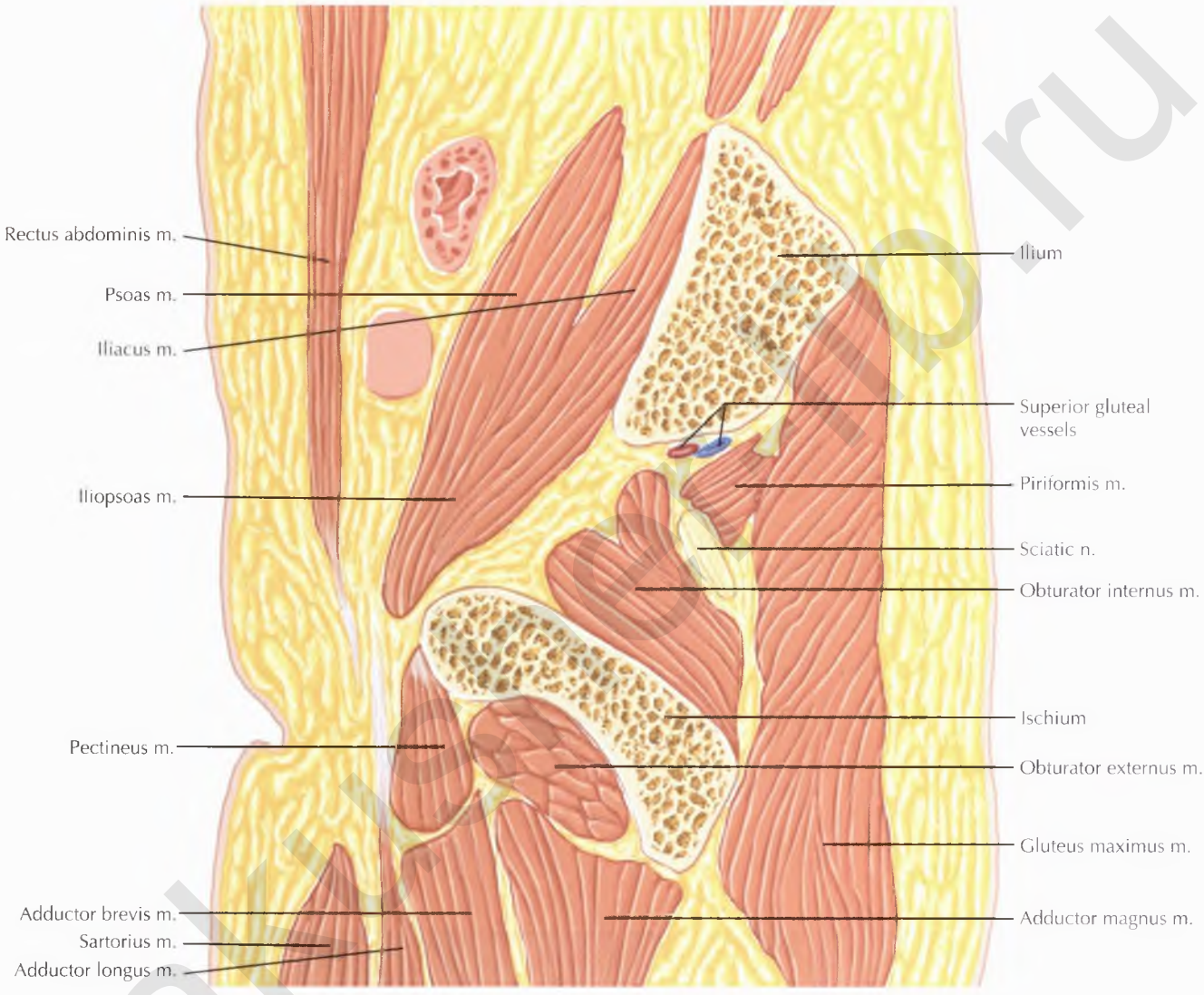

PATHOLOGIC PROCESS

Piriformis syndrome is caused by irritation of the sciatic nerve by the adjacent piriformis muscle, causing buttock pain and referred pain along the sciatic nerve distribution.

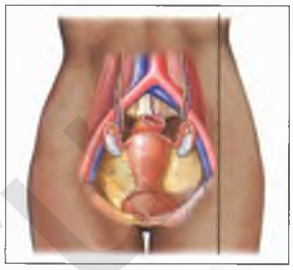

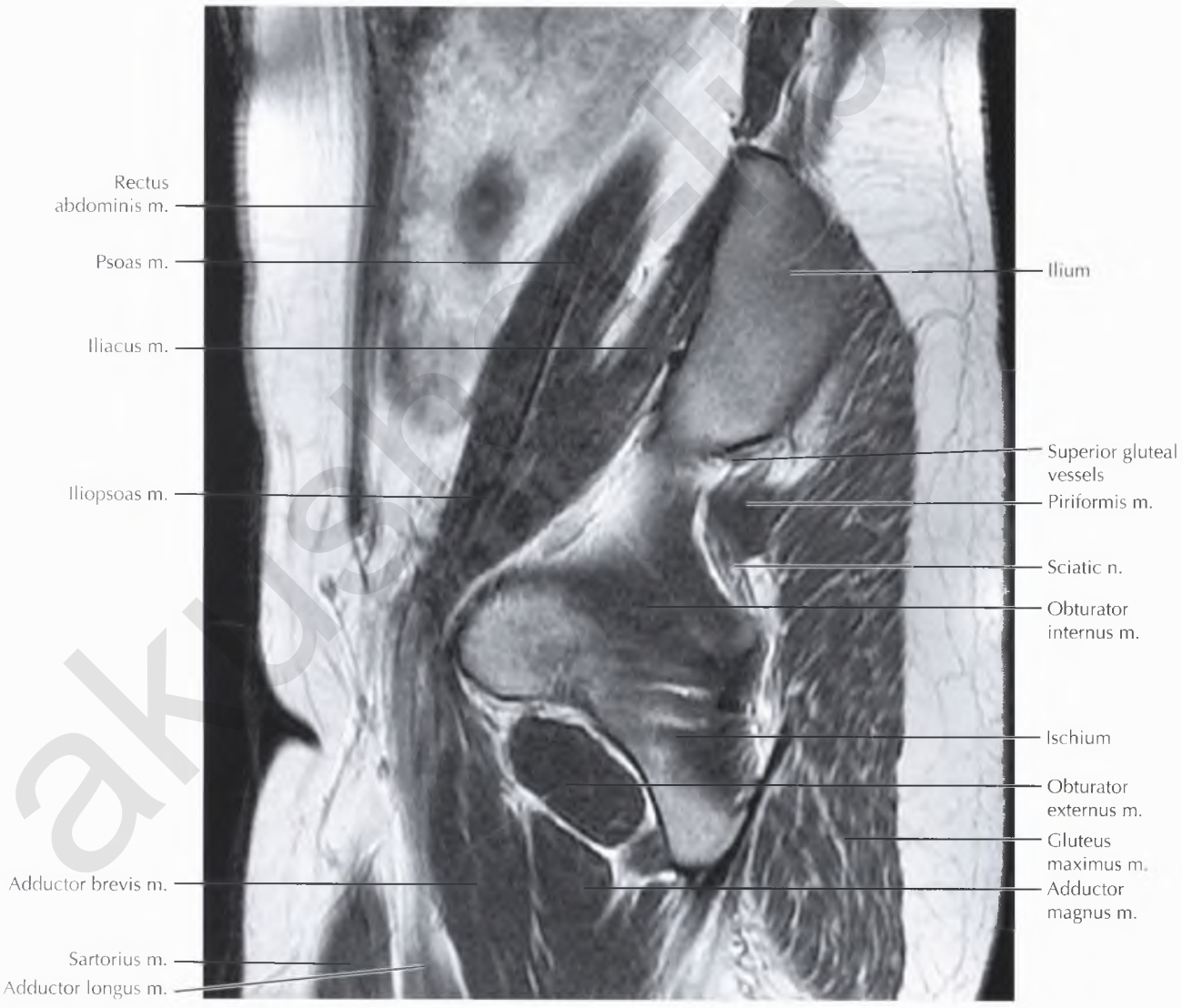
Rectus abdominis m.
Psoas m.
Iliacus m.
Iliopsoas m.
Adductor brevis m.
Sartorius m.
Adductor longus m.
Ilium
Superior gluteal vessels
Piriformis m.
Sciatic n.
Obturator internus m.
Ischium
Obturator externus m.
Gluteus maximus m.
Adductor magnus m.

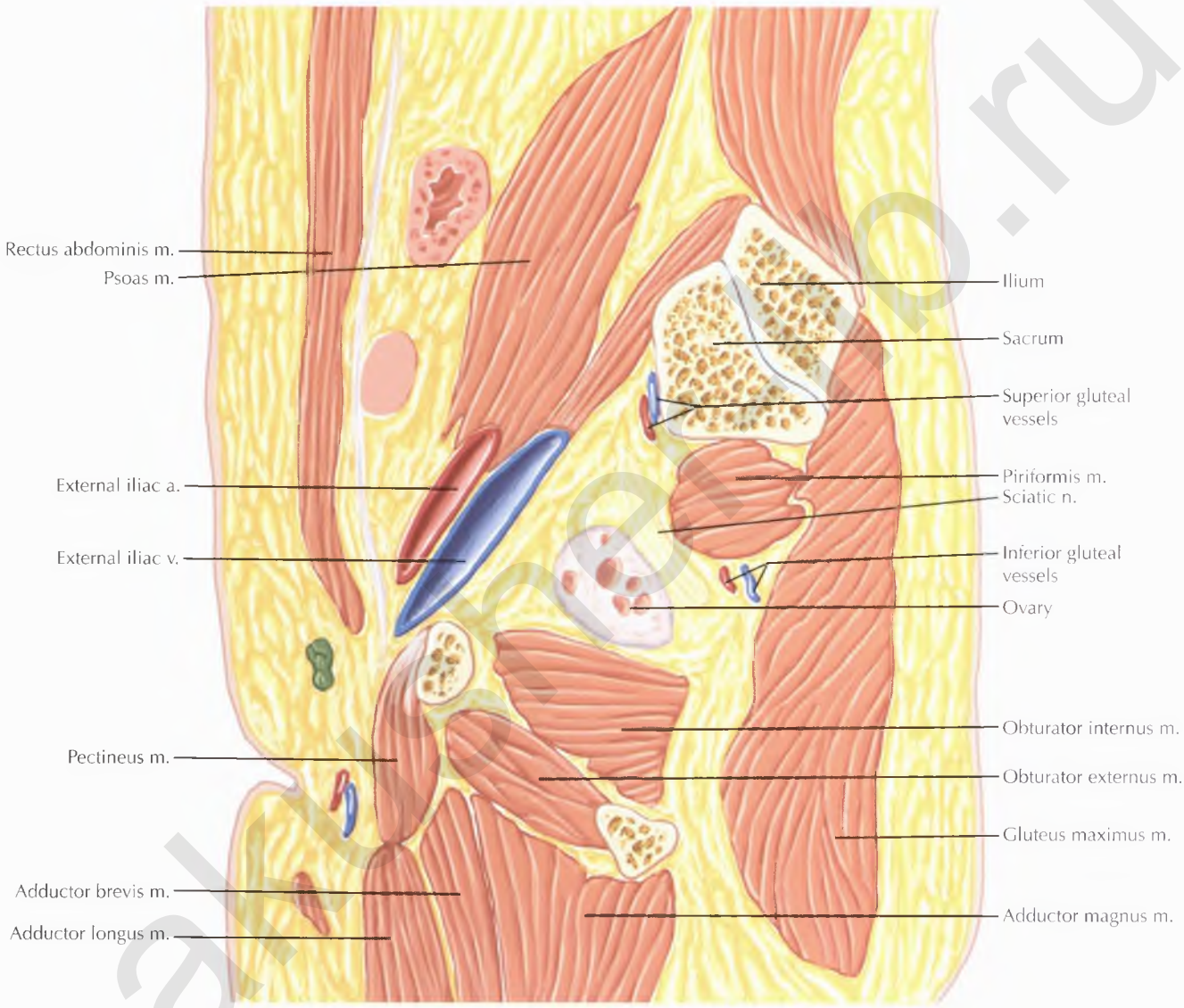
Rectus abdominis m.
Psoas m.
External iliac a.
External iliac v.
Pectineus m.
Adductor brevis m.
Adductor longus m.
Ilium
Sacrum
Superior gluteal vessels
Piriformis m.
Sciatic n.
Inferior gluteal vessels
Ovary
Obturator internus m.
Obturator externus m.
Gluteus maximus m.
Adductor magnus m.

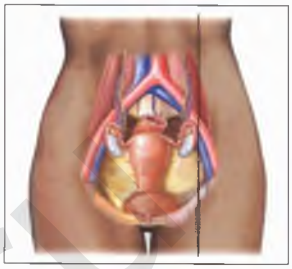

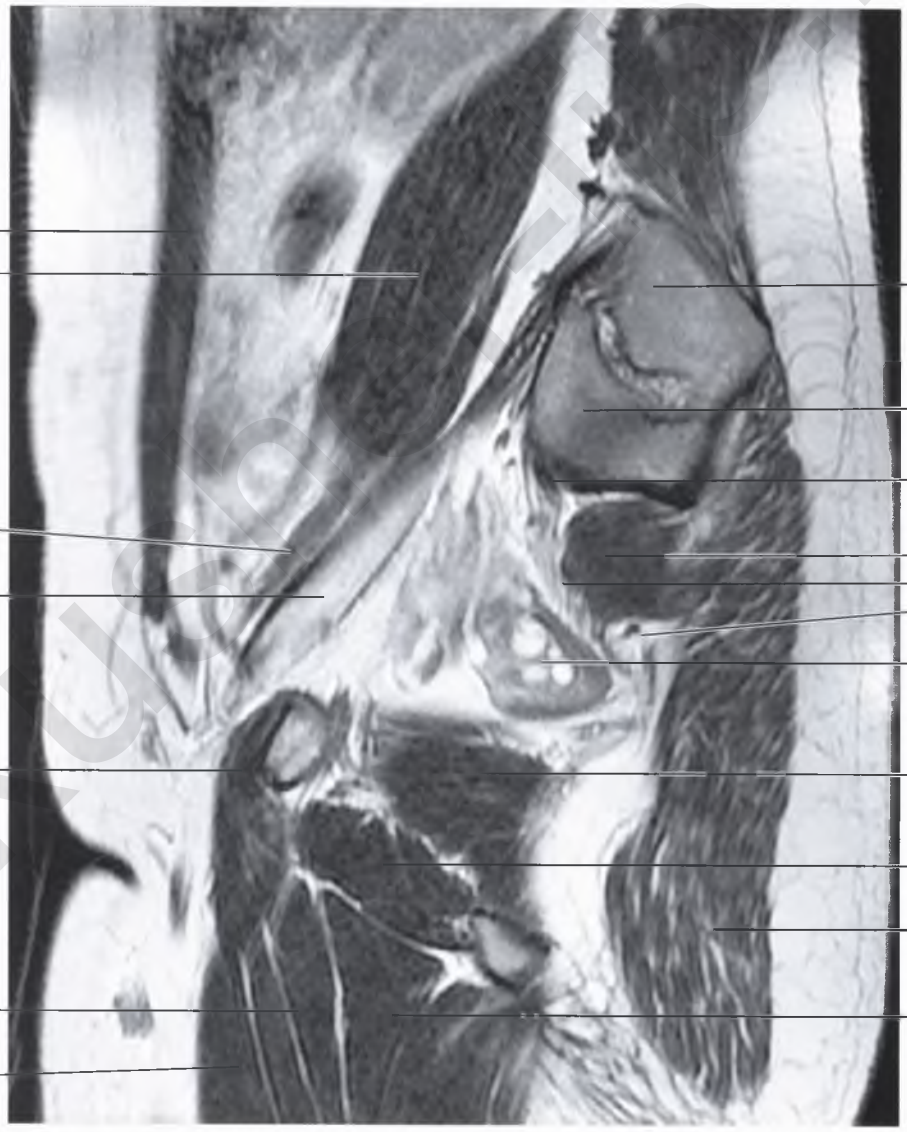
Rectus abdominis m.
Psoas m.
External iliac a.
External iliac v.
Pectineus m.
Adductor brevis m.
Adductor longus m.
Ilium
Sacrum
Superior gluteal vessels
Piriformis m.
Sciatic n.
Inferior gluteal vessels
Ovary
Obturator internus m.
Obturator externus m.
Gluteus maximus m.
Adductor magnus m.

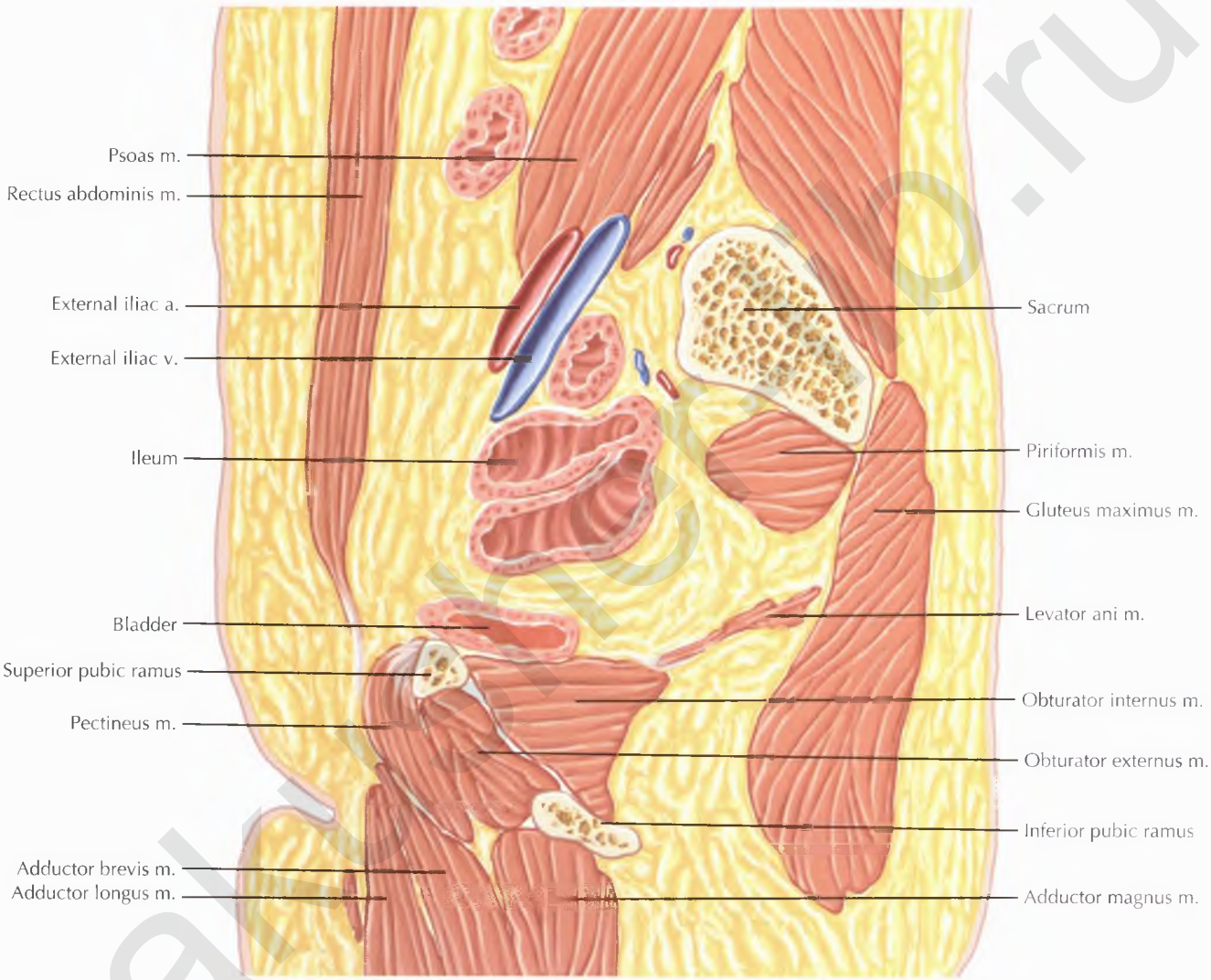
Psoas m.
Rectus abdominis m.
External iliac a.
External iliac v.
Ileum
Bladder
Superior pubic ramus
Pectineus m.
Adductor brevis m.
Adductor longus m.
Sacrum
Piriformis m.
Gluteus maximus m.
Levator ani m.
Obturator internus m.
Obturator externus m.
Inferior pubic ramus
Adductor magnus m.

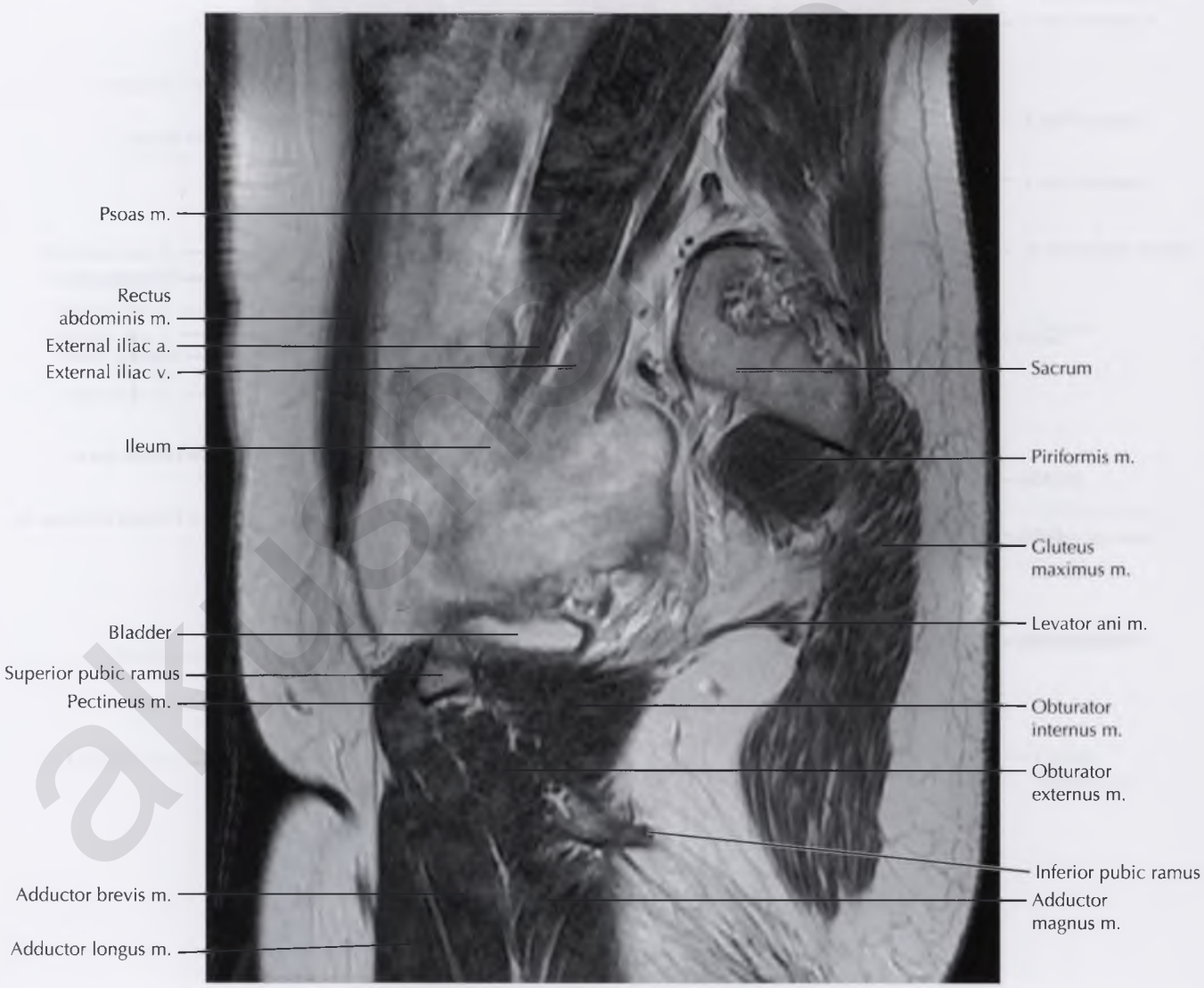
Psoas m.
Rectus abdominis m.
External iliac a.
External iliac v.
Ileum
Bladder
Superior pubic ramus
Pectineus m.
Adductor brevis m.
Adductor longus m.
Sacrum
Piriformis m.
Gluteus maximus m.
Levator ani m.
Obturator internus m.
Obturator externus m.
Inferior pubic ramus
Adductor magnus m.

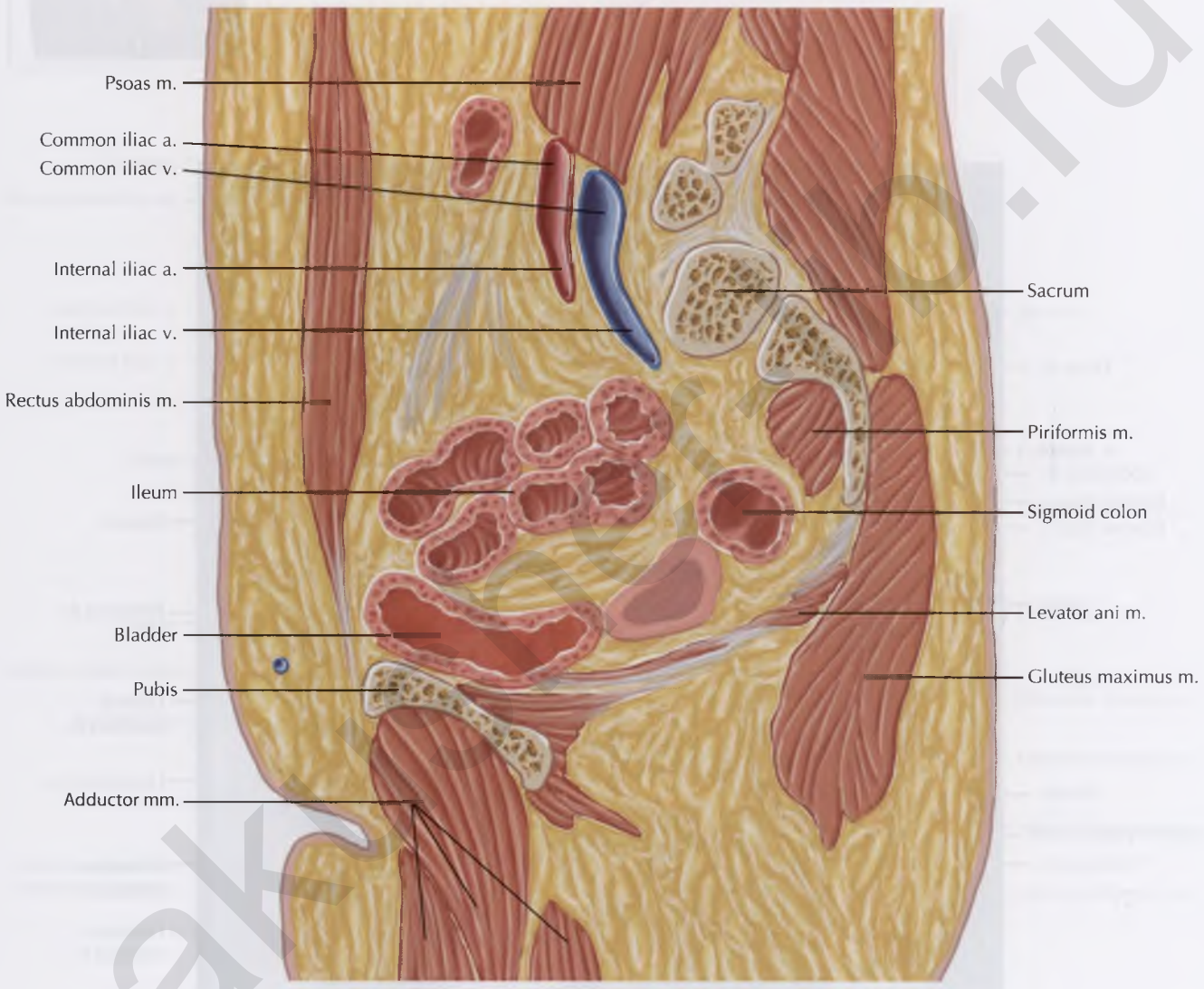
Psoas m.
Common iliac a.
Common iliac v.
Internal iliac a.
Internal iliac v.
Rectus abdominis m.
Ileum
Bladder
Pubis
Adductor mm.
Sacrum
Piriformis m.
Sigmoid colon
Levator ani m.
Gluteus maximus m.

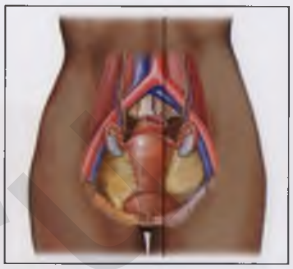

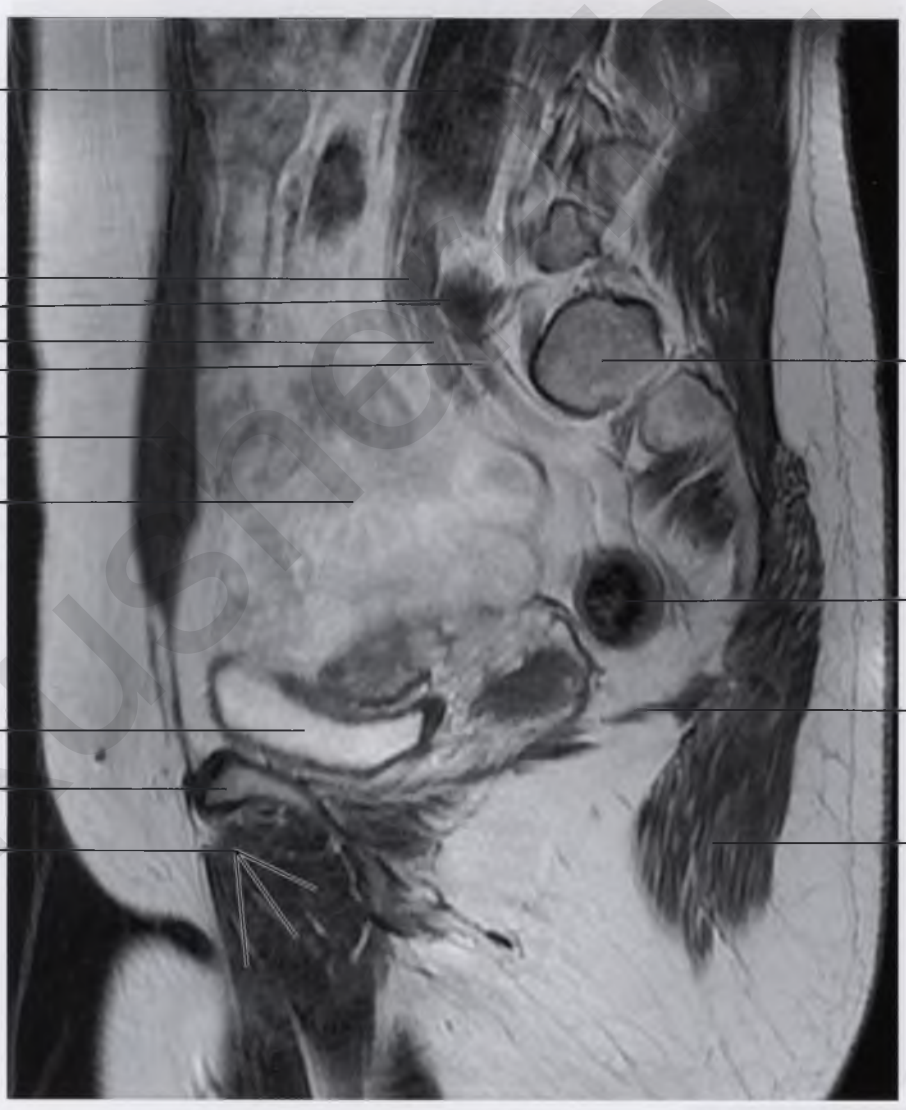
Psoas m.
Common iliac a.
Common iliac v.
Internal iliac a.
Internal iliac v.
Rectus abdominis m.
Ileum
Bladder
Pubis
Adductor mm.
Sacrum
Sigmoid colon
Levator ani m.
Gluteus maximus m.

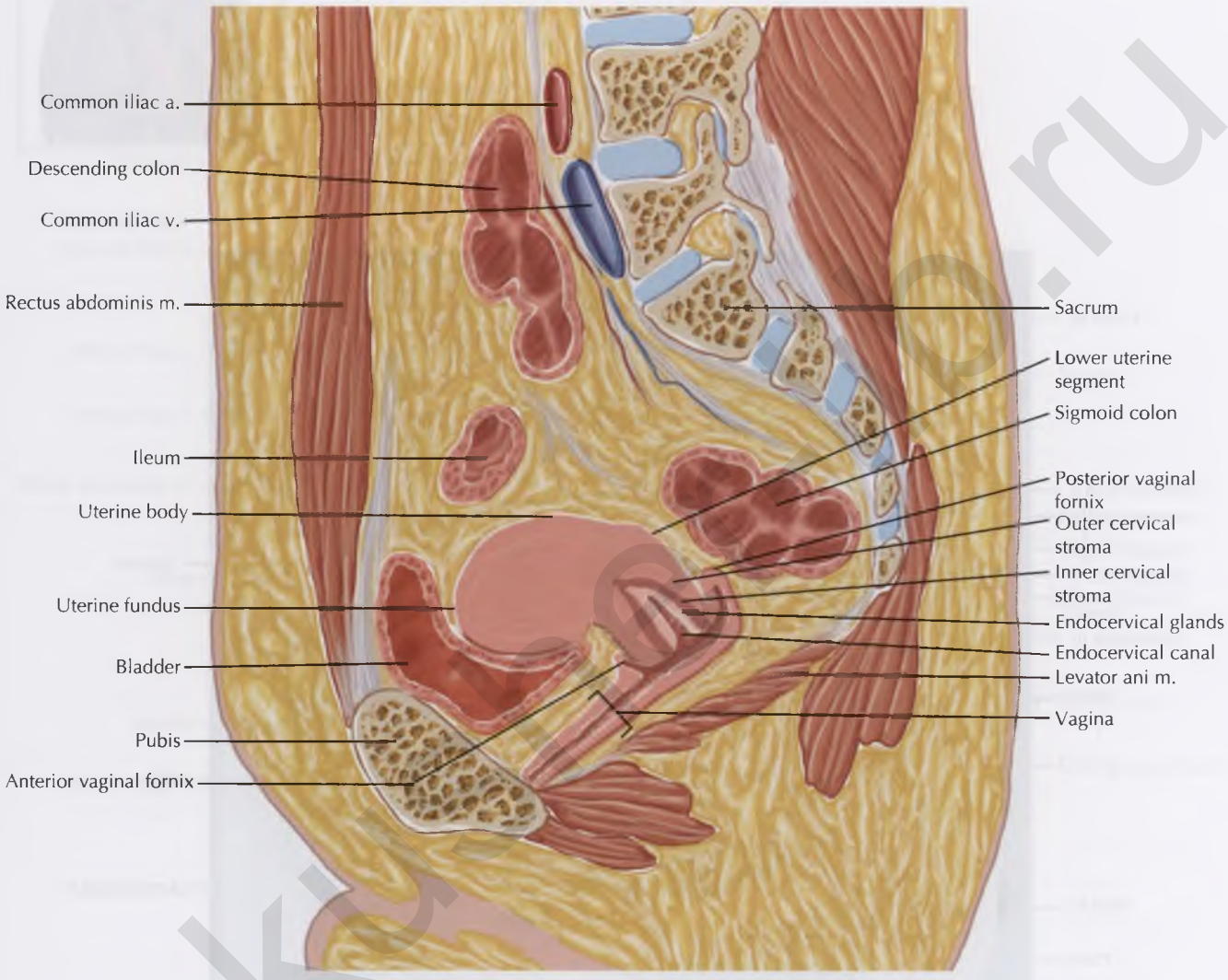

NORMAL ANATOMY

The uterus is divided into the uterine fundus, the uterine body, and the lower uterine segment. The position of the uterus is often described based on the flexion and version of the uterus, with *flexion* referring to the axis of the uterine body relative to the cervix, and *version* referring to the axis of the cervix relative to the vagina. In this case, the uterus is anteverted and anteflexed, which is the most common position.

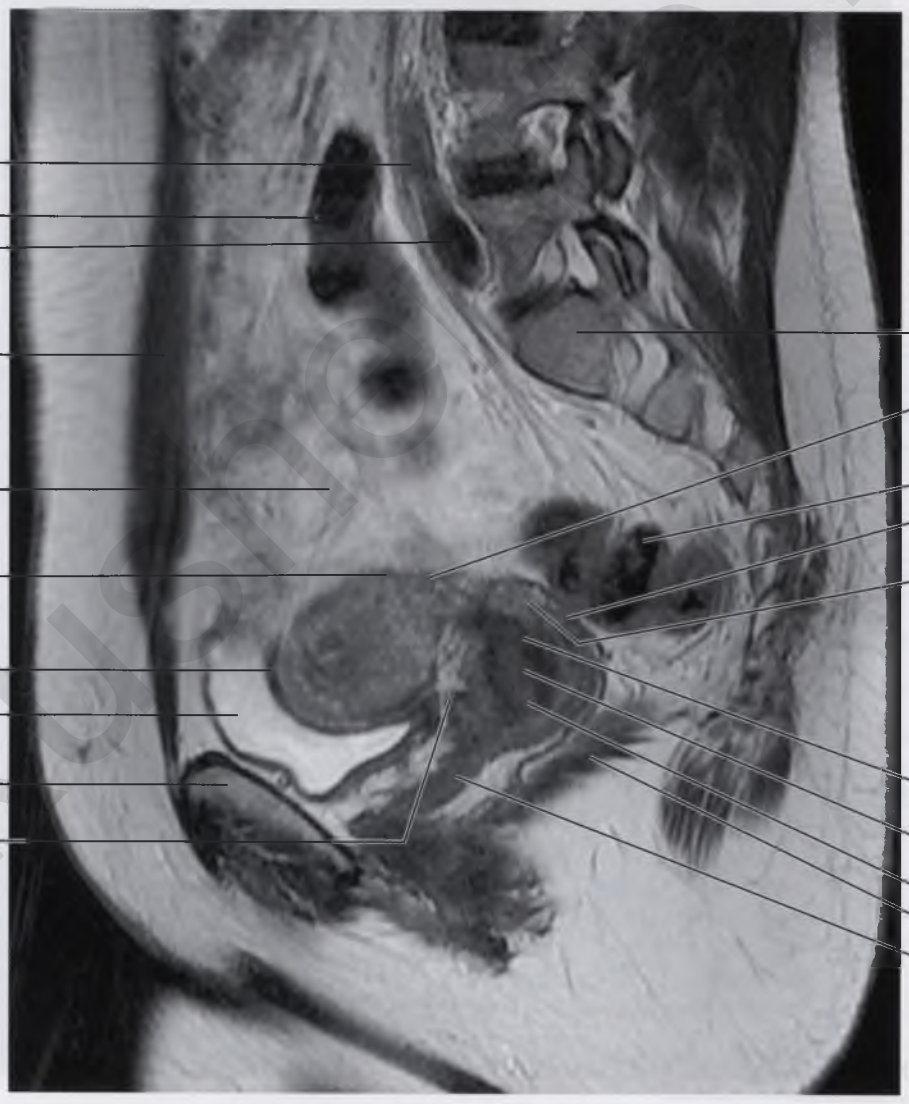

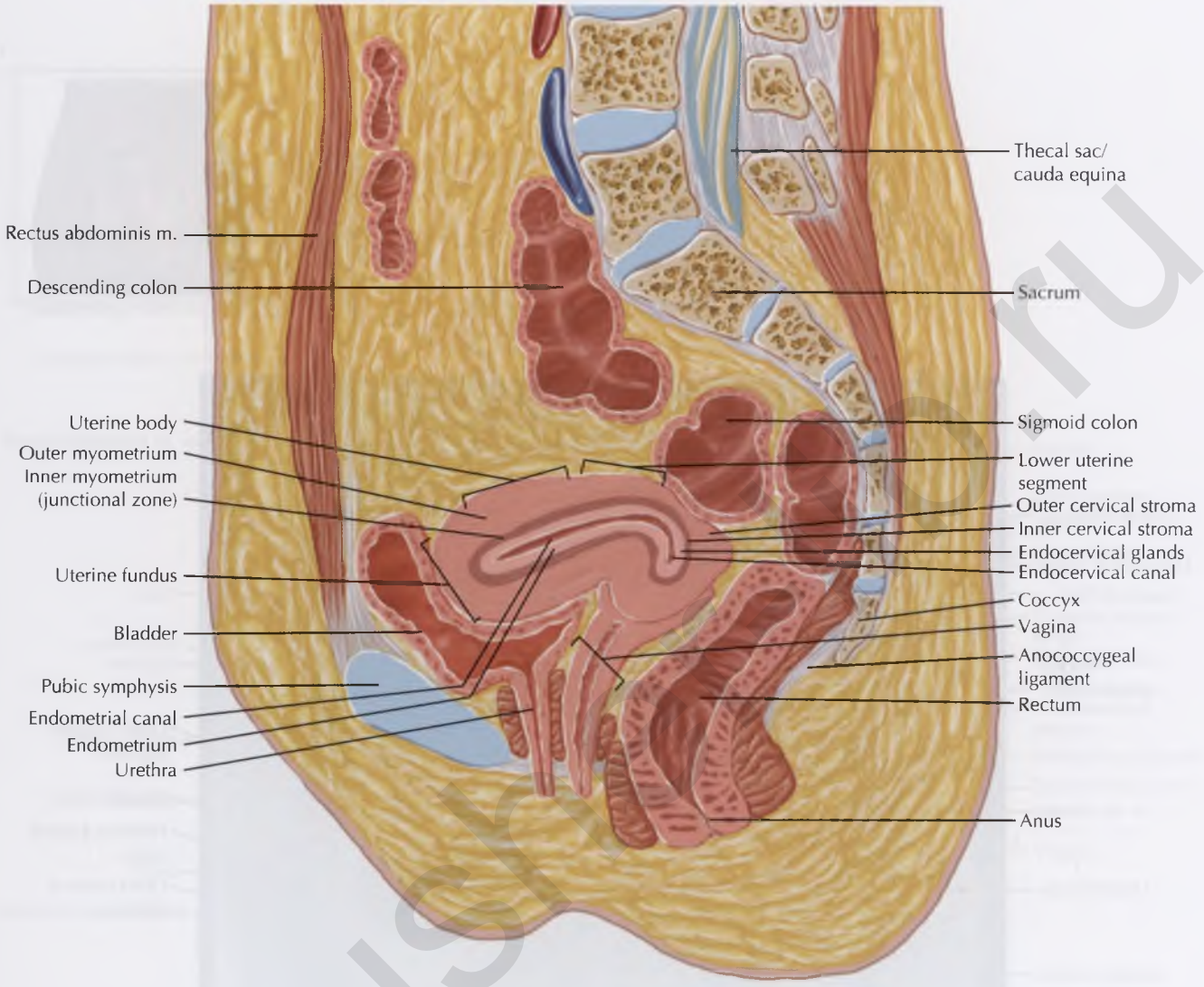

NORMAL ANATOMY

The thickness of the junctional zone and endometrium should be assessed on sagittal (long-axis) T2-weighted images through the uterus. The inner myometrium (or junctional zone) normally measures less than 12 mm in thickness. Endometrial thickness varies depending on the phase of the menstrual cycle, appearing thin (1-4 mm) during menstruation and reaching maximal thickness (up to about 20 mm) during the secretory phase. The postmenopausal endometrium should be thin and normally measures less than 5 mm.

PATHOLOGIC PROCESS

In *adenomyosis* the junctional zone is thickened, measuring 12 mm or greater, and often contains small, high-signal-intensity foci on T1-weighted and T2-weighted MR images, corresponding to ectopic hemorrhagic endometrial glands.

Focal endometrial thickening or signal abnormality raises suspicion for endometrial hyperplasia, endometrial carcinoma, or an endometrial polyp.

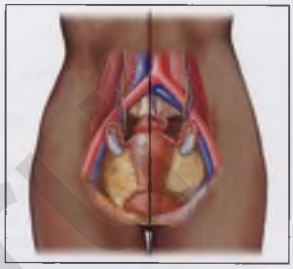

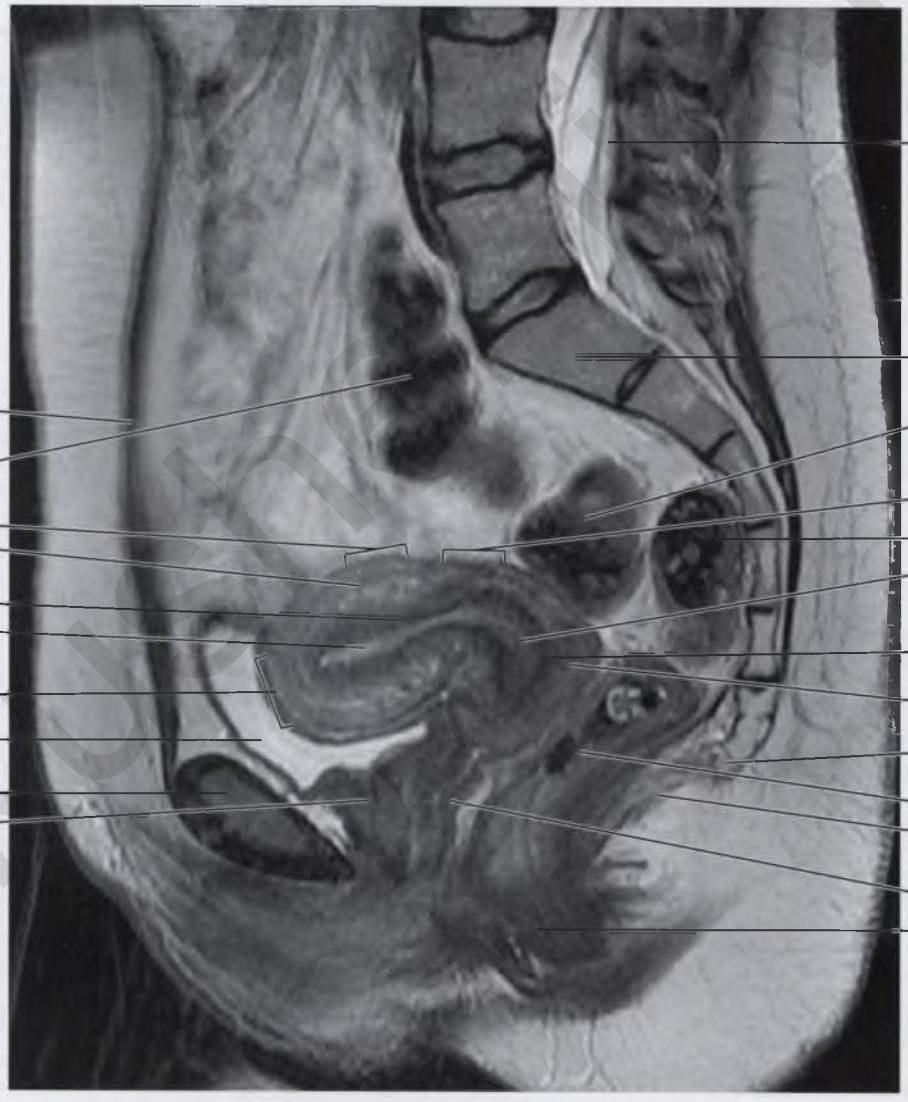
Thecal sac/
cauda equina
Sacrum
Rectus
abdominis m.
Descending colon
Sigmoid colon
Lower uterine
segment
Uterine body
Outer myometrium
Inner myometrium
(junctional zone)
Endometrium and
endocervical canal
Rectosigmoid colon
Endocervical
glands and
endocervical canal
Inner cervical
stroma
Uterine fundus
Outer cervical
stroma
Bladder
Coccyx
Pubic symphysis
Urethra
Rectum
Anococcygeal
ligament
Vagina
Anus

Index

C

D

E

F

G

H

I

J

K

L

M

N

O

P

Q

R

S

T

U

V

X

Z

NETTER'S Correlative Imaging
Abdominal and Pelvic Anatomy

with Online Access at www.NetterReference.com

DREW A. TORIGIAN, MD, MA, AND MARY KITAZONO HAMMELL, MD

Visualize normal anatomy of the abdomen and pelvis like never before with the unparalleled coverage in this outstanding volume of the *Netter's Correlative Imaging* series. Beautiful and instructive **Netter paintings** and **illustrated cross-sections created in the Netter style** are presented side by side with **high-quality patient MR images** to help you envision and review both gastrointestinal and genitourinary anatomy section by section.

- **View organs, vessels, and peritoneal anatomy** through MR, MRA, MRV, and MRCP imaging in a variety of planes, **complemented with a detailed illustration of each slice** done in the instructional and aesthetic Netter style.
- **Find anatomical landmarks quickly and easily** through comprehensive labeling and concise text highlighting key points related to the illustration and image pairings.
- **Correlate patient data to idealized normal anatomy**, always in the same view with the same labeling system.
- **Access NetterReference.com** where you can quickly and simultaneously scroll through images and illustrations.

In-depth coverage, access to correlated images online, and concise, descriptive text make this unique atlas a **comprehensive, one-stop normal-anatomy reference** for today's busy body-imaging specialists.

Activate at
www.NetterReference.com

Netter's Correlative Imaging Series

Recommended
Shelving
Classification
Radiology
Anatomy

ISBN 978-1-4377-3654-0

9 781437 736540

ELSEVIER
SAUNDERS

elsevierhealth.com